

LATE-HOLOCENE LAKE DIATOM-INFERRED PALAEOCLIMATE
FROM CENTRAL TURKEY

by

JESSIE WOODBRIDGE

A thesis submitted to the University of Plymouth
in partial fulfilment for the degree of

DOCTOR OF PHILOSOPHY

School of Geography

Faculty of Science

April 2009

Abstract

Late-Holocene Lake Diatom-Inferred Palaeoclimate from Central Turkey

Jessie Woodbridge

In the semi-arid environment of the Eastern Mediterranean, water can be a limiting resource and its availability is influenced by different climate factors. Knowledge of late Holocene water balance is limited for this region. Lake systems and organisms respond to environmental variability and can be used as a proxy for palaeoclimate. The aims of this research project were to reconstruct late Holocene palaeoclimate using diatom frustules preserved within crater lake sediments in central Turkey. Two lakes (Nar Gölü and Kratergöl), located in the same climate region, were selected for this purpose. Modern lake samples and sediment cores collected between 1999-2006 were subsampled at high resolution for diatom analysis. Nar Gölü provided an uninterrupted annually-laminated late Holocene sequence covering the last 1720 years. The varied lake sedimentation rate of Kratergöl was evident in sediment core coarse sandy sections and the sequence was thought to represent the mid-late 20th century.

A diatom-salinity transfer function was employed using existing training sets from the European Diatom Database to infer past water balance. The reconstruction was calibrated with instrumental meteorological data. Reconstructed salinity was limited by poor analogue matching between the palaeo-diatom assemblage and the modern training set. This was partly associated with the presence of a previously undescribed diatom genus (newly named *Clipeoparvus anatolicus*), which was highly abundant in the Nar

modern environment and sediment record. Additional methods to extract palaeoenvironmental information from the diatom record were explored. This included calibrating diatom DCA axes with instrumental temperature in order to reconstruct palaeo-temperature, identifying mono-specific diatom bloom events *in situ* on core thin section slides, calculating diatom biovolume, concentration, diversity and grouping species according to their habitat preferences. Comparison of the Nar and Kratergöl records highlighted the advantages of annually laminated lake sediments for palaeoenvironmental research and the limitations of sediment sequences from lakes with a varied sedimentation rate and poor chronological control.

The primary meteorological control on the Nar diatom population was identified as summer temperature, via the link with lake water salinity. The Nar diatom sequence was compared with an oxygen isotope (palaeo-evaporation) and pollen record (human land use) from the same sediment cores and palaeoclimate reconstructions from other sites and regions. Nar diatoms and oxygen isotopes revealed that Cappadocia experienced high aridity prior to AD 540 and mono-specific diatom bloom events have become increasingly common during the most recent ~400 years. A diatom assemblage shift at AD 2001 also indicated a recent change in the system. Human land use evident in the pollen sequence may have influenced the diatom relationship with climatic variability in the later part of the record. The Kratergöl diatom record indicated environmental variability throughout the mid-late 20th century; however, interpretations were limited due to chronological discrepancies. The annually laminated Nar diatom record has provided a detailed account of palaeoenvironmental variability in central Anatolia throughout the late Holocene and contributes towards our understanding of Eastern Mediterranean palaeoclimate.

Contents	Page
<i>Copyright Statement</i>	<i>i</i>
<i>Title Page</i>	<i>ii</i>
<i>Abstract</i>	<i>iii</i>
<i>Contents</i>	<i>v</i>
<i>Figures</i>	<i>xiv</i>
<i>Tables</i>	<i>xxii</i>
<i>Plates</i>	<i>xxv</i>
<i>Abbreviations</i>	<i>xxvi</i>
<i>Acknowledgements</i>	<i>xxviii</i>
<i>Author's declaration</i>	<i>xxix</i>
Chapter 1: Introduction	1
1.0 Late Holocene Eastern Mediterranean climate	1
1.1 Lake palaeoenvironmental archives	7
1.2 Diatom palaeoenvironmental indicators	9
1.3 Aims and objectives	12
1.4 Thesis outline	13
Chapter 2: Literature Review	
Lake Diatoms and Eastern Mediterranean Climate	15
2.0 Introduction	15
Part I: Palaeolimnology and Diatoms	15
2.1 Lacustrine environments	15
2.1.1 <i>Lake hydrology, biogeochemistry and climate</i>	17
2.1.2 <i>Palaeolimnology</i>	19
2.2 Diatoms as palaeo-indicators	20

2.2.1	<i>Lake diatoms</i>	20
2.2.2	<i>Lake hydrology, biogeochemistry and diatoms</i>	21
2.2.3	<i>Diatom-inferred climate reconstructions</i>	23
2.2.4	<i>Numerical techniques</i>	24
2.2.5	<i>Limitations</i>	27
2.2.6	<i>Additional diatom analysis methods</i>	30
2.3	Summary	32
Part II: Eastern Mediterranean Climate		33
2.4	Introduction	33
2.5	Factors controlling Eastern Mediterranean climate	34
2.5.1	<i>North Atlantic Oscillation</i>	34
2.5.2	<i>North Sea Caspian Pattern</i>	36
2.5.3	<i>Arctic Oscillation</i>	36
2.5.4	<i>Southern Oscillation</i>	37
2.5.5	<i>Indian Monsoon</i>	37
2.6	Instrumental meteorological records	37
2.6.1	<i>Spatial variability</i>	38
2.6.2	<i>Temporal variability</i>	41
2.7	Holocene palaeoclimate reconstructions	44
2.7.1	<i>Lake sediment archives</i>	44
2.7.2	<i>Non-lake archives</i>	46
2.7.3	<i>Holocene climate history</i>	48
2.8	Summary	49
Chapter 3: Methodology		51
3.0	Introduction	51

3.1	Site selection	51
3.2	Fieldwork methods	57
3.2.1	<i>Diatom sampling</i>	57
3.2.2	<i>Seston sediment traps</i>	58
3.2.3	<i>Water sampling</i>	62
3.2.4	<i>Glew core collection</i>	62
3.2.5	<i>Archived lake cores</i>	63
3.2.6	<i>Bathymetry</i>	65
3.3	Laboratory methods	65
3.3.1	<i>Nar Gölü core chronology</i>	65
3.3.2	<i>Kratergöl chronology</i>	66
3.3.3	<i>Core sub-sampling</i>	66
3.3.4	<i>Kratergöl sediment analysis</i>	67
3.3.5	<i>Diatom subsampling</i>	68
3.3.6	<i>Sediment traps and modern samples</i>	69
3.3.7	<i>Diatom analysis</i>	69
3.3.8	<i>Light microscopy (LM)</i>	71
3.3.9	<i>Scanning electron microscopy (SEM)</i>	71
3.3.10	<i>Diatom identification and taxonomy</i>	72
3.3.11	<i>NAR01/02 core thin sections</i>	72
3.4	Data presentation and analysis	73
3.4.1	<i>Presentation of stratigraphic data</i>	73
3.4.2	<i>Data transformation and correlation analysis</i>	73
3.4.3	<i>Diatom concentration and biovolume</i>	74
3.4.4	<i>Diatom species diversity</i>	75

3.4.5	<i>Diatom habitat preferences</i>	75
3.4.6	<i>Detrended Correspondence Analysis (DCA)</i>	76
3.4.7	<i>Transfer functions</i>	76
3.4.8	<i>Sediment dating</i>	78
3.4.9	<i>Meteorological data, climate indices and palaeoclimate records</i>	78
3.5	Summary	80
Chapter 4: Site Descriptions		81
4.0	Introduction	81
4.1	Regional characteristics	81
4.1.1	<i>Central Anatolian climate</i>	81
4.1.2	<i>Geological setting</i>	83
4.1.3	<i>Human activity</i>	85
4.2	Lake site descriptions	85
4.2.1	<i>Water chemistry and hydrology</i>	86
4.2.2	<i>Geomorphology and sedimentation</i>	93
4.2.3	<i>Vegetation</i>	94
4.3	Summary	95
Chapter 5: Results: Nar Gölü		97
5.0	Introduction	97
5.1	Diatom identification and taxonomy	97
5.2	Modern diatom assemblage	98
5.2.1	<i>Lake habitats</i>	98
5.2.2	<i>Sediment traps</i>	103
5.3	Palaeo-records	110

5.3.1	<i>Sediment lithology</i>	110
5.3.2	<i>Core chronology</i>	113
5.3.3	<i>Diatom stratigraphy</i>	115
5.3.4	<i>Detrended Correspondence Analysis</i>	119
5.3.5	<i>Concentration and total biovolume</i>	121
5.3.6	<i>Species diversity</i>	122
5.3.7	<i>Habitat preferences</i>	122
5.3.8	<i>Comparison of the NAR01/02 and NAR06 records</i>	123
5.3.9	<i>Biovolume</i>	128
5.3.10	<i>NAR01/02 core thin sections</i>	134
5.3.11	<i>Environmental reconstructions</i>	141
5.3.12	<i>Analogue matching</i>	147
5.3.13	<i>Nar DI-conductivity with and without C. anaticus and bloom species</i>	148
5.3.14	<i>Reconstructed and instrumentally-measured conductivity</i>	155
5.4	Summary	156
Chapter 6: Results: Kratergöl		158
6.0	Introduction	158
6.1	Diatom identification and taxonomy	158
6.2	Modern diatom assemblage	159
6.3	Palaeo-record	164
6.3.1	<i>Lithology and sedimentation</i>	164
6.3.2	<i>Chronology</i>	165
6.3.3	<i>Diatom stratigraphy</i>	171
6.3.4	<i>Detrended correspondence analysis</i>	174

6.3.5	<i>Diatom concentration and total biovolume</i>	176
6.3.6	<i>Species diversity</i>	178
6.3.7	<i>Habitat preferences</i>	178
6.3.8	<i>Environmental reconstruction</i>	178
6.3.9	<i>Analogue analysis</i>	180
6.3.10	<i>Diatom biovolume</i>	181
6.4	Summary	183
Chapter 7: Diatom stratigraphical and environmental change		185
7.0	Introduction	185
7.1	Diatom species ecology	185
7.1.1	<i>Modern diatom assemblages</i>	185
7.1.2	<i>Relationship between modern and fossil assemblages</i>	186
7.2	Lake sedimentation	189
7.2.1	<i>The Nar Gölü varve cycle</i>	189
7.2.2	<i>Nar diatom blooms</i>	193
7.2.3	<i>Nar diatom blooms and nutrients</i>	198
7.2.4	<i>Diatom seasonality</i>	199
7.2.5	<i>Kratergöl diatom seasonality and sedimentation</i>	201
7.3	Palaeoenvironmental change	202
7.3.1	<i>Nar Gölü</i>	202
7.3.2	<i>Kratergöl</i>	216
7.3.3	<i>Comparison of Nar and Kratergöl diatom records</i>	220
7.4	Nar Gölü multi-proxy comparisons	221
7.4.1	<i>Oxygen isotopes</i>	221
7.4.2	<i>Pollen</i>	227

7.5	Summary	231
Chapter 8: Eastern Mediterranean Palaeoclimate		232
Part I: Diatom and Meteorological Records		232
8.0	Introduction	232
8.1	Meteorological records from central Turkey	233
8.2	Diatom relationship with meteorological records	234
8.3	Correlation analysis of diatom and meteorological records	237
8.3.1	<i>Annual averages</i>	237
8.3.2	<i>Seasonal averages</i>	240
8.3.3	<i>Monthly averages</i>	251
8.4	Water balance	254
8.4.1	<i>Aridity index</i>	254
8.4.2	<i>Cumulative water balance</i>	257
8.5	Summary	260
Part II: Palaeoclimate Reconstruction		262
8.6	Introduction	262
8.7	Pre-instrumental palaeoenvironmental change	262
8.7.1	<i>Diatom-inferred summer temperature</i>	263
8.7.2	<i>Nar multi-proxy inferred palaeoclimate</i>	265
8.7.3	<i>Kratergöl environmental change</i>	271
8.7.4	<i>Limitations of the palaeo-environmental reconstructions</i>	272
8.8	Controls on EM climate and the Nar Gölü diatom record	273
8.8.1	<i>Northern Hemisphere (NH) temperature and precipitation</i>	273
8.8.2	<i>Atmospheric circulation patterns</i>	278
8.9	Palaeoclimate reconstructions	283

8.9.1	<i>Lake-inferred palaeoclimate</i>	283
8.9.2	<i>Tree-ring-inferred palaeoclimate</i>	285
8.9.3	<i>Central Anatolian historical climate records</i>	286
8.9.4	<i>Comparisons with other DI-conductivity records</i>	290
8.10	Summary	294
Chapter 9: Conclusion		297
9.0	Introduction	297
9.1	Diatom-inferred environmental change	298
9.1.1	<i>Modern environment</i>	298
9.1.2	<i>Diatom assemblage analysis methods</i>	299
9.2	Late Holocene climate reconstruction	302
9.2.1	<i>Palaeoclimate inferences</i>	302
9.2.2	<i>Factors controlling EM climate</i>	306
9.3	Suitability of sites and methodology	306
9.4	Further work	308
References		311
Appendices		357
Appendix 1:	Nar Gölü diatom species illustrations and taxonomy	357
Appendix 2:	Kratergöl diatom species illustrations and taxonomy	365
Appendix 3:	Nar Gölü and Kratergöl diatom cell dimensions and biovolume	368
Appendix 4.1:	NAR06 species DCA ordination plots	373
Appendix 4.2:	NAR01/02 species DCA ordination plots	374
Appendix 4.3:	ACM99 species DCA ordination plots	379
Appendix 5.1:	NAR01/02 min. DC and matching analogues	381

Appendix 5.2:	NAR06 min. DC and matching analogues	384
Appendix 5.3:	ACM99 min. DC and matching analogues	386
Appendix 6.1:	Nar Gölü diatom habitat, salinity and ecological preferences	387
Appendix 6.2:	Kratergöl diatom habitat, salinity and ecological preferences	390
Appendix 7.1:	Nar Gölü diatom conductivity optima (EDDI)	391
Appendix 7.2:	Kratergöl diatom conductivity optima (EDDI)	392
Appendix 8:	Relationships between Nar diatom record and gridded meteorological data	393
Appendix 9:	Woodbridge <i>et al.</i> (<i>submitted to Diatom Research</i>) Morphology and ecology of a new centric diatom from Cappadocia (central Turkey)	398

Figures	Page
1.1 Map of the Mediterranean region highlighting dominating atmospheric circulation patterns.	2
1.2 IPCC report: records of Northern Hemisphere temperature variation during the last 1300 years (AD 700-2000).	5
1.3 Lake water chemistry and diatom response to climatic changes.	7
1.4 The process involved in palaeoclimate reconstruction from lake diatoms.	11
2.1 Structure of a maar lake illustrating hydrological inputs/outputs and stratified water layers.	16
2.2 Turkish precipitation regions based on geographical distribution of rainfall regimes.	40
2.3 Mean annual precipitation totals for Turkey.	40
2.4 Mean annual temperature for Turkey.	41
2.5 Mean annual aridity for Turkey.	41
2.6 Average summer and winter temperature plotted with total annual precipitation for the period AD 1960-2007 recorded at Nevşehir meteorological station (Turkey).	43
2.7 Average summer and winter temperature plotted with total annual precipitation for the period AD 1926-2006 recorded at Ankara meteorological station (Turkey).	43
3.1 Map of Turkey highlighting the location of lake sites (Nar Gölü and Kratergöl) and meteorological stations.	52
3.2 Diagram of sediment traps installed at Nar Gölü.	59
3.3 Nar Gölü sampling locations.	61
3.4 Diagram of Kratergöl.	64

3.5	Flow diagram illustrating the preparation procedure for diatom analysis of lake sediments.	70
4.1	1967-2007 mean climate data from Nevşehir meteorological station.	82
4.2	1927-2007 mean climate data from Ankara meteorological station.	82
4.3	Geological setting of the Central Anatolian Volcanic Province.	84
4.4	a) Nar water temperature depth profiles.	89
	b) Nar water conductivity (mScm ⁻¹) depth profiles.	89
	c) Nar water pH depth profiles.	89
4.5	a) Kratergöl water temperature depth profile.	92
	b) Kratergöl Dissolved oxygen content and pH depth profile.	92
	c) Kratergöl Chloride depth profile.	92
5.1	Modern Nar diatom assemblage: species percentages.	101
5.2	Modern Nar diatom assemblage: species biovolume.	101
5.3	Modern Nar diatom concentration and total biovolume.	102
5.4	Diatom rarefaction of modern Nar samples and different sediment depths in the NAR01/02 palaeo-record.	102
5.5	Sediment trap diatom stratigraphy (%) with rarefaction and valve concentration.	107
5.6	Sediment trap diatom stratigraphy plotted according to biovolume.	108
5.7	DCA ordination plot for Nar sediment trap and modern diatom samples.	109
5.8	Photographs of the Nar master sequence (NAR01/02) and NAR06 section.	111
5.9	Comparison of ¹³⁷ Cs, ²¹⁰ Pb and varve chronology from the NAR01 sediment record.	114
5.10	Age-depth relationship for varve chronology from the NAR01/02 sediment sequence.	114

5.11	NAR06 diatom stratigraphy. The assemblage has been stratigraphically zoned through cluster analysis.	117
5.12	NAR01/02 diatom stratigraphy. The assemblage has been stratigraphically zoned through cluster analysis.	118
5.13	NAR06 DCA ordination plot. Samples plotted on axes 1 and 2 with symbols corresponding to cluster analysis zones.	120
5.14	NAR01/02 DCA ordination plot. Samples plotted on axes 1 and 2 with symbols corresponding to cluster analysis zones (excluding <i>S. parvus</i>).	121
5.15	a) NAR06 diatom stratigraphy presented with DCA axes 1 and 2, rarefaction, concentration, total biovolume and % benthic taxa.	125
	b) The most recent 85 VY of the NAR01/02 decadal record for comparison with the NAR06 annual record, presented with rarefaction, concentration and total biovolume.	126
5.16	NAR01/02 diatom stratigraphy presented with DCA axes 1 and 2, rarefaction, concentration, total biovolume , % benthic taxa, grey scale value and carbon/nitrogen ratio (C:N).	127
5.17	SEM image of <i>Campylodiscus clypeus</i> with <i>Nitzschia paleacea</i> and <i>Clupeoparvus anatolicus</i> specimens.	128
5.18	NAR06 diatom stratigraphy plotted according to biovolume with DCA axes 1 and 2.	131
5.19	NAR01/02 diatom stratigraphy plotted according to biovolume with DCA axes 1 and 2.	132
5.20	DCA ordination plot for NAR06 diatom biovolume data. Symbols correspond to percentage data cluster analysis zones.	133

5.21	DCA ordination plot for NAR01/02 diatom biovolume data. Symbols correspond to percentage data cluster analysis zones.	134
5.22	NAR01/02 core thin section stratigraphy with measurements of white carbonate, brown organic, grey clastic, diatom bloom and total varve thickness for the most recent 78 VY (AD 1924-2002).	138
5.23	NAR01/02 core thin section stratigraphy with measurements of white carbonate, brown organic, grey clastic, diatom bloom and total varve thickness for the last 900 VY (AD 1100-2002).	139
5.24	NAR01/02 thin section diatom bloom and clastic event frequency per hundred years for the last 900 varve years (AD 1100-2000).	140
5.25	NAR01/02 thin section average white and brown layer and varve thickness per hundred years for the last 900 varve years (AD 1100-2000).	140
5.26	NAR06 diatom stratigraphy with reconstructed conductivity and total phosphorus based on the combined training sets from EDDI using weighted averaging and the MAT.	145
5.27	NAR01/02 diatom stratigraphy with reconstructed conductivity and total phosphorus based on the combined training sets from EDDI using weighted averaging and the MAT.	146
5.28	NAR06 diatom stratigraphy with reconstructed conductivity based on bloom species <i>N. paleacea</i> and <i>S. acus</i> only.	151
5.29	NAR06 species % recalculated omitting bloom species and <i>C. anatolicus</i> with reconstructed conductivity omitting bloom species (<i>N. paleacea</i> and <i>S. acus</i>) and <i>C. anatolicus</i> .	152
5.30	NAR01/02 diatom stratigraphy with reconstructed conductivity omitting bloom species (<i>N. paleacea</i> , <i>S. acus</i> and <i>S. parvus</i>) and <i>C. anatolicus</i> .	153

5.31	NAR01/02 diatom stratigraphy with reconstructed conductivity based on bloom species (<i>N. paleacea</i> , <i>S. acus</i> and <i>S. parvus</i>) only.	154
6.1	Modern Kratergöl diatom assemblage: species percentages.	161
6.2	Modern Kratergöl diatom assemblage: species biovolume.	161
6.3	Modern Kratergöl sample diatom concentration and total biovolume.	162
6.4	Diatom rarefaction of modern Kratergöl samples and different sediment depths in the ACM99 palaeo-record.	162
6.5	DCA ordination plot for modern diatom samples according to habitat and collection date.	163
6.6	ACM99 carbon content and particle size analysis. Total, inorganic and organic carbon concentrations are presented with percentage of sand and silt+clay.	165
6.7	a) ACM99 total and unsupported ^{210}Pb , ^{137}Cs and ^{241}Am activity profiles (Bq/Kg) and metal species concentration (mg/Kg).	169
	b) ACM99 unsupported ^{210}Pb , ^{137}Cs and ^{241}Am activity profiles (Bq/Kg) and metal species concentration (mg/Kg) relative to diatom concentration.	170
6.8	Diatom stratigraphy of the ACM99 record. The assemblage has been zoned according to cluster analysis.	173
6.9	ACM99 DCA ordination plot. Diatom samples plotted on axes 1 and 2 with symbols corresponding to cluster analysis zones.	175
6.10	ACM99 diatom stratigraphy presented with DCA axes 1 and 2, rarefaction, diatom concentration, total diatom biovolume, % benthic taxa and DI-conductivity by WA-inv. and W-MAT.	177
6.11	ACM99 diatom stratigraphy plotted according to biovolume with DCA axes 1 and 2.	182

6.12	ACM99 diatom sample biovolume DCA ordination plot with zones corresponding to percentage data cluster analysis.	183
7.1	Comparison of Nar modern sample concentration and total biovolume with different sediment depths in the NAR01/02 palaeo-record.	187
7.2	Comparison of Kratergöl modern sample concentration and total biovolume with different sediment depths in the ACM99 palaeo-record.	188
7.3	NAR01/02 thin section micrograph illustrating carbonate, diatom bloom of <i>S. parvus</i> and organic layer.	193
7.4	NAR01/02 thin section micrograph illustrating pale yellow <i>S. parvus</i> bloom (~750 VY).	194
7.5	NAR06 diatom stratigraphy presented with DI-conductivity, DCA axes 1 and 2 and the NAR01/02 oxygen isotope record.	223
7.6	NAR01/02 diatom stratigraphy with DI-conductivity and diatom DCA axes 1 and 2. Presented with NAR01/02 pollen and oxygen isotope stratigraphy and pollen DCA axes 1 and 2.	224
8.1	Nevşehir average summer temperature plotted with NAR06 diatom DCA axis 2 for the period AD 1960-2006.	248
8.2	Total Nevşehir autumn precipitation plotted with NAR06 <i>S. acus</i> percentage for the period AD 1960 to 2006.	248
8.3	Nevşehir spring minimum temperature plotted with NAR06 DI-conductivity (OB) for the period AD 1960-2006.	249
8.4	Nevşehir average summer temperature plotted with DI-conductivity (B) using an eight-year running average for the period AD 1964-2003.	249
8.5	Ankara annual total precipitation plotted with NAR06 DI-conductivity (B) for the period AD 1927-2006.	250

8.6	Ankara total autumn precipitation plotted with NAR06 DI-conductivity (AS) for the period AD 1931-2003 using an eight-year running average.	250
8.7	Minimum July Nevşehir temperature plotted with NAR06 DCA axis 2 for the period AD 1960-2006.	252
8.8	Aridity index plotted with NAR06 DCA axis 1 (AS) smoothed using an eight-year running average for the period AD 1943-2003.	256
8.9	Aridity index plotted with NAR06 DCA axis 1 (OB) using an eight-year running average for the period AD 1943-2003.	257
8.10	Cumulative lake water balance: precipitation/evaporation, plotted with NAR01/02 isotopes for the period AD 1940-2006.	259
8.11	Cumulative lake water balance: precipitation/evaporation, plotted with NAR06 diatom DCA axis 1 (OB) for the period AD 1940-2006.	259
8.12	Scatter plot of average Nevşehir summer temperature (°C) and NAR06 DCA axis 1.	263
8.13	Nevşehir average summer temperature plotted with NAR06 DCA axis 1 for the period AD 1960-2006.	264
8.14	NAR01/02 DI-summer temperature, conductivity and oxygen isotopes plotted for the period AD 290-2000 with Mann and Jones's (2003) NH temperature reconstruction (AD 290-1994).	266
8.15	Deviation from mean Nar DI-summer temperature, conductivity and Northern Hemisphere reconstructed temperature for the period AD 1000-2000.	277
8.16	October NAOI plotted with NAR06 diatom DCA axis 2 for the period AD 1950-2006.	280

8.17	December NCPI plotted with NAR06 DI-conductivity (OB) for the period AD 1948-2006.	281
8.18	Tree-ring-inferred precipitation plotted with NAR06 DI-conductivity, temperature and NAR01/02 oxygen isotopes for the period AD 1927-2006.	288
8.19	Tree-ring-inferred precipitation plotted with NAR01/02 DI-conductivity, temperature and oxygen isotopes for the period AD 1690-1990.	289
8.20	DI-conductivity from Moon Lake (USA) (AD 286-1980), Lake Naivasha (East Africa) (AD 883-1993) and Nar Gölü (AD 290-2000).	293
9.1	The processes involved in palaeoclimate reconstruction from lake diatoms. Additional diatom analysis methods employed in this research project are highlighted.	301
Appendix 4.1		
	NAR06 DCA ordination plots. a) <i>A. minutissimum</i> , b) <i>N. paleacea</i> , c) <i>C. anatolicus</i> , d) <i>S. acus</i> .	373
Appendix 4.2		
	NAR01/02 DCA ordination plots. a) <i>A. minutissimum</i> , b) <i>S. acus</i> , c) <i>N. paleacea</i> , d) <i>G. olivaceum</i> , e) <i>N. cryptotenella</i> , f) <i>N. af. fonticola</i> , g) <i>N. oblonga</i> , h) <i>R. abbreviata</i> , i) <i>A. crenulata</i> , j) <i>A. libyca</i> , k) <i>C. anatolicus</i> , l) <i>N. elkab</i> , m) <i>N. paleacea</i> , n) <i>C. meneghiniana</i> , o) <i>F. construens</i> var. <i>venter</i> , p) <i>N. halophila</i> , q) <i>N. af. palea</i> , r) <i>R. operculata</i> .	374
Appendix 4.3		
	Kratergöl ACM99 DCA ordination plots. a) <i>N. frustulum</i> , b) <i>N. af. fonticola</i> , c) <i>F. fasciculata</i> , d) <i>E. paludosa</i> var. <i>subsalina</i> , e) <i>C. placentula</i> , f) <i>A. veneta</i> , g) <i>N. sigma</i> .	379

Appendix 7.1

Nar species conductivity optima based on % abundance at lakes sites in the EDDI combined salinity training set. **a)** *A. minutissimum*, **b)** *C. meneghiniana*, **c)** *F. construens*, **d)** *N. paleacea*, **e)** *S. acus*, **f)** *S. parvus*. 391

Appendix 7.2

Kratergöl species conductivity (\log_{10}) optima based on % abundance at lakes sites in the EDDI combined salinity training set. **a)** *C. placentula*, **b)** *E. paludosa var. subsalina*, **c)** *F. fasciculata*, **d)** *N. fonticola*. 392

Tables

3.1	Nar Gölü and Kratergöl lake characteristics.	56
4.1	Nar Gölü water chemistry averaged for the period 2001-2008.	88
4.2	Nar Gölü major ion water chemistry (mg/lcm^{-1}).	88
4.3	Water chemistry data recorded at Kratergöl during summer.	91
4.4	Kratergöl major ion chemistry (g/l^{-1}).	91
5.1	Sediment trap details.	104
5.2	NAR06 and NAR01/02 core sections stratigraphically tied according to varve years and calendar age.	110
5.3	NAR06 main diatom zones (according to cluster analysis) with depth, calendar age and a summary of the diatom community.	115
5.4	NAR01/02 main diatom zones (according to cluster analysis) with depth, calendar age and a summary of the diatom community.	116
5.5	Nar species groups according to habitat preferences.	123

5.6	Training set and model performance comparisons using datasets from the European Diatom Database (EDDI) and studies by Gasse <i>et al.</i> (1995), Gell (1997) and Laird <i>et al.</i> (1998).	142
5.7	Comparison of DI-conductivity based on all species, bloom species, non-bloom species and instrumentally measured conductivity at Nar Gölü between AD 1999 and 2006.	156
6.1	ACM99 cluster analysis diatom zones according to depth with a summary of dominant species.	172
6.2	Average percentage of ACM99 fossil sample assemblage represented in modern lake diatom-conductivity training sets from EDDI.	180
7.1	Model of the seasonal varve cycle at Nar Gölü based on sediment material, colour, composition and origin.	192
7.2	Summary of inferences derived from the Nar diatom records.	204
7.3	Significant relationships between different analyses of the NAR01/02 palaeo-record.	214
7.4	Significant relationships between different analyses of the NAR06 diatom and the most recent 80 years of the NAR01/02 thin section palaeo-records.	215
7.5	Summary of inferences derived from the ACM99 diatom palaeorecord.	217
7.6	Significant relationships between the oxygen isotope (NAR01/02) and diatom (NAR01/02 and NAR06) records from Nar Gölü.	227
7.7	Significant relationships between the pollen and diatom (NAR01/02) records from Nar Gölü.	229

8.1	Relationships between annual average climate data from Ankara meteorological station and the NAR06 diatom and NAR01/02 thin section records.	237
8.2	Relationships between annual average climate data from Nevşehir meteorological station and the NAR06 diatom and NAR01/02 thin section records.	238
8.3	Relationships between Ankara spring and summer meteorological data and the NAR06 diatom and NAR01/02 thin section records.	242
8.4	Significant relationships between Ankara autumn and winter meteorological data and the NAR06 diatom and NAR01/02 thin section records.	243
8.5	Relationships between Nevşehir spring and summer meteorological data and the NAR06 diatom and NAR01/02 thin section records.	244
8.6	Relationships between Nevşehir autumn and winter meteorological data and the NAR06 diatom and NAR01/02 thin section records.	244
9.1	Summary of palaeoclimate inferences from the Nar palaeo-record based on diatoms, oxygen isotopes and pollen with other proxy and documentary records.	305

Appendix 8: Table 1

Relationships between annual average gridded climate data for central Anatolia and the NAR01/02 diatom thin section record.	393
---	-----

Appendix 8: Table 2

Relationships between annual average climate data for the grid containing Nar Gölü and the NAR01/02 diatom thin section record.	393
---	-----

Appendix 8: Table 3

Relationships between spring and summer gridded climate data from central Anatolia and the NAR01/02 thin section diatom record. 394

Appendix 8: Table 4

Relationships between autumn and winter gridded climate data for central Anatolia and the NAR01/02 thin section diatom record. 394

Appendix 8: Table 5

Relationships between spring and summer climate data for the grid containing Nar Gölü and the NAR01/02 thin section diatom record. 395

Appendix 8: Table 6

Relationships between autumn and winter climate data for the grid containing Nar Gölü and the NAR01/02 thin section diatom record. 395

Appendix 8: Table 7

Seasonal relationship between gridded climate data for central Anatolia and the NAR06 diatom record. 396

Appendix 8: Table 8

Seasonal relationship between climate data for the grid containing Nar Gölü and the NAR06 diatom record. 397

Plates

- 2.1 *Rhopalodia operculata.* 21
- 2.2 *Cyclotella meneghiniana.* 21
- 3.1 Nar Gölü photographed facing south. 53
- 3.2 Kratergöl photographed facing north. 53
- 3.3 Aerial view of Nar Gölü. 54

3.4	Nar Gölü catchment facing south west.	54
3.5	Aerial view of Kratergöl.	55
3.6	Kratergöl catchment facing north east.	55
3.7	Photograph of a sediment trap and a Perspex tube containing lake sediment collected throughout the course of a year.	60
3.8	Messenger-operated gravity corer containing the NAR06 core section.	63
5.1	<i>C. anaticus</i> : valve view (SEM).	98
5.2	<i>C. anaticus</i> : girdle view (SEM).	98
7.5	NAR/02 thin section micrograph illustrating <i>S. acus</i> bloom layer.	195
7.6	NAR01/02 thin section micrograph illustrating <i>N. paleacea</i> bloom layer.	195

Abbreviations

ACM99:	Lake core collected from Kratergöl in 1999
AI:	Aridity index
AO (I):	Arctic oscillation (index)
B, OB, AS:	Bloom species, omitting bloom species and all species
CCA:	Canonical correspondence analysis
Combined salinity:	EDDI diatom-salinity combined modern training set
Combined TP:	EDDI diatom-total phosphorus combined modern training set
DCA:	Detrended correspondence analysis
DI:	Diatom-inferred
EDDI:	European Diatom Database
EM:	Eastern Mediterranean
ENSO (SO):	El Niño (southern oscillation)
IC:	Inorganic carbon

IPCC:	Intergovernmental Panel on Climate Change
KD1:	ACM99 diatom zone 1
KD2:	ACM99 diatom zone 2
KD3:	ACM99 diatom zone 3
KD4:	ACM99 diatom zone 4
KLB:	Krammer and Lange-Bertalot (1991; 1997; 2000)
LIA:	Little Ice Age
LM:	Light microscope
MCA:	Medieval Climate Anomaly
Min. DC:	Minimum dissimilarity coefficient
NAO (I):	North Atlantic oscillation (index)
NAR01/02:	Lake cores collected from Nar Gölü between 2001 and 2002
NAR06:	Lake core collected from Nar Gölü in 2006
NCP(I):	North Sea-Caspian pattern (index)
ND1:	NAR01/02 diatom zone 1
ND1a:	NAR06 diatom zone a
ND1b:	NAR06 diatom zone b
ND1c:	NAR06 diatom zone c
ND1d:	NAR06 diatom zone d
ND2:	NAR01/02 diatom zone 2
ND3:	NAR01/02 diatom zone 3
ND4:	NAR01/02 diatom zone 4
NH:	Northern Hemisphere
OC:	Organic carbon
P/E:	Precipitation/evaporation

RMSEP:	Root mean square error prediction
SEM:	Scanning electron microscope
TC:	Total carbon
VY:	Varve year
WA (TOL) (inv.):	Weighted averaging (tolerance down-weighed) with
(classical)	inverse/classical deshrinking
(W) MAT (c dist ²):	(Weighted) Modern analogue technique
	(by squared chord distance)

Acknowledgements

This Ph.D. was funded by a University of Plymouth scholarship. The aims of the research were to contribute to knowledge and improve understanding of Eastern Mediterranean palaeoclimate. A number of individuals contributed to the outcome of this research project. I would like to thank Adam Fisher for continued support throughout the duration of my studies and for volunteering fieldwork assistance, my supervisors Neil Roberts and Martin Kent for support, encouragement and guidance, and the thesis examiners, Phil Barker (University of Lancaster) and Ralph Fyfe (UoP) for helpful comments and advice. Additionally, the UoP Quaternary Environments Research Group, School of Geography technical and administrative staff and the Cartographic Resources Unit provided valuable advice and assistance, in particular Ann Kelly, Jamie Quinn, Tim Absalom, Brian Rogers, Katie Head, Kev Solman, Debbie Bauckham and Richard Hartley.

I would also like to thank a number of individuals who shared their knowledge and offered advice including Matt Jones (University of Nottingham), Jane Reed (University of Hull), Katie Szkornik (University of Keele), Becky Turner and Wil Marshall (UoP). I am extremely grateful to the team of researchers who conducted fieldwork in Turkey between 1999-2008 and collected a number of lake cores used in this project. Fieldwork in Turkey was supported with a grant from The British Institute at Ankara and attendance of the INQUA conference in Cairns (Australia) was part funded by the Quaternary Research Association. The Natural History Museum (London), in particular Eileen Cox, assisted with the naming of a new diatom genus and various people offered useful advice at the annual British Diatomists' Meeting and through responding to posts on Diatom-L list server. Furthermore, I would like to thank my family for their encouragement and a number of friends at the UoP including Maria, Heather, Lauren, Lou, Susie and Shabnam, who have provided support and welcome distractions from work throughout the last few years.

Author's Declaration

At no time during the registration for the degree of Doctor of Philosophy has the author been registered for any other University award without prior agreement of the Graduate Committee. This study was financed with the aid of a studentship from the School of Geography (University of Plymouth). Relevant scientific seminars and conferences were regularly attended at which work was often presented; external institutions were visited for consultation purposes and a paper was prepared for publication.

Publications and conference presentations:

Woodbridge, J., Roberts, N. and Cox, E.J. (*submitted to Diatom Research*)

Morphology and ecology of a new centric diatom from Cappadocia (central Turkey).

Woodbridge, J. Diatom-inferred late Holocene climate variability from central Turkey.

7th International Postgraduate Quaternary Research Association Symposium (Liverpool, UK), Aug. 2008. Oral presentation.

Woodbridge, J. Diatom-inferred late Holocene climate variability from a crater lake in central Turkey. *British Diatomists' Meeting (Lake District, UK), Oct. 2007.* Oral presentation.

Woodbridge, J. and Roberts, N. Diatom-inferred late Holocene climate variability from a crater lake in central Turkey. *International Quaternary (INQUA) Conference (Cairns, Australia), Jul.-Aug. 2007.* Oral Presentation.

Woodbridge, J. and Roberts, N. Late Holocene lake diatoms and climate variability in central Turkey. *Quaternary Environments and the Human Past (University of Manchester, UK), May 2007.* Poster presentation.

Woodbridge, J. and Roberts, N. Late Holocene Lake Diatoms and Climate Variability in Central Turkey. *British Diatomists' Meeting (Malham Tarn, UK), Oct. 2006.* Poster presentation.

Roberts, N., Reed, J.M., **Woodbridge, J.**, Turner, R., Leng, M.J. and Eastwood, W. Replicating proxy-climate records: a lake sediment based study from the east Mediterranean. *HOLIVAR Conference (University College London, UK), Jun. 2006.* Poster presentation.

Woodbridge, J. Testate amoebae as hydrological indicators within experimental microcosms. *Postgraduate Quaternary Research Association Symposium (Plymouth, UK), Aug.-Sept. 2005.* Oral Presentation.

Courses attended:

June 2005: Introduction to Diatom Analysis. Run by Prof. R. Battarbee, Dr. Viv Jones and others. Environmental Change Research Centre, University College London.

Further funding obtained:

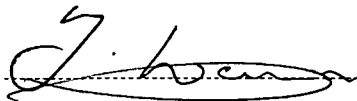
August 2006: £500 British Institute at Ankara travel grant.

August 2007: £600 Quaternary Research Association INQUA conference fund.

January 2009: Fully funded place to attend the joint UCL-Lanzhou "Tracking Environmental Change Using Lake Sediments" summer school to be held in August 2009.

Word count of main body of thesis:

59,213 (including tables and figure, plate and table captions)

Signed 

Date 9/4/09

Chapter 1

Introduction

1.0 Late Holocene Eastern Mediterranean climate

The Holocene climate of the Eastern Mediterranean (EM) has fluctuated in terms of temporal trends and regional variability. The EM has a complex climatic history, due to the influence of atmospheric circulation patterns associated with surrounding continents, ocean conditions and regional variability in factors such as topography. Much of the EM is classified as arid or semi-arid and drought has been a typical feature of the Holocene climate, with prolonged dry episodes affecting various regions. Mann (2002) identified that the dominant pattern of influence on EM temperature is the North Atlantic Oscillation (NAO) (Figure 1.1). The region is also influenced by atmospheric circulation patterns associated with both high latitude and tropical locations, such as the Indian Monsoon. Continental central Turkey has a long record of human occupation (Roberts, 1990), is characterised by diverse climate types and regimes (Türkeş *et al.*, 1995) and is likely to be sensitive to future climate changes, due to the impacts of drought on water resource availability.



Figure 1.1 Map of the Mediterranean region highlighting dominating atmospheric circulation patterns (adapted from Bolle, 2003).

In countries surrounding the EM basin, human land use has been extensive throughout the Holocene. For example, the Neolithic settlement of Çatalhöyük in the Konya Plain (central Turkey) was dated to 9000 cal. years BP (Eastwood *et al.*, 2006). Human activity in Turkey has been continuous since this time, with many civilisations developing and collapsing in the region. Pollen and archaeological records indicate evidence of human impact on the landscape of Turkey throughout the last ~4000 years, with increasing forcing on natural environments throughout recent centuries (e.g. Roberts *et al.*, 2001; Wick *et al.*, 2003; Eastwood *et al.*, 2006). Consequently, the EM provides an ideal location to analyse the relationship between human activity, climate and environmental change.

Recent global climatic warming is thought to be associated with increasing anthropogenic activity, in particular industrialisation (since ~AD 1840 in Europe) (Jones and Mann, 2002). The Intergovernmental Panel on Climate Change (IPCC) Fourth Assessment Report (Allali *et al.*, 2007) highlighted that future climate change is expected to result in increased temperatures, drought and wildfires with impacts on health, water availability, tourism and crop productivity in southern Europe and the EM region. Arid and semi-arid regions were identified as areas at great risk, particularly regarding water resource availability. According to Bolle (2003), the frequency and amplitude of extreme climatic events has recently increased in the Mediterranean region and this will have severe consequences for ecosystems, economy and human life. Turkish climate trends indicate decreased precipitation in some regions since the 1960s (Türkeş, 2003). Keyantash and Dracup (2002) described drought as the world's costliest disaster, which affects the highest number of people globally. Water resource availability and management is a particularly important issue for societies inhabiting semi-arid regions.

Knowledge of pre-instrumental palaeoclimatic variability is required in order to analyse whether the climate trends of the last few centuries (~AD 1800-2000) are significant in the context of the past (Luterbacher *et al.*, 2004) and to identify the precursors for climate shifts. Additionally, understanding the impacts of climate change on water availability allows predictions concerning the environmental responses to projected climate variability (Yano *et al.*, 2007). The last 2000 years are particularly significant in terms of understanding the impact of human activity on the environment and evaluating how societies have adapted to climatic changes in the past.

Various methods are employed to reconstruct palaeoclimate through utilising natural archives, such as tree-rings, cave speleothems and lake and marine sediments. Northern Hemisphere climate reconstructions typically reveal a Medieval Climatic Anomaly (MCA) (preceding and during the 10th to 14th centuries), a Little Ice Age (LIA) (throughout the 16th to mid-19th centuries) and recent warming (since ~AD 1840) (Jones and Mann, 2002) (Figure 1.2). The last 200-300 years has been termed the Anthropocene epoch (Crutzen and Stoermer, 2000; Zalasiewicz *et al.*, 2008). The epoch is defined by the time period during which human influence has had most dramatic impact on the natural environment, predominantly as a result of industrialisation. Limited high-resolution palaeoclimatic information covering the last 2000 years is available for the EM. Whether the EM experienced similar palaeoclimatic trends to other regions has implications for understanding present climate patterns and planning for future variability.

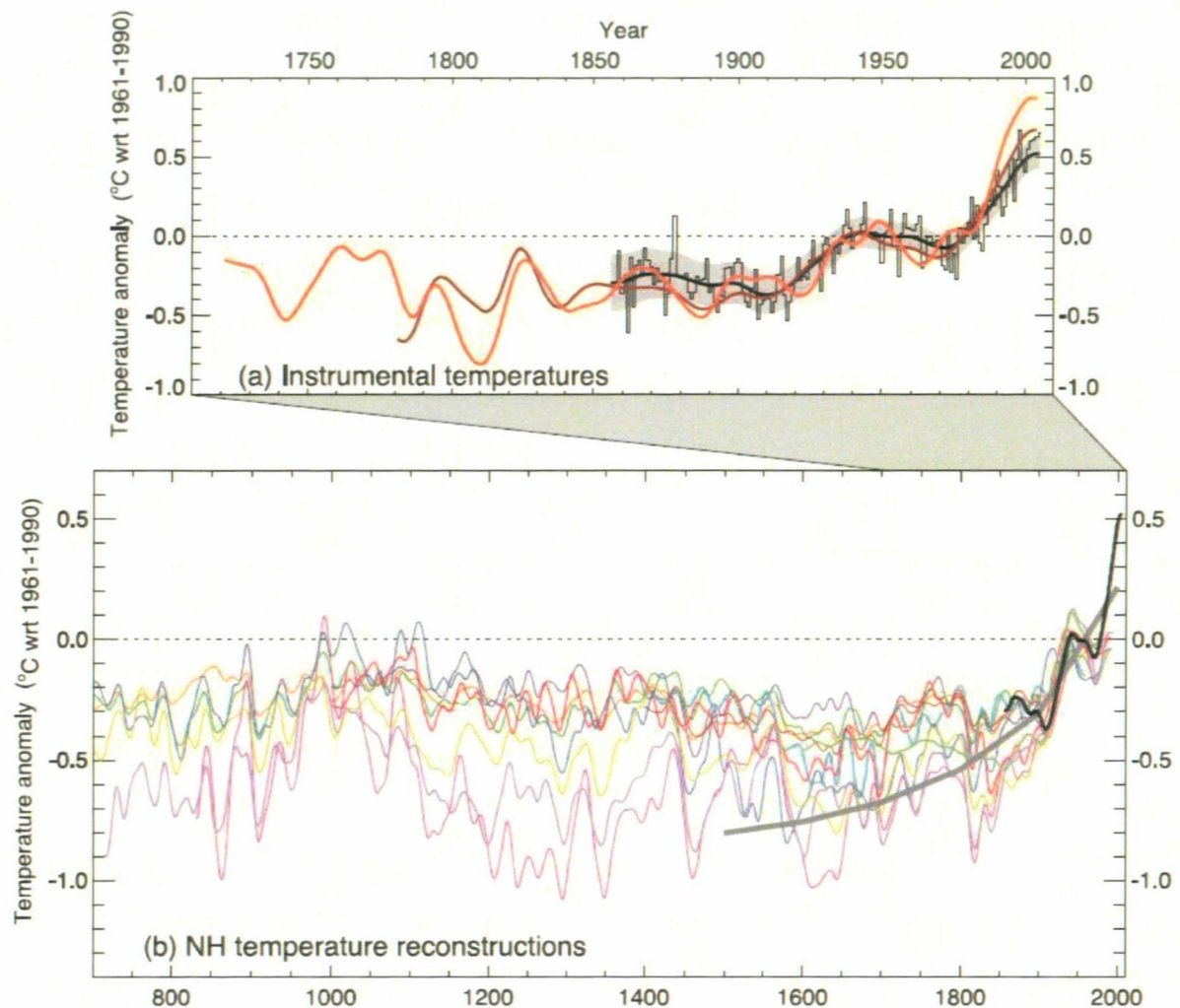


Figure 1.2 IPCC report: records of Northern Hemisphere temperature variation during the last 1300 years (AD 700-2000). (a) Annual average instrumental temperature records from 4 European stations (orange line), terrestrial temperatures (brown line), and land and marine temperatures (black line) (grey shading represents error). (b) Reconstructions using multiple climate proxy records based on research conducted between 1998 and 2006 and plotted with instrumental temperature (black line). Full details are available in Jensen and Overpeck (2007).

The IPCC Fourth Assessment Report (Jansen and Overpeck, 2007) discussed the valuable contribution of palaeoclimate research to understanding climatic trends and

past variability. Recent temperature increases are evident in both instrumental records and numerous Northern Hemisphere temperature reconstructions (Figure 1.2). In particular, these records emphasise increased temperatures during the late 20th century. The majority of the climate reconstructions discussed in the report concentrated on temperature variability. This presents a need for more high-resolution reconstructions concerning palaeo-precipitation and evaporation, which are important climate factors in semi-arid regions and are linked with water availability. Additionally, Luterbacher *et al.* (2004) highlighted the need for the spatio-temporal coverage of high-resolution, accurately dated proxy evidence to be extended in the Mediterranean region.

The present semi-arid climate of Turkey, combined with predicted future climatic changes associated with greenhouse gas (GHG) emissions, has led to concerns about the impacts of climate change upon society. According to the IPCC report, difficulties remain in reliably simulating and attributing observed temperature changes to natural or human causes. At smaller scales, factors such as land use change and pollution complicate the detection of anthropogenic warming influence on physical and biological systems (Jensen and Overpeck, 2007). Therefore high-resolution research focusing on areas where data are limited, and attempting to separate natural from human-induced environmental changes, is required.

Mann (2002) considered a number of recent climate trends particularly in the EM and Southwest Asia (Near East) and acknowledged that recent temperature increases associated with anthropogenic activity have been masked by natural variability. According to Mann (2002), this will not be the case in the future, due to stronger projected trends in global warming. Therefore, Turkey is located in an area that may be

particularly sensitive to future climate change. Mann *et al.* (1999) suggested that further research is needed to extend detailed palaeoclimate reconstructions to the EM region.

1.1 Lake palaeoenvironmental archives

Variability in climatic factors, such as temperature and precipitation, is reflected by shifts in lake hydrology and chemistry. This information is recorded in lake sediment through biotic population changes and geochemical alterations (Figure 1.3). An extensive archive of environmental information is provided by lake sediments, which allows various palaeoecological and geochemical techniques to be employed for analysis of temporal changes in climate. In particular, annually-laminated sediments allow high-resolution analyses and offer a powerful tool for reconstructing palaeoenvironmental change.

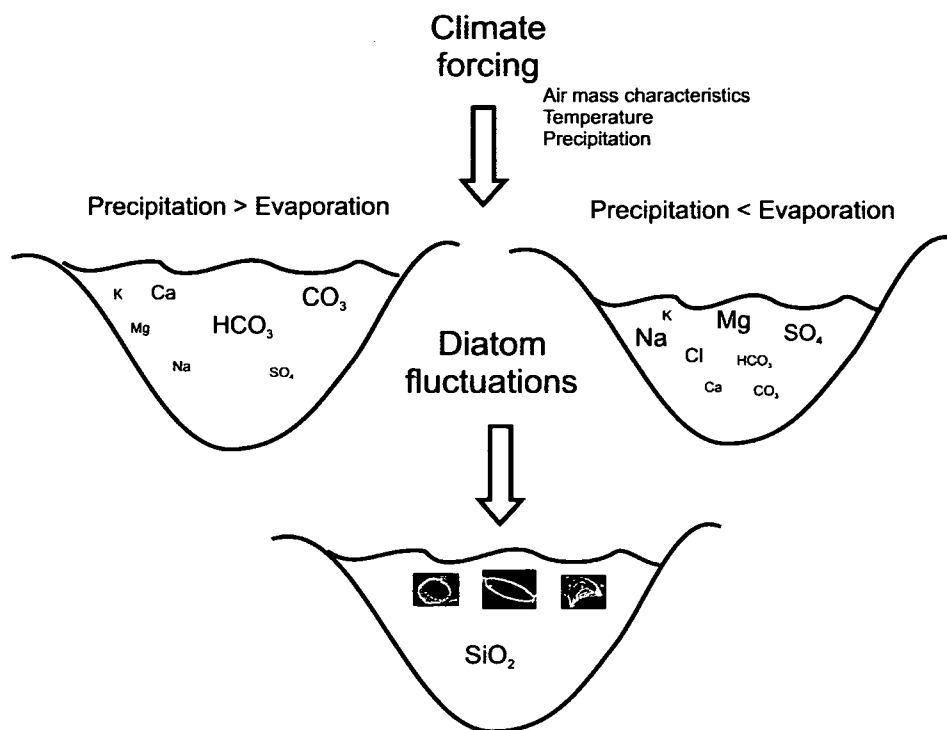


Figure 1.3 Lake water chemistry and diatom response to climatic changes (adapted from Fritz *et al.*, 1999).

Previous EM palaeolimnological climate reconstructions have identified that the climate of the region has become increasingly arid since the early Holocene. For example, diatom fossils have indicated increasing trends in lake water salinity and climatic aridity (e.g. Kashima, 1994, 2003; Reed *et al.*, 1999; Roberts *et al.*, 2001). Oxygen isotopes have also become increasingly positive, indicating drier late Holocene climatic conditions in records from Eski Acıgöl in central Turkey (Roberts *et al.*, 2001; Jones *et al.*, 2007). Furthermore, a trend towards increased aridity throughout the last 1300 years was identified in lake pollen and oxygen isotope records from southwest Turkey (Eastwood *et al.*, 1999, 2006). However, the majority of previous research was based on long time scales and analyses were conducted at relatively low-resolution. Therefore further research is required to improve understanding of recent climatic change in the EM at high-resolution.

Varved (laminated) lake sediments form in highly seasonal environments and can provide an annual record of environmental fluctuations (Lamoureux, 2001), due to visible changes in the sediment composition associated with variation in lake processes and productivity. Within this research project, two continental volcanic crater lakes, located in semi-arid central Turkey, have been identified as suitable sites to study EM palaeoclimate. Nar Gölü is annually laminated for the last 2000 years and its water chemistry is thought to relate to the balance between precipitation and evaporation. The varved sediment profile permits a high-resolution sampling strategy and annual calibration with meteorological records. Kratergöl is a hypersaline lake with non-varved sediments and could provide a comparative record of environmental change.

Lake sediment cores offer potential for multiple proxy analyses from the same sequence, such as methods employing palaeoecological indicators and geochemical proxies. Multi-proxy studies allow records to be compared and validated against one another. For example, Roberts *et al.* (2001) and Eastwood *et al.* (2006) used a combination of lake proxy indicators, e.g. diatoms, oxygen isotopes and pollen, to reconstruct palaeoclimate in Turkey. Jones (2004), Jones *et al.* (2005, 2006), England (2006) and England *et al.* (2008) analysed the oxygen isotope and pollen profiles of Nar Gölü at high-resolution and identified oscillations between wetter/drier climate and that human land use has been extensive in the region throughout the last 2000 years. Potential exists for the application of additional proxy analysis of Nar Gölü sediments to evaluate the relative impacts of human activity and climate factors on the environmental history of the lake and improve understanding of EM palaeoclimate.

1.2 Diatom palaeoenvironmental indicators

Diatoms are unicellular algae that respond to fluctuations in climate-related limnological variables through assemblage changes associated with different species' ecological preferences (Smol and Cumming, 2000). For example, changes in temperature and precipitation affect lake hydrology resulting in dilution or concentration of salts leading to a diatom response (Figure 1.3). Diatom-inferred (DI) conductivity has successfully been employed to surmise palaeoclimate by Fritz *et al.* (1990) and Laird *et al.* (1998) in North America, Gell and Gasse (1994) in Australia, Gasse *et al.* (1997) and Verschuren *et al.* (2000) in Africa, Reed (1998) and Reed *et al.* (2001) in Spain and Reed *et al.* (1999) and Roberts *et al.* (2001) in Turkey. Diatoms preserved within annually-laminated lake sediments therefore offer a potentially powerful tool for palaeoclimate reconstruction. Within this research project, diatom

fossils from Nar Gölü and Kratergöl sediment cores will be utilised as a proxy for water chemistry.

Transfer functions are frequently employed to derive palaeoclimatic information from fossil species assemblages. Training sets of modern species-environment relationships (e.g. diatom assemblages and lake water conductivity) based on a range of lakes are used to infer palaeoenvironmental conditions from the fossil species assemblage preserved in the lake sediment (Figure 1.4). Calibration with meteorological records for the instrumental period provides a cross-check for interpreting pre-instrumental reconstructions in terms of climatic variability (Battarbee *et al.*, 2001). Additionally, a range of numerical analyses can be employed to derive palaeoenvironmental change from diatom assemblages. For example, detrended correspondence analysis (DCA) can be used to observe assemblage change through time.

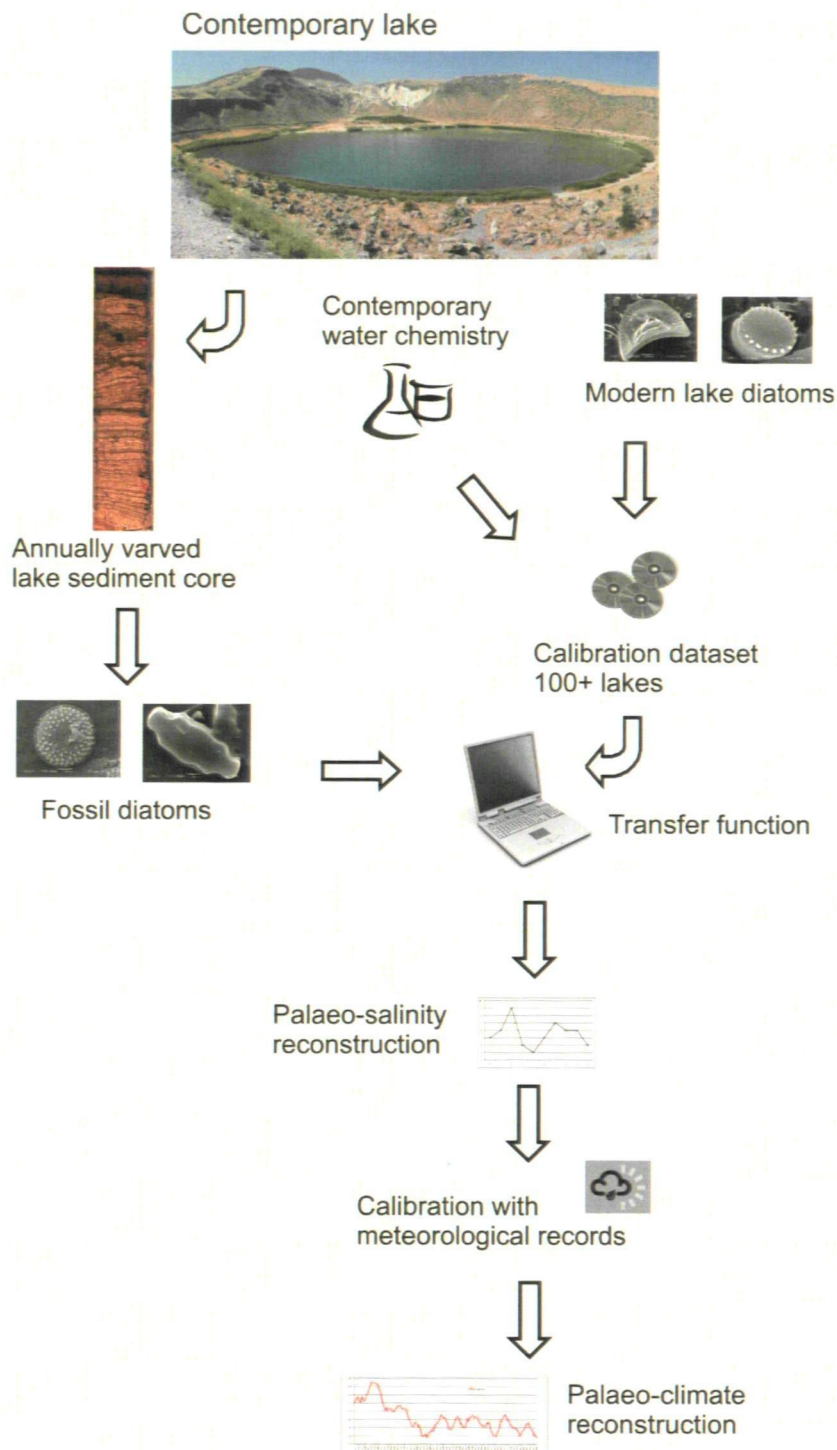


Figure 1.4 The process involved in palaeoclimate reconstruction from lake diatoms (adapted from Hall and Smol, 1999).

1.3 Aims and objectives

The primary aim of this research project is to reconstruct variability in EM late Holocene climate from diatom assemblages preserved within lake sediment from Nar Gölü and Kratergöl. A secondary aim is to explore different numerical analysis techniques to derive palaeoenvironmental information from diatom assemblages. The palaeoclimate reconstructions will contribute towards understanding of temporal variability in long-term climatic fluctuations in the EM region.

Hypotheses

1. Lake diatoms provide sensitive indicators of climate and water resource variability in the Eastern Mediterranean region.
2. Diatom-inferred climate variability during the late Holocene has significantly exceeded the range recorded during the period of instrumental observations (i.e. last century).

The aims will be achieved through a number of objectives:

- Examine modern diatom populations through lake sampling, sediment traps and water chemistry in order to understand species seasonality and the relationship between the modern and palaeo-assemblages.
- Analyse temporal changes in diatom species assemblages at decadal resolution through subsampling core sections covering the late Holocene from two crater lakes.
- Apply the diatom data to an existing transfer function from the European Diatom Database in order to derive a conductivity reconstruction.

- Calibrate an annual record of diatom assemblage change with instrumental meteorological records.
- Explore novel diatom assemblage analysis methods made possible by the presence of annually-laminated lake sediment.
- Explore numerical analyses to extract palaeoenvironmental information from the diatom assemblages.
- Compare and incorporate the results of different diatom numerical analyses to infer lake environmental change and palaeoclimate.
- Compare diatom-inferred (DI) environmental change with other proxy records for the same lake sediment cores and other lake and non-lake proxy climate reconstructions.
- Analyse the relationships between DI-environmental change and atmospheric circulation patterns, in order to identify possible controls on EM palaeoclimate.

1.4 Thesis outline

This chapter (1) has provided an introduction to various aspects of the research. Chapter 2 includes a two-part review of the literature surrounding the use of lake diatoms as palaeoclimate indicators and trends in EM climate. The next chapter provides a discussion of site selection, reviews methodological approaches employed and describes the different procedures followed (Chapter 3). This is followed by a discussion of the study sites with regard to their lake catchment characteristics (Chapter 4). The next chapters present the results from Nar Gölü (Chapter 5) and Kratergöl (Chapter 6). Chapter 7 includes interpretation of diatom analysis results. In Chapter 8: Part I comparisons are made with instrumental meteorological records from Turkey. Results are then discussed in terms of palaeoclimate and comparisons are made with other

records from Nar Gölü and various regions (Chapter 8: Part II). The global atmospheric circulation patterns associated with EM climatic variability are then considered. Chapter 9 includes a discussion of conclusions drawn from the investigation and makes suggestions for further research.

Chapter 2

Literature Review: Lake Diatoms and Eastern Mediterranean Climate

2.0 Introduction

This chapter comprises two subsections, which form the basis of the research. Part I introduces the subject areas of limnology/palaeolimnology and includes a review of the literature surrounding the use of diatoms from lake sediments as palaeoclimatic indicators. Part II describes the issues surrounding late Holocene climate change in relation to the Eastern Mediterranean region.

Part I Palaeolimnology and Diatoms

2.1 Lacustrine environments

Lakes comprise inland water bodies that form through tectonic, volcanic, glacial and other processes (Horne and Goldman, 1994) and vary with regard to their geomorphology, biogeochemistry and ecology. A lake's catchment comprises the area surrounding the basin from which water drains. Catchment characteristics influence the nutrient and chemical status of the lake and impact on the biota inhabiting the system.

Lake water balance relates to the hydrological inflow and outflow and is linked to variability in climatic factors, such as rainfall and temperature (Figure 2.1). Lake residence time relates to the duration taken for water to circulate through the system and is calculated by dividing lake volume by the sum of water inflows and outflows. Open and closed-basin lakes differ in their sensitivity to climatic fluctuations. Open systems lose water partly via surface outlets; therefore water level remains relatively constant.

Closed systems, common in semi-arid regions where evaporation exceeds precipitation, are highly influenced by climate, due to the fact that evaporation is the main process by which water leaves the system (Wetzel, 2001). The hydrochemistry of closed-basin lakes is therefore greatly influenced by the balance between precipitation and evaporation.

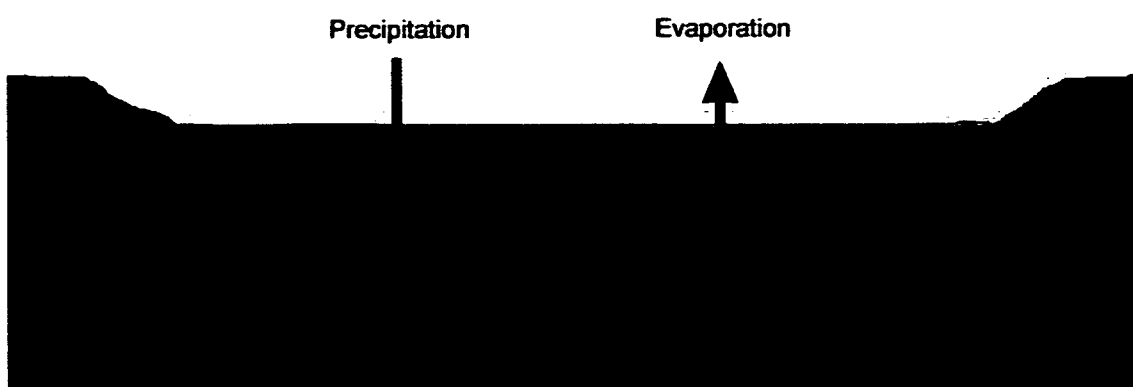


Figure 2.1 Structure of a maar lake illustrating the hydrological inputs/outputs and stratified water layers.

Lake water is frequently separated into non-mixing layers as a result of vertical temperature and chemical differences (Figure 2.1). A typical stratified lake comprises three layers, termed the epilimnion (top), metalimnion/thermocline (middle layer where temperature rapidly changes) and hypolimnion (bottom) (Brönmark and Hansson, 2005). These layers are often thermally and chemically stratified and change position throughout the year in a cyclic pattern. Deeper water layers receive a limited supply of atmospheric oxygen and light, which can restrict colonization by benthic organisms; this allows sediment to remain undisturbed. The sharp salinity and temperature gradients

associated with steep-sided, deep basins with a small surface area provide suitable conditions for water to become stratified (Wetzel, 2001).

Stratified lake systems, with anoxic bottom waters and limited bioturbation, provide ideal conditions for the formation of annually laminated sediments or varves. This involves distinct deposition patterns related to regional seasonality, forming a repetitive, cyclic pattern (O'Sullivan, 1983). Varve couplets, typically a few millimeters thick, comprise a light/dark sequence of organic material and inorganic sediment, which accumulates during different seasons, associated with processes occurring in the system. Varved lake sequences can provide a consistent record of past environmental change and a useful sediment dating tool (Lamoureux, 2001). Maar lakes are often stratified and form within volcanic craters, which result when ground water makes contact with rising magma (phreatic eruptions). This leads to the formation of steep sided U-shaped basins, which can be deep in relation to their surface area (Wetzel, 2001). These systems provide suitable conditions for the formation of varved sediments.

2.1.1 Lake hydrology, biogeochemistry and climate

Lacustrine environments are highly sensitive to climatic variability, responses to which are evident in hydrological and chemical fluctuations. Such relationships are complex and related to the lake's geomorphological, hydrological and chemical characteristics. Lake water chemistry is dependent on various factors, such as the parent rock type, topography, vegetation and human land use in the region (Horne and Goldman, 1994). Solutes accumulate in lake systems through inflow of water and rock weathering. The major ions in a lake system typically include magnesium, sodium, potassium, calcium, carbon, sulphate, iron and silica (Wetzel, 2001). Specific Electrical Conductivity (SEC)

is a measure of the total concentration of all dissolved ions and can be used as a proxy for salinity. Fluctuations in ionic composition affect biota inhabiting the lake. The relative importance of these ions to lake biota differs seasonally, for example, spring-blooming diatoms are dependent on silica and nutrient availability. Silica enters lake systems through surface and ground water. Greatest concentrations occur in ground water that is in contact with volcanic rocks (Wetzel, 2001); therefore maar lakes are particularly silica-rich. Lake carbonates are derived from inorganic and biogenic sources. In carbonate-bicarbonate lake systems photosynthetic CO_2 consumption by plants and algae results in increased lake water pH, which leads to calcium carbonate precipitation (CaCO_3) and accumulation in sediments (Bronmark and Hansson, 2005). This process often occurs during early summer following algal blooms.

When solutes become concentrated, saline lakes form. Such lakes are common in semi-arid regions. Concentration of ions occurs when the outflow of water is restricted and evaporation exceeds inflows, which remain sufficient to sustain the standing body of water (Hammer, 1986). Sodium (Na) is often the dominating ion in the system and different lakes vary with regard to their brine type. Saline lake systems are characterised, on the basis of dominating anionic concentrations, as carbonate, chloride or sulphide brine type water (Wetzel, 2001). Eugster and Hardie (1978) devised a lake brine type classification system based on the relative proportions of different anions and cations in the system. Brine evolution results from inflow of water, chemical weathering and evaporative concentration leading to precipitation of minerals (Eugster and Hardie, 1978). In seasonal environments, lake salinity alters throughout the year. Freshening takes place following spring snow melt and conductivity increases as a result of enhanced evaporation during summer. Winter ice contains mainly freshwater; therefore

remaining lake water can become concentrated in salts during this season (Hammer, 1986). Knowledge of the relationship between a contemporary lake and various climate and non-climate-related factors is required for reliable environmental interpretations, based on palaeolimnological analyses.

2.1.2 Palaeolimnology

Palaeolimnology is the study of the physical, chemical and biological information stored in lake deposits (Smol *et al.*, 2001). Lake sediment is composed of autochthonous material, formed within the system, and allochthonous matter, produced outside of the lake (Brönmark and Hansson, 2005). This material provides a valuable tool for understanding past and present lake conditions. Sediment dating permits changes in palaeo-lake conditions to be interpreted temporally. For example, varve counting and radioisotopic dating methods are used to date different sediment depths. Varve counting has been employed as a reliable dating method in various studies. For example, Wick *et al.* (2003) performed palaeolimnological analyses on a continually laminated sequence from Lake Van in eastern Turkey. Climatic factors, combined with anthropogenic influences and basin characteristics, determine the types of organisms that are capable of existing within the lake. The sensitivity of biological organisms to changing lake conditions leads to information about the palaeoenvironment, such as water depth and salinity levels, being preserved in fossil assemblages (Battarbee *et al.*, 2001). Palaeoenvironmental reconstructions can be performed through lake sediment analysis. This allows present and future environmental change to be evaluated in the context of past variability.

2.2 Diatoms as palaeo-indicators

Biological indicators can provide extensive palaeoclimatic information. Various palaeoecological proxy methods are applied to preserved material within lake cores to infer past climatic cycles and trends. Diatoms respond to changes in the ecological characteristics of an environment and are a key component of lake ecosystems.

2.2.1 Lake diatoms

Diatoms (class: Bacillariophyceae) are photosynthetic, microscopic, eukaryotic algae that are well preserved in fossil deposits from lakes (Stoermer and Smol, 1999) (e.g. Plates 2.1 and 2.2). Diatoms comprise two siliceous valves, or frustules, joined by girdle bands and form a single cell. Taxonomic distinctions are primarily made through identification of frustule size, shape and cell wall features. Within lakes, diatoms inhabit various niches, including the water column as plankton, attached to various substrata, such as sand, plants and seston, and as benthos on the lake bottom or margins. The benthos are split into epilithon, epiphyton, epipsammon and epipelon. Epilithon live attached to stones and pebbles, and have many species in common with the epiphyton, which attach to a host plant and are restricted by the growing season. Epipsammon attach to sand grains at the lake margin and are a very distinctive community composed of small, firmly-attached, adnate taxa. Epipelon is associated with seston at various depths within the water column and bottom mud, which also includes a specialised community of mainly motile raphid taxa (Battarbee *et al.*, 2001).

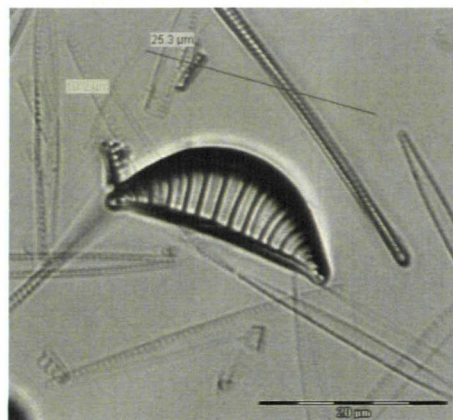


Plate 2.1 *Rhopalodia operculata*.

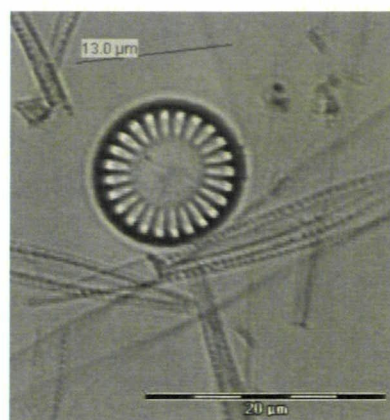


Plate 2.2 *Cyclotella meneghiniana*.

Diatom assemblages are often diverse and ubiquitous in lakes and other aquatic environments. Additionally, species respond rapidly to water chemical changes and are identifiable to high taxonomic levels, which has led to their frequent use as a palaeoenvironmental proxy (Battarbee, 1991). Diatoms are often the most dominant algal group in lake ecosystems and can account for over 50% of primary production (Stoermer and Smol, 1999). Therefore their importance to ecosystem processes is paramount. As a component of autochthonous material, diatoms are dependent on specific limnological conditions.

2.2.2 Lake hydrology, biogeochemistry and diatoms

Changes in lake hydrology and biogeochemistry alter the productivity and distribution of biota inhabiting the system. Due to the differing tolerances and affinities of taxa, diatom distribution and species composition is dependent upon a number of climate-sensitive limnological variables, for example, light availability, temperature, pH, nutrient status, and salinity. Diatoms are particularly sensitive to changes in lake salinity and taxa show dissimilar optima along salinity gradients (Fritz *et al.*, 1999). The sensitivity of diatoms to salinity is a direct result of osmotic stress and is also associated

with physiological factors, such as the effects of altered salinity on nutrient absorption efficiency (Saros and Fritz, 2000).

Kilham *et al.* (1986; 1996) discussed the importance of understanding the responses of different diatom species to seasonal resource ratios for more detailed interpretation of palaeo-records and identified that climatic change can alter nutrient loadings resulting in alterations to diatom assemblages. For example, different species are favoured by changes in ratios of Si:P and N:P and resource competition theory can be used to predict the distribution of different species.

Diatom frustules are composed of silica (SiO_2) and growth is therefore reliant on silica availability in the lake. Increased temperature and precipitation results in accelerated chemical rock weathering, which enhances the availability of silica for diatom population growth. Populations are also greatly dependent on lake nutrient supply, which is often a limiting factor for phytoplankton growth. When phosphate levels are high, diatoms are prolific and deplete silica resources.

Diatom species assemblages alter seasonally as a response to lake physical and chemical changes. Diatom populations are also affected by competition with other algal groups, such as dinoflagellates and blue-green algae. Additionally, fungal, zooplankton, viral and bacterial predation and parasitism influence diatom population dynamics (Horne and Goldman, 1994). The differing abilities of diatom species to compete and tolerate factors such as grazing pressure and low nutrient availability in summer, results in altered species assemblages throughout the course of a year. Diatoms also differ in their response to lake variables, depending on their cell volume. For example, Snoeijs *et al.*

(2002) identified that large diatoms respond more strongly to salinity variability. The combined effects of different factors, and the specific basin ecology, interact and result in a complex diatom response, which requires careful interpretation.

2.2.3 Diatom-inferred climate reconstructions

Diatoms provide a powerful tool to infer past lake hydrological conditions quantitatively and have frequently been used to reconstruct palaeo-conductivity, moisture availability and climate. Coring methods are used to obtain a profile of sediment from the lake bed (Glew *et al.*, 2001) and analyse temporal change in diatom species assemblages by substituting 'space' for 'time'.

When using biological indicators, it is important to ensure that the species composition reflects changes in the limnological variables of interest and that fossil records are reliable and interpretable (Stoermer and Smol, 1999). Multiproxy methods, such as those combining diatom with pollen analysis and geochemical techniques, allow records to be validated and compared, which improves understanding of the lake system and palaeoenvironmental conditions.

Sediment traps can be used to collect material suspended within the water column in hollow tubes. This material is called 'seston' and is composed of organic and inorganic particulate matter. Sediment traps can be particularly useful to diatomists as a means of providing an integrated sample of the present-day lake flora for direct comparison with sediment core samples, plankton and benthos (Battarbee *et al.*, 2001). Seston traps have been used in various studies concerning lake diatom communities; for example,

Cameron (1995) used sediment traps to compare the quality of the diatom fossil record with the modern lake flora.

Transformation of modern diatom communities into the fossil record is controlled by a complex array of site specific taphonomic processes that operate both in the water column and in sediments (Flower, 1993). In addition, laboratory preparation techniques may initiate further breakage or frustule dissolution. Various limnological variables influence diatom preservation in sediment. Dissolution has varied affects of different diatom taxa and can reduce the reliability of palaeoenvironmental interpretations (Barker *et al.*, 1991; Barker, 1992).

Anderson (1995) highlighted that, prior to the development of robust transfer functions, fossil diatom data were interpreted subjectively. Birks (1998) discussed the progress of numerical tools in palaeolimnology and highlighted that, throughout the 1990s, palaeolimnology changed from a predominantly qualitative, descriptive subject to a quantitative, analytical science. This was accredited chiefly to major developments in applied statistics and high temporal resolution sampling and dating.

2.2.4 Numerical techniques

Diatom species count data, derived from light microscope slides containing processed sediment, are converted into percentages for multivariate statistical analysis. The first stage in interpreting diatom stratigraphical data involves dividing the lake sediment sequence into assemblage zones using methods such as cluster analysis (Birks, 1995). This allows zonation and major assemblage changes in the record to be identified by partitioning samples from different sediment depths into subsets based on their

similarity. Detrended Correspondence Analysis (DCA) (Hill and Gauch, 1980) is also used to assess the similarity between samples or species visually.

Transfer functions involve using relationships between modern diatom species and environmental variables (i.e. water chemistry) to infer ecological conditions from fossil diatom assemblages (Battarbee *et al.*, 2001). In the development of a transfer function, calibration training sets are compiled from selected lakes representing a gradient for the environmental variable of interest, e.g. salinity. Various statistical methods are used to analyse lake training sets, including Canonical Correspondence Analysis (CCA), weighted averaging (WA) and the modern analogue technique (MAT). CCA is an ordination technique that allows species characteristic of specific water chemical conditions to be identified (Jongman *et al.*, 1995). For the transfer function to be effective, the environmental variable of interest needs to explain a significant proportion of the variance in the species compositional data (Battarbee *et al.*, 2001).

Models are employed to produce reconstructions from fossil assemblages based on the modern species-environment data. WA) is used to determine taxa tolerances for an environmental variable and is the most widely utilised method in diatom transfer functions. WA involves establishing an optimum value for each species (weighted by its relative abundance) for a specific environmental variable by analysing its dominance in lakes in the training set along with water chemistry data. This optimum value is applied to the species weighting in the fossil assemblage in order to infer palaeoecological conditions. WA is disadvantaged by the tendency of reconstructions to follow the distribution of the dominant species. The MAT performs the reconstruction based on an average of a number of the closest analogue sites (lakes with a similar species

assemblage) and therefore avoids this problem to an extent. However, MAT is limited by its susceptibility to the effects of autocorrelation, i.e. the tendency of sites in close proximity to resemble one another, which can produce incorrect results (Telford and Birks, 2005).

The predictive ability of the transfer function can be evaluated by examining the relationship between observed and predicted values. This is reflected by the r value, which provides a measure of the strength of this relationship. The Root Mean Square Error of Prediction (RMSEP) is a cross-validation measure of the performance of the training set, i.e. the predictive error (Birks, 1995). However, due to over-estimation of the predictive ability of models, errors are often produced when the same data are used to predict the values. Various computer-based methods have been developed to reduce the effects of this, e.g. jack-knifing and bootstrapping. This involves leaving random samples out of the data set and observing the predictive ability of the model (Birks, 1998). Ensuring that fossil taxa are well represented in the modern training set is also an important factor, as the reconstructed values are likely to be more reliable if most fossil species are present in the modern lakes (Birks *et al.*, 1990). The MAT can be used to produce a numerical definition of the similarity between the modern and fossil samples (Battarbee *et al.*, 2001).

Once a reconstruction has been performed, the reliability of inferred values, based on fossil samples, needs to be assessed (Birks, 1995). This can be achieved using analogue matching methods described by Birks *et al.* (1990) and Bartlein and Whitlock (1993). The MAT uses a dissimilarity measure to numerically compare biological assemblages in fossil samples with those in modern samples (Birks, 1995). The MAT can be used to

assess whether fossil samples have a good modern analogue in the training set based on a comparison of the fossil and modern sample minimum dissimilarity coefficients (min. DC) (e.g. Laird *et al.*, 1998). Fossil samples with min. DC values in the extreme 10 and 5% of the modern training set are identified as having ‘no good’ or ‘no close’ analogues in the modern environment (Birks, 1995). Therefore reconstructions for these samples are likely to be unreliable.

An alternative method to assess the reconstruction involves comparing inferred values with instrumental meteorological records. Correlation and regression allow the relationship between diatom populations and other factors to be explored and quantified. Comparison of reconstructed values with meteorological records is possible only when high-resolution diatom data are available for the instrumental period. Significant correlation between climate factors and diatom-inferred (DI) conductivity validates inferences from the pre-instrumental DI-conductivity record (Birks, 1995). Laird *et al.* (1998) identified a strong link between diatom-inferred conductivity, instrumentally measured lake conductivity and water level in the Northern Great Plains (USA) and employed a WA transfer function to reconstruct pre-instrumental conductivity.

2.2.5 Limitations

There are a number of limitations associated with the use of diatoms as a palaeoenvironmental research tool and their use requires a number of assumptions. Fritz (2008) highlighted that the response of lakes to non-climatic factors results in non-linear responses to climate and changes associated with the lake ageing process may alter the response to a given climate perturbation, resulting in non-stationarity in the diatom response. Additionally, a relationship derived from contemporary data may not be

relevant throughout the lake's history. There are also a number of problems associated with differential species dissolution and poor preservation of fossil diatoms in certain lake conditions (Barker *et al.*, 1991; Barker, 1992). Battarbee *et al.* (2005) suggested that as little as 1% of the phytoplankton may be preserved in sediment and that failure to take such factors into account can undermine the use of diatoms for palaeoclimatic reconstruction.

The application of transfer functions also requires a number of initial assumptions, for example, the species in the modern and fossil datasets have not altered significantly, biota present are related to the ecological conditions and environmental variables are related to climatic factors (Imbrie and Webb, 1981). Gasse *et al.* (1997) highlighted a number of potential problems associated with the use of diatoms to infer palaeo-conductivity, for instance, representation of the species assemblages, distortion of the ecological signal, and non-climatic hydrological factors that may alter water chemistry. Additionally, problems arise when species are not normally distributed. For example, a population may be truncated or bimodal in its response to an environmental variable.

When applying training sets compiled from different regions to that of the fossil samples, a number of additional issues arise. Problems can be associated with the differing temporal and spatial responses of species to environmental variables, taxonomic harmonisation between researchers and issues surrounding the presence of dominant fossil species that do not have an analogue in the modern training set. Lakes within different global regions differ with regard to their calcium and carbonate ions (Wetzel, 2001); therefore chemical responses to climate also vary. Saros and Fritz (2000) identified that the growth rates of different diatom species differed in response to

changing salinity, brine types and nitrogen form (NH_4^+ versus NO_3^-). For example, species exhibited lower growth rates in sulphate in comparison with bicarbonate brine type lakes. Factors such as rock weathering and volcanic products may also alter the ionic composition of maar lake water and affect the diatom relationship with salinity. Martin-Del Pozzo *et al.* (2002) identified increased Na^+ , Ca_2^+ , SiO_2 and Mg_2^+ concentrations in spring water prior to volcanic activity. Therefore it is important to combine information from multiple proxies and consider additional biostratigraphic and lithological data when inferring palaeoclimate from diatom assemblages. Although a number of limitations exist, there is still great potential for the use of diatoms in palaeoenvironmental research.

The European Diatom Database (EDDI) was created to provide an extensive archive of diatom-environment information and allow reconstructions to be performed using collections of training sets from Europe, Africa and Asia (Juggins, 2008). The combined salinity training set comprises data from East Africa, North Africa and Spain. There is potential for such databases to expand and a global diatom resource to be created. Birks (1998) suggested a number of future advances involving improved statistical techniques and computer technology. For example, there is potential for calibration training sets to take into consideration the varied responses of a species to an environmental variable. Battarbee *et al.* (2001) highlighted the need to strengthen understanding of diatom habitats and ecology to permit higher precision climate reconstructions and Fritz (2008) suggested that increased coordination of efforts is needed to generate regionally robust climate reconstructions.

2.2.6 Additional diatom analysis methods

A number of other analytical methods can be employed to infer palaeoenvironmental information from diatom assemblages. For instance, in addition to conductivity, diatoms are also employed to infer palaeo-temperature, pH and nutrient status of lakes. An oxygen isotope signal is also recorded in frustule silica, which can be used to infer palaeo-lake water balance based on the ratio of $^{18}\text{O}/^{16}\text{O}$ associated with changing temperature and precipitation (e.g. Leng and Barker, 2006; Barker *et al.*, 2007).

Diatoms can also be employed to reconstruct palaeo-silica-cycling from lakes (Street-Perrott and Barker, 2008) with implications for understanding palaeoenvironmental change.

Calculation of diatom concentration and total cell biovolume (biological volume) provides information regarding past productivity and allows the relative importance of different species in the population to be analysed. Wolfe (2003) calculated diatom cell biovolume and species diversity in conjunction with a WA transfer function for summer water temperature, in order to analyse the response to climate change. Species cell dimensions and volumes are likely to vary between lakes. There are positive and negative aspects to using percentage data and biovolume. Percentages allow an individual specie's relative contribution to the community to be calculated and are useful when applying transfer functions. However, percentages do not account for variability in species cell volume and productivity. As proportions are relative, assemblage change is masked by extreme abundances of small diatoms and bloom species. Maximum specific growth time has been identified as decreasing with increasing algae cell size (Mizuno, 1991), which results in large species being observed less frequently and leads to incorrect ecological interpretations. Although biovolume

accounts for actual biomass, this reduces the importance of smaller species cell number, which may lead to important information about fecundity being lost. A combination of percentage and biovolume data provides more detailed information about the assemblage.

Estimating species diversity can also provide palaeoenvironmental information. For example, greater diversity may indicate increased system disturbance due to the changing number of habitat types available. Gell and Gasse (1994) recognised greater species diversity in lakes of lower salinity; this is likely to relate to the fact that fewer species are able to tolerate extreme conditions. Species can also be grouped according to their habitat preferences. For instance, the ratio of planktonic to littoral/benthic diatom species can be used as a proxy for past water level (e.g. Barker *et al.*, 1994).

Varved sediments permit a number of additional analytical methods. Measurements of varve thickness and analysis of sub-layers can provide information about palaeo-productivity and different events occurring in the lake. Romero-Vianna *et al.* (2008) derived a climate signal from sediment varve thickness. Distinct single-species diatom bloom events can also be microscopically visible on thin section slides prepared directly from a varved sediment core and can provide valuable information about assemblage seasonality. Additionally, the installation of sediment traps in a lake allows material deposited at different times of year to be studied and seasonality in the diatom population to be analysed. For example, Hausmann and Pienitz (2007) highlighted the need to reconstruct seasonal variability in past climate and identified differences in a lake's sub-annual response to climate using sediment traps.

2.3 Summary

Lacustrine environments are sensitive to environmental fluctuations and can provide sediment archives of palaeoecological information. Biological indicators are useful tools to reconstruct palaeoenvironmental change and strengthen understanding of past climate variability. The extensive literature surrounding diatoms as palaeoclimate indicators focuses on diverse global locations and provides a strong foundation on which to base future research. Transfer functions offer a powerful tool to reconstruct palaeo-conductivity from diatom assemblages. Interpretations of such reconstructions can be improved by employing additional methods to analyse temporal change in the diatom community, comparison with different proxy data and instrumental meteorological records.

Part II Eastern Mediterranean Climate

2.4 Introduction

In semi-arid regions, palaeoecological information derived from the sediment archives of closed-basin lakes can reveal long-term patterns in the intensity, duration and frequency of climatic changes (Fritz *et al.*, 1999). Analysis of the modern climate regime can be employed to understand palaeoclimate from lake sediment records. The Eastern Mediterranean (EM) includes a number of European, North African and Southwest Asian countries and surrounding marine basins (Chapter 1: Figure 1.1). Turkey occupies the region where the continents of Europe and Asia meet. This region is topographically elevated in comparison with neighbouring countries, and is predominantly mountainous, with a broad plateau (1000-2000 m above sea level) (Sansal, 2005). Turkey is bordered by the Mediterranean, Black, and Aegean Seas. Fairbridge *et al.* (1997) highlighted the 'special position' of Anatolia (central Turkey) linked to its geologic history, elevation and the position of surrounding marine basins, which combine to create a unique climatological setting.

Human settlement has been extensive and continuous throughout the Holocene in Turkey, with many civilisations developing on the Anatolian peninsula. Anthropogenic activity has played an important role in shaping the landscape of the EM, predominately through agriculture. Roberts *et al.* (2004) highlighted that spatio-temporal complexity exists in human impact on the region due to the combined impacts of climatic fluctuations and social factors. Water is a sensitive resource for humans inhabiting drylands, due to the risk of drought and negative consequences of decreased moisture availability (Cullen *et al.*, 2002). Drought events have had dramatic social,

environmental and economic impacts on present and past societies (Fritz *et al.*, 1999). Therefore it is important to understand patterns in past water resource availability.

2.5 Factors controlling Eastern Mediterranean climate

In order to make inferences about EM palaeoclimate, it is necessary to understand present trends and factors affecting variability. According to Rossignol-Strick (1993), the present climate of the EM is dependent on conditions in central and southern Asia, central Europe, Africa, the Mediterranean Sea and the Atlantic Ocean. Turkey is situated in a transition zone that is under the influence of various atmospheric disturbances and weather types (Türkeş *et al.*, 1995). For example, the North Atlantic Oscillation (NAO) and the North Sea Caspian Pattern (NCP) have important influences in the climate of the region. The Southern Oscillation (SO), the Arctic Oscillation (AO) and the Indian Monsoon have been identified as exerting less influence on EM climate. The influence of changing strength and intensity of these pressure systems on seasonal climate at annual to centennial timescales, combined with regional factors, such as Turkey's high elevation, the presence of mountain ranges and marine basins, create a specific climatological setting. Additionally, climate forcing associated with human activity, such as increased GHGs and changes in land use, may have impacted upon EM climatic variability.

2.5.1. North Atlantic Oscillation

The NAO has been identified as the pressure system exerting greatest influence on Turkish climate, particularly during winter. The NAOI (Index) is related to the surface pressure alteration between the Azores High and the Icelandic Low. Negative phase of the NAOI is associated with increased storm tracks entering the Mediterranean basin

and consequently impacts upon EM climate. Türkeş and Erlat (2003; 2005) investigated climatological responses to the NAOI at 78 weather stations in Turkey. Significant relationships were identified between climate data and positive or negative NAOI phases at most stations. A number of time periods throughout the instrumental period were identified as having experienced widespread, severe drought and these were linked to extreme NAOI. Additionally, Mann (2002) identified the dominant pattern of influence on Middle Near Eastern Temperature (MNET) as the NAO. Over the past several decades, the NAOI has steadily strengthened. Cullen *et al.* (2002) suggested that this trend accounts for increased temperature over parts of Europe and Asia.

During periods of positive NAOI, the North Atlantic westerlies, which provide moisture for the EM, shift northwards, creating drier conditions in Turkey (Komuscu, 2001). Türkeş (1998) suggested that downward trends in Turkish precipitation since the 1970s could be attributed to a further northward shift of the polar front from its normal position, as a result of the more eastward extension of the drought-dominated subtropical anticyclones from the Azores to the EM. When the NAOI is high, wetter conditions prevail throughout northern Europe and drier conditions occur in Mediterranean Europe, with the opposite effect during low NAOI (Osborn, 2008). Karabörk *et al.* (2005) identified that winter NAO influences precipitation and stream flow patterns in Turkey and that temperature appears to be less sensitive to the NAO.

A teleconnection 'see-saw' oscillation pattern has been identified in atmospheric pressure distribution and spatial precipitation variability between the east and west Mediterranean (Roberts *et al.*, 2004). Oldfield and Thompson (2004) identified negative correlation in winter (NDJF) precipitation (AD 1855-1990) between meteorological

stations in Western Europe and the EM. Wet winters in the west correspond with dry winters in the east. This relationship is likely to relate to shifts in the NAO and implies that Turkey may experience opposite precipitation patterns to those typical of Western Europe.

2.5.2 North Sea Caspian Pattern

The NCP Index (NCPI) represents the atmospheric teleconnection between the North Sea and the northern Caspian Sea region (Southwest Asia) (Kutiel and Benaroch, 2002). The influence of this pressure system is more pronounced in winter and negative phases relate to higher pressure over the Caspian Sea. Positive and negative phases of the NCPI were identified by Kutiel and Türkeş (2005) as significantly related to temperature in the EM, Anatolia (central Turkey) and Southwest Asia. Greatest influence of the NCP was recognised on the temperature regime of continental central Turkey; however, the relationship with precipitation was less clear and subject to considerable spatial variability.

2.5.3 Arctic Oscillation

The AO represents atmospheric pressure changes between the Arctic and northern middle latitudes. Türkeş and Erlat (2008) evaluated the relationship between Turkish climate and the AO Index (AOI). Significant relationships were identified between winter temperatures and the AOI at 70 Turkish meteorological stations. Türkeş and Erlat (2008) identified that the AO pattern forms warm signals in Turkey by increasing westerly and south-westerly circulation carrying Atlantic and northernmost African warm air into the EM.

2.5.4 Southern Oscillation

The SO represents seasonal fluctuations in air pressure differences between Tahiti (South Pacific) and Darwin (north coast of Australia). Cold/warm SO phases (El Niño and La Niña) are related to various climatic events in the South Pacific region. Dry conditions in the EM have been associated with warm SO events (Türkeş, 1998). The SO was recognised as a climate feature in the EM by Mann (2002) and identified as having a weak and inconsistent influence on the region. Alpert *et al.* (2005) suggested that shifts in the SO lead to changes in Mediterranean circulation patterns and are associated with rainfall extremes in the EM.

2.5.5 Indian Monsoon

The Indian monsoon is associated with the seasonal temperature difference between the Eurasian land mass and surrounding oceans and has been identified as a teleconnection influencing summer climate in central Anatolia (Lionello *et al.*, 2006 b; Jones *et al.*, 2006). Liu and Yanai (2001) recognised that greater intensity of monsoon rains from tropical Africa to India lead to warmer conditions in western Asia and Alpert *et al.* (2005) identified that an enhanced Indian Monsoon is linked to increased summer temperatures in the EM. Increased monsoon rainfall results from low pressure systems over southern Asia; this strengthens the northerly and north-easterly airflows from warm/dry central Asia, resulting in increased drought in the EM (Jones *et al.*, 2006).

2.6 Instrumental meteorological records

The present climate of Turkey is temporally and spatially variable. Coastal locations have a mild Mediterranean climate, while the inland Anatolian plateau experiences extremes of hot summer, cold winter and low rainfall (Reed *et al.*, 1999). Sub-regions

vary considerably with regard to their temperature and precipitation regimes (Türkeş, 1998).

2.6.1 Spatial variability

The climatic regime of the Mediterranean is spatially variable due to the presence of many sharp orographic features, such as islands, gulfs and peninsulas (Lionello *et al*, 2006 b). Regional temperature and precipitation variability in Turkey results from the influence of local topography, elevation and regional distances from surrounding marine basins. Türkeş (1998) identified several precipitation regions in Turkey associated with rainfall geographical control and seasonality (Figure 2.2). Spatial variability in precipitation between these regions is highlighted by measured differences in total rainfall (Figure 2.3). For example, central areas experience an annual rainfall total of 400 mm, whereas coastal regions receive around 800 mm. Türkeş (1995) identified highest mean temperatures in the south and in coastal regions, whereas the east and central areas experience a cooler climate (Figure 2.4), which is mainly associated with elevation changes. Extreme seasonality exists in the temperature and precipitation regimes of Turkey. For example, summer temperatures reach as high as 30°C in central Anatolia, whereas winters are typically cold and snowy due to the high elevation. Spring precipitation accounts for over 30% of the annual total in central regions, while summer accounts for less than 5% (Türkeş, 2003).

Droughts, involving prolonged periods of reduced water availability (Wilhite, 2000), are a typical climatic feature of semi-arid Turkey. Inland continental areas with little vegetation cover are described by Bolle (2003) as particularly sensitive to increased temperatures, due to the lack of water for evaporative cooling and absence of plants for

CO₂ fixation. The intensity of droughts and regional susceptibility can be quantified using aridity indices. Türkeş (2003) defined spatial variability in the aridity index of Turkey (Figure 2.5) based on the ratio of evapotranspiration to precipitation and identified central areas as the most arid. Throughout much of Turkey, evapotranspiration is greater than precipitation; therefore semi-arid and dry sub-humid climate conditions dominate the continental interior of the country (Türkeş 1998).

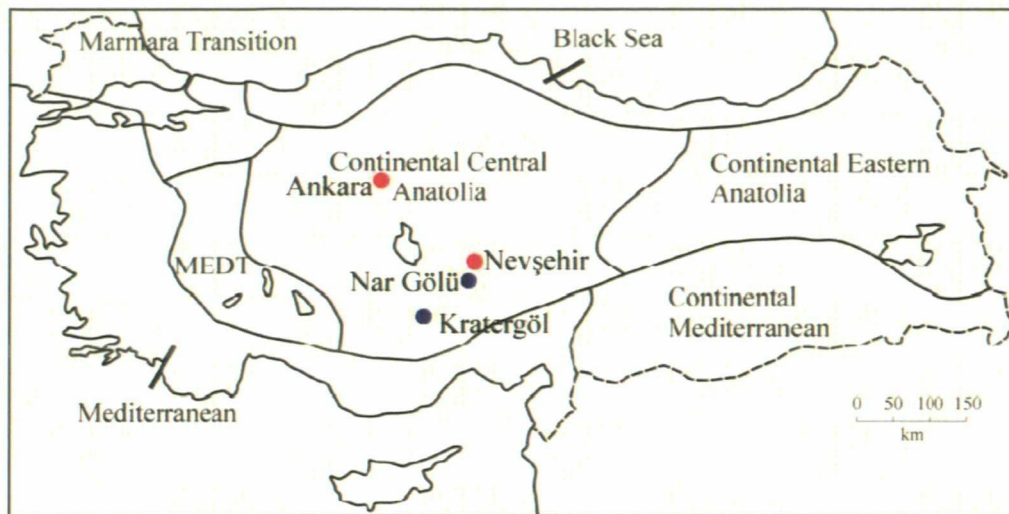


Figure 2.2 Turkish precipitation regions based on geographical distribution of rainfall regimes. Data from Türkeş (1998; 2003), redrawn by Jones (2004). Blue circles highlight locations of lake sites in this study.

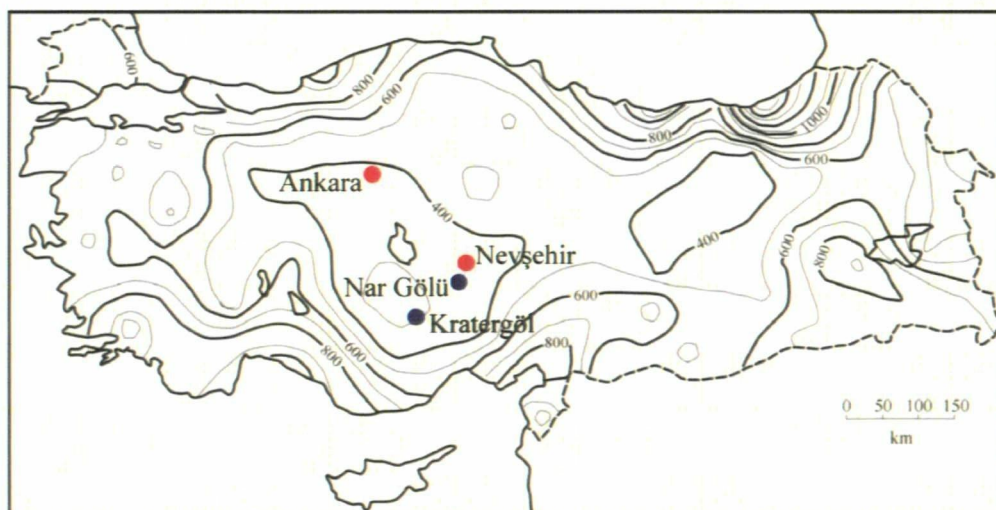


Figure 2.3 Mean annual precipitation totals for Turkey. Data from Türkeş (1998; 2003), redrawn by Jones (2004). Blue circles highlight locations of lake sites in this study.

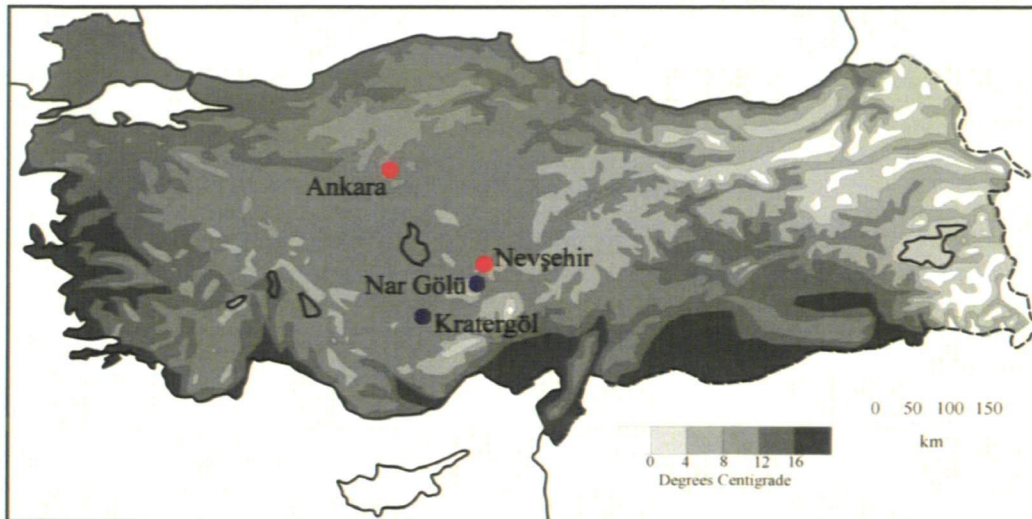


Figure 2.4 Mean annual temperature for Turkey. Data from Türkeş (1995), redrawn by Jones (2004). Blue circles highlight locations of lake sites in this study.

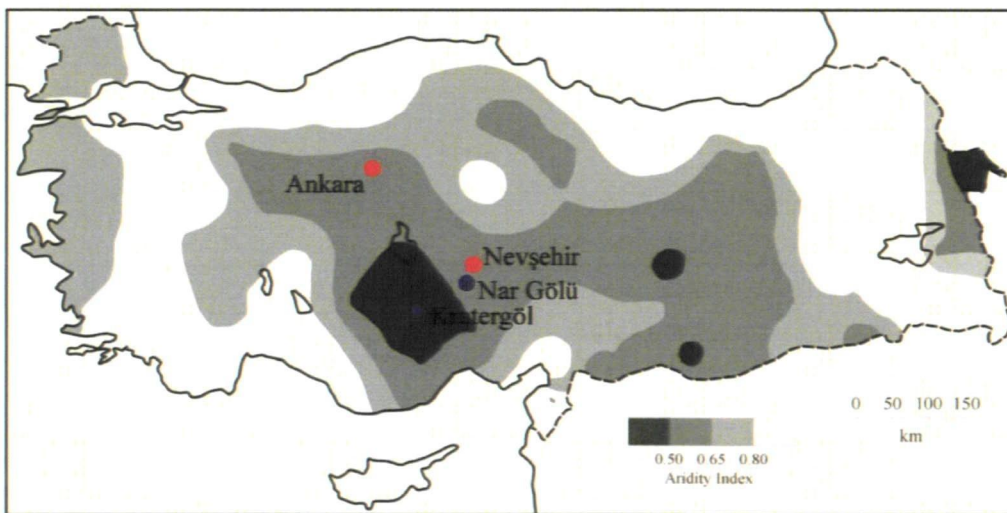


Figure 2.5 Mean annual aridity for Turkey. Data from Türkeş (2003), redrawn by Jones (2004). Blue circles highlight locations of lake sites in this study.

2.6.2 Temporal variability

Considerable temporal variability throughout the late Holocene has been identified in meteorological records and palaeoclimate reconstructions from the Mediterranean region (Luterbacher *et al.*, 2006). Xoplaki *et al.* (2006) claimed that the hot summers of

the decade 1994–2003 in the Mediterranean were unprecedented in the context of the last 500 years. Türkeş (2003) acknowledged that annual and winter precipitation have decreased over a considerable part of Turkey since the early 1970s and identified a general tendency from the humid conditions of the 1960s towards the recent dry sub-humid climate of the region. Additionally, annual, winter and spring mean temperatures have increased in many areas of Turkey, particularly in the south, whereas summer and autumn temperatures have decreased over the northern and continental regions (Türkeş *et al.*, 2002).

Figures 2.6 and 2.7 illustrate recent climate trends recorded at two meteorological stations in Turkey (Ankara and Nevşehir) based on average summer and winter temperature and total annual precipitation records from the 20th century. The Ankara record illustrates a general increasing trend in winter temperature between 1927 and 2007 and a recent rise in summer temperature. Total precipitation recorded at Ankara has increased throughout this period. The Nevşehir record shows a recent increase in summer temperatures and a decrease in total precipitation.

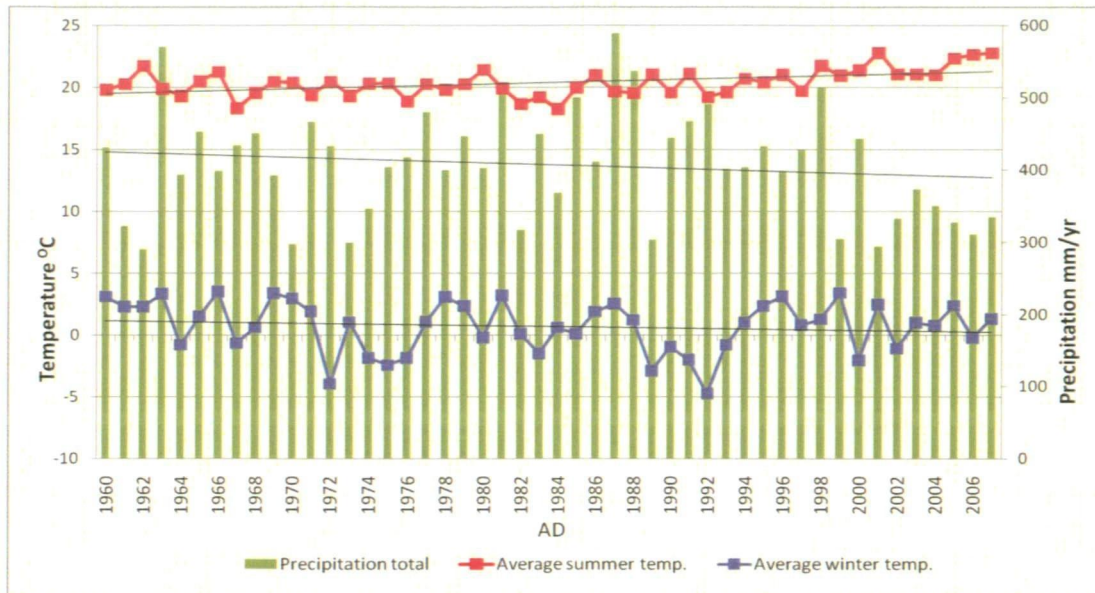


Figure 2.6 Average summer and winter temperature plotted with total annual precipitation for the period AD 1960-2007 recorded at Nevşehir meteorological station (Turkey) (data from Turkish State Meteorological Service).

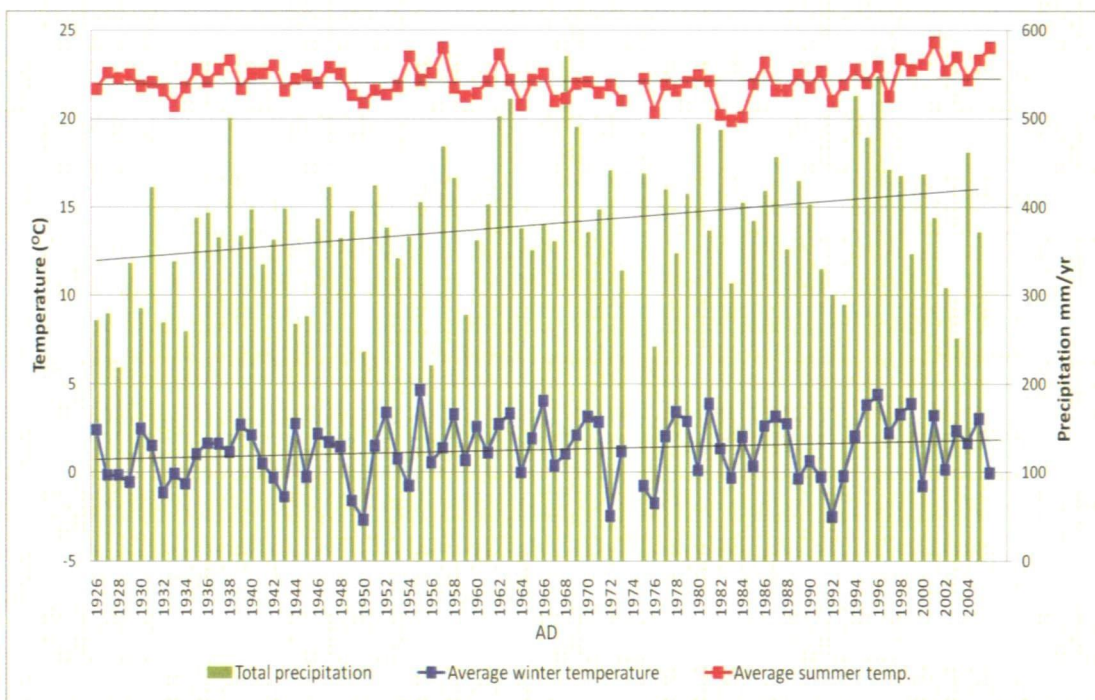


Figure 2.7 Average summer and winter temperature plotted with total annual precipitation for the period AD 1926-2006 recorded at Ankara meteorological station (Turkey) (data from Turkish State Meteorological Service).

2.7 Holocene palaeoclimate reconstructions

Spatial and temporal changes in the trends and intensity of factors controlling EM climate, combined with regional influences, have resulted in climatic variability throughout the Holocene (~11.7 ka). Previous palaeoenvironmental research in the EM has often involved low-resolution descriptive studies based on relatively long time scales; for example, Cohen and Erol (1969), Rossignol-Strick (1993), Erol (1978; 1997), Erinc (1978), Harrison and Digerfeldt (1993), Landmann *et al.* (1996), Fairbridge *et al.* (1997), Fontugne *et al.* (1999) and Akgün *et al.* (2007). Low resolution studies lack the advantage of calibration with instrumental meteorological records made possible through high-resolution sampling.

Due to the wide range of natural proxies available, the Mediterranean region presents an ideal location for climate reconstructions, in particular for analysing present climate extremes in relation to pre-instrumental periods (Luterbacher *et al.*, 2006). Numerous natural archives, including lake sediment, vegetation, tree rings and cave speleothems, have been utilised as palaeoclimate indicators in the EM.

2.7.1 Lake sediment archives

Changes in vegetation, hydrology and the nature of lake sediment are reflected in proxies such as pollen, diatoms and geochemical records. Within semi-arid regions, changes to the diatom assemblage often reflect drought frequency. Diatoms have been utilised as a climate proxy in Turkish lakes by numerous researchers including Reed *et al.* (1999), Eastwood *et al.* (1999), Roberts *et al.* (1999; 2001) and Kashima (1996; 2003).

Kashima (1996; 2003) identified a strong relationship between measured and diatom-inferred conductivity and highlighted the potential for reconstructing diatom-inferred palaeo-conductivity fluctuations in Turkish closed inland lakes in order to understand Late Quaternary climate change. Reed *et al.* (1999) recognised an inverse relationship between lake level and diatom-inferred conductivity in Turkish lakes. Such research has illustrated the sensitivity of lake diatoms to climatic fluctuations. However, these studies involved relatively long time scales and were disadvantaged by poor diatom preservation (Reed *et al.*, 1999) and limited chronological control.

Oxygen and carbon isotopes recorded in lake sediments are frequently used as a proxy for precipitation and evaporation. The ratio of ^{18}O to ^{16}O , related to the evaporative removal of lighter isotopes, indicates wet and dry shifts in climate associated with drought frequency. In Turkey, this method has been employed by Leng (1999; 2001), Roberts *et al.* (1999; 2001), Wick *et al.* (2003) Eastwood *et al.* (2006) and Jones *et al.* (2005; 2006; 2007; 2008). Jones *et al.* (2005) recognised significant relationships between the oxygen isotope record from Nar Gölü crater lake in central Turkey, summer temperature and evaporation. However, it was highlighted that interpretations of isotopic records in lake sediments are often over-simplified (Jones *et al.*, 2008). Therefore a combination of proxy analyses can provide more reliable climate reconstructions.

Pollen preserved in lake sediments can provide detailed records of past landscape change, human activity and climate variability. A number of pollen studies based in Turkey have been largely descriptive and have involved long timescales; for example, Bottema and Woldring (1990), Bottema (1995), Rossignol-Strick (1993) and Roberts *et*

al. (1997; 1999; 2001). More recent studies have employed higher-resolution sampling, for example, England *et al.* (2008), Wick *et al.* (2003) and Eastwood *et al.* (2006). England *et al.* (2008) compared pollen, stable isotopes and charcoal records from Nar Gölü crater lake in central Turkey and identified that pollen and charcoal relate to human land use and do not coincide with changes in the isotope record, which is associated with climate variability.

Palaeoclimate reconstructions from lakes can be complex due to the influence of regional variability and specific basin characteristics. Interpreting Holocene pollen records is complicated by the combined impacts of climatic forcing and human land use on vegetation change. For example, Eastwood *et al.* (2006) highlighted that agreement between isotopic and pollen data was limited in a lake study in southwest Turkey, which is likely to be associated with human land use and the slower response time of vegetation to climatic changes in comparison with isotopes. This lack of agreement was also recognised during the late Holocene by Wick *et al.* (2003) in a lake study from northeast Turkey. Therefore multiproxy reconstructions from lakes need to be interpreted in relation to the changing impacts of human activity, the different response time of indicators, regional factors and basin characteristics.

2.7.2 Non-lake archives

Tree-rings are frequently used as a proxy for palaeo-rainfall, due to the fact that growth rates respond to changes in available moisture. Similarly to lake varves, tree-rings allow annual-resolution research; however, the temporal extent of this method is limited by tree life-span (e.g. the last ~900 years) and the fact that growth only represents one season rather than annual climate. According to Luterbacher *et al.* (2006),

dendroclimatology is still in its early stages of development in the EM. Several recent studies have successfully employed this method. For example, D'Arrigo and Cullen (2001), Touchan *et al.* (2003; 2007), Akkemik *et al.* (2005), Akkemik and Aras (2005) and Sarris *et al.* (2007) reconstructed precipitation and drought during the last millennium in Turkey, based on tree-ring data and identified a number of wet/dry trends.

Isotopes recorded in cave speleothems offer detailed records of palaeoclimate that can be dated with high precision and act as a proxy for precipitation and temperature. Bar-Matthews *et al.* (1997; 1999; 2000; 2004) researched EM palaeoclimate using carbon and oxygen isotopes from speleothems in Israel and identified events that coincide with northern latitude climate variability. Recent work has employed cave speleothems as a palaeoenvironmental indicator in Turkey (Baker *et al.*, 2008). Additionally, isotopic signals have been derived from Mediterranean marine foraminifera (e.g. Rohling *et al.*, 2004) and marine coral from the Red Sea (e.g. Felis *et al.*, 2003) in order to infer palaeoclimatic change.

Documentary records can provide information relating to extreme climatic events. Intense and prolonged drought episodes have been recorded in Turkey in relation to their impacts on agriculture and society. Kuniholm (1990) discussed the historically recorded extreme drought in the Ankara province during AD 1873-1874, which resulted in the death of 20,000 people out of a population of 52,000. Documentary records can be useful for validating proxy reconstructions and evaluating the impacts of climate shifts on human populations.

2.7.3 Holocene climate variability

The Holocene period, which followed the cold/dry Younger Dryas, is characterised by a transition to warmer conditions and increased humidity. Numerous lake sediment studies, such as Harrison and Digerfeldt (1993), Roberts *et al.* (2001), Reed *et al.* (1999), Wick *et al.* (2003), and Jones *et al.* (2007), based in the EM, have identified wet conditions during the early Holocene, associated with high lake levels, followed by drier climate throughout the late Holocene (since ~5000–4000 yr BP). For instance, higher diatom-inferred conductivity, more positive oxygen isotope values, and changes in core lithology were identified in lake sediment from the Konya Basin (central Turkey) by Reed *et al.* (1999) during the late Holocene. Kashima (2003) also identified higher diatom-inferred salinity during the late Holocene in a record from the Konya Basin. Similarly, more positive oxygen isotope values were recognised during this period in Eski Acıgöl (central Turkey) by Roberts *et al.* (2001) and Jones *et al.* (2007), which indicate a transition to a more arid climatic regime.

Rossignol-Strick (1993) reviewed a number of low-resolution pollen records from the EM and recognised a period of rising oak abundance at the beginning of the Holocene, associated with increased temperatures and moisture. The vegetation record was recognised as reflecting increasing human interference throughout the most recent 5000 years. According to Wick *et al.* (2003), based on a pollen multiproxy lake study in eastern Turkey, the impact of human land use has intensified during the most recent 600 years.

Several studies have highlighted the frequency of drought events in the EM throughout the Holocene. For example, Staubwasser and Weiss (2006) identified dry periods

around 8,200, 5,200 and 4,200 yr BP. Many climate events have been marked by sudden changes in climate. For example, Jones *et al.*, (2006) identified dry periods (AD 300-500 and 1400-1950) and wetter intervals (AD 560-750 and 1000-1350), in sediment from Nar Gölü crater lake, associated with rapid shifts in oxygen isotope values. In a Turkish tree-ring record, Touchan *et al.* (2003; 2007) identified humid episodes ~AD 1518 and 1587 and a particularly dry period from AD 1195 to 1264. Akkemik and Aras (2005) reconstructed April to August precipitation from tree-rings in south-central Turkey for the period AD 1689-2000. A number of drought years and wetter intervals were identified. Additionally, Sarris *et al.* (2007) recognised a recent drying trend in the EM based on tree growth and precipitation data from Samos Island (SW Turkey) and highlighted that this pattern has been more pronounced since the summer of AD 2000. Therefore proxies that permit high-resolution studies and allow reliable dating control, such as tree-rings, can provide detailed information about recent climate change and can reveal short-term shifts in conditions. Diatom populations alter throughout the course of a year and are sensitive to a range of limnological factors. Diatoms preserved within annually laminated lake sediments have not been utilised to their full potential as indicators of Holocene climate change in Turkey.

2.8 Summary

The EM has a varied climate regime, which is influenced by a number of regional and global factors. The region also has a complex climate history and provides an interesting link between neighbouring continents. Turkey's extensive collection of lakes provide a useful resource for studying climate change. In order to quantify current and future anthropogenic influence on climate, the last 2000 years are of particular interest, particularly in relation to the present and pre-industrial era (Luterbacher *et al.*, 2006). In

light of recent climate anomalies, the late Holocene is a particularly important time period, which requires further research. This presents a need for more quantitative proxy climate reconstructions concentrating on recent centuries. Lake diatoms have proven to be a powerful tool to reconstruct palaeoclimate. Annually-varved lake sediments allow high-resolution sampling and calibration with instrumental meteorological records. The lack of high-resolution EM late Holocene climate reconstructions highlights the need for further research to focus on recent millennia and utilise proxies that permit high-resolution research.

Chapter 3

Methodology

3.0 Introduction

This chapter includes a discussion of site selection criteria and describes the field and laboratory procedures followed for the contemporary and palaeo-limnological analysis of the Nar Gölü and Kratergöl diatom assemblages.

3.1 Site selection

Turkey was identified as a suitable location to research Eastern Mediterranean palaeoclimate, due to the availability of natural palaeoenvironmental archives and the fact that this area provides a climatic link between Europe and Asia. During the late 1990s, a number of lakes in the central Anatolia region were identified via a regional survey as potential useful indicators of environmental change (Roberts *et al.* unpublished). Following this, between 1999 and 2002, core sequences were collected from various lakes in Anatolia and analyses undertaken. Within this project, two extant lakes were identified as suitable sites to investigate palaeoenvironmental change through diatom analysis in order to obtain information concerning palaeoclimatic variability. Nar Gölü (Nar lake) (Figure 3.1) is a stratified, closed-basin crater-lake that provides a high-resolution record of environmental change due to the annually-laminated nature of the sediments. A reliable chronology has been established for the Nar sediment sequence and pollen (England *et al.*, 2008) and oxygen isotope (Jones *et al.*, 2005, 2006) records have previously been derived from the sediment archive; this will allow multiproxy comparisons with the diatom record. A second closed basin, Kratergöl (Crater-lake), located in the same climatological region as Nar Gölü, was

chosen as a comparison site. However, no previous palaeoenvironmental research has been carried out for this site.



Figure 3.1 Map of Turkey highlighting the location of lake sites Nar Gölü and Kratergöl (blue circles) and meteorological stations located at Nevşehir and Ankara (black circles).

Volcanic crater-lakes (maars) can offer an excellent resource for studying palaeoclimatic change. Lake sediments are likely to experience limited disturbance in this kind of system. This suggests that Nar and Kratergöl may provide a detailed, uninterrupted record of past environmental change. Analysis of multiple lake sites permits reconstruction of regional climate variability and changes in the palaeo-records can be attributed to catchment or climate-related factors.

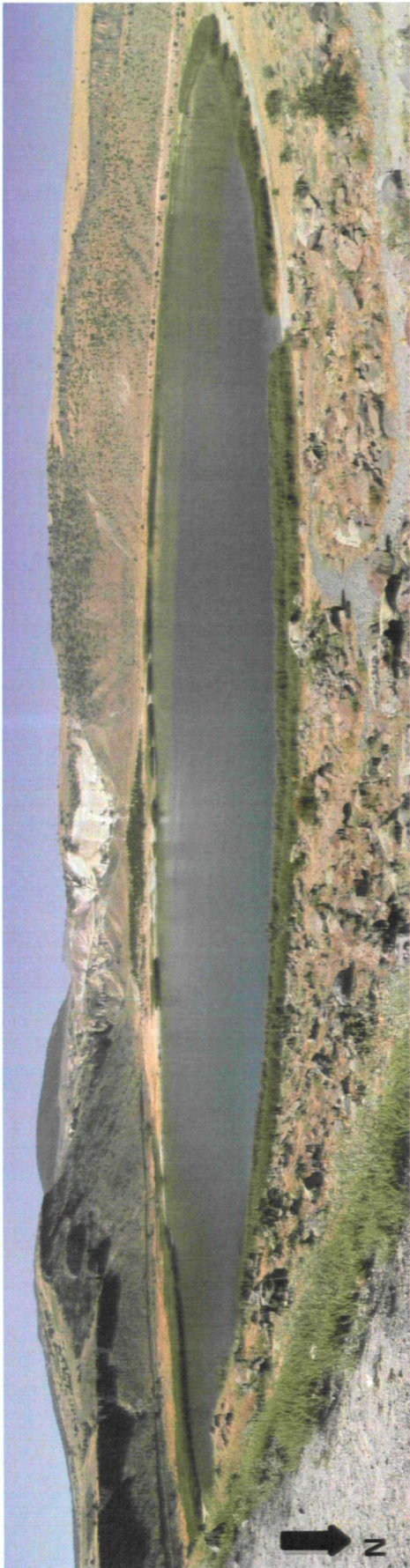


Plate 3.1 Nar Gölü photographed facing south.



Plate 3.2 Kratergöl photographed facing north.



Plate 3.3 Aerial view of Nar Gölü (Google Earth, 2007).



Plate 3.4 Nar Gölü catchment facing south west (Google Earth, 2007).

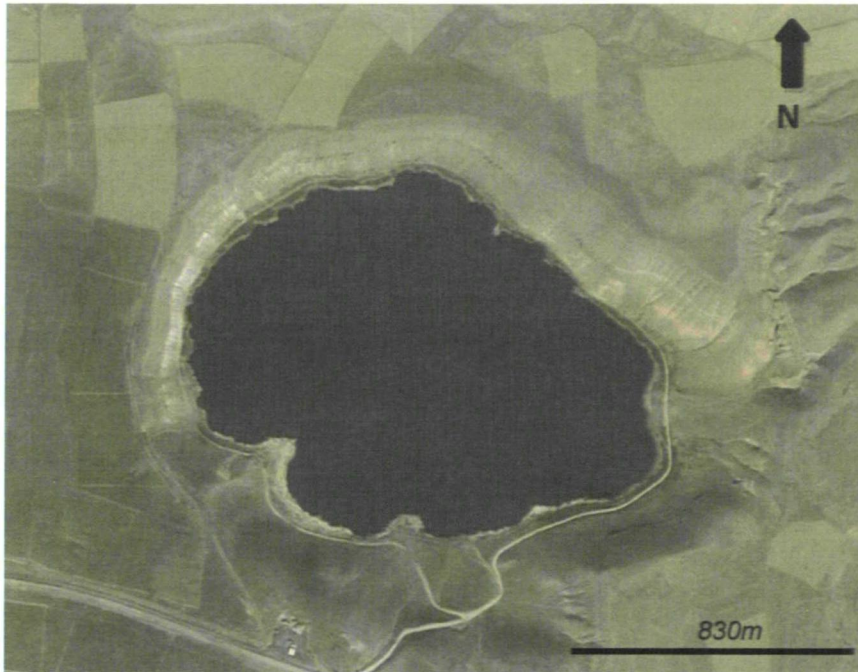


Plate 3.5 Aerial view of Kratergöl (Google Earth, 2007).

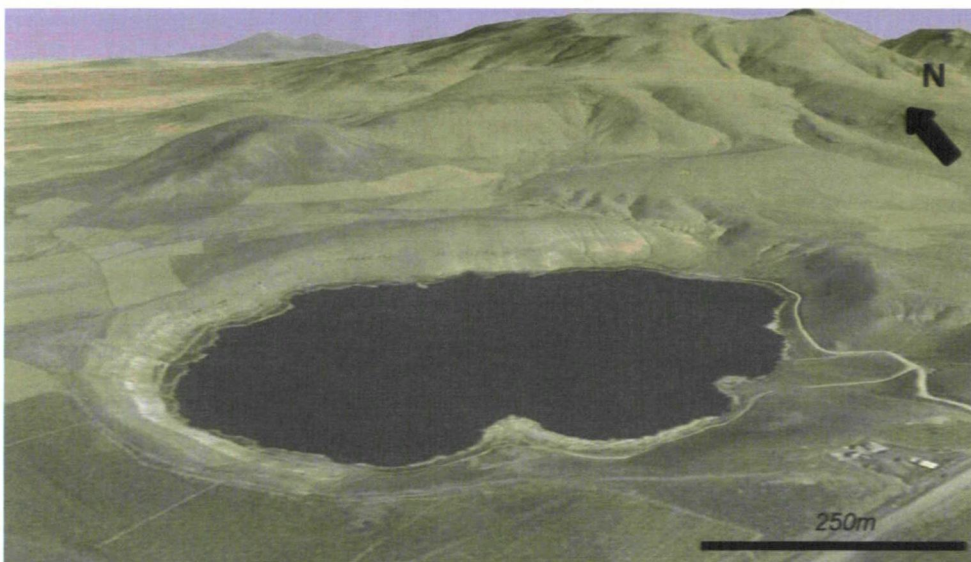


Plate 3.6 Kratergöl catchment facing north east (Google Earth, 2007).

Nar Gölü and Kratergöl are both located at considerable height above sea level (Table 3.1) and at a similar distance from surrounding marine basins. Therefore similarities are likely to exist in the lakes' response characteristics to climatic variability. Türkeş (1996) identified that the distance to marine basins, elevation and the presence of mountain ranges are the most important features influencing spatial variability in Turkish

precipitation. Nar and Kratergöl were selected in order to compare two sequences from the same climate region.

Site	Lake area (m ²)	Lake volume (m ³)	Catchment area (m ²)	Residence time (yrs)	Elevation (m above sea level)	Water depth (m)
Nar Gölü	5.6x10 ⁵	7.7x10 ⁶	2.4x10 ⁶	8-11 yrs	1363	26m (2001) 22.6 (2008)
Kratergöl	1.4x10 ⁶	7.0x10 ⁷	3.0x10 ⁶	-	950	76.5 (Dumont, 1981)

Table 3.1 Nar Gölü and Kratergöl lake characteristics. Including data from Jones (2004), England (2006) and Dumont (1981).

The sediment profiles from Nar and Kratergöl provide records corresponding to the late Holocene period. These sequences provide potential for high-resolution analysis of relatively recent climate variability. Dissimilarities exist in the lake sedimentology of the sites. The Nar record is annually-laminated while Kratergöl sediments include coarse-grained facies that may relate to within-lake mass movements of sediments. The different lake sedimentation regimes permitted a comparison of the suitability of different sites for palaeoecological research. Preliminary investigations revealed that diatom preservation is very good within the lake sediments of Nar Gölü and Kratergöl. Therefore an opportunity was presented for analyses leading to the reconstruction of palaeo-conductivity and climate.

3.2 Fieldwork methods

Modern lake samples were collected from Nar and Kratergöl between 2006 and 2008, in order to study the lake's contemporary diatom ecology and add to an archive of recent water chemistry recordings. Core material was collected in 2006 for palaeoecological analysis and combined with archived sediment sequences collected between 1999 and 2002.

3.2.1 Diatom sampling

Diatoms inhabit various niches within lake environments. Sampling living diatoms allows understanding of the relationship between modern communities, water chemistry and fossil assemblages. A number of lake sample locations were chosen to represent different environments and provide information regarding diatom species habitat preferences, taphonomy and preservation. During summer 2006-2008, Nar Gölü and Kratergöl macrophyte material, bottom mud and surface gravel was sampled and plankton was collected with the use of a plankton-net for diatom analysis. Samples were stored in polythene bags or plastic bottles and refrigerated on return from the field. Additionally, modern plant, gravel/pebble and bottom mud diatom samples were collected from Kratergöl by Barker *et al.* during summer 1992. Ideally diatom samples should be collected during various seasons to provide a complete picture of the community (e.g. Marchetto and Musazzi, 2001). However, due to fieldwork limitations, this was not possible. Sediment traps collect lake material throughout the course of a year and offered an additional method for studying the modern diatom assemblage.

3.2.2 Seston sediment traps

Sediment traps were used to study the diatom community at Nar Gölü, to examine seasonality in species composition in order to understand the modern environment and to aid interpretation of the palaeo-diatom record. Lake sediment traps at Nar Gölü were collected and replaced annually (2001-2007) and have been subject to diatom analysis. The traps were suspended on ropes at different depths within the water column (Figure 3.2). Floats were connected to the traps and the ropes were anchored to the lake bed to maintain position (Jones, 2004). Individual traps comprised an inner Perspex tube, encased within plastic guttering, with a funnel inserted to allow sediment to collect in the tube. Plate 3.7 includes an example of a retrieved intact sediment trap with visible colour changes associated with seasonality.

In summer 2006, two traps were installed at two points in the lake, at depths of 5 m and 15 m below the water surface (Figure 3.3). Water depth was measured at site A as 20.7 m and at site B as 22.5 m using a Garmin Fish Finder. The deepest part of the lake was selected, as sedimentation is expected to be most consistent here. In summer 2006, one sediment trap was retrieved intact (installed in July 2005) from the lake. Two sediment traps were collected from Nar in summer 2007. However, mixing of these samples had occurred and stratigraphic integrity was lost. Sediment traps installed in 2007 were unfortunately lost during the course of the year.

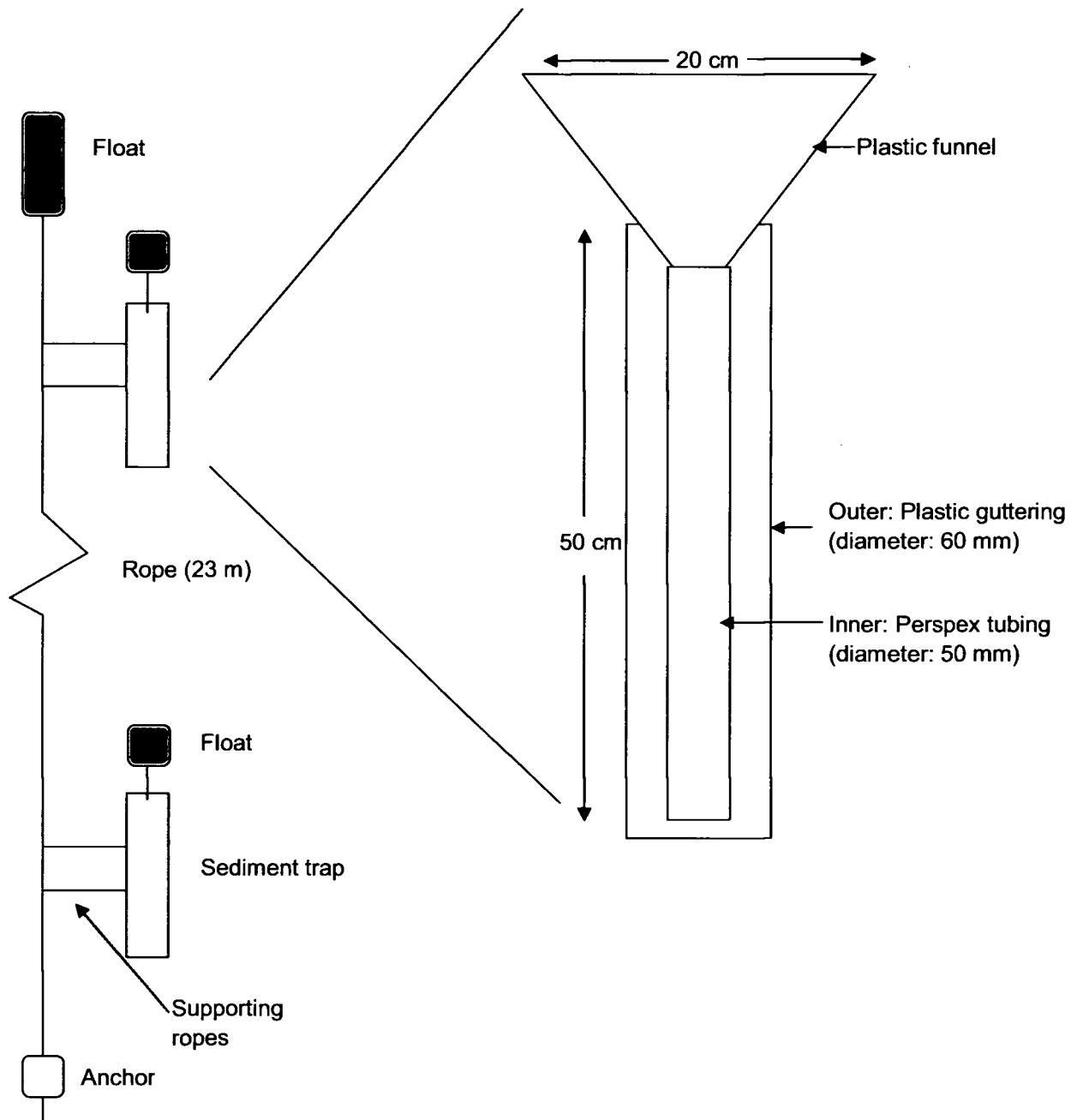


Figure 3.2 Diagram of sediment traps installed at Nar Gölü (diagram not to scale).

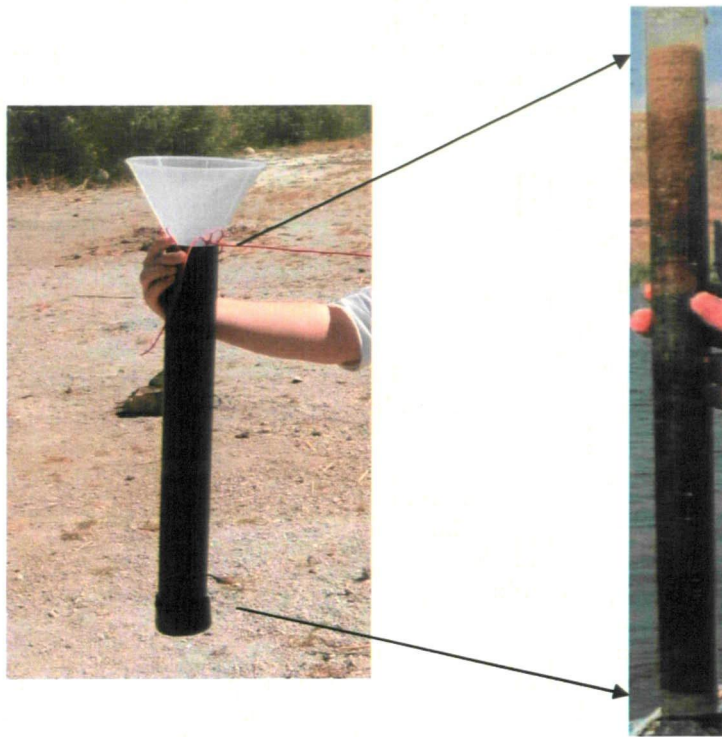


Plate 3.7 Photograph of a sediment trap (2006) and a Perspex tube containing lake sediment collected throughout the course of a year (Jones, 2004).

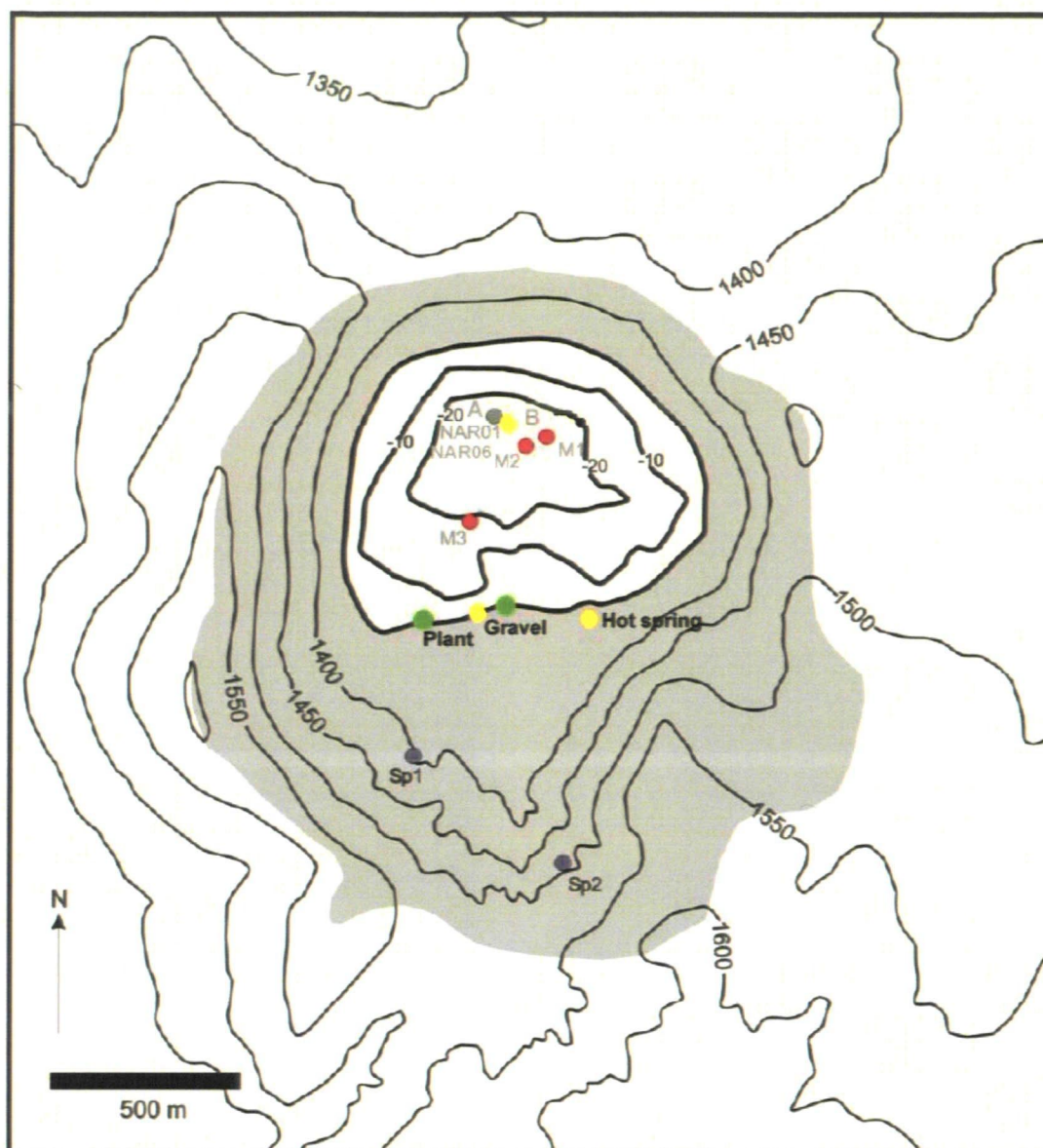


Figure 3.3 Nar Gölü catchment (shaded area) and sampling locations. 2001 coring site: NAR01 (grey circle); 2002 coring sites: M1, M2 and M3 (NAR02) (red circles) (Jones, 2004). 2006 sediment trap A installed in vicinity of NAR01 and sediment trap B installed near M1. 2006 and 2008 gravel and plant samples collected at southwest margin (green circles). NAR06 Glew core collected in vicinity of NAR01 sampling point. Yellow circles illustrate 2006 and 2008 water sample collection points.

3.2.3 Water sampling

In order to understand the modern environmental conditions of the lake, it is necessary to monitor water chemistry. Temperature, pH, and conductivity readings were taken at Nar Gölü during summer 2006 and 2008 and added to a database of previous measurements collected between 1999 and 2005. Readings were taken at various points in and around the lake, using a K&M 7002 pH measuring instrument and a 330I conductivity meter. Locations were chosen in order to compare various lake habitats and analyse stratification of water layers. The specific water chemistry of Nar was analysed using samples collected in 1999 and 2008, through laboratory titration methods (Golterman *et al.*, 1978). Samples from Kratergöl were analysed in 1999 by Reed *et al.* using similar methods.

3.2.4 Glew core collection

Studying lake core material allows analysis of temporal changes in the diatom population. A short core was collected from Nar in summer 2006 (NAR06) and correlated with a master core sequence retrieved between 1999 and 2002 (NAR01/02). Nar lake depth was measured using a Garmin Fish Finder and confirmed using pre-measured rope. A suitable site for core retrieval was selected (Figure 3.3) and a 36 cm core section (NAR06) was collected using a messenger-operated gravity corer (Glew *et al.*, 2001) during summer 2006 (Plate 3.8). The coring device was dropped into the water in order to penetrate and retrieve sediment from the lake bed. A metal messenger was dispatched down the rope to seal material in the tube and allow the sediment water interface to be retrieved intact. The device was then pulled to the surface and lake bottom water was removed with a pipette. Oasis foam was inserted to absorb water and

prevent mixing. Bungs were then placed into the ends of the tube, which was securely taped for transport.



Plate 3.8 Messenger-operated gravity corer (Glew *et al.*, 2001) containing the NAR06 core section (summer, 2006).

3.2.5 Archived lake cores

Between 1999 and 2002, a number of lake cores were collected by Roberts *et al.* from Nar Gölü and Kratergöl, using lake bed morphology to select suitable sites (Figure 3.3). The deepest part of the lake was chosen to represent the longest and least disturbed part of the record (England, 2006). A combination of Livingstone (Livingstone, 1955), Mackereth (Mackereth, 1969) and Glew (Glew, 1991) corers were used to retrieve a 376 cm sequence from Nar Gölü (NAR01/02) (Chapter 5: Figure 5.8). Cores were extruded, cut into half lengths and stored in guttering at 4°C, (Jones, 2004; England, 2006). A short core of 59 cm was collected from the deepest part of Kratergöl (ACM99) by Roberts *et al.* during summer 1999, using a Mackereth corer (Figure 3.4).

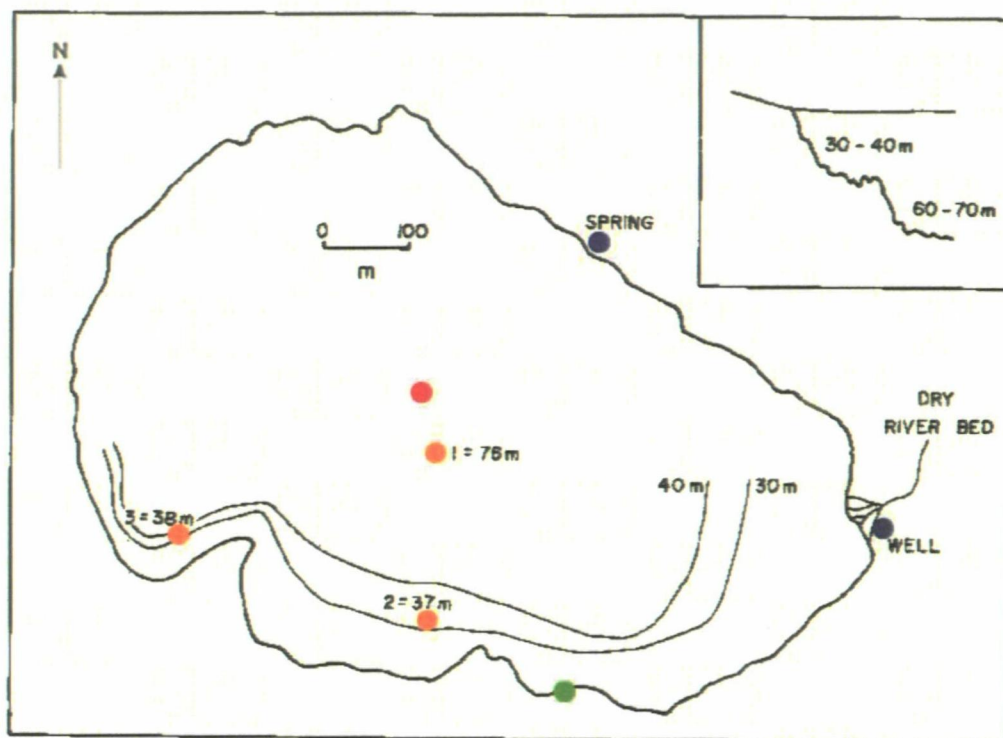


Figure 3.4 Diagram of Kratergöl highlighting the bathymetry of the southern bays and water depth (orange circles), a spring and well (blue circles) and a dry river bed (Dumont, 1981). 1999 and 2008 sampling locations (red circle highlights approximate location of ACM99 core retrieval site and green circle represents 2008 diatom sampling location).

Core samplers were chosen to suit the sediment type and retrieval requirements. The Mackereth is a pneumatically driven piston corer designed to collect long, in this case 1 or 3 m, uninterrupted sediment and was chosen for this purpose (Glew *et al.*, 2001). A messenger-operated gravity Glew corer was chosen to retrieve the most recent sediment, as this allows the sediment-water interface to be recovered. A Livingstone corer was chosen to retrieve deeper sediment, as this device allows undisturbed penetration of more compact material (Glew *et al.*, 2001). These devices allow sediment profiles of similar diameter to be retrieved from differing depths and sections to be stratigraphically correlated with one another.

3.2.6 Bathymetry

Research at Nar Gölü, which took place between 1999 and 2002, involved studying the lake bathymetry (Figure 3.3). A depiction of lake-bed morphology was constructed through taking depth measurements using a Garmin Fish Finder along a range of transects across the lake. This information allowed the deepest and flattest part of the lake to be selected for coring and calculations were made regarding lake volume and hydrology (Jones, 2004). Nar Gölü margins are shallower (~10 m) in relation to the central area (~20 m). Kratergöl bathymetry was studied by Dumont (1981) (Figure 3.4). A water depth of 76 m was identified with two sub-surface cliffs in the southern bays. The depth of the north section of the lake was not analysed. Therefore a complete picture of Kratergöl bathymetry is not available.

3.3 Laboratory methods

3.3.1 Nar Gölü core chronology

A master sequence was compiled from the various Nar core sections with the use of varve chronological techniques (Lamoureux, 2001). This involved counting varves, comparing lamination patterns between core sections and radioisotope dating. In order to establish a varve chronology for Nar, two people counted laminations within 6 cm sections to reach agreed lamina counts for the 1999-2002 core sections (NAR01/02) (Jones, 2004). The same method was applied to the NAR06 section. Prior to archiving in cold stores, pins were inserted into cores to correspond with specific lamination counts and allow future analyses to follow the established chronology. Radioactive isotopes can be used as reliable dating tools. ^{210}Pb and ^{137}Cs analysis of the top 50 cm of the Nar core sequence and sediment trap material revealed that varve couplets are

deposited annually (Jones, 2004). Dating of the Nar sediment record was carried out at the University of Liverpool Environmental Radioactivity Laboratory using direct gamma assay.

3.3.2 *Kratergöl chronology*

In order to interpret palaeoecological archives when varves are not present, accurate sediment chronologies are required (Appleby, 2001). Sediment samples from Kratergöl were analysed for ^{210}Pb , ^{137}Cs and ^{241}Am concentration at the University of Plymouth Consolidated Radio-isotope Facility (CoRiF) using a planar gamma spectrometer. Samples were freeze-dried, homogenised and stored in sealed containers for three weeks to allow ^{214}Pb to reach radioactive equilibration. The detectors were calibrated using samples of known radioactivity. ^{210}Pb was determined via its gamma emissions at 46.5 keV, ^{226}Ra by the 295 keV and 352 keV γ -rays emitted by its daughter isotope ^{214}Pb and ^{137}Cs was measured by its emissions at 662 keV (Appleby, 2001). Additionally, the presence of metals in sediments can be used as a dating tool. For example, high concentration of total lead is associated with intensification of industrial processes. For metal analysis, sediment samples were ground and sieved. The fraction below 150 μm was digested using concentrated nitric acid and analyses were carried out at the University of Plymouth using a Varian 725ES ICP/OES.

3.3.3 *Core sub-sampling*

The NAR06 core was extruded in the laboratory and cut in half lengthways using cheese wire to reveal the stratigraphy. The two sections were transferred into lengths of plastic half guttering covered with cling film. The exposed core half sections were then cleaned, photographed, described, and laminations were counted. Sections were labelled

and stored in plastic bags below 4°C. A similar procedure was followed for the 1999-2002 Nar cores. The Kratergöl core (ACM99) was subsampled on retrieval into 2 cm sections and stored below 4°C in polythene bags for future analyses.

High-resolution subsamples were obtained from the archived NAR01/02 core sequence and NAR06 section for diatom analysis. Long-term storage schemes must take into account the avoidance of warm temperatures, light and loss of moisture from the core (Glew *et al.*, 2001). There are many issues to consider when using archived sediment material. For example, problems associated with sediment contamination, drying and shrinkage. It was evident that NAR01/02 core shrinkage had occurred due to water loss; however, the stratigraphic profiles remained intact. When the material was fresh, NAR01/02 sections were described, photographed and pinned, according to specific lamination counts (Jones, 2004). Therefore it was possible for sampling to follow the previously established chronology.

3.3.4 Kratergöl sediment analysis

The Kratergöl core sequence was described according to grain size, material type and colour. Carbon content and particle size analysis provides information about processes that have occurred in the lake and improves understanding of radiometric and palaeoecological data. The organic carbon content of lake sediment can be used as a proxy for productivity and the quantity of inorganic carbon gives a measure of the amount of carbonate in the system. Samples from Kratergöl were analysed for carbon content using a Smimadzu TOC-500 carbon analyser in the School of Geography (University of Plymouth). In order to measure total carbon (TC) and inorganic carbon (IC), samples were combusted at 1000°C and the amount of CO₂ produced was

measured. The quantity of organic carbon was calculated by subtracting IC from TC. Samples were analysed using the high-temperature catalytic oxidation method in a Skalar Primacs carbon analyser.

Knowledge of the particle size distribution of lake sediment allows inferences to be made concerning the nature of the parent material, sediment transport and processes that have occurred in the lake. A laser particle size analyser was used to evaluate changes in the stratigraphy of the Kratergöl sediment in the School of Geography (University of Plymouth). Standard procedures were followed and three subsamples for the range 2000–4 μm and one for the 80–0.1 μm range were analysed. Sediment was heated in hydrogen peroxide to remove organics and remaining material was sieved to eliminate the >2 mm fraction prior to analysis. The percentage of sand, silt and clay was determined for each sample depending on the particle size distribution.

3.3.5 Diatom subsampling

Subsamples for diatom analysis were obtained by cutting fragments of laminations from Nar core half sections using a scalpel. Three varve year (VY) samples, of approximately 0.5 cm^3 , were taken at ten year intervals for the entire 1720 VY Nar master sequence (NAR01/02) (AD 280–2001). A decadal sampling strategy was chosen to match the hydrological response time of the lake system (8–11 year residence time). A three VY sampling strategy was adopted to reduce ‘noise’ in the diatom record and for practical reasons involving subsampling. For example, when sampling deeper, highly-compacted sediments, it can be difficult to select individual lamina and it is possible that contamination may occur between successive laminations. Annual subsamples, representing the most recent 80 VY (AD 1926–2006), were taken from the NAR06 core.

The fresh, near-surface sediment of the NAR06 core was suitable for sampling individual lamina. An annual strategy was adopted for comparison with twelve-monthly meteorological records matching this time period.

Subsampling the Kratergöl core (ACM99) involved taking a representative portion of approximately 1 g from each polythene bag containing a 2 cm sediment section. Dating and sediment analysis methods were employed to establish the temporal resolution of the 2 cm samples.

3.3.6 Sediment traps and modern samples

Sediment material was extruded from the Perspex tubing of the seston traps and sliced into 1 cm sections for storage in polythene bags. Subsamples of approximately 1 g were taken for diatom analysis at 2 and 4 cm resolution, depending on the length of the section. This sampling method was chosen to reveal seasonality in the diatom flora. Appropriate subsamples of approximately 1 g or 2 ml were taken from the modern lake macrophyte, gravel, plankton and bottom mud samples for diatom analysis.

3.3.7 Diatom analysis

A diatom analysis preparation procedure was selected to suit the sediment type, remove unwanted material and allow preservation of valves (Figure 3.5). The process followed standard procedures adapted from Battarbee (1986) and Battarbee *et al.* (2001).

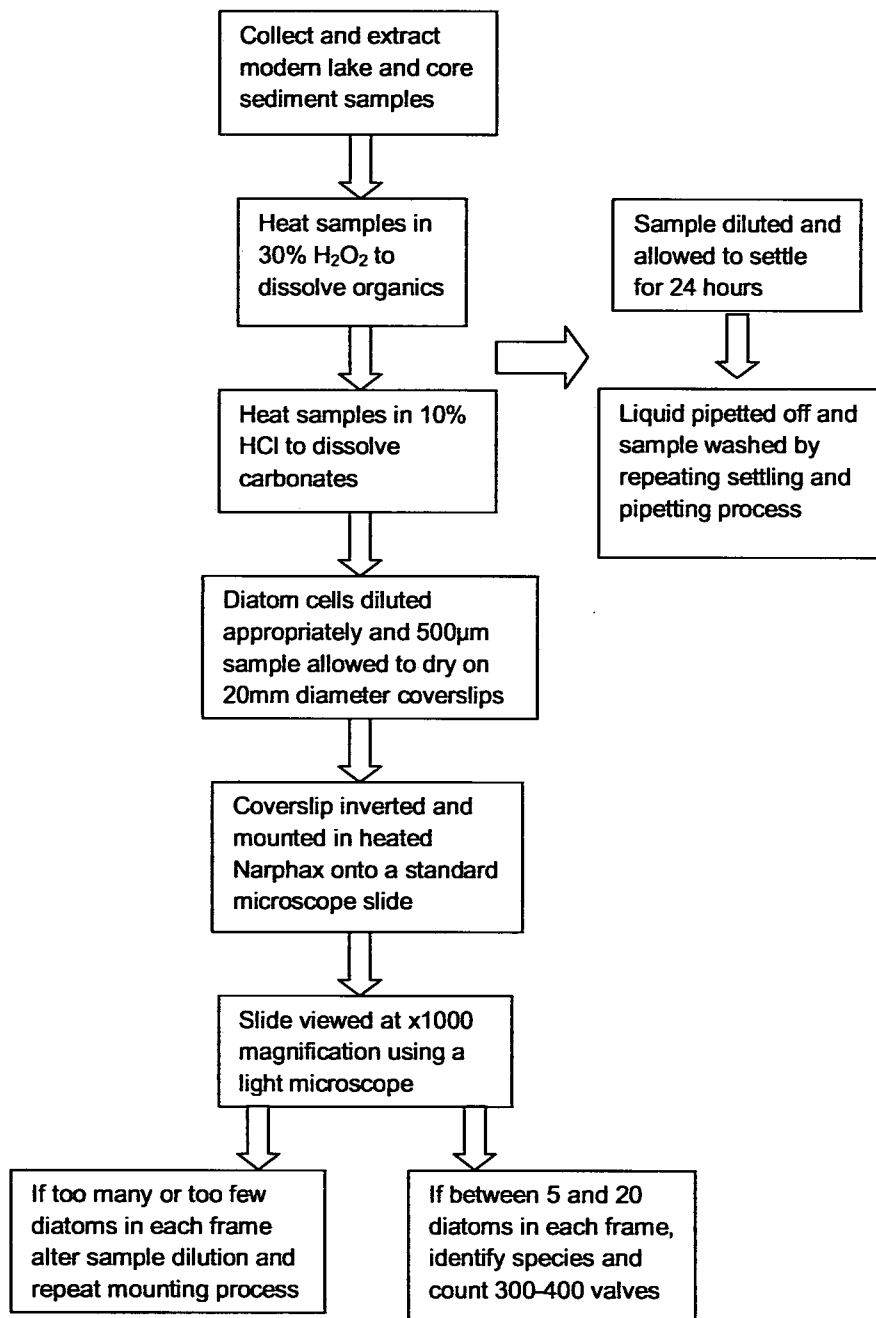


Figure 3.5 Flow diagram illustrating the preparation procedure for diatom analysis of lake sediments (adapted from Battarbee *et al.* 2001).

3.3.8 Light microscopy (LM)

Prepared diatom slides were viewed using an Olympus BX50 LM at x1000 magnification (oil immersion). 300-400 diatom valves were counted in transects on each slide and the number of viewing frames was recorded. Battarbee *et al.* (2001) recommend a count of between 300 and 600 valves. Tests were conducted when counting Nar and Kratergöl diatoms to ensure that the valve number was appropriate to represent the species assemblage. The results revealed that new species were not likely to be encountered after the first 300 valves were identified. A consistent counting method was developed and adapted to suit different species. For example, a number of long, thin diatoms were often broken, e.g. *Synedra acus*; therefore individual ends were counted and the total divided by two. Only the central area of species such as *Navicula oblonga* and *Cymbella cistula*, was sometimes preserved; therefore centres were counted and fragments ignored. LM analysis was supported with the use of an eyepiece reticule for measuring diatoms, a Leica DFC280 microcam and analySIS computer software (1986-2002) for photographing diatoms.

3.3.9 Scanning electron microscopy (SEM)

SEM allows higher precision taxonomic classification through the identification of structures not visible with a LM. For SEM analysis, a small drop of prepared diatom sample in suspension was evaporated directly on an aluminium stub. Samples were then coated with gold ready for inspection (Battarbee *et al.*, 2001). Photomicrographs were taken at ~x10,000 magnification using a JEOL 5600 low vacuum SEM at the University of Plymouth Electron Microscopy Center and a Phillips XL30 field emission SEM at the Natural History Museum (London).

3.3.10 *Diatom identification and taxonomy*

Diatom species identification is principally made on the basis of frustule size, shape, raphe presence and striae arrangement (Battarbee *et al.*, 2001). Literature sources for species identification primarily included Krammer and Lange-Bertalot (1991; 1997; 2000) and the European Diatom Database (Juggins, 2008). Numerous additional sources were consulted including Round *et al.* (1992), Gasse (1986), Hartley (1996), Cox (1996), Hustedt and Jensen (1985), Germain (1981), Barber and Haworth (1994) and journal articles from *Diatom Research* (Serieyssol and Kociolek, 1985-2008). A number of diatomists assisted with identification through responding to posted images on the diatom list server (Sweets, 1995-2008), through discussions at the annual British Diatomists' Meeting and support with studying literature at the Natural History Museum (London).

3.3.11 *NAR01/02 core thin sections*

Core thin sections for the most recent ~900 VY were prepared from the NAR01/02 sequence in 2002 by Elizabeth Hunt (University of Plymouth). Lengths of core sections comprising 17 lamina were impregnated in epoxy resin, glued onto microscope slides, ground to 30 µm thickness and enclosed with a coverslip (England, 2006). Thin sections allowed individual varves to be analysed *in situ* and the diatom assemblage to be observed without disturbance to the sediment. Sections were analysed and species identified using an Olympus BX50 LM. Organic brown, white carbonate, grey clastic, and diatom bloom layers were measured using an eyepiece reticule at x40 and x400 magnification. Measurements were taken, in order to infer lake productivity, identify patterns in the blooms of different diatom species and make comparisons with traditionally prepared diatom material. Due to the presence of additional organic

material, it was not possible to identify the majority of diatom species on the thin section slides. However, distinct single species diatom bloom layers appeared frequently, which provided insights into diatom community seasonality.

3.4 Data presentation and analysis

3.4.1 Presentation of stratigraphic data

Diatom species percentages were calculated using Excel (Microsoft, 2007) and plotted on stratigraphic diagrams using C2 data analysis software (Juggins, 2003) in order to observe temporal change in the assemblage composition. A suitable collection of dominant taxa were selected for presentation based on species relative percentages in the population. Species representing at least 5% and 3% of the population in at least one sample were identified as representing >90% of the total population at Nar and Kratergöl respectively. Therefore all species above these values have been included in stratigraphic diagrams.

Hierarchical cluster analysis arranges samples into groups based on their similarity using a hierarchy to illustrate the relationship between the different groups (Kovach, 1995). This method was employed in order to reveal zones in the sequence and identify temporal change in the assemblage. Stratigraphically constrained cluster analysis was performed using TILIA (TG View: version 2.0.2) (Grimm, 2004) and sample groups were plotted as zones on stratigraphic diagrams.

3.4.2 Data transformation and correlation analysis

Multivariate data are often not normally distributed and are therefore mathematically transformed in order to normalise data for easier analysis and reduce extreme variability

(Kovach, 1995). The logarithm transformation method is suitable for continuous data and was therefore selected to transform different features of the diatom data, such as reconstructed conductivity, diatom biovolume and concentration. Species biovolume data were also power transformed in order to compare the extreme size variability of different species.

Correlation analysis was employed to assess whether relationships exist between different features of the diatom assemblage, meteorological variables and to explore similarities with other proxy records from Nar Gölü. Pearson's correlation for parametric data is recognised as the most powerful technique in correlation analysis (Shaw and Wheeler, 2000) and is a suitable method for exploring relationships in continuous data with a true zero, such as percentages. Data were normalised using a \log_{10} transformation and the direction, strength and significance of relationships was signified by an r and p -value.

3.4.3 *Diatom concentration and biovolume*

Information regarding the concentration and biovolume of diatoms within a sediment sample aids interpretation of palaeoecological data. Diatom concentration varies in sediment cores as a result of numerous factors. This includes variability in diatom productivity, the efficiency of diatom transport to the sediment, dissolution of frustules and the rate of sediment accumulation (Battarbee *et al.*, 2001). Concentrations were determined by calculating the number of diatoms on a LM coverslip and using the sample dilution and volume to derive the number of diatoms per gram of wet sediment. The Nar sediment accumulation rate is almost linear; therefore data were plotted without accounting for changes in sedimentation rate.

Diatom species cell sizes often vary considerably. Consequently percentage and concentration data may be misleading (Wolfe, 2003). Therefore diatom data were converted to biovolume for comparison with percentage diagrams. Biovolume was calculated by measuring the dimensions of individual diatom species, calculating average width, length or diameter and using Biovol computer software (Kirschtel, 1996) to determine cell volume. Due to the extreme variation between species volumes, data were power or \log_{10} transformed using PC-ORD (McCune and Mefford, 1999) and Excel (Microsoft, 2007) for plotting and analysis. Total biovolume provides an estimation of diatom productivity and was calculated for each sample based on the sum of species biovolumes.

3.4.4 Diatom species diversity

Species richness was estimated for the modern and fossil diatom assemblages using Analytic Rarefaction software (version 1.3, Holland, 2003). Rarefaction estimates diversity given a specific cell count. This method is effective when total counts differ between samples, such as in the Nar assemblage when blooming species dominated the diatom population. This allowed species diversity throughout the last 1720 years to be analysed in terms of environmental change and in relation to the modern lake assemblage.

3.4.5 Diatom habitat preferences

Diatom species are frequently grouped according to their ecological preferences. For example, the ratio of planktonic to benthic species can be employed to infer past lake level. Decreased water level is likely to create more habitats for benthic taxa and higher

water depth will provide a larger niche for planktonic diatoms (Wolin and Duthie, 1999). Within this project, many modern diatom species were identified as inhabiting multiple lake habitats. For example, numerous planktonic species were also encountered in epiphytic environments. Therefore species were grouped and the percentage of benthic taxa was calculated in order to provide additional information regarding past ecological conditions.

3.4.6 Detrended Correspondence Analysis (DCA)

DCA (Hill and Gauch, 1980) is an indirect ordination method that involves classifying samples or species into groups on the basis of their similarity (Kent and Coker, 1992). This technique was used to plot modern and fossil lake diatom samples in ordination space using PC-ORD (McCune and Mefford, 1999). Sample similarity was analysed to infer patterns associated with environmental change. DCA was performed on percentage and biovolume data and results were displayed in ordination graphs and plotted on stratigraphic diagrams. DCA axis scores plotted against depth provide an estimate of species turnover (e.g. Barker *et al.*, 2003; Keatley *et al.*, 2006). Axes were selected for presentation based on the relative percentage of variability in the assemblage explained by each of the axes.

3.3.7 Transfer functions

Transfer functions use the relationship between individual diatom taxa and the environmental variable of interest (e.g. conductivity) to infer palaeoclimate from fossil assemblages (Battarbee *et al.*, 2001). Nar and Kratergöl palaeo-diatom data were applied to existing transfer function training sets provided by the European Diatom Database (Juggins, 2008) using C2 computer software version 1.3 (Juggins, 2003). This

involved uploading an appropriate training set, corresponding environmental data and the fossil dataset and running the transfer function in order to reconstruct palaeo-conductivity. The transfer function output provides reconstructed values on a \log_{10} scale; therefore values were subject to an antilog function to derive conductivity (μS^{-1}). Data were plotted on stratigraphic diagrams and patterns analysed. Inferences were then made concerning the relationship between conductivity and climate.

Nar Gölü and Kratergöl are not thought to have experienced extensive agriculture in their catchments throughout the late Holocene; however, surrounding areas are likely to have been influenced by human land use, particularly at Nar. Due to the fact that both lakes have circumneutral pH water and are concentrated closed-basins in a semi-arid region, conductivity is considered an important factor driving diatom assemblage change. Therefore palaeoenvironmental reconstructions were performed using diatom-conductivity training sets. Training sets were selected based on the percentage of fossil sample species represented in the modern data set, the number of sites in which these species were present and the model performance (r and RMSEP values). The r value provides a measure of the strength of the relationship between observed and expected values and the Root Mean Square Error of Prediction (RMSEP) indicates prediction errors. Combined datasets were identified as containing a greater number of matching analogue species in comparison with regional datasets. The combined salinity training set is a composite dataset comprising 387 modern samples collected from East Africa, North Africa, Spain and the Caspian region (Central Asia) between 1960 and 1996 (Juggins, 2008). Salinity varies between sites within the training set from a minimum of 133 and maximum of 333,021 $\mu\text{g}/\text{l}^{-1}$.

Weighted Averaging (WA) is a commonly employed model in diatom-conductivity reconstructions (e.g. Gasse *et al.*, 1995; 1997). Within this study, WA with inverse deshrinking gave the highest r and lowest RMSEP values and was therefore selected as the most suitable model. The Modern Analogue Technique (MAT) reduces the weighting of dominant species and is suitable when large modern datasets are available. The MAT was also employed to infer palaeo-conductivity and compared with the WA reconstruction. The reliability of the reconstruction was assessed using the MAT to evaluate how well the fossil samples match the modern training set (Birks, 1995, Laird *et al.*, 1998).

3.4.8 Sediment dating

Kratergöl radioisotopic data (^{210}Pb , ^{137}Cs , and ^{241}Am) were plotted on stratigraphic diagrams using C2 (Juggins, 2003). Interpretations were based on the changing activity of the radioisotopes with depth. Kratergöl dating was complicated by the varied lake sedimentation rate and the limited stratigraphic integrity of the core (Chapter 6: Section 6.3.2). The chronology of the NAR01/02 sequence was established using a composite model that best fits all of the radiometric data (Jones, 2004).

3.4.9 Meteorological data, climate indices and palaeoclimate records

Meteorological data have been recorded at various stations in Turkey throughout the last 80 years and were obtained from the Turkish State Meteorological Service. Instrumental records of temperature, humidity and precipitation were compared with the diatom records, in order to aid the use of palaeoecological data for reconstructing pre-instrumental climate variability (e.g. Laird *et al.*, 1996; 1998). High-resolution gridded meteorological data obtained from the University of East Anglia Climate Research Unit

(Mitchell and Jones, 2005) were also compared with the diatom records. These global records provide high-resolution grids of monthly climate data based on interpolated values for all regions in relation to data from surrounding stations. The relationship between meteorological data and the diatom records was explored using correlation analysis.

The ratio of precipitation to evaporation relates to lake conductivity and is thought to influence the diatom assemblage. Based on meteorological data, an aridity index (AI) was calculated (Türkeş, 2003) by dividing precipitation by evaporation ($AI=P/E$) (mm/yr). The equation is typically based on precipitation divided by potential evapotranspiration; however, as the lake catchments are sparsely vegetated, evaporation was used as an alternative. The temporal relationship between AI and the diatom assemblage was explored. Precipitation included total annual values recorded at Ankara meteorological station. Evaporation calculations were based on the relationship between air temperature, altitude, latitude, wind speed and dew point temperature recorded at Ankara and other stations in the vicinity of Nar Gölü (Jones, 2004). In addition to the aridity index, cumulative water balance was calculated by addition of cumulative deviation from mean P/E in order to account for moisture accumulated during previous years.

Climate indices, including North Atlantic Oscillation, North Sea-Caspian Pattern, Arctic Oscillation, Southern Oscillation and Asian Monsoon, have frequently been identified as important drivers of Turkish climate (e.g. Türkeş and Erlat, 2003; 2005; Kutiel and Türkeş, 2005; Alpert *et al.*, 2005). These data were downloaded from various internet sources (Chapter 8) and correlated with the diatom records in order to analyse whether

atmospheric circulation patterns influence the assemblages. Additionally, previous palaeoenvironmental reconstructions were downloaded from various online resources for comparison with the Nar and Kratergöl records (Chapter 8).

3.5 Summary

The methodology was developed to suit the aims of the research and achieve a number of objectives. Lake sites were selected on the basis of their comparability and suitability to palaeoclimate research. Field methods allowed a representative sample of the modern diatom communities to be analysed and temporal change throughout the last 1720 years to be evaluated. Laboratory procedures were adapted and developed to suit the different sediment types. Data analysis followed standard methods and involved exploring a number of additional avenues, such as core thin sections, to derive palaeoenvironmental information from the diatom assemblages.

Chapter 4

Site Descriptions

4.0 Introduction

This chapter includes a description of generic features of the study site region and provides information about each of the lakes in relation to their catchment hydrology, water chemistry, geology and vegetation.

4.1 Regional characteristics

4.1.1 Central Anatolian climate

The climate of central Turkey is continental, semi-arid, sub-humid and dry (Kutiel and Türkeş, 2005). Nar Gölü and Kratergöl are located in the Continental Central Anatolian precipitation region (Türkeş, 1998). This continental setting limits the buffering effect of marine basins against climate extremes. Combined with the high elevation of Cappadocia, this leads to extreme temperature variations between summer and winter. Average Nevşehir summer (JJA) and winter (DJF) temperatures are 20.3°C and 0.4°C respectively. Figures 4.1 and 4.2 illustrate average monthly temperature and precipitation data recorded at Ankara (1927-2007) and Nevşehir (1967-2007) meteorological stations. The records reveal similar temperature and precipitation regimes in these different regions. Extremes of temperature are illustrated by the August high of 33°C and January low of -10°C at Nevşehir during this period. Average total precipitation at Ankara is 375 mm/year and at Nevşehir, this figure is 407 mm/year. Highest rainfall occurs between December and May, with an average of 55.6 mm at

Nevşehir in May and 6.1 mm in August. Humidity is highly related to temperature, with higher readings during colder periods.

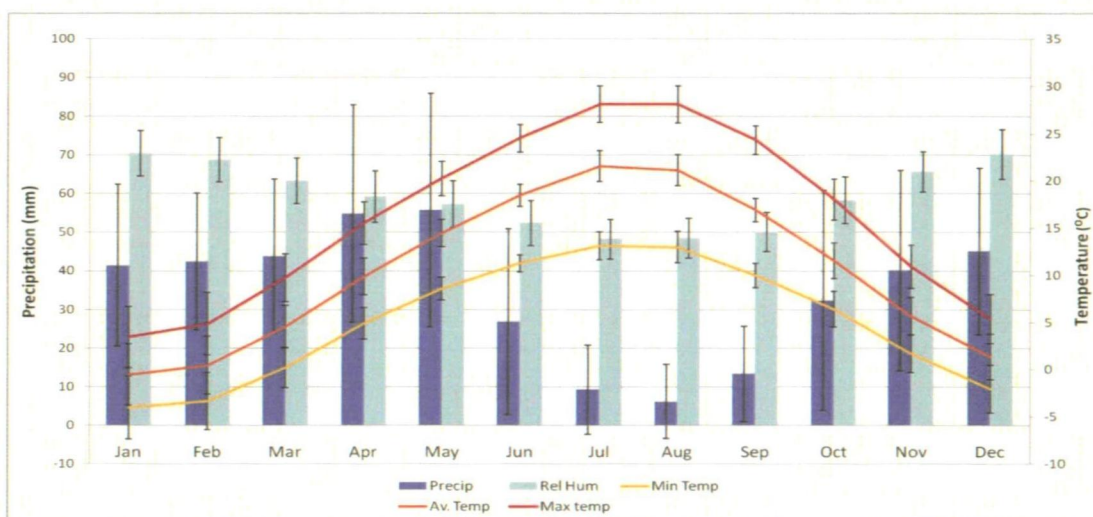


Figure 4.1 1967-2007 mean climate data (relative humidity, total precipitation and minimum, average and maximum temperature) from Nevşehir meteorological station (Turkey) (data from Turkish State Meteorological Service).

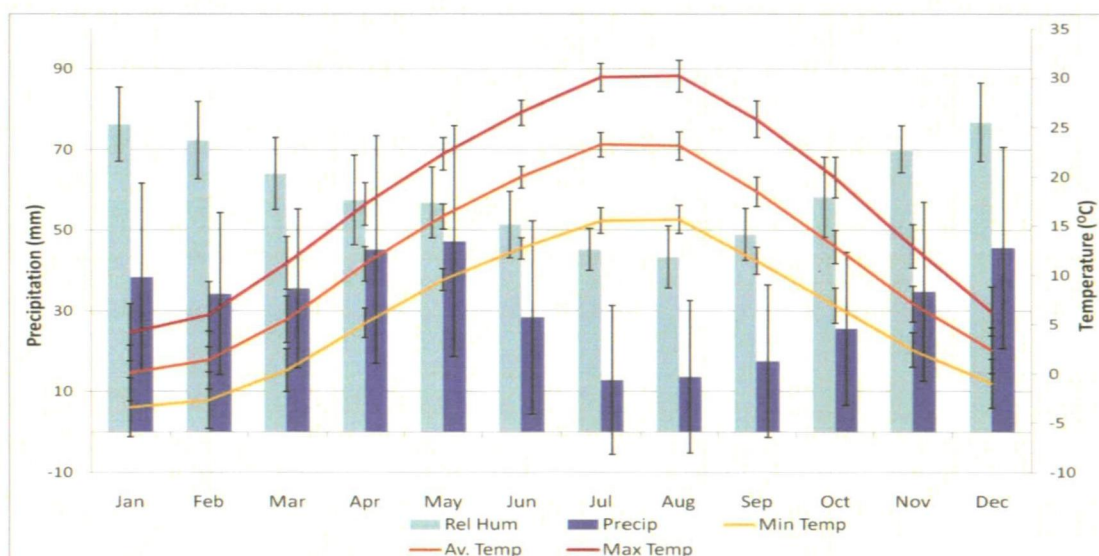


Figure 4.2 1927-2007 mean climate data (relative humidity, total precipitation and minimum, average and maximum temperature) from Ankara meteorological station (Turkey) (data from Turkish State Meteorological Service).

4.1.2 Geological setting

The Central Anatolian Volcanic Province (CAVP) or Cappadocian volcanic province (Figure 4.3) comprises several eruptive centres and covers the area between Tuz Gölü, the Konya Plain and the Taurus Mountains. Cappadocian volcanism is of basaltic type and relatively young (<35 ka) (Kuzucuoğlu *et al.*, 1998). This extensive volcanic region of Neogene-Quaternary age extends between Aksaray, Niğde, Nevşehir and Kayseri. Numerous lake basins of Miocene-Pliocene and Quaternary age have formed in the CAVP as a result of faulting and volcanism (Karabıyıkoglu *et al.*, 1999). Volcanic tephra within lacustrine records from lakes in Konya and Eski Acıgöl in central Anatolia was analysed by Kuzucuoğlu *et al.* (1998), who identified several eruptions during the Late Glacial and Holocene periods. The age of the evolution of the CAVP has been dated between 13.5 Ma to the Holocene period.

Turkey has experienced numerous minor and major earthquakes throughout the Holocene. For example, central regions were affected by the well documented earthquake of AD 1170 in the EM (Guidoboni *et al.*, 2004). However, Erdik *et al.* (2001) highlighted that Central Anatolia does not possess major tectonic elements capable of generating high magnitude earthquakes. Therefore the sediment records from Kratergöl and Nar are unlikely to have been notably affected by earthquake events throughout the last 2000 years.

Nar Gölü is located in the Göllüdağ-Acıgöl volcanic complex of the CAVP. Evidence from Eski Acıgöl (near Nevşehir) has revealed that Cappadocia was volcanically active until the Late Glacial to Lower-Mid Holocene period (~5000 BP) (Kuzucuoğlu *et al.*, 1998). Kratergöl, situated on the Konya Plain, exists within the region of an extensive

palaeolake on the southern edge of the Anatolian plateau. Lake Konya reached its maximum ~23,000-17,000 BP (Karabiyikoğlu *et al.*, 1997) and following this period, the lake level declined due to decreased precipitation and higher temperatures (Roberts, 1982). Throughout the Holocene, this area has experienced periods of drought and renewal of lakes (Karabiyikoğlu *et al.*, 1997). Kratergöl is an example of a maar lake, situated in the Karapınar volcanic field. This region, dated to Late Pleistocene age, is located to the southwest of the Karacadağ volcanic complex and represents the southwestern extension of the CAVP (Karabiyikoğlu *et al.*, 1997).

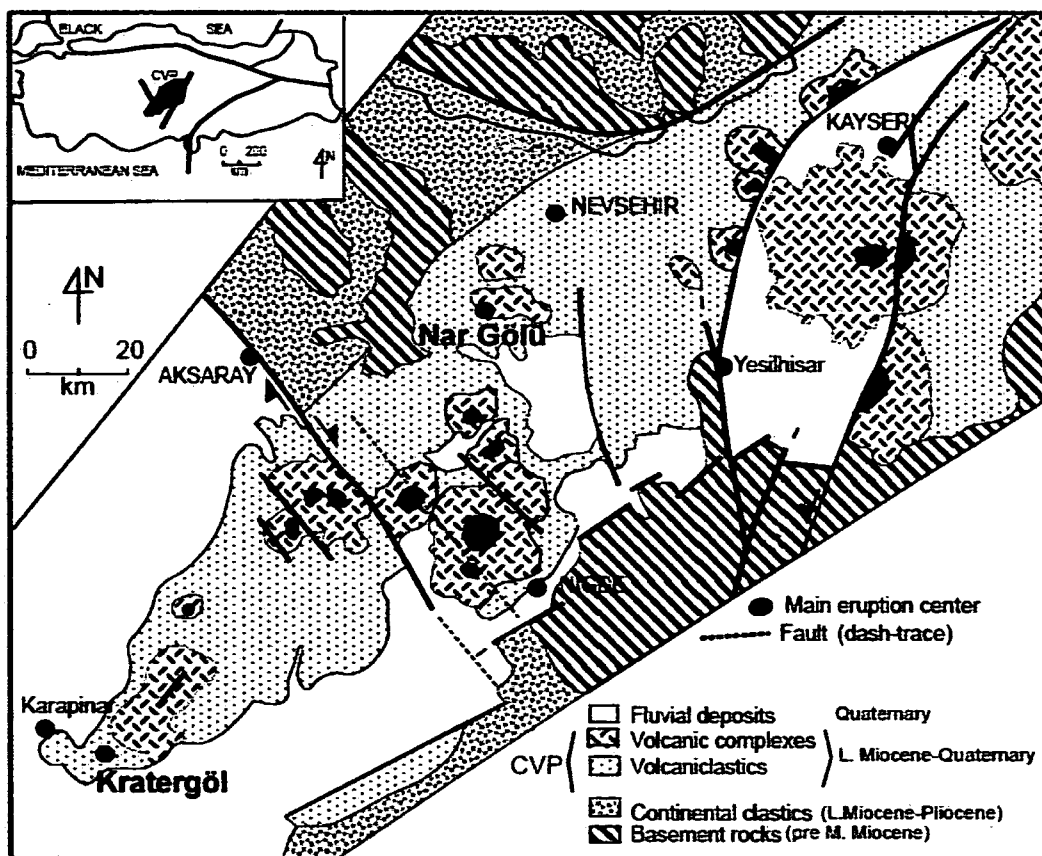


Figure 4.3 Geological setting of the Central Anatolian Volcanic Province (Toprak, 1998). Nar Gölü and Kratergöl highlighted (blue circles).

4.1.3 Human activity

Central Anatolia has experienced considerable human activity throughout the previous 2000 years. There is extensive evidence of human-induced alteration to natural vegetation in pollen records (e.g. Bottema and Woldring, 1990; Wick *et al.*, 2003; Eastwood *et al.*, 2006 and England *et al.*, 2008). Erinc (1978) discussed the various impacts of human activity on the natural landscape of Turkey and highlighted deforestation, over-grazing and soil erosion, associated with agriculture, as some detrimental consequences. Bottema and Woldring (1990) identified the Beyşehir Occupation (BO) Phase, starting towards the end of the fourth millennium BP and continuing until the end of the second millennium BP, as involving an advanced form of agriculture in Turkey with consequences for the natural environment, which is evident in numerous palaeo-pollen records. The lake sediment records from Nar Gölü and Kratergöl are also likely to contain evidence of human activity.

4.2 Lake site descriptions

Nar Gölü (38°22'30"N; 34°27'30"E) (Chapter 3: Plates 3.1, 3.3 and 3.4) is relatively small and deep and is located in the Cappadocia region of central Anatolia in east-central Turkey (30 km southwest of the city of Nevşehir). Kratergöl (37°42'49.21"N; 33°39'55.58"E) (Chapter 3: Plates 3.2, 3.5 and 3.6), located on the Konya Plain in western Anatolia (Turkey), is a relatively small, deep hyper-saline lake situated in a volcanic semi-desert area near the town of Karapınar (Dumont, 1981). The systems are likely to exert comparable responses to environmental change, due to similarities in catchment characteristics and the fact that the lakes are located in a semi-arid region.

4.2.1 Water chemistry and hydrology

Nar Gölü has been annually surveyed and a database of water chemistry monitoring has been collected throughout the last decade. However, Kratergöl has not been monitored as extensively throughout this time period. Additionally, recent bathymetrical investigations have been carried out at Nar but not at Kratergöl. Therefore the lakes differ with regard to knowledge of their recent hydrochemical fluctuations and geomorphology.

Nar Gölü

The chemical and hydrological nature of a lake system determines the sedimentation regime and biota capable of inhabiting the ecosystem. Nar lake volume was calculated as 7,692,360 m³ in July 2001 and the lake water residence time has been estimated as 8-11 years (Jones, 2004). Water depth readings revealed that Nar water level decreased by 3.4 m between 2001 and 2008. This may be a consequence of evaporation exceeding water inflow and implies that the regional climate is becoming increasingly arid.

Jones (2004) developed a hydrological model for Nar Gölü and calculated that 178,080 m³ of rainfall enters the lake directly from precipitation and 570,412 m³ of water is lost via evaporation annually. Due to the closed-basin structure of Nar, an important output of water is via evaporation, which was calculated as accounting for 40-60% of the water flux leaving the lake (Jones, 2004). The lake catchment is not used for irrigation purposes. Only 24-33% of the water entering the lake was calculated as originating directly from precipitation, which suggests that the remainder is derived from groundwater flow and the cold-water springs around the catchment edge. There is also an alluvial fan extending into the southern margin of the lake, which may account for a

portion of water flow. The fact that precipitation is not the main water input has implications for the strength of the relationship between lake hydrology and climate. The lake-climate relationship is not straightforward and may be altered by a number of catchment characteristics and the impacts of human land use. For example, snow melt during spring is likely to impact on lake ionic concentrations and human land use may alter the nutrient status of the lake.

Lake water chemistry readings collected between summer 1999 and 2008 demonstrate that Nar is weakly alkaline to circum-neutral and brackish (Tables 4.1 and 4.2). Summer 2008 water chemistry analyses revealed 0.046 mg/l^{-1} of nitrite in a sample from 0.5 m water depth and 0.023 mg/l^{-1} at 20 m. No biologically available phosphate was found in the water samples; therefore this appears to be a limiting nutrient in the lake during summer. The order of dominating ions in Nar lake water is: $\text{Na}^+ > \text{Mg}^{2+} > \text{K}^+ > \text{Ca}^{2+} > \text{Sr}^{2+}$ and $\text{Cl}^- > \text{SO}_4^{2-} > \text{SiO}_2$. Eugster and Hardie (1978) devised a brine type classification system for saline lakes based on water chemical composition according to relative percentages of anions and cations. In the Nar system, the major anion is Na^+ (52.9%) and the major cation is Cl^- (82%). The system is also dominated by K^+ (20%) and Mg^{2+} (14.3%). Carbonate levels were not directly measured but are thought to be important in the system. High bicarbonate alkalinity at Nar is indicated by the fact that phenolphthalein alkalinity is less than half that of total alkalinity. Therefore, according to Eugster and Hardie's (1978) classification, the system is $\text{CO}_3\text{-(SO}_4\text{)-(Cl)-Mg-(Na)}$ brine type.

Fluctuating temperature, pH and conductivity with water depth illustrates that Nar lake water is stratified, with similar results in 2001, 2002 and 2008 (Figure 4.4 a-c). Greatest change in all variables occurred between 5 and 15 m; this implies that the thermocline is

positioned at this depth in the water column. However, field research has only taken place during summer; therefore it is not known whether mixing occurs at any time during the year or whether the thermocline changes position. Summer temperature readings at different Nar lake water depths has remained consistent through time, whereas conductivity increased between 2001 and 2002 and then decreased in 2008 and lake water pH increased between 2001 and 2008.

Water sample location	Depth (m)	Temperature (°C)	Conductivity (mScm ⁻¹)	pH
Lake centre (ave. 2001-2008)	0cm	23.3	3.3	7.9
	10m	18.2	3.6	7.3
	20m	12.4	3.4	6.8
Hot springs		32.5	3.4	6.6
Cold springs		14.15	0.11	7.6

Table 4.1 Nar Gölü water chemistry averaged for the period 2001-2008 (including data from Jones, 2004).

Lake water sample location	Centre 1999	Hot spring 1999	Centre 0.5m depth 2008	Centre 20m depth 2008
mg/l ⁻¹				
Cl ⁻	970.0	830.0		
Na ⁺	380.0	374.8		
SO ₄ ²⁻	154.0	155.0	160.7	163.4
K ⁺	144.4	145.1		
Mg ²⁺	103.4	106.0		
Ca ²⁺	59.8	72.4		
SiO ₂	58.14	54.69	79.2	72.9
Sr ²⁺	31.3	28.9		
Phosphate			0.000	0.000
Nitrate			0.046	0.023
Phenolphthalein alkalinity	83.84	31.44	54.3	4.2
Total alkalinity	455.90	445.42	591.5	645.8

Table 4.2 Nar Gölü major ion water chemistry (mg/l⁻¹) summer 1999 (analysis by Jane Reed) and summer 2008 (analyses conducted at the University of Plymouth).

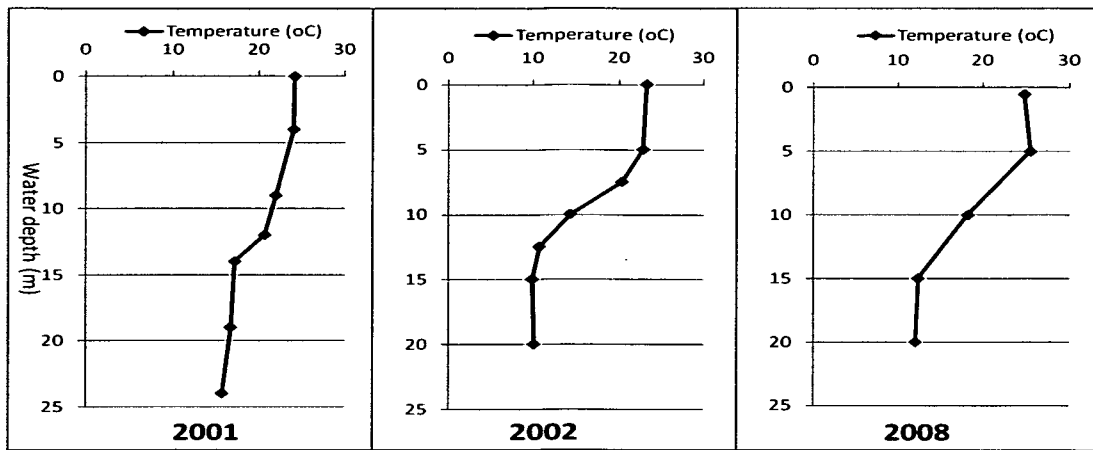


Figure 4.4 a) Nar water temperature depth profile (summer 2001, 2002, 2008).

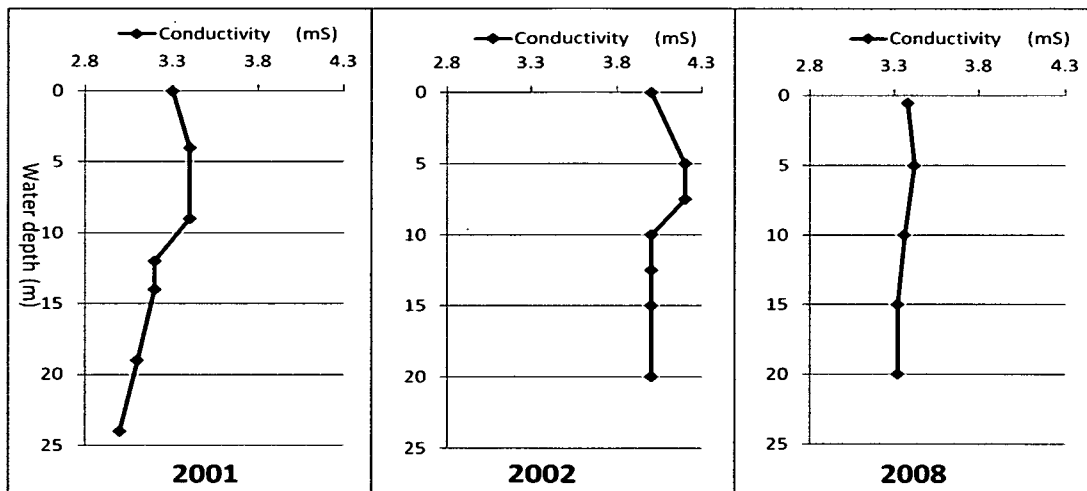


Figure 4.4 b) Nar water conductivity (mS cm^{-1}) depth profile (summer 2001, 2002, 2008).

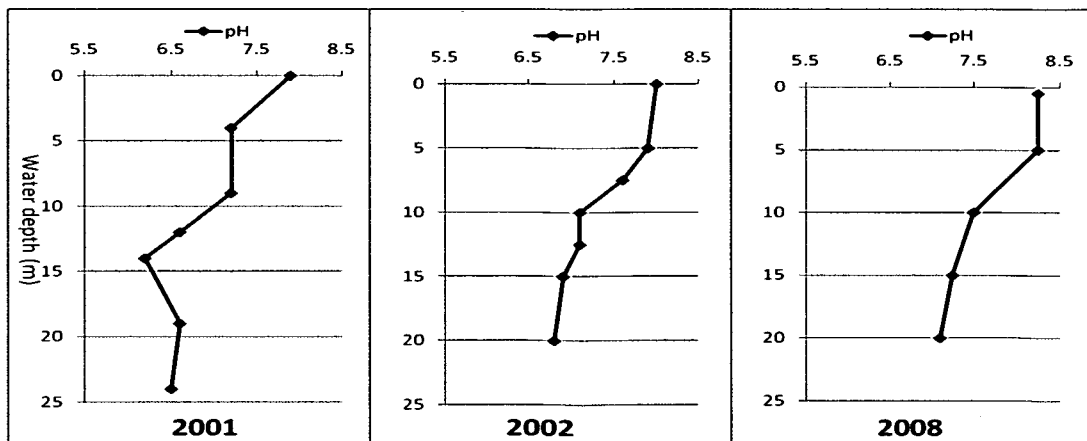


Figure 4.4 c) Nar water pH depth profile (summer 2001, 2002, 2008).

Kratergöl

The Konya plain is fed by precipitation, ground-water inflow and discharge from an inflowing stream. An irrigation network has been implemented in the region, which has led to decreased underground water-table level (Karabiyikoğlu *et al.*, 1997). In 1973, a lake water depth of 76.5 m was recorded at Kratergöl (Dumont, 1981). The lake is closed and likely to be hydrologically linked to climate. Dumont (1981) recognised that the lake level recedes annually and this results in the formation of brine pools along the rims, which evaporate and leave a salt crust. Fieldwork conducted in summer 2008 revealed that the lake level has decreased by approximately 5 m since 1999. Tables 4.3 and 4.4 summarise water chemical analyses carried out at Kratergöl during 1999/2008 and by Dumont (1981). Lake water is hyper-saline and dominated by major anion Na^+ (88%) and cation Cl^- (81.6%) with important ions Mg^+ (9.6%) and SO_4^- (16%), therefore the lake is of Na^+ - Cl^- brine type.

Kratergöl chemistry recordings taken during summer 1999 suggest that lake pH and conductivity differs between the surface and bottom water. A more thorough water chemistry investigation was undertaken by Dumont (1981), during which the lake was identified as having anoxic bottom water and being stratified for temperature, pH and chloride, with a sudden change in conditions at around 30-50 m water depth (Figure 4.5 a, b and c), which may relate to the thermocline. Therefore it appears that the system is stratified for at least part of the year. Comparing 1970s data from Dumont's (1981) study with the 1999 and 2008 recordings has revealed that the pH of the lake has decreased slightly and conductivity has increased. This suggests that the system has become less alkaline and aridity has increased, which may be associated with calcium

and magnesium precipitation as a result of altered lake water chemistry. However, very few recordings were taken and different instruments were used; therefore it is difficult to draw conclusive inferences from these comparisons.

Sample location	Water depth (m)	July temp. (°C)	pH	Conductivity (mS/cm ⁻¹)
1999				
Surface	0.6	21.0	8.3	77.2
Bottom	68.0		7.7	80.5
2008				
Surface		28.0	7.98	83.5

Table 4.3 Water chemistry data recorded at Kratergöl during summer 1999 (analysis by Jane Reed) and 2008.

Lake surface	g/l ⁻¹
Cl ⁻	34.63
Na ⁺	21.27
SO ₄ ⁼	6.94
Mg ⁺⁺	2.33
HCO ₃ ⁻	0.83
K ⁺	0.40
Ca ⁺⁺	0.155

Table 4.4 Kratergöl major ion chemistry g/l⁻¹ (Dumont, 1981).

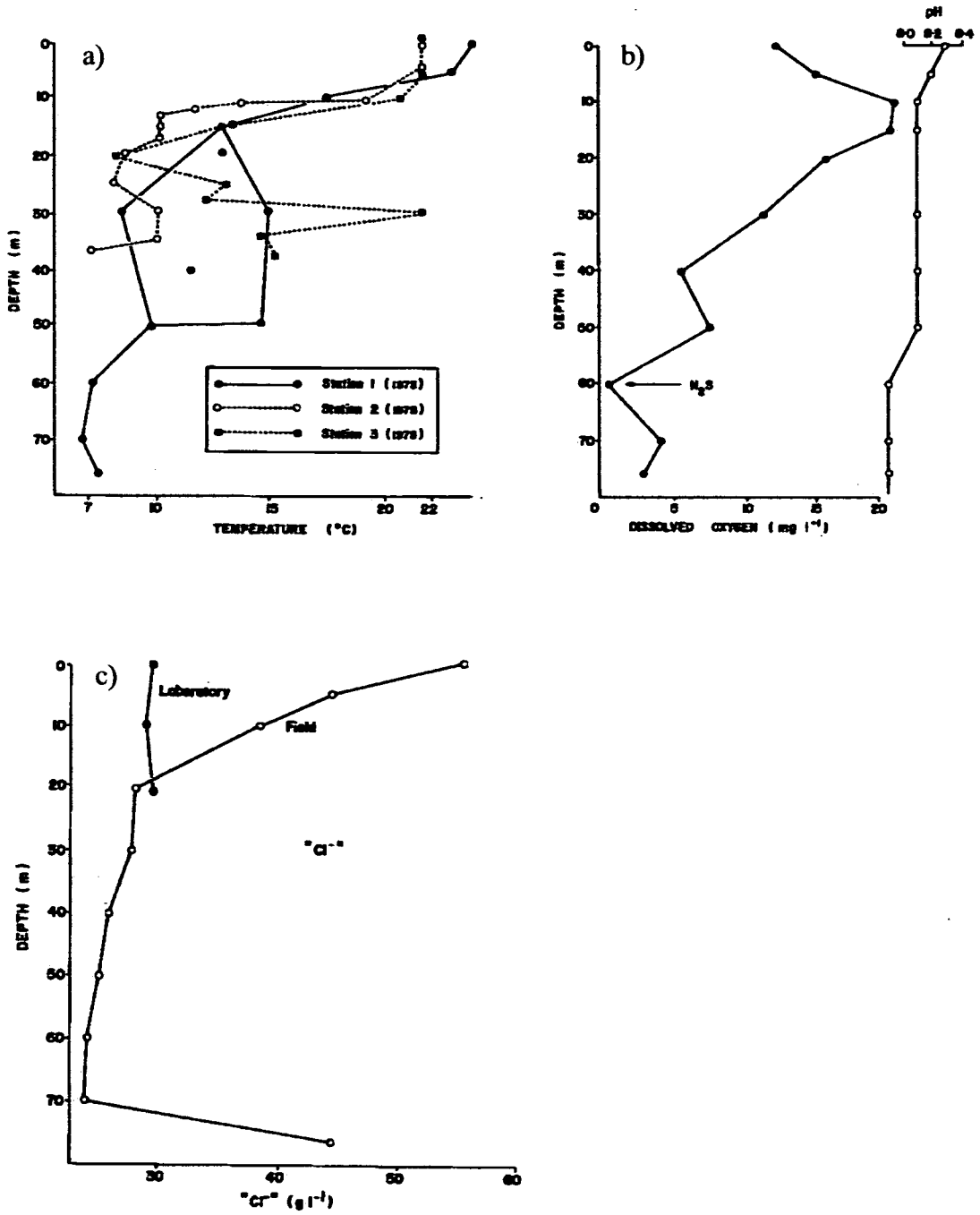


Figure 4.5 Kratergöl water temperature depth profile, b) dissolved oxygen content and pH depth profile, c) chloride depth profile (Dumont, 1981).

4.2.2 Geomorphology and sedimentation

Lake geomorphology controls the drainage nature, inputs of nutrients and the residence time of a lake. These patterns govern the distribution of dissolved gases, nutrients and organisms (Wetzel, 2001). The lake sedimentation regime is associated with catchment-related factors and seasonality.

Nar Gölü

Nar has a distinctly closed catchment with crater rims rising to 200 m above the lake (England, 2006) (Chapter 3: Plates 3.3 and 3.4). The lake has a simple inverse bowl morphology, steep north, east and west scree slopes and a faulted basalt intrusion on the eastern and western sides. The southern margin is less steep and a fan-delta is present (Roberts and Karabıyıkoglu, 2004).

The seasonal climate, combined with lake stratification and anoxic bottom waters, has resulted in the formation of annual varves in the sediments of Nar Gölü. The stratigraphic similarities recognised between core sections collected from different areas of Nar suggest that sedimentation is constant across the central area of the lake.

Sediment traps and radiometric dating confirmed that laminations form annually (Jones, 2004; Jones *et al.*, 2005). Based on sediment trap analysis, Jones (2004) identified that sedimentation involves an organic period in autumn, winter and spring, followed by calcium carbonate deposition in late spring and early summer. Carbonate laminae fluctuate in colour between whiter fine grained aragonite (<5 µm in size) and calcite polyhedral crystals (10-40 µm in size) (Roberts and Karabıyıkoglu, 2004). Dark laminae remain relatively consistent in colour throughout the sequence with slight changes between browner/greener material, which is mainly composed of diatoms.

Kratergöl

Kratergöl characteristics are outlined in Chapter 3: Table 3.1. The lake shorelines are relatively straight along the northern rim and in the south two basaltic peninsulas create deep bays (Chapter 3: Plates 3.5 and 3.6). The south and east rims of the lake are gentle sloping and steep cliffs are present at the north and west margins (Dumont, 1981). The morphology of the two bays includes a near-shore underwater cliff at 30-40 m depth, and a second cliff some distance from the shore at a depth of 60-70 m. Although the lake water is stratified and bottom waters are anoxic, as evidenced by the high organic content, conditions for the formation of annual varves are not present. This may be associated with seasonal mixing and other processes occurring in the lake.

4.2.3 Vegetation

Photographs of the lake sites (Chapter 3: Plates 3.1 and 3.2) illustrate considerably more vegetation at Nar in comparison with Kratergöl. This may be due to the hyper-saline Kratergöl lake water limiting plant growth. It appears that human agricultural and pastoral land use has been more intense and consistent at Nar during recent history, in comparison with Kratergöl. Therefore Nar's catchment is likely to be more disturbed.

Nar Gölü

Steppe (e.g. drought-tolerant shrubs) is the dominant vegetation cover in Cappadocia and dry forests sparsely populate the region (Kutiel and Türkeş, 2005). The vegetation surrounding Nar Gölü has been described by England (2006) (Chapter 3: Plate 3.1). The lake margins are fringed by *Phragmites* (reed/grass) and emergent *Juncus* (rushes), excluding the southern border, where hot springs are present. Vegetation does not inhabit the steep crater slopes. However, further afield, on the northern periphery, there

are cultivated agricultural plots of *Cicer arietinum* (chick peas), *Lycopersicon esculentum* (tomatoes) and *Cucurbita pepo* (squash). Additionally, grazing takes place around the elevated edge of the lake crater. *Pinus* (pine), planted approximately 20 years ago, populates the southern edge of the lake along with *Platanus* (sycamore) and *Populus* (poplar), in the area occupied by the alluvial fan. Degraded scrub woodland, comprising *Quercus cerris* (Turkish oak) and various other tree species, occupies higher elevated areas around the lake. There are a number of fallow or abandoned agricultural plots on the eastern periphery of the lake and cultivation of cereals (*Triticum* and *Secale*) takes place on surrounding land (England, 2006).

Kratergöl

The natural vegetation of the Konya Plain is steppic (Karabıyıkoglu *et al.*, 1997). However, a great deal of irrigation, deforestation, agriculture and grazing has taken place outside the catchment, which has altered the landscape. The Kratergöl basin, catchment and surrounding area is sparsely vegetated (Chapter 3: Plate 3.2). A small number of shrubs are present on the slopes surrounding the lake, sparsely distributed fringing macrophytes surround the water margin and there is currently no agricultural activity in the catchment. Stromatolites, which are organosedimentary structures formed by microbial activity (Papineau *et al.*, 2005), surround the periphery of the lake.

4.3 Summary

Nar Gölü provides an ideal site from which to conduct palaeolimnological investigations, mainly owing to the annually-laminated nature of the lake sediments. Nar and Kratergöl were selected for palaeoecological research, as the lakes have a number of similarities; for example, both have well preserved diatom assemblages and

similar basin characteristics. Additionally, the sites are located in a continental volcanic region and have experienced the same climate history. The fact that the two lakes have dissimilar sedimentation regimes implies that they may provide an interesting comparison with regard to the suitability of different lake types for palaeoclimatic investigations.

Chapter 5

Results: Nar Gölü

5.0 Introduction

This chapter presents and describes results from the modern and palaeo-diatom analysis of Nar Gölü.

5.1 Diatom identification and taxonomy

Diatom species identifications were primarily based on the Krammer and Lange-Bertalot (1991; 1997; 2000) (KLB) taxonomic key and illustrations (see Chapter 4 for a list of additional literature sources consulted). Key distinguishing features of species that occurred at greater than 5% abundance are described in Appendix 1. Specific taxonomic problems are summarised and presented with illustrations (see Appendix 3 for a complete species list). Detailed species descriptions are not included and are available in KLB.

The Nar diatom species assemblages were relatively diverse and a number of issues arose regarding the taxonomy of certain taxa. For example, identification of the *Achnantheidium minutissimum* species group presented problems due to variations in cell size, shape and ornamentation. It was not possible to confidently split varieties of this species; therefore specimens were grouped. Numerous small *Fragilaria* spp. presented problems due to the presence of valves with features belonging to different species. For instance, specimens were encountered with size range and shape corresponding to *F. elliptica* and striae arrangement suiting *F. construens* var. *venter*. Numerous extremely variable *Nitzschia* diatoms were also difficult to identify due to the presence of

transitional features that appeared to belong to different species and forms.

Additionally, a previously undescribed taxon, newly named as *Clipeoparvus anatolicus*, was highly abundant in the Nar modern and palaeo-environment (see Appendix 9: paper submitted to *Diatom Research*). Describing this species and determining its ecological tolerance will allow future work to utilise it as a palaeoenvironmental indicator. *C. anatolicus* is a small (<10 µm), non-chain forming, heavily silicified centric diatom of non-planktonic life-form (Plates 5.1 and 5.2). Encountering this diatom presented opportunity to describe a new taxon. However, this also created problems associated with the lack of matching analogue species in modern training sets for environmental reconstructions.

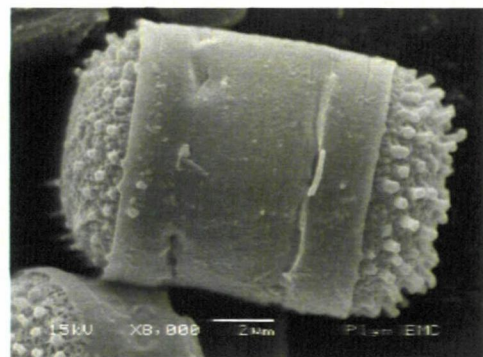
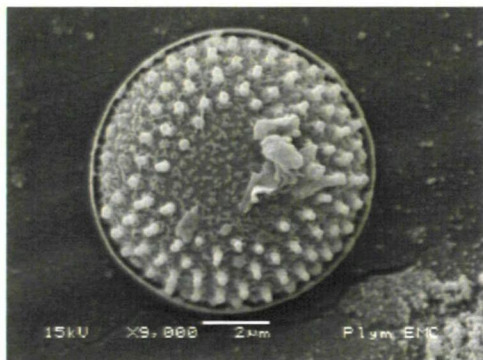


Plate 5.1 *C. anatolicus*: valve view (SEM). **Plate 5.2** *C. anatolicus*: girdle view (SEM).

5.2 Modern diatom assemblage

5.2.1 Lake habitats

Basin shape influences the type of diatoms inhabiting the lake. For example, the Nar south shore is gradual sloping and gravelly, which creates an extended littoral area for macrophytes and epiphytic diatoms to colonise. The lake is also relatively deep and the north, east and west margins are steep-sloping; therefore planktonic species were

expected to dominate the assemblage. Diatoms are limited to the photic zone for photosynthesis. Consequently, the deeper parts of the lake are not colonised. Figure 5.1 summarises the plankton (water), episammon (gravel), epiphyton (plant), epilithon (rock) and epipelon (bottom mud) diatom communities at Nar during summer 2006-2008, according to species percentage data. The macrophyte samples were dominated by *C. anatolicus* and *A. minutissimum*. It appears that these species live part of their life cycle epiphytically at Nar and colonise macrophytes on the lake fringe.

Abundant species in the gravel samples included *C. anatolicus*, *Navicula cincta*, *Achnanthes lanceolata*, *Nitzschia palea*, *Navicula cryptocephala* and *Achnanthes exigua* var. *exigua*. These are mainly motile, raphid diatoms typical of this environment. The bottom mud samples were dominated by *Synedra acus*, *C. anatolicus* and *N. paleacea* and the rock scraping contained abundant *A. minutissimum*. *Asterionella formosa* was absent from the sediment traps and palaeorecord. However, this species dominated the 2007 plankton sample, along with *C. anatolicus*, *A. minutissimum*, *S. acus* and *Synedra ulna*. This suggests that *A. formosa* may suffer dissolution within the water column or has only recently appeared as a dominant species in the system. *C. anatolicus* was abundant in all modern habitats; this may be due to its high productivity at the time of sampling (summer) and not reflect the species' true habitat preferences.

The modern samples have been described according to species percentage abundance. An additional method involves adjusting percentage data according to the cell biovolume of different species (Figure 5.2). When plotted according to biovolume, species inhabiting the epiphyton and bottom mud became more important in the assemblage. Therefore it appears that larger species inhabit these environments.

Additionally, the weighting of species altered according to biovolume. For example, large *Rhopalodia spp.* and *Synedra spp.* became more important in the assemblage. Smaller species, such as *Achnanthes* taxa, inhabiting the Nar gravel and plankton carried less weighting according to biovolume.

Figures 5.3 and 5.4 illustrate the concentration, total biovolume (sum of species volume) and species diversity of the modern samples. Species diversity (rarefaction) was greatest in the plant and gravel samples. This implies that these environments create a niche suitable for a range of species and may accumulate diatoms washed-in from other environments. The bottom mud and plant samples possessed the greatest concentration and total biovolume suggesting that diatoms are more prolific in these environments during summer.

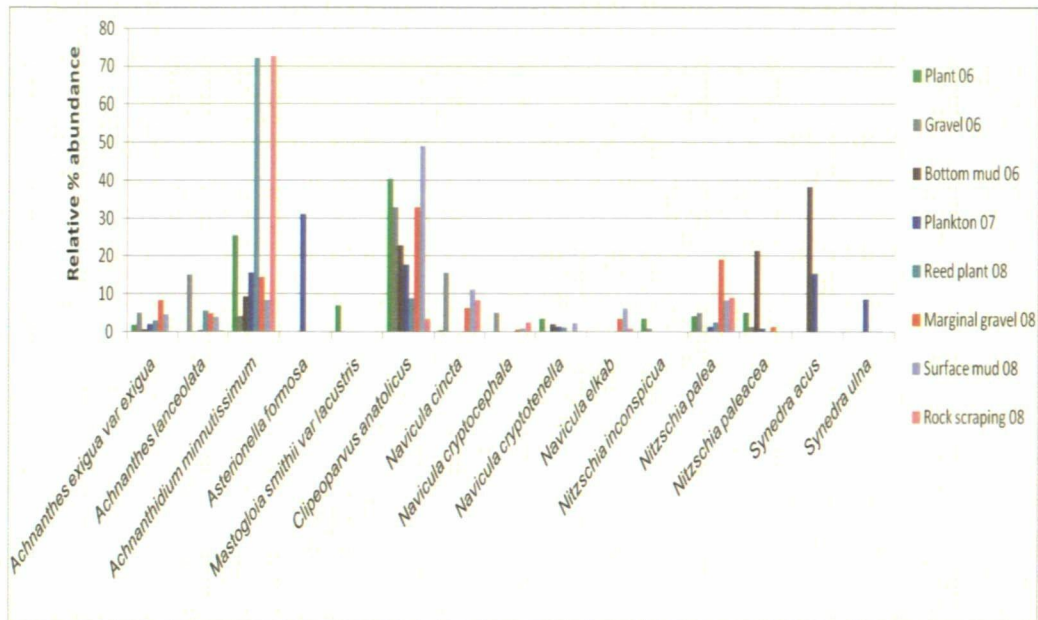


Figure 5.1 Modern diatom assemblage: species percentages presented according to habitat and collection date (species included account for >3% of the population in at least one sample).

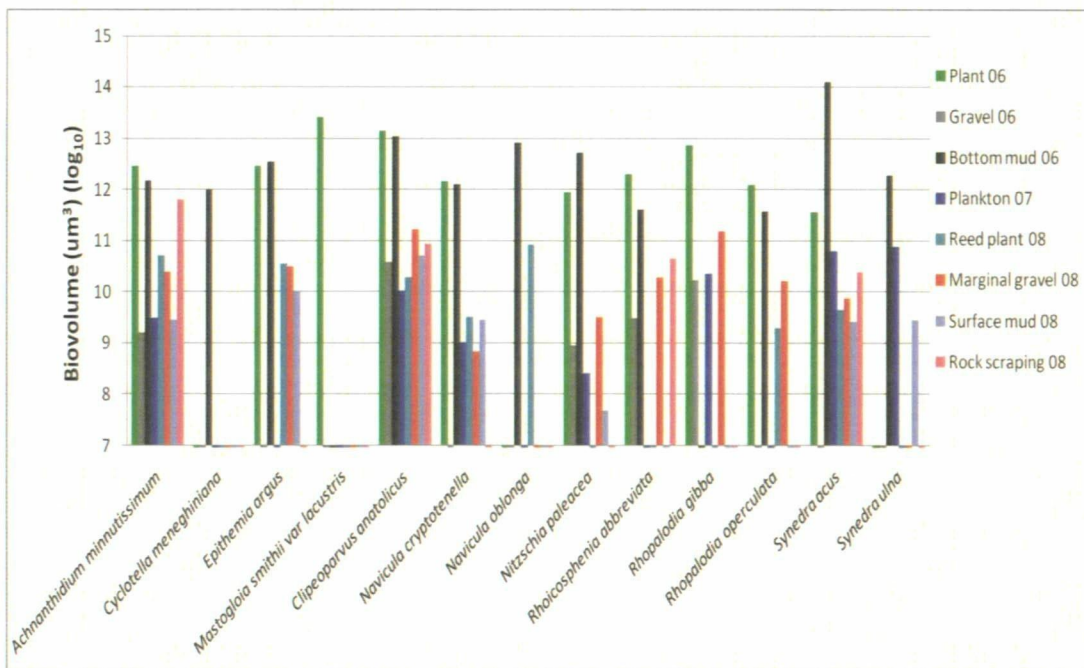


Figure 5.2 Modern diatom assemblage: species biovolume (μm^3) (\log_{10}) presented according to habitat and collection date (species included account for $>1.0\text{e}^{+06}$ in at least one sample).

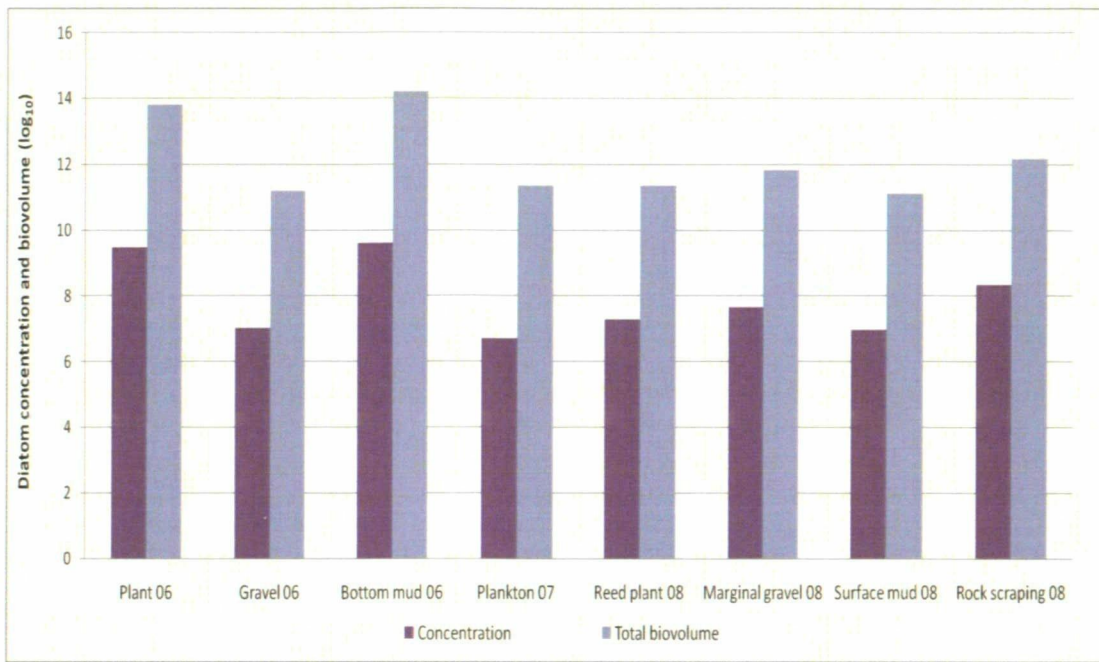


Figure 5.3 Modern sample diatom concentration (diatoms/g wet sediment, log₁₀) and total biovolume (sum of species biovolume, (µm³), log₁₀) calculated according to cell volume.

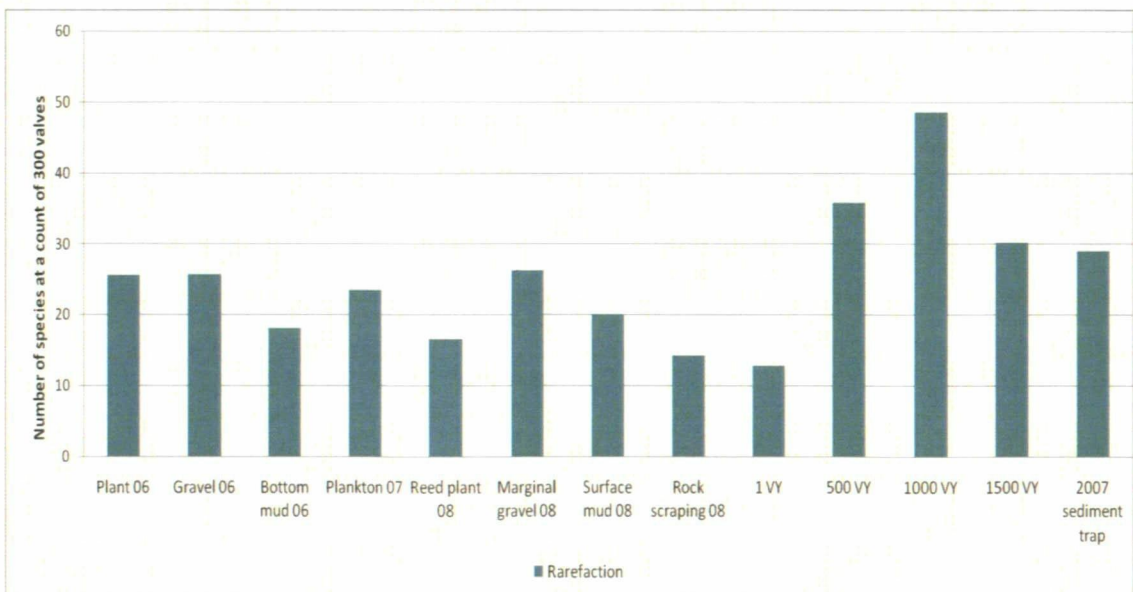


Figure 5.4 Diatom rarefaction (species diversity) of modern Nar samples and different sediment depths in the NAR01/02 palaeo-record according to varve year (VY) before AD 2001.

Detrended Correspondence Analysis (DCA) was performed on modern diatom samples in order to analyse the assemblage similarity between different lake environments (Figure 5.7). The ordination plots revealed that the 2008 plant and rock scraping assemblages were similar to one another and distinct from other samples. This is due to the same collection date and littoral location of these samples. The 2008 gravel and surface mud and 2006 plant and bottom mud samples are all positioned high on DCA axis 1. The 2007 plankton and 2006 gravel assemblages were distinct from other modern samples. The relative differences between the samples confirm that diatom species exhibit differing habitat preferences at Nar. However, the presence of species in multiple habitats suggests that many taxa are able to exist within various niches.

Habitat inferences based on modern samples are limited by the possibility that species preferences may not be represented accurately. Sampling times were limited to summer and it is likely that species were identified in habitats other than their ideal niche. For example, epipelagic species may live amongst dead or resting cells derived from other lake habitats. Planktonic diatoms within lakes often exist as meroplankton, i.e. they spend part of their life cycle resting on the sediment, and benthic taxa can be observed re-suspended in the water column (Battarbee *et al.*, 2001). Analysis of the modern environment has provided general information regarding the diatom community, productivity and diversity.

5.2.2 Sediment traps

Sediment traps were installed during summer and collected annually from Nar between 2002-2007 (Table 5.1). Traps were situated at two positions in the lake at different water depths (Chapter 3: Figure 3.3). The lithology of 2002-2004 sediment traps at Nar

was analysed by Jones (2004) and England (2006) in order to infer the lake sedimentation regime. Jones (2004) identified colour changes at different depths within the traps, associated with organic carbon content and carbonate lithology. A period dominated by diatoms was recognised, followed by calcium carbonate deposition, as a result of lowered lake water pH associated with increased photosynthesis. The photic zone was identified as the location where carbonate precipitation occurs due to the association between plankton productivity and light availability. Decreased organic content was evident in traps near the water surface, as a result of oxidation, and traps at lower water depth had higher carbon content due to anoxic conditions.

Date installed in lake	Date collected from lake	Depth in water column (m)	Length of section (cm)	Notes
Sept 2006	Aug 2007	5	N/A	Sample amalgamated
Sept 2006	Aug 2007	15	N/A	Sample amalgamated
July 2005	Sept 2006	-	26	Sediment mixed in tube
July 2004	July 2005	-	22.5	
July 2002	July 2003	10	8	
July 2002	July 2003	15	5	

Table 5.1 Sediment trap details.

Traps were installed and collected from the lake during summer and were therefore expected to contain sediment representing late summer and autumn, followed by winter, the spring diatom bloom and the top of the trap should represent early summer. The sediment trap diatom stratigraphy (based on percentage data) is presented in Figure 5.5. The 2006-2007 traps were not recovered intact. Samples therefore represent an amalgamated annual flora from two depths within the water column.

The community of the 2006-2007 trap positioned at 5 m water depth differed slightly from the 15 m trap. For example, *C. anaticus* was more abundant in the higher trap, due to the species association with macrophytes and the photic zone. Increased *A. minutissimum* within the 2005-2006 trap appears related to periods of decreased *C. anaticus* and vice versa. There was a high proportion of *S. acus* in the 2002-2003 and 2004-2005 traps that was not recognised in 2005-2006 and 2006-2007. This implies that the bloom of this species had already occurred when the trap was installed, as evidenced by its high abundance in the 2006 bottom mud sample (Figure 5.1). In the 2003-2004 traps, an increase in *S. acus* appeared to be associated with a decrease in *C. anaticus*.

The concentration of diatoms/g of wet sediment does not show any clear pattern between the different sediment traps (Figure 5.5). However, it appears that valve concentration increased towards the top of the traps, suggesting that diatom productivity is highest during early summer, when the traps were collected from the lake. This may relate to blooms of *S. acus*. Species diversity (rarefaction) remains relatively consistent through the traps; this implies that diatom diversity has not altered seasonally at Nar during the last six years. This is not supported by NAR01/02 core thin sections, which reveal large mono-specific diatom blooms (Section 5.3.10). This could be associated with the changing seasonal ratio of silica and phosphorus.

Sediment trap data plotted according to species biovolume (Figure 5.6) altered the relative weighting of a number of species. *S. acus* remained dominant; however, the relative quantity of *A. minutissimum* and *C. anaticus* decreased in relation to species such as *Navicula halophila*, *Navicula oblonga* and *Rhopalodia gibba*, which became more significant in the assemblage. Total biovolume showed similar patterns to diatom

concentration, with slightly increased values towards the top of the traps, implying that diatoms at Nar are more productive in summer.

The similarity between sediment traps and modern samples is illustrated in Figure 5.7 DCA ordination plot. Data were plotted on DCA axes 1 and 2. Greatest similarity exists between samples from the same trap, regardless of depth within the trap. For example, samples from the 2005-2006 trap are all positioned high on DCA axis 1. Therefore there do not appear to be any clear seasonal patterns; this suggests that inter-annual similarities are more significant than assemblages associated with specific seasons. However, inter-annual assemblage similarities may also be associated with mixing of sediment within the traps through their installation in the lake and during transport to the laboratory.

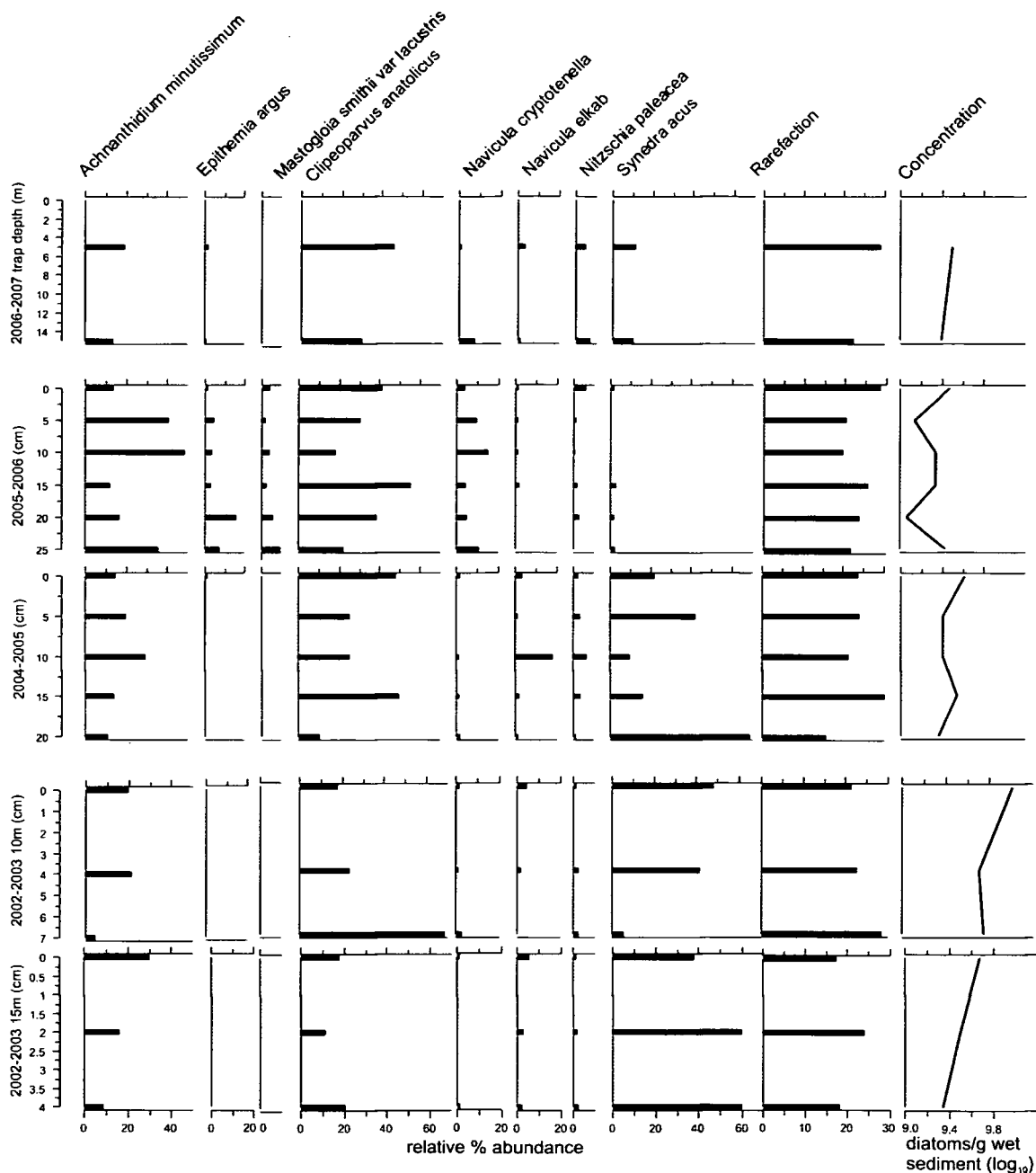


Figure 5.5 Sediment trap diatom stratigraphy with rarefaction and valve concentration

(log₁₀). Amalgamated samples from water depth 5 m and 15 m traps shown for 2007.

All other traps are plotted according to sediment depth within the trap.

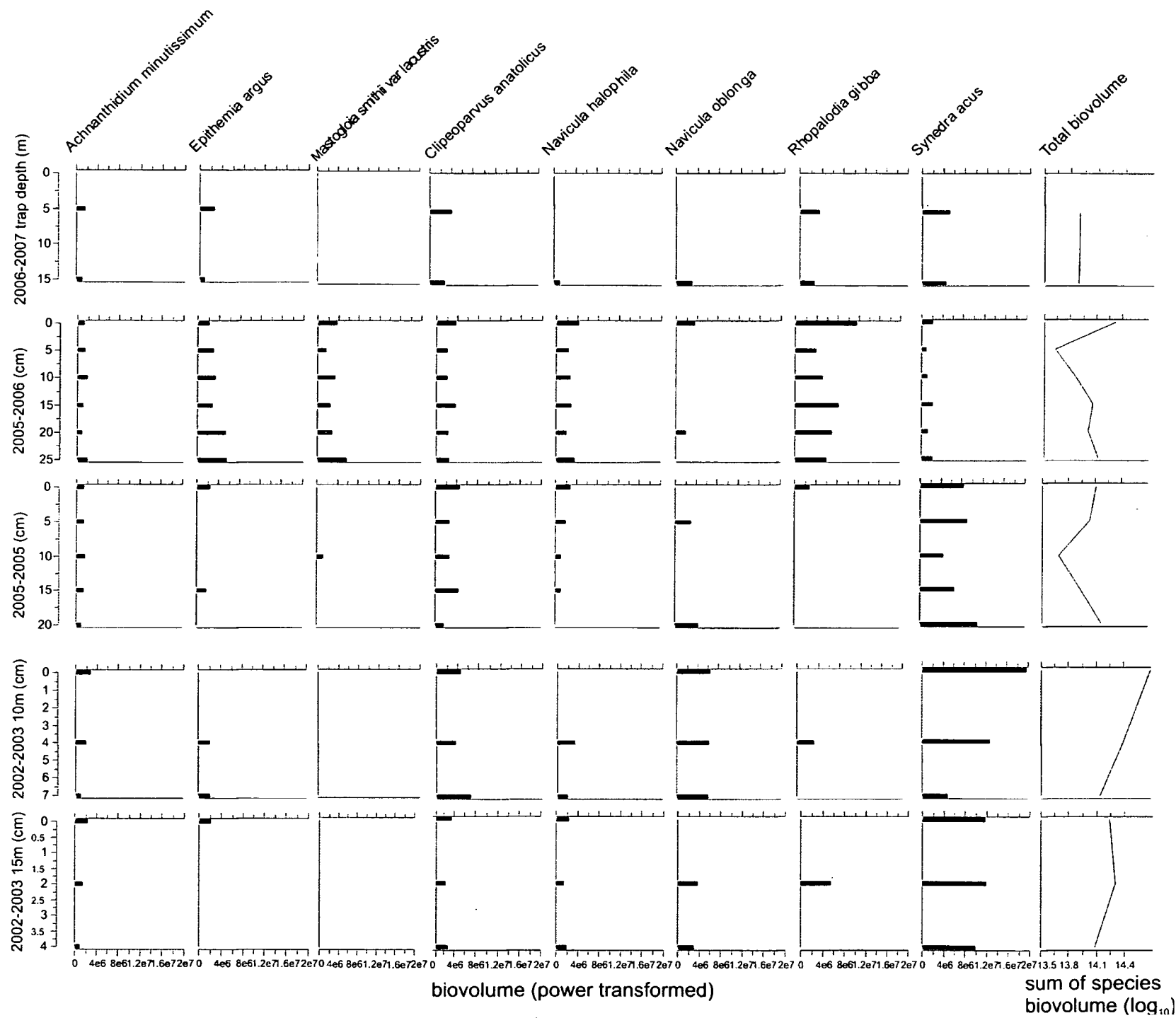


Figure 5.6 Sediment trap diatom stratigraphy plotted according to biovolume (μm^3) (power transformed) (species plotted $>2.0\text{e}^{+06}$ on a maximum scale of 2.0e^{+07}) with total biovolume (μm^3) (\log_{10}). Amalgamated samples from water depth 5 m and 15 m traps shown for 2007. All other traps are plotted according to sediment depth within the trap.

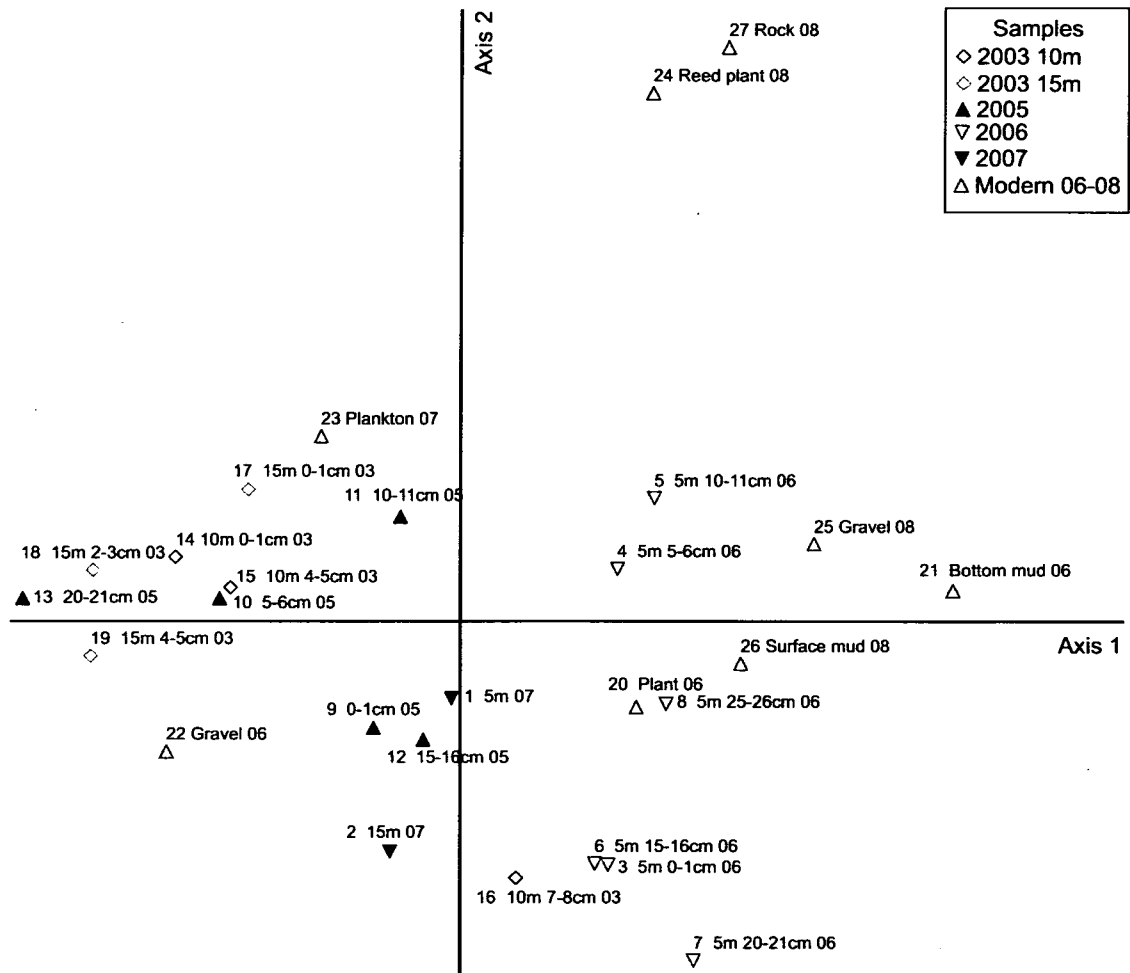


Figure 5.7 DCA ordination plot for Nar sediment trap and modern diatom samples according to sample number, depth, habitat and collection date.

5.3 Palaeo-records

5.3.1 Sediment lithology

The 376 cm core master sequence (NAR01/02) (Table 5.2) is entirely laminated with additional sporadic grey clastic layers of varying width. Annual varve couplets are composed of light coloured (white) lamina containing mainly carbonate and dark brown layers comprising organic material and diatoms (Jones, 2004). The sequence includes 1725 VYs representing the period AD 276-2001. The NAR06 core section was tied with this sequence and contributes 80 VY (AD 1927-2006). Figure 5.8 illustrates the entire Nar master sequence comprising stratigraphically tied sections.

Section number	Section code	Subsection length (cm)	Varve year (before AD 2001)	Cal age (AD)
Plym	NAR06	0-25	0-80 (before AD 2006)	1927-2006
1	NAR01 GB	0-20	0-31	1969-2001
2	NAR01 FB	16-27.5	31-44	1956-1969
3	NAR02 M11	38-71	44-108	1892-1969
4	NAR01 LCb	6-25	108-181	1819-1892
5	NAR01 LA 1	14-89	181-562	1438-1819
6	NAR01	33.5-89	562-890	1110-1438
7	NAR02 M2/3	40-83	890-1087	913-1110
8	NAR02 M3/3	36-90	1087-1310	690-913
9	NAR02 BIII	50-55	1310-1370	640-690
10	NAR02 CIII	17-82	1370-1725	276-640

Table 5.2 NAR06 and NAR01/02 core sections stratigraphically tied according to varve years and calendar age.

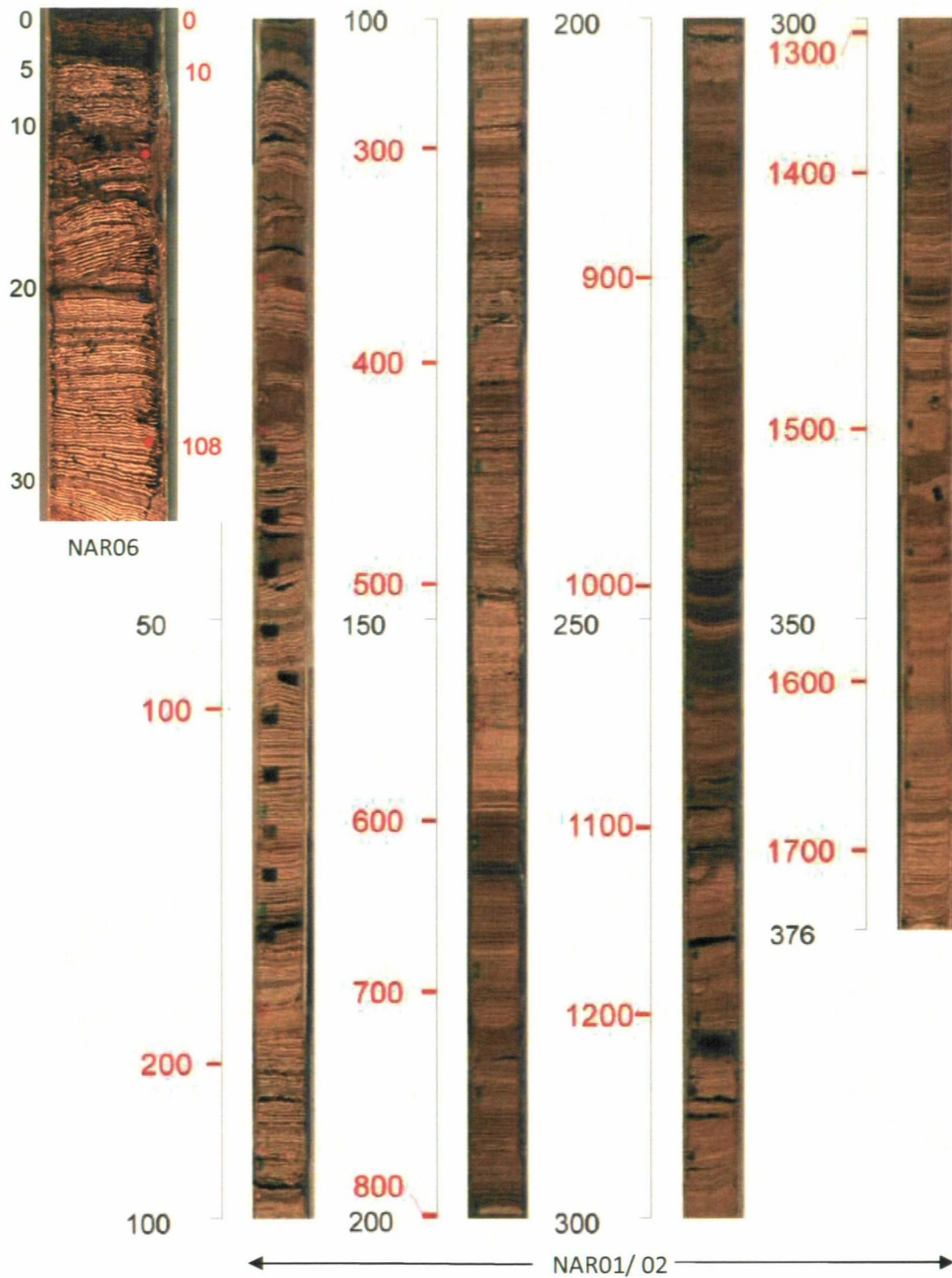


Figure 5.8 Photographs of the Nar 376 cm master sequence (NAR01/02) with depth (cm) (black figures) and varve years before AD 2001 (red figures) (Jones, 2004).

The NAR06 section is presented with depth (cm) and VY before AD 2006.

Matching stratigraphic lamination patterns are evident between the NAR01/02 and NAR06 sections, with corresponding varve counts and diatom assemblages. This implies that sediment accumulation and lithology is uniform across the lake bottom. However, the sections differ with regard to grey clastic layer thickness, which were thicker in the NAR01/02 sections, implying that events associated with clastic layers, such as sediment slumping and in-wash, are not consistent across the lake basin.

The lithology of the NAR01/02 carbonate sequence was evaluated through greyscale (colour change) and organic lamina were analysed for their carbon to nitrogen (C:N) ratio (Figure 5.16) (Jones, 2004). Greyscale indicates changes in calcium carbonate mineralogy associated with the percentage of calcite and aragonite in the system. Lighter coloured sediment occurred between 1720-1470 VY (AD 280-540). This was followed by darker sediment, with a subsequent change to even darker sediment between 1130-990 VY (AD 870-1010), lighter sediments followed until 600 VY (AD 1400) and a significant change to much lighter sediments was evident until 10 VY (AD 1990), when sediments became darker once again.

The C:N ratio of the organic laminae refers to the amount of carbon and nitrogen in the system and has remained relatively consistent throughout the record with occasional peaks and a larger increase at 120 VY (AD 1880). This could relate to increased plant cover or catchment in-wash and may be associated with increased agricultural land use and precipitation (Jones, 2004). The organic brown layers remain relatively consistent in colour throughout the entire sequence.

5.3.2 Core chronology

The NAR01/02 sequence chronology was established using varve counting and radioisotopic dating techniques (Jones, 2004) (Figure 5.9). ^{210}Pb and ^{137}Cs were employed to date the most recent 50 VY and an age/depth model was produced (Figure 5.10) in order to predict the age of deeper sediments. Varves were confirmed as annually deposited using ^{210}Pb and sediment trap analysis. Two peaks were identified in the ^{137}Cs activity profile, highlighting the 1963 ‘bomb spike’ and the 1986 Chernobyl incident (Appleby, 2001), at depths of ~28.5 and ~6 cm. The radioisotope chronology was off-set from the uppermost varve chronology by five years. The age-depth relationship revealed that sedimentation at Nar is almost constant, which provided confidence for interpreting varves in terms of calendar years. Varve counting identified 1725 individual laminations and the sequence was converted to a calendar record dating from AD 276 to AD 2001. Stratigraphically correlating the NAR06 section with the NAR01/02 sequence allowed a calendar scale (AD 1927-2006) to be applied to this record.

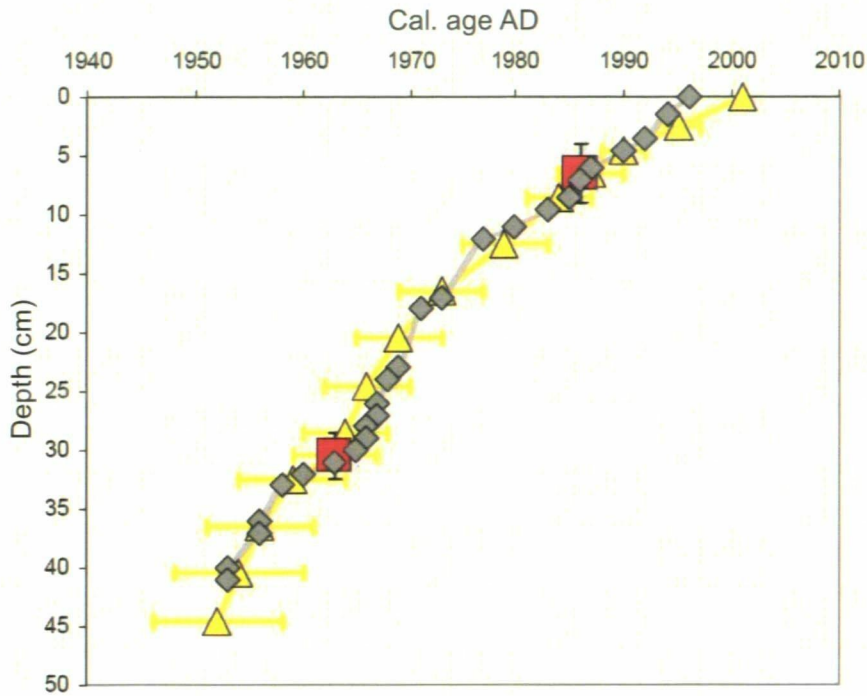


Figure 5.9 Comparison of ^{137}Cs (red squares), corrected ^{210}Pb chronology (yellow line) and varve chronology (grey line) from the NAR01 sediment record (Jones, 2004).

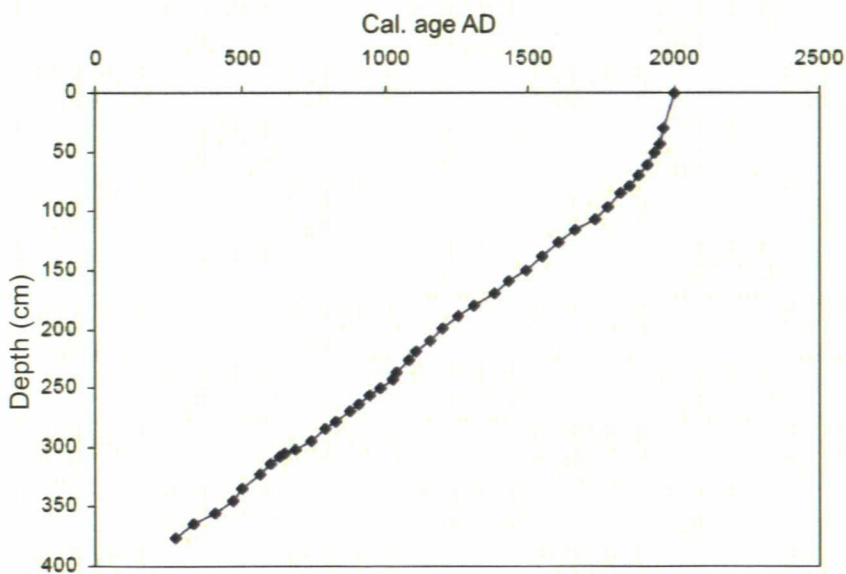


Figure 5.10 Age-depth relationship for varve chronology from the NAR01/02 sediment sequence (Jones, 2004).

5.3.3 Diatom stratigraphy

The NAR01/02 and NAR06 fossil diatom sequences are presented and described according to VY before AD 2001/2006 and calendar age AD. The NAR06 sequence (Figure 5.11) was divided into four zones using stratigraphically constrained cluster analysis (Table 5.3). *N. paleacea* was the dominant diatom species throughout the record, this species fluctuated considerably contributing between 0% and near 100% to the population at different depths. Zone ND1d was dominated by *A. minutissimum* and *S. acus*. The transition to zone ND1c involved decreased values of these species and dominance of *N. paleacea*. Zone ND1b began with renewed dominance of *A. minutissimum* and *S. acus*, followed by abundant *N. paleacea*. Throughout this zone, *A. minutissimum* gradually decreased and *S. acus* regained dominance during the most recent 15 VY. ND1a was markedly different from preceding zones and was characterised by the disappearance of *N. paleacea* and a sudden increase in *C. anaticus* and *S. acus*.

Zone	Depth (VY)	Calendar age (AD)	Dominant diatom species
ND1a	5-1	2001-2006	<i>C. anaticus</i> and <i>S. acus</i>
ND1b	60-6	1947-2001	<i>A. minutissimum</i> , <i>N. paleacea</i> and <i>S. acus</i>
ND1c	70-61	1937-1946	<i>N. paleacea</i>
ND1d	80-71	1927-1936	<i>A. minutissimum</i> and <i>S. acus</i>

Table 5.3 NAR06 main diatom zones (according to cluster analysis) with depth, calendar age and a summary of the diatom community.

The longer NAR01/02 diatom record was divided into four zones using cluster analysis (Table 5.4) (Figure 5.12), *N. paleacea* and *S. acus* fluctuated considerably with values

reaching extreme high and low percentages between successive decadal samples. Zone ND4 was markedly different from all successive periods and was dominated by *Cyclotella meneghiniana*, *Fragilaria construens* var. *venter* and *Rhopalodia operculata*. Zone ND3 began with an abrupt species assemblage change. This was reflected by the disappearance of species typical of ND4, dominance of *C. anaticus* and increasing values of *N. paleacea*. Similar species to those abundant in ND4 dominated zones ND2 and ND1. Zone ND2 was distinguished by extremely high, short-lived values of *S. parvus* between 798-757 VY (AD 1205-1246). *C. anaticus* declined gradually throughout zones ND2 and ND1 with a slight increase ~AD 2000. *A. minutissimum* gradually increased throughout ND1 and decreased at AD 2000. ND1 comprised species typical of the NAR06 record and indicates that the modern species assemblage was established at ~500 VY depth.

Zone	Depth (VY)	Calendar age (AD)	Dominant diatom species
ND1	520-1	1480-2000	<i>A. minutissimum</i> , <i>S. acus</i> and <i>N. paleacea</i>
ND2	1010-530	990-1470	<i>N. paleacea</i> , <i>S. parvus</i> and <i>C. anaticus</i>
ND3	1460-1020	550-980	<i>C. anaticus</i> and <i>N. paleacea</i>
ND4	1720-1470	290-540	<i>C. meneghiniana</i> , <i>F. construens</i> var. <i>venter</i> and <i>R. operculata</i>

Table 5.4 NAR01/02 main diatom zones (according to cluster analysis) with depth, calendar age and a summary of the diatom community.

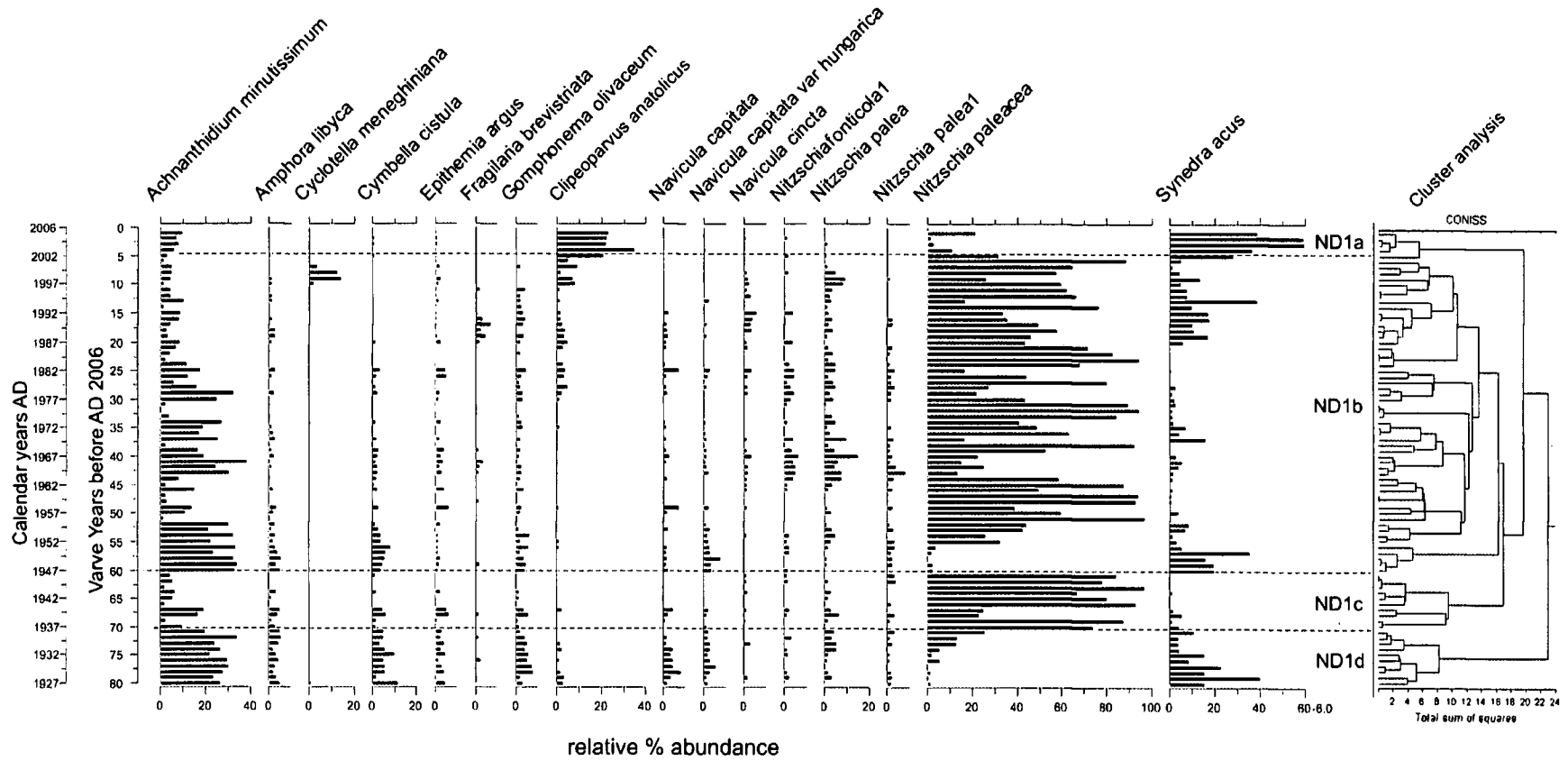


Figure 5.11 NAR06 diatom stratigraphy. Species included represent >5% of the population within at least one sample. The assemblage has been stratigraphically zoned through cluster analysis.

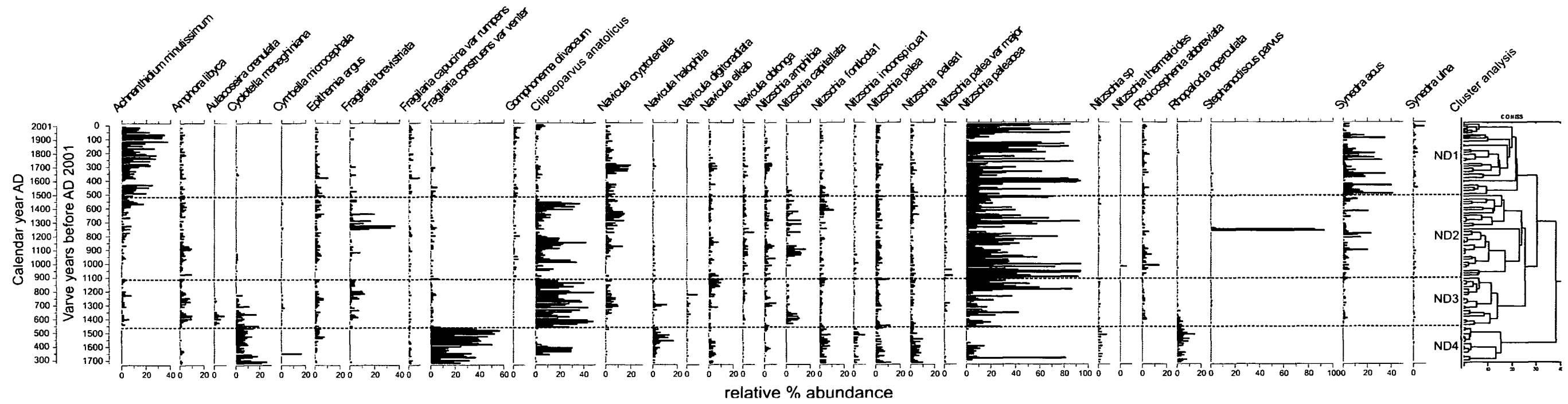


Figure 5.12 NAR01/02 diatom stratigraphy. Species included represent >5% of the population within at least one sample. The assemblage has been stratigraphically zoned through cluster analysis.

5.3.4 Detrended Correspondence Analysis

DCA was performed on the NAR01/02 and NAR06 diatom records (Figures 5.13 and 5.14) in order to reveal the similarity between samples from different core depths. The percentage of variance explained by NAR06 DCA axes 1 and 2 was 42.9%, 12.9%. The most distinct zones were ND1a (plotted high on NAR06 axis 1 and 2) and ND1d (plotted low on NAR06 axis 2). Zones ND1b and ND1c were less distinct. Ordination plots, with sample symbol size weighted according to species abundances (Appendix 4.1), reveal which zones were associated with particular taxa. These plots indicate that *A. minutissimum* and *N. paleacea* split the similarity between samples from zone ND1d. Recent change in the assemblage is illustrated by the higher weighting of *C. anaticus* and *S. acus* in zone ND1a.

The NAR01/02 ordination plot for axes 1 and 2 revealed clear zonation of samples in relation to their species assemblages. The extremely dissimilar samples comprising *S. parvus* blooms masked patterns in the plots and were subsequently removed from the data set. The percentage of variation within the data explained by NAR01/02 axes 1 and 2 was 51.1 and 19.8%. The most dissimilar zone was ND4, positioned high on NAR01/02 axis 1. This is also evident in the stratigraphic diagram (Figure 5.12), highlighting the period of greatest variation in the diatom assemblage. ND1 is reasonably distinct in the DCA plot and ND2 and ND3 are less distinctive. DCA data presented stratigraphically (Figure 5.16) revealed that NAR01/02 axis 1 accounts for the major change in the assemblage between zones ND4 and ND3, whereas axis 2 appears to represent more recent variability in the record. NAR01/02 ordination plots, with sample symbols weighted to species abundance, are illustrated in Appendix 4.2.

Although *A. minutissimum* and *S. acus* occur along with *N. paleacea* in zone 1, samples

associated with *N. paleacea* are plotted low on NAR01/02 axis 1 and samples associated with *A. minutissimum* and *S. acus* are plotted high on the same axis.

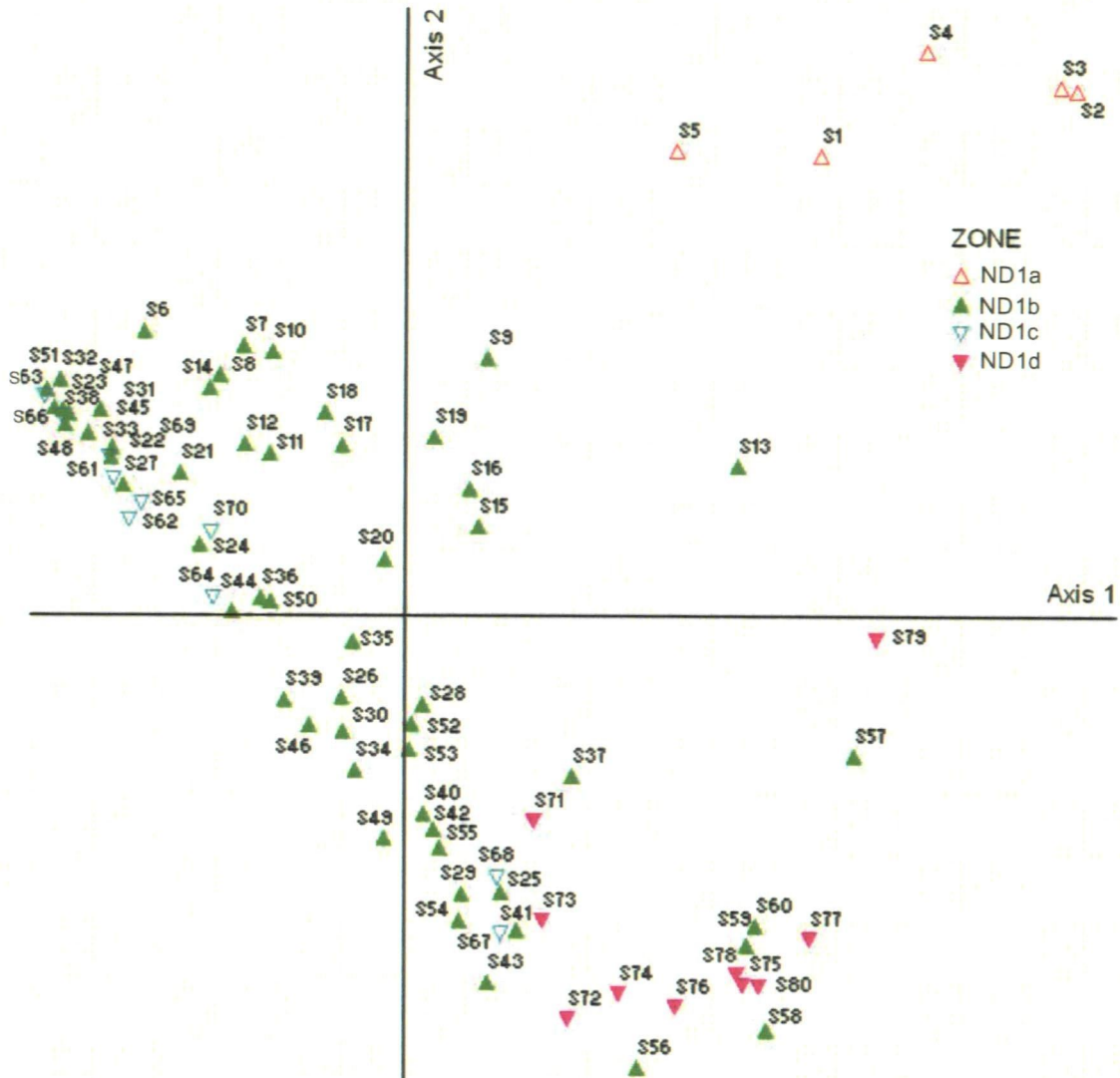


Figure 5.13 NAR06 DCA ordination plot. Samples plotted on axes 1 and 2 with symbols corresponding to cluster analysis zones.

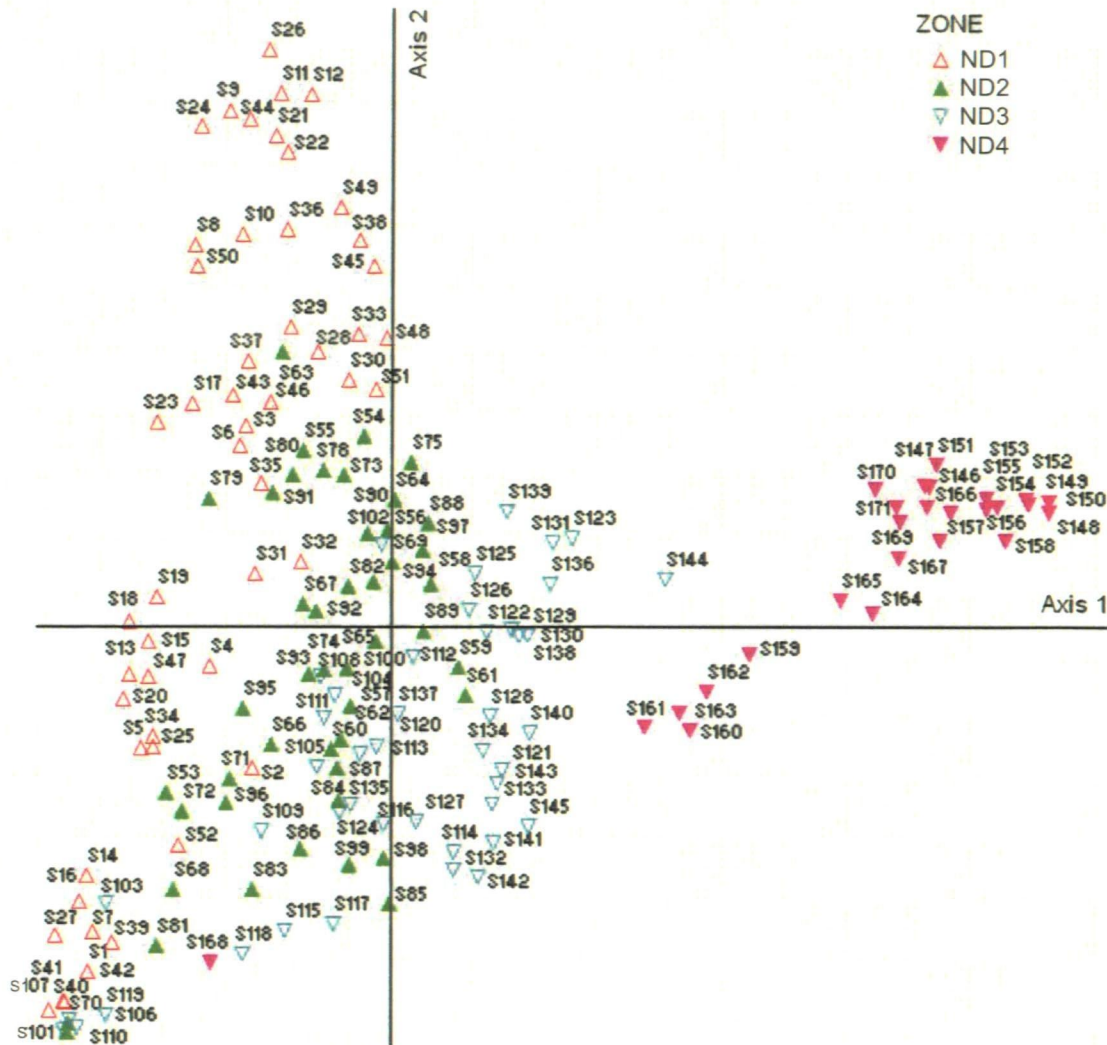


Figure 5.14 NAR01/02 DCA ordination plot. Samples plotted on axes 1 and 2 with symbols corresponding to cluster analysis zones (excluding *S. parvus*).

5.3.5 Concentration and total biovolume

Temporal change in diatom cell concentration and the total biovolume of all species within a sample can provide information about palaeo-productivity. Diatom concentration and total biovolume have been plotted on a \log_{10} scale (Figures 5.15 and 5.16) for the NAR01/02 and NAR06 records in order to reveal relative changes in the number of valves (concentration) and total biovolume (productivity) of diatoms through time. The Nar sedimentation rate is near linear (Figure 5.10); therefore data were not

adjusted for changes in lake sediment accumulation. Throughout the NAR06 record, concentration showed an upwards trend towards the most recent sediments and was significantly correlated with *N. paleacea* abundance ($r=0.692$, $p=0.000$). Concentration appeared to increase when *N. paleacea* was more dominant and total biovolume increased when *S. acus* was abundant. This is associated with the larger size of *S. acus* and the fact that *N. paleacea* blooms with extremely high cell numbers. Concentration and total biovolume fluctuated throughout the NAR01/02 record; however, changing values did not correspond with any major zone boundaries.

5.3.6 Species diversity

The diversity of diatom species within each sample is expressed by the number of species predicted by rarefaction at a count of 300 valves. The NAR06 record (Figure 5.15, a) illustrates that periods of higher diatom concentration were associated with decreased diversity ($r=-0.852$, $p=0.000$) and higher *N. paleacea* abundance. NAR01/02 species diversity (Figure 5.16) was also greatly associated with the dominant species *N. paleacea* ($r=-0.813$, $p=0.000$) and diatom concentration ($r=0.738$, $p=0.000$), indicating that more productive periods were less diverse. This implies that *N. paleacea* blooms swamp the community and drive diversity down. Rarefaction indicates increased diversity during zone ND3 and a recent decrease through ND1.

5.3.7 Habitat preferences

Diatom species were grouped according to habitat preferences (Table 5.5) based on their niche recognised in supporting literature (e.g. Gasse, 1986) and modern sampling at Nar. Grouping taxa according to habitat preferences was problematic, due to the wide niches of many species. The percentage of benthic taxa fluctuated throughout the

records and is presented in Figures 5.15 (a) and 5.16. In the NAR06 record, the percentage of benthic taxa decreased in the most recent sediments. Within the NAR01/02 sequence, benthic taxa abundance fluctuated considerably and was influenced by the dominance of *N. paleacea*.

Benthos	Plankton	Plankton/Epiphyton
<i>Amphora libyca</i>	<i>Aulacoseira crenulata</i>	<i>Achnanthydium minutissimum</i>
<i>Cymbella cistula</i>	<i>Cyclotella meneghiniana</i>	<i>Clupeoparvus anaticus</i>
<i>Cymbella microcephala</i>	<i>Stephanodiscus parvus</i>	<i>Fragilaria brevistriata</i>
<i>Epithemia argus</i>	<i>Nitzschia paleacea</i>	<i>Fragilaria capucina</i> var <i>rumpens</i>
<i>Gomphonema olivaceum</i>	<i>Synedra acus</i>	<i>Fragilaria construens</i> var <i>venter</i>
<i>Navicula capitata</i>	<i>Synedra ulna</i>	<i>Nitzschia amphibia</i>
<i>Navicula capitata</i> var <i>hungarica</i>		<i>Nitzschia capitellata</i>
<i>Navicula cincta</i>		<i>Nitzschia fonticola</i> 1
<i>Navicula cryptotenella</i>		<i>Nitzschia inconspicua</i> 1
<i>Navicula digitoradiata</i>		<i>Nitzschia palea</i>
<i>Navicula elkab</i>		<i>Nitzschia palea</i> 1
<i>Navicula halophila</i>		<i>Nitzschia palea</i> var <i>major</i>
<i>Navicula oblonga</i>		<i>Nitzschia thermaloides</i>

Table 5.5 Nar species groups according to habitat preferences.

5.3.8 Comparison of the NAR01/02 and NAR06 records

Figure 5.15 (b) illustrates the most recent 85 VY of the NAR01/02 decadal record for comparison with the NAR06 annual core. The two sequences reveal similarities regarding their diatom assemblages. For example, *N. paleacea* and *A. minutissimum* dominate both records. A simultaneous shift to lower *A. minutissimum* and higher *N. paleacea* is evident in both records (zone ND1c) providing evidence that the sequences

are stratigraphically tied. The recent rise in *C. anatolicus* is also apparent at the top of the NAR01/02 record (AD 2000). The comparison graph (Figure 5.15 b) highlights that considerable detail is lost in the NAR01/02 record due to the decadal sampling resolution. The period AD 2002-2006 is not covered in the NAR01/02 record; therefore the most recent assemblage change involving higher *C. anatolicus* and *S. acus* is not evident. Comparing the rarefaction, concentration and total biovolume graphs has revealed that the same associations with *N. paleacea* exist in both records. The NAR01/02 decadal resolution allows more general trends to be observed, which are masked in the NAR06 annual record.

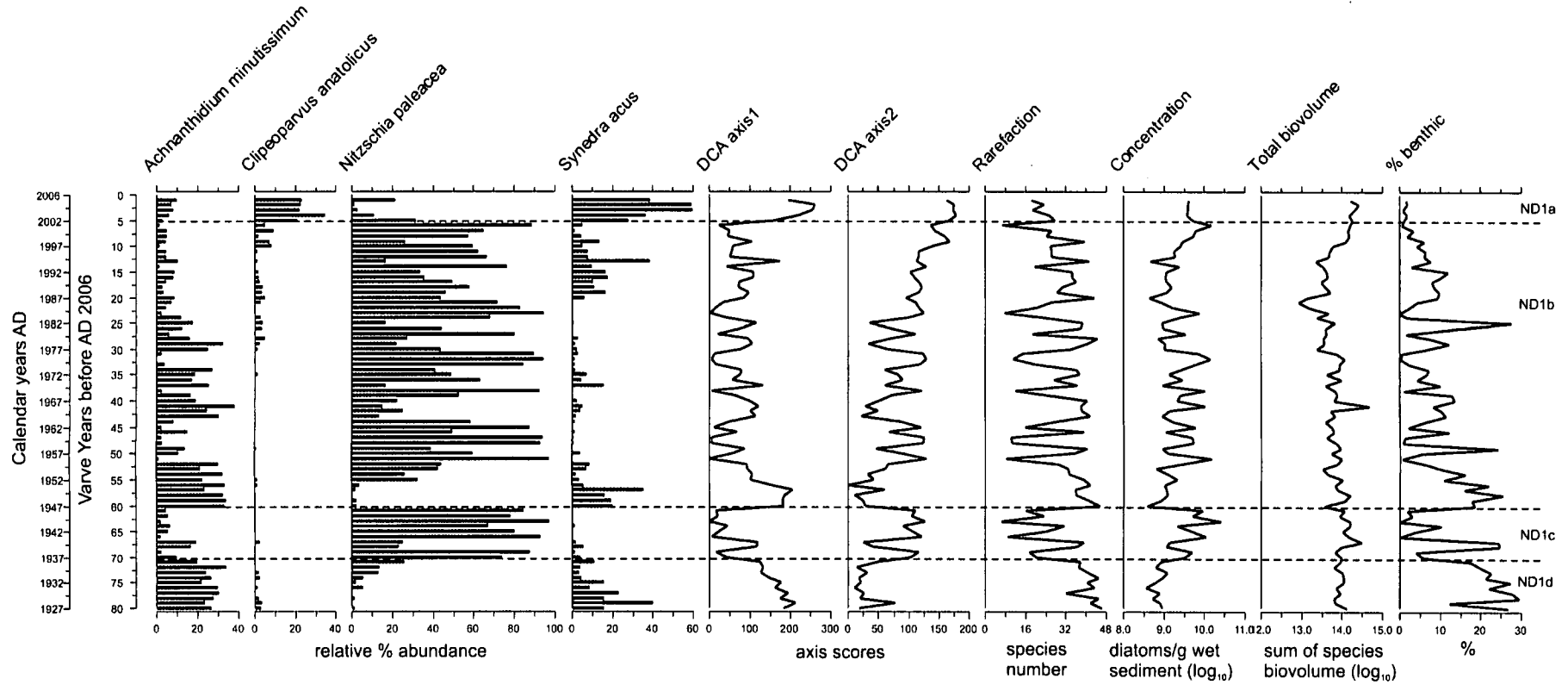


Figure 5.15 (a) NAR06 diatom stratigraphy (species >10%) presented with DCA axes 1 and 2, rarefaction, concentration (diatoms/g wet sediment) (\log_{10}), total biovolume (μm^3) (\log_{10}) and % benthic taxa.

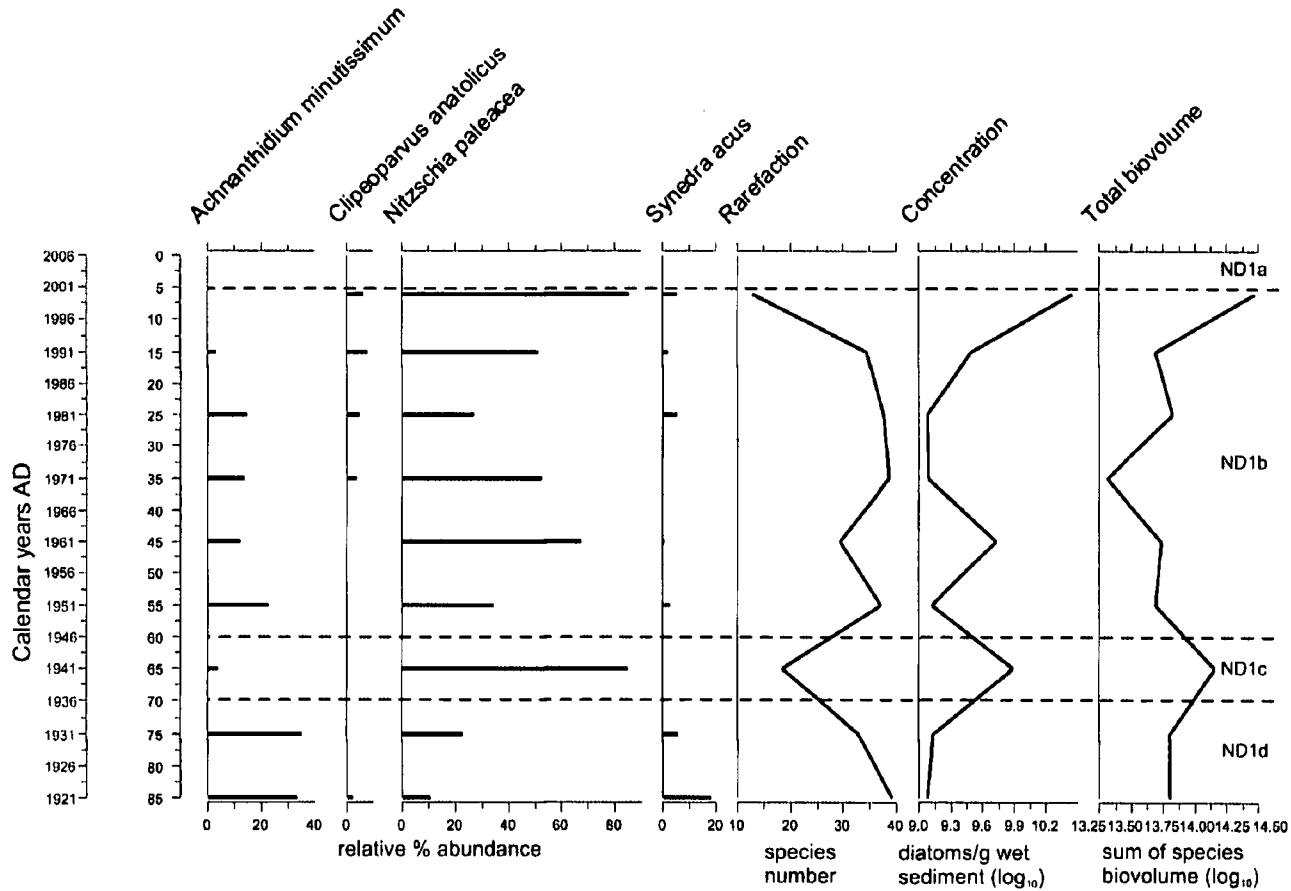


Figure 5.15 (b) The most recent 85 VY of the NAR01/02 decadal record (species >10% in NAR06 record) for comparison with the NAR06 annual record, presented with rarefaction, concentration (diatoms/g wet sediment) (\log_{10}) and total biovolume (μm^3) (\log_{10}).

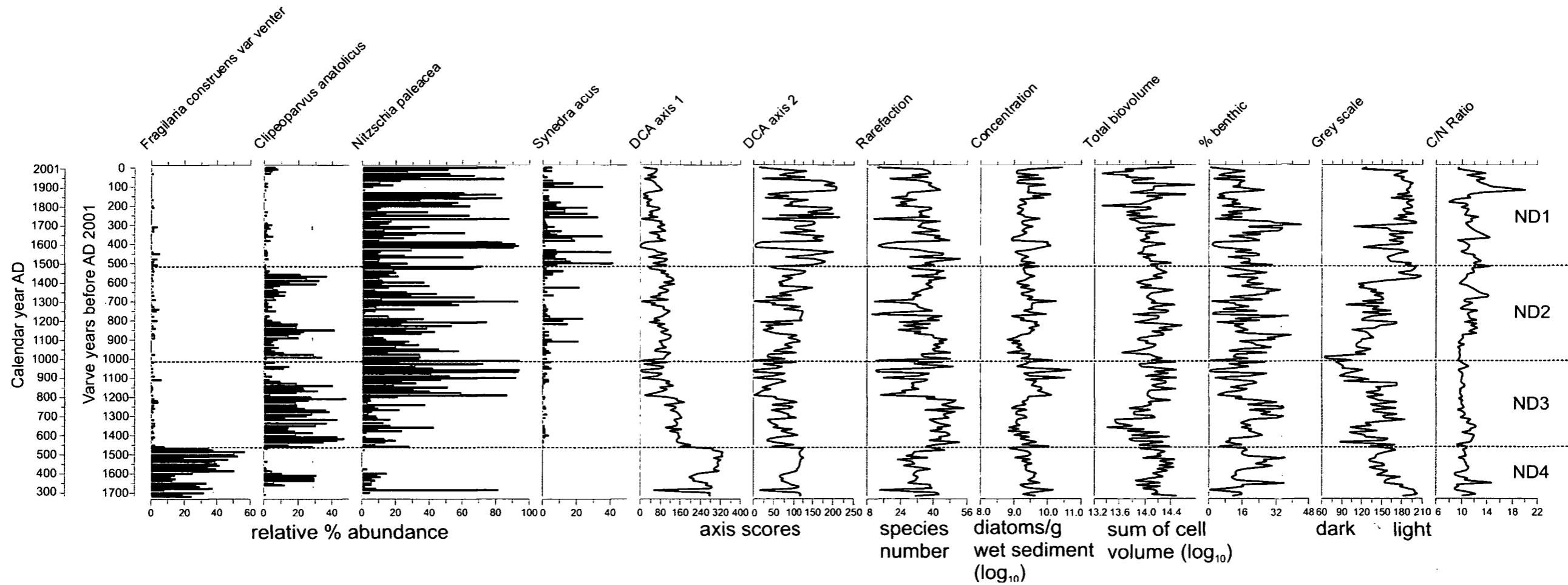


Figure 5.16 NAR01/02 diatom stratigraphy (species >10%) presented with DCA axes 1 and 2, rarefaction, concentration (diatoms/g wet sediment) (\log_{10}), total biovolume (μm^3) (\log_{10}), % benthic taxa, grey scale value and carbon/nitrogen ratio (C:N).

5.3.9 Biovolume

Nar diatom species cell dimensions and biological-volume (biovolume) varied considerably. For example, *Campylodiscus clypeus* has a volume of $57,020 \mu\text{m}^3$, whereas *Cymbella microcephala* has a volume of just $13 \mu\text{m}^3$ (see Appendix 3 for species dimensions and biovolume). In percentage counts, one cell of these differently sized species carries the same weighting. Figure 5.17 illustrates the extreme variation in diatom cell size at Nar; *C. clypeus* is pictured with a *N. paleacea* ($59 \mu\text{m}^3$) specimen on the left and some *C. anatolicus* ($113 \mu\text{m}^3$) examples to the right. Species biovolume was calculated for the NAR01/02 and NAR06 samples in order to provide an alternative to percentage data and analyse diatom palaeo-productivity.

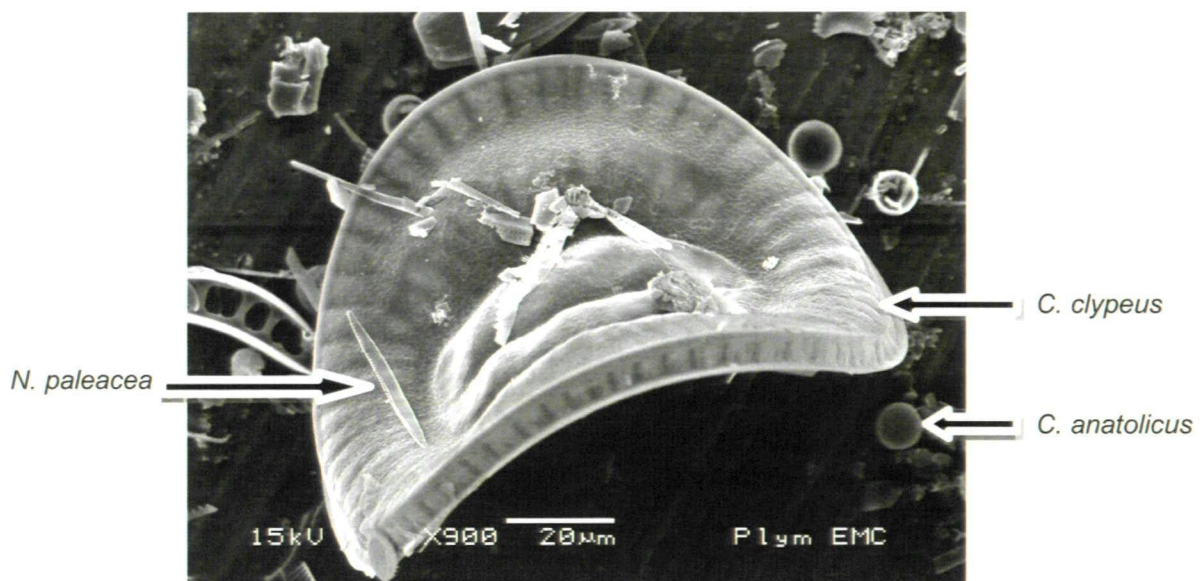


Figure 5.17 SEM image of *Campylodiscus clypeus* with *Nitzschia paleacea* and *Clupeoparvus anatolicus* specimens to illustrate variation in diatom cell size and biovolume.

Biovolume data for the NAR06 record revealed increased weighting of *C. clypeus* and *R. gibba* (Figure 5.18). Zones ND1d and ND1c were characterised by *Pinnularia*

viridis, another species not recognised as significant according to percentage data.

Smaller species, abundant in the percentage diagrams, such as *C. anaticus*, were not as significant in the NAR06 biovolume graph. *N. paleacea* has decreased weighting and *N. oblonga* is an important member of the diatom population through all zones.

Although the weighting of species altered according to biovolume, the zone boundaries remain unchanged. Therefore it appears that environmental fluctuations influenced both smaller and larger diatom species simultaneously at Nar. The biovolume NAR06 DCA ordination plot (Figure 5.20) revealed a similar pattern to that based on percentage data, with samples from ND1a most dissimilar to other samples. Zones ND1b and ND1c appeared more distinct from one another; this is associated with the increased weighting of *N. oblonga* and *C. clypeus* in ND1c.

The diatom stratigraphy of the NAR01/02 record is plotted according to biovolume in Figure 5.19. Overall biostratigraphic change is similar to percentage data. However, the relative weighting of certain smaller/larger species altered considerably. The major assemblage change between zones ND4 and ND3 is evident through species that were not dominant in the percentage diagrams. For example, according to biovolume, *C. clypeus* and *N. halophila* characterise ND4, along with *R. operculata* and *C. meneghiniana*. This zone is also associated with lower values of *N. oblonga* and *R. gibba*, common in ND3. Small species, that were abundant according to percentage data, are no longer as significant (e.g. *N. paleacea*, *C. anaticus* and *F. construens* var. *venter*). The DCA ordination plot for NAR01/02 biovolume data (Figure 5.21) highlights the distinct composition of ND4, associated with the fact that this zone was composed primarily of larger species. Zone ND1, composed mainly of smaller species, merges with ND2 and ND3 in the ordination plot, due to smaller diatoms carrying less

weight. Additionally, the biovolume data are less ‘noisy’ than percentages; this appears to be associated with the decreased weighting of the small bloom species *N. paleacea*. Considering these patterns, it appears that biovolume can provide valuable additional information about diatom assemblage change.

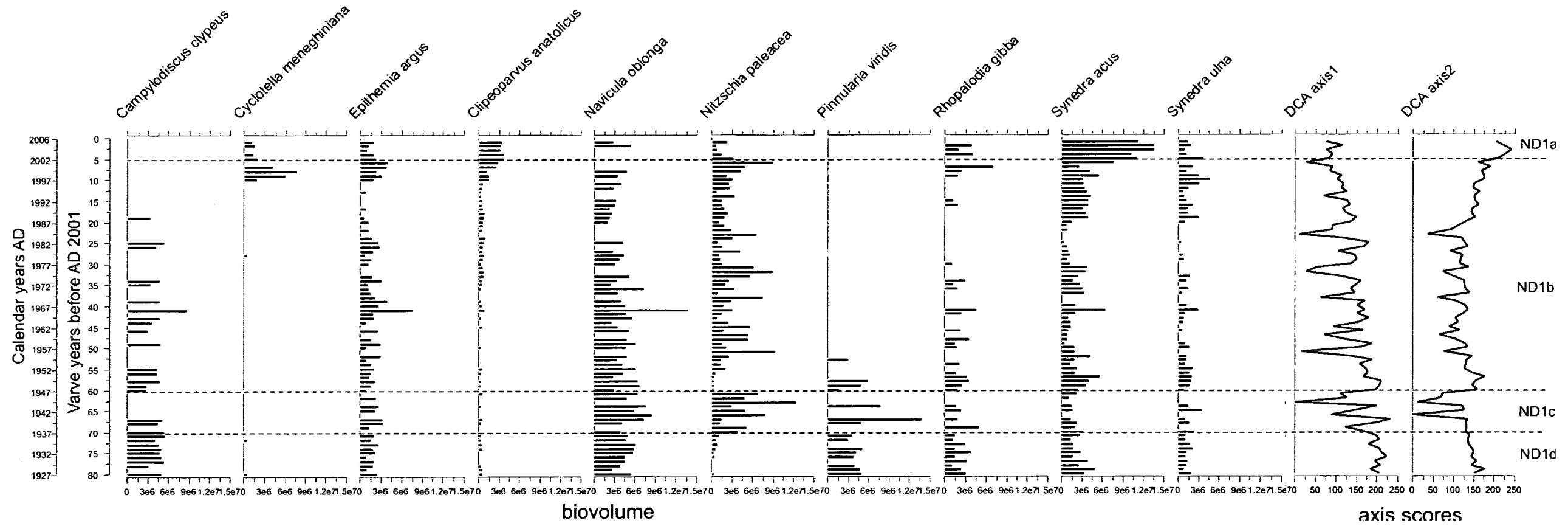


Figure 5.18 NAR06 diatom stratigraphy plotted according to biovolume (μm^3) (power transformed) with DCA axes 1 and 2 based on biovolume. Species included have a maximum of at least $5.0e^{+06}$ (μm^3). All species are plotted on the common scale $0-5.0e^{+07}$ (μm^3).

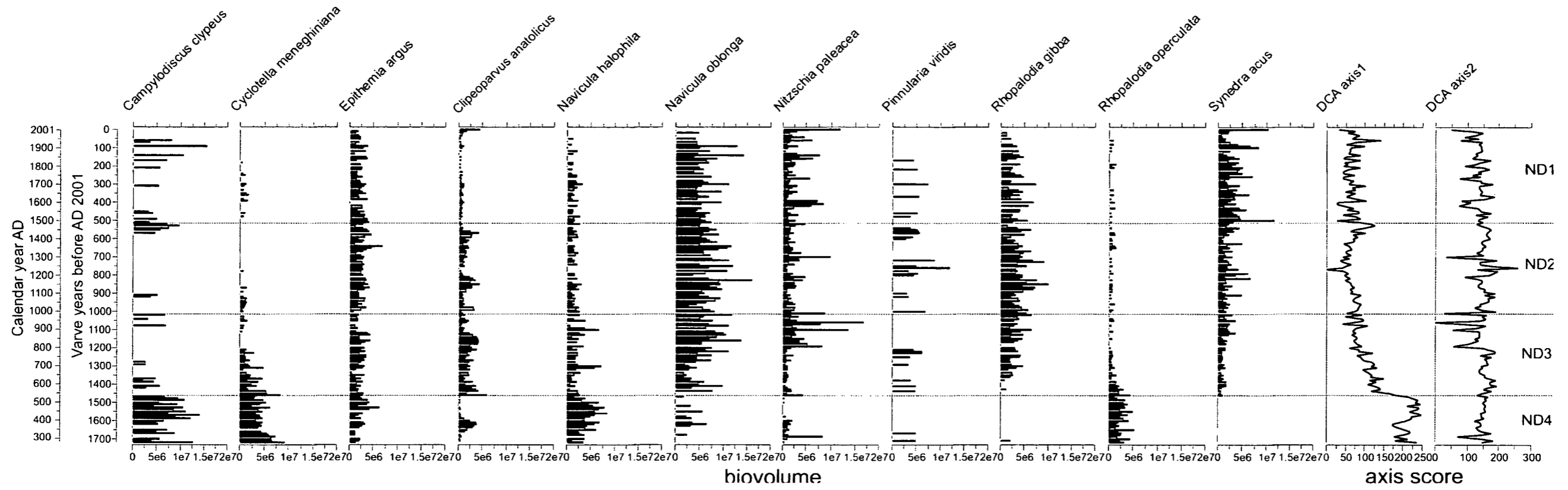


Figure 5.19 NAR01/02 diatom stratigraphy plotted according to biovolume (μm^3) (power transformed) with DCA axes 1 and 2 based on biovolume. Species included have a maximum of at least $3.6e^{+06}$ (μm^3). All species are plotted on the common scale $0-2.0e^{+07}$ (μm^3).

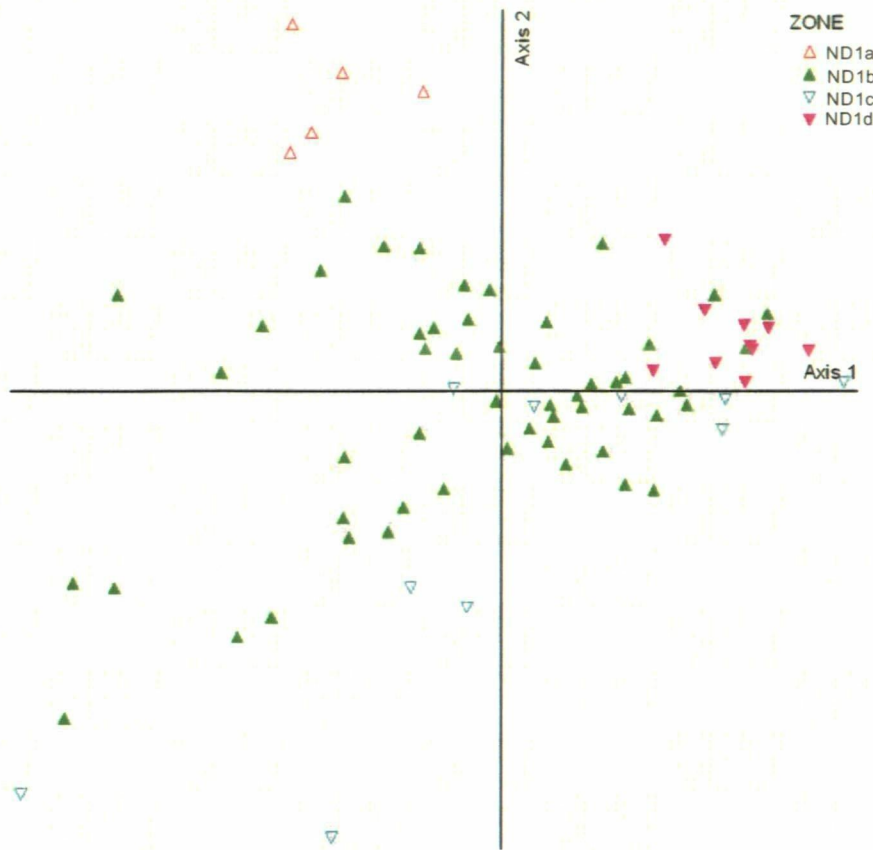


Figure 5.20 DCA ordination plot for NAR06 diatom biovolume data. Symbols correspond to percentage data cluster analysis zones.

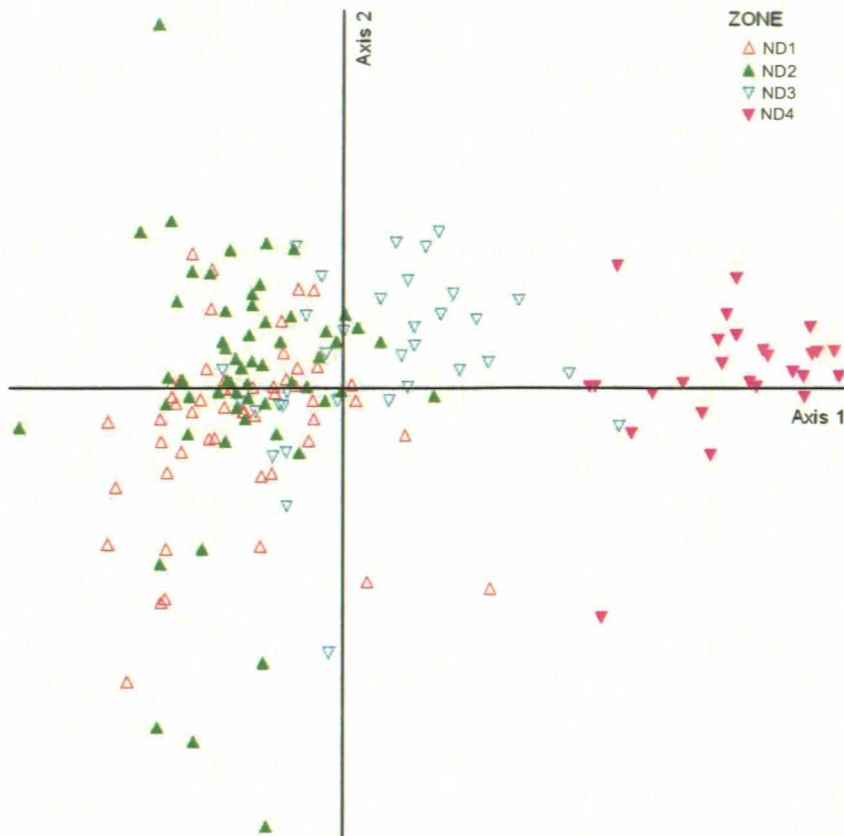


Figure 5.21 DCA ordination plot for NAR01/02 diatom biovolume data. Symbols correspond to percentage data cluster analysis zones.

5.3.10 NAR01/02 core thin sections

Core thin section slides comprise undisturbed 30 μm thick sediment (each slide included ~17 lamina subsections) from the NAR01/02 sequence for the last ~900 years (AD 1100-2002). Thin sections allowed the diatom assemblage to be microscopically observed *in situ*. Varves comprise carbonate (white), grey clastic, brown organic (containing a mixture of diatom species) and distinct single species diatom bloom layers. The changing thickness of varve sub-layers and frequency of bloom events was analysed for comparison with percentage data and to provide additional information about the diatom palaeo-assemblage.

The diatom stratigraphy of the NAR01/02 thin sections is presented in Figures 5.22 and 5.23. The amalgamated widths (μm at x40 magnification) of specific layers within a varve are displayed for the most recent 80 VY and the last 900 VY. The graphs reveal that distinct bloom layers of *N. paleacea* and *S. acus* are common within the Nar sediment profile and *S. parvus* bloomed for ~20 VY (AD 1205-1246). White layers illustrate the volume of carbonate in the system and brown layers, composed primarily of diatoms, non-siliceous algae and other organic and inorganic material, give an indication of productivity. Grey clastic layers contained little organic material and may represent turbidite events, which involve sudden movement and deposition of sediment within the lake.

The 80 VY thin section graph (Figure 5.22) revealed that *N. paleacea* bloomed throughout the record, *S. acus* bloomed between 30-14 VY (AD 1974-1990) and carbonate and varve thickness increased during the most recent 5 VY (AD 1999-2002). Comparison of this diagram with the NAR06 diagram (Figure 5.11) has revealed that *N. paleacea* and *S. acus* blooms are far more frequent in the percentage record in comparison with the core thin sections. This may be due to the possibility that blooms need to be extremely large in order to form a distinct layer within the varve and therefore only particularly high blooms are recorded in the thin sections. The number of *N. paleacea* blooms comprising above 80% of the population in the NAR06 graph (15) is equal to the number of blooms observed in the thin sections during the most recent 80 VY. Higher percentages of *S. acus* began at 20 VY (AD 1987) in the NAR06 graph. This does not coincide with the appearance of *S. acus* blooms in the thin sections beginning at 32 VY (AD 1970), which implies that this part of the thin section record

does not reliably reflect the sediment cores or other species may have altered the relative percentage of *S. acus* during this period.

The 900 VY thin section record (Figure 5.23) revealed that white/brown layers and varve thickness increased throughout this period. *S. acus* blooms have become increasingly common since 500 VY (AD 1500). This coincided with the rise of this species in zone ND1 (Figure 5.12) evident in the percentage data. *N. paleacea* blooms have become more common since 230 VY (AD 1770). The *S. parvus* blooms ~750 VY (AD 1230) coincided with the timing of increased percentages of this species in the NAR01/02 record. However, the bloom layer thickness of this small species is not as extreme as the high cell counts. Similarities also exist between different characteristics of the diatom assemblage and the thin section measurements. For example, varve thickness is positively correlated with NAR06 diatom concentration ($r=0.339$, $p=0.003$) and negatively correlated with species diversity ($r=-0.234$, $p=0.042$), indicating that thicker varves contain a greater number of cells and a less diverse diatom assemblage.

Figure 5.24 illustrates temporal change in the frequency of thin section species bloom events and clastic layer formation. Single species blooms have become increasingly frequent throughout the last ~400 VY (AD 1600), most commonly involving *N. paleacea*. The frequency of clastic events has also increased during the most recent 100 VYs of the record. Figure 5.25 shows the average thickness of varve thin section sub-layers throughout the NAR01/02 record. White and brown layers were relatively consistent in thickness throughout the last 900 years, with a slight increase during the most recent 200 VYs; this is likely to be associated with decreased compaction and higher water content of sediments nearer the profile surface. Varve thickness has

increased throughout the last 400 VYs; this is associated with the increasing number of diatom bloom events during this period.

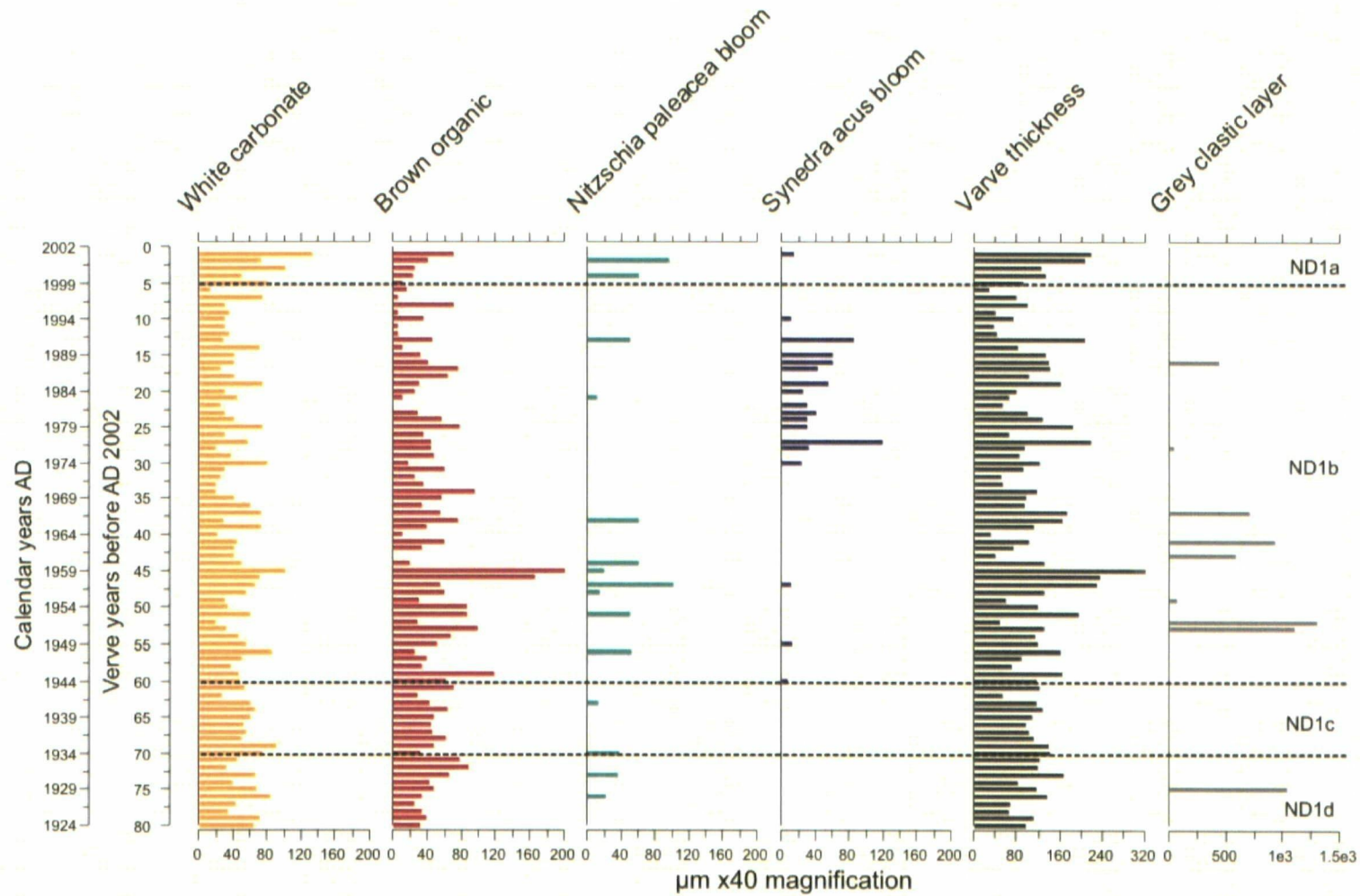


Figure 5.22 NAR01/02 core thin section stratigraphy with measurements of white carbonate, brown organic, grey clastic, diatom bloom and total varve thickness for the most recent 80 VY (AD 1924-2002).

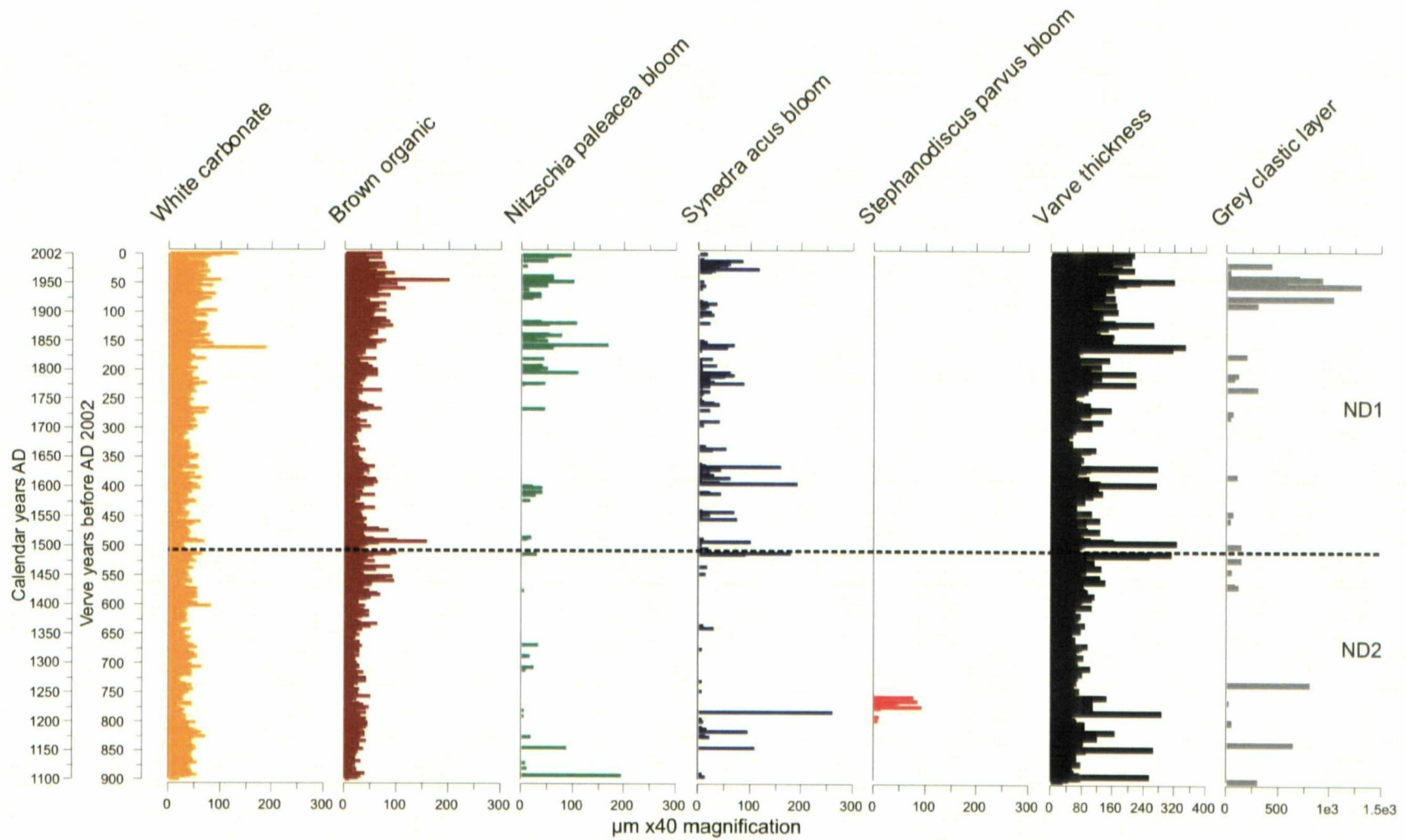


Figure 5.23 NAR01/02 core thin section stratigraphy with measurements of white carbonate, brown organic, grey clastic, diatom bloom and total varve thickness for the last 900 VY (AD 1100-2002).

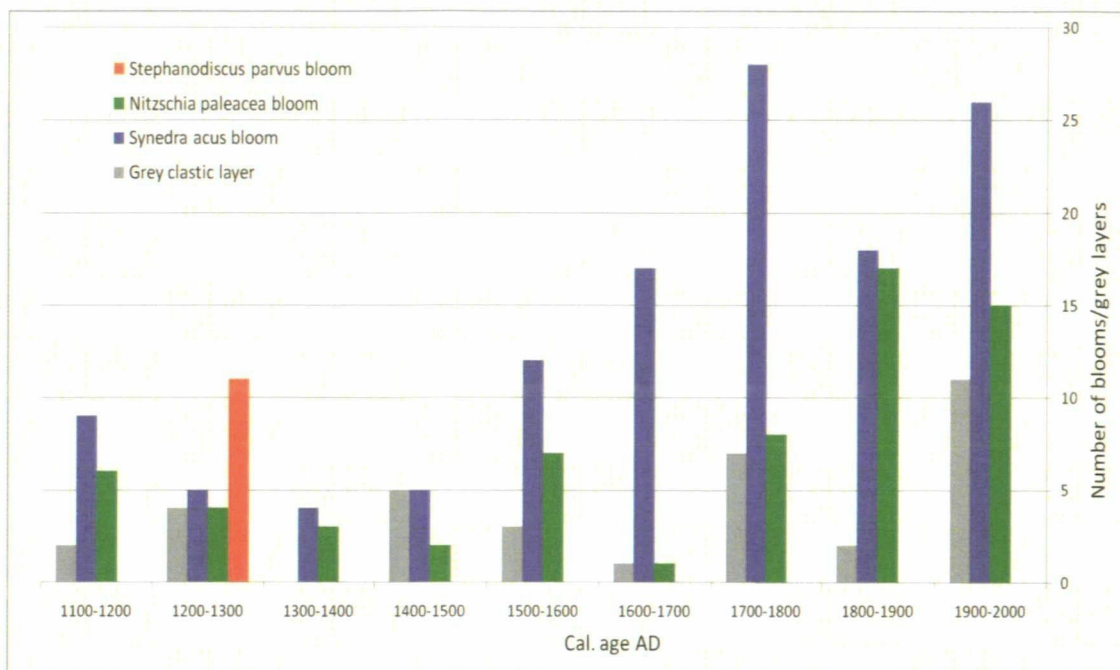


Figure 5.24 NAR01/02 thin section diatom bloom and clastic event frequency per hundred years for the last 900 varve years (AD 1100-2000).

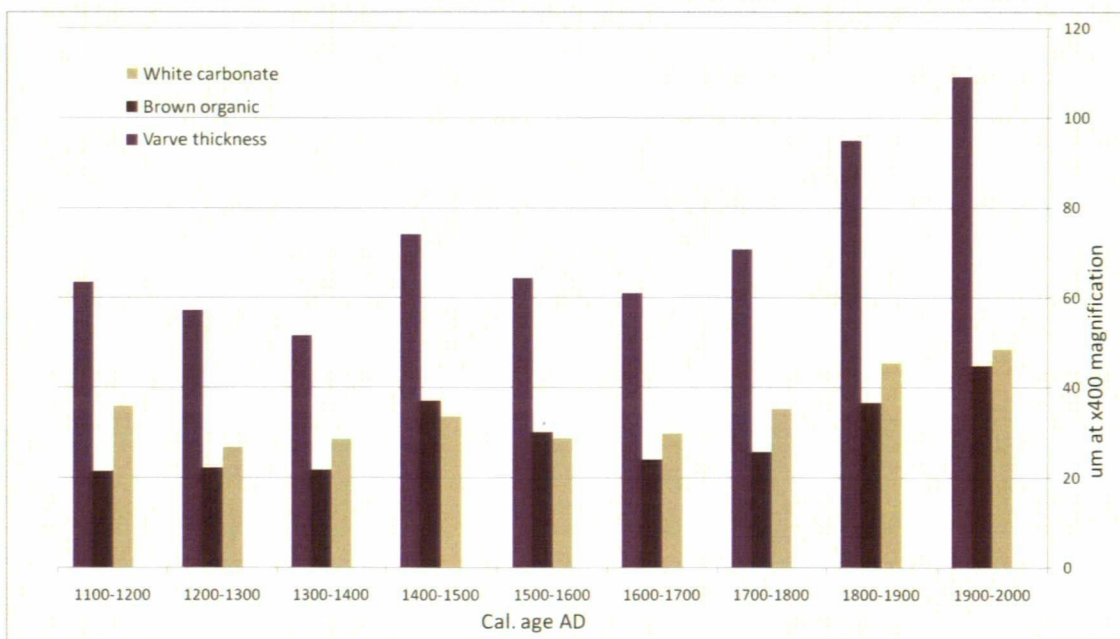


Figure 5.25 NAR01/02 thin section average white/brown layer and varve thickness (μm at x40 magnification) per hundred years for the last 900 varve years (AD 1100-2000).

5.3.11 Environmental reconstructions

Transfer functions were employed in order to infer palaeo-conductivity and total phosphorus (TP) from the Nar fossil diatom assemblages. Reconstructed diatom-inferred (DI) conductivity and TP for the NAR01/02 and NAR06 records, based on training sets from the European Diatom Database (EDDI) (Juggins, 2008), are presented in Figures 5.26 and 5.27. The combined salinity modern training set was identified as possessing the highest number of matching analogue diatom species in the Nar fossil assemblage using the modern analogue technique (MAT) (Table 5.6). The MAT was used to calculate the percentage of the diatom assemblage in each fossil sample represented in the modern training set and an average was taken for all samples. Weighted Averaging (WA) with inverse deshrinking and (Weighted) W-MAT by squared chord distance were identified as the models with highest predictive ability (r) and lowest prediction errors (RMSEP). In comparison with diatom-inferred conductivity r and RMSEP values in transfer function research in Africa by Gasse *et al.* (1995), in Australia by Gell (1997) and in North America by Laird *et al.* (1998), the EDDI datasets have similar predictive ability, i.e. r values in the range of 0.8. However, the EDDI training sets have higher prediction errors with RMSEP values higher than those in the literature.

Training set and model	Ave. % fossil sample in training set NAR01/02	Ave. % fossil sample in training set NAR06	<i>r</i> value	<i>f</i> _{boot-strapped} (1000)	RMSEP μS^{-1} (\log_{10})
Combined salinity (EDDI participants, 1960-1996)	74.4	90.57			
WA Inv			0.85	0.77	0.47
WMAT c dist²			0.80	0.80	0.45
African salinity (F. Gasse, 1960-1986)	70	88.65			
WA Inv			0.84	0.76	0.46
WMAT c dist²			0.79	0.79	0.45
CASPIA salinity (S. Juggins and J. Reed, 1996)	55.98	66.23			
WA TOL Inv			0.92	0.83	0.54
WMAT c dist²			0.80	0.80	0.58
Spanish salinity (J. Reed, 1990-1993)	34.28	35.79			
Combined TP (EDDI participant, 1900-1998)	69.38	85.58			
WA TOL Inv			0.76	0.69	0.33
WMAT c dist²			0.72	0.73	0.31
Gasse <i>et al.</i> (1995)					
WA Inv			0.8	0.8	0.3
WA Classical			0.9	0.8	0.2
Laird <i>et al.</i> (1998) WA			0.99		
Gell (1997) WA			0.79		0.29

Table 5.6 Training set and model performance comparisons using datasets from the European Diatom Database (EDDI) (Juggins, 2008) and diatom-conductivity reconstruction studies by Gasse *et al.* (1995), Gell (1997) and Laird *et al.* (1998).

Specific Electrical Conductivity (SEC) (μS^{-1}) provides a measure of total water solutes and can be used as a proxy for salinity in concentrated lake systems. Reconstructed conductivity values by WA for the NAR06 record (Figure 5.26) fluctuated and appeared highly related to the abundance of *N. paleacea*. The MAT gave a similar pattern with

increasing conductivity values in the most recent sediment. Conductivity values, based on WA models, appear related to the dominant species, *N. paleacea*. The MAT gives less weighting to the dominant species and reconstructs conductivity based on an average of the 10 closest matching analogue sites.

WA reconstructions for the NAR01/02 record indicated fluctuating conductivity throughout the last 1720 VYs with a significant period of elevated values in zone ND4 (Figure 5.27). Reconstructions based on W-MAT also indicated a period of higher conductivity in zone ND4, with fluctuating levels throughout zones ND3, ND2 and ND1. Reconstructed conductivity varied throughout the NAR01/02 record between a maximum of $5,531 \mu\text{S}^{-1}$ at 1560 VY (AD 450) and a minimum of $124 \mu\text{S}^{-1}$ at 0 VY (AD 2000). Average diatom-inferred (DI)-conductivity during ND4 = $3,545 \mu\text{S}^{-1}$, ND3 = $1,078 \mu\text{S}^{-1}$, ND2 = $569 \mu\text{S}^{-1}$ and ND1 = $485 \mu\text{S}^{-1}$. This implies that Nar lake water has become less concentrated throughout the last 1720 VYs or shifts in brine type could have altered the relationship between conductivity and salinity.

Average DI-conductivity for the NAR06 record was $422 \mu\text{S}^{-1}$. This value is similar to the average reconstructed conductivity for NAR01/02 zone ND1. However, reconstructed conductivity at AD 2000 differs between the NAR06 ($197 \mu\text{S}^{-1}$) and NAR01/02 records, such discrepancies are likely to be associated with the three and one-year sampling difference between the sequences. The fact that the reconstructions are similar highlights that the cores replicate. Although absolute values may not have been reconstructed correctly, it is possible to observe relative fluctuations in conductivity levels. The fact that one of the most dominant species, *C. anatolicus*, does not have a modern analogue, presents problems when reconstructing conductivity.

Therefore reconstructed values for samples where this species is dominant have been interpreted with caution.

Diatom-transfer functions can also be used to infer palaeo-lake nutrient levels (e.g. Barker *et al.*, 2005). A number of species at Nar, such as *N. paleacea*, are interpreted as indicators of nutrient enrichment. Therefore, transfer function reconstructions were carried out for total phosphorus (TP) using the EDDI combined TP training set. The best model performance was identified as tolerance down-weighted WA with inverse deshrinking and W-MAT with squared chord distance (Table 5.6).

TP reconstructions for the NAR01/02 record suggested that the transition between zones ND4 and ND3 experienced an increase in TP with higher levels also apparent in the most recent sediments (Figures 5.26 and 5.27). WA and the MAT provided comparable results. Similar TP values were reconstructed for AD 2000 in the NAR06 ($184 \mu\text{g/l}^{-1}$) and NAR01/02 ($207 \mu\text{g/l}^{-1}$) records. Reconstructed TP for the NAR06 record revealed a general increasing trend towards the most recent sediment. TP ranged in the NAR01/02 record between $272 \mu\text{g/l}^{-1}$ at 1550 VY (AD 560) and $37 \mu\text{g/l}^{-1}$ at 120 VY (AD 1880), which corresponds with the peak in the C:N ratio. The average for ND4 = $130 \mu\text{g/l}^{-1}$, ND3 = $141 \mu\text{g/l}^{-1}$, ND2 = $138 \mu\text{g/l}^{-1}$ and ND1 = $107 \mu\text{g/l}^{-1}$. Summer 2008 chemistry analysis revealed Nar lake water to contain no biologically-available phosphate. This implies that reconstructed TP values are likely to be unreliable or summer values are not representative of annual average lake phosphorus levels. TP may increase during spring following thermocline breakdown.

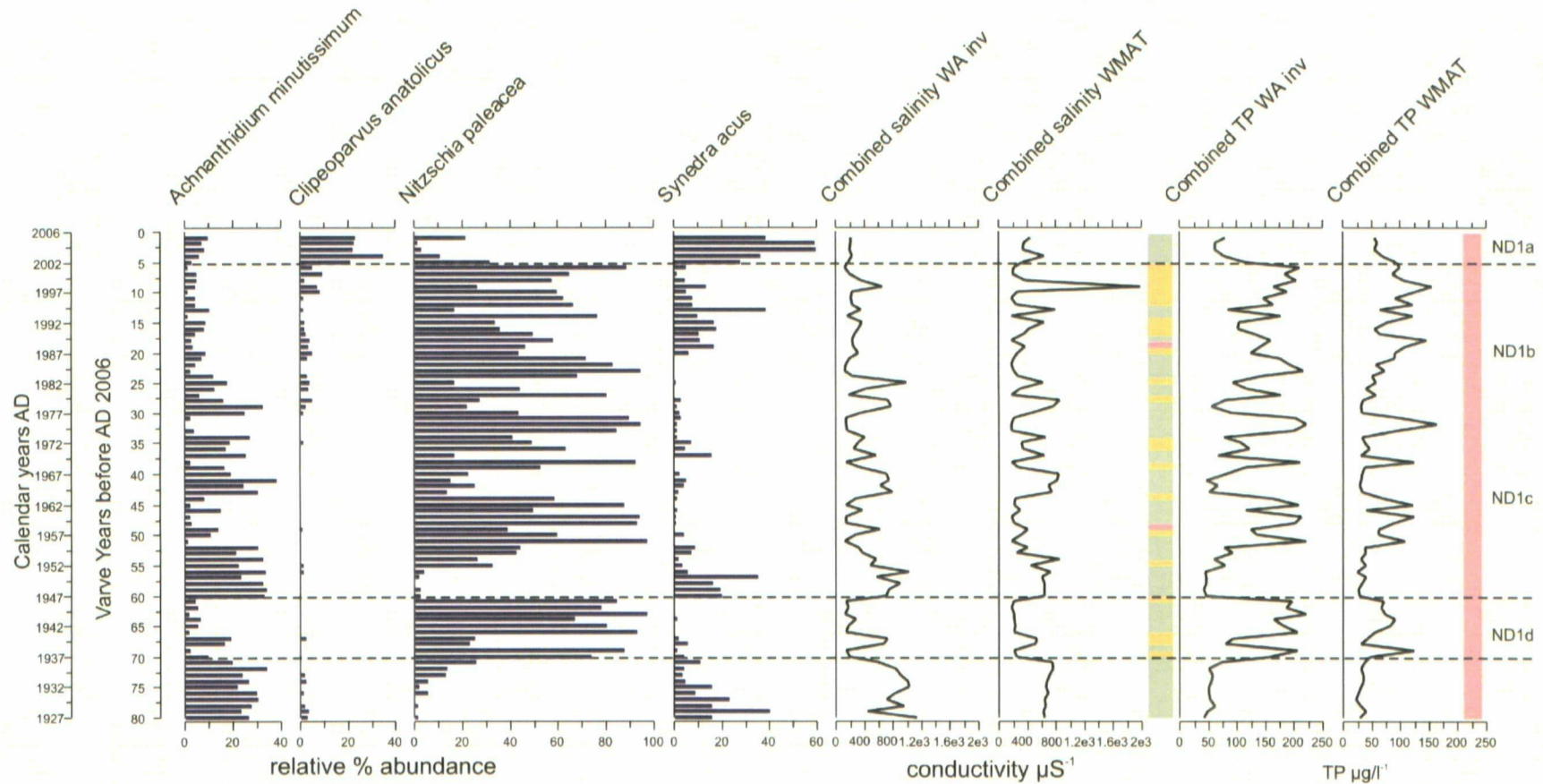


Figure 5.26 NAR06 diatom stratigraphy (species >20%) with reconstructed conductivity (μS^{-1}) and total phosphorus (TP) ($\mu\text{g/l}$) based on the combined training sets from EDDI using weighted averaging and the MAT. Coloured bars represent sample analogue matching with modern training set (green = good modern analogue, yellow = no good analogue and pink = no close analogue).

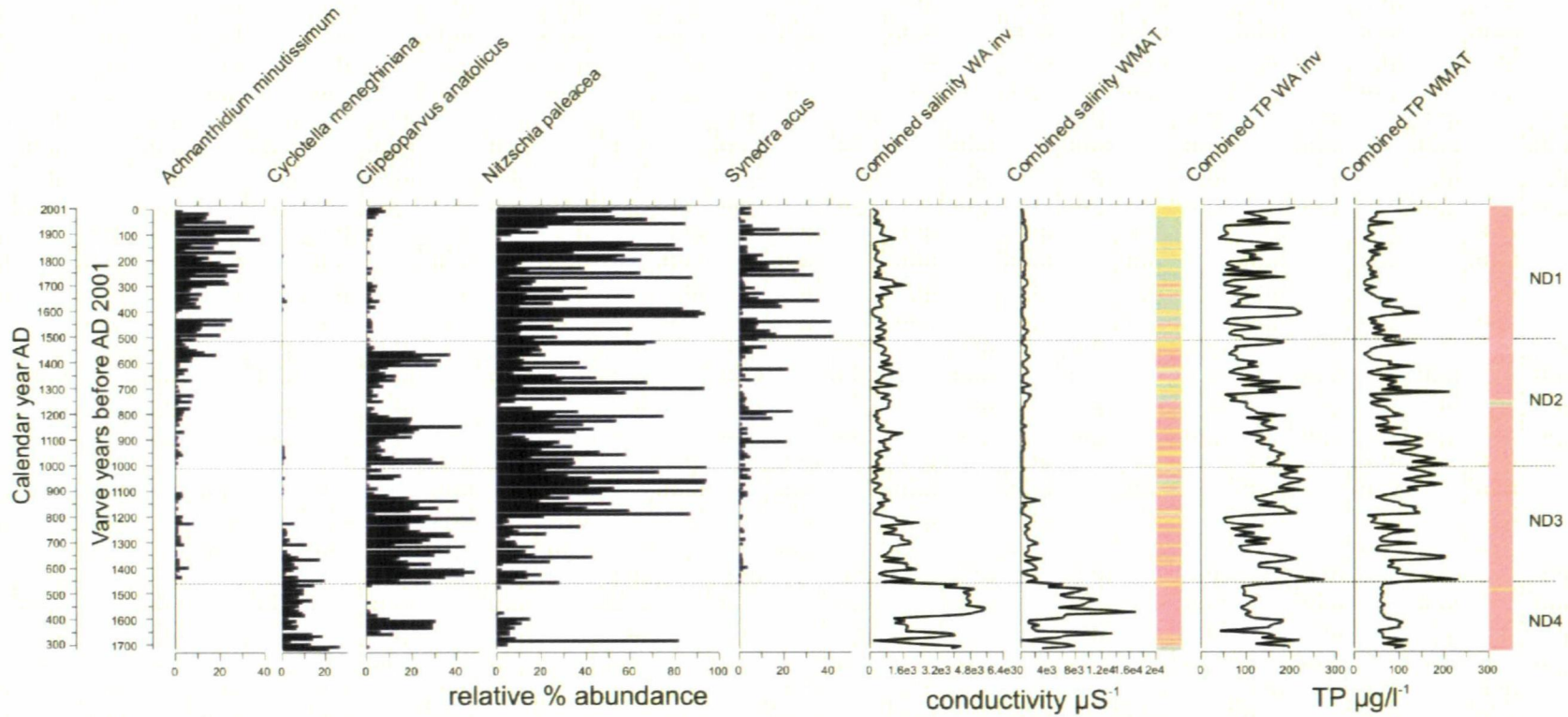


Figure 5.27 NAR01/02 diatom stratigraphy (>20%) with reconstructed conductivity (μS^{-1}) and total phosphorus (TP) ($\mu\text{g/l}$) based on the combined training sets from EDDI using weighted averaging and the MAT. Coloured bars represent sample analogue matching with modern training set (green = good modern analogue, yellow = no good analogue and pink = no close analogue).

5.3.12 Analogue matching

Analogue analysis can be performed to evaluate how sufficiently fossil samples are represented in the modern diatom training set (Laird *et al.*, 1998) and thus assess the reliability of the reconstruction. This was achieved by calculating and comparing the minimum dissimilarity coefficients (min. DC) of fossil and training set samples using the MAT. The extreme 5% and 10% min. DC of the modern samples was used to define critical values to determine whether fossil samples have a good modern analogue (Birks, 1995). These values were identified as 121 and 109 respectively for the combined salinity training set. Fossil samples with a high min. DC contain species that are not well represented in the modern environment. Such samples were identified as having 'no good' (>109) and 'no close' (>121) modern analogues in the training set. Samples with a min. DC below 109 were considered to have a 'good' modern analogue.

Analogue matching for each fossil sample is presented on the coloured bars in Figures 5.26 and 5.27. Green bars illustrate samples with a 'good', yellow indicates 'no good' and red represents 'no close' modern analogue. Only 26.9% of the fossil samples in the NAR01/02 dataset were identified as possessing a good modern analogue in the training set. The highest number of no good analogues occurred when *C. anaticus* was dominant and in zone ND4. Therefore conductivity reconstruction for these zones should be interpreted with caution. 70% of fossil samples within the NAR06 record possessed a good modern analogue; therefore reconstructed conductivity for this record can be interpreted with greater confidence.

Assessing the reliability of the TP reconstruction for the NAR01/02 record revealed that 98.2% of fossil samples had no close modern analogue and all of the NAR06 samples

had no close analogue. Consequently, the TP reconstructions are considered unreliable. The only fossil samples with a good modern analogue were those that experienced a bloom of *S. parvus* at a depth of 750-760 VY; therefore reconstructed TP for this period may be more reliable.

5.3.13 Nar DI-conductivity with and without *C. anaticus* and bloom species

Bloom species (*N. paleacea*, *S. acus* and *S. parvus*) can swamp the diatom assemblage and result in extreme variability in the relative percentages of different species.

Differences may also exist in the palaeo-climate signal from bloom species and the remainder of the diatom assemblage. Additionally, *C. anaticus* had no analogue in the modern training set and reduced the relative percentages of species with good matching analogues. Consequently, conductivity reconstructions have been performed firstly omitting *C. anaticus*, *N. paleacea*, *S. acus* and *S. parvus* from the assemblage and secondly based on bloom species only.

Non-analogue problems, associated with the presence of the new species (*C. anaticus*), were identified early in the counting process. Therefore total counts were made large enough for analyses to still be statistically viable when removing *C. anaticus* from the dataset. However, bloom species comprise a high proportion of many counts. Omitting these species has resulted in some sample counts of just 30 valves or less. Therefore results need to be interpreted with caution, as the small counts are not statistically robust. Additionally, as bloom species are not prolific every year, this has resulted in samples lacking a bloom event remaining at ~300 valves and samples with a bloom having severely reduced counts. Species percentages were

recalculated, based on bloom species only and omitting bloom species. When values were not recalculated, a similar reconstruction was produced.

The NAR01/02 combined salinity transfer function was run omitting *C. anaticus* from the dataset. This did not alter the reconstruction, as this species would have been ignored by the transfer function initially. However, the number of good modern analogue samples increased to 35.7%, in comparison with 26.9% when this species was included in the dataset. Therefore, even when *C. anaticus* was removed from the dataset, there were still a significant number of samples without a good modern analogue. For the NAR06 record, the number of good modern analogues with *C. anaticus* alone omitted was 73.8% and with both *C. anaticus* and the bloom species omitted, there were no good and no close modern analogues. Therefore the NAR06 reconstruction omitting bloom species is statistically unreliable. Coloured bars are included to highlight samples with extremely low valve counts as a result of removing or including only bloom species (pink = total valve count less than 50 and green = total valve count more than 50).

The NAR06 reconstruction based on bloom species alone revealed conductivity peaks at 80-75 VY (AD 1927-1932), 63-55 VY (AD 1944-1952) and in the most recent 5 VY (AD 2002-2006) (Figure 5.28). It appears that *N. paleacea* is a species that favours low salinity and high nutrients, whereas *S. acus* favours higher salinity and low nutrients. Reconstructed conductivity for the NAR06 record, omitting bloom species revealed peaks in conductivity at 65 VY (AD 1942), 28 VY (AD 1979) and 10-7 VY (AD 1997-2000) (Figure 5.29). The peak around AD 2000 is related to the appearance of *C. meneghiniana*, which is an indicator of higher conductivity.

The conductivity reconstruction for the NAR01/02 record (Figure 5.30), omitting bloom species, has revealed that zone ND4 remains distinct, with a period of higher conductivity and an additional smaller peak in conductivity in zone ND3 between 1200-1100 VY (AD 800-900). Conductivity levels remained relatively stable throughout the remainder of the record. The reconstruction, based on bloom species alone, differed considerably from the original reconstruction (Figure 5.31). Percentages were not recalculated due to the absence of bloom species in ND4. The same pattern as that in the NAR06 record is evident, with *N. paleacea* relating to periods of decreased conductivity and increased nutrients and *S. acus* indicating periods of increased conductivity and decreased nutrients. Throughout zone ND4, when only *N. paleacea* was present and often in small numbers, the reconstruction does not appear to have performed correctly. This is probably due to the fact that the reconstruction could not be performed on extremely low values of one species. Conductivity levels fluctuate greatly throughout the record, in accordance with variations in the percentages of different bloom species. Although reconstructions omitting bloom species are likely to be unreliable, this has provided additional information about the palaeoenvironment for consideration.

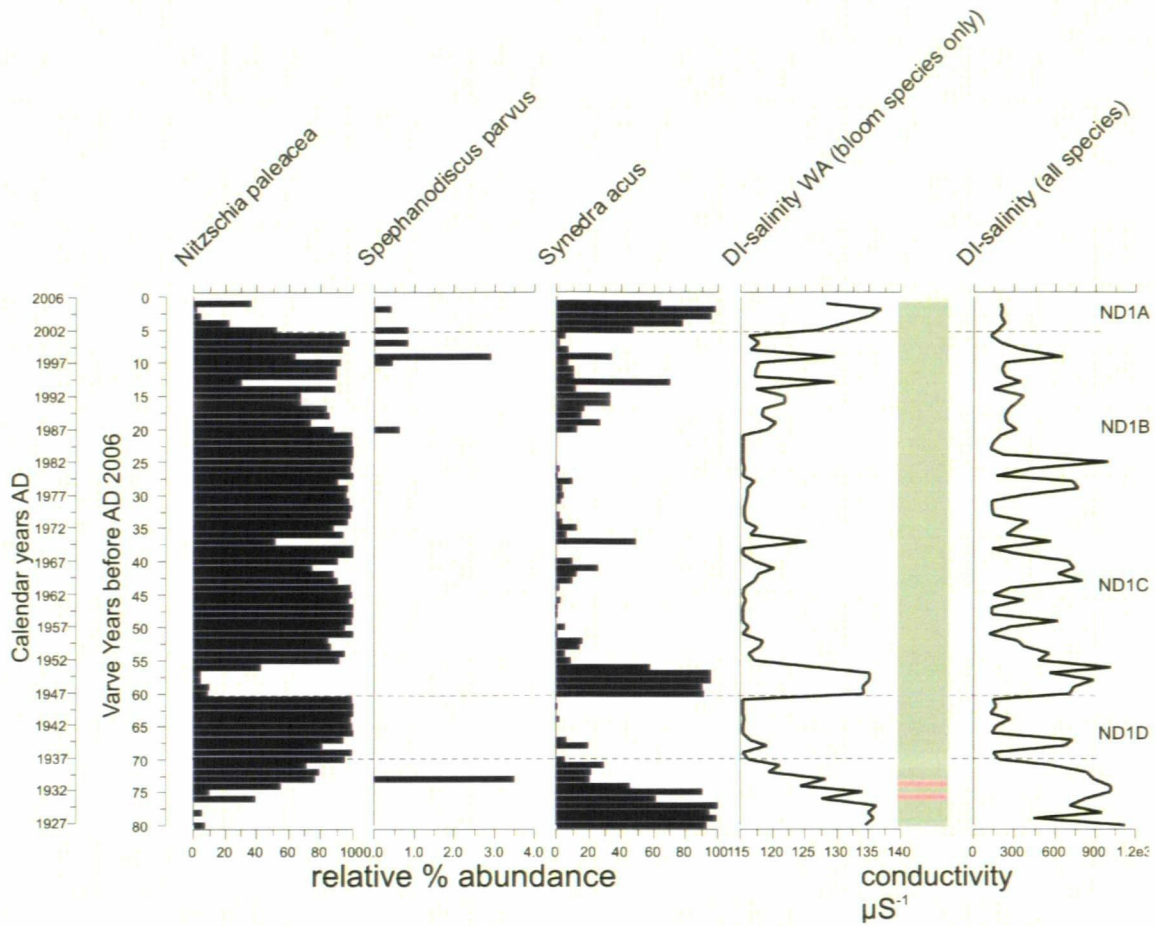


Figure 5.28 NAR06 diatom stratigraphy with reconstructed conductivity based on bloom species *N. paleacea* and *S. acus* only. Coloured bar highlights samples with a diatom valve count above 50 (green) and below 50 (pink).

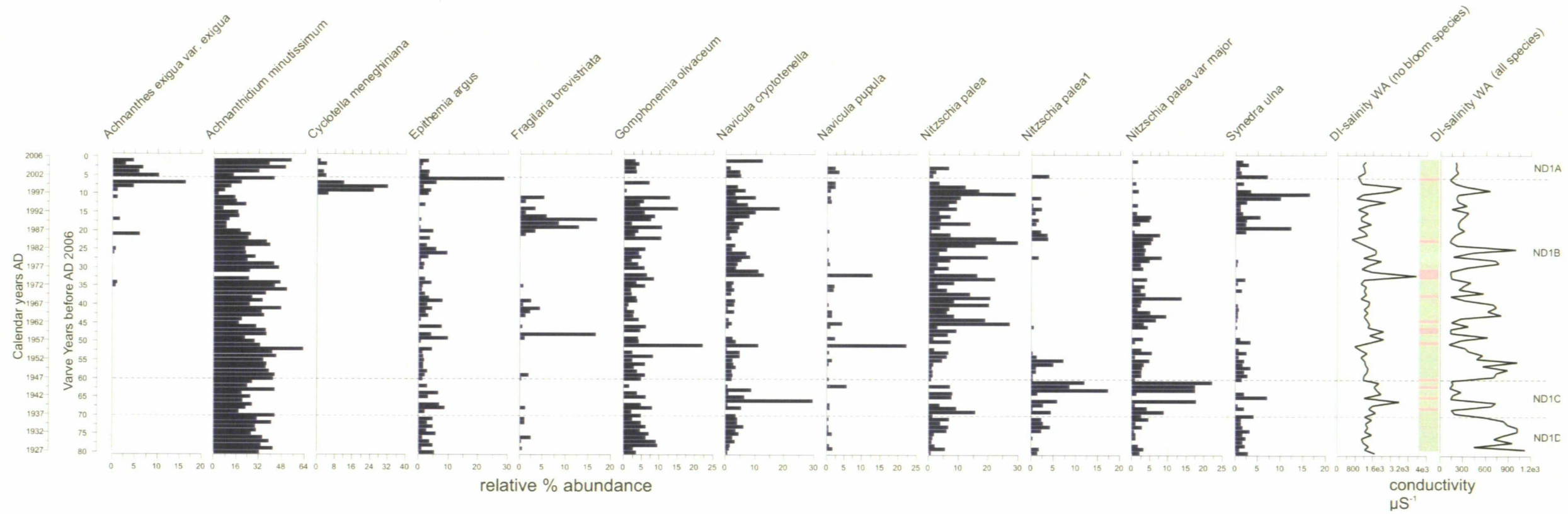


Figure 5.29 NAR06 species % recalculated omitting bloom species and *C. anaticus* with reconstructed conductivity omitting bloom species (*N. paleacea* and *S. acus*) and *C. anaticus*. Coloured bar highlights samples with a diatom valve count above 50 (green) and below 50 (pink).

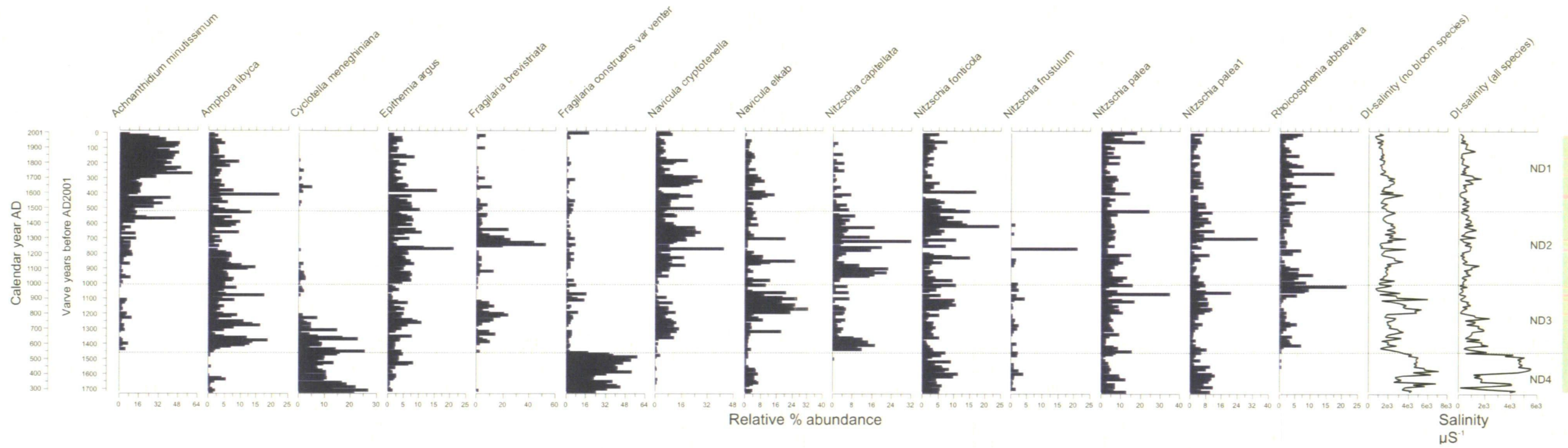


Figure 5.30 NAR01/02 diatom stratigraphy with reconstructed conductivity omitting bloom species (*N. paleacea*, *S. acus* and *S. parvus*) and *C. anatolicus*. Coloured bar highlights samples with a diatom valve count above 50 (green) and below 50 (pink).

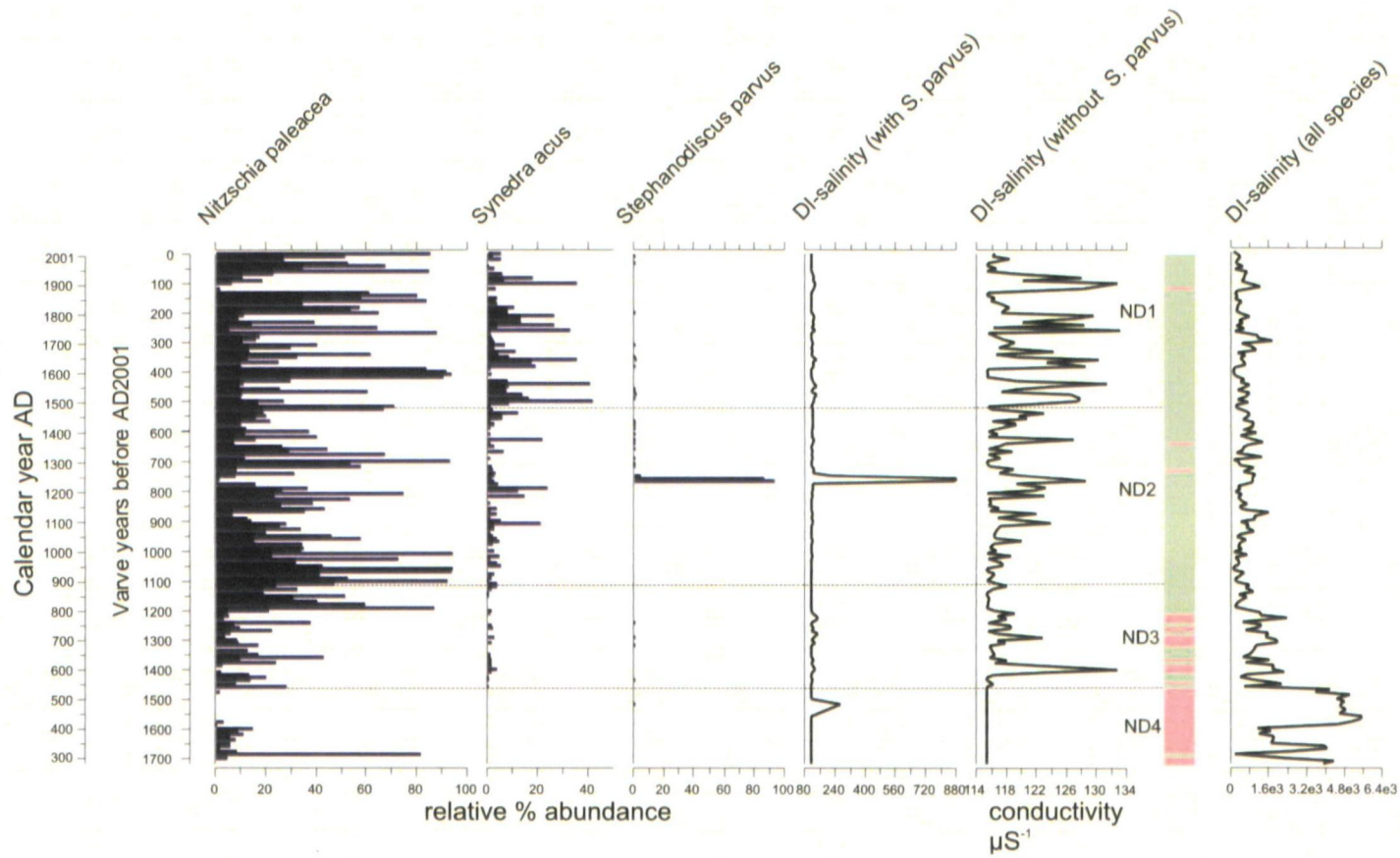


Figure 5.31 NAR01/02 diatom stratigraphy with reconstructed conductivity based on bloom species (*N. paleacea*, *S. acus* and *S. parvus*) only. Coloured bar highlights samples with a diatom valve count above 50 (green) and below 50 (pink).

5.3.14 Reconstructed and instrumentally-measured conductivity

Comparing reconstructed and instrumentally measured conductivity for the most recent eight years suggests that the transfer function has not performed well, as reconstructed values do not correspond with instrumental data (Table 5.7). Contemporary average conductivity at Nar has been recorded at $3,350 \mu\text{S}^{-1}$. This is approximately eight times higher than the reconstruction based on all diatom species predicts. Low-salinity indicator diatom bloom species (*N. paleacea* and *S. acus*), which are associated with short time periods (e.g. spring or summer), drive reconstructed conductivity values down. Leng *et al.* (2001) suggested that depleted lake isotope values occurred as a result of the spring snow thaw in a central Anatolian lake. Snow melt could dilute lake water temporarily at Nar and allow low-salinity indicators to bloom in spring.

DI-conductivity based on non-bloom species provided values closest to the contemporary environment for most of the year; however, absolute values are still drastically underestimated. Therefore it appears that the reconstruction could be inaccurate. However, as the most recent samples did not have a good modern analogue, due to abundance of *C. anatolicus*, the reconstruction is likely to be unreliable for these samples. This may not apply to other core depths, when a higher number of good modern analogue species were present. Also, the dataset of modern lake conductivity recordings is small, and only included recordings during summer, whereas reconstructed conductivity represents an annual average. Therefore it is not possible to derive definite conclusions when comparing instrumental data with reconstructed conductivity.

The key difference between the bloom and non-bloom reconstructions is the difference in absolute conductivity values. The reconstruction based on all species results in values

closer to the bloom species reconstruction as these taxa were more dominant in the assemblage and drove conductivity values down. The Nar diatom assemblage appears to have a bimodal relationship with lake water salinity due to the differing preferences of bloom and non-bloom species. This may account for the limited correspondence between summer measured and DI-conductivity.

Calendar year AD	Reconstructed conductivity μS^{-1}			Measured conductivity μS^{-1}
	All species	Bloom species	Non-bloom species	
2006	207	128	1285	3350
2005	209	137	1119	
2004	201	135	1192	
2003	238	131	1223	
2002	184	127	934	4100
2001	122	116	1004	3200
2000	197	118	1094	2900
1999	352	117	2856	2500

Table 5.7 Comparison of DI-conductivity based on all species, bloom species, non-bloom species and instrumentally measured conductivity at Nar Gölü between AD 1999 and 2006 (data not available for 2003-2005).

5.4 Summary

This chapter has provided a summary of modern diatom taxonomy and presented data from the contemporary and palaeo-diatom assemblages of Nar Gölü. Records revealed that the diatom species assemblages have fluctuated throughout the past 1720 years. The most significant changes in the records include a species shift at AD 540-550 and during the most recent 5 years (AD 2001-2006). These periods have been highlighted by DCA and cluster analysis. Temporal variation in diatom concentration, total biovolume,

species diversity and percentage benthic taxa appears to be driven by the changing abundance of dominant species *N. paleacea*.

Biovolume offered an additional method for presenting data and provided further information about assemblage change. For example, larger species were identified as responding to environmental variation simultaneously with smaller taxa. Core thin sections offered a unique tool for studying the assemblage *in-situ* and revealed that diatom bloom events have become more frequent at Nar throughout the most recent 100 years. The application of the diatom data to transfer functions from EDDI revealed a period of enhanced DI-conductivity prior to AD 550. However, reconstructions were limited by the poor fit of many fossil samples to the modern training sets. Bloom species drive DI-conductivity down and appear to relate to fresher conditions in the lake. A combination of diatom assemblage analyses and presentation methods has provided complementary information to aid interpretations.

Chapter 6

Results: Kratergöl

6.0 Introduction

This chapter presents and describes results from the modern and palaeo-diatom analysis of Kratergöl.

6.1 Diatom identification and taxonomy

The diatom species assemblage was described primarily according to Krammer and Lange-Bertalot (1991; 1997; 2000). Samples from Kratergöl contained lower species diversity than those from Nar Gölü and fewer problematic taxa were present. All species observed in the modern Kratergöl environment were also represented in the sediment record. Key distinguishing features of species that occurred at greater than 3% abundance are described in Appendix 2. Taxonomic issues are summarised and presented with illustrations (see Appendix 3 for a complete species list).

Taxonomic problems arose regarding certain Kratergöl species groups. For example, transitional types were frequently observed between *Amphora coffeaeformis* and *Amphora veneta*. Additionally, numerous *Nitzschia* species presented identification problems. For example, specimens of characteristic *Nitzschia fonticola* shape frequently lacked the distinguishing feature of this species, a gap in the fibulae at the raphe mid-point. Valves were frequently encountered without a gap and occasionally two valves of the same diatom differed with regard to fibulae spacing. Identification of the majority of

Kratergöl species was straightforward. However, some specimens were extremely rare and therefore lacked adequately preserved features from which to make identifications.

6.2 Modern diatom assemblage

The modern lake environment of Kratergöl provides habitats for a variety of diatom groups. Figure 6.1 illustrates the percentage abundance of diatom species (>3%) for two stone/pebble lake samples (epilithic), four plant (epiphytic) samples and one bottom mud sample (epipelon) collected in 1992 by P. Barker. Five samples collected in 2008 include a water sample (plankton), surface mud (epipelon), gravel (epilithon), filamentous algae (epiphyton) and an exposed stromatolite comprising primarily microorganisms and biofilms.

The 1992 epilithic community was primarily composed of *Navicula complanata*, which was not common in the sediment record. This may be due to the species' delicately silicified structure limiting preservation. Other 1992 epilithic species included *Fragilaria fasciculata*, *A. veneta* and *Nitzschia cf. fonticola*. These are mainly motile, benthic taxa typical of this environment. The 2008 epilithic sample was dominated by a diverse diatom assemblage including *N. cf. fonticola*, *Cocconeis placentula*, *F. fasciculata* and *A. veneta*. The 1992 epiphytic community was dominated by *C. placentula* and *F. fasciculata*. Similarly, the 2008 epiphyton was dominated by these two species. The 1992 epipelon contained abundant *N. cf. fonticola*, *A. veneta*, *F. fasciculata* and *Nitzschia sigma*. These species are mainly typical adnate, benthic taxa. 2008 epipelon was also diverse with abundant *N. fonticola*, *F. fasciculata*, *C. placentula* and *Rhopalodia constricta*. The 2008 plankton was dominated by *F. fasciculata* and *N. cf. fonticola*, implying that these species inhabit the water column in addition to other

habitats. Diatoms were also abundant in the stromatolite sample. *F. fasciculata* dominated this assemblage; this may be due to the species' high abundance at the time of sampling. A common epipellic species in the sediment record, *Entomoneis paludosa* var. *subsalina*, was rare in the modern environment. This suggests that this taxon is not favoured by modern Kratergöl conditions. However, the absence of this species may also be associated with sampling time and locations.

The relative weighting of modern species altered when data were plotted according to cell biovolume (Figure 6.2). The importance of smaller species typical of the modern epilithic and epipellic environments decreased (e.g. *N. complanata*) according to biovolume, whereas the weighting of larger species increased (e.g. *R. constricta*). Calculation of diatom concentration and total biovolume allowed information regarding the productivity of different lake environment to be derived. Due to the lack of sample weights, frame counts and dilution data, the 1992 modern samples are not plotted according to diatom concentration and biovolume. Figure 6.3 illustrates that diatom concentration and total biovolume was lowest in the 2008 plankton and epilithic samples. Rarefaction (Figure 6.4) indicates similar diversity of species in the 1992 and 2008 epilithic and epipellic samples. Lowest diversity is evident in the epiphytic samples from 1992 and 2008. Therefore epiphytic environments appear to provide a niche for more specialist species; however, this is also associated with the limited niche and that fact that there is less chance of dead cells accumulating on macrophytes in comparison with other habitats. Rarefaction is negatively related to concentration and total biovolume; therefore greater diatom cell numbers are associated with decreased diversity.

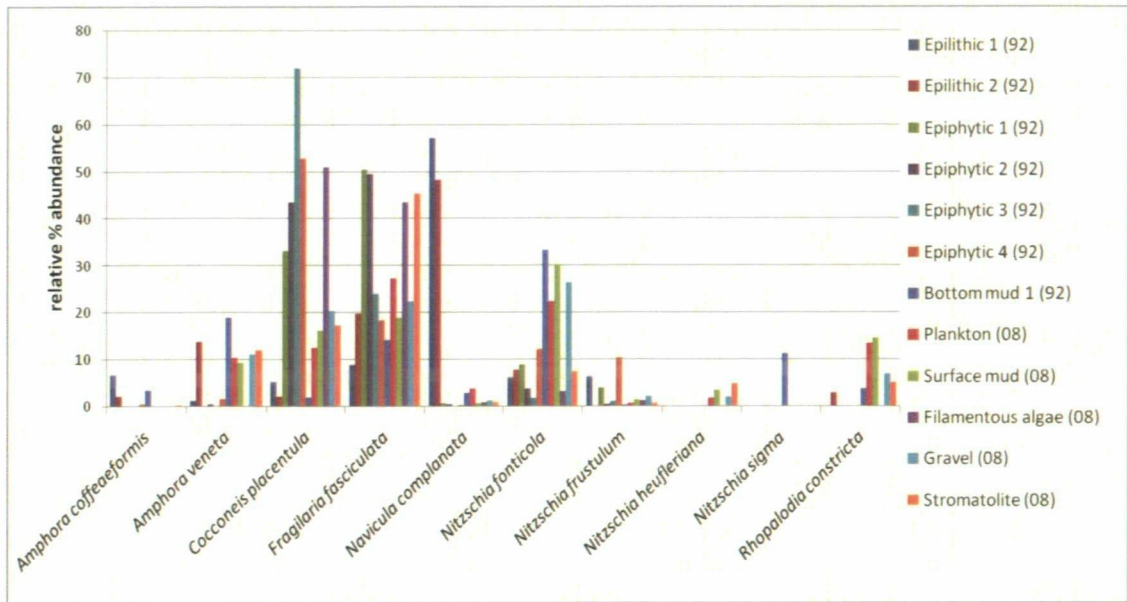


Figure 6.1 Modern Kratergöl diatom assemblage (>3%). Species percentages presented according to habitat and collection date.

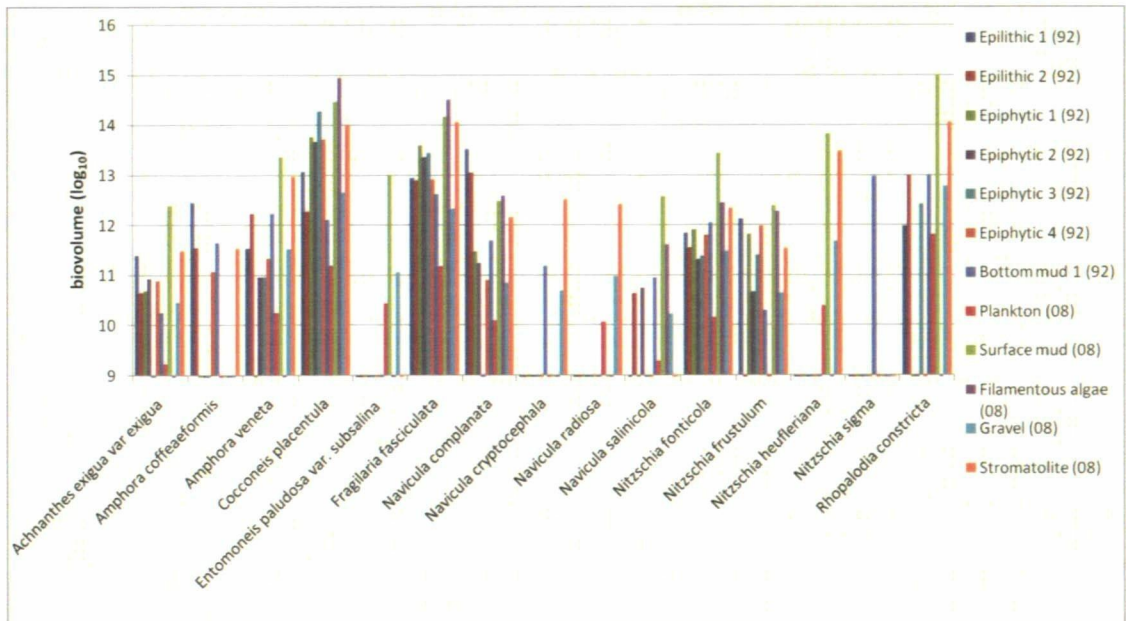


Figure 6.2 Modern Kratergöl diatom assemblage (>3%). Species biovolume (μm^3) (\log_{10}) presented according to habitat and collection date (species included account for >12 \log_{10} within at least one sample).

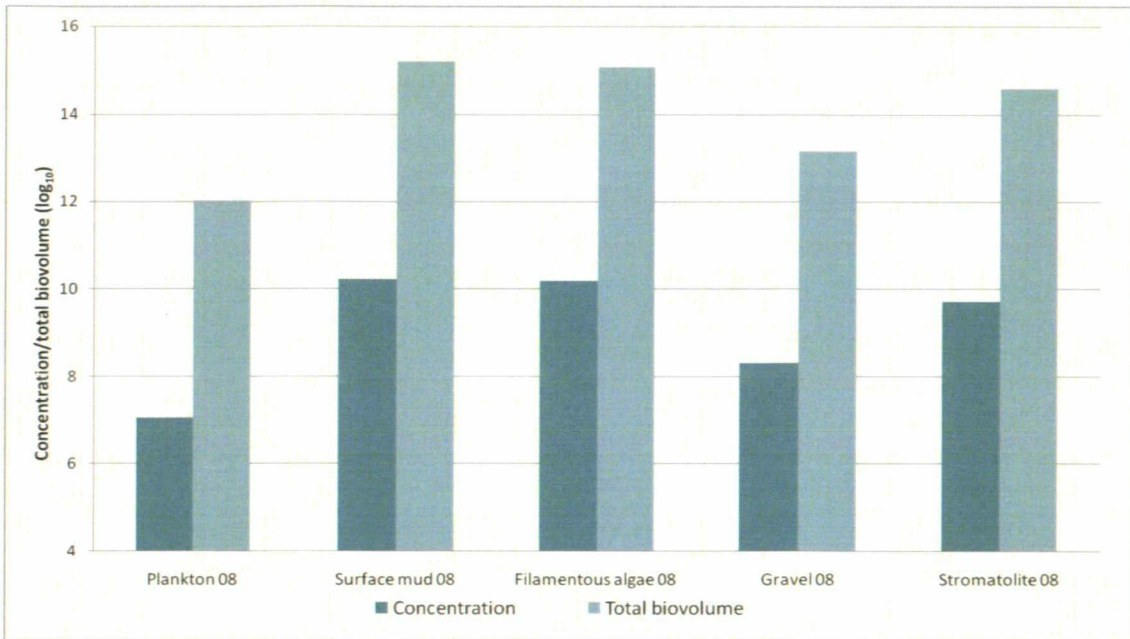


Figure 6.3 Modern Kratergöl sample diatom concentration (diatoms/g wet sediment log₁₀) and total biovolume (µm³) (log₁₀).

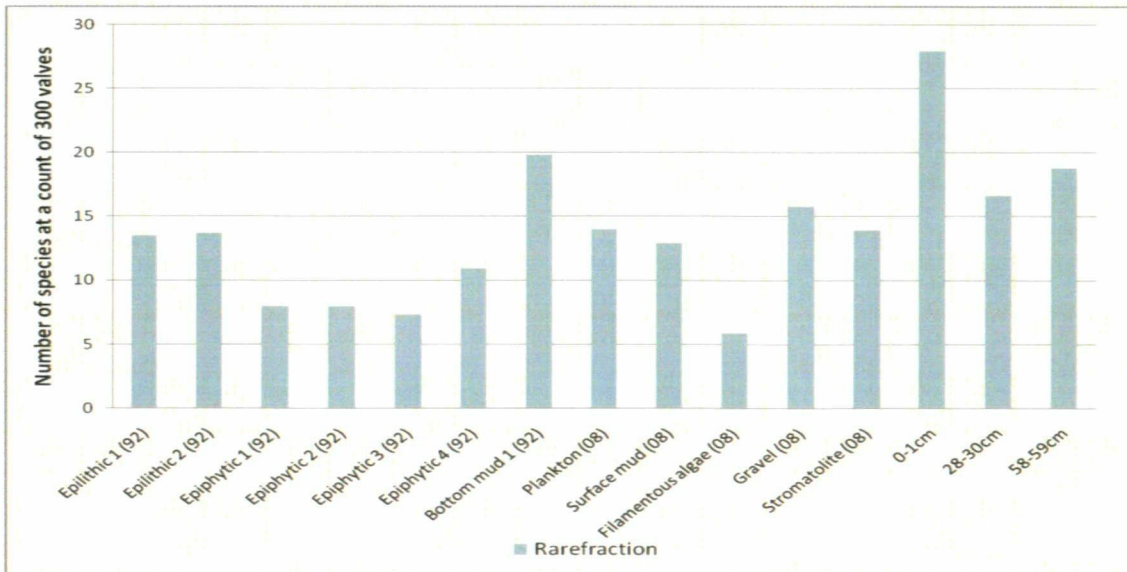


Figure 6.4 Diatom rarefaction (species diversity) of modern Kratergöl samples and different sediment depths in the ACM99 palaeo-record.

The similarity between modern samples with regard to species assemblage is illustrated in the DCA ordination plot (Figure 6.5). The 1992 and 2008 epiphytic samples are

positioned low on axis 1 and the 1992 epilithic and epipellic samples are clustered high on axis 1. The 2008 plankton, epilithon and epipelon samples are positioned at the centre of the graph. This zonation suggests that each of these environments hosts specific species and assemblages altered between the two collection dates.

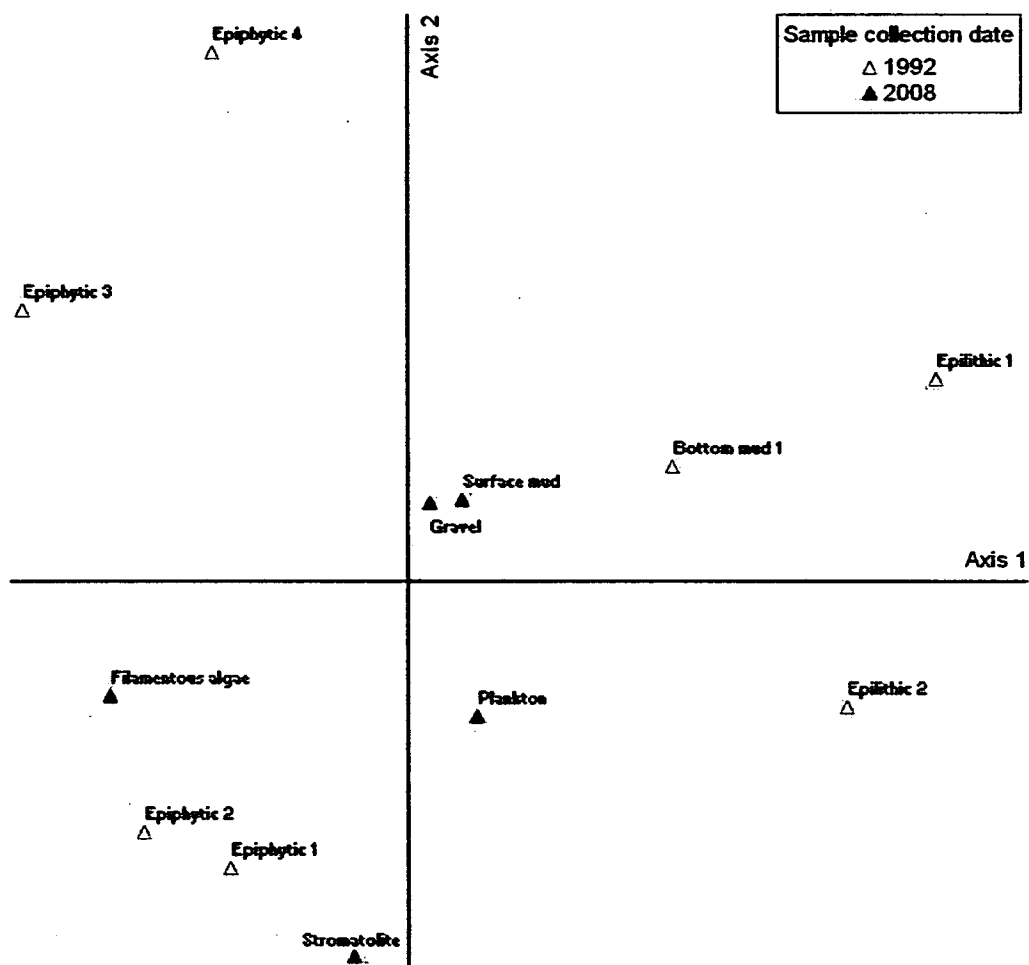


Figure 6.5 DCA ordination plot for modern diatom samples according to habitat and collection date.

6.3 Palaeo-record

6.3.1 Lithology and sedimentation

The Kratergöl core section (ACM99) comprised a 59 cm sequence of non-laminated lake sediment, which varied with regard to material type and composition. Core lithology has been described according to diatom zones established by cluster analysis (see Table 6.1 for zone depths). The core section containing older sediment (zone KD4) was composed mainly of silt and clay and had high carbon content (Figure 6.6). This was followed by a period (zone KD3) of increased sand and low carbon values. Zone KD2 varied in composition, with lower sand percentage and a subsequent rise, associated with an increase and decrease in carbon content. Zone KD1 had high sand and low carbon values (Figure 6.6), which decreased within the most recent sediments when silt, clay and carbon increased.

The sandy sections (KD3 and KD1) (36-16 cm and 12-2 cm) may represent within-lake events that resulted in the sudden deposition of sediment. The sedimentation regime appears to be characterised by periods of high organic content with clays and silts, interrupted by turbidite events resulting in high sand percentage and low carbon values. Lake bathymetry includes submerged shelves and bays (Dumont, 1981), which may collapse and lead to the sudden movement and deposition of sediment. Sediment is also likely to derive from the delta on the east side of the lake (Chapter 3: Plate 3.5). This may account for the sandy sections in the sequence. Lake water is stratified and the hypolimnion is anoxic. However, the sedimentation regime is not uniform and varves are not formed.

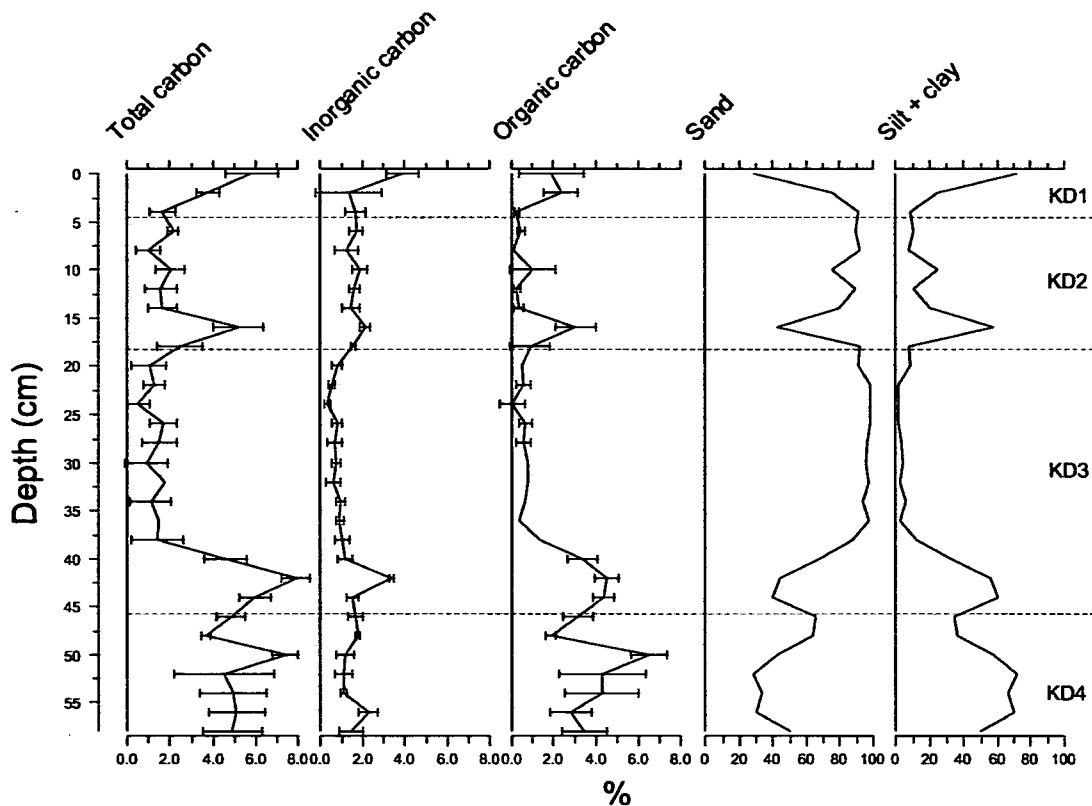


Figure 6.6 ACM99 carbon content and particle size analysis. Total, inorganic and organic carbon concentrations are presented with percentage of sand and silt+clay.

6.3.2 Chronology

Establishment of a chronology for the ACM99 profile was attempted using radionuclides (Appleby, 2001) and metal analysis dating techniques (Renberg *et al.*, 2001; 2002) (Figures 6.7 a and b). Problems arose when interpreting results, due to the relatively low activity measured, the possibility of vertical radionuclide migration or sediment mixing and the lack of comparison datasets in the region. There are also uncertainties as to whether the top section of the core was retained during sampling. Kratergöl is a deep lake (~70 m); therefore core retrieval was problematic. The absence of replicate sections means that it is not possible to confirm whether the core represents a complete stratigraphy. Diatom concentration (valves/g wet sediment) was used as a

proxy for relative sediment accumulation rate. This method required the assumption that assemblage productivity remains relatively constant through time. Diatom concentration decreased in accordance with the sandy sections; this ‘dilution’ implies a sharp rise in sedimentation rate during these periods.

The decay rate of ^{210}Pb is frequently used to date lake sediment profiles (Appleby, 2001). Additionally, peaks in ^{137}Cs and ^{241}Am activity can signal the timing of the period of nuclear weapons testing or ‘bomb spike’ (AD 1963 in the Northern Hemisphere) and the Chernobyl nuclear accident (AD 1986). Thus, ^{137}Cs and ^{241}Am profiles are used to date lake sediments covering the late 20th century. Unsupported ^{210}Pb activity was highest at the surface of the ACM99 profile but decayed rapidly to very low levels after 4 cm. This rapid decay of ^{210}Pb may suggest that sediment accumulation rate is extremely slow at Kratergöl, as each ^{210}Pb half life represents a 22 year period. Alternatively, this may be related to core stratigraphic problems. The coarse-grained lithology of the core does not support this and implies rapid deposition between 36-16 and 12-2 cm; therefore it appears that the ^{210}Pb profile is likely to be unreliable and the ^{137}Cs and ^{241}Am activity may provide a more reliable dating tool for the ACM99 record.

Other sediment profiles in the region (central Turkey) contain evidence of the ^{137}Cs bomb test spike and Chernobyl nuclear fallout (e.g. Nar Gölü, see Chapter 5); therefore these events should also be evident in the ACM99 record. The ^{137}Cs activity peaked in the most recent sediment and at 10 cm, with a smaller peak at 44 cm; this pattern is also reflected in the ^{241}Am profile. ^{137}Cs has been identified as a radionuclide that migrates within lake sediment profiles leading to dating problems (Putyrskaya and Klemm, 2007).

The fact that ^{241}Am corresponds suggests that ^{137}Cs is unlikely to have migrated vertically within the sediment as, according to Zaccone *et al.* (2007), ^{241}Am binds to particles and does not migrate through sediment (Appleby, 2001). However, ^{241}Am values were extremely low in the ACM99 record and are therefore likely to be unreliable (Figure 6.7 a). Consequently, it is not clear whether or not ^{137}Cs may have migrated through the profile. Additionally, Abril (2004) highlighted that simple dating methods based on the identification of ^{137}Cs fallout peaks may not provide reliable sediment chronologies and the varied sedimentation rate of Kratergöl will have affected relative radionuclide concentrations through the sequence.

The ^{137}Cs peak at 44 cm may represent the 1963 bomb test spike (Figure 6.7 b). Higher values at 12 cm and near the profile surface could also represent fallout from the 1986 Chernobyl accident with continued input from the catchment towards the top of the core. Ketterer *et al.* (2004) highlighted that the signature left by the bomb spike is less significant than the Chernobyl incident; the ACM99 pattern corresponds with this hypothesis. However, ^{241}Am is more commonly associated with nuclear weapons testing (Ketterer *et al.*, 2004), the peak at 44 cm implies that this period represents 1963. However, radionuclides were also detected below this depth in the profile; these are likely to represent error recordings or may be the result of sediment mixing. The sandy sections are considered to relate to sudden turbidite events and the periods with high carbon content are thought to represent slower accumulation. Therefore it appears that the bottom of the profile could relate to ~AD 1920/30; this implies an average sedimentation rate of ~1 cm/year throughout the 59 cm sequence.

These interpretations may be unreliable, due to the possibility that low radionuclide levels in the sandy sections could be the result of increased sedimentation rate; therefore the peaks at the profile surface, 10 and 44 cm may not be significant. Radionuclide activity and metal concentrations decreased through the sandy sections and are likely to have been diluted by the turbidite events (sub-surface sediment movement) between 36-16 cm and 12-2 cm. Putyrskaya and Klemm (2007) discussed the effect of sediment deposition rate on radionuclide profiles and also identified a period of very low activity during a turbidite event. ACM99 data were plotted using diatom concentration as a substitute for sedimentation rate in order to account for this. However, radionuclide levels were extremely low through the sandy section; therefore trends may still not have been revealed accurately. Additionally, the assumption that changes in diatom cell number are predominantly associated with lake sedimentation may not be accurate.

In addition to radionuclides, dating was also carried out using metal analysis and spherical carbonaceous particles (SCPs) associated with fossil fuel combustion. SCPs were not detected in the ACM99 record; this is likely to be associated with the fact that the lake is not situated in an industrial location. Total lead (Pb) was expected to reveal the beginning of industrial emissions during the 19th century and a post WWII peak (~1950) (Renberg *et al.*, 2001; 2002). Peaks in the metal species corresponded with patterns associated with carbon content and particle size data, e.g. higher carbon and silt+clay content corresponded with Pb peaks. Therefore metal concentration is mainly associated with catchment processes and sedimentation. Considering the different analysis methods, it appears that the most reliable dating tool for the ACM99 record may be ¹³⁷Cs. However, sediment mixing may have occurred during core recovery and the varied lake sedimentation rate reduces the reliability of the radionuclide profile.

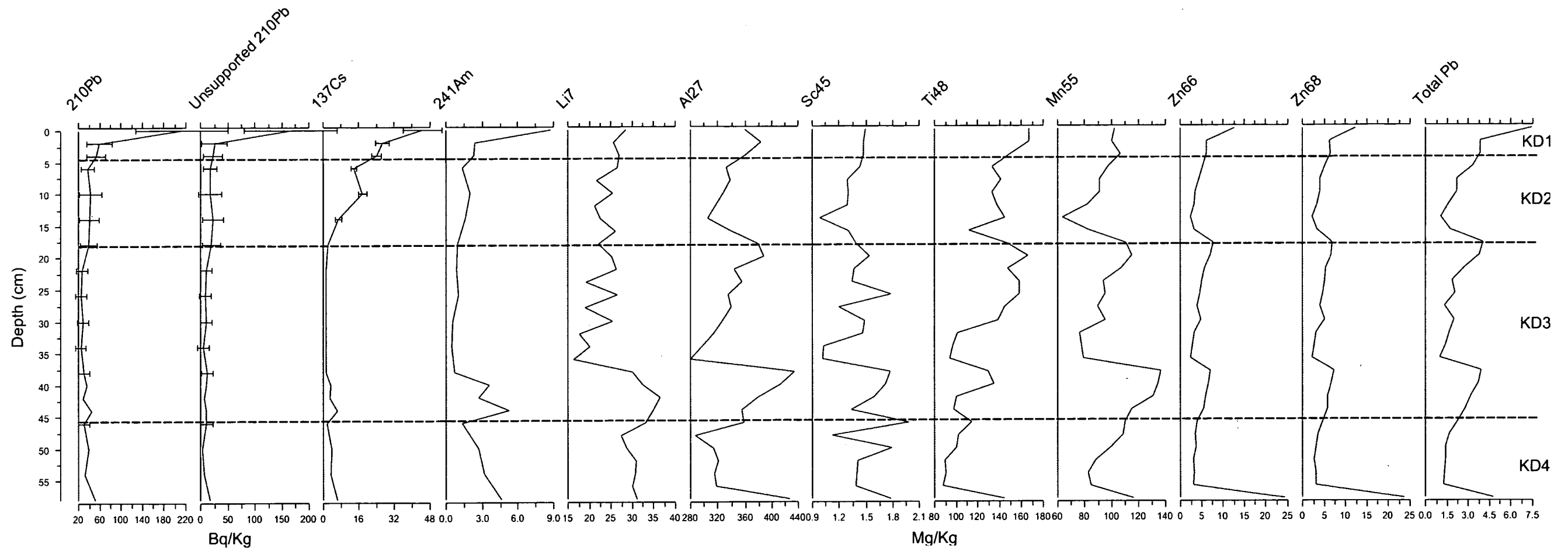


Figure 6.7 a) ACM99 total and unsupported ^{210}Pb , ^{137}Cs and ^{241}Am activity profiles (Bq/Kg) and metal species concentration (mg/Kg) (error values not provided by detector for all samples).

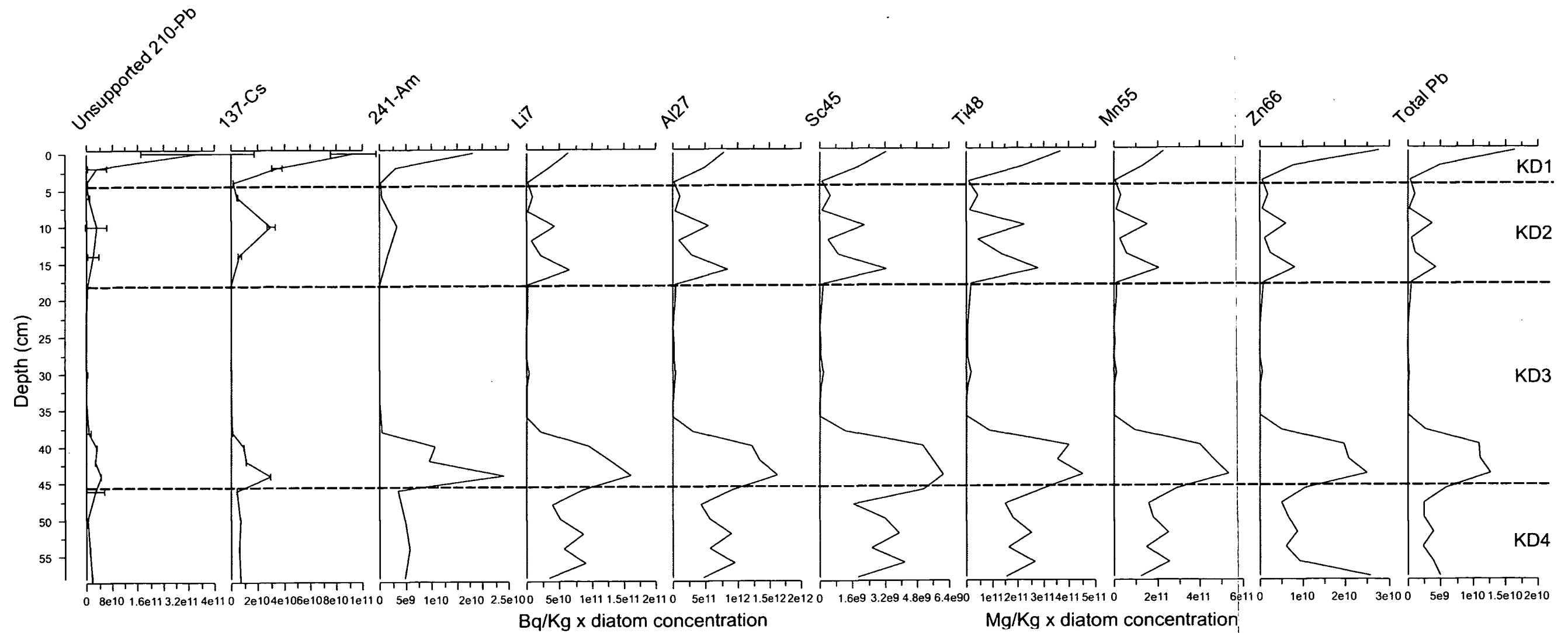


Figure 6.7 b) ACM99 unsupported ^{210}Pb , ^{137}Cs and ^{241}Am activity profiles (Bq/Kg) and metal species concentration (mg/Kg) relative to diatom concentration (diatoms/g wet sediment) (error values not provided by detector for all samples).

6.3.3 Diatom stratigraphy

The Kratergöl palaeo-record was dominated by four key diatom species, *E. paludosa* var. *subsalina*, *C. placentula*, *F. fasciculata* and *N. cf. fonticola*. The relative percentages of these species fluctuated throughout the record. Diatom stratigraphy of the ACM99 sequence was split into four zones using stratigraphically constrained cluster analysis (Figure 6.8). The species assemblage composition remained relatively consistent throughout the sequence with changing percentages of certain dominant species (Table 6.1). Zone KD4 was dominated by *C. placentula*, *E. paludosa* var. *subsalina*, *F. fasciculata* and *N. cf. fonticola*. The shift to zone KD3 involved disappearance of *E. paludosa* var. *subsalina*, increased values of *N. cf. fonticola* and a slight increase in *A. veneta* and *A. coffeaeformis*. The transition to zone KD2 was characterised by renewed dominance of *E. paludosa* var. *subsalina*, decreased *C. placentula* and *F. fasciculata*, increased *N. frustulum* and a gradual decrease in *A. veneta* and *A. coffeaeformis*. KD1 involved decreased *E. paludosa* var. *subsalina* and increased *N. cf. fonticola*.

The ACM99 record differed from the Nar Gölü diatom sequence. Kratergöl experienced relatively gradual increases/decreases of species between sample depths and the extreme bloom events typical of Nar were not present. No Kratergöl taxa reached above 60% in the record and there were no total species shifts evident. This is partly associated with the longer time period covered by the Nar sequence and the different sampling strategies, i.e. annual/three-VY at Nar and 2 cm at Kratergöl. These differences are also likely to be associated with variation between the lake ecosystems.

Kratergöl diatom (KD) zone	Depth (cm)	Dominant diatom species
KD1	0-4	<i>C. placentula</i> , <i>N. cf. fonticola</i> , <i>F. fasciculata</i> and <i>N. frustulum</i> .
KD 2	6-18	<i>C. placentula</i> , <i>E. paludosa</i> var. <i>subsalina</i> <i>F. fasciculata</i> and <i>N. frustulum</i> .
KD 3	20-46	<i>A. veneta</i> , <i>C. placentula</i> , <i>N. cf. fonticola</i> , <i>F. fasciculata</i> and <i>N. frustulum</i> .
KD 4	48-59	<i>C. placentula</i> , <i>E. paludosa</i> var. <i>subsalina</i> , <i>N. cf. fonticola</i> , <i>F. fasciculata</i> and <i>N. frustulum</i> .

Table 6.1 ACM99 cluster analysis diatom zones according to depth with a summary of dominant species.

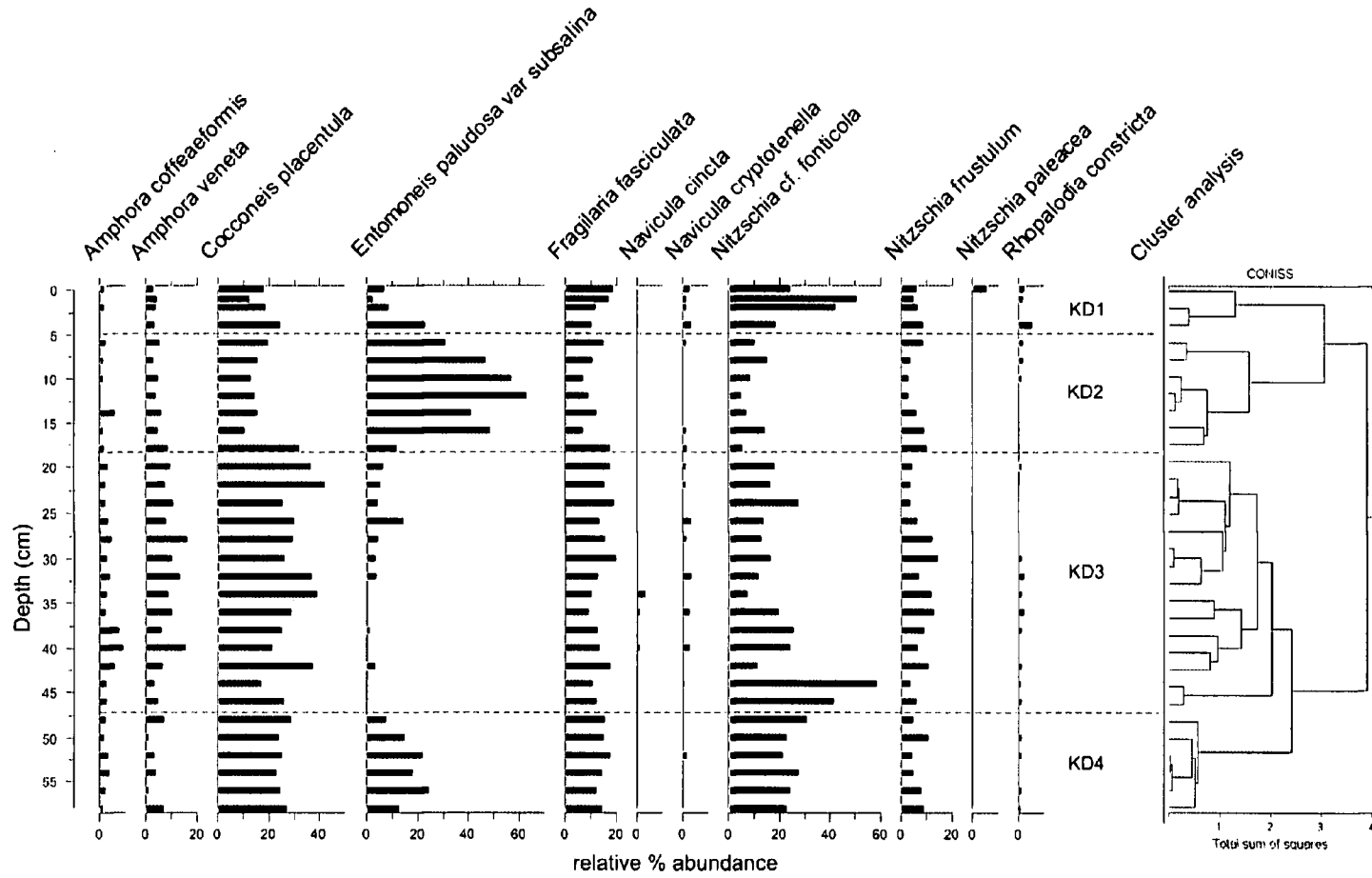


Figure 6.8 Diatom stratigraphy of the ACM99 record. Species included represent >3% of the population within at least one sample. The assemblage has been zoned according to cluster analysis.

6.3.4 Detrended Correspondence Analysis (DCA)

DCA was performed in order to explore patterns in the ACM99 dataset. Similarities between samples from different depths in the core sequence are illustrated in the DCA ordination plot (Figure 6.9). The percentage of variation explained by axes 1 and 2 was 24.1% and 6%. The most distinct zone was KD2 involving increased *E. paludosa var. subsalina*, with samples clustered high on axis 1; this period experienced greatest variation in the diatom assemblage. Zones KD3 and KD4 were also distinct and greatest sample dissimilarity occurred in KD1, implying environmental change during this period. DCA axis 1, plotted stratigraphically (Figure 6.10), illustrates greatest change to the record in zones KD1 and KD2. Axis 2 highlights variability in the assemblage throughout zone KD4.

Ordination plots weighted according to species abundance are illustrated in Appendix 4.3. The plots reveal which species characterise different zones. *N. frustulum* is specific to zone KD3, *N. cf. fonticola* characterises zone KD1 and *F. fasciculata* is abundant in all zones. *E. paludosa var. subsalina* is common in zone KD2 and *C. placentula* and *A. veneta* are specific to KD2 and KD3.

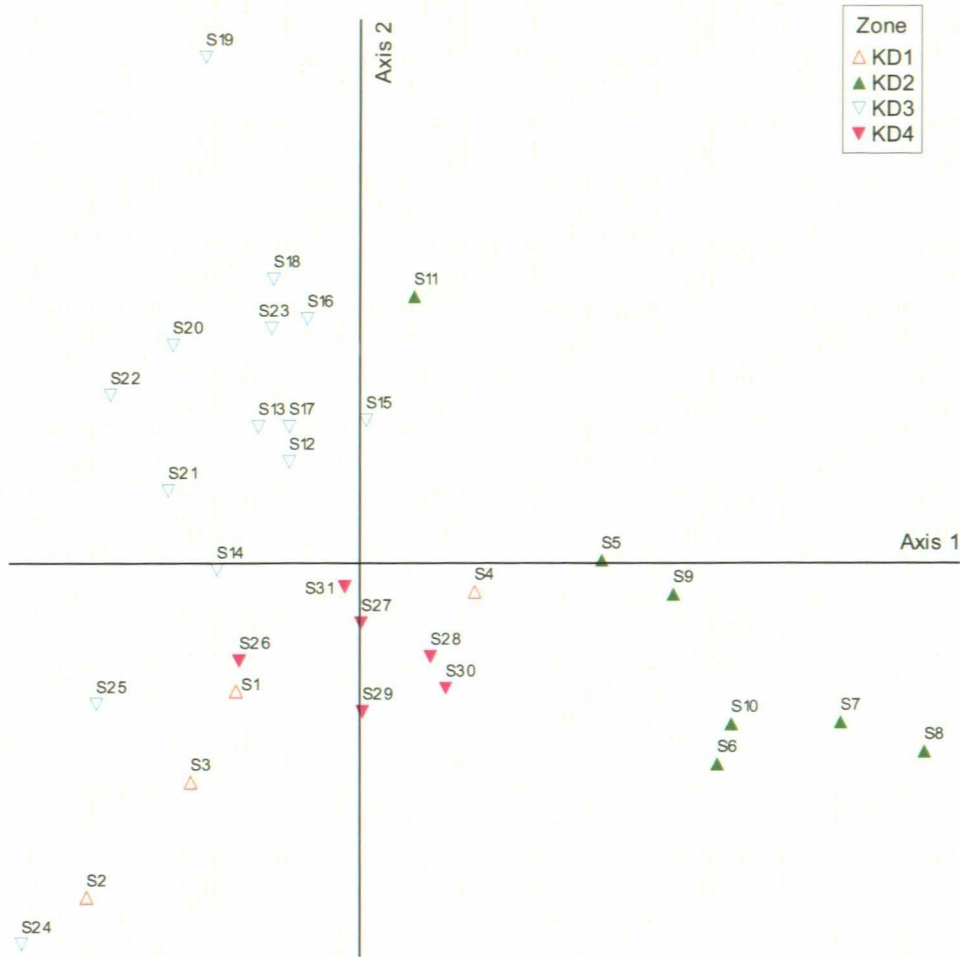


Figure 6.9 ACM99 DCA ordination plot. Diatom samples plotted on axes 1 and 2 with symbols corresponding to cluster analysis zones.

6.3.5 Diatom concentration and total biovolume

Diatom concentration and total biovolume were highest in zones KD4, KD2, the beginning of KD3 and within the most recent sediment (Figure 6.10). Lower concentration and biovolume values between 18 and 36 cm correspond with the largest sandy section in the core; this indicates that sediment was deposited rapidly during this period. The decline in concentration and total biovolume during zone KD3 was significantly correlated with increased species diversity ($r=-0.378$, $p=0.036$). Thus, the same pattern to that observed at Nar is apparent, i.e. greater concentration of diatoms is associated with lower diversity. Diatom concentration was also significantly related to carbon content ($r=0.792$, $p=0.000$) and particle size distribution (e.g. negatively correlated with sand content: $r=-0.832$, $p=0.000$). Therefore it appears that concentration and biovolume relate to lake sedimentation rate and may not realistically represent productivity in the system. This illustrates that diatom concentration is affected by basin processes and associated with the amount of carbon in the system.

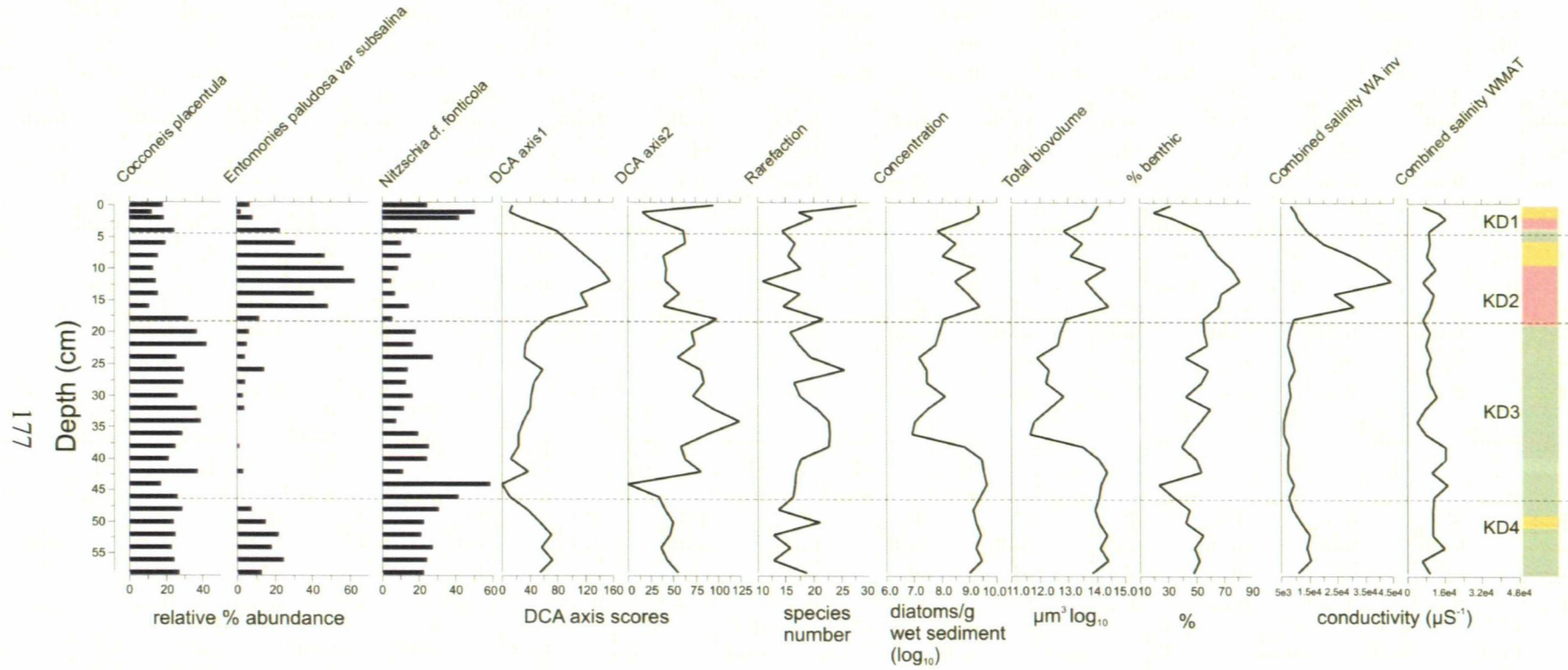


Figure 6.10 ACM99 diatom stratigraphy (>20%) presented with DCA axes 1 and 2, rarefaction, diatom concentration (\log_{10}), total diatom biovolume (μm^3) (\log_{10}), % benthic taxa and DI-conductivity (μS^{-1}) by WA-inv. and W-MAT. Coloured bars represent sample analogue matching with modern training set (green = good modern analogue, yellow = no good analogue and pink = no close analogue).

6.3.6 Species diversity

Diatom diversity is reflected by rarefaction species number estimations, which highlight periods of change in the system (Figure 6.10). Rarefaction fluctuated through the ACM99 record between 12 and 25 species peaking at 24 cm and at the top of the core. Lowest diversity is evident at 10 cm, associated with dominance of *E. paludosa* var. *subsalina*. Total diatom biovolume is significantly negatively correlated with rarefaction ($r=-0.378$, $p=0.036$); therefore more productive periods were dominated by certain taxa.

6.3.7 Habitat preferences

The relative percentage of benthic taxa (Figure 6.10) fluctuated through the record, with lowest values in KD4, KD3 and KD1 and higher values in KD2, in relation to the changing dominance of different species. The percentage of benthic taxa was significantly related to carbon content and particle size distribution. This implies that basin processes are associated with diatom life form and the type of species dominating the community.

6.3.8 Environmental reconstructions

Diatom-inferred (DI) conductivity was reconstructed for the ACM99 sequence, using training sets from EDDI (Juggins, 2008). The combined salinity training set was identified as possessing the highest number of matching modern analogue species using the Modern Analogue Technique (MAT) (Table 6.2). Models that performed best were identified by their r and RMSEP values (see Chapter 5; Section 5.3.11) and included Weighted Averaging with inverse deshrinking (WA-inv.) and Weighted (W) MAT.

DI-conductivity by WA-inv. revealed lower conductivity values during zones KD4 and KD3, the shift to KD2 involved greatly enhanced values, and KD1 experienced a return to lower levels. Conductivity varied between a maximum of $44,426 \mu\text{S}^{-1}$ at 12 cm and a minimum of $5,984 \mu\text{S}^{-1}$ at 36 cm. Average conductivity for zone KD4= $12,918 \mu\text{S}^{-1}$, KD3= $7,875 \mu\text{S}^{-1}$, KD2= $28,419 \mu\text{S}^{-1}$ and KD1= $11,110 \mu\text{S}^{-1}$. Variability in WA reconstructed conductivity levels was associated with the abundance of dominant species *E. paludosa var. subsalina* (Figure 6.10). The percentage of this species is highly correlated with the DI-conductivity record ($r=0.98$, $p=0.000$). *E. paludosa var. subsalina* was present in only two of the modern training set sites; therefore reconstructed values based on the species relationship with environmental variables is limited. The MAT bases the reconstruction on an average of the 10 closest analogue sites (lakes) and therefore reduces this problem. However, the MAT reconstruction was accompanied by large errors. W-MAT revealed fluctuating conductivity throughout the record and a notable decrease around 33 cm (mid-way through zone KD3). MAT reconstructed conductivity values fluctuated between a maximum of $17,585 \mu\text{S}^{-1}$ at 44 cm and a minimum of $4,163 \mu\text{S}^{-1}$ at 34 cm. The average for zone KD4= $10,927 \mu\text{S}^{-1}$, KD3= $10,821 \mu\text{S}^{-1}$, KD2= $9,315 \mu\text{S}^{-1}$ and KD1= $11,649 \mu\text{S}^{-1}$.

The major difference between the WA and MAT reconstructions is the decreased weighting given to *E. paludosa var. subsalina* by the MAT and the lower variability in the MAT reconstructed values. Analogue matching (Section 6.3.9) revealed that fossil samples, where *E. paludosa var. subsalina* was abundant, did not have a 'good' modern analogue in the training set. Although this species was not common in the modern training set, it may still represent an important environmental change in the sediment profile. Therefore WA may provide a more reliable record of palaeo-conductivity.

However, samples with ‘no good’ or ‘no close’ modern analogue need to be interpreted with caution. Modern Kratergöl conductivity was recorded instrumentally as 83,500 μS^{-1} in 2008 and 77,200 μS^{-1} in 1999. DI-conductivity for the top of the ACM99 core, representing 1999, was 8,624 μS^{-1} according to WA and 6,890 μS^{-1} for the MAT. The EDDI training sets drastically underestimated modern lake conductivity; therefore reconstructions need to be interpreted with caution. Although absolute values may not have been reconstructed correctly, relative changes in conductivity provide information about palaeoenvironmental change.

Training set (EDDI)	Ave. % fossil sample represented in modern training set
Combined salinity	95.15
African salinity	94.51
CASPIA salinity	52.13
Spanish salinity	72.08
Combined TP	48.14

Table 6.2 Average percentage of ACM99 fossil sample assemblage represented in modern lake diatom-conductivity training sets from EDDI.

6.3.9 Analogue matching

The reliability of the reconstruction was assessed using the MAT. The dissimilarity (min. DC) of fossil samples was compared with the combined salinity modern training set min. DC. Critical values were defined by the min. DC of the training set second and fifth percentiles (see Chapter 5, Section 5.3.12). 67.7% of the Kratergöl fossil samples had a ‘good’ modern analogue. Therefore reconstructions can be interpreted with confidence that the majority of fossil species are represented in the modern training set. The coloured bar in Figure 6.10 highlights samples with a ‘good’ (green), ‘no good’

(yellow) and 'no close' (pink) analogue site. Samples with no good analogue are clustered around zone KD2 dominated by *E. paludosa var. subsalina*. The fact that this species does not have a good modern analogue requires reconstructed conductivity for this zone to be interpreted with caution.

6.3.10 Diatom biovolume

In order to account for variability in species valve size and volume, diatom stratigraphic data have also been plotted according to cell biovolume. The biovolume graph (Figure 6.11) reveals that zone KD3 experienced a decrease in the volume of all diatom species between 16 and 36 cm. Therefore the period of decreased *E. paludosa var. subsalina*, which characterised zone KD3, is less significant. This period coincided with the sandy section in the profile; therefore decreased cell volume could be an artefact of increased lake sedimentation rate. According to biovolume, the relative weighting of larger species (e.g. *C. placentula*) increased and the importance of smaller species (e.g. *N. cf. fonticola*) decreased. Biovolume zone boundaries do not remain the same as those defined by percentage data. This is associated with the fact that diatom biovolume is greatly related to lake sedimentation rate, i.e. faster sedimentation dilutes the number of diatoms accumulating in the sediment. The biovolume DCA ordination plot (Figure 6.12) illustrates that samples are less distinct according to their cluster analysis zones. Samples from KD3 show greatest dissimilarity to other depths indicating greatest variability according to biovolume. Biovolume DCA plotted stratigraphically also revealed greatest change in the assemblage throughout zone KD3 (Figure 6.11).

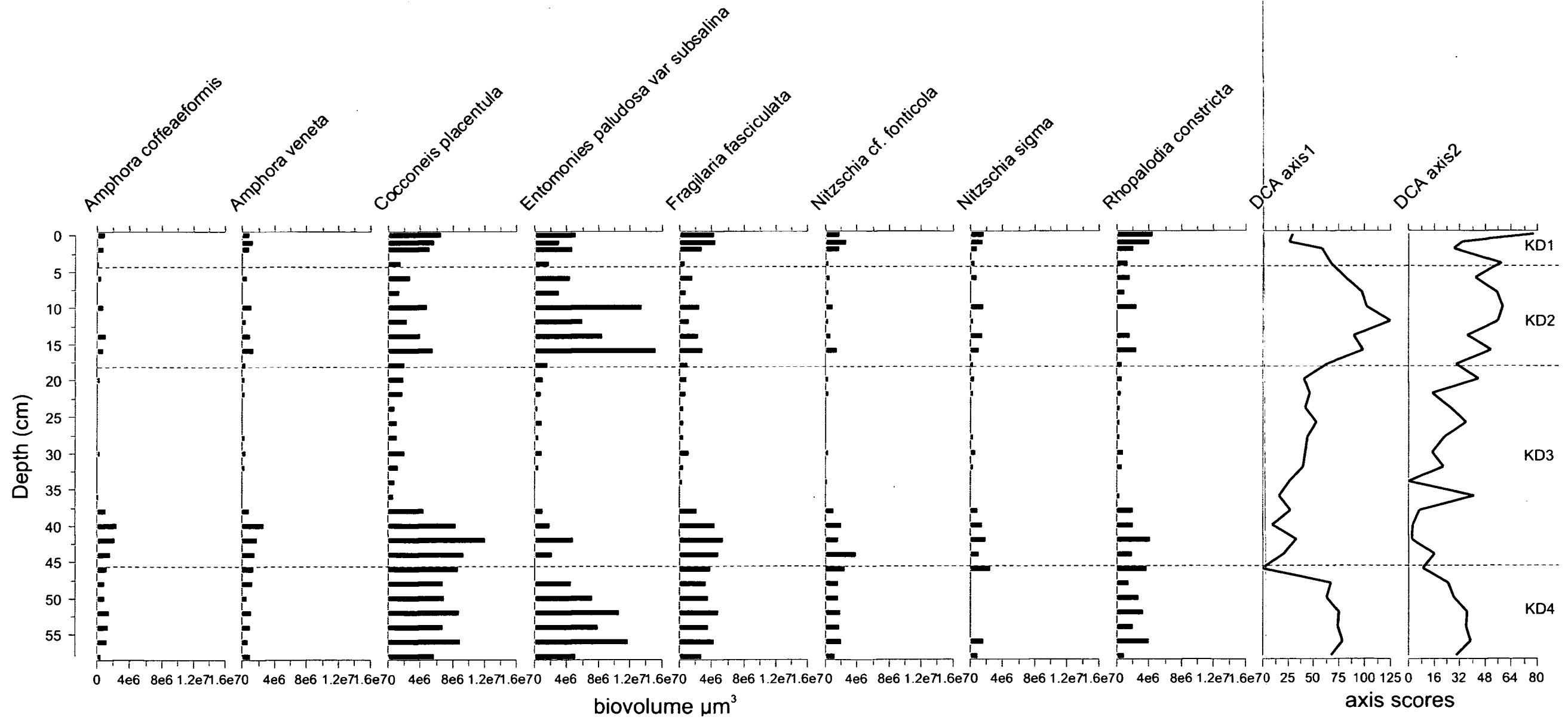


Figure 6.11 ACM99 diatom stratigraphy plotted according to biovolume (μm^3) (power transformed) with DCA axes 1 and 2. Species included have a maximum biovolume of at least $2.0e^{+06}$ within at least one sample.



Figure 6.12 ACM99 diatom sample biovolume DCA ordination plot with zones corresponding to percentage data cluster analysis.

6.4 Summary

This chapter summarised the modern diatom taxonomy of Kratergöl and presented data from the contemporary and palaeo-diatom assemblages. The ACM99 core section appears to represent sediment accumulated throughout the 20th century. The bottom of the sequence may relate to the 1920/1930s, the upper section with the late 1980s and it appears that the very top of the core may have been lost during retrieval. The sediment

profile is interrupted by sandy sections (37-17 cm) of low carbon content and diatom concentration, which are thought to represent major within-lake sedimentation events.

The diatom palaeo-assemblage is well represented in the modern environment and the dominance of key species varied throughout the record. According to cluster analysis and DCA, the diatom stratigraphy was split into four zones. The most significant period of change in the record involved increased abundance of *E. paludosa* var. *subsalina* during zone KD2 (17-4 cm); this may relate to a period of environmental change and higher salinity in the lake system. Species diversity (rarefaction) is associated with the abundance of three dominating species and concentration/total biovolume is related to the lake sedimentation rate. Species biovolume data revealed that zone KD3 experienced greatest variability in the diatom assemblage, with extremely low cell volume throughout this period. The transfer function reconstruction revealed that zone KD2 experienced a period of enhanced conductivity. However, discrepancies exist between values derived from the WA and MAT reconstructions and KD2 does not possess good matching analogues in the modern training set.

Despite superficial similarities between the lake sites, Kratergöl has a very different sediment record to the annually-laminated Nar sequence. Results suggest that the Kratergöl record is highly related to the lake sedimentation regime and interpretations are limited by discrepancies associated with the core integrity. Regardless of these limitations, there are changes evident in the diatom record, which are likely to be associated with environmental change.

Chapter 7

Diatom Stratigraphical and Environmental Change

7.0 Introduction

This chapter provides an interpretation of the Nar Gölü and Kratergöl diatom records and associated numerical analyses.

7.1 Diatom species ecology

Palaeoenvironmental inferences based on diatom assemblages require knowledge of species ecology. Details of taxon habitat, conductivity optima and ecological preferences for Nar and Kratergöl species at greater than 5% and 3% abundance were obtained primarily from the European Diatom Database (Juggins, 2008), Gasse (1986), Round (1984), Round *et al.* (1992) and Kelly *et al.* (2005) and are presented in Appendix 6.1 and 6.2.

7.1.1 Modern diatom assemblages

Nar epibenthic/epilithic habitats were mainly dominated by a diverse mixture of small diatom species (Chapter 5: Figure 5.1). For example, the widespread and abundant species *A. minutissimum*, which favours low to moderate conductivity and moderate nutrient levels and the non-planktonic diatom *C. anatolicus*, which is thus far unique to the Nar population and appears to favour brackish, circum-neutral conditions. Plankton and epiphyton samples were dominated by more specialised assemblages and larger taxa. Dominant blooming species identified in core thin sections include the cosmopolitan diatom *N. paleacea*, which is an indicator of low to moderate conductivity

levels and nutrient enrichment and the epiphytic/planktonic species *S. acus*, which signifies dilute conditions. The dominance of *A. formosa*, which has been recognised as an indicator of increased nutrients (Barker *et al.*, 2005), in the 2007 plankton may be associated with nutrient enrichment or recent disturbance in the lake system.

Abundant species in the modern Kratergöl assemblage included many large taxa that favour higher conductivity than species at Nar. The modern environment was dominated by the widely-distributed, pioneer, benthic/epiphytic species *C. placentula* (Chapter 6: Figure 6.1), which has a wide conductivity range. The high salinity indicators *F. fasciculata* and *N. complanata* and the fresh/brackish species *N. fonticola*, which colonises a variety of habitats and tolerates a range of water chemical conditions also dominated the modern Kratergöl environment.

Nar diatoms appear to derive from two sources associated with different seasons; the background assemblage includes taxa from numerous habitats, such as benthic and epiphytic niches. These species have been identified in organic layers on thin section slides and represent a diverse population. Other Nar diatoms are associated with bloom events, which do not occur every year, cover short time durations and involve high cell concentration of a single species. The Kratergöl assemblage does not appear to include bloom species and the community mainly comprises benthic taxa.

7.1.2 Relationship between modern and fossil assemblages

Interpretation of palaeo-diatom records requires understanding of the relationship between modern and fossil assemblages. In order to evaluate whether a representative sample of the modern diatom population is preserved in sediments, diatom

concentration, biovolume and rarefaction (species diversity) were compared with the lake sediment records.

Nar diatom concentration and total biovolume were lower in the modern surface mud in comparison with different sediment depths in the palaeo-record (Figure 7.1). This is associated with the fact that fossil samples contain an amalgamated annual diatom assemblage, whereas modern samples only include one habitat. Modern bottom mud, which represents diatoms from various habitats, had similar concentration and biovolume to the sedimentary record. Therefore the fossil assemblage is considered representative of the diatom community inhabiting the lake. This provides confidence for inferring past environmental conditions from fossil diatoms. Kratergöl concentration and biovolume was slightly lower in fossil samples in comparison with the modern environment (Figure 7.2). This implies that not all valves are preserved in the sediment or diatoms are currently more productive in the lake than in the past, which may be associated with allochthonous inputs.

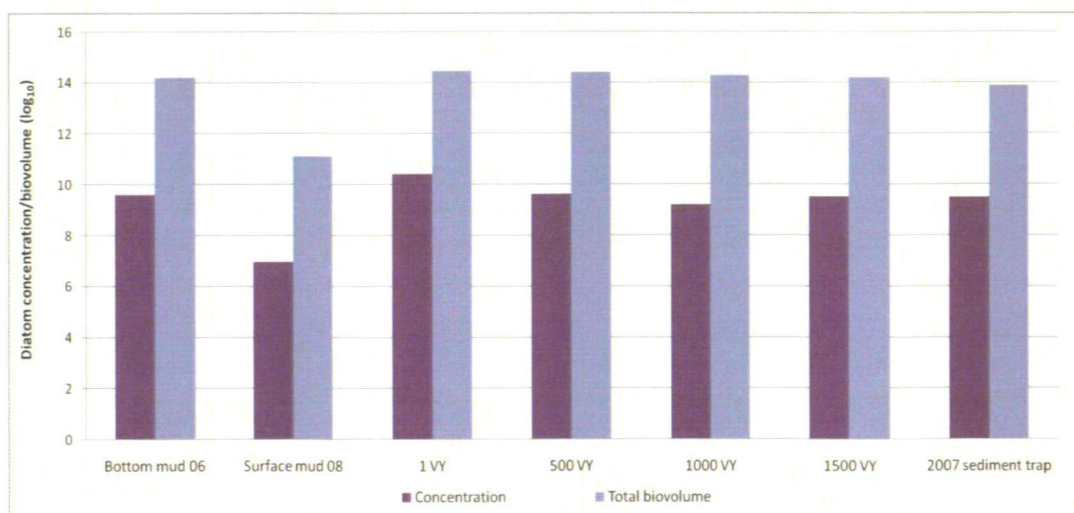


Figure 7.1 Comparison of Nar modern sample concentration (log₁₀) and total biovolume (μm^3) (log₁₀) with different sediment depths in the NAR01/02 palaeo-record.

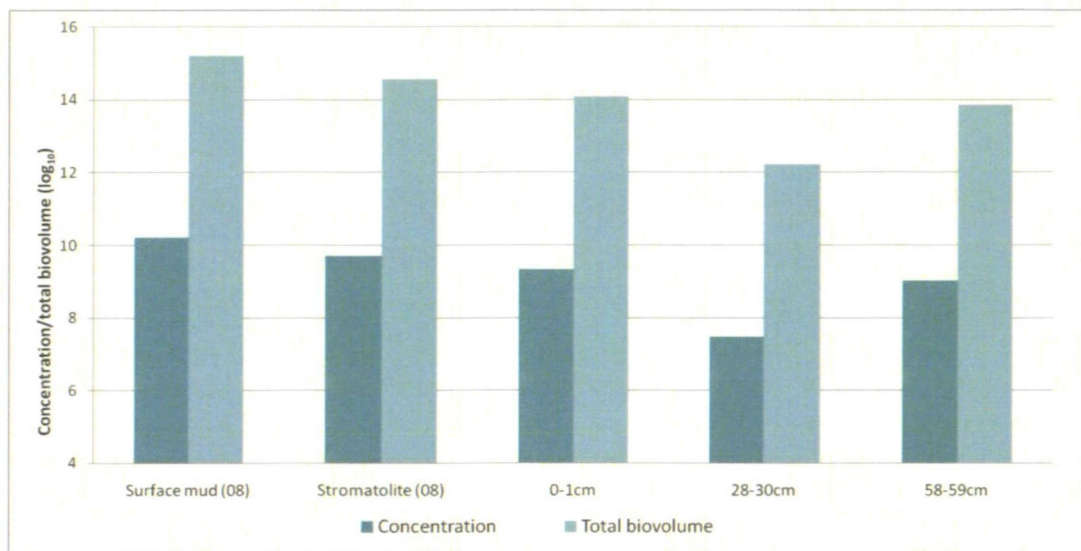


Figure 7.2 Comparison of Kratergöl modern sample concentration (\log_{10}) and total biovolume (μm^3) (\log_{10}) with different sediment depths in the ACM99 palaeo-record.

Nar samples contained higher diversity of species in comparison with Kratergöl, indicating that this site provides niches for a more varied assemblage. Modern samples only included one habitat sampled during one season, whereas fossil samples contained an amalgamated one/three year or ~ 1 g sediment sample. Therefore species diversity is greater in the fossil samples of both Nar and Kratergöl in comparison with the contemporary environment (Chapter 5: Figure 5.4 and Chapter 6: Figure 6.4).

The Nar and Kratergöl palaeo-diatom assemblages are well represented in the modern lake environments. Only one species was identified in the modern environment, *A. formosa*, which was not observed in fossil samples from Nar. Similarly, within Kratergöl modern samples, only one species was not represented in the fossil record, *N. complanata*. The two species that are not preserved in the lake sediments are delicately silicified and are likely to have suffered dissolution in the water column or they may not

have been present in the palaeo-environment. The fact that the majority of diatom species are represented in both records implies that diatom dissolution is not significant in these lakes. The Kratergöl fossil assemblages for all zones and the Nar assemblages of the most recent ~500 years are well represented in the modern lake environments. However, the diatom community of zone ND4 is not represented in the modern lake; this is associated with changing ecological conditions.

In addition to standard light microscope slides, Nar diatoms were also identified in core thin sections comprising undisturbed lake sediment (NAR01/02). Although it was not possible to clearly identify all diatom species on the thin section slides, a basic comparison between the modern, fossil and *in situ* thin section species revealed that the assemblages were very similar. Therefore the laboratory preparation procedure did not lead to selective dissolution of certain taxa. However, a higher frequency of intact cells of species such as *C. clypeus* and *S. acus* was observed in the thin sections; this implies that valves may become fragmented during the preparation process. Such problems were overcome through employing counting techniques that accounted for cell fragments.

7.2 Lake sedimentation

7.2.1 The Nar Gölü varve cycle

Lake sedimentation involves seasonal deposition of autochthonous matter, such as zooplankton and phytoplankton at various stages of decay, and material associated with chemical processes, such as biogenic calcite precipitation. Additionally, allochthonous material, including organics from the catchment, e.g. pollen, particulate matter (such as clays and carbonates) are incorporated in lake sediment. Maar lake sediments also

contain material derived from crater weathering, volcanic ash (tephras) and siliciclastic and volcanoclastic turbidites derived from the margins of the crater (Cohen, 2003).

Nar sediment varves comprise multiple layers of white/brown material associated with different lake processes. According to O'Sullivan's (1983) varve formation system, sediments at Nar include biogenic/calcareous lamina and, linked to the presence of mono-specific diatom bloom lamina, varves are seasonally-laminated. The Nar varve cycle is occasionally interrupted by relatively thick grey clastic layers. O'Sullivan (1983) highlighted that the formation of clastic layers is associated with allochthonous material from the catchment.

Nar laminated varves represent lake sediment accumulated throughout the course of a year (Table 7.1). Diatoms are an important component of the sediment and alter in concentration and species composition seasonally (Section 7.2.4). Organic material, including algal remains (such as diatoms), pollen and organic detritus is deposited during spring, summer and autumn. These layers form in a cyclic pattern with calcite layers. Within Nar sediments, the white carbonate layer was identified by Jones (2004) as representing late spring/early summer, therefore the deposition timing of other varve sub-layers can be interpreted in relation to this. According to Dittrich *et al.* (2004), carbonate precipitation lasts approximately one month following diatom blooms. Brown varve sub-layers at Nar accumulate throughout the course of the year and appear to represent slower disposition of organic plant and algal remains with a mixture of non-blooming diatom species.

Diatom production is typically greatest in spring and can be continuous throughout the year (Wetzel, 2001). Nar single-species diatom bloom events involved extremely high cell numbers and occurred on average once in every two-three years. The sequence of sediment deposition events is highlighted in Figure 7.3. Stratification of Nar lake water was identified during summer. It is not known whether the thermocline breaks-down at any point during the course of a year.

Season	Material	Colour	Composition	Origin
Spring	Organic detritus, often preceded or succeeded by a mono-specific diatom bloom	Organics appear brown Diatom blooms appear pale yellow Large diatom blooms may appear green when viewing core material directly	Plant, algal, pollen and other organic detritus Diatom blooms are composed of silica and often involve high abundance of <i>N. paleacea</i>	Autochthonous organic material produced within the lake
Late spring/ early summer	Calcium carbonate	White lamina	Calcite or aragonite depending on the evaporative status of the lake	Autochthonous carbonate precipitated as a result of photosynthetically-lowered lake water pH following the spring diatom bloom
Summer	Organic detritus and diatoms	Brown organic	Plant, algal, pollen and diatom remains	Autochthonous organic material
Autumn	Organic detritus, occasionally preceded or succeeded by a mono-specific diatom bloom	Organics appear brown Diatom blooms appear pale yellow	Plant, algal and other organic detritus Diatom blooms often involve high abundance of <i>S. acus</i>	Autochthonous organic material
Winter	Organic detritus	Lighter/darker brown associated with dominant material, e.g. algal/plant	Plant, algal and other organic detritus	Autochthonous organic material
Non-seasonal	Clastic	Consistently grey	Clays and particulate matter	Allochthonous catchment in-wash or sub-surface sediment slumping

Table 7.1 Model of the seasonal varve cycle at Nar Gölü based on sediment material, colour, composition and origin.

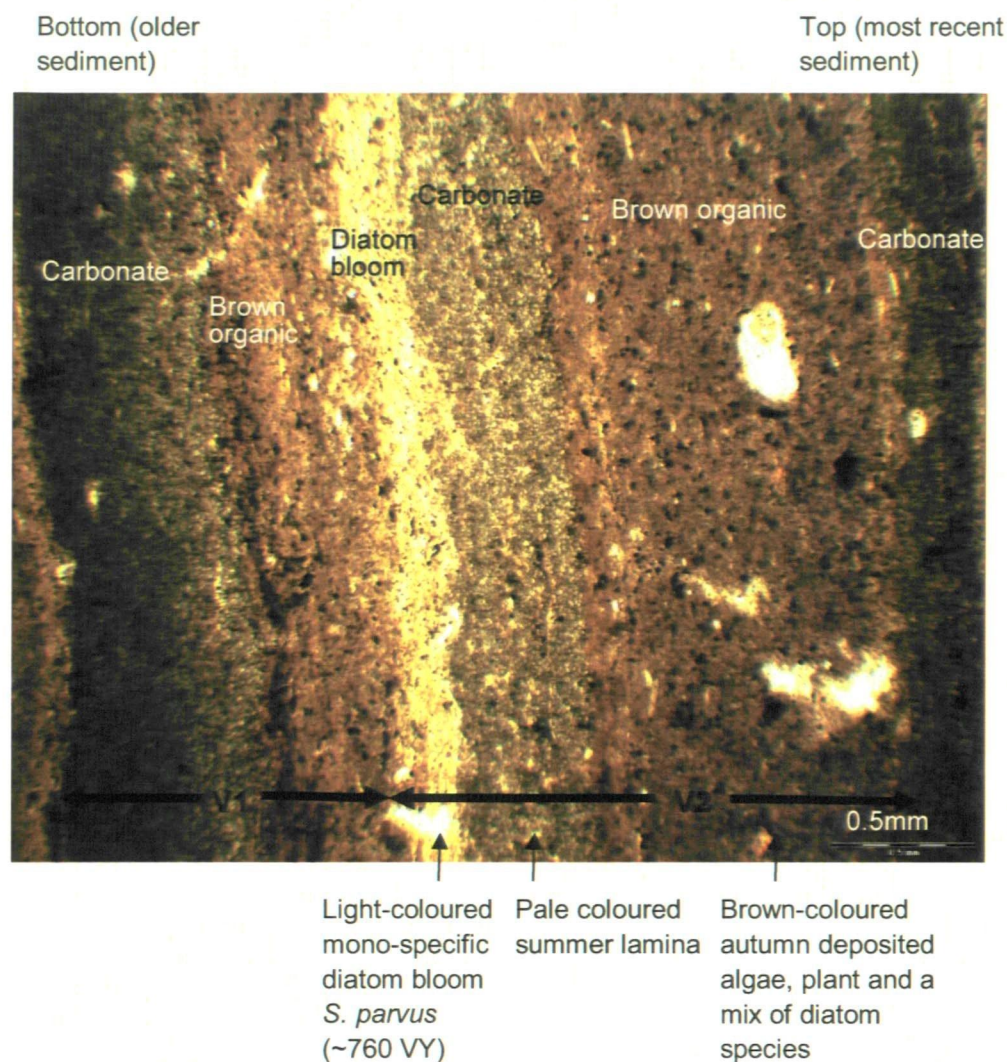


Figure 7.3 NAR01/02 thin section micrograph illustrating carbonate (appears grey/white), diatom bloom of *S. parvus* (pale yellow) and organic layer (brown).

7.2.2 Nar diatom blooms

When viewing the Nar diatom assemblage *in situ* on thin sections slides, it was possible to observe bloom events of specific taxa, which form distinct layers within varves during periods when no other material or species are deposited. Bloom species include *N. paleacea* (Figure 7.6), *S. acus* (Figure 7.5) and *S. parvus* (Figure 7.4). It is possible that other species bloom; however, this may be masked on the thin section slides by organic material deposited simultaneously. Additionally, thin section slides did not

cover the period AD 290-1100. Mono-specific blooms of the dominant planktonic species *C. meneghiniana* may have dominated the assemblage in the early part of the record.

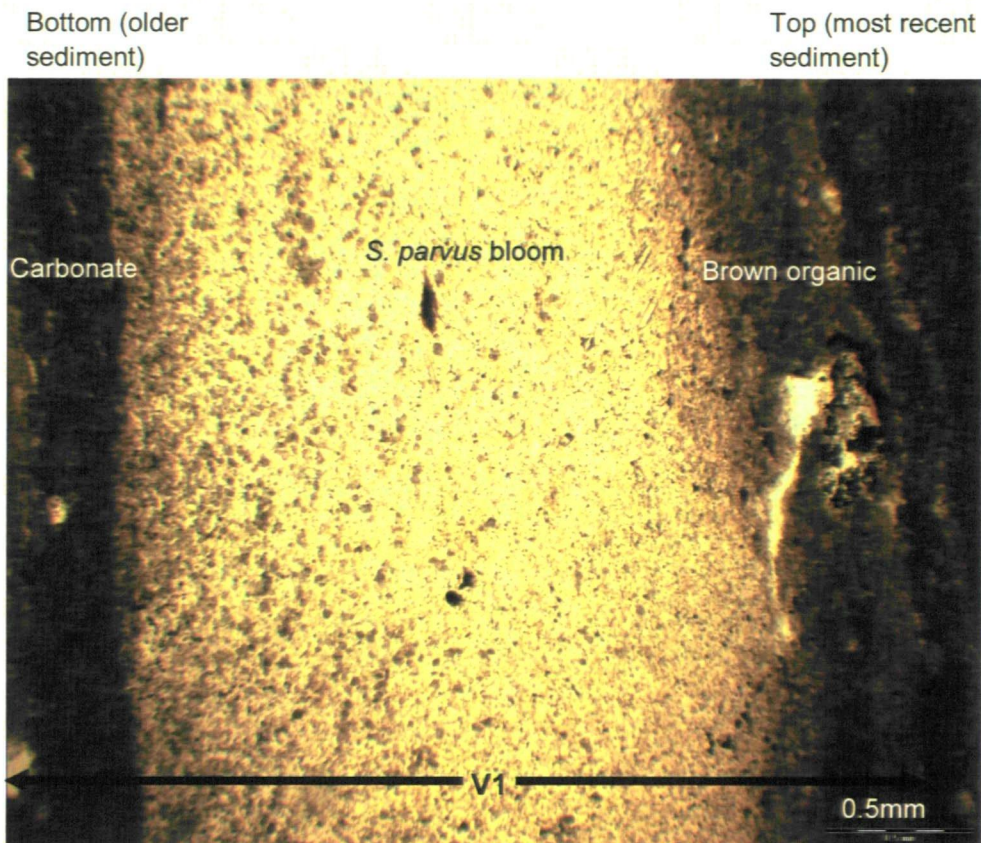


Figure 7.4 NAR01/02 thin section micrograph illustrating pale yellow *S. parvus* bloom (~750 VY).

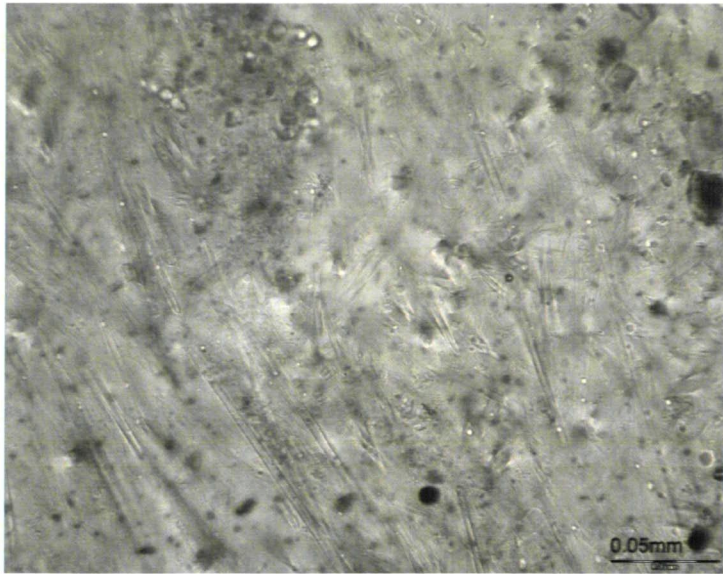


Plate 7.5 NAR/02 thin section micrograph illustrating *S. acus* bloom layer (2 VY).

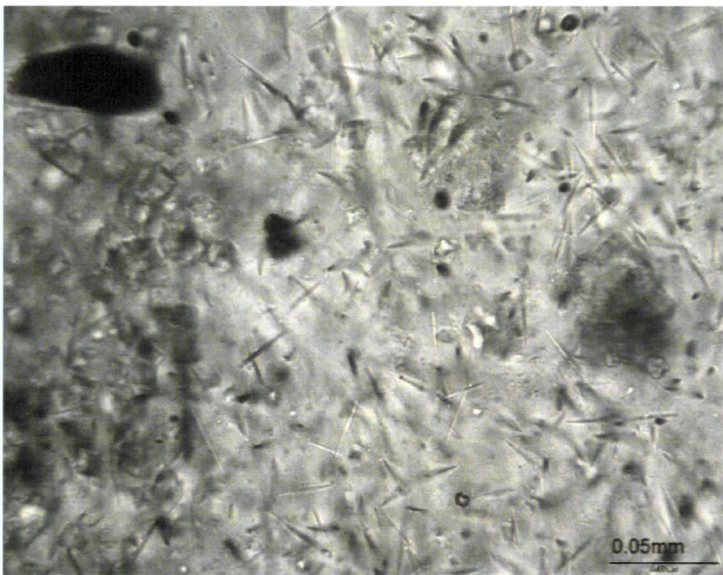


Plate 7.6 NAR01/02 thin section micrograph illustrating *N. paleacea* bloom layer (1 VY).

Within the core thin sections, a mixture of diatom species was identified as blooming immediately before the white carbonate layer (Figure 7.3). This sometimes involved mono-specific *N. paleacea* blooms. However, blooms of this species did not always precede the carbonate layer. *S. acus* appeared shortly after the beginning of organic

deposition and was followed by a thicker brown organic layer. Therefore it appears that *N. paleacea* often blooms during spring, prior to carbonate precipitation, and *S. acus* blooms during the period when organic plant material is deposited, which could relate to spring or autumn. However, the timing of large bloom events of these species was not always consistent through the year. *S. parvus* bloomed over a ~20 varve year period (798-757 varve years (VY), AD 1205-1246) (Figure 7.4) and was not identified in such extreme high cell numbers again throughout the entire record. This species bloomed for extended sub-annual periods of time and was frequently abundant throughout the carbonate layer. Therefore *S. parvus* may bloom during spring/early summer, when carbonate is precipitated. The sudden abundance of *S. parvus* may be associated with other processes occurring in the lake rather than seasonality. For example, *S. parvus* is a eutrophic taxon that favours low conductivity and may have increased in abundance following enhanced nutrient supply or lowered salinity level, allowing it to out-compete other blooming species. Kilham and Kilham (1990) identified that *Stephanodiscus* species dominate when the supply ratio of Si:P is relatively low. This implies that the Nar blooms of *S. parvus* could be associated with increased phosphorus levels in the system.

The appearance of bloom species may represent specific changes in the lake system. *S. acus* and *N. paleacea* are frequently described as spring and summer blooming diatoms (e.g. Ishihara *et al.*, 2003, Mackay *et al.*, 2005, Tsukada *et al.*, 2006 and Brüchmann and Nengendank, 2004). *S. acus* has also been described by Mackay *et al.* (2005) as an opportunistic species, able to increase its net growth when other species cannot. This species also favours high nutrient concentration (Baier *et al.*, 2004). Therefore *S. acus* may bloom when conditions are unfavourable for *N. paleacea*.

According to the Nar sediment traps, *S. acus* is productive throughout the year. Distinct bloom events were not identified; however, increased diatom concentration and biovolume towards the sediment trap surface may represent blooms of *S. acus* (Chapter 5: Figures 5.5 and 5.6). Sediment traps could lose stratigraphic integrity throughout their instalment in the lake or during transport to the laboratory. Alternatively, material may be lost through the duration of the trap's instalment in the lake. *N. paleacea* and *S. parvus* have not bloomed during the last six years and were therefore not present in the sediment traps. Changing abundance of diatoms is also affected by blooms of other algae; this may affect seasonality in the sediment traps.

Kilham *et al.* (1986) linked the changing dominance of *Nitzschia*, *Synedra* and *Stephanodiscus* species to alterations in Si:P ratios. For example, *Stephanodiscus* and *Synedra* species predominated at extreme ends of the Si:P gradient and *Nitzschia* species dominated at intermediate values. Changes in the lake nutrient regime, which may be associated with nutrient recycling in the system and partly related to climatic variability, could account for some of the seasonal and centennial variability observed in the Nar diatom bloom species record.

Diatom bloom species are associated with a short time period, are prolific when nutrient availability increases and drive DI-conductivity down in the palaeorecord. Their low conductivity optima imply that they should not be able to bloom in the brackish Nar environment. A possible explanation for their presence could be associated with the spring snow-melt, which may result in lowered lake water conductivity, creating conditions suitable for *N. paleacea* to bloom when nutrient availability increases.

7.2.3 Nar diatom blooms and nutrients

Seasonal changes in water temperature can lead to thermocline breakdown. This allows nutrient-rich deeper water to mix with surface layers (Round, 1984) and may initiate blooms of diatom species, such as *N. paleacea*, which favour higher nutrient levels. Diatom bloom events have increased in frequency at Nar during the most recent 100 years (Chapter 5: Figure 5.24). Plankton blooms are typically associated with eutrophic conditions (Hall and Smol, 1999). Nutrient enrichment leads to decreased diatom species diversity, which is apparent during bloom events, when *N. paleacea* dominates over 90% of the population. However, decreased values of other species during *N. paleacea* blooms are a statistical artefact of relative percentage calculations. Therefore species diversity may not actually decrease when *N. paleacea* blooms.

A number of Nar diatom species are described as favouring high nutrient conditions (Appendix 6.1). Natural eutrophication can result from forest fires and climatic changes, such as drought, which may concentrate lake water nutrients and lead to increased nutrient-rich ground water supply (Hall and Smol, 1999). However, natural eutrophication is normally gradual and enhanced nutrient supply is usually associated with human activity, particularly sewage disposal, farming and soil erosion (Hall and Smol, 1999). It is possible that local agricultural practice may have resulted in increased nutrient supply at Nar. However, farming around the lake is presently limited and many plots are currently abandoned. According to England (2006) and England *et al.* (2008), the pollen record from Nar signifies that the wider environment is influenced by much anthropogenic activity, such as forest clearance and periods of intensified agriculture. Additionally, volcanic influx of geothermal groundwater can lead to nutrient influx.

Therefore it appears that Nar may have experienced periods of enhanced nutrient levels throughout the last 1720 years as a consequence of different factors.

7.2.4 Diatom seasonality

Information about diatom community seasonality at Nar has been derived from modern samples, sediment traps and thin sections. The dominance of different diatom species altered throughout the sediment trap sequences; however, these changes were not uniform between the different traps representing six years of sedimentation (Chapter 5: Figure 5.5). For example, the 2002-2003 10 m water depth trap contained greatest abundance of *C. anaticus* at the bottom and low values of *S. acus*; this pattern was reversed in the 2004-2005 trap. Therefore it appears that sediment traps at Nar may record changes in diatom productivity but do not always record changes in species seasonality clearly.

There appear to be some discrepancies between the dominance of certain species in the Nar sediment traps, palaeo-records and modern samples. For example, the 2007 plankton sample contained abundant *S. acus* and this species was also dominant in the NAR06 percentage record between 2003 and 2006 (Chapter 5: Figure 5.17). *S. acus* dominance was expected to be reflected in the sediment traps. However, the 2005 and 2003 traps do not contain *S. acus*; therefore these traps may not represent the entire year of sedimentation. *S. acus* represents over 30% of the population between 2002 and 2006 in the NAR06 percentage record. These discrepancies highlight that dissimilar information can be derived from different diatom community analysis methods.

In addition to the ecological preferences and life-forms of individual species, there are a number of additional factors governing diatom population dynamics. For example, diatoms interact with other algal and non-algal groups and are affected by factors such as predation and parasitism. These interactions have not been investigated at Nar or Kratergöl. Therefore literature sources have been consulted in order to understand how such interactions may influence the diatom assemblages in the study sites.

Wetzel (2001) summarised phytoplankton population succession throughout the course of a year in a typical temperate lake and described changes in the diatom population in relation to the dominance of other organisms. During mid-winter, zooplankton grazing pressure of diatoms is low and decreased temperatures and moderate nutrient availability leads to dominance of small phytoplankton, particularly flagellates. Algal species that tolerate low nutrient and light levels can out-compete many diatom species for resources in winter. During late winter, light availability improves with increasing dominance of dinoflagellates and small centric diatoms. During spring, nutrient levels are typically high and light availability is variable; therefore diatom biomass increases rapidly leading to a peak in productivity. The spring maximum is typically dominated by one diatom species and green algae. The bloom is usually short lived, lasting typically one to two months. During summer, light availability increases and nutrients decline, particularly phosphorus, resulting in decreased phytoplankton biomass. Zooplankton grazing increases during this period. Other algal species, tolerant of increased grazing pressure, then prevail. During late summer, zooplankton populations decline, which is followed by an abundance of chrysophytes and green algae. If silica levels remain sufficient, green algae are often replaced by large diatoms. A second phytoplankton maximum during autumn, typically involving diatoms, is usually not as

pronounced as the spring bloom. An abrupt decline in phytoplankton occurs following autumn.

The applicability of Wetzel's (2001) examples based on typical temperate lakes is limited when comparing with the semi-arid environments of Nar and Kratergöl. The climate of central Anatolia is strongly seasonal; therefore the diatom populations are likely to be influenced by many of the successive seasonal patterns and intra-species interactions described by Wetzel (2001). The impacts of sub-annual conditions may be more pronounced in the Nar and Kratergöl records as a result of greater seasonal climatic variability. The Nar assemblages appear to be affected by changing nutrient levels throughout the year, which allow diatom bloom species (*N. paleacea* and *S. acus*) to out-compete other algae. Bloom events coincide with increased diatom concentration, which is enhanced towards the top of the sediment traps (Chapter 5: Figure 5.5); this represents spring and summer. When key nutrients (e.g. phosphate) become depleted other algae may dominate the Nar assemblage. Silica availability is not a limiting factor for diatoms at Nar and Kratergöl due to its availability in the volcanic rock type. Additionally, the diatom blooms may end due to increased parasitism or zooplankton grazing during summer. In the Nar thin sections, diatom blooms involving two different species are frequently evident throughout the year. These are likely to represent the spring and autumn blooms described by Wetzel (2001).

7.2.5 Kratergöl diatom seasonality and sedimentation

The Kratergöl diatom assemblage is greatly influenced by the variable lake sedimentation rate. O'Sullivan (1983) suggested that varve formation requires flat-bottomed lake beds to avoid slumping. The fact that Kratergöl is not flat-bottomed,

according to Dumont's (1981) analysis of the southern bays, could be the reason for the absence of varves in the lake sediment. The Kratergöl sequence was non-laminated and sediment traps were not installed in the lake. Therefore seasonality in the Kratergöl diatom assemblage is not well understood. The diatom percentage data imply that Kratergöl does not appear to experience sudden blooms of certain species resulting in extreme abundance of different taxa through the palaeo-record. However, interpretations are limited as it not clear how many years are represented by each ACM99 sample and processes in the lake that may smooth the signal, such as sediment reworking, are not well understood. Seasonal variability in the Kratergöl assemblage is likely to be affected by many of the factors discussed by Wetzel (2001), such as intra-species interactions and changing light and nutrient availability.

Dominant Kratergöl species have been identified as prolific during different seasons. For example, according to Reynolds (1993), *Fragilaria* species often contribute significantly to lake algal biomass during late summer. *F. fasciculata* was recognised as highly abundant at Kratergöl during the summer sampling time. According to Round (1984), *C. placentula* often exists within a relatively simple diatom community dominated by a few species, typically epiphytically, with seasonally continued growth. These assemblage types were recognised at Kratergöl.

7.3 Palaeoenvironmental change

7.3.1 Nar Gölü

Diatoms are well preserved throughout the entire Nar palaeo-sequence. This suggests that conditions that lead to poor diatom preservation have not occurred in the lake throughout the last 1720 years. For example, extreme lake shallowing leads to

dissolution and breakage of diatom frustules (Battarbee *et al.*, 2001) and extreme alkalinity can initiate silica dissolution. Palaeoclimatic inferences have been drawn from the Nar diatom zones based on the various analysis methods (Table 7.2).

Nar diatom zone	Sediment colour	Diatom ecology	Diatom concentration, biovolume, % benthic and diversity	DCA axes 1 and 2	Thin sections Bloom frequency	DI-conductivity (all species, blooms and omitting blooms)
ND1 AD 1480-2000 (520-1 VY) a, b, c, d AD 1927- 2006(80-1 VY)	Consistently light (aragonite) with a shift to dark at AD 2000 (calcite) (2008 sediment trap suggests return to aragonite)	Continued abundance of lower salinity indicators and planktonic bloom species (<i>N. paleacea</i> , <i>A. minutissimum</i> and <i>S. acus</i>) with a shift at AD 2000 to dominance of non-planktonic/epiphytic <i>C. anatolicus</i> and <i>S. acus</i> .	Similar to zone ND2 Recent increased biovolume of higher salinity indicator <i>C. meneghiniana</i>	Axis 2 highlights increasing variability related to blooming species	Increased frequency of large mono-specific bloom events (~30/100 years) Thicker varve layers Higher frequency of clastic layers	Consistently low conductivity Averages: A: 485 μS^{-1} B: 121 μS^{-1} OB: 1,588 μS^{-1}
ND2 AD 990-1470 (1010-530 VY)	Shift to lighter at AD 990 and very light at AD 600 (aragonite)	Continued dominance of bloom species and appearance of widespread <i>A. minutissimum</i>	Concentration, total biovolume, diversity and % benthic reflect highly fluctuating values of <i>N. paleacea</i>	Axis 1 indicates stable diatom population	Gradual increasing frequency of large mono-specific bloom events (~10/100 years)	Consistently low conductivity Averages: A: 569 μS^{-1} B: 118 μS^{-1} OB: 2,048 μS^{-1}
ND3 AD 550-980 (1460-1020 VY)	Shift to darker at AD 540 (calcite) Return to lighter at AD 600	Appearance of bloom species and lower salinity indicators <i>N. paleacea</i> and <i>S. acus</i>	Diversity decreased Concentration and biovolume increased with higher abundance of <i>N. paleacea</i>	Axis 1 indicates a slower period of change	N/A	Decreased DI-conductivity Averages: A: 1,078 μS^{-1} B: 118 μS^{-1} OB: 2,664 μS^{-1}
ND4 AD 290-540 (1720-1470 VY)	Light Aragonite	High salinity and disturbance indicators <i>C. meneghiniana</i> , <i>F. construens</i> var. <i>venter</i> and <i>R. operculata</i>	Concentration and total biovolume stable Large species dominate Lower species diversity	Major shift in DCA axis 1 at AD 540	N/A	Elevated DI-conductivity Averages: A: 3,545 μS^{-1} B: 115 μS^{-1} OB: 4,580 μS^{-1}

Table 7.2 Summary of inferences derived from the Nar diatom records. DI- conductivity based on A=all species, B=bloom species only and OB=omitting bloom species.

Zone ND4 (AD 290-540, 1720-1470 VY)

Throughout this period, the Nar palaeo-diatom record was dominated by the widespread pioneering species *F. construens* var. *venter* (Chapter 5: Figure 5.12), which tolerates a wide range of water chemistry and is associated with disturbance and increased turbidity (see Appendix 7.1 for species conductivity optima according to the EDDI combined salinity training set). The centric, widespread planktonic species *C. meneghiniana*, which is an indicator of higher salinity levels and tolerates a wide range of alkalinity, also dominated this period. The higher conductivity optima of species during this period indicate that lake level was low and disturbance was high, which may be associated with an arid climate or catchment disturbance as a result of human activity. This period experienced the highest conductivity levels in the last 1720 years, suggesting a lower lake level. However, the DI-conductivity reconstruction for this zone was accompanied by poor analogue matching; this is attributed to the presence of *R. operculata*.

The absence of known diatom bloom species (*N. paleacea* and *S. acus*) during this time indicates that these species were not able to tolerate higher salinity levels or were out-competed by other blooming algae and diatoms. According to biovolume, dominant species in this zone are also indicators of higher conductivity, e.g. *C. clypeus* ($8,162 \mu\text{S}^{-1}$) and *N. halophila* ($5,639 \mu\text{S}^{-1}$), which has been described as a species that can survive extreme saline conditions (Round, 1984), and *R. operculata*, which is a common epiphytic taxon that often favours shallower water depth (Round, 1984). Larger diatom species were important during this period (e.g. *R. operculata* and *C. clypeus*) in comparison with ND3. The lake environmental change leading to zone ND3 impacted upon both large and smaller diatoms (Chapter 5; Figure 5.19). Lake sediment mineralogy alters as a response to changes in evaporation. For example, aragonite

relates to more evaporated conditions and calcite indicates lower evaporation. This zone was dominated by lighter sediment (aragonite), which indicates increased evaporation in agreement with the drier environment identified by the diatoms.

The percentage of benthic species was lower in ND4 in comparison with later zones. However, the opposite pattern was expected; drier zone ND4 should have involved lower lake levels and thus a higher proportion of benthic species. It seems that the relationship between diatom life-form and water level is not straightforward at Nar, as species appear to inhabit multiple niches.

Zone ND3 (AD 550-980, 1460-1020 VY)

The beginning of this zone involved a major diatom assemblage shift. According to Gasse *et al.* (1997), abrupt species shifts occur when a limnological threshold has been reached, which may represent a gradually changing climate rather than a rapid climate shift. Therefore the Nar assemblage change may represent a gradual climate shift during the preceding time period.

The appearance of the widespread blooming species *N. paleacea*, which has lower conductivity optima than ND4 species, can also be indicative of eutrophic conditions. This implies that the lake may have become more productive. This was accompanied by dominance of the new taxon identified in the modern Nar environment (*C. anatolicus*), which may indicate conditions similar to the present. Biovolume also highlights the appearance of lower salinity indicators *S. acus*, epiphytic/epipelic *R. gibba* (optimum: $916 \mu\text{S}^{-1}$) and *N. oblonga*. This indicates a shift to lower conductivity levels, possible nutrient enrichment, increased water depth and decreased turbidity.

The shift from zone ND4 to ND3 is reflected by an increase in species diversity, associated with the lack of bloom species in zone ND4 and a significant shift in NAR01/02 DCA axis 1 (Chapter 5; Figure 5.16). DI-conductivity decreased through this zone with increasing abundance of *N. paleacea*, indicating freshening of the system. However, the reliability of the reconstruction was reduced by the appearance of the non-analogue species *C. anaticus* during this period. Although *S. acus* and *N. paleacea* have low conductivity optima in the combined salinity training set, the upper range of these species reaches well above their optima (Appendix 7.1). Therefore reconstructed values may be misleading. Additionally, DI-conductivity may not reflect the environmental preferences of many species in the lake during periods dominated by bloom species, which results in low diversity assemblages.

A colour shift to darker laminae (calcite) was identified in the carbonate greyscale measurements at AD 540 simultaneously with the major shift in the diatom assemblage. Increased calcite indicates decreased evaporation and a possible climatic change. This was followed by a return to lighter sediment, signifying enhanced evaporation towards the latter stage of this zone.

Zone ND2 (AD 990-1470, 1010-530 VY)

Increasing values of *S. acus* indicate lower conductivity levels with increasing abundance of the widespread freshwater/brackish species *A. minutissimum* during the latter period of ND2. The sudden bloom of the freshwater, eutrophic, planktonic species *S. parvus* at 750 VY may be indicative of higher nutrient levels and implies a sudden change in environmental conditions. Biovolume signifies a stable environment through

this zone, with continued dominance of lower salinity indicators *N. oblonga*, *R. gibba* and *S. acus*. This relates to dilute conditions and deeper water level. Bloom species increased in abundance throughout this period, with extreme fluctuating levels. This highlights seasonal variability in the assemblage and higher nutrient availability. Additionally, NAR01/02 DCA axes, diatom rarefaction, concentration and total biovolume remained relatively consistent through this zone, indicating a relatively stable population.

DI-conductivity remained consistently low throughout this period. *S. parvus* has a narrow conductivity range (Appendix 7.1), which may account for the absence of this species throughout the majority of the record. DI-conductivity is positively correlated with rarefaction and negatively correlated with diatom concentration; this indicates that the assemblage is more diverse and less productive during drier periods. However, this pattern is largely associated with the changing dominance of *N. paleacea*, which has a large impact on species diversity and concentration.

A shift to lighter carbonate greyscale (increased evaporation) occurred at 990 VY (AD 1010) simultaneously with the diatom zone boundary involving decreased *C. anatolicus* and increased *N. paleacea*. A further colour shift to extremely light sediment occurred at 600 VY (AD 1400) simultaneously with the disappearance of *C. anatolicus*. A significant negative relationship was identified between grey scale measurements and the abundance of *C. anatolicus* (Tables 7.3 and 7.4). Therefore *C. anatolicus* relates to darker sediment, which is rich in calcite and may indicate a wetter environment. However, there are further controls on carbonate colour change other than shifts in calcite/aragonite mineralogy; therefore this relationship is not straightforward.

Additionally, a positive relationship was identified between grey scale and *S. acus* and *A. minutissimum*. As colour changes mainly relate to the degree of evaporation, this implies that *C. anaticus*, *S. acus* and *A. minutissimum* may show a secondary response to changes in evaporation and is reflected in the significant relationship between grey scale and DCA axis 2 (Figure 7.3). The organic carbon content (C:N ratio) of each varve layer (Jones, 2004) is negatively correlated with diatom NAR01/02 DCA axis 1 and positively related to *A. minutissimum* percentage (Tables 7.3 and 7.4). Although these correlations are not 'strong', it appears that temporal changes in the carbonate sediment colour and organic carbon content are related to diatom assemblage fluctuations.

Zone ND2 represents the first half of the thin section record (900-1 VY, AD 1100-2000). This period experienced lower frequency of mono-specific diatom bloom events (~10 per 100 years) in comparison with ND1. Nar does not experience extreme values of blooming diatom species every year. Therefore during non-diatom bloom years, other algae may have dominated the spring/autumn assemblages. Varve thickness remained relatively consistent throughout this zone with peaks associated with diatom bloom events. This indicates consistent lake productivity and that variable diatom biomass is associated with mono-specific blooms.

Zone ND1 (AD 1480-2006) (NAR01/02: 520-1 VY) (NAR06: 80-1 VY)

The transition to zone ND1 involved disappearance of *C. anaticus* and significantly greater abundance of *S. acus* and *A. minutissimum*. According to Mackay *et al.* (2005), *S. acus* is an opportunistic species; therefore this taxon may dominate when conditions become unfavourable for other species. *N. paleacea* favours higher nutrient levels and

reduced abundance of this species may have resulted from decreased nutrients in the system or changes in disturbance. *N. paleacea* peaks are accompanied by increased diatom concentration and decreased diversity highlighting the blooming life-form of this species. *A. minutissimum* inhabits various environments, tolerates moderate nutrient levels and low conductivity. Therefore increased values of this species may represent a slight freshening of the system or a decrease in nutrient levels. NAR01/02 DCA axis 2 highlights increasing population variability through this zone associated with periods of *N. paleacea* blooms. Consequently rarefaction, total biovolume and percentage benthic are more variable, indicating environmental change in the system.

DI-conductivity remains consistently low throughout zone ND1. The most recent (post AD 2000) change in the assemblage was dominated by *C. anatolicus*, which does not have a modern analogue in the EDDI salinity training set. Therefore conductivity has not been reliably reconstructed for this period. However, the decrease in *N. paleacea* could be interpreted as signifying increased conductivity levels. This would correspond with the fact that lake level has recently decreased.

Biovolume highlights continued dominance of *N. oblonga*, *R. gibba* and *S. acus* through ND1, with periods of increased high-conductivity indicator *C. clypeus*. This may indicate recent enhanced aridity. However, the importance of *C. clypeus* has been underestimated by the DI-conductivity reconstruction, due to its relatively large size and lower cell numbers.

Mono-specific diatom bloom events became increasingly common throughout zone ND1 (~30 per 100 years) according to the core thin sections. Such events may be

associated with changing nutrient supply or system disturbance and indicate an environment impacted by increasing human activity. Thin section total varve thickness is positively correlated with NAR06 diatom concentration (Table 7.4) and white carbonate and brown organic layers are significantly related to different numerical analyses of the diatom record e.g. rarefaction and diatom concentration ($r=0.344$, $p=0.002$). This implies that varve thickness can be used as a proxy for diatom productivity and thicker varve layers are associated with diatom bloom events, which result in decreased species diversity and increased autochthonous carbon production in the lake. Total varve thickness has increased throughout the last ~200 VY (AD 1800), implying that this period has experienced greater productivity and may relate to increased nutrient supply. However, thicker more recently deposited varves also relate to decreased compaction and increased water content of near surface sediment.

During the last 80 years bloom species have dominated the Nar record. *S. acus* and *A. minutissimum* were abundant in zone ND1d and *N. paleacea* dominated the assemblage of ND1c, indicating a fresh environment with conditions suitable for mono-specific diatom blooms, i.e. high nutrient availability during spring. A significant assemblage change occurred between zones ND1b and ND1a (AD 2002-2006), when dominant species *N. paleacea* and *A. minutissimum* were replaced by *C. anaticus* and *S. acus*. This may represent a recent change in the system. According to biovolume (Chapter 5: Figure 5.18), the assemblage change in zone ND1a is also significant (AD 2000). Biovolume revealed that *P. viridis*, a large epiphytic/benthic species with a wide salinity range, is characteristic of zones DN1d and ND1c and *C. clypeus* dominated zones ND1d, c and b. Increased values of *C. meneghiniana* during the most recent 11 years

(~AD 1997-2006) may indicate recent increased aridity or a change in the lake water N:P ratio.

The fact that the most recent five years have experienced an increase in *S. acus* and decrease in *N. paleacea* implies that the system is becoming more evaporated and other factors associated with disturbance may have altered. However, summer instrumental readings at the lake during the last nine years have not revealed an increase in conductivity. According to Kilham *et al.* (1986) nitrogen limitation is frequently associated with dominance by cyanobacteria. Marcarelli *et al.* (2006) examined how salinity and nutrient supply interact to control phytoplankton community composition in saline lakes. Salinity controls whether N₂-fixing cyanobacteria are present in the phytoplankton community, which leads to changes in nutrient limitation with consequences for the diatom community. Therefore salinity may be influencing nutrient availability at Nar and therefore relates to the changing dominance of *S. acus* and *N. paleacea*.

Relatively low species diversity often reflects a stable system and higher diversity relates to an environment where disturbance increases competition and creates niches for a more varied assemblage. This is illustrated by Connell's (1978) intermediate disturbance hypothesis, which predicts that maximum species diversity is reached at intermediate disturbance levels. Wolfe (2003) identified this relationship in diatom communities. Decreased values of *N. paleacea*, associated with higher diversity, may represent periods of disturbance. Therefore, low values of *N. paleacea* in zone ND4 and in the most recent 5 years (zone ND1a) (Chapter 5: Figures 5.11 and 5.12) may represent greater disturbance in the system.

DI-conductivity was enhanced in ND1d and appeared to increase when *N. paleacea* was lower. However, the recent disappearance of *N. paleacea* (ND1a) did not result in higher DI-conductivity. This zone was accompanied by poor analogue matching due to dominance of *C. anaticus*. There is a positive relationship between NAR06 DI-conductivity and the percentage of benthic species (Table 7.4). This implies that during periods of increased salinity, the number of benthic niches increases due to decreased water level. Additionally, there is a weak positive relationship between NAR06 DI-conductivity and greyscale value indicating that conductivity changes relate to carbonate sediment colour changes. DI-conductivity is also negatively related to varve thickness suggesting that drier periods, involving higher salinity, were less productive and resulted in decreased material being deposited on the lake bed.

A shift in greyscale to darker carbonate sediment (calcite) was identified at AD 2000 (Chapter Figure 5.16). Darker sediment is also evident in the most recent six years of the NAR06 profile (1-6 VY, AD 2000-2006) and relates to decreased evaporation. This coincided with a recent shift in the diatom assemblage involving increased *C. anaticus*. Sediment traps collected in 2008 contained lighter sediment (aragonite), which suggest the lake is now becoming more evaporated. The C:N ratio is consistent throughout the majority of the 1720 year record with a significant peak at 120 VY (AD 1880). This coincided with disappearance of *N. paleacea* for ~50 years. Lower nitrogen in the system during this period may have led to other diatoms and algal blooming species out-competing *N. paleacea*.

Variable	Total biovolume	Rare fraction	DCA axis 1	DCA axis 2	Varve thickness	<i>N. paleacea</i> blooms	<i>S. acus</i> blooms	Clastic layers	% benthic	DI-cond.	Grey scale	C:N ratio
Diatom conc.	0.150 0.000	0.0738 0.000	0.0258 0.000	0.0563 0.000	0.130 0.205	-0.105 0.308	0.074 0.468	-0.124 0.226	0.0594 0.000	0.0735 0.000	-0.069 0.368	0.122 0.236
Total biovolume		0.0178 0.020	0.0159 0.039	-0.028 0.713	-0.013 0.897	-0.093 0.367	-0.005 0.963	-0.143 0.164	0.053 0.495	0.0196 0.010	-0.114 0.136	0.174 0.089
Rarefaction			0.030 0.000	0.0514 0.000	-0.162 0.113	0.038 0.715	-0.095 0.352	0.101 0.327	0.0607 0.000	0.0894 0.000	-0.056 0.469	0.038 0.717
DCA axis 1					-0.182 0.078	-0.040 0.703	-0.113 0.276	-0.000 0.999	0.0374 0.000	0.0913 0.000	-0.006 0.936	0.0217 0.005
DCA axis 2					-0.072 0.486	0.002 0.984	-0.036 0.729	0.068 0.510	0.0495 0.000	0.0273 0.000	0.0406 0.000	0.007 0.946
Varve thickness						0.0477 0.000	0.0786 0.000	-0.194 0.057	-0.173 0.089	-0.134 0.191	0.148 0.147	0.097 0.345
<i>N. paleacea</i> blooms							0.0326 0.000	-0.027 0.796	-0.028 0.783	-0.016 0.878	-0.022 0.832	-0.084 0.415
<i>S. acus</i> blooms								-0.055 0.596	-0.132 0.197	-0.129 0.208	0.098 0.338	0.068 0.508
<i>A. minutissimum</i> %									0.078 0.313	0.0848 0.000	0.0536 0.000	0.0247 0.000
<i>C. anaticus</i> %									0.188 0.065	0.0224 0.030	0.0219 0.004	0.081 0.430
<i>S. acus</i> %									0.016 0.880	-0.086 0.402	0.0251 0.000	-0.038 0.714
<i>N. paleacea</i> %									0.0682 0.000	0.0860 0.000	-0.031 0.762	-0.003 0.976
Clastic layers									0.050 0.630	-0.039 0.701	-0.024 0.817	-0.066 0.523
% benthic										0.0595 0.000	-0.134 0.191	0.119 0.244
DI-cond.											-0.089 0.385	0.108 0.292
Grey scale												0.116 0.257

Table 7.3 Significant relationships between different analyses of the NAR01/02 palaeo-record (Pearson's correlation, significant relationships ($p < 0.05$) highlighted).

Variable	Total biovolume	Rare fraction	DCA axis 1	DCA axis 2	Varve thickness	<i>N. paleacea</i> blooms	<i>S. acus</i> blooms	Clastic layers	% benthic	DI-cond.	Grey scale	C:N ratio
Diatom conc.	0.464 0.000	-0.852 0.000	-0.550 0.000	0.633 0.000	0.339 0.003	0.220 0.056	-0.020 0.865	-0.237 0.039	-0.713 0.00	-0.432 0.000	-0.163 0.162	-0.023 0.847
Total biovolume		-0.127 0.263	0.251 0.025	0.040 0.727	0.120 0.302	0.201 0.082	-0.229 0.047	0.007 0.952	0.078 0.493	0.142 0.210	0.063 0.590	0.182 0.121
Rare fraction			0.617 0.000	-0.707 0.000	-0.234 0.042	-0.169 0.145	-0.024 0.838	0.196 0.089	0.753 0.000	0.445 0.000	0.162 0.166	0.142 0.229
DCA axis 1					-0.214 0.063	-0.158 0.172	-0.063 0.586	0.240 0.037	0.561 0.000	0.598 0.000	0.193 0.097	0.199 0.089
DCA axis 2					0.355 0.002	0.182 0.115	0.177 0.125	-0.316 0.005	-0.843 0.000	-0.838 0.000	-0.458 0.000	-0.201 0.087
Varve thickness						0.442 0.000	0.396 0.000	-0.428 0.000	-0.373 0.001	0.322 0.005	0.128 0.274	0.152 0.230
<i>N. paleacea</i> blooms							0.005 0.966	-0.118 0.311	-0.155 0.180	-0.151 0.182	0.029 0.808	0.191 0.131
<i>S. acus</i> blooms								-0.136 0.242	-0.149 0.198	-0.149 0.189	-0.092 0.431	-0.329 0.008
<i>A. minutissimum</i> %									0.714 0.000	0.812 0.000	0.359 0.002	0.272 0.019
<i>C. anatolicus</i> %									-0.234 0.037	-0.159 0.158	-0.335 0.003	-0.416 0.001
<i>S. acus</i> %									0.044 0.698	0.040 0.725	-0.035 0.763	0.123 0.333
<i>N. paleacea</i> %									-0.725 0.000	-0.87 0.000	-0.193 0.096	-0.134 0.291
Clastic layers									0.386 0.001	0.180 0.111	0.052 0.655	0.127 0.316
% benthic										0.88 0.000	0.302 0.008	0.229 0.069
DI-cond.											0.234 0.043	0.196 P=0.121
Grey scale												0.279 0.025

Table 7.4 Significant relationships between different analyses of the NAR06 diatom and the most recent 80 years of the NAR01/02 thin section palaeo-records (Pearson's correlation, significant relationships ($p < 0.05$) highlighted).

7.3.2 Kratergöl

Dominant diatom species in the Kratergöl palaeo-assemblage have been described in numerous texts as being associated with marine or high salinity environments, e.g. *E. paludosa* var. *subsalina*, *F. fasciculata*, *N. complanata*, *N. salinicola*, *N. frustulum* and *R. constricta*. The Kratergöl palaeo-record did not experience any complete species shifts (Chapter 6: Figure 6.8). Therefore, throughout the time period covered, a critical threshold in water chemistry was not reached to initiate a large diatom response. DI-conductivity values are negatively correlated with rarefaction implying that, during periods of higher conductivity, diatom species diversity decreased. This relationship was also recognised by Gell and Gasse (1994) and may result from fewer species being capable of tolerating extreme high lake salinity levels. Palaeoenvironmental inferences based on different Kratergöl analyses are summarised in Table 7.5.

Zone	Sediment lithology	Diatom ecology	Diatom concentration, biovolume, diversity and DCA	Conductivity reconstruction (μS^{-1})
KD1 4-0 cm	Turbidite followed by return to higher organics and silt+clay	Assemblage dominated by <i>N. cf. fonticola</i> indicating shift to higher nutrients or lower salinity	Higher species diversity indicating shift to more disturbed environment Increase in concentration and biovolume	Return to lower conductivity Average: WA: 11,110 MAT: 11,649
KD2 18-6 cm	Increased organics, silt and clay followed by turbidite	Dominance of <i>E. paludosa var. subsalina</i> indicating reduced nutrients or increased salinity	Increased concentration and biovolume and lower diversity Greatest period of change in DCA axis 1	Period of extremely high conductivity accompanied by poor analogue matching Average: WA: 28,419 MAT: 9,315
KD3 46-20 cm	Sandy turbidite event with low organic content	Disappearance of planktonic <i>E. paludosa var. subsalina</i> , which favours high salinity and low nutrients	Lower concentration and biovolume of diatoms	Consistently lower conductivity Average: WA: 7,875 MAT: 10,821
KD4 59-48 cm	Organic rich silt and clay	High salinity indicators including epiphytic, epipellic and planktonic species	High diatom concentration and total biovolume	Slightly enhanced conductivity Average: WA: 12,918 MAT: 10,927

Table 7.5 Summary of inferences derived from the ACM99 diatom palaeo-record.

Zone KD4 (59-48 cm)

This zone was dominated by high conductivity indicators representing a range of habitats including epiphytic/epipellic *C. placentula*, *F. fasciculata* and *N. cf. fonticola* and planktonic *E. paludosa var. subsalina*. *C. placentula* is a fast growing, widespread species that remains relatively consistent in abundance throughout the entire sequence. *E. paludosa var. subsalina* is typical of higher salinity and lower nutrient levels.

This period experienced slightly enhanced conductivity in comparison with the following zone, indicating higher aridity. Sediment included organic-rich silt and clay, which are associated with higher diatom concentration and total biovolume during this period. Large species dominated the Kratergöl assemblage; therefore when plotted according to biovolume the same species dominated the population.

Zone KD3 (46-20 cm)

Planktonic *E. paludosa* var. *subsalina*, was replaced by the widely distributed epipellic/epiphytic species *C. placentula* and *N. cf. fonticola*. This indicates a change to higher nutrient availability, lower salinity or variability in habitat availability, which may have allowed these species to out-compete *E. paludosa* var. *subsalina*.

Diatom concentration and total biovolume dramatically decreased between 36 and 20 cm. This occurred during an inferred turbidite event involving increased sedimentation rate and may not have resulted in a significant change in diatom productivity. This was accompanied by lower organic content and increased sand. Diatom concentration appears to be highly related to the lake sedimentation rate. However, species composition is not clearly related to sedimentation and may reflect other environmental factors. The percentage of benthic species also increased throughout the sandy section. This implies that benthic diatoms may have been deposited simultaneously with this material. Although the diatom assemblage appears greatly related to sedimentation rate, when considering the changing abundance of the three dominant species, it seems that they may also be responding to changes in lake water chemistry. This zone also experienced consistently lower conductivity indicating a fresher system.

Zone KD2 (18-6 cm)

E. paludosa var. subsalina dominated this zone and may indicate an environmental change involving reduced nutrient availability, allowing this species to out-compete other diatoms. This change in the assemblage may be associated with increasing salinity levels in the system and decreased nutrients. The fact that *E. paludosa var. subsalina* is a planktonic species also implies that lake level could have been higher, providing a suitable niche for this taxon. This zone began with increased organics, silt and clay followed by a sandy layer. This coincided with increased diatom concentration and biovolume and lower species diversity, reflected by the greatest period of change in DCA axis 1.

DI-conductivity was greatly enhanced during this period, indicating more arid conditions and a more saline lake environment. However, this was accompanied by poor analogue matching with the modern training set. The conductivity reconstruction (WA) for this period followed the abundance of dominant species *E. paludosa var. subsalina*. Due to the fact that *E. paludosa var. subsalina* only occurred twice in the modern training set, this species may not be a reliable indicator. According to the MAT, a significant environmental change did not occur during this period.

Zone KD1 (4-0 cm)

N. cf. fonticola replaced *E. paludosa var. subsalina* in the top 4 cm of the profile. *N. cf. fonticola* has slightly lower salinity optima and favours eutrophic waters. Therefore this change in the population may be associated with freshening of the system or increased

nutrient levels. This period also coincided with a return to lower DI-conductivity levels. Sediment analysis revealed a turbidite event, followed by return to higher organics, silt+clay and an increase in diatom concentration, biovolume and species diversity during this period. This may be associated with recent disturbance, which can provide habitats for a more diverse species assemblage. Rarefaction is negatively correlated with total biovolume ($r=-0.378$, $p=0.036$); the same relationship was observed at Nar, i.e. when productivity is greater, species diversity decreases ($r=-0.468$, $p=0.008$). It appears that the Kratergöl palaeo-diatom assemblage has responded to environmental change. However, the absence of a reliable chronology makes inferring temporal variability problematic.

7.3.3 Comparison of Nar and Kratergöl diatom records

Nar Gölü represents a lake with an extremely well resolved and stratigraphically consistent sediment profile, whereas Kratergöl has experienced a varied sedimentation rate. Consequently, inferences were limited for Kratergöl, due to problematic coring and chronological discrepancies. There are some similarities between the diatom records from the two sites. For example, a recent assemblage change is evident at both lakes, which could be associated with disturbance in the system, such as altered nutrient status or climatic change. However, the most recent sediment studied from Kratergöl appears to be at least ten years older than that from Nar. Similarities between the records also exist in the negative relationships between diatom concentration and species diversity, suggesting that this is a characteristic trait of diatom communities. The species assemblage of Nar is more diverse and contains a number of eutrophic species, whereas Kratergöl diatom taxa are all indicators of the extreme high conductivity levels. It seems

that when water salinity levels are extremely high, such as in Kratergöl, this leads to a less diverse assemblage, due to the smaller number of species capable of tolerating such extreme conditions. Nar has experienced greater diatom assemblage fluctuations throughout the palaeo-record. As the Kratergöl sequence may only represent the late 20th century, it is not directly comparable with the NAR01/02 record. The Kratergöl and NAR06 records both indicate environmental variability in central Anatolia throughout the 20th century. However, the timing of events could not be compared due to the absence of a reliable chronology for Kratergöl. The most notable conclusion, when comparing these two sites, is that stratigraphic integrity can vary greatly between sediment profiles from different lakes.

7.4 Nar Gölü multi-proxy comparisons

Oxygen isotope and pollen analyses of the NAR01/02 sediment sequence have been compared with the NAR01/02 diatom record in order to improve understanding of palaeo-environmental change. The NAR06 sequence was not subject to isotope and pollen analyses. Therefore the most recent 80 VYs of the NAR01/02 isotope and pollen records have been compared with the NAR06 diatom data.

7.4.1 Oxygen isotopes

The changing ratio of ¹⁸O to ¹⁶O isotopes in a lake system relates to the evaporative removal of lighter isotopes, which reflects changes in temperature, relative humidity and precipitation and can be used to infer palaeoclimate. More positive oxygen isotope values indicate periods of increased evaporation and thus drier climatic conditions, whereas more negative values signify a wetter climate. Diatoms and isotopes have been

utilised as complementary proxies in various studies. For example, Reed *et al.* (1999) identified a link between DI-conductivity and oxygen isotopes in Turkish lakes. Jones (2004) and Jones *et al.* (2005; 2006) identified that evaporation is an important driver of lake water isotope ratios at Nar Gölü and revealed a number of rapid shifts between wet and dry episodes throughout the last 1720 years (Figures 7.5 and 7.6).

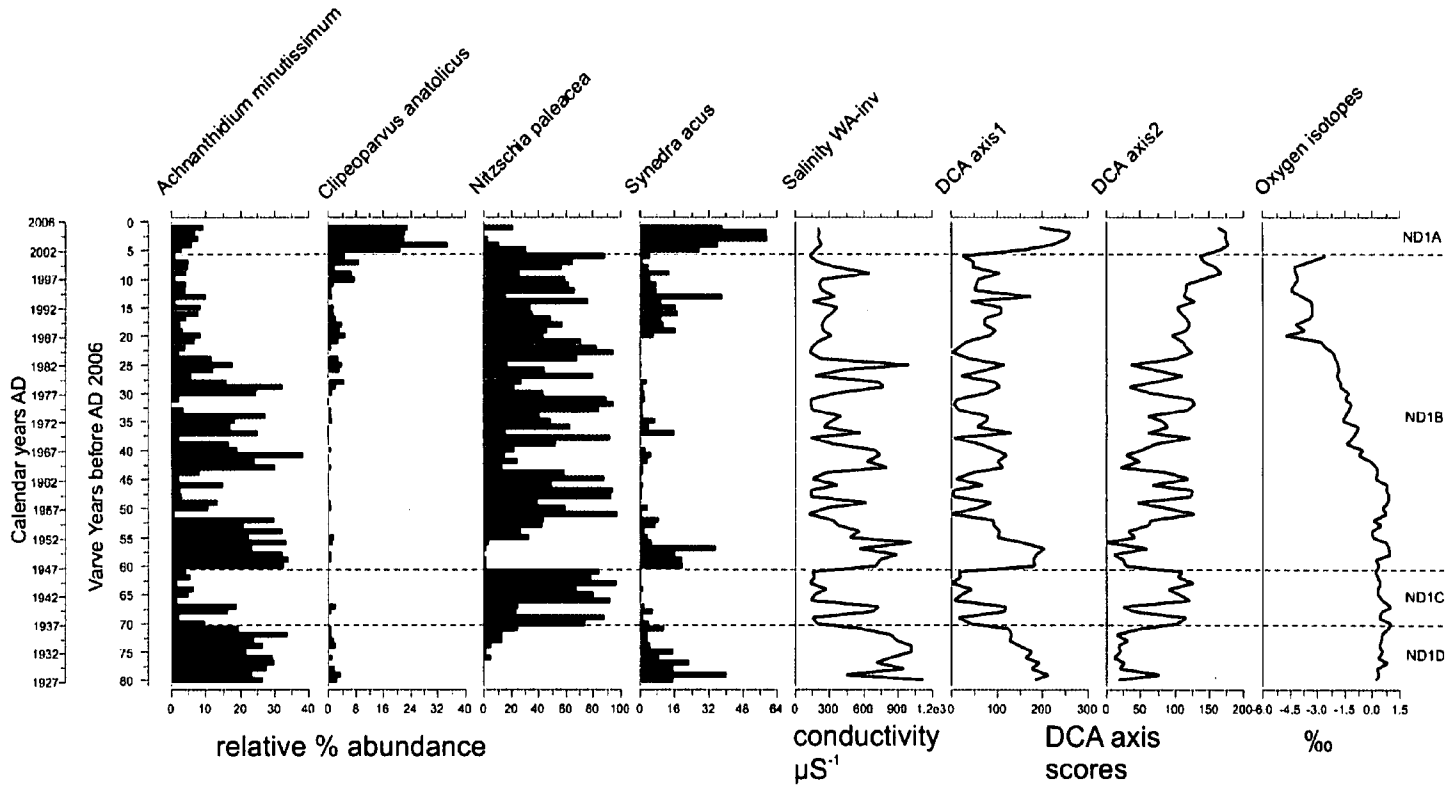


Figure 7.5 NAR06 diatom stratigraphy (>40%) presented with DI-conductivity, DCA axes 1 and 2 and the NAR01/02 oxygen isotope record.

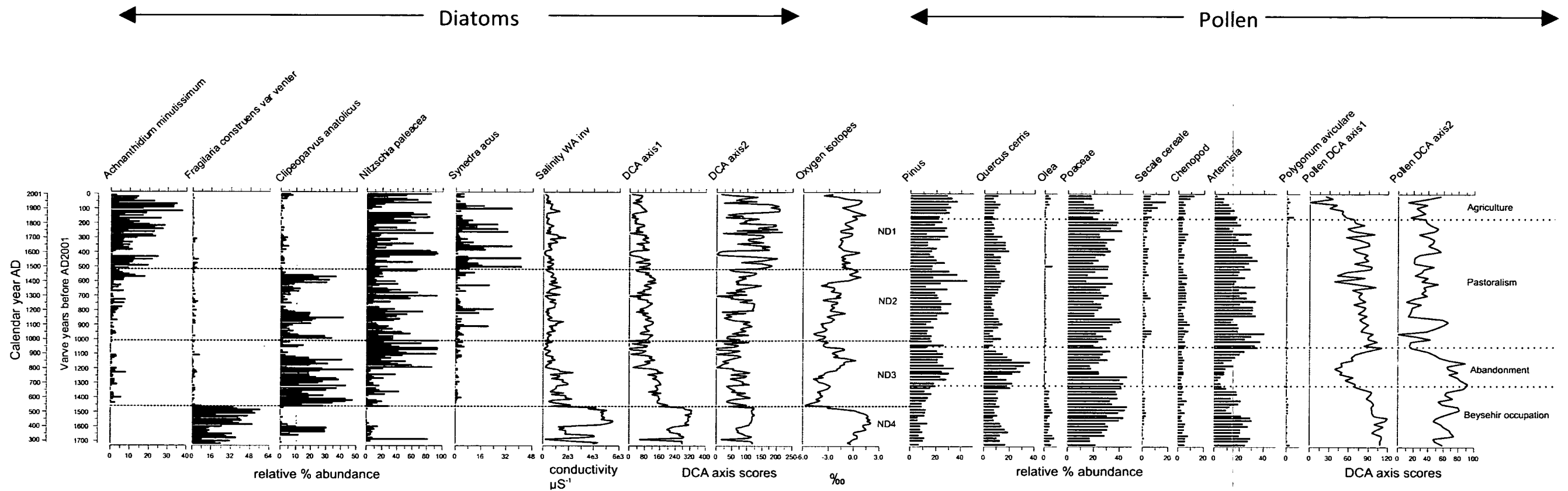


Figure 7.6 NAR01/02 diatom (>40%) stratigraphy with DI-conductivity and diatom DCA axes 1 and 2. Presented with NAR01/02 pollen and oxygen isotope stratigraphy and pollen DCA axes 1 and 2.

Diatom zones are illustrated with fine dotted lines and pollen zones are highlighted by coarse dotted lines.

Three large shifts from positive to negative oxygen isotope values were identified between AD 486-561, AD 1393-1429 and AD 1949-1987. The most positive isotope values occurred during diatom zones ND4 and part of ND1. Similarly, DI-conductivity was elevated during zone ND4. The most significant diatom assemblage change occurred simultaneously, with the most important shift to more negative isotopes at AD 540. Therefore it appears that diatoms and oxygen isotopes responded in a similar manner to changes in the lake system during this period and both indicate a shift from drier conditions prior to AD 540 to a wetter/fresher environment. However, more positive isotopes during zone ND1 were not accompanied by a return to the diatom species that dominated zone ND4.

The relationship between the diatom assemblage and lake water chemistry may have altered in zone ND1, due to increased human activity and changing nutrient levels, or changes in lake chemistry may not have reached a critical threshold to result in a diatom species shift. According to Gasse *et al.* (1997), due to the impacts of threshold effects on diatom populations, periods of stable DI-conductivity may not indicate a stable climate but rather signify that a critical threshold has not been reached to initiate a species shift. Comparison of the NAR06 diatom record with the most recent 80 VY of the NAR01/02 oxygen isotope record highlighted that isotopes show a smoothed response to climate and diatom assemblage fluctuations are more variable. This is associated with the affect of bloom events on the conductivity reconstruction and the 'smoothed' relationship between oxygen isotopes and lake residence time (8-11 years).

The oxygen isotope record is significantly correlated with a number of numerical analyses derived from the diatom assemblage (Table 7.6). Isotopes and DI-conductivity

are positively correlated, implying that more positive isotopes are related to more saline conditions. Isotopes are also correlated with all NAR06 and NAR01/02 diatom DCA axes, indicating a significant relationship with the diatom population. The isotope record is also negatively correlated with NAR06 rarefaction, thus suggesting that drier environmental conditions result in decreased species diversity. This relates to the fact that fewer species are capable of tolerating extreme conditions. In addition, isotopes are significantly correlated with the percentage of important diatom species in the NAR01/02 record (Table 7.6). This indicates that the climatic drivers of oxygen isotope shifts also initiate a response in these diatom species. However, the relationships are not 'strong' and r values are not particularly high.

Diatoms may record additional information about lake environmental change in comparison with oxygen isotopes. This is associated with the fact that the diatom record includes numerous species, which have differing seasonal relationships with climate and other limnological variables. Isotopes provide a smoothed record of environmental change, as they relate to the residence time of the lake (8-11 years) and represent spring/summer conditions. Both diatom and isotopes highlight that the largest change in the sequence involved a shift to fresher conditions at AD 540.

NAR06 and NAR01/02	NAR01/02 oxygen isotopes	
	1-80 VY	1-1720 VY
DI-cond.	0.342 P=0.004	0.164 0.032
Diatom conc.	-0.029 P=0.811	0.234 P=0.002
Total biovolume	0.456 P=0.000	0.205 0.007
Rare faction	0.123 P=0.309	-0.393 0.000
DCA axis 1	0.274 P=0.022	0.233 P=0.002
DCA axis 2	-0.507 P=0.000	0.182 P=0.018
Varve thickness	-0.142 P=0.240	0.300 P=0.004
<i>N. paleacea</i> blooms	-0.044 P=0.720	0.216 P=0.041
<i>S. acus</i> blooms	-0.422 P=0.000	0.045 P=0.676
<i>A.</i> <i>minutissimum</i> %	0.407 P=0.000	0.251 P=0.001
<i>C. anatolicus</i> %	-0.570 P=0.000	-0.371 P=0.000
<i>S. acus</i> %	0.069 P=0.569	-0.011 P=0.883
<i>N. paleacea</i> %	-0.248 P=0.038	0.025 P=0.749
Clastic layers	0.201 P=0.095	-0.187 P=0.077
% benthic	0.365 P=0.002	-0.149 P=0.052
Grey scale	0.493 P=0.000	0.534 P=0.000
C:N ratio	0.589 P=0.000	0.126 P=0.103

Table 7.6 Significant relationships between the oxygen isotope (NAR01/02) and diatom (NAR01/02 and NAR06) records from Nar Gölü (Pearson's correlation, significant relationships ($p < 0.05$) highlighted) (only variables showing significant relationships included).

7.4.2 Pollen

Pollen is frequently employed as a proxy for natural, climate-related and human-induced landscape vegetation change. England (2006) and England *et al.* (2008) analysed the pollen profile of the NAR01/02 sequence and suggested that human

activity has been the main driver of vegetation change in the Nar catchment throughout the last 1720 years. Four principal land-use phases are highlighted by pollen DCA axes 1 and 2 (Figure 7.6). These phases were described by England *et al.* (2008): 1 - early Byzantine landscape characterised by cereals and tree crops (AD 290-670); 2 - landscape abandonment and woodland establishment (AD 670-950); 3 - cereal-based agriculture and pastoralism (AD 950-1830); 4 - agricultural intensification (AD 1830-present). Comparison of the pollen zones with the NAR01/02 diatom stratigraphy revealed no obvious relationship in the response of these proxies (Figure 7.6).

Additionally, England *et al.* (2008) recognised that oxygen isotope data from Nar did not coincide with pollen-inferred land-use and landscape changes. The most significant shifts in the pollen record included the period of abandonment and recent agricultural intensification. The fact that these episodes are not reflected in the diatom or isotope records may be related to the different response characteristics of these proxies or the fact that human land use has masked the climate signal in the pollen record.

Despite the absence of obvious relationships between the diatom and pollen records, correlation analysis revealed a number of weak significant patterns (Table 7.7). DCA axis scores plotted stratigraphically for the pollen data are likely to predominantly represent change through the record associated with human land use. Pollen DCA axes 1 and 2 are significantly correlated with DI-conductivity and diatom NAR01/02 DCA axes 1 and 2. This implies similarities in the response characteristics of these proxies to environmental change.

	Pollen DCA axis 1	Pollen DCA axis 2	<i>Pinus</i> %	<i>Poaceae</i> %	<i>Secale cereal</i> %	<i>Avena triticum</i> %	<i>Hordeum</i> %	<i>Sanguisorba</i> %
DI-cond.	0.403 P=0.000	0.395 P=0.000	-0.405 P=0.000	0.171 P=0.239	0.339 P=0.001	-0.228 P=0.034	-0.287 P=0.007	0.503 P=0.000
Diatom conc.	0.227 P=0.035	-0.242 P=0.093	0.142 P=0.329	-0.287 P=0.007	0.172 P=0.237	0.215 P=0.138	0.054 P=0.714	-0.153 P=0.295
Total biovolume	0.085 P=0.562	-0.137 P=0.349	0.011 P=0.943	-0.274 P=0.011	-0.274 P=0.057	-0.130 P=0.374	-0.231 P=0.110	-0.092 P=0.528
DCA axis 1	0.521 0.000	0.207 P=0.158	0.001 P=0.992	0.159 P=0.280	-0.374 P=0.009	-0.251 P=0.085	-0.381 P=0.008	0.222 P=0.129
DCA axis 2	0.433 P=0.000	0.076 P=0.607	0.115 P=0.436	0.094 P=0.523	0.094 P=0.523	-0.102 P=0.490	0.062 P=0.677	0.028 P=0.849
<i>N. paleacea</i> %	-0.105 P=0.473	-0.127 P=0.383	-0.072 P=0.625	0.222 P=0.040	0.267 P=0.064	0.196 P=0.177	0.197 P=0.175	-0.121 P=0.407

Table 7.7 Significant relationships between the pollen and diatom (NAR01/02) records from Nar Gölü (Pearson's correlation, significant relationships ($p < 0.05$) highlighted) (only variables showing significant relationships included).

A number of correlations have been identified between individual pollen species and the diatom record. For example, the abundance of *Pinus* (pine) is negatively related to DI-conductivity, indicating that more saline, drier periods correspond with decreased *Pinus* pollen influx. As pine has only recently been planted in the Nar catchment, and fossil *Pinus* pollen is likely to have travelled considerable distances, the abundance of this pollen species at Nar relates to regional rather than local environmental change.

Additionally, *Poaceae* (grass) correlates with *N. paleacea* percentage and a number of pollen species relate to various characteristics of the diatom population. For example, *Poaceae* percentage is negatively related to diatom concentration and total biovolume, indicating that when algae are more productive, grasses are less abundant. The percentages of cereal pollen, which relates to human land use, such as *Secale cereale* (rye), *Avena triticum* (wheat) and *Hordeum* type (barley) are negatively related to DI-conductivity. These relationships imply that during periods of increased lake salinity, agricultural practice decreased. Additionally, the drought-tolerant shrub *Sanguisorba*

(salad burnet) is positively correlated with DI-conductivity, suggesting that this species was prolific during drier episodes.

Although the major zone boundaries do not coincide, it appears that some diatom and pollen species may respond simultaneously to environmental change. However, these relationships are not 'strong' and correlations do not apply to all pollen and diatom species. Additionally, deciphering whether human land-use drives salinity change or salinity variability relates to climate and consequently alters human agricultural practice is complicated. The relationship between diatoms and pollen appears to be complex and is likely to be related to numerous human land-use, climate-related and limnological variables. The lack of direct relationships may relate to the different response times of vegetation to environmental variability and the fact that floristic change relates more closely to human activity.

Laird *et al.* (1996) identified that periods of greater fire frequency can relate to enhanced DI-conductivity. The charcoal record from Nar Gölü (Turner, 2007) revealed lowest fire frequency during the early part of the record and higher incidence during the most recent 80 years. Therefore there does not appear to be a link between DI-conductivity and fire frequency at Nar. Additionally, no clear relationship has been identified between the charcoal and Nar oxygen isotope record. Based on the pollen record, England (2006) recognised that changes in charcoal concentration were associated with human occupancy and land use.

7.5 Summary

The diatom records from Nar Gölü and Kratergöl have provided various insights into palaeo-environmental change. Nar diatoms are diverse and include a background assemblage in addition to bloom species, which are associated with short-time periods and relate to seasonality or changes in lake nutrient availability. Kratergöl contains a less diverse assemblage and appears to lack bloom species; this implies a relatively consistent environment with specialised taxa. Nar and Kratergöl modern assemblages are well represented in the fossil records and should therefore provide detailed information about palaeoenvironmental change.

The Kratergöl diatom assemblage is clearly affected by the variable lake sedimentation rate and is typical of the high-salinity environment. The Kratergöl palaeo-sequence experienced a period of enhanced DI-conductivity between 18-6 cm and a recent assemblage shift (4-0 cm). Nar lake sedimentation involves a seasonal cycle of carbonate, diatom and organic material deposition. The Nar diatom relationship with salinity is not straightforward. Key interpretations from the Nar palaeo-record include a major dry event prior to AD 540 and a recent change in the lake environment since AD 2000. The change to a wetter environment at AD 540 coincided with a shift to more negative isotopes. However, a return to positive isotopes at AD 1400 was not accompanied by a species shift in the diatom record. The pollen sequence revealed that, throughout the last 1720 years, vegetation shifts have not been synchronous with isotope and diatom population changes at Nar. Variability in the different proxy records are likely to relate to a combination of climatic and non-climatic factors.

Chapter 8

Eastern Mediterranean Palaeoclimate

Within this chapter, the results of the palaeoenvironmental analyses of Nar Gölü and Kratergöl are analysed and discussed in terms of Eastern Mediterranean palaeoclimate.

Part I Diatom and Meteorological Records

8.0 Introduction

Pre-instrumental diatom-inferred (DI) palaeoclimate reconstructions can be validated through calibration of the most recent part of the record covering the instrumental period, with meteorological records. For example, Laird *et al.* (1998) identified a strong link between lake DI-conductivity and an index of North American drought based on meteorological data, revealing that more saline time periods relate to enhanced aridity. This provided validation for employing the relationship to infer pre-instrumental palaeoclimate from DI-conductivity. Part 1 of this chapter includes presentation and discussion of the relationships between meteorological data from central Anatolia and the NAR06 diatom record for the most recent 80 years (AD 1927-2006). The high-resolution of the diatom sequence allowed the relationship with instrumental meteorological data to be analysed annually. Due to the absence of a comprehensive chronology and variability in lake sedimentation rate, relationships between meteorological variables and the Kratergöl diatom record (ACM99) have not been analysed.

8.1 Meteorological records from central Turkey

Instrumental meteorological records are available from various regions of Turkey dating from AD 1926 to the present (data from Turkish State Meteorological Service). Turkish climate trends, highlighted in Chapter 2 (Figures 2.6 and 2.7), have revealed recent warming and variable precipitation between different regions throughout the past 80 years (Türkeş, 2003). Meteorological data chosen for comparison with the Nar diatom sequence include records from stations located in Ankara and Nevşehir (Chapter 3: Figure 3.1). Ankara has the longest climate record, dating from AD 1926 and extending to the present. However, this station is located 230 km from the lake site and therefore may not realistically reflect climate in the Nar region. Nevşehir was also selected for comparison, as this station is in closer proximity to Nar Gölü (30 km) and has a complete record dating back to AD 1959 and extending to the present. Meteorological data include monthly recordings of minimum, average and maximum temperature, relative humidity and total precipitation.

Correlation analysis revealed that Nevşehir and Ankara temperature are strongly related (e.g. annual average: $r=0.93$, $p=0.000$). Therefore these regions experience similar temperature regimes and are likely to reflect conditions at Nar. However, precipitation (annual total: $r=0.055$, $p=0.729$) and relative humidity (annual average: $r=0.372$, $p=0.015$) are not strongly related between Nevşehir and Ankara. Consequently, interpreting rainfall trends with the Nar diatom record is problematic, due to the spatially variable nature of this climate factor. Additionally, data from meteorological stations can be unreliable due to recording errors and diatoms are affected by the cumulative influence of climate. Therefore the absence of significant relationships with

the Nar record cannot be assumed to imply that diatoms have not responded to climatic variability.

High-resolution gridded climate data were obtained from the University of East Anglia (UEA) Climate Research Unit (CRU) web resource (Mitchell and Jones, 2005). Data from meteorological stations are often of low spatial resolution. Gridded meteorological data provide information for all land areas, by calculating values based on means from surrounding stations. Each half-degree grid square provides time-series values of temperature, precipitation and other meteorological variables (AD 1902-2002). The grid square containing Nar Gölü and data averaged for the 48 grids covering central Anatolia were compared with the diatom record for the period AD 1927-2002. Precipitation is highly variable between regions; therefore interpolated gridded data may more reliably reflect rainfall in the Nar catchment in comparison with records from meteorological stations.

8.2 Diatom relationship with meteorological records

Diatom species assemblages are affected by numerous limnological variables, which fluctuate through time as a result of climatic changes. Consequently, numerical analyses of the Nar diatom palaeo-record were expected to show significant relationships with Turkish meteorological data. Variability in precipitation, temperature and relative humidity affect lake water balance and chemistry and consequently influence the diatom assemblage. Smol (2001) highlighted that temperature has important impacts on lake diatom populations. Such relationships may be direct or indirect; for example, direct effects are associated with species temperature optima and indirect effects involve the influence of temperature on lake water chemistry. The diatom relationship with

meteorological factors is complicated by the possibility that different species have dissimilar threshold responses to climatic variables (Reed *et al.*, 1999). Gradual change in a meteorological variable may not initiate a diatom response until a threshold is reached. This may appear as a sudden assemblage change in palaeo-records.

The Nar oxygen isotope record was identified by Jones (2004) and Jones *et al.* (2005; 2006) as most strongly related to central Anatolia summer temperature and relative humidity. Therefore the impact of summer evaporation on the Nar system appears to be an important factor affecting lake conditions. The diatom assemblage is also likely to be influenced by variability in summer temperature and relative humidity.

Nar diatom numerical analyses include species percentages, DCA axes, species diversity (rarefaction), valve concentration, total biovolume and DI-conductivity, which are greatly affected by the changing abundance of the dominant bloom species *N. paleacea* and *S. acus*. Therefore relationships between diatom numerical analyses and meteorological variables are likely to reflect changes in the frequency of bloom events. *N. paleacea* was identified in core thin sections as a predominantly spring/summer blooming species and *S. acus* usually bloomed during autumn. Therefore these species were expected to correspond with meteorological data for these seasons. The relationships between meteorological data and DI-conductivity and DCA axes based on non-bloom species (OB) reduced the influence of *N. paleacea* and *S. acus* and revealed additional influences of climate on the diatom record.

Diatoms are most prolific in lakes during spring, summer and autumn (Wetzel, 2001). Therefore strongest relationships were expected with these seasons. However, the

majority of the observed relationships between diatoms and meteorological data for all seasons were not 'strong'. Calculation of running averages (smoothing) for selected time periods can reduce 'noise' in datasets and reveal general trends between variables. For example, Bigler and Hall (2003) smoothed meteorological data prior to comparison with a DI record of July temperature, in order to remove high inter-annual variability. The strength of correlations was higher when central Anatolia meteorological data and Nar diatom records were smoothed using an eight-year running average to match the lake residence time (8-11 years). The influence of variability in meteorological factors during successive years will affect the lake system for the duration of the residence time and this should also influence the diatom response. However, interpretations based on the relationship between smoothed data may be unreliable due to issues of temporal autocorrelation between sample depths. Therefore unsmoothed correlations were considered more reliable.

The Nevşehir meteorological time series (47 years) is shorter than Ankara (80 years). This is likely to alter observed trends with the diatom dataset. Gridded data were expected to show similar relationships between temperature and the Nar diatom record to metrological station records. However, the results of correlation analyses between the diatom record and gridded data were weaker and less consistent than those with data from meteorological stations. Therefore interpretations are primarily based on observed relationships between Nar diatoms and Nevşehir and Ankara meteorological station data.

8.3 Correlation analysis of diatom and meteorological records

8.3.1 Annual averages

Annual average temperature, precipitation and relative humidity were calculated from meteorological data in order to explore relationships with temporal changes in the diatom population. NAR06 diatom DCA axes summarise assemblage change throughout the year and were expected to relate to annual average meteorological data. A number of statistically significant relationships were identified (Tables 8.1 and 8.2). However, the majority of these correlations were not ‘strong’. Therefore additional factors are likely to influence the diatom assemblage.

	Annual average				
	Min. temp.	Ave. temp.	Max. temp.	Rel. humidity	Total Precipitation
DI-conductivity (B)	-0.027 0.811	0.015 0.897	-0.020 0.863	-0.277 0.014	-0.353 0.001
DCA axis 1 (AS)	0.036 0.749	0.034 0.763	0.023 0.838	-0.231 0.041	-0.304 0.006
DCA axis 2 (AS)	0.246 0.028	0.222 0.049	0.021 0.855	0.143 0.208	0.136 0.232
<i>N. paleacea</i> %	-0.006 0.955	0.014 0.903	-0.020 0.858	0.208 0.066	0.254 0.024
<i>C. anaticus</i> %	0.243 0.030	0.202 0.074	0.056 0.626	0.040 0.725	-0.058 0.614
<i>S. acus</i> %	0.127 0.260	0.136 0.233	0.018 0.876	-0.218 0.053	-0.283 0.011
<i>N. paleacea</i> bloom	0.248 0.031	0.314 0.006	0.197 0.090	-0.074 0.530	-0.073 0.534
Varve thickness	0.267 0.020	0.213 0.067	0.075 0.523	-0.068 0.563	-0.066 0.571
Clastic layer	-0.192 0.097	-0.161 0.167	0.017 0.882	-0.076 0.515	-0.228 0.049

Table 8.1 Relationships between annual average climate data from Ankara

meteorological station and the NAR06 diatom and NAR01/02 thin section records.

Pearson’s correlation r and p -values presented with significant relationships highlighted ($p < 0.05$). Only diatom numerical analyses that showed a significant relationship included.

	Annual average				
	Min. temp.	Ave. temp.	Max. temp.	Rel. humidity	Total Precipitation
DI-conductivity (B)	0.228	0.244	0.310	0.089	-0.162
	0.123	0.099	0.034	0.554	0.277
Concentration	0.187	0.274	0.251	-0.059	0.392
	0.209	0.063	0.089	0.693	0.006
Total biovolume	0.270	0.328	0.353	-0.106	0.438
	0.067	0.024	0.015	0.478	0.002
A. minutissimum %	0.040	0.014	-0.053	0.314	-0.014
	0.790	0.927	0.722	0.032	0.926
N. paleacea bloom	0.310	0.338	0.375	-0.038	-0.255
	0.043	0.027	0.013	0.810	0.099

Table 8.2 Relationships between annual average climate data from Nevşehir

meteorological station and the NAR06 diatom and NAR01/02 thin section records.

Pearson's correlation r and p -values presented with significant relationships highlighted ($p < 0.05$). Only diatom numerical analyses that showed a significant relationship included.

The annual average Nevşehir climate data were not significantly correlated with the NAR06 diatom DCA axes. However, positive relationships were evident between Nevşehir annual average temperature and total diatom biovolume (Table 8.2). This implies that diatoms are more prolific when temperatures are higher. Annual average Ankara temperature was significantly correlated with NAR06 diatom DCA axis 2, whereas precipitation and relative humidity were correlated with DCA axis 1 (Table 8.1). The percentage of a number of diatom species also showed significant relationships with annual meteorological data. For example, increased Ankara precipitation was related to higher *N. paleacea* abundance and minimum temperature was correlated positively with *C. anatolicus* percentage. However, all relationships were relatively 'weak' and the precipitation record from Ankara may not reliably reflect rainfall in the Nar catchment.

The diatom assemblages were not significantly related to the annual average gridded climate data. This implies that the instrumental meteorological data provide a more realistic record of climate change. DI-conductivity based on the entire assemblage (AS) was not significantly correlated with the annual average climate data. However, the fact that DCA axes were correlated with meteorological data implies that changes in the diatom record relate to climatic variability and that DI-conductivity may not have been reconstructed accurately. Alternatively, the climatic link with lake water salinity may not be straightforward. Annual average, spring and winter Ankara relative humidity and winter precipitation were negatively correlated with DI-conductivity based on bloom species (B). Therefore it appears that bloom species respond to periods of increased temperature and decreased precipitation. Mono-specific blooms may reflect temporally diluted lake water in spring, leading to dominance of species that favour low conductivity. This could also relate to increased regional precipitation during winter and spring, which may result in increased nutrient delivery to the lake via ground water flow. DCA (OB) was not highly correlated with the meteorological data and the DI-conductivity bloom species (B) range was very small. Therefore patterns with meteorological data are difficult to interpret. The DI-conductivity (OB) range was larger and values were similar to the modern lake. Therefore this record may more reliably reflect climatic change.

Relationships between annual average Ankara and Nevşehir meteorological data and the thickness (μm) of carbonate, organic, diatom bloom and clastic layers of the NAR01/02 thin sections are summarised in Tables 8.1 and 8.2. Bloom layers of *N. paleacea* and *S. acus* were expected to show the same relationship with meteorological variables as percentage data, i.e. positive correlations with temperature. Positive relationships were

identified between Ankara temperature and *N. paleacea* blooms and varve thickness, implying that diatom bloom events are associated with warmer conditions and that increased temperatures relate to higher lake productivity. The lack of significant trends with precipitation is likely to be associated with spatial variability of this factor between the lake catchment and meteorological stations.

8.3.2 Seasonal averages

The observed relationships between the Nar diatom assemblage and central Anatolia annual average meteorological data were not strong or consistently significant. In order to analyse whether the diatom assemblage is controlled by sub-annual climate trends, the meteorological data were averaged according to seasons (spring: March, April and May; summer: June, July and August; autumn: September, October and November; winter: December, January, and February). Strongest relationships were expected with spring, summer and autumn, when diatoms are most prolific in the lake.

Analysis of the Nevşehir seasonal climate dataset (Tables 8.5 and 8.6) revealed strongest relationships between diatom NAR06 DCA axes and summer temperature (e.g. Figure 8.1). Therefore it appears that summer temperature has greatest meteorological influence on the Nar diatom assemblage. Relationships observed between NAR06 DCA axes, the percentages of dominant species and the meteorological data are strongly related, as these taxa drive change in the DCA axes. For example, NAR06 DCA axis 1 is primarily driven by *N. paleacea*. Various other numerical analyses of the diatom record were significantly correlated with the Nevşehir seasonal meteorological data. For instance, valve concentration, total biovolume and the percentages of *C. anatolicus* and *S. acus* were positively related to summer temperature,

implying that these species favour warmer conditions, which leads to increased diatom productivity. This is likely to be associated with the impact of summer evaporation on lake water chemistry.

Analysis of the Ankara seasonal climate data also revealed that the highest number of significant correlations occurred between NAR06 diatom DCA axes and summer temperatures (Tables 8.3 and 8.4). However, relationships were not 'strong', implying that Ankara meteorological data is less reflective of the Nar catchment. *C. anatolicus* percentage was positively correlated with Ankara temperature and relative humidity and therefore appears to favour warmer/moist conditions. According to the relationship between *C. anatolicus* and greyscale, discussed in Chapter 7 (section 7.3.1), this species favours a wetter environment. Therefore higher abundance of *C. anatolicus* could be interpreted as relating to a warmer/wetter climate. *S. acus* was identified in core thin sections as usually blooming during autumn. This species is positively related to autumn precipitation (Figure 8.2), implying that *S. acus* is more productive when autumn rainfall is greater.

	Spring (MAM)					Summer (JJA)				
	Min. temp.	Ave. temp.	Max. temp.	Relative humidity	Total precip.	Min. temp.	Ave. temp.	Max. temp.	Relative humidity	Total precip.
DI-conductivity	-0.115	-0.040	0.026	-0.111	-0.079	<u>0.272</u>	-0.216	-0.149	-0.045	0.022
	0.310	0.722	0.821	0.329	0.487	<u>0.015</u>	0.056	0.189	0.694	0.846
DI-conductivity (B)	0.030	0.143	0.130	<u>0.273</u>	-0.157	0.015	0.140	0.025	-0.095	-0.126
	0.791	0.206	0.249	<u>0.015</u>	0.166	0.894	0.217	0.825	0.403	0.267
DCA axis 1	0.046	0.127	0.122	<u>0.272</u>	-0.115	0.006	0.072	-0.009	-0.029	-0.100
	0.686	0.260	0.281	<u>0.015</u>	0.312	0.957	0.530	0.939	0.801	0.380
DCA axis 2	<u>0.281</u>	0.156	0.017	0.075	0.095	<u>0.484</u>	<u>0.327</u>	0.126	<u>0.226</u>	0.021
	<u>0.012</u>	0.167	0.881	0.512	0.407	<u>0.000</u>	<u>0.003</u>	0.267	<u>0.045</u>	0.852
<i>N. paleacea</i> %	0.008	-0.062	-0.082	<u>0.225</u>	0.087	0.101	0.051	0.077	0.015	0.058
	0.944	0.586	0.467	<u>0.046</u>	0.444	0.376	0.652	0.499	0.892	0.612
<i>A. minutissimum</i> %	-0.157	-0.041	0.055	-0.156	-0.117	<u>0.322</u>	-0.193	-0.058	-0.199	-0.071
	0.163	0.720	0.627	0.169	0.306	<u>0.004</u>	0.088	0.612	0.078	0.536
<i>C. anaticus</i> %	0.216	0.159	0.063	-0.067	0.029	<u>0.420</u>	<u>0.317</u>	0.121	<u>0.259</u>	0.065
	0.054	0.159	0.577	0.555	0.799	<u>0.000</u>	<u>0.004</u>	0.290	<u>0.021</u>	0.569
<i>S. acus</i> %	0.200	<u>0.235</u>	0.157	<u>0.297</u>	-0.099	0.217	<u>0.245</u>	0.071	-0.022	-0.132
	0.075	<u>0.036</u>	0.163	<u>0.008</u>	0.385	0.054	<u>0.030</u>	0.536	0.846	0.245
<i>N. paleacea</i> bloom	<u>0.238</u>	<u>0.261</u>	0.204	0.006	-0.063	<u>0.438</u>	<u>0.449</u>	<u>0.325</u>	-0.167	-0.046
	<u>0.039</u>	<u>0.023</u>	0.077	0.961	0.594	<u>0.000</u>	<u>0.000</u>	<u>0.004</u>	0.152	0.693
Varve thickness	0.173	0.194	0.121	-0.069	0.021	<u>0.332</u>	<u>0.302</u>	0.193	-0.044	-0.061
	0.134	0.092	0.297	0.557	0.858	<u>0.004</u>	<u>0.009</u>	0.098	0.708	0.600
Carbonate	0.126	0.098	-0.008	-0.075	0.093	<u>0.291</u>	0.171	0.005	0.074	-0.010
	0.277	0.398	0.946	0.524	0.428	<u>0.011</u>	0.142	0.967	0.526	0.933
Clastic layer	-0.124	-0.034	0.084	-0.029	-0.074	<u>0.257</u>	-0.082	0.056	-0.121	-0.200
	0.285	0.773	0.470	0.806	0.528	<u>0.026</u>	0.485	0.631	0.302	0.085

Table 8.3 Relationships between Ankara spring and summer meteorological data and the NAR06 diatom and NAR01/02 thin section records. Pearson's correlation r and p -values presented with significant relationships highlighted ($p < 0.05$). Only diatom numerical analyses that showed a significant relationship are included.

	Autumn (SON)					Winter (DJF)				
	Min. temp.	Ave. temp.	Max. temp.	Relative humidity	Total precip.	Min. temp.	Ave. temp.	Max. temp.	Relative humidity	Total precip.
DI-conductivity	-0.178 0.116	0.052 0.648	0.110 0.336	-0.221 0.050	0.277 0.013	-0.062 0.585	-0.020 0.861	0.047 0.683	-0.113 0.319	-0.011 0.926
DI-conductivity (B)	-0.002 0.987	0.098 0.392	0.038 0.737	-0.062 0.585	-0.142 0.211	-0.201 0.076	-0.184 0.104	-0.154 0.177	0.340 0.002	0.262 0.020
DCA axis 1	-0.026 0.817	0.075 0.513	0.028 0.809	-0.052 0.647	-0.145 0.202	-0.100 0.381	-0.081 0.479	-0.036 0.754	0.271 0.016	0.235 0.037
DCA axis 2	0.324 0.004	0.018 0.878	-0.119 0.296	0.345 0.002	0.276 0.014	0.136 0.234	0.087 0.445	0.020 0.861	-0.200 0.077	-0.071 0.531
N. paleacea %	0.092 0.422	-0.063 0.579	-0.057 0.621	0.104 0.360	0.211 0.062	0.076 0.506	0.47 0.681	-0.009 0.939	0.227 0.044	0.161 0.157
A. minutissimum %	0.240 0.033	0.013 0.911	0.091 0.423	0.284 0.011	0.263 0.019	-0.074 0.515	-0.020 0.863	0.041 0.717	0.026 0.817	-0.013 0.907
C. anaticus %	0.223 0.049	0.048 0.673	-0.065 0.567	0.250 0.026	0.049 0.667	0.093 0.415	0.061 0.593	0.040 0.726	0.270 0.016	-0.110 0.333
S. acus %	0.139 0.220	0.078 0.495	-0.051 0.658	0.103 0.368	0.053 0.645	-0.075 0.509	-0.080 0.484	-0.075 0.511	0.350 0.002	0.332 0.003
N. paleacea bloom	0.301 0.009	0.205 0.077	0.048 0.684	-0.015 0.900	0.151 0.194	0.057 0.627	0.036 0.759	0.007 0.952	-0.065 0.578	0.054 0.648
S. acus bloom	-0.091 0.437	-0.217 0.062	0.256 0.027	0.147 0.209	0.192 0.099	-0.125 0.286	-0.135 0.249	-0.155 0.185	-0.072 0.537	-0.077 0.513
Varve thickness	0.289 0.012	0.172 0.141	0.069 0.559	0.038 0.745	0.093 0.427	0.049 0.679	0.013 0.911	-0.076 0.516	-0.112 0.338	-0.030 0.799
Carbonate	0.313 0.006	0.181 0.120	0.117 0.317	0.002 0.985	0.029 0.808	0.038 0.745	0.016 0.893	-0.068 0.561	0.302 0.008	-0.077 0.513
Clastic layer	-0.210 0.070	-0.045 0.701	0.081 0.489	-0.165 0.156	0.275 0.017	-0.219 0.059	-0.183 0.116	-0.106 0.365	0.070 0.552	0.005 0.969

Table 8.4 Significant relationships between Ankara autumn and winter meteorological data and the NAR06 diatom and NAR01/02 thin section records. Pearson's correlation r and p -values presented with significant relationships highlighted ($p < 0.05$). Only diatom numerical analyses that showed a significant relationship are included.

	Spring (MAM)					Summer (JJA)				
	Min. temp.	Ave. temp.	Max. temp.	Rel. hum.	Total precip.	Min. temp.	Ave. temp.	Max. temp.	Rel. hum.	Total precip.
DI-conductivity (OB)	<u>0.291</u> <u>0.047</u>	0.219 0.139	0.189 0.204	0.097 0.515	0.196 0.187	0.089 0.550	0.009 0.954	0.033 0.824	0.039 0.796	0.088 0.558
DI-conductivity (B)	0.091 0.543	0.212 0.153	0.278 0.058	-0.125 0.404	-0.185 0.214	<u>0.485</u> <u>0.001</u>	<u>0.468</u> <u>0.001</u>	<u>0.463</u> <u>0.001</u>	0.235 0.112	-0.288 0.050
DCA axis 1	-0.002 0.987	0.123 0.410	0.193 0.193	-0.169 0.257	-0.271 0.066	<u>0.330</u> <u>0.023</u>	<u>0.300</u> <u>0.041</u>	<u>0.294</u> <u>0.045</u>	0.151 0.311	-0.141 0.344
DCA axis 2	0.078 0.600	0.163 0.275	0.222 0.134	0.118 0.429	0.013 0.928	<u>0.525</u> <u>0.000</u>	<u>0.499</u> <u>0.000</u>	<u>0.528</u> <u>0.000</u>	<u>0.380</u> <u>0.008</u>	-0.256 0.083
Concentration	0.268 0.069	0.232 0.116	0.180 0.226	0.097 0.517	0.063 0.674	0.261 0.076	<u>0.306</u> <u>0.036</u>	<u>0.294</u> <u>0.045</u>	-0.111 0.459	-0.252 0.088
Total biovolume	0.252 0.088	0.282 0.055	0.277 0.059	-0.029 0.844	-0.124 0.406	<u>0.434</u> <u>0.002</u>	<u>0.404</u> <u>0.005</u>	<u>0.386</u> <u>0.007</u>	-0.015 0.919	-0.157 0.293
A. minutissimum %	0.021 0.888	-0.007 0.964	-0.036 0.811	-0.169 0.256	-0.075 0.616	-0.229 0.121	-0.208 0.162	-0.258 0.080	<u>0.348</u> <u>0.016</u>	0.111 0.459
C. anaticolicus %	-0.058 0.699	0.078 0.602	0.161 0.278	-0.031 0.834	-0.182 0.220	<u>0.434</u> <u>0.002</u>	<u>0.451</u> <u>0.001</u>	<u>0.487</u> <u>0.001</u>	0.241 0.103	-0.204 0.170
S. acus %	0.101 0.498	0.227 0.124	<u>0.289</u> <u>0.049</u>	-0.145 0.331	-0.245 0.097	<u>0.485</u> <u>0.001</u>	<u>0.443</u> <u>0.002</u>	<u>0.435</u> <u>0.002</u>	0.231 0.118	-0.245 0.098
N. paleacea bloom	0.301 0.050	<u>0.350</u> <u>0.022</u>	<u>0.349</u> <u>0.022</u>	0.024 0.878	-0.084 0.594	<u>0.443</u> <u>0.003</u>	<u>0.457</u> <u>0.002</u>	<u>0.425</u> <u>0.004</u>	0.103 0.511	-0.114 0.466
S. acus bloom	<u>0.334</u> <u>0.029</u>	0.159 0.307	0.049 0.754	-0.171 0.273	-0.004 0.980	0.151 0.333	0.043 0.786	0.007 0.967	-0.109 0.485	-0.011 0.945
Varve thickness	<u>0.337</u> <u>0.027</u>	0.214 0.168	0.164 0.295	0.007 0.967	0.091 0.564	0.255 0.098	0.264 0.088	0.229 0.140	0.029 0.854	-0.033 0.833

Table 8.5 Relationships between Nevşehir spring and summer meteorological data and the NAR06 diatom and NAR01/02 thin section records. Pearson's correlation r and p -values presented with significant relationships highlighted ($p < 0.05$). Only diatom numerical analyses that showed a significant relationship are included.

	Autumn (SON)					Winter (DJF)				
	Min. temp.	Ave. temp.	Max. temp.	Relative humidity	Total precip.	Min. temp.	Ave. temp.	Max. temp.	Relative humidity	Total precip.
Concentration	0.237 0.108	<u>0.295</u> <u>0.044</u>	<u>0.317</u> <u>0.030</u>	-0.144 0.333	<u>0.499</u> <u>0.000</u>	-0.048 0.750	-0.015 0.923	0.021 0.888	0.023 0.880	-0.129 0.387
Total biovolume	0.259 0.079	<u>0.307</u> <u>0.036</u>	<u>0.309</u> <u>0.035</u>	-0.126 0.398	<u>0.417</u> <u>0.004</u>	0.025 0.866	0.050 0.737	0.113 0.450	-0.118 0.430	-0.175 0.241
C. anaticolicus %	0.072 0.631	0.033 0.827	0.129 0.287	<u>0.301</u> <u>0.040</u>	0.122 0.416	-0.052 0.727	-0.030 0.841	0.056 0.710	<u>0.302</u> <u>0.039</u>	-0.263 0.074
S. acus %	0.131 0.379	0.087 0.561	0.117 0.434	0.268 0.068	<u>0.289</u> <u>0.049</u>	-0.057 0.702	-0.045 0.763	0.019 0.900	-0.167 0.263	<u>0.300</u> <u>0.040</u>
S. acus bloom	-0.244 0.115	<u>0.355</u> <u>0.019</u>	<u>0.393</u> <u>0.009</u>	<u>0.324</u> <u>0.034</u>	0.294 0.056	-0.260 0.092	-0.334 0.028	<u>0.362</u> <u>0.017</u>	0.154 0.323	-0.101 0.521

Table 8.6 Relationships between Nevşehir autumn and winter meteorological data and the NAR06 diatom and NAR01/02 thin section records. Pearson's correlation r and p -

values presented with significant relationships highlighted ($p < 0.05$). Only diatom numerical analyses that showed a significant relationship are included.

The relationships between DI-conductivity based on all species (AS), bloom-species (B) (*N. paleacea* and *S. acus*) and non-bloom species (OB) and the seasonal Nevşehir and Ankara meteorological records were analysed in order to evaluate whether specific climate factors have varying effects on DI-conductivity based on diatom species with different life-forms and seasonal preferences (Tables 8.3-8.6). DI-conductivity (OB) was weakly positively related to Nevşehir spring temperature (Figure 8.3) and (B) was positively correlated with summer temperature. The difference in relationships observed with bloom and non-bloom species suggests that bloom taxa are mainly affected by summer temperature, particularly *N. paleacea*, whereas non-bloom species relate to spring temperature. This may be associated with lake stratification and thermocline breakdown leading to enhanced nutrient supply in spring. However, correlations were relatively 'weak'; therefore this relationship is not straightforward and may have altered through time as a result of changes in lake level and the stratification regime.

Analysis of the relationship between smoothed (using an eight-year running average) DI-conductivity (AS, OB and B) and meteorological data revealed a number of significant relationships and more general trends between the datasets. The majority of DI-conductivity correlations were positive with temperature and negative with precipitation, highlighting that periods of enhanced lake water salinity relate to a drier climate. Figure 8.4 shows smoothed Nevşehir summer temperature and DI-conductivity (B) ($r=0.880$, $p=0.000$). An increasing trend is evident between AD 1990-2006, suggesting that bloom species have responded to drier climatic conditions. Figure 8.6

illustrates smoothed autumn precipitation and DI-conductivity (AS) ($r=-0.751$, $p=0.000$) and highlights that rainfall may have important impacts on the diatom assemblage; this may be associated with the water balance of previous seasons. There were stronger relationships between DI-conductivity (B) in comparison with (OB). This implies that climatic control is more pronounced over the bloom species. This is also related to the fact that bloom species have dominated the assemblage of the last 80 years.

Relationships between seasonal average gridded data and the diatoms record were not as strong as those from meteorological stations (Appendix 8). Analyses similarly revealed strongest correlations with summer temperature. Gridded precipitation data were expected to more reliably reflect rainfall in the Nar catchment. Winter precipitation from the Nar grid was positively correlated with core thin section organic layer thickness, indicating that wetter winters lead to increased organic sedimentation. However, relationships were 'weak', implying that precipitation alone is not an important variable affecting the diatom population or interpolated values are not an accurate reflection of rainfall at Nar.

Core thin sections revealed a number of relationships with seasonal meteorological data. However, r values were low, implying other controls influence sub-layer thickness. *N. paleacea* thin section bloom layer thickness was positively correlated with spring, summer and autumn Nevşehir and Ankara temperature (Tables 8.3-8.6). The strongest and most significant relationship was evident with summer temperature, highlighting that this species favours warmer conditions. Additionally, total varve, *S. acus* and

carbonate layer thickness were positively correlated with spring, summer and autumn temperatures.

The positive relationship between varve thickness and temperature is associated with the appearance of bloom events, which result in thicker varves. Annual total precipitation was also negatively correlated with the thickness of thin section clastic layers. This implies that decreased precipitation could be associated with conditions that lead to accumulation of clastic material.

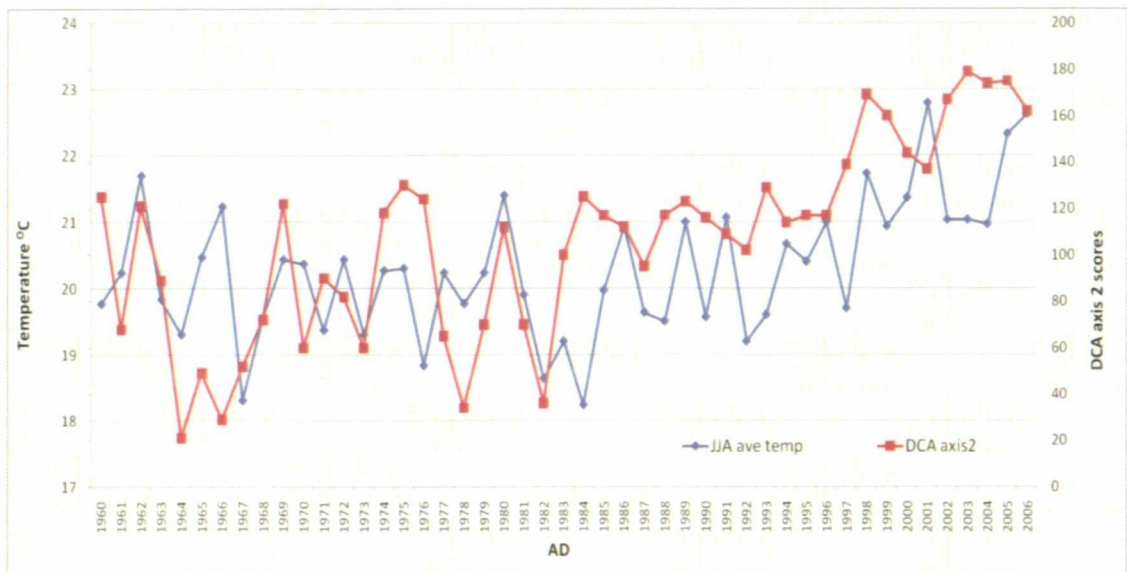


Figure 8.1 Nevşehir average summer temperature plotted with NAR06 diatom DCA axis 2 for the period AD 1960-2006 ($r=0.499$, $p=0.000$).

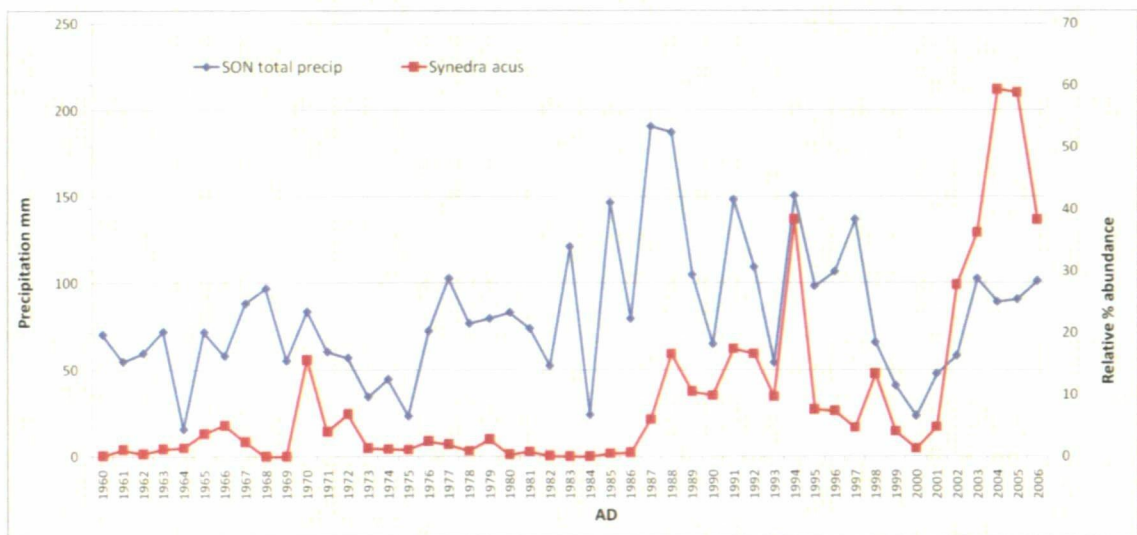


Figure 8.2 Total Nevşehir autumn precipitation plotted with NAR06 *S. acus* percentage for the period AD 1960 to 2006 ($r=0.289$, $p=0.049$).

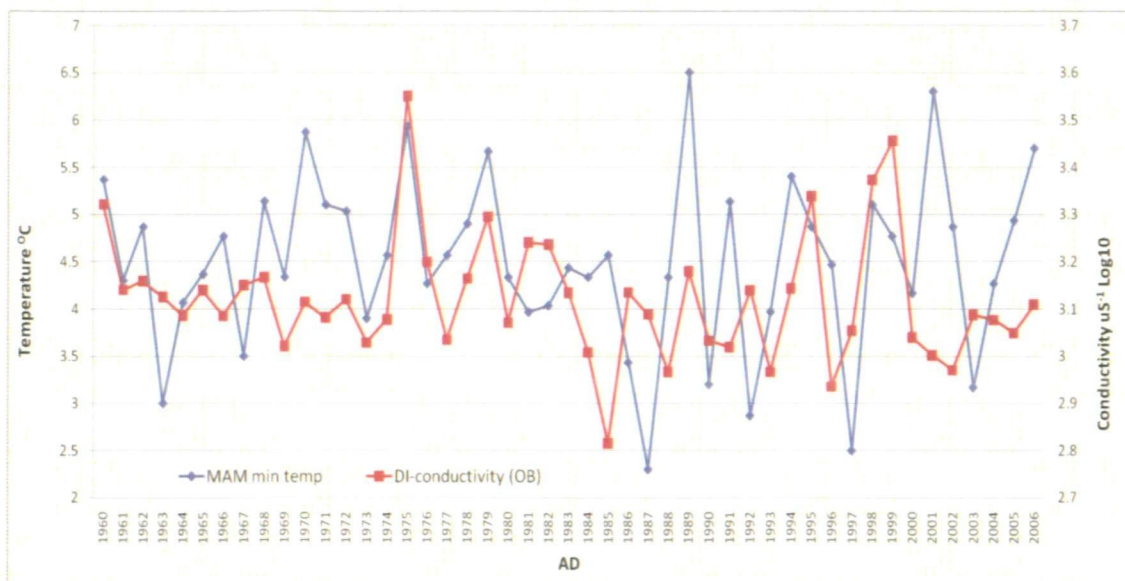


Figure 8.3 Nevşehir spring minimum temperature plotted with NAR06 DI-conductivity (OB) for the period AD 1960-2006 ($r=0.291$, $p=0.047$).

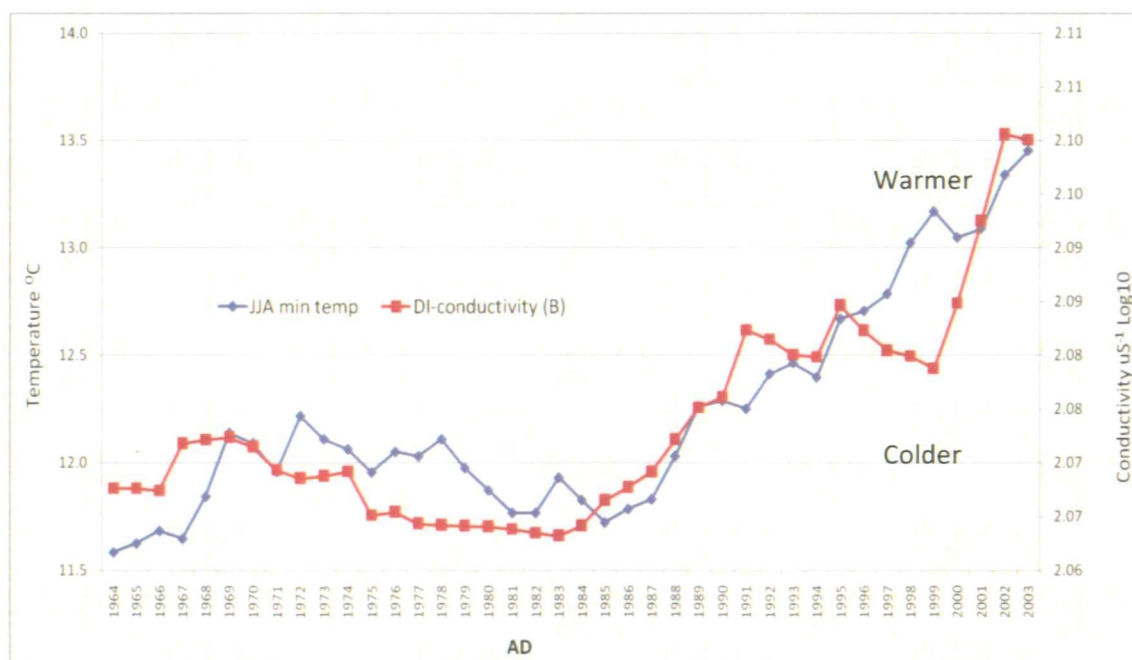


Figure 8.4 Nevşehir minimum summer temperature plotted with DI-conductivity (B) using an eight-year running average for the period AD 1964-2003 ($r=0.880$, $p=0.000$).

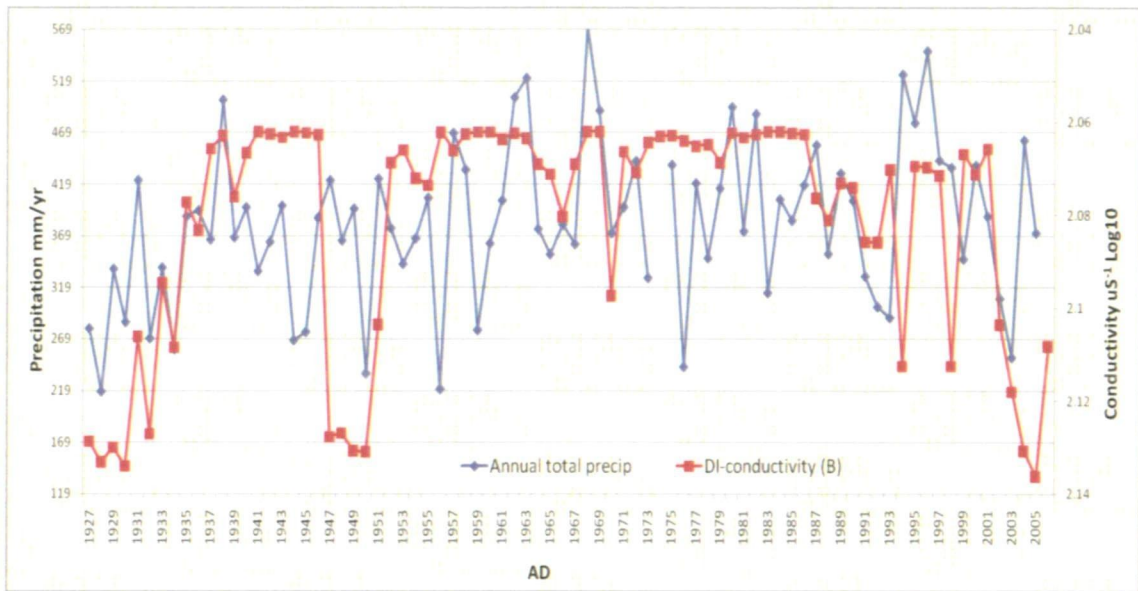


Figure 8.5 Ankara annual total precipitation plotted with NAR06 DI-conductivity (B) for the period AD 1927-2006 (conductivity axis reversed to highlight negative relationship) ($r=-0.353, p=0.001$).

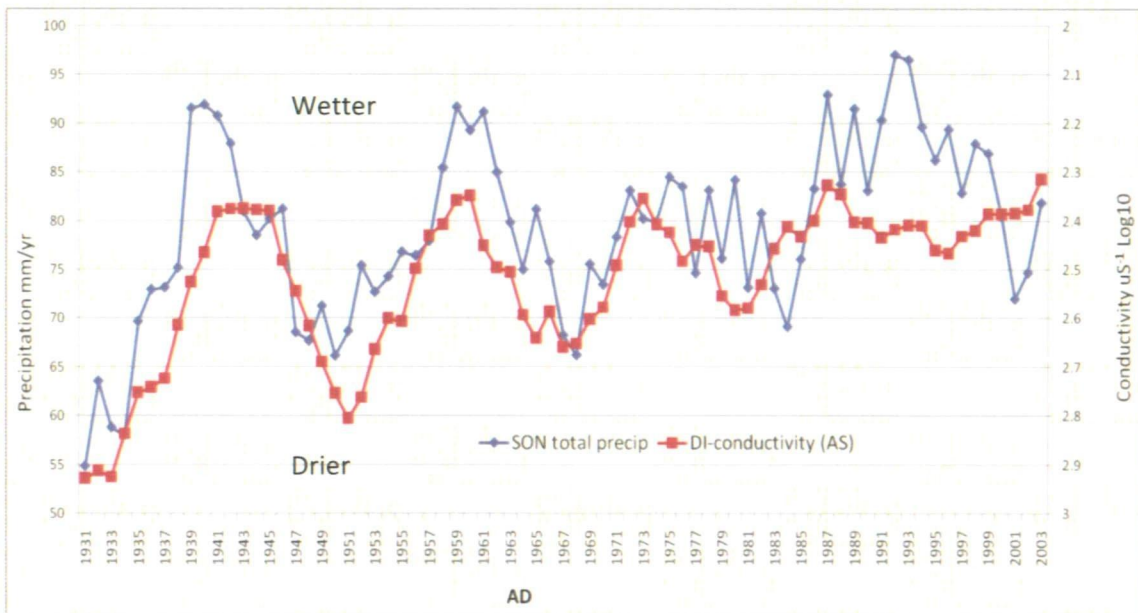


Figure 8.6 Ankara total autumn precipitation plotted with NAR06 DI-conductivity (AS) for the period AD 1931-2003 using an eight year running average (conductivity axis reversed to highlight negative relationship) ($r=-0.751, p=0.000$).

8.3.3 Monthly averages

Seasonal environments lead to successive patterns in diatom population dynamics throughout the course of a year (Wetzel, 2001). Temporal changes in sub-annual conditions favour blooms of certain species, which can last for short time periods. Correlation analyses were carried out in order to reveal whether the climate conditions of particular months have a more pronounced influence on the NAR06 diatom record.

Strongest and most consistently significant relationships were identified between the Nar diatom record and Nevşehir June, July and August temperatures, e.g. minimum July temperature and NAR06 DCA axis 2 ($r=0.406$, $p=0.005$) (Figure 8.7). Similarly, Bigler and Hall (2003) identified that lake DI-July temperature compared well with smoothed meteorological records. Summer temperatures were also correlated significantly with many numerical analyses of the Nar diatom record. For example, June temperature and rarefaction ($r=-0.341$, $p=0.019$) and diatom concentration ($r=0.336$, $p=0.021$). This implies that higher temperature during this month is associated with lower species diversity and higher diatom concentration, which is likely to be associated with mono-specific diatom blooms.

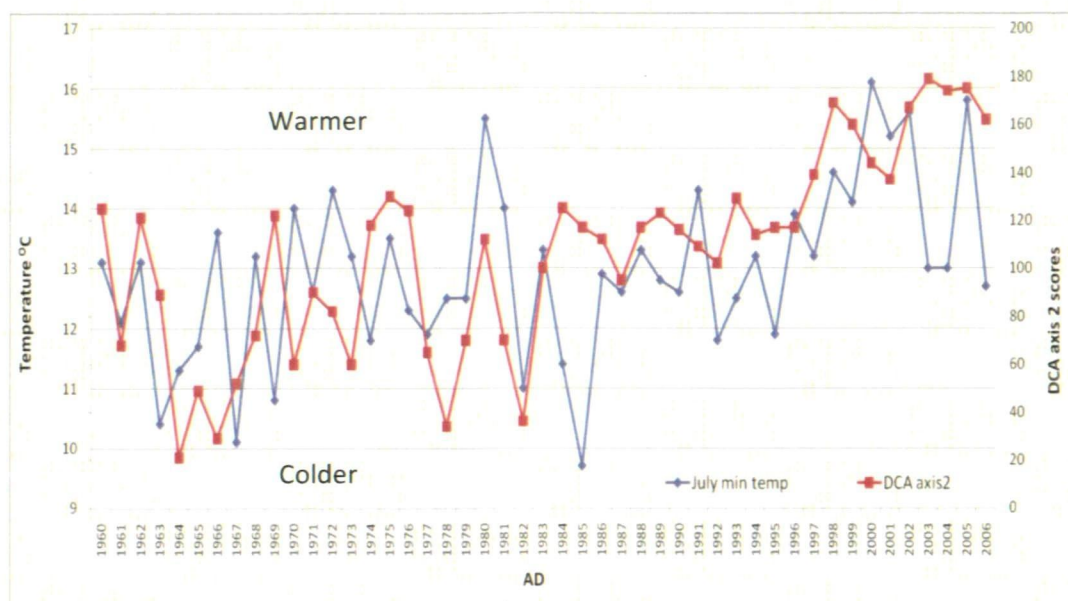


Figure 8.7 Minimum July Nevşehir temperature plotted with NAR06 DCA axis 2 for the period AD 1960-2006 ($r=0.406$, $p=0.005$).

The most frequent correlations with precipitation occurred between October and March, implying that rainfall during these months influences the diatom community. For example, March precipitation was significantly related to NAR06 DCA axis 3 ($r=0.318$, $p=0.030$). NAR06 DCA axis 2 was also significantly correlated with July ($r=0.401$, $p=0.005$) and August ($r=0.396$, $p=0.006$) relative humidity. However, relationships were not 'strong' and other factors are likely to influence the diatom population. It appears that the main climatic drivers of the Nar diatom population are July-August temperature and relative humidity, due to the influence on evaporation, and October-March precipitation.

Similar relationships were expected to exist between monthly meteorological data and core thin section sub-layer thickness. *N. paleacea* bloom layers were positively correlated with Ankara March and June to September temperature with the strongest

relationship between average June temperature and bloom thickness ($r=0.446$, $p=0.000$). Similarly, *N. paleacea* blooms were positively correlated with Nevşehir March and June to September temperatures with the strongest relationship between March temperature and bloom thickness ($r=0.421$, $p=0.005$). This corresponds with evidence from the core thin section analyses, which revealed that this species blooms during spring. *S. acus* blooms were positively correlated with April minimum temperature ($r=0.429$, $p=0.004$), implying that this species may be prolific during spring in addition to autumn. White carbonate layer and varve thickness were also positively correlated with July ($r=0.319$, $p=0.005$ and $r=0.371$, $p=0.001$) and September temperature ($r=0.295$, $p=0.010$ and $r=0.330$, $p=0.004$). This highlights that carbonate is precipitated in spring/early summer and that changing temperatures could be associated with this process. Warmer temperatures may be associated with higher carbonate precipitation and greater lake productivity.

There were fewer relationships between the thin section layers and maximum temperature suggesting that minimum temperatures are a more important factor affecting the lake environment. The only relationship with monthly precipitation occurred between *S. acus* blooms and June ($r=0.259$, $p=0.025$) and October precipitation ($r=0.246$, $p=0.033$). Additionally, January and April precipitation were positively correlated with brown organic layer thickness ($r=0.355$, $p=0.020$ and $r=0.313$, $p=0.041$), implying that increased rainfall during these months leads to overall greater lake productivity. Although correlations were not 'strong', the thin sections relationships with meteorological data suggest that layer thickness is mainly related to summer temperature variability. The relationship between the diatom assemblage and meteorological data is complex and is likely to be influenced by a combination of

climatic and non-climatic factors. Additionally, interpretations are limited, as diatoms are more likely to be influenced by the cumulative effects of meteorological factors.

8.4 Water balance

Relationships between the diatom assemblage and meteorological factors are related to the lake hydrology and residence time. Nar diatoms may respond to cumulative water availability throughout an 8-11 year period and changes in ground water flow.

Fluctuations in temperature and precipitation influence the water balance of the region. This affects lake level and results in diatom population changes. Calculation of water balance based on meteorological data can provide an indication of relative lake level change. An aridity index and cumulative water balance were calculated for a 66 year period (AD 1940-2006), based on central Anatolia meteorological records, for comparison with the Nar diatom sequence.

8.4.1 Aridity index

Aridity indices, based on the relationship between precipitation and evaporation, can be used to analyse the degree to which DI-conductivity is a reliable proxy for palaeoclimate. For example, Laird *et al.* (1998) compared a record of DI-conductivity from Devil's Lake (North America) with the Bhalme-Mooley Drought Index (BMDI), which is based on cumulative percentage departure from long-term mean rainfall. A highly significant relationship was identified between DI-conductivity and summer BMDI through the 20th century ($r=0.49$, $p<0.01$). Analyses of central Anatolia meteorological records have indicated that the Nar diatom assemblage is influenced by temperature and precipitation variability. Therefore the Nar DI-conductivity record has been interpreted primarily as a proxy for palaeo-water balance/aridity.

Türkeş (2003) created an aridity index (AI) to determine dry-land types in Turkey, based on the current ratio between annual average total precipitation (P) and potential evapotranspiration (PE) ($AI=P/PE$) (mm/yr). An AI based on meteorological data from central Anatolia was calculated using this method for the period AD 1940-2006. The semi-arid environment of Cappadocia is sparsely vegetated; consequently evapotranspiration from vegetation is currently not likely to have a considerable impact on total evaporation. Therefore evaporation (E) was used as an alternative to potential evapotranspiration in the AI calculation ($AI=P/E$). Evaporation (mm/yr) was calculated for Nar, based on the relationship between air temperature, altitude, latitude, wind speed and dew point temperature from Ankara, Niğde and Derinkuyu meteorological stations (Jones, 2004) located 230, 45 and 25 km from Nar Gölü respectively.

Criteria used by Türkeş (2003) to define the aridity of different regions of Turkey were used to identify drier/wetter episodes through the period AD 1940-2006. AI values below 1.00 represent annual moisture deficit, values between 0.05-0.20 are defined as arid, 0.20-0.50 are semi-arid and 0.50-0.65 are dry sub-humid. Throughout the last 66 years, the climate of central Anatolia has been predominantly semi-arid with occasional arid years (Figure 8.8). Enhanced aridity leads to concentration of lake water salinity; therefore DI-conductivity was expected to be negatively correlated with AI. However, AI did not show any strong or highly significant relationships with the diatom record. When smoothed with an eight-year running average AI was significantly correlated with various numerical analyses of the diatom record, e.g. NAR06 DCA axis 1 (OB) ($r=0.533, p=0.000$) (Figure 8.9) and NAR06 DCA axis 1 (AS) ($r=-0.368, p=0.003$) (Figure 8.8), which shows a possible diatom response to increased aridity since AD

1998. Therefore more general trends in the climate record appear to relate to lake water balance.

The absence of clear relationships between Nar diatoms and the AI may be associated with the fact that the aridity of each year has been calculated based on annual precipitation and temperature, without accounting for the moisture balance of previous years. Therefore, cumulative water balance was calculated for comparison with the Nar diatom record.

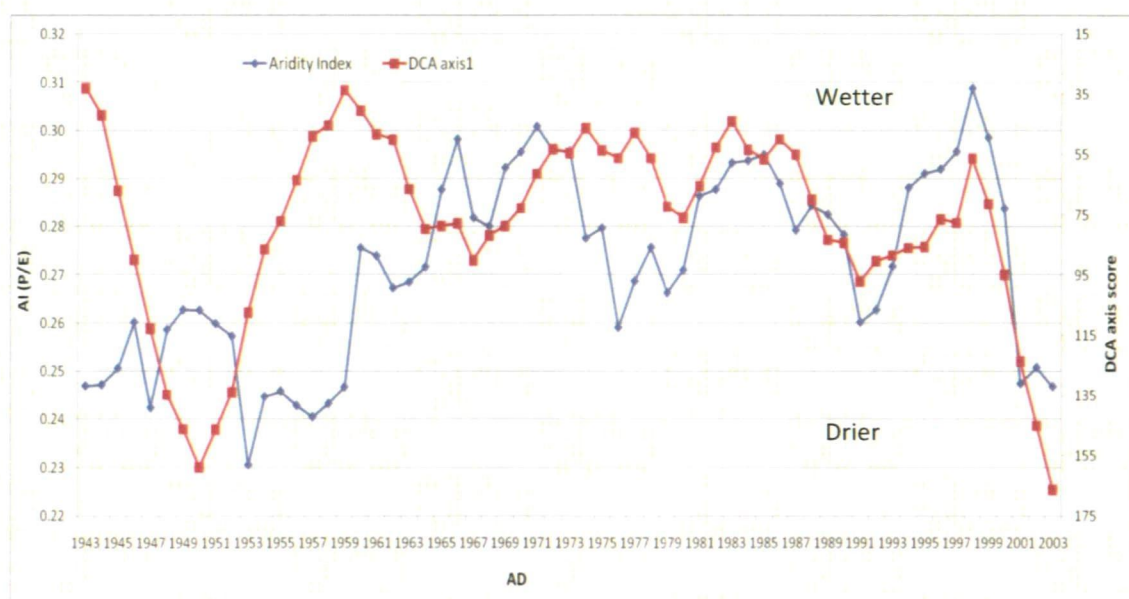


Figure 8.8 Aridity index plotted with NAR06 DCA axis 1 (AS) smoothed using an eight-year running average for the period AD 1943-2003 (AI axis reversed to highlight the negative relationship) ($r=-0.368$, $p=0.003$).



Figure 8.9 Aridity index plotted with NAR06 DCA axis 1 (OB) using an eight-year running average for the period AD 1943-2003 ($r=0.533$, $p=0.000$).

8.4.2 Cumulative water balance

Cumulative lake water balance was calculated for Nar by adding deviation from mean P/E (aridity index) and P-E (moisture deficit) for each successive year for the entire time series and according to the eight year residence time (AD 1940 = 0). The first few data points in the series may not reliably reflect cumulative water balance, as values for the period preceding 1940 were not available. Ankara precipitation was selected as this station showed more significant relationships with the Nar diatom sequence. This calculation allowed information regarding the cumulative effect of precipitation and evaporation to be taken into account and provides an indication of lake level fluctuations.

The strongest relationship was identified between cumulative deviation from mean P/E (based on an eight year residence time) and NAR06 DCA axis 1 (OB) ($r=0.512$, $p=0.000$) (Figure 8.11). DI-conductivity was not significantly correlated with

cumulative water balance; this implies that DCA of the diatom record provides a more reliable record of palaeoclimate. The climatic link is highlighted by the 'strong' correlation of cumulative water balance and oxygen isotopes ($r=-0.729$, $p=0.000$) (Figure 8.10), which provide a record of palaeo-evaporation. This implies that more evaporated conditions indicated by oxygen isotopes relate to decreased lake water level, which is reflected by shifts in the non-blooming diatom population. When smoothed with an eight-year running average, a number of additional significant relationships emerged between water balance and the diatom record e.g. cumulative P-E (based on eight-year residence time) and DI-conductivity ($r=-0.476$, $p=0.000$) and existing relationships became stronger (e.g. oxygen isotopes: $r=-0.819$, $p=0.000$). This implies that DI-conductivity provides a record of lake level change and oxygen isotopes are highly related to cumulative water balance. The stronger relationship with isotopes implies that they may provide a clearer palaeoclimate record. The significant relationship between isotopes and DI-conductivity suggests that diatoms also respond to climate variability.

The observed relationships with cumulative P/E imply that the pre-instrumental period can also be interpreted in terms of palaeo-water balance. The 'strong' relationship with oxygen isotopes highlights that this proxy relates to lake water balance. The 'weaker' relationship with diatoms implies that taxa are also influenced by climate and additional factors affect assemblage change.

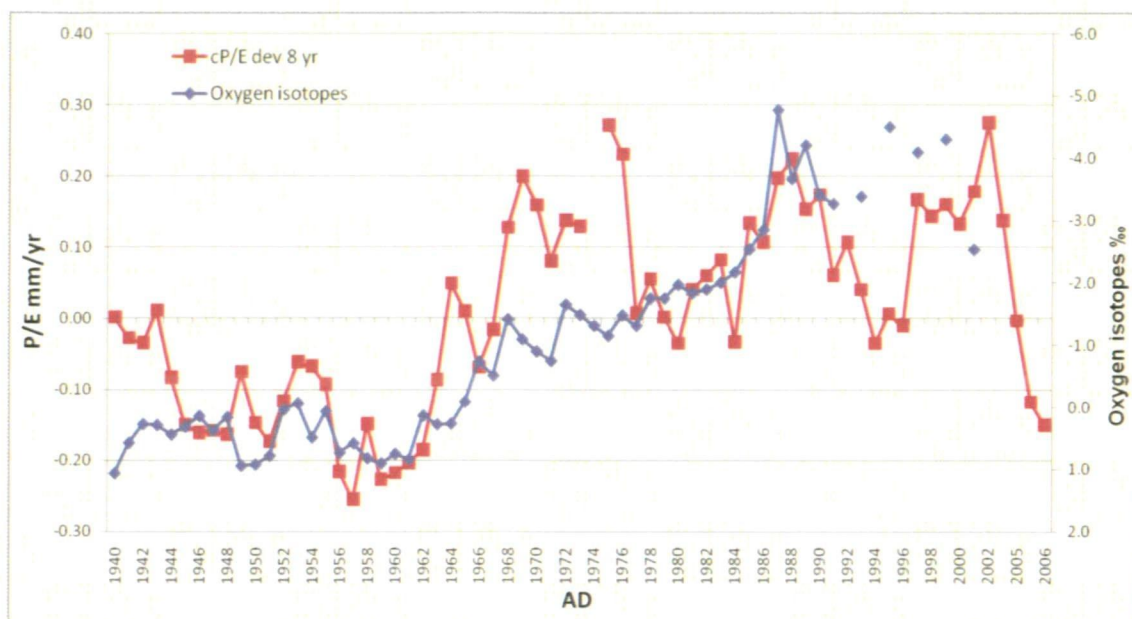


Figure 8.10 Cumulative lake water balance: precipitation/evaporation (cumulative calculation based on eight year lake residence time) plotted with NAR01/02 isotopes for the period AD 1940-2006. (Oxygen isotope axis reversed to highlight negative relationship).

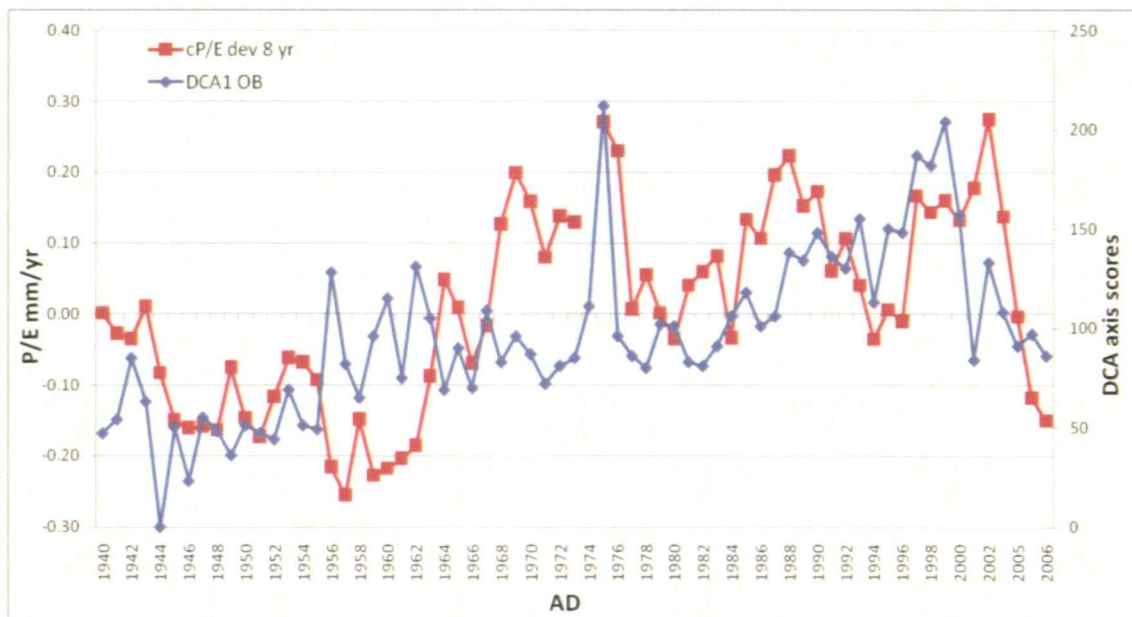


Figure 8.11 Cumulative lake water balance: precipitation/evaporation (cumulative calculation based on eight year lake residence time) plotted with NAR06 diatom DCA axis 1 (OB) for the period AD 1940-2006.

8.5 Summary

Throughout the past 80 years (AD 1927-2006), summer temperature appears to have been one of the main factors driving change in the Nar diatom assemblage. Nar oxygen isotopes were also most strongly correlated with summer temperatures and relative humidity (Jones, 2004; Jones *et al.*, 2005). This implies that a primary climatic control over the Nar Gölü system is summer temperature. Similarly, Keatley *et al.* (2006) attributed recent diatom assemblage change in Canadian lakes to climatic warming. The link between Nar diatom assemblage fluctuations and precipitation variability was less clear. This is likely to be associated with spatial variability of this climatic variable, leading to meteorological stations not reliably reflecting rainfall in the Nar catchment. Many correlations between diatoms and meteorological data were not 'strong'. Therefore the diatom assemblage is likely to be influenced by a combination of climatic and non-climatic variables. This could be related to factors associated with human land use, which can alter nutrient availability, and the complex response of diatoms to environmental change.

NAR06 DCA axes 2 (B, OB and AS) related positively to summer temperature, i.e. higher axis scores corresponded with elevated temperature and vice versa. Therefore both bloom and non-bloom species are most strongly affected by this variable.

Similarly, analyses of thin section relationships with meteorological records and gridded climate data revealed most consistent and strongest relationships with summer temperature. *N. paleacea* was consistently recognised as associated with warmer temperatures in thin section bloom layers and percentage data correlations with meteorological station and gridded climate records. Additionally, *S. acus* was identified

as related to higher autumn rainfall and *C. anatolicus* appeared to favour warmer/wetter conditions.

Cumulative lake water balance based on the eight-year residence time is most strongly related to diatom DCA axis 1 (OB). This climatic link is highlighted by the relationship between water balance and the Nar oxygen isotope record. Key relationships between DI-conductivity (B, OB and AS) and meteorological data revealed that enhanced lake water salinity relates to higher temperature and lower rainfall. However, the DI-conductivity (B and OB) reconstructions may not be reliable as a consequence of low sample counts and poor analogue matching, resulting from removal of species groups from the datasets (Chapter 5; Section 5.3.13).

Stronger relationships were expected with spring meteorological data, as diatoms are typically most prolific during this season (Wetzel, 2001). The absence of significant correlations may be associated with other algal species dominating the spring assemblage and additional factors influencing the diatom relationship with climate. Turkey may experience shorter seasons in comparison with other regions, such as the temperate environments described by Wetzel (2001), in particular, spring may only include a short time period. The stronger, more consistent relationships with summer may be associated with the significant impacts of summer temperature on lake water evaporation, which may have important direct and indirect impacts on the diatom population. Additionally, the stronger trends with Ankara precipitation in comparison with Nevşehir were not expected. Such relationships may exist, due to the effects of run-off and regional precipitation affecting groundwater flow. This may also be associated with the longer timescale of the Ankara record.

Part II Palaeoclimate Reconstruction

8.6 Introduction

The Nar Gölü palae-diatom records indicate considerable environmental variability in central Anatolia throughout the last 1720 years. Significant relationships were identified between the annual NAR06 (AD 1927-2006) diatom record and Turkish meteorological data for the last 80 years (Chapter 8). This implies that the decadal NAR01/02 pre-instrumental diatom record (AD 290-2000) can be interpreted as a proxy for climate.

8.7 Pre-instrumental palaeoenvironmental change

Palae-diatom assemblages offer a rich archive of environmental information. Diatom relationships with lake variables and climate vary between species, alter through time and are affected by a combination of factors, such as changing lake nutrient supply. Correlation analysis of diatom and meteorological data revealed strongest and most significant relationships between NAR06 diatom DCA axes and summer temperature. This relationship is likely to be indirect and associated with the effects of summer temperature on the diatom response to changes in lake water salinity. The absence of relationships between transfer function DI-conductivity and meteorological data is partly related to poor analogue matching with the modern EDDI (European Diatom Database) combined salinity training set. Therefore NAR01/02 diatom DCA axes were used to infer temperature change and additional palaeoenvironmental information was drawn from inferences based on species ecology and diversity, core thin sections, diatom concentration and biovolume. Although each method is subject to limitations, a combination of analyses revealed general patterns in environmental change throughout the record. In addition to a combination of diatom numerical techniques, multiproxy

analyses were used to validate palaeoenvironmental inferences.

8.7.1 Diatom-inferred summer temperature

Regression of the diatom relationship with instrumental meteorological data can be used to infer fluctuations in a specific variable for the pre-instrumental period. Strongest correlation was identified between instrumental summer temperature and NAR06 diatom DCA axes 1 and 2 based on all taxa, which is primarily driven by the changing abundance of bloom species *N. paleacea* (Figure 8.12). A regression equation was calculated for the relationship and applied to pre-instrumental NAR1/02 DCA axis 1 in order to infer palaeo-temperature (regression equation: JJA ave. temp. = $19.9 + 0.00498 \times \text{NAR06 DCA axis 1}$). Figures 8.12 and 8.13 show the relationship between NAR06 DCA axis 1 and summer temperature. Values of NAR01/02 DCA axis 1 were applied to the equation in order to infer pre-instrumental summer temperature. However, this was limited by differences between NAR06 and NAR01/02 DCA axis 1, i.e. the 1 VY and 3 VY sampling resolutions.

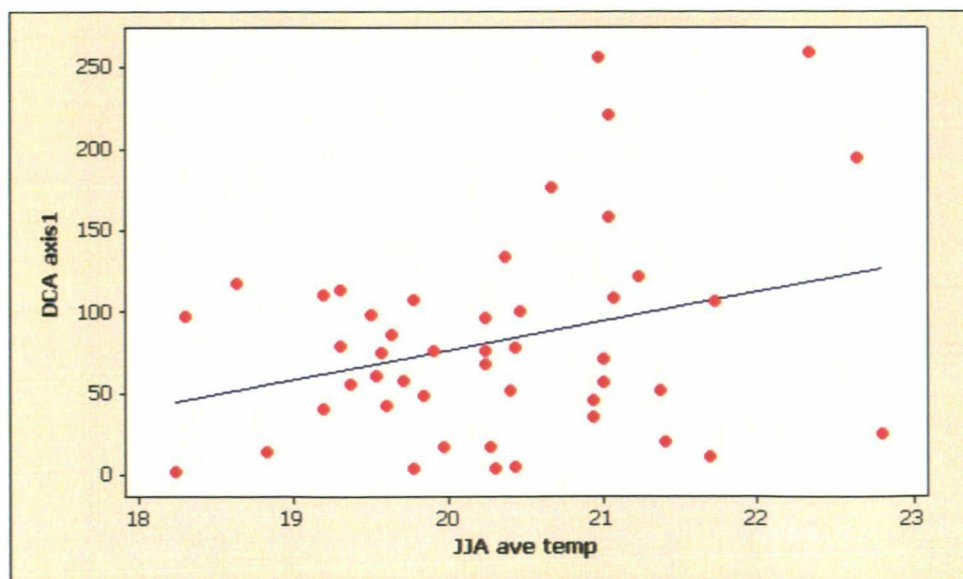


Figure 8.12 Scatter plot of average Nevşehir summer temperature (°C) and NAR06 DCA axis 1 ($r=0.300$, $p=0.041$).

analyses were used to validate palaeoenvironmental inferences.

8.7.1 Diatom-inferred summer temperature

Regression of the diatom relationship with instrumental meteorological data can be used to infer fluctuations in a specific variable for the pre-instrumental period. Strongest correlation was identified between instrumental summer temperature and NAR06 diatom DCA axes 1 and 2 based on all taxa, which is primarily driven by the changing abundance of bloom species *N. paleacea* (Figure 8.12). A regression equation was calculated for the relationship and applied to pre-instrumental NAR1/02 DCA axis 1 in order to infer palaeo-temperature (regression equation: JJA ave. temp. = $19.9 + 0.00498 \times \text{NAR06 DCA axis 1}$). Figures 8.12 and 8.13 show the relationship between NAR06 DCA axis 1 and summer temperature. Values of NAR01/02 DCA axis 1 were applied to the equation in order to infer pre-instrumental summer temperature. However, this was limited by differences between NAR06 and NAR01/02 DCA axis 1, i.e. the 1 VY and 3 VY sampling resolutions.

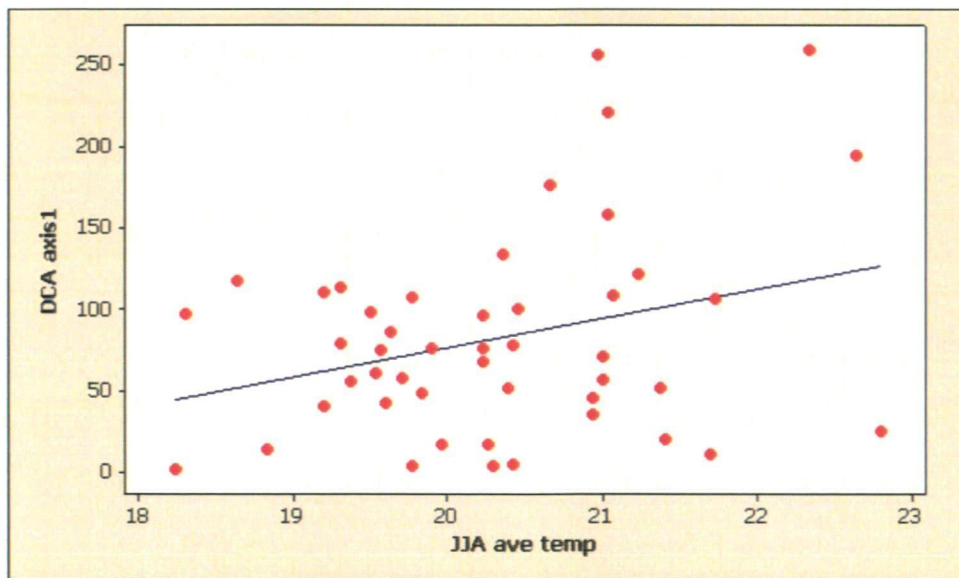


Figure 8.12 Scatter plot of average Nevşehir summer temperature (°C) and NAR06 DCA axis 1 ($r=0.300$, $p=0.041$).

has been used to infer palaeoclimate in conjunction with other diatom numerical analyses.

8.7.2 *Nar multi-proxy inferred palaeoclimate*

NAR01/02 DI-temperature, conductivity and the oxygen isotope record (Jones *et al.*, 2005; 2006) (Figure 8.14) all indicate a major change in the system ~AD 540. This involved a shift to lower DI-temperature, more negative oxygen isotopes (lower evaporation) and decreased DI-conductivity, which indicates higher water availability. DI-temperature and conductivity suggest that average summer conditions may have been between 2 and 4°C warmer and lake water between 2 and >4 times more saline during the period prior to AD 540. Dominant diatom species in this zone favoured higher lake water salinity and disturbance. For example, the period AD 290-540 was dominated by *F. construens var. venter*, *R. operculata* and *C. meneghiniana* (until ~AD 800) also indicating a drier climate during this time. Dominant diatom species then shifted to taxa, such as *N. paleacea*, which favour lower salinity, simultaneously with the shift to lower isotope-inferred evaporation.

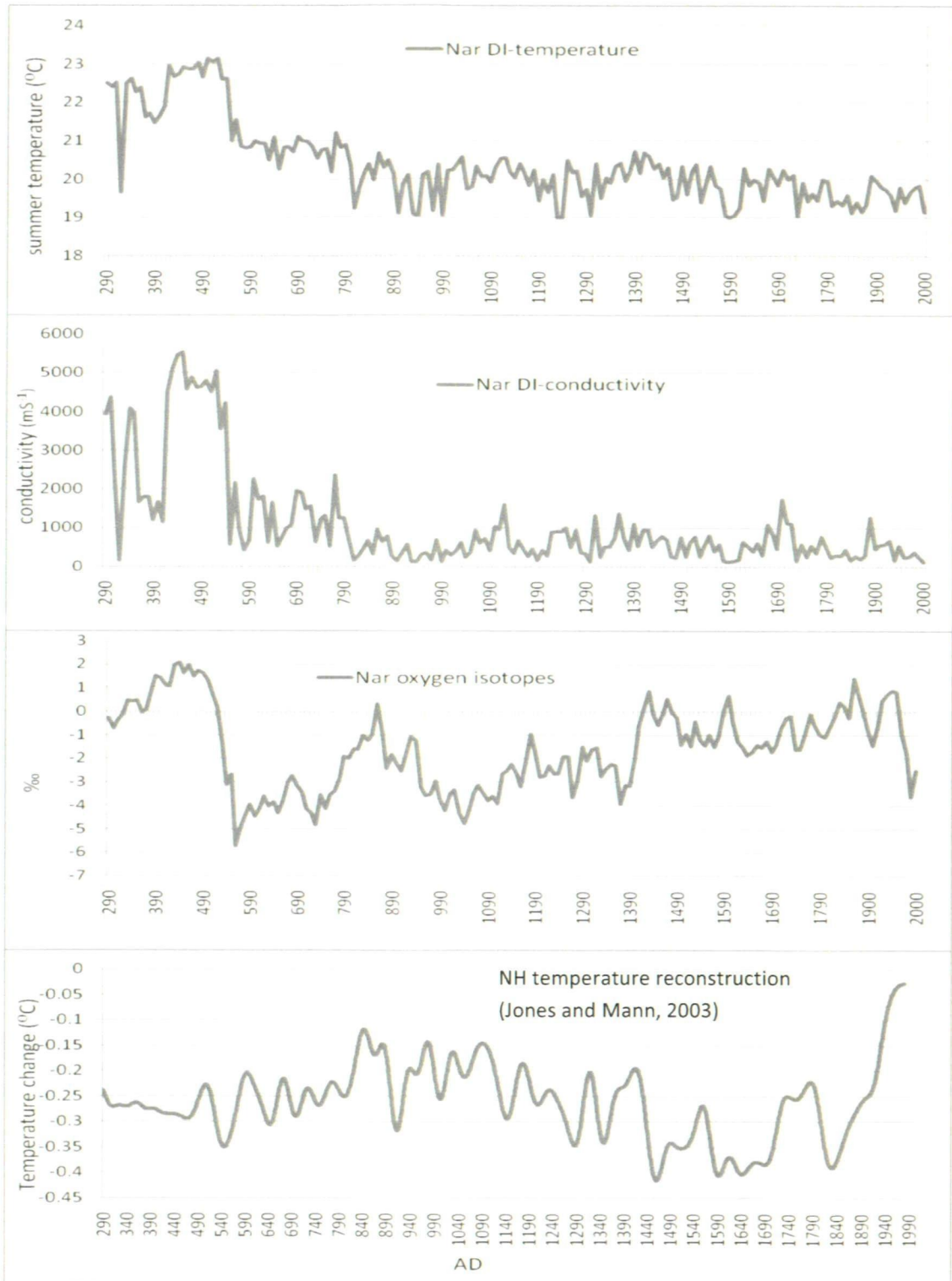


Figure 8.14 NAR01/02 DI-summer temperature, conductivity and oxygen isotopes plotted for the period AD 290-2000 with Mann and Jones’s (2003) NH temperature reconstruction (AD 290-1994).

These inferences are supported by the presence of *Olea* pollen in the early part of the NAR01/02 record, which decreased ~AD 700 and may indicate that conditions became cooler as olive trees cannot tolerate extreme cold winters (England *et al.*, 2008). The Nar pollen sequence revealed that the arid episode prior to AD 540 involved a landscape dominated by herbs, drought-tolerant sparse trees and agricultural pollen indicators. Therefore diatom and isotope-inferred arid conditions between AD 290-540 do not appear to have inhibited human occupation and agriculture in the Nar catchment. This implies that humans may have adapted to climatic changes and continued to utilise the land during this time. Rosen and Rosen (2001) suggested that with the development of sedentary societies, the solutions for adapting to climatic change became more complex throughout the late Holocene. Roberts *et al.* (2004) highlighted that during non-drought conditions, the Mediterranean climate still experienced strong seasonality, with extremely dry summers, and past societies were well adapted to this regime. This is reflected by the typical drought-tolerant vegetation of the Mediterranean (Roberts and Wright, 1993). Alternatively, rainfall during the vegetation growing season may have remained adequate or sufficient ground water could have been retained in the catchment to support plant growth during this arid phase. Therefore it appears that the vegetation response to extreme climatic events is complex and masked by human land use. This also appears to be evident in the diatom record.

Following the lake freshening period (~AD 540-560), diatom and oxygen isotopes diverged through the record showing dissimilar trends. This coincided with the appearance of blooming diatom species, which were the main drivers of the DCA axes and conductivity reconstruction. Therefore these species may mask the diatom relationship with climate. Oxygen isotopes revealed a shift to drier conditions ~AD 800.

However, DI-conductivity and temperature decreased at this point. Discrepancies may exist between the isotope and diatom records due to the differing sensitivity of the proxies to climatic variability, alterations in other limnological factors and the possibility that water chemistry thresholds were not reached to initiate a diatom response. Isotopes indicated a return to enhanced aridity at ~AD 1400, whereas diatoms signified a less variable environment.

The pollen record indicates that the wider Nar catchment has been subject to almost continuous human land use throughout the past 1720 years (England, 2006; England *et al.*, 2008). This is likely to have impacted on lake conditions and the diatom assemblage and may be responsible for the divergence observed between diatom and oxygen isotope records throughout the sequence. The pollen record revealed a number of changes in human land use. This included agricultural abandonment between AD 670-950 and an agricultural crisis during the 12th century (England *et al.*, 2008), which coincided with a period of increased DI-temperature and a reduction in agricultural pollen indicators between AD 1640-1680, representing a problematic period for agriculture (England, 2006).

The NAR01/02 pollen DCA axes, which summarise vegetation change throughout the last 1720 years, were not significantly correlated with the oxygen isotope record ($p > 0.05$) and pollen zone boundaries did not coincide with diatom assemblage shifts (Chapter 7: Figure 7.6). This implies that diatoms and vegetation could have dissimilar response times and sensitivity to environmental changes. Similarly, the pollen record from Eski Acıgöl in central Turkey (Roberts *et al.*, 2001) revealed human-induced shifts in vegetation patterns and Eastwood *et al.* (2006) recognised divergence between pollen

and isotope-inferred palaeoclimate during the last 3-4 millennia in a lake sediment record from Gölhisar (southwest Turkey). Divergence between records was attributed to the increasing impact of human land use and the different response time of vegetation to climatic changes. Similar patterns have been identified in other pollen records from the Mediterranean (e.g. Lamb and van der Kaars, 1995; Wick *et al.*, 2003). However, the timing of increased human impact differs regionally. Barker *et al.* (1994) identified climatically-induced lake level change in a diatom record from the Middle Atlas (Morocco) and only recognised human-induced catchment disturbance during the 20th century.

Diatom concentration and biovolume were positively correlated with instrumental temperature and higher values may indicate increased aridity between AD 400-540, 790-990, 1140 and ~1900 (Chapter 5: Figure 5.16). Additionally, mono-specific diatom bloom layers evident in core thin sections (Chapter 5: Figure 5.23) increased in frequency within more recent sediments (~AD 1600-2000) and may relate to environmental variability during this time or changes in lake nutrient supply. Lamina thickness was used as a palaeo-climate proxy by Romero-Viana *et al.* (2008), who identified strong correlation between varve width from a Spanish lake sediment sequence and instrumental precipitation. NAR01/02 core thin section varve thickness was positively correlated with instrumental temperature. Therefore increased varve thickness throughout the last 300 years may relate to warmer climatic conditions. However, thicker varves are also associated with diatom blooms which drive DI-temperature and conductivity values down in the reconstruction. Additionally, interpretations based on Nar lamina thickness are limited by the influence of decreased sediment compaction nearer the profile surface.

A significant event in the Nar diatom record involved sudden elevated values of *S. parvus* (AD 1205-1246). This was not reflected in the oxygen isotope and pollen records and may represent a specific change in water chemistry, leading to conditions that favour this diatom species over other blooming algae. Another short-lived and abrupt biotic shift was identified in the Nar record by England (2006) between AD 999-1001. This involved a dramatic increase in the abundance of a chlorophyte algal species (*Pediastrum boryanum*), which indicates shallowing of the lake. Both events were unique in the record and imply that the system has experienced abrupt and short-lived changes throughout the last 1720 years.

More recent species ecological changes in the Nar record appear to relate to factors other than salinity fluctuations. Reed *et al.* (1999) identified that *C. cistula* and *A. minutissimum* are typical of shallow waters with abundant aquatic macrophytes in Turkish lakes. According to biovolume, the large taxon *C. cistula* became increasingly abundant in the Nar record after ~AD 1630 and *A. minutissimum* after ~AD 1300, which may relate to increased fringing macrophyte cover due to warmer temperatures or enhanced nutrients and lake level decrease. Increased dominance of the non-planktonic/epiphytic new taxon *C. anatolicus* between AD 550 and 1500 and during the most recent five years (AD 2001-2006) could also indicate enhanced macrophyte cover. *N. paleacea* is a planktonic species that favours higher nutrient levels. The increasing dominance of this taxon between AD 540 and 2000, along with *S. acus* between AD 950-2000, indicates higher lake levels in relation to the period prior to AD 540 and possibly increased nutrient supply. Combined inferences from the different proxies and

diatom numerical analyses have provided various insights into the palaeoclimate of the region.

8.7.3 Kratergöl environmental change

Kratergöl diatom-inferred environmental change was not analysed on a calendar time scale, due to problems with the ACM99 core chronology and the variable lake sedimentation rate. This prevented reliable comparisons with other proxy records, meteorological data and atmospheric circulation patterns. Furthermore, instrumentally measured and DI-conductivity differed considerably, which also made climatic inferences problematic. Diatom valve concentration and biovolume were reflective of the varied lake sedimentation rate.

Although the ACM99 chronology was uncertain, variability through the record relates to temporal changes in the lake environment. DI-conductivity indicates a less arid climate between 59 and 18 cm core depth, followed by a shift to extremely high DI-conductivity and increased percentage of *E. paludosa* var. *subsalina* signifying more arid conditions between 16 and 4 cm. This was followed by a return to decreased DI-conductivity in the most recent sediment (Chapter 6: Figure 6.10). The profile is thought to represent the 20th century and may therefore relate to increased temperatures during this time period or decreased ground water level as a consequence of irrigation. Lake level recordings indicated that Kratergöl water depth has decreased throughout the past decade (AD 1999-2008). However, as the ACM99 core was collected in 1999, recent climatic change was not recorded in the profile.

Analysis of the Kratergöl sequence has highlighted the suitability of annually-laminated lake sediments, such as those present at Nar, to palaeoclimate reconstruction and the problems that can be encountered when non-laminated archives from lakes with a varied sedimentation rate are used in palaeoenvironmental research.

8.7.4 Limitations of the palaeo-environmental reconstructions

Numerous assumptions are required in order to infer climate from palaeolimnological analyses. Recognising the limitations that result from these assumptions is important when considering the reliability of inferences. Fluctuations in water level affect different individual chemical variables in addition to total conductivity and the diatom assemblage is influenced by a combination of limnological factors. Lags in the lake response to climate change may also affect the observed relationships and non-climatic factors are likely to influence both the lake system and the diatom response to environmental change. For example, human land use may have affected the nutrient status, chemistry and water level of the lake, thus influencing the diatom and oxygen isotope relationships with climate.

Additionally, changes in the catchment groundwater regime throughout time may have altered the diatom response to climatic variability. Reconstructing climate from DI-conductivity is complicated by the possibility that salinity may not be linearly coupled to lake level or the balance between precipitation and evaporation (Fritz *et al.*, 1999). For example, Saros and Fritz (2000) identified that the growth rates of different diatom species differed in response to changing salinity, brine types and nitrogen form. Additionally, the balance between precipitation and evaporation may not be the only driver of Nar lake level and the presence of freshwater and saline springs may have

altered lake conductivity through time. Consequently, the response of diatoms to changing water balance may not always reflect climate variability.

Inferences based on DI-temperature are limited by various factors. For instance, relationships between the diatom assemblages and variables, such as instrumental temperature, are not straightforward and issues of temporal autocorrelation between sample depths may give unrealistic correlations with meteorological data. It was not possible to estimate errors for the NAR01/02 DI-temperature record, as variability predicted for the calibration period may not reflect the magnitude of change in the pre-instrumental record. The use of linear regression to produce the DI-temperature reconstruction is also limited by the possibility that the diatom response to climate change is non-linear and related to threshold effects (Reed *et al.*, 1999).

The majority of numerical analyses explored, e.g. diatom concentration, species diversity, biovolume, DCA axes and DI-conductivity were all greatly influenced by the abundance of *N. paleacea*. Therefore palaeoclimatic inferences for periods of the record dominated by this taxon may mask the climate signal from other diatom species.

8.8 Controls on EM climate and the Nar Gölü diatom record

8.8.1 Northern Hemisphere (NH) temperature and precipitation

Reconstructions of NH temperature for the last 2000 years have revealed characteristic climatic episodes, which may be reflected by changes in the Nar palaeo-record. The Medieval Climatic Anomaly (MCA), which involved warmer climate preceding and during the 10th to 14th centuries and the Little Ice Age (LIA), associated with colder conditions throughout the 16th to mid-19th century, have been identified in

palaeoclimatic proxy records from Europe (e.g. Gil *et al.*, 2006), Greenland (e.g. Jensen *et al.*, 2004), Africa (e.g. Verschuren *et al.* 2000), North America (e.g. Laird *et al.*, 1996; 1998; Fritz *et al.*, 1999), Russia (e.g. Mackay *et al.*, 2005) and various other locations. In order to compare the timing of these events with the Nar diatom record, the last 1000 years have been analysed separately and deviation-from-mean data are presented to allow general shifts between warmer/colder periods to be identified.

The MCA may relate to the period of increased DI-conductivity and temperature between AD 1050-1550 at Nar (Figure 8.15). However, aridity at this time is not significant when compared with the period in the Nar record prior to AD 540 (Figure 8.14). The LIA may relate to lower Nar DI-conductivity evident at ~AD 1600 and 1830, indicating a fresher system and lower DI-temperature between AD 1550-2000. However, this episode was interrupted by drier periods. Diatom bloom species are the principal drivers of the DI-temperature reconstruction for the majority of the record. The change to lower DI-temperature at ~AD 1600 is reflected by the fact that mono-specific diatom bloom layers became more common in the core thin section record at this time.

The MCA and LIA are not clear in the Nar DI-conductivity record but may be apparent in the DI-temperature reconstruction. Mann and Jones's (2003) NH temperature reconstruction and Nar DI-temperature both indicate a shift from a generally warmer to a cooler climate at ~AD 1450 (Figure 8.15). However, the fact that this pattern is not clear in other analyses from the Nar sediment record reduces the reliability of interpretations based on DI-temperature. In contrast, the Nar oxygen isotope record revealed opposite to typical MCA and LIA conditions (Jones, 2004). Therefore it is not

certain whether typical NH climate trends occurred simultaneously in central Anatolia. Jones (2004) recognised that positive isotopes (drier climate) at Nar corresponded with periods of decreased NH temperature and vice versa ($r=-0.538$, $p=0.000$). This suggests that central Anatolia experiences opposite conditions to the NH average. This negative relationship with NH temperature also appears to be reflected in part of the Nar DI-conductivity record (AD 290-1400) ($r=-0.455$, $p=0.001$). However, the isotopes and diatoms reflect moisture balance. Therefore increased NH temperature may have involved warm/wet climate in Turkey and lower NH temperature may relate to cooler/drier Turkish climate.

A teleconnection 'see-saw' oscillation pattern has been identified in atmospheric pressure distribution and spatial precipitation variability between the east and west Mediterranean (Roberts *et al.*, 2004). Oldfield and Thompson (2004) suggested that the same teleconnection pattern is likely to exist in millennial-long proxy records. Additionally, Xoplaki *et al.* (2006) identified negative correlation between precipitation in the western and northern Mediterranean and the NAOI, whereas a positive trend was identified in the southeast Mediterranean. This 'see-saw' pattern may account for some of the trends identified in the Nar record.

The lack of clear MCA and LIA periods in the Nar diatom record implies that the timing of these events may have differed in the EM in comparison with Western Europe. Jones and Mann (2004) emphasised that terms such as the LIA and MCA have limited use for describing the climate of the past millennium due to the dramatic differences between regions. Researchers attempt to identify these episodes in palaeo-records when they may actually be specific to Western Europe/North America and regional variability is likely

to be underestimated (Jones and Mann, 2004). According to Bradley and Jones (1992), the LIA was a complex period, which varied between regions and involved decade-long cold episodes, separated by warmer intervals. This appears to correspond with the Nar deviation from mean DI-temperature record (Figure 8.15). In a comparison of globally distributed palaeoclimate records, Mayewski *et al.* (2004) recognised limitations of the terms MCA and LIA and alternatively termed episodes 'periods of rapid climate change'. This may more reliably reflect variability throughout the Nar palaeo-records.

Recent climatic warming (since ~AD 1840) is not clearly evident in the Nar diatom sequence. However, Turkish meteorological records reveal that higher temperatures have occurred in central Anatolia during the 20th century. Recent warming could be reflected by DI-conductivity and temperature between AD 1850-1920; however, values then decrease. Nar core thin sections indicate increased varve thickness between 1840-2002, which may also relate to recent climatic warming.

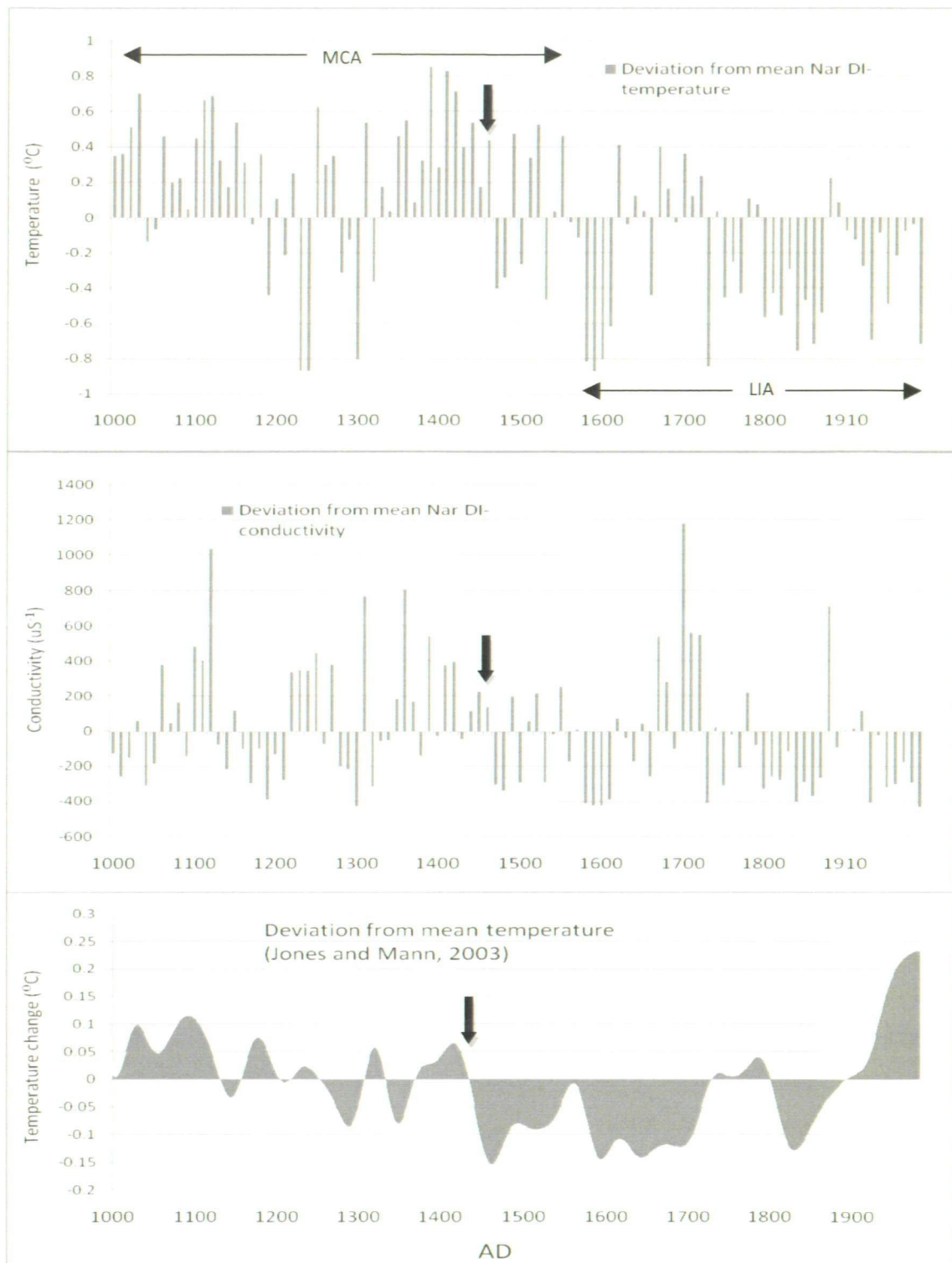


Figure 8.15 Deviation from mean Nar DI-summer temperature, conductivity and Northern Hemisphere reconstructed temperature (Mann and Jones, 2003) for the period AD 1000-2000. Arrows highlight correspondence between the records.

8.8.2 Atmospheric circulation patterns

Global temperature changes influence atmospheric circulation patterns, which result in climatic shifts that may differ in their characteristics and timing between regions. The influence of different atmospheric circulation patterns on the climate of central Anatolia alters seasonally. During winter, low pressure systems (depressions) associated with polar regions dominate in their influence on Turkish climate with origins in the North Atlantic (e.g. the North Atlantic Oscillation and the North Sea-Caspian Pattern) (Kutiel and Türkeş, 2005) and the Arctic (e.g. the Arctic Oscillation) (Türkeş and Erlat, 2008). In summer, high-pressure systems associated with tropical regions, such as Asia and the Southern Hemisphere (e.g. the Indian Monsoon and Southern Oscillation), have a greater influence on Turkish climate (Karabörk and Kahya, 2003; Jones *et al.*, 2006) and are particularly associated with drought events.

Changes in the diatom and isotope records from Nar are likely to be associated with shifts in different atmospheric circulation patterns. Enzel *et al.* (2003) identified that the potential causes for wet and dry episodes in the EM are rooted in the larger-scale NH atmospheric circulation. Diatoms are most prolific during spring, early summer and autumn. Consequently, atmospheric circulation patterns determining weather patterns during these seasons should have greater influence on the Nar diatom assemblage. Additionally, cumulative annual precipitation impacts on moisture availability of following time periods; therefore atmospheric pressure distribution during all seasons may influence the diatom population.

North Atlantic Oscillation (NAO)

The NAO is related to the surface pressure alteration between the Azores High and the Icelandic Low and is an important driver of EM climate (Kutiel and Türkeş, 2005).

During positive NAO years, Turkey experiences significantly drier climate, and during negative phases wetter conditions dominate (Dünkoleh and Jacobeit, 2003, Türkeş and Erlat, 2003; 2005). This is evident in the negative relationship between the NAOI (index) and central Anatolia gridded meteorological data for the period AD 1950-2002 (NAOI and mean temperature: $r=-0.389$, $p=0.004$).

Analysis of the relationship between the NAOI (Osborn, 2008) and the NAR06 diatom record between AD 1950-2006 revealed that October NAOI is correlated most frequently with the diatom sequence (NAR06 DCA axis 2: $r=-0.338$, $p=0.010$) (Figure 8.16). Additionally, January and February NAOI were weakly related to the diatom assemblage and there were no significant correlations with any other months. The impact of the NAO on Turkish climate is more pronounced during October-March and affects water availability during the following spring, when diatoms are typically most prolific. Therefore more positive NAOI phases may be associated with lower precipitation in Turkey. However, Touchan *et al.* (2003) and Akkemik and Aras (2005) did not identify any significant relationships between central Anatolian tree-ring-inferred precipitation and the NAOI. The absence of strong relationships with the Nar diatom record implies that there are additional controls on EM climate and the diatom assemblage.

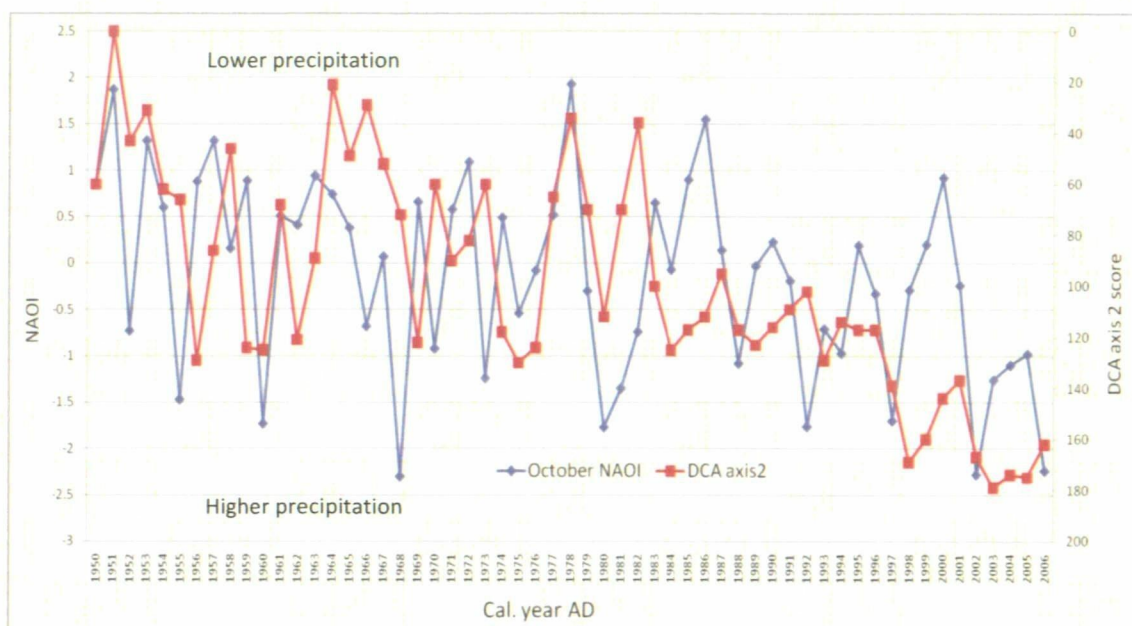


Figure 8.16 October NAOI plotted with NAR06 diatom DCA axis 2 for the period AD 1950-2006 (DCA axis reversed to highlight the negative relationship) ($r=-0.338$, $p=0.010$).

North Sea-Caspian Pattern (NCP)

The NCPI (index) represents the atmospheric teleconnection between the North Sea and the northern Caspian region (Kutiel and Benaroch, 2002). Kutiel and Türkeş (2005) identified the NCP as a particularly important factor influencing the climate of Cappadocia, especially during winter months. Temperatures during negative NCPI were considerably higher than periods of positive NCPI and no influence on the precipitation regime of the region was identified. According to Kutiel and Benaroch (2002), negative episodes of the NCPI bring an increased south-westerly anomaly circulation towards the Balkans, Middle East and western Turkey, resulting in above normal temperatures and below normal precipitation. The opposite occurs during positive NCPI episodes. The NCPI (Harding, 2006) was weakly correlated with numerical analyses of the NAR06 diatom record for the period AD 1948-2005. For example, higher temperature (lower

December NCPI) was associated with enhanced non-bloom species DI-conductivity (OB) ($r=-0.283$, $p=0.032$) (Figure 8.17). Similar trends between the records are evident with peaks in 1975/76 and 1999 relating to drier conditions. Therefore it appears that winter NCP may exert some influence on the Nar diatom community via the connection with temperature. The absence of correlations with summer, spring and autumn could be associated with the NAO and NCP having more pronounced impacts on the winter climate of Turkey and their effects on water availability during seasons following winter.

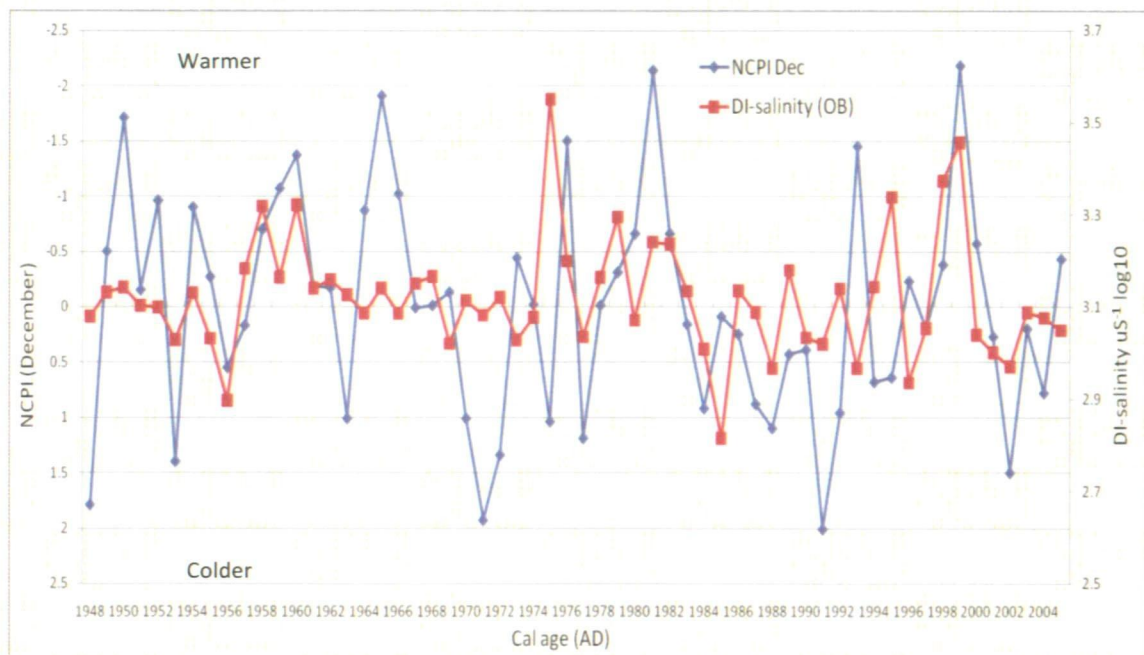


Figure 8.17 December NCPI plotted with NAR06 DI-conductivity (OB) for the period AD 1948-2006 (NCPI axis reversed to highlight the negative relationship) ($r=-0.283$, $p=0.032$).

Tropical teleconnections

The Indian Monsoon is associated with the seasonal temperature difference between the Eurasian land mass and surrounding oceans and has been recognised as a teleconnection

influencing summer climate in central Anatolia (Jones *et al.*, 2006). Liu and Yanai (2001) identified that greater intensity of monsoon rains from tropical Africa to India lead to warmer conditions in western Asia. Increased monsoon rainfall results from low pressure systems over southern Asia. This strengthens the northerly and north-easterly airflows from warm/dry central Asia, resulting in increased drought in the EM (Jones *et al.*, 2006).

Analysis of the relationship between the Indian monsoon (Sontakke *et al.*, 1993) and Ankara meteorological data revealed that higher monsoon rainfall weakly relates to increased temperatures and lower precipitation in central Turkey (e.g. average September temperature and monsoon rainfall $r=-0.257$, $p=0.031$). However, these relationships were not strong or frequent and no significant correlations were identified between monsoon rainfall and the diatom record. Jones (2004) and Jones *et al.*, (2006) identified a negative relationship between the Nar oxygen isotope record and Indian and African monsoon rainfall between AD 1900 and 2000, indicating that decreased evaporation (wetter conditions) at Nar is associated with drier climate in India and the Sahel region of Africa and increased monsoon rainfall is related to drier conditions in Turkey. Therefore it appears that the Indian Monsoon influences the climate of central Anatolia, however, this is not reflected directly by changes in the Nar diatom record.

Southern Oscillation (SO) represents the difference in air pressure between Tahiti (South Pacific Ocean) and Darwin (North coast of Australia) and exerts various influences upon global climate. Alpert *et al.* (2005) identified relationships between EM rainfall extremes and tropical systems, such as El Niño (ENSO), and Karabörk and Kahya (2003) recognised significant responses in Anatolian precipitation to extreme SO

phases. However, SO has also been identified as having a weaker relationship with Turkish climate in comparison with the NAOI (Karabörk *et al.*, 2005).

Analysis of the Nar diatom and isotope relationship with the seasonal ENSO index (US Dept. of Commerce, 2008) between AD 1950 and 2006 revealed no significant relationships ($p > 0.05$). However, strengthening of the ENSO throughout this period may be associated with increased temperatures in the EM. Türkeş (1998) identified that warm (La Niña) and cold (El Niño) SO event responses are characterised by decreased rainfall in Turkey. Cold events were also related to increased rainfall in central Anatolia. Therefore it appears that the relationship between SO and Turkish climate is complicated. The absence of strongly significant relationships between the diatom record and atmospheric circulation patterns does not necessarily imply that these factors are not important drivers of central Anatolian climate. The most important drivers are likely to be the NAO, NCP and Indian Monsoon with little influence from other circulation patterns.

8.9 Palaeoclimate reconstructions

The magnitude and frequency of change in the proxy records from Nar Gölü may be influenced by both climatic and non-climatic factors on local and regional scales. Comparisons have been made with palaeoclimate records from the EM and additional global regions in order to identify how similarly the sequences from Nar resemble other proxy reconstructions.

8.9.1 Lake-inferred palaeoclimate

A number of lake sites in the EM contain sedimentary palaeoclimate records that are

affected by the same atmospheric circulation patterns as those influencing the climate of central Anatolia. However, few studies from the EM, other than those from Nar, have focused on the last 2000 years at high-resolution, therefore comparisons are limited.

Palaeolimnological climate reconstructions in Turkey have highlighted the incidence of drought and increasing impact of human activity throughout the late Holocene. For example, Roberts *et al.* (2001) and Jones *et al.* (2007) recognised late Holocene aridity in a record from Eski Acıgöl in central Turkey and Wick *et al.* (2003) identified intensification of human activity at Lake Van (northeast Turkey) throughout the past 600 years. Additionally, Eastwood *et al.* (2006) identified a trend towards increased climatic aridity throughout the last 1300 years in lake pollen and isotope records from southwest Turkey. Higher DI-conductivity during the late Holocene in central Turkey was also recognised by Reed *et al.* (1999). However, these long-term, low-resolution records cannot be compared with the detailed climatic variability evident in the Nar record throughout the last 2000 years.

The sedimentology of northwest Anatolian lakes was employed as a proxy for palaeo-water balance by Kazancı (2005) from lakes on the southern coast of the Sea of Marmara (Leroy *et al.*, 2002). Increased organic matter within lake sediment was interpreted as representing drier climatic episodes. Similarly, Nar diatom concentration and varve thickness were positively correlated with instrumental temperature, implying greater lake productivity during drier climatic periods. Kazancı (2005) identified a number of dry episodes throughout the Holocene, with decreasing duration towards the present. Shorter duration dry periods were also recognised in the latter part of the Nar record (Figure 8.14). Kazancı (2005) recognised two dry intervals between AD 400-

700. The beginning of this dry event coincided with the rise to maximum aridity in the Nar DI-conductivity and temperature records. However, freshening at Nar indicated by diatoms and oxygen isotopes, occurred ~160 years before that inferred from lakes in northwest Anatolia. The second dry event identified by Kazancı (2005) occurred between AD 1200-1470 and coincided with a period of warmer Nar DI-summer temperature (Figure 8.19). However, the shift in isotopes ~AD 1400 to more arid conditions is not evident in Kazancı's (2005) reconstruction. These comparisons imply that similar climate trends throughout the last 2000 years may have been recorded in sediments from different regions of Turkey and the duration and timing of drought events may vary regionally.

8.9.2 Tree-ring-inferred palaeoclimate

Studies of temporal change in tree-ring width based in Turkey have provided high-resolution records of palaeo-precipitation. Tree-ring research benefits from high-resolution reconstructions and reliable chronologies. These factors, combined with the climatic links with vegetation growth rate and lake level, make tree-ring records suitable for comparison with the annually-laminated Nar sediment record. The palaeo-records from Nar were compared with Akkemik and Aras's (2005) 305-year April-August precipitation reconstruction from the upper and northern part of the Western Taurus Mountains in south-central Turkey (~190 km from Nar Gölü) (Figures 8.18 and 8.19). This region was expected to experience a similar climate regime to that of Cappadocia.

Akkemik and Aras's (2005) tree-ring record was correlated with the aridity index calculated for central Anatolia ($r=0.361$, $p=0.007$), Nar DI-conductivity ($r=-0.412$, $p=0.000$) and oxygen isotopes ($r=-0.840$, $p=0.000$) for the period AD 1927-2001/2006.

Therefore higher tree-ring-inferred precipitation relates to periods of lower aridity. The particularly strong relationship with the isotopes implies that both proxies are greatly influenced by regional water balance. The NAR06 DI-conductivity and tree-ring records show a pattern of increased precipitation corresponding with decreased lake water salinity between AD 1950 and 1986 (Figure 8.18). This trend is also evident in more negative oxygen isotopes since 1960.

Nar isotopes and the tree-rings also revealed a simultaneous shift to lower moisture availability ~1987/1988. Additionally, the two lowest periods in tree-ring-inferred precipitation (AD 1696 and 1890) may corresponded with the two episodes of highest NAR01/02 DI-conductivity and temperature during this period (~AD 1700 and 1880) (Figure 8.19). At AD 1880 there was also a peak in the NAR01/02 C:N ratio, DI-total phosphorus (Chapter 5: Figures 5.16 and 5.27) and high-nutrient favouring *N. paleacea* disappeared from the record. These trends indicate low nutrient levels in the Nar catchment at this time. Correspondence between the Nar palaeo-records and tree-ring-inferred precipitation implies that the Nar lake system relates to regional hydrology.

8.9.3 Central Anatolian historical climate records

Documentary evidence of historical events has been utilised to study past climate trends in Turkey. Touchan *et al.* (2007) identified that extreme phases in a tree-ring-precipitation reconstruction from south-central Turkey coincided with historical events in the region. Based on documentary evidence, Kuniholm (1990) described the late 16th and early 17th centuries in Anatolia as unstable climatically, politically and socially. This was partly attributed to cumulative drought during this period. This coincided with the agricultural crisis identified in the Nar pollen record between 1500-1700, which

corresponded with higher Nar DI-conductivity, temperature and lower tree-ring inferred precipitation (~AD 1700 in Akkemik and Aras's (2005) record: Figure 8.19).

Documentary records indicate that drought events were accompanied by famine and increased fire frequency in central Anatolia. The effects of such episodes were highlighted by Kuniholm (1990), who discussed the extreme drought in the Ankara province between AD 1873-1874, which resulted in the death of 81% of the cattle, 97% of the sheep and 20,000 people out of a population of 52,000 and caused extensive migration. This event coincided with an upward trend in Nar DI-conductivity and temperature (Figure 8.19). Therefore documentary records can provide validation for the use of palaeolimnological analysis to infer palaeoclimate. It appears that extreme climatic events with consequences for human society may have been recorded in the sediments of Nar Gölü.

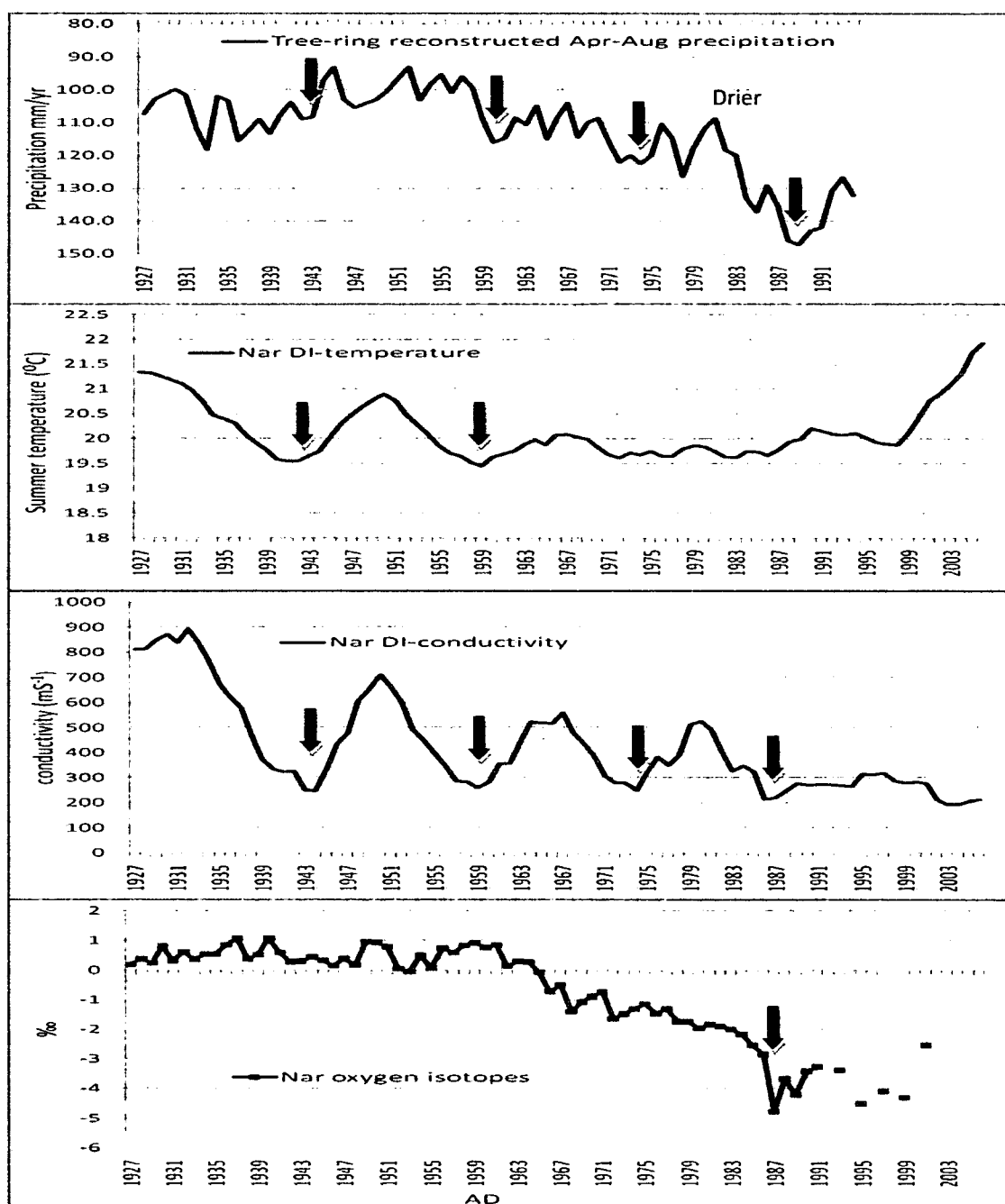


Figure 8.18 Tree-ring-inferred precipitation (axis reversed) (Akkemik and Aras, 2005) plotted with NAR06 DI-conductivity, temperature and NAR01/02 oxygen isotopes for the period AD 1927-2006. Data smoothed using 8 year running average to match residence time of Nar (isotopes naturally smoothed). Arrows highlight corresponding climatic episodes between the records.

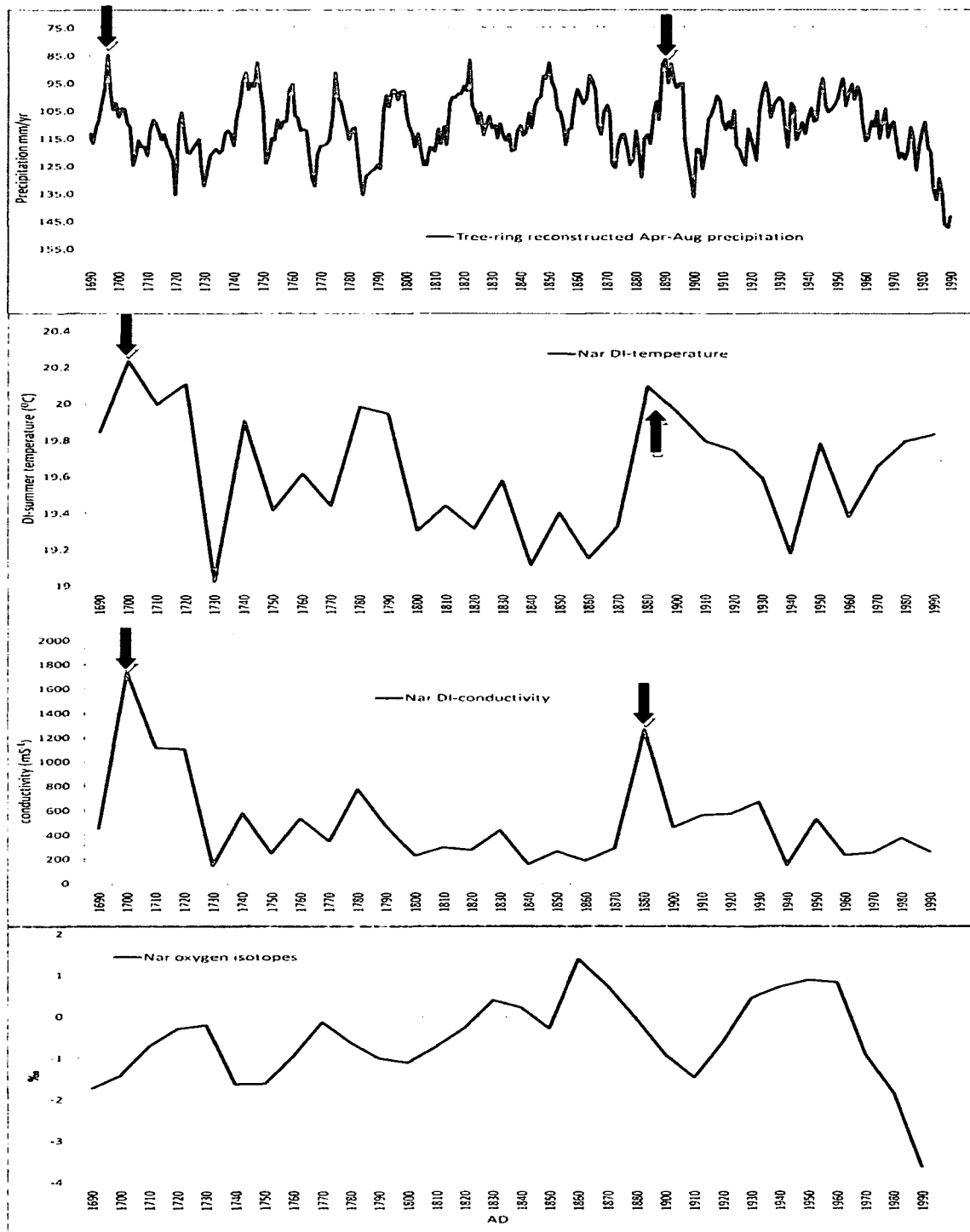


Figure 8.19 Tree-ring-inferred precipitation (axis reversed) (Akkemik and Aras, 2005) plotted with NAR01/02 DI-conductivity, temperature and oxygen isotopes for the period AD 1690-1990. Arrows highlight corresponding climatic episodes between the records.

8.9.4 Comparisons with other DI-conductivity records

Atmospheric circulation patterns that affect the climate of the EM also influence trends in other global regions. Diatoms have been utilised as a climate proxy in various locations, allowing methodological comparisons with Nar. Shifts in pressure distribution and circulation patterns are likely to have dissimilar impacts on different global regions. The Nar DI-conductivity sequence can be compared with similar records from different continents in order to analyse temporal and spatial trends in inferred palaeoclimate.

Drought frequency and intensity was reconstructed at high-resolution by Laird *et al.* (1996; 1998) and Fritz *et al.* (1999) from Moon Lake in the Northern Great Plains (USA) for the last 2300 years based on lake DI-conductivity (Figure 8.20) (Laird *et al.*, 2008). This sub-decadal record has many methodological similarities to the diatom sequence from Nar Gölü. For example, both lakes are hydrologically-closed systems and located in continental drought-prone regions with climatic regimes linked to North Atlantic Oscillation. In the Great Plains, extreme droughts were identified in higher frequency prior to AD 1200, with pronounced dry episodes between AD 200-370, 700-850 and 1000-1200, during the MCA. Laird *et al.* (1996) suggested that the atmospheric anomalies that result in drought today were more frequent and persistent in the past. The DI-conductivity records from Moon Lake and Nar Gölü revealed that North America and the EM experienced more extreme droughts in the past in relation to the climate of the last ~800 years. This may be associated with changes in atmospheric circulation patterns that affect both continents.

Verschuren *et al.* (2000) used diatoms and multiproxy analyses of Lake Naivasha to analyse rainfall and drought frequency in equatorial East Africa during the past 1100 years (Figure 8.20). A drier climate was identified during the MCA (AD 1000-1270) and a wetter climate was evident during the LIA (AD 1270-1850) with three interruptions. As in the Nar and Moon Lake records, greater intensity droughts were identified in the past with a generally more arid climate prior to ~AD 1300. The Nar sequence indicates a shift to generally wetter conditions ~AD 1450. However, this shift is not significant when compared with the arid period prior to AD 540. This may relate to more local drought variability.

Barker *et al.* (1994) identified significant periods of lake water level regression during the mid-late Holocene in a diatom-inferred lake level reconstruction from North Africa (Middle Atlas Mountains, Morocco). An abrupt period of water level regression was recognised at ~1800 BP (~AD 200). This may coincide with the period of maximum aridity in the Nar record prior to AD 540. Russell *et al.* (2007) recognised that the timing of drought episodes from other regions of Africa did not follow the trend identified by Verschuren *et al.* (2000) and highlighted that century-scale climate changes over the African continent have a strongly regional nature. This highlights that regional variability exists in the timing of climatic changes.

A DI-conductivity record for the last 1600 years was derived from the Aral Sea (central Asia) by Austin *et al.* (2007) using the combined salinity dataset from EDDI. This same training set was used to reconstruct Nar DI-conductivity. Three episodes of lake level regression were identified by Austin *et al.* (2007) at AD 300-440, 1195-1355 and 1780-2000. These episodes were attributed to changes in human activity, natural water

movements and climatic variability. The timing of the first dry event coincided with the period of greatly enhanced aridity indicated by diatoms and oxygen isotopes at Nar and the second period may coincide with generally drier climate in the DI-temperature record (Figure 8.15). The most recent dry episode in Austin *et al.*'s (2007) record was not reflected in the Nar sequence. However, isotopes do appear to have become increasingly positive since ~AD 1780. According to Austin *et al.* (2007), levels of the Dead Sea declined from ~AD 300 to as late as 450, which corresponded with regression of the Aral Sea. This period of higher aridity, indicated by lower water level of the Dead and Aral Seas, may correspond with the arid period revealed by diatoms and oxygen isotopes at Nar before AD 540. Therefore it appears that the climate patterns that affect Asia, Africa and North America also influence variability in central Anatolia. However, the timing and magnitude of events varies and shifts in circulation patterns may have dissimilar consequences for different global regions.

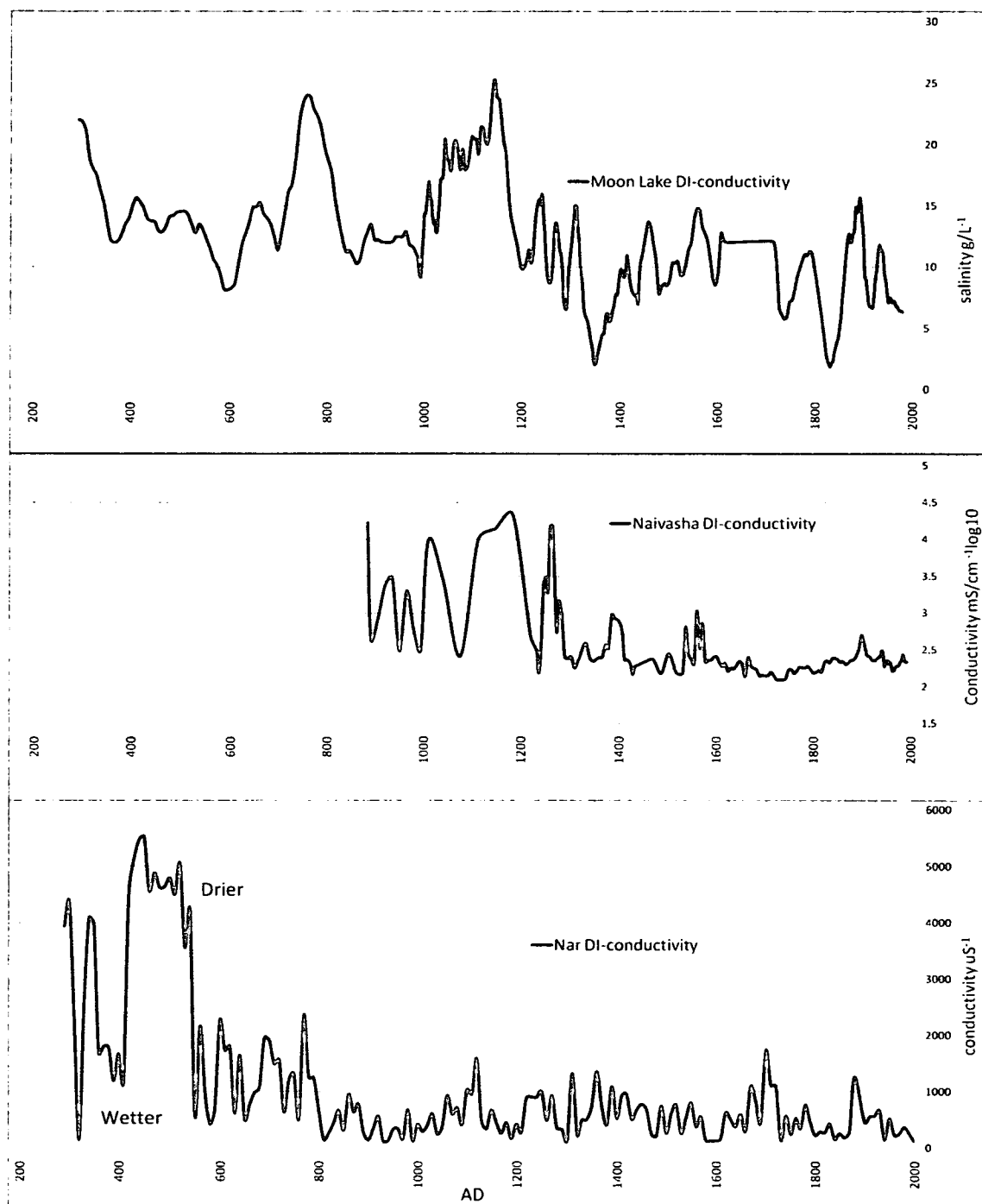


Figure 8.20 DI-conductivity from Moon Lake (USA) (Laird *et al.*, 1996) (AD 286-1980), Lake Naivasha (East Africa) (Verschuren *et al.*, 2000) (AD 883-1993) and Nar Gölü (AD 290-2000).

8.10 Summary

The EM has experienced drier/warmer and wetter/colder climatic episodes throughout the late Holocene. Palaeoenvironmental inferences based on the Kratergöl diatom record were limited by problems with the core chronology and the varied lake sedimentation rate. Therefore palaeoclimate interpretations have focused on the Nar Gölü record. Nar DI-conductivity is thought to provide a record of palae-aridity in central Anatolia. However, inferences based on the reconstruction were limited by poor analogue matching with the modern EDDI combined salinity training set. A combination of analysis methods including DI-temperature, based on the relationship between meteorological records and diatom DCA axes, and measurement of lamination sub-layer thickness using core thin sections has provided supplementary palaeoenvironmental information. Further palaeoclimatic inferences were based on diatom concentration, biovolume and species ecology. Absolute values of the DI-conductivity and temperature reconstructions were limited by statistical issues. Therefore a multiproxy approach, employing palaeo-evaporation oxygen isotope and human land use pollen indicators has allowed a clearer record of palaeoclimate to be constructed through identifying consistent trends and general patterns between datasets.

It appears that winter teleconnections with the NAOI and NCPI have greatest influence on the Nar diatom record and are important drivers of EM climate. Summer teleconnections did not show a clear relationship with the Nar diatoms. However, oxygen isotopes were identified as significantly influenced by tropical teleconnections, such as the Indian Monsoon. Winter teleconnections (the NAO and NCP) may have a more pronounced influence on the Nar diatom assemblage due to the link with groundwater availability during following months, which may alter lake water salinity

and nutrient levels. Drought episodes in central Anatolia appear to be associated with more positive NAOI, negative NCPI, enhanced Indian Monsoon and increased ENSO events. These climate features may have been more pronounced in the past during prolonged dry periods.

Throughout the last 1720 years, the Nar DI-conductivity and temperature records revealed maximum aridity between AD 310-540 and a shift to a wetter/cooler climate at AD 540 and 800. This was followed by a change to lower aridity with numerous less extreme wetter/drier episodes throughout the last 1200 years. The latter part of the record was dominated by mono-specific diatom bloom events identified in core thin sections, which are important drivers of assemblage change. Nar diatoms and oxygen isotopes provided a similar record of environmental change in the early part of the record. The Nar pollen sequence relates to human activity and does not show clear relationships with other proxies. However, the pollen record revealed that human land use may have had increasing impacts on the diatom record throughout the latter part of the sequence.

Comparisons between the Nar record and NH temperature reconstructions revealed that the timing of the MCA and LIA climatic events were regionally variable and, according to the oxygen isotope record, Turkey may have experienced opposite to average NH climate over the last 2000 years. This corresponds with the 'see-saw' pattern of precipitation distribution recognised in various studies between the west and east Mediterranean. Alternatively, the DI-temperature reconstruction over the last 1000 years could be interpreted as relating to the MCA between ~AD 1000-1500 and the LIA

between ~AD 1600 and 2000. However, these episodes are not significant in relation to the arid period prior to AD 540.

Comparisons with central Anatolian tree-ring-inferred precipitation revealed similarities with Nar DI-temperature, conductivity and oxygen isotopes in the timing of drought events and changes in aridity. Similarities were also identified in the timing of drought periods in sediments from Nar and a study based on north Anatolian lakes. Lower levels of the Dead and Aral Seas may correspond with the arid period prior to AD 540 in the Nar record. DI-conductivity records from East Africa, North America, Asia and Turkey, including Nar, have revealed that prolonged, extreme droughts were a more typical climate feature of the past and may be associated with shifts in atmospheric circulation patterns. The timing and magnitude of shifts between arid and wetter periods varies between different global locations.

Nar Gölü appears to have altered through time from a lake that is primarily driven by changes in climate, illustrated by the link between DI-conductivity and oxygen isotopes in the early part of the record, to a system dominated by high-nutrient-favouring diatom bloom species influenced by other factors. This is likely to be associated with human land use evident through the Nar pollen record. The Nar record has provided detailed evidence of palaeoenvironmental change and implies that central Anatolia has a variable late Holocene climatic history.

Chapter 9

Conclusion

9.0 Introduction

This research project aimed to reconstruct Eastern Mediterranean (EM) late-Holocene climate variability at high-resolution. The EM was identified as an area that is particularly sensitive to climatic fluctuations, due to the impacts of limited water resources upon past and present societies and the fact that EM drought intensity is predicted to increase in the future (Allali *et al.*, 2007). Diatom fossils preserved within lake sediments were identified as a suitable proxy to reconstruct palaeoclimate. This is due to the globally recognised relationship between diatom community structure and climate-related limnological variables, such as salinity.

Nar Gölü and Kratergöl located in central Anatolia provided well preserved diatom assemblages within their late Holocene lake sediment archives and are thought to have hydrological regimes that relate to the balance between precipitation and evaporation. Nar Gölü was identified as a particularly appropriate site from which to conduct high-resolution palaeoclimatic research, due to the presence of annually-laminated lake sediments. The modern diatom community and temporal changes in the species assemblage throughout the last 1720 years were investigated. The application of an existing transfer function from the European Diatom Database (EDDI) to the diatom data allowed a record of palaeoconductivity to be derived, from which palaeoclimatic inferences could be made. A combination of numerical analyses, including core thin section sub-layer measurements, calculation of diatom concentration, biovolume, species diversity and the use of DCA (Detrended Correspondence Analysis) axes to

reconstruct pre-instrumental temperature were employed. The annually-laminated nature of the lake sediment archives used in this study permitted opportunities to explore different laboratory and numerical analyses. This allowed additional palaeoenvironmental information to be extracted from the diatom population. Consequently, the hypothesis: *Lake diatoms provide sensitive indicators of climate and water resource variability in the Eastern Mediterranean region* (Chapter 1: Section 1.3) can be accepted. An oxygen isotope (Jones, 2004; Jones *et al.*, 2005; 2006) and pollen record (England, 2006; England *et al.*, 2008) from the same sediment sequence provided supplementary palaeoenvironmental information and a number of palaeoclimate inferences were drawn.

9.1 Diatom-inferred environmental change

9.1.1 Modern environment

Analysis of the modern diatom assemblages through sediment trap and lake habitat sampling revealed that the palaeo-diatom population was well represented in the contemporary environment and that frustule dissolution is not an issue at Nar or Kratergöl. Diatom taxa inhabiting these systems have previously been identified as indicators of lake water salinity variability (Appendix 6.2). Additionally, a number of species were identified in the modern environment of Nar that are typically indicators of high nutrient conditions. Therefore it is likely that the diatom relationship with climate may not be straightforward and human activity in the catchment may have affected the system. Core thin sections revealed that diatom bloom events involving extremely high abundance of *N. paleacea* and *S. acus* frequently occur at Nar, particularly during spring, early summer and autumn. Further investigation, such as sub-annual lake monitoring, is required to fully understand the precursors for and significance of Nar

diatom blooms. A previously undescribed centric diatom taxon (*Clipeoparvus anaticus*) of non-planktonic life-form was also identified in the modern environment of Nar Gölü and was highly abundant at various stages in the palaeo-record (Appendix 9).

9.1.2 Diatom assemblage analysis methods

Numerical methods employed for the palaeoenvironmental analyses of the Nar sediments were made possible by the presence of annually-laminated varves, which allowed calibration with meteorological data and core thin section examination of sub-annual lake processes. The Nar diatom palaeo-record was used to infer lake conductivity throughout the last 1720 years and the Kratergöl record for part of the 20th century. This was limited by poor modern analogue matching with Nar diatom taxa, the applicability of the training set lakes to the study sites and the differences between instrumentally measured and diatom-inferred (DI) conductivity. Consequently, a number of additional analysis techniques were explored. Figure 9.1 includes a modified version of the diatom analysis-climate reconstruction diagram presented in Chapter 1 (Figure 1.4) based on the additional numerical analyses explored in this study.

The diatom numerical analysis methods employed have different strengths and weaknesses. For example, DI-temperature, based on DCA axes, is limited by the fact that the calibration period is not reflective of variability in the pre-instrumental period. DI-environmental change, DCA axes, diatom concentration, biovolume and species diversity were closely related to the fluctuating abundance of dominant bloom species *N. paleacea*. Therefore palaeo-environmental information based on other species may have been masked by this taxon. A multi-proxy approach, involving comparisons of the

diatom data with an oxygen isotope and pollen record from the same sequence permitted a clearer picture of palaeoenvironmental and climatic change.

The discovery of the new diatom genus (*C. anatolicus*) within the modern and palaeoenvironments of Nar presented opportunity to formally describe this taxon and contribute to knowledge of diatom species diversity. However, this also presented problems, as this species was not included in the EDDI modern diatom-salinity training set and its ecological preferences are not well known. Therefore interpretations of periods of the record where this taxon was prolific were limited.

Core thin section analysis revealed the sequence of events and processes involved in varve formation at Nar. Diatom bloom species were identified as distinct layers, which represent sub-seasonal changes in lake conditions. Bloom species drove reconstructed DI-conductivity values down and greatly influenced all numerical analyses. Therefore DCA and conductivity reconstructions were also performed on non-bloom species only. However, when bloom species were removed, valve counts became very low for many samples and numerical analyses were consequently not always reliable. Additionally, calibration with meteorological records permitted identification of variables, such as summer temperature, which have greatest affects on the diatom population.

Kratergöl diatoms were well preserved and species were adequately represented in the modern environment. Additionally, the assemblage was well matched with the EDDI combined salinity training set. Therefore this lake had the potential to provide an interesting record of palaeoclimate. However, due to chronological problems, palaeoclimate interpretations from the Kratergöl sediment record were limited. The fact

that measured and DI-conductivity at this site differed considerably also made climatic inferences problematic.

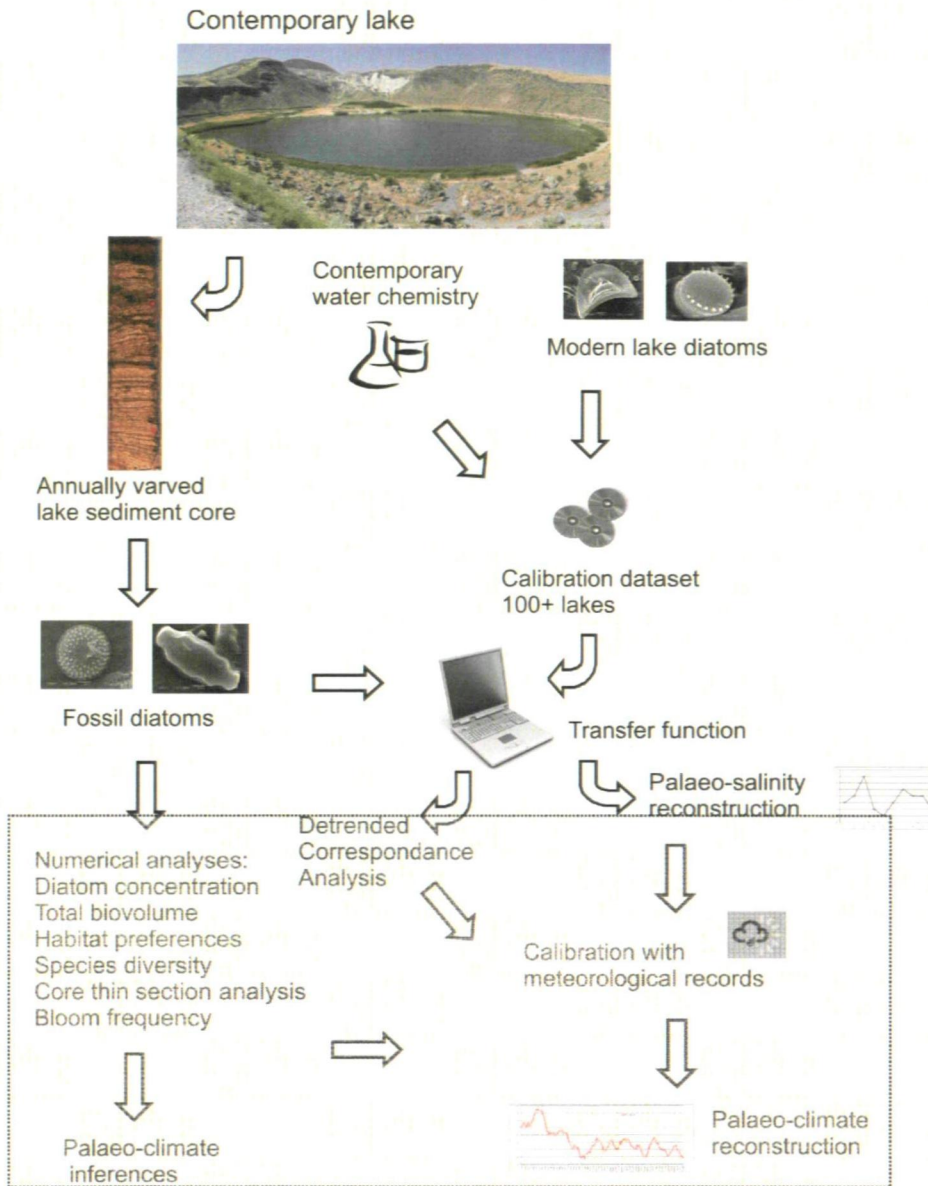


Figure 9.1 The processes involved in palaeoclimate reconstruction from lake diatoms (adapted from Hall and Smol, 1999). Additional diatom analysis methods employed in this research project are highlighted in the shaded box.

9.2 Late Holocene climate reconstruction

The diatom records revealed that the water chemistry of Nar Gölü fluctuated throughout the last 1720 years. Analyses of the Nar sediment profile revealed a number of consistent events between the different proxy records, which are summarised in Table 9.1.

9.2.1 Palaeoclimate inferences

Multi-proxy analyses revealed that Nar sediments provide evidence of palaeoclimatic variability and changes in human land use in central Anatolia throughout the last 1720 years. Analysis of the relationship between the NAR06 diatom record and central Anatolia meteorological data revealed that summer temperature is the main factor driving change in the diatom population. This is associated with the diatom relationship with lake water salinity and the impacts of summer evaporation on the hydrological status of the lake. Other diatom assemblage data and meteorological factors, such as autumn precipitation and *S. acus* percentage, were significantly correlated. However, many of the relationships were not 'strong' and the diatom community is probably influenced by a combination of climatic and non-climatic factors.

DI-temperature, conductivity, species ecology and the oxygen isotope record all indicated a major dry period prior to AD 540 (Table 9.1), followed by an apparent abrupt shift to a fresher lake system and wetter climate. Therefore the hypothesis:

Diatom-inferred climate variability during the late Holocene has significantly exceeded the range recorded during the period of instrumental observations (i.e. last century)

(Chapter 1: Section 1.3) can be accepted. The major climatic change indicated by the diatoms and isotopes at AD 540 was not reflected in the Nar pollen record. This may be

associated with the drought-tolerant EM vegetation and the ability of human inhabitants to adapt to dry climatic periods (Rosen and Rosen, 2001). After AD 800, the palaeoclimate signal from the diatoms and oxygen isotopes diverged. Oxygen isotopes indicated opposite to typical Northern Hemisphere (NH) climate trends throughout the last 1000 years, possibly due to the oscillating 'see-saw' pattern of precipitation distribution recognised between the western and eastern Mediterranean basin (Oldfield and Thompson, 2004). However, DI-temperature appeared to correspond with the timing of the Medieval Climatic Anomaly (MCA) and Little Ice Age (LIA) in the NH and revealed typical trends of these periods, i.e. warmer climate between ~AD 1000-1450 and cooler conditions between ~AD 1450-2000. However, these inferences were limited due to the limitations of the DI-temperature reconstruction.

Increasing isotope-inferred aridity since AD 1400 was not reflected in the diatom record. Diatom species associated with nutrient enrichment and bloom events increased during the most recent ~1000 years (e.g. *N. paleacea* and *S. acus*), especially since AD 1500. This may be associated with increasing human activity and land use in the Nar catchment. Core thin sections also indicated increased varve thickness since AD 1840, possibly relating to warmer temperatures. The recent assemblage shift in the diatom record at AD 2001 (NAR06) appears to represent a response to recent environmental variability. This period, however, is not covered in the oxygen isotope and pollen records, which only include the period prior to AD 2001 (NAR01/02).

Although the Kratergöl core (ACM99) chronology was unreliable, variability through the record is related to temporal changes in the lake environment. DI-conductivity indicated a less arid climate in the earlier part of the record, followed by a shift to more

arid conditions, and a subsequent return to a wetter climate in the most recent sediment. However, as the core was collected in 1999, this record did not reflect the most recent environmental change. Calculation of diatom concentration and biovolume highlighted the varied lake sedimentation rate, with decreased values during the deposition of high sand and low organic content material. Lake level recordings taken in 1999 and 2008 indicated that water depth has decreased throughout the past decade. This may be associated with warmer temperatures and decreased rainfall throughout this time period or groundwater level lowering as a result of irrigation. Further investigation is required to evaluate whether recent lake level lowering has initiated a diatom response.

Comparisons between Nar and other lake diatom records from the EM were limited due to the absence of high-resolution research covering the last 2000 years in this region. However, numerous records of lower resolution, based on longer time scales, indicate that climatic aridity increased throughout the late Holocene. Tree ring-inferred precipitation from south-central Turkey showed similarities with the Nar record. For example, two dry events indicated by tree-rings at AD 1696 and 1890, appear to correspond with highest Nar DI-conductivity and temperature during this period (AD 1700 and 1880). Additionally, the historically documented drought of the late 16th and early 17th centuries corresponded with the agricultural crisis in the Nar pollen record and increased diatom, oxygen isotope and tree-ring inferred aridity. Comparisons of the Nar sequence with DI-conductivity reconstructions from North America, East Africa and Asia revealed that prolonged droughts appear to have been a more typical climate feature of the period prior to ~800 BP and that the timing and duration of climatic shifts was not consistent between different locations.

Nar diatom zone	Diatoms	Oxygen isotopes (Jones <i>et al.</i> , 2005; 2006)	Pollen (England <i>et al.</i> , 2008)	Other proxy records
<p>ND1</p> <p>AD 1480-2000</p> <p>a, b, c, d</p> <p>AD 1927-2006</p>	<p>Shift at AD 2001 to dominance of non-planktonic <i>C. anatolicus</i> and low-salinity indicator <i>S. acus</i>. Increasing dominance of <i>A. minutissimum</i> and diatom bloom species. Increased diatom concentration and varve thickness possibly related to warmer temperature during the most recent ~400 years. Shorter duration and lower magnitude wetter/drier episodes. DI-temperature indicates possible LIA between ~AD 1600-2000. Possible drought period evident in DI-temperature and conductivity ~AD 1880.</p>	<p>Increasing moisture availability since the 1960s and a shift to higher aridity at AD 1987/88. Shift to more positive isotopes (increased aridity) between AD 1400-1980. Opposite to typical NH LIA climate.</p>	<p>Recent agricultural intensification (AD 1830-present). Decreased agricultural pollen indicators between ~AD 1500-1700 indicating an agricultural crisis.</p>	<p>Tree-ring-inferred precipitation (Akkemik and Aras, 2005) corresponded with isotopes, indicating increasing rain since the 1960s and a decrease at 1987/88. Drought evident in tree-ring record ~AD 1700. Agricultural crisis evident in documentary records ~AD 1700 and 1870/80 (Kuniholm, 1990).</p>
<p>ND2</p> <p>AD 990-1470</p>	<p>Appearance of mono-specific diatom blooms of <i>N. paleacea</i> and <i>S. acus</i> in core thin sections. DI-temperature indicates possible MCA between ~AD 1000-1500. Abrupt change to elevated values of <i>S. parvus</i> (AD 1205-1246).</p>	<p>Decreased isotopes between ~AD 900-1400 (less arid). Opposite to typical NH MCA climate.</p>	<p>Cereal-based agriculture and pastoralism (AD 950-1830). Abrupt change to elevated values of a chlorophyte algal species between AD 999-1001.</p>	<p>Drought period evident in north Anatolian lakes between AD 1200-1470 (Kazancı, 2005).</p>
<p>ND3</p> <p>AD 550-980</p>	<p>Further decrease in DI-conductivity and temperature (aridity) ~AD 780. Dominance of low-salinity indicator diatoms and new taxon (<i>C. anatolicus</i>). Shift to increased water availability at AD 540-550.</p>	<p>Return to more positive isotopes at AD 700-800 (drier climate). Shift to lower aridity at AD 540-550.</p>	<p>Agricultural abandonment between AD 670-950. Decreased olive tree pollen from ~AD 700 possibly associated with colder climate.</p>	<p>DI-conductivity records from North America (Laird <i>et al.</i>, 1996) and East Africa (Verschuren <i>et al.</i>, 2000) indicate increased frequency and duration of droughts prior to ~AD 1200.</p>
<p>ND4</p> <p>AD 290-540</p>	<p>Period of maximum aridity in DI-conductivity and DI-temperature records. Dominance of high-salinity indicator diatom species.</p>	<p>More positive isotopes indicating period of maximum aridity.</p>	<p>Abundant cereals and tree crops (AD 290-670). Higher abundance of olive tree pollen.</p>	<p>Drought period in north Anatolian lakes between AD 400-700 (Kazancı, 2005).</p>

Table 9.1 Summary of palaeoclimate inferences from the Nar palaeo-record based on diatoms, oxygen isotopes and pollen with other proxy and documentary records.

9.2.2 Factors controlling EM climate

Various atmospheric circulation patterns have been identified as exerting influence on the climate of central Anatolia. Winter teleconnections (the North Atlantic Oscillation and the North Sea-Caspian Pattern) appeared to have greater influence of the Nar diatom assemblage in comparison with teleconnections (the Indian Monsoon and El Niño Southern Oscillation) associated with summer drought. This possibly relates to the effect of October-March rainfall on cumulative moisture availability at Nar. By contrast, the Nar oxygen isotope record was related to summer teleconnections, particularly the Indian Monsoon (Jones *et al.*, 2006). Therefore the climate of central Anatolia is likely to be influenced by a combination of atmospheric circulation patterns. Recent EM climate trends have involved increased temperatures and decreased precipitation. Drought periods in central Anatolia and the EM have previously been associated with more positive NAO, negative NCP, enhanced Indian Monsoon and increased ENSO events. Understanding how these atmospheric circulation patterns influence EM climate variability is important for recognising precursors of future drought events.

9.3 Suitability of sites and methodology

Nar Gölü and Kratergöl are closed-basin lakes located in a semi-arid region. The Nar sediment sequence was annually-laminated and stratigraphically constant, whereas the sedimentology of Kratergöl was variable and problems were encountered when attempting to date the core profile. The Nar sequence provided a highly-resolved record of the last 1720 years while Kratergöl is thought to include only the mid-late 20th century. Analysis of these two sites has highlighted the advantages of laminated sediments and the limitations of reconstructing climate using lakes with varied

sedimentation rate. As a result of this, it was not possible to reliably compare the records from the two sites.

When addressing the suitability of the sites and methods, issues of representation require consideration. Numerous stratigraphically consistent cores collected from Nar between 1999 and 2006 ensured that the lake core sequence was representative of the basin. Only one core section was analysed from Kratergöl, which may not have been representative of the lake basin. Therefore Nar provided a more coherent record of palaeoclimate. However, the Nar sequence may not necessarily always be representative of the climate of central Turkey. Events specific to the Nar catchment may have influenced the lake sediment palaeo-record. This was explored through comparisons of the Nar record with other palaeoclimate reconstructions.

Interpretation of temporal changes in the Nar diatom community for the pre-instrumental climate period required a number of assumptions. For example, the same relationships between the lake system, diatom assemblage and climatic variables were presumed to have existed in the past. Variability in these relationships can reduce the reliability of palaeoclimatic inferences. Diatom-conductivity and salinity-climate relationships may not be straightforward at Nar and require further investigation through modern lake monitoring.

Exploration of different numerical techniques provided novel methods to interpret temporal diatom assemblage change. DI-conductivity was reconstructed without accounting for all Nar species due to poor analogue matching with the EDDI training set. This was particularly an issue during periods of the record dominated by the new

taxon (*C. anatolicus*). DCA axes summarised diatom assemblage change through time. Regression analysis between the DCA axes and instrumental temperature permitted a climate reconstruction based on all species.

Furthermore, calculation of diatom concentration, biovolume, species diversity and evaluation of taxa ecological preferences provided supplementary palaeoenvironmental information. Comparisons with other proxy records relating to climate variability and human land use revealed some dissimilar trends and allowed validation of consistent climatic inferences. This project has shown that the relationships between diatom assemblages and environmental change are not straightforward and highlighted the benefits of multiproxy analyses for identifying consistent or contrasting palaeoenvironmental trends.

9.4 Further work

This research has highlighted that annually varved lake sediments offer an excellent resource for palaeoenvironmental research. The lack of high-resolution palaeoclimatic records covering the last 2000 years in the EM emphasises that further work is required focusing on this time scale, in order to analyse whether the sequence from Nar is typical of the region. Sub-decadal monitoring of Nar diatom, water chemistry and lake level change is required to understand the hydrological and species relationships with salinity. Additionally, this would allow the precursors for diatom bloom events to be identified and information regarding what such episodes imply about palaeoclimate to be derived. Furthermore, potential exists to increase the length of the palaeo-record and analyse whether prolonged drought periods were also a typical climatic feature during earlier periods of the Holocene in central Anatolia. Replicate core sections are required from

Kratergöl in order to evaluate whether the ACM99 section is reflective of the basin, derive a more reliable chronology and extend the record further back in time.

Diatom assemblage data are information-rich, as individual species are prolific during different seasons and have dissimilar relationships with a range of limnological variables. Sub-annual lake monitoring would allow species life-cycles to be explored and aid detailed interpretation of palaeoecological data. Additionally, there is potential to evaluate temporal changes in non-diatom algae through pigment analyses and derive a palaeoclimate signal. The oxygen isotope signal recorded in diatom frustules could also provide further information on palaeoevaporation. Further analyses of Nar sediments could involve counting bloom and non-bloom taxa separately, in order to perform reliable DCA and DI-conductivity reconstructions based on species with different life forms.

The conductivity reconstruction was limited by poor analogue matching and dissimilarities between lake types in the combined salinity EDDI training set and Nar and Kratergöl. There is potential to apply a diatom-salinity training set based on Turkish lakes (work in progress, Reed, *pers. com.*) to the diatom record and more reliably reconstruct palaeo-conductivity. Calculation of diatom biovolume gave extra weighting to larger species and revealed additional information about assemblage change.

Therefore there is also potential to design a training set based on diatom biovolume. Conductivity or total phosphate reconstructions would thus reflect diatom productivity rather than fecundity. Core thin section analysis provided a novel technique to explore the diatom population *in situ*. This method could be further explored; for example, through detailed analysis of the diatom population and identification of other material,

such as plant and algal remains. These opportunities for further research highlight that the laminated lake sediments of Nar Gölü have provided a useful resource for understanding EM palaeoclimate.

References

- Abril, J. M. (2004) Constraints on the use of ^{137}Cs as a time-marker to support CRS and SIT chronologies. *Environmental Pollution*. 129, 31–37.
- Akgün, F., Kayseri, M.S. and Akkiraz, M.S. (2007) Palaeoclimatic evolution and vegetational changes during the Late Oligocene-Miocene period in the Western and Central Anatolia (Turkey). *Palaeogeography, Palaeoclimatology, Palaeoecology*. 253, 56-106.
- Akkemik, Ü. and Aras, A. (2005) Reconstruction (AD 1689-1994) of April-August precipitation in the southern part of central Turkey. *International Journal of Climatology*. 25, 537-548. NAOO Satellite and Information Service, National Climate Data Centre US Dept. of Commerce. [Online: <http://www.ncdc.noaa.gov/paleo/metadata/noaa-tree-2660.html>]. Accessed: 10/08/2008.
- Akkemik, Ü., Dagdeviren, N. and Aras, A. (2005) A preliminary reconstruction (AD 1635-2000) of spring precipitation using oak-tree rings in the western Black Sea region of Turkey. *International Journal of Biometeorology*. 49, 297.
- Allali, A., Bojariu, R., Diaz, S., Elgizouli, I., Griggs, D., Hawkins, D., Hohmeyer, O., Pateh Jallow, B., Kajfež-Bogataj, L., Leary, N., Lee, H. and Wratt, D. (Eds) (2007) *Intergovernmental Panel on Climate Change IPCC Fourth Assessment*

- Report: Climate Change Synthesis*. [Online: http://www.ipcc.ch/pdf/assessment-report/ar4/syr/ar4_syr.pdf]. Accessed: 03/04/08.
- Alpert, P., Price, C., Krichak, S.O., Ziv, B., Saaroni, H., Osetinsky, I., Barkan, J. and Kishcha, P. (2005) Tropical tele-connections to the Mediterranean climate and weather. *Advances in Geosciences*. 2, 157-160.
- Anderson, N.J. (1995) Using the past to predict the future: lake sediments and the modelling of limnological disturbances. *Ecological Modelling*. 78, 149-172.
- Appleby, P.G. (2001) Ch. 9: Chronostratigraphic techniques in recent sediments. In: Last, M. and Smol, J.P. (Eds) *Tracking Environmental Change Using Lake Sediments. Vol 1: Basin Analysis, Coring and Chronological Techniques*. Kluwer Academic Publishers: Netherlands. 171-203.
- Austin, P., Mackay, A., Palagushkina, O. and Leng, M. (2007) A high-resolution diatom-inferred palaeoconductivity and lake level record of the Aral Sea for the last 1600 years. *Quaternary Research*. 67, 383-393.
- Baier, J., Lucke, A., Negendank, J.F.W., Schleser, G.H. and Zolitschka, B. (2004) Diatom and geochemical evidence of mid-to-late Holocene climatic changes at Lake Holzmaar, West-Eifel (Germany). *Quaternary International*. 113, 81-96.
- Baker, A., Eastwood, W., Fairchild, I., Jex, C. and Leng, M. (2008) Conference abstract: Calibrating speleothems ^{18}O against instrumental climate data. *ESF MedCLIVAR workshop, Piza, Italy*. [Online:

<http://www.geog.plymouth.ac.uk/research/groups/SpeakerAbstracts.pdf>].

Accessed: 13/01/09.

- Barber, H.G. and Haworth, E.Y. (1994) *A Guide to the Morphology of the Diatom Frustule: with a Key to the British Freshwater Genera*. Freshwater Biological Association: UK.
- Barker, P.A. (1992) Differential diatom dissolution in Late Quaternary sediments from Lake Manyara, Tanzania: an experimental approach. *Journal of Paleolimnology*. 7, 235-251.
- Barker, P.A., Gasse, F., Roberts, N. and Taieb, M. (1991) Taphonomy and diagenesis in diatom assemblages; a Late Pleistocene palaeoecological study from Lake Magadi, Kenya. *Hydrobiologia*. 214, 267-272.
- Barker, P.A., Roberts, N., Lamb, H.F., van der Kaars, S. and Benkaddour, A. (1994) Interpretation of lake-level change from diatom life form in Lake Sidi Ali, Morocco. *Journal of Palaeolimnology*. 12, 223-234.
- Barker, P.A., Williamson, D., Gasse, F. and Gilbert, E. (2003) Climatic and volcanic forcing revealed in a 50,000-year diatom record from Lake Massoko, Tanzania. *Quaternary Research*. 60, 368-376.
- Barker, P.A., Pates, J.M., Payne, R.J. and Healey, R.M. (2005) Changing nutrient levels in Grasmere, English Lake District, during recent centuries. *Freshwater Biology*. 50, 1971-1981.

- Barker, P.A., Leng, M.J., Gasse, F. and Huang, Y. (2007) Century-to-millennial scale climatic variability in Lake Malawi revealed by isotope records. *Earth and Planetary Science Letters*. 261, 93-103.
- Bar-Matthews, M. Ayalon, A. and Kaufman, A. (1997) Late Quaternary palaeoclimate in the eastern Mediterranean region from stable isotope analysis of speleothems at Soreq Cave (Israel). *Quaternary Research*. 47, 155-168.
- Bar-Matthews, M., Ayalon, A., Kaufman, A. and Wasserburg, G.J. (1999) The eastern Mediterranean palaeoclimate as a reflection of regional events: Soreq Cave, Israel. *Earth and Planetary Science Letters*. 166, 85-95.
- Bar-Matthews, M., Gilmour, M., Ayalon, A., Vax, A., Kaufmann, A., Frumkin, A. and Hawkesworth, C. (2000) Variation of palaeoclimate in the eastern Mediterranean region – as derived from speleothems in various climate regimes in Israel. *Journal of Conference Abstracts*. Cambridge Publications: UK. 5, 194.
- Bar-Matthews, M. and Ayalon, A. (2004) Chpt. 18: Speleothems as palaeoclimate indicators, a case study from Soreq Cave located in the eastern Mediterranean region, Israel. In: Battarbee, R.W., Gasse, F. and Stickley, C.E. (Eds) *Past Climate Variability through Europe and Africa*. Springer: Netherlands. 363-391.
- Bartlein, P.J. and Whitlock, C. (1993) Palaeoclimate interpretation of the Elk Lake pollen record. In: Bradbury, J.P. and Dean W.E. (Eds) *Elk Lake Minnesota*:

Evidence for rapid climate change in the north-central United States. Geological Society of America: USA. 276, 275-293.

Battarbee, R.W. (1986) Diatom Analysis. In: Berglund, B.E. (Ed.) *Handbook of Holocene palaeoecology and palaeohydrology*. Wiley: Chichester. 527-570.

Battarbee R.W. (1991) Recent palaeolimnology and diatom-based environmental reconstruction. In: Shane, L.C.K. and Cushing, E.J. (Eds) *Quaternary Landscapes*. University of Minnesota Press: Minneapolis. 129-173.

Battarbee, R.W. (2000) Palaeolimnological approaches to climate change, with special regard to the biological record. *Quaternary Science Reviews*. 19, 107-124.

Battarbee, R.W., Jones, V.J., Flower, R.J., Cameron, N.G. and Bennion, H. (2001) Chapter 8: Diatoms. In: Smol, J. (Ed.) (2001) *Tracking Environmental Change Using Lake Sediments, Vol 3: Terrestrial, Algal and Siliceous Indicators*. Kluwer Academic Publishers: Netherlands. 155-202.

Battarbee, R.W., Gasse, F. and Stickley, C.E. (2004) *Past Climate Variability through Europe and Africa*. Springer: Netherlands.

Battarbee, R.W., Mackay, A.W., Jewson, D.H., Ryves, D.B. and Sturm, M. (2005) Differential dissolution of Lake Baikal diatoms: correction factors and implications for palaeoclimatic reconstruction. *Global and Planetary Change*. 46, 75-86.

- Bigler, C., Larocque, I., Peglar, S.M., Birks, H.J.B. and Hall, R.I. (2002) Quantitative multiproxy assessment of long-term patterns of Holocene environmental change from a small lake near Abisko, northern Sweden. *The Holocene*. 12, 481-496.
- Bigler, C. and Hall, R.I. (2003) Diatoms as quantitative indicators of July temperature: a validation attempt at century-scale with meteorological data from northern Sweden. *Palaeogeography, Palaeoclimatology, Palaeoecology*. 189, 147-160.
- Bigler, C., von Gunten, L., Lotter, A.F., Hausmann, S., Blass, A., Ohlendorf, C. and Sturm, M. (2007) Quantifying human-induced eutrophication in Swiss mountain lakes since AD 1800 using diatoms. *The Holocene*. 17, 1141-1154.
- Binney, H. (2004) *Human Impact on Lake Ecosystems and the role of Palaeolimnology*. [Online: <http://www.geog.ucl.ac.uk/ecrc/limpacs/outline.htm>] Accessed: 19/02/05.
- Birks, H.J.B. (1995) Ch 6: Quantitative palaeoenvironmental reconstructions. In: Maddy, D. and Brew, J.S. (Eds) *Statistical Modelling of Quaternary Science Data: Technical guide no. 5*. Quaternary Research Association: Cambridge. 161-254.
- Birks, H.J.B. (1998) Numerical tools in palaeolimnology: progress, potentialities and problems. *Journal of Palaeolimnology*. 20, 307-332.
- Blass, A., Bigler, C., Grosjean, M. and Sturm, M. (2007) Lake Silvaplana, Switzerland annual biogenic silica and temperature reconstruction. *IGBP PAGES/World Data*

- Centre for Palaeoclimatology, NOAA/NCDC Paleoclimatology Program. [Online: ftp://ftp.ncdc.noaa.gov/pub/data/paleo/paleolimnology/europe/switzerland/silvapla_na2007.txt]. Accessed: 10/08/2008.
- Blinn, D.W. and Bailey, P.C.E. (2001) Land use influence on stream water quality and diatom communities in Victoria, Australia: a response to secondary salinisation. *Hydrobiologia*. 466, 231-244.
- Bolle, H.J. (Ed.) (2003) *Mediterranean Climate: Variability and Trends*. Springer-Verlag: Germany.
- Bottema, S. (1995) The Younger Dryas in the Eastern Mediterranean. *Quaternary Science Reviews*. 14, 883-891.
- Bottema, S., Entjes-Nieborg, G. and van Zeist, W. (Eds) (1990) *Man's Role in the Shaping of the Eastern Mediterranean Landscape*. Balkema: Rotterdam.
- Bottema, S. and Woldring, H. (1990) Cht. 19: Anthropogenic indicators in the pollen record of the Eastern Mediterranean. In: Bottema, S., Entjes-Nieborg, G. and van Zeist, W. (Eds) *Man's Role in Shaping the Eastern Mediterranean Landscape*. Balkema: Netherlands. 231-264.
- Bottema, S. and Woldring, H. (1997) Late Quaternary vegetation and climate of southwestern Turkey: part II. In: Nüzhet, H., Kukla, G. and Weiss, H. (Eds) *NATO ASI Series: Third Millennium BC Climate Change and Old World Collapse*. Springer-Verlag: Berlin Heidelberg. 149, 489-515.

- Bradley, R.S. and Jones, P.D. (Eds) (1992) *Climate Since A.D. 1500*. Chapman and Hall: New York.
- Brönmark, C. and Hansson, L. (2005) *The Biology of Lakes and Ponds*. Oxford University Press: UK.
- Brüchmann, C. and Negendank, J.F.W. (2004) Indication of climatically induced natural eutrophication during the early Holocene period, based on annually laminated sediment from Lake Holzmaar, Germany. *Quaternary International*. 123-125, 117-134.
- Cameron, N.G. (1995) The representation of diatom communities by fossil assemblages in a small acid lake. *Journal of Palaeolimnology*. 14, 185-223.
- Cini Castagnoli, G., Bernasconi, S.M., Della Monica, P. and Taricco, C. (1999) 700 year record of the 11 year solar cycle by planktonic foraminifera of a shallow water Mediterranean core. *Advances in Space Research*. 24, 233-236.
- Cleve-Euler, A. (1922) Cited in: Battarbee, R.W., Jones, V.J., Flower, R.J., Cameron, N.G., Bennion, H., Carvalho, L. and Juggins, S. (2001) Cht. 8: Diatoms. In: Smol, J.P., Birks, H.J.B. and Last, W.M. (Eds) *Tracking Environmental Change Using Lake Sediments. Vol 3: Terrestrial, Algal and Siliceous Indicators*. Kluwer Academic Publishers: Netherlands. 155-202.

- Cohen, A.S. (2003) *Palaeolimnology: The History and Evolution of Lake Systems*.
Oxford University Press: UK.
- Cohen, R.H. and Erol, O. (1969) Aspects on the palaeogeography of central Anatolia.
The Geographical Journal. 135, 388-398.
- Connell, J.H. (1978) Diversity in tropical rainforests and coral reefs. *Science*. 199,
1302-1310.
- Cox, E.J. (1996). *Identification of Freshwater Diatoms from Live Material*. Chapman
and Hall: UK.
- Crawford, R.M. (1978) The taxonomy and classification of the diatom genus *Melosira*
C. A. Agardh. III *Melosira lineate* (Dillw.) C. A. Ag. and *M. varians* C. A. Ag.
Phycologia. 17, 237-250.
- Crawford, R.M. (1988) Reconsideration of *Melosira arenaria* and *M. teres*; resulting in
a proposed new genus *Ellerbeckia*. In: Round, F.E. *Algae and the Aquatic*
Environment. Biopress Ltd: Bristol. 413-433.
- Crutzen, P.J. and Stoermer, E.F. (2000) The 'Anthropocene'. *Global Change*
Newsletter. 41, 17-18.
- Cullen, H.M., Kaplan, A., Arkin, P.A. and Demenocal, P.B. (2002) Impact of the North
Atlantic Oscillation on Middle Eastern climate and stream flow. *Climate Change*.
55, 315-338.

- D'Arrigo, R. and Cullen, H.M. (2001) A 350-year (AD 1628-1980) reconstruction of Turkish precipitation. *Dendrochronologia*. 19, 169-177.
- Davies, S. J., Metcalfe, S. E., Caballero, M. and Juggins, S. (2002) Developing diatom-based transfer functions for central Mexican lakes. *Hydrobiologica*. 476, 199-213.
- Di Lauro, A., Fernex, F., Fierro, G., Ferrand, J.L., Pupin, J.P. and Gasparro, J. (2004) Geochemical approach to the sedimentary evolution of the Bay of Nice (NW Mediterranean Sea). *Continental Shelf Research*. 24, 223-239.
- Dittrich, M., Kurz, P. and Wehrli, B. (2004) The role of autotrophic picocyanobacteria in calcite precipitation in an oligotrophic lake. *Geomicrobiology Journal*. 21, 45-53.
- Dixit, S.S., Smol, J.P., Kingston, J.C. and Charles, D.F. (1992) Diatoms: powerful indicators of environmental change. *Environmental Science and Technology*. 26, 23-33.
- Dumont, H.J. (1981) Kratergöl, a deep hypersaline crater-lake in the steppe zone of western-Anatolia (Turkey), subject to occasional limno-meteorological perturbations. *Hydrobiologica*. 82, 271-279.
- Dünkeloh, A. and Jacobeit, J. (2003) Circulation dynamics of Mediterranean precipitation variability 1948-98. *International Journal of Climatology*. 23, 1843-1866.

- Eastwood, W.J., Roberts, N., Lamb, H.F. and Tibby, J.C. (1999) Holocene environmental change in southwest Turkey: a palaeoecological record of lake and catchment-related changes. *Quaternary Science Reviews*. 18, 671-695.
- Eastwood, W.J., Leng, M.J., Roberts, N. and Davis, B. (2006) Holocene climate change in the eastern Mediterranean region: a comparison of stable isotope and pollen data from a lake record in southwest Turkey. *Journal of Quaternary Science*. 22, 327-341.
- Embassy of the Republic of Turkey (1999) Country profile. *Republic of Turkey, Turkish Embassy*. [Online: <http://www.turkishembassy.org/countryprofile/>]. Accessed: 10/12/05.
- England, A. (2006) *Late Holocene Palaeoecology of Cappadocia (Central Turkey): an Investigation of Annually Laminated Sediments from Nar Gölü Crater Lake*. Ph.D. thesis: University of Birmingham.
- England, A., Eastwood, W.J., Roberts, C.N., Turner, R. and Haldon, J.F. (2008) Historical landscape change in Cappadocia (central Turkey): a palaeoecological investigation of annually-laminated sediments from Nar lake. *Holocene*. 18, 1229-1245.
- Enzel, Y., Bookman, R., Sharon, D., Gvirtzman, H., Dayan, R., Ziv, B. and Stein, M. (2003) Late Holocene climates of the Near East deduced from Dead Sea level

- variations and modern regional winter rainfall. *Quaternary Research*. 60, 263-273.
- Erdik, M., Biro, Y. and Durukal, E. (2001) *Assessment of Earthquake Hazard in Turkey and Neighbouring Regions*. American Geophysical Union: USA. 42, 1125-1138.
- Erinc, S. (1978) Changes in the physical environment in Turkey since the end of the Last Glacial. In: Brice, W.C. (Ed.) (1978) *The Environmental History of the Near and Middle East since the Last Ice Age*. Academic Press: London. 87-100.
- Erol, O. (1978) The Quaternary history of the lake basins of central and southern Anatolia. In: Brice, W.C. (Ed.) *The Environmental History of the Near and Middle East since the Last Ice Age*. Academic Press: London. 111-139.
- Erol, O. (1997) Geomorphologic arguments for mid-to-late Holocene environmental change in Central Anatolian (pluvial) lake basins. In: Nüzhet, H., Kukla, G. and Weiss, H. (Eds) *NATO ASI Series: Third Millennium BC Climate Change and Old World Collapse*. Springer-Verlag: Berlin Heidelberg. 49, 321-350.
- Esper, J., Wilson, R.J.S., Frank, D.C., Moberg, A., Wanner, H. and Luterbacher, J. (2005) Climate: past ranges and future changes. *Quaternary Science Reviews*. 24, 2164-2166.
- Eugster, H.P. and Hardie, L.A. (1978) Cht 8: Saline lakes. In: Lerman, A. (Ed.) *Lakes, Chemistry, Geology, Physics*. Springer-Verlag: New York. 237-293.

- Fairbridge, R., Erol, O., Karaca, M. and Yilmaz, Y. (1997) Background to mid-Holocene climate change in Anatolia and adjacent regions. In: Nüzhet, H., Kukla, G. and Weiss, H. (Eds) *NATO ASI Series: Third Millennium BC Climate Change and Old World Collapse*. Springer-Verlag: Berlin Heidelberg. 49, 595-510.
- Falciatore, A. and Bowler, C. (2002) Revealing the molecular secrets of marine diatoms. *Annual Review of Plant Biology*. 53, 109-130.
- Felis, T., Rimbu, N., Lohmann, G., Kuhnert, H. and Patzold, J. (2003) Reconstructions of Middle Eastern climate from Red Sea corals. *Geophysical Research Abstracts*. 5, 05023.
- Fleitmann, D. (2007) Holocene to Late-Pleistocene paleoclimatic changes in Turkey and the eastern Mediterranean recorded in speleothems. *Institute of Geological Sciences, University of Bern*. [Online: <http://www.earthsci.unibe.ch/snf/climate.htm>]. Accessed: 29/04/08.
- Flower, P.J. (1993) Diatom preservation: experiments and observations on dissolution and breakage in modern and fossil material. *Hydrobiologia*. 269-270, 473-484.
- Fontugne, M., Kuzucuoğlu, C., Karabiyikoğlu, M., Hatté, C. and Pastre, J.-F. (1999) From pleniglacial to Holocene: a ¹⁴C chronostratigraphy of environmental changes in the Konya Plain, Turkey. *Quaternary Science Reviews*. 18, 573-591.

- Foster, I.D.L., Mighall, T.M., Proffitt, H., Walling, D.E. and Owens, P.N. (2006) Post-depositional ^{137}Cs mobility in the sediments of three shallow coastal lagoons, SW England. *Journal of Paleolimnology*. 35, 881-895.
- Frignani, M., Langone, L., Ravaioli, M., Sorgente, D., Alvisi, F. and Albertazzi, S. (2005) Fine-sediment mass balance in the eastern Adriatic continental shelf over a century time scale. *Marine Geology*. 222-223, 113-133.
- Fritz, S.C. (1990) Twentieth-century salinity and water-level fluctuations in Devils Lake, North Dakota: test of a diatom based transfer function. *Journal of Limnology and Oceanography*. 8, 1771-1781.
- Fritz, S.C. (2008) Deciphering climate history from lake sediments. *Journal of Paleolimnology*. 39, 5-16.
- Fritz, S.C., Juggins, S. and Battarbee, R.W. (1993) Diatom assemblages and ionic characterisation of lakes of the northern great-plains, North America – a tool for reconstructing past salinity and climate fluctuations. *Canadian Journal of Fisheries and Aquatic Sciences*. 50, 1844-1856.
- Fritz, S.C., Cumming, B.F., Gasse, F. and Laird, K.R. (1999) Cht 3: Diatoms as indicators of hydrologic and climate change in saline lakes. In: Stoermer, E.F. and Smol, J.P. (1999) *The Diatoms: Applications for the Environmental and Earth Sciences*. Cambridge University Press: UK. 205-226.

- Gasse, F. (1986) *Bibliotheca Diatomologica: East African Diatoms*. Gebrüder Borntraeger: Berlin.
- Gasse, F., Juggins, S. and Khelifa, B.B. (1995) Diatom-based transfer functions for inferring hydrochemical characteristics of African palaeolakes. *Palaeogeography, Palaeoclimatology, Palaeoecology*. 117, 31-54.
- Gasse, F., Barker, P.A., Gell, P.A., Fritz, S.C. and Chalif, F. (1997) Diatom-inferred salinity of palaeolakes, an indirect tracer of climate change. *Quaternary Science Reviews*. 16, 547-563.
- Gell, P.A. (1997) The development of a diatom database for inferring lake salinity, western Victoria, Australia: towards a quantitative approach for reconstructing past climates. *Australian Journal of Botany*. 45, 389-423.
- Gell, P.A. and Gasse, F. (1994) Relationships between salinity and diatom flora from some Australian saline lakes. *Proceedings of the 11th International Diatom Symposium*. 17, 631-647.
- Gerdes, G., Petzelberger, B.E.M., Scholz-Bottcher, B.M. and Streif, H. (2003) The record of climate change in the geological archives of shallow marine, coastal and adjacent lowland areas of Northern Germany. *Quaternary Science Reviews*. 22, 101-124.
- Germain, H. (1981) *Flore Des Diatomées, eaux douces et saumâtres*, Société Nouvelle Des éditions Boubée: Paris.

- Gil, I.M., Abrantes, F. and Hebbeln, D. (2006) The North Atlantic Oscillation forcing through the last 2000 years: spatial variability as revealed by high-resolution marine diatom records from N and SW Europe. *Marine Micropaleontology*. 60, 113–129.
- Glew, J.R. (1991) Miniature gravity corer for recovering short sediment cores. *Journal of Paleolimnology*. 5, 285-287.
- Glew, J.R., Smol, J.P. and Last, W.M. (2001) Cht 5: Sediment core collection and extrusion. In: Last, M. and Smol, J.P. (Eds) *Tracking Environmental Change Using Lake Sediments. Vol 1: Basin Analysis, Coring and Chronological Techniques*. Kluwer Academic Publishers: Netherlands. 73-105.
- Golterman, H.L., Clymo, R.S. and Ohnstad, A.M. (1978) *IBP Handbook No. 8: Methods for Physical and Chemical Analysis of Fresh Water*. J.B. Lippincott: USA.
- Grimm, E.C. (2004) *TGVIEW version 2.0.2*. (Computer Software). Illinois State Museum, Research and Collections Center: Springfield, USA.
- Guidoboni, E., Bernardini, F., Comastri, A. and Boschi, E. (2004) The large earthquake on 29 June 1170 (Syria, Lebanon and central southern Turkey). *Journal of Geophysical Research-Solid Earth*. 109, B7.

- Hall, R.I. and Smol, J.P. (1999) Cht. 6: Diatoms as indicators of lake eutrophication. In: Stoermer, E.F. and Smol, J.P. (Eds) (1999) *The Diatoms: Applications for the Environmental and Earth Sciences*. Cambridge University Press: UK. 128-168.
- Hammer, U.T. (1986) *Saline Lake Ecosystems of the World*. Dordrecht: Lancaster.
- Harding, A. (2006) North Sea Caspian Pattern (NCP). *UEA Climate Research Unit*. [Online: <http://www.cru.uea.ac.uk/~andrewh/ncp.html>]. Accessed: 10/08/2008.
- Harrison, S.P. and Digerfeldt, G. (1993) European lakes as palaeohydrological and palaeoclimatic indicators. *Quaternary Science Reviews*. 12, 233-248.
- Hartley, B. (1996) *An Atlas of British Diatoms*. Henry Ling Ltd: UK.
- Hausmann, S. and Pienitz, R. (2007) Seasonal climate inferences from high-resolution modern diatom data along a climate gradient: a case study. *Journal of Paleolimnology*. 38, 73-96.
- Heim, C., Nowaczyk, N.R., Negendank, J.F.W., Leroy, S.A.G. and Ben-Avraham, Z. (1997) Near East desertification: evidence from the Dead Sea. *Naturwissenschaften*. 84, 398-401.
- Hill, M.O. and Gauch, H.G. (1980). Detrended Correspondence Analysis: an improved ordination technique. *Vegetatio*. 42, 47-58.

- Holland, S.M. (2003) *Analytic Rarefaction version 1.3*. (Computer Software). UGA Stratigraphy Lab. [Online: <http://www.uga.edu/~strata/software/anRareReadme.html>] Accessed: 10/01/08.
- Horne, A.J. and Goldman, C.R. (1994) *Limnology: Second Edn*. McGraw-Hill Book Co: Singapore.
- Hustedt, F. and Jensen, N.G. (1985) *The Pennate Diatoms: A Translation of Hustedt's 'Die Kiesselslgen, 2 Teil.'* Koeltz Scientific Books: Germany.
- Imbrie, J. and Webb, T. III (1981) Transfer functions: calibrating micropalaeontological data in climatic terms. In: Berger, A. (Ed.) *Climatic Variations and Variability: Facts and Theories*. D. Reidel: Dordrecht. 125-134.
- Ishihara, S., Kato, M., Tanimura, Y. and Fukusawa, H. (2003) Varved lacustrine sediments and diatom assemblages of Lake Fukami, central Japan. *Quaternary International*. 105, 21-24.
- Jansen, E. and Overpeck, J. (2007) Ch. 6: Palaeoclimate. *IPCC Fourth Assessment Report: Working Group I "The Physical Science Basis"*. [Online: <http://www.ipcc.ch/pdf/assessment-report/ar4/wg1/ar4-wg1-chapter6.pdf>]. Accessed: 03/04/08.
- Jensen, K.G., Kuijpers, A., Koc, N. and Heinemeier, J. (2004) Diatom evidence of hydrographic changes and ice conditions in Igaliku Fjord, South Greenland, during the past 1500 years. *The Holocene*. 14, 152-164.

- Jones, M.D. (2004) *High-Resolution Records of Climate Change from Lacustrine Stable Isotopes through the Last Two Millennia in Western Turkey*. Ph.D. thesis: University of Plymouth.
- Jones, M.D., Leng, M.J., Roberts, C.N. and Türkeş, M. (2005) A coupled calibration and modelling approach to the understanding of dry-land lake oxygen isotope records. *Journal of Palaeolimnology*. 34, 391-411.
- Jones, M.D., Roberts, C.N., Leng, M.J. and Türkeş, M. (2006) A high-resolution Late Holocene lake isotope record from Turkey and links to North Atlantic and monsoon climate. *Geology*. 34, 361-364.
- Jones, M.D., Roberts, C.N. and Leng, M.J. (2007) Quantifying climatic change through the last glacial-interglacial transition based on lake isotope palaeohydrology from central Turkey. *Quaternary Research*. 67, 463-473.
- Jones, M.D. and Roberts, C.N. (2008) Interpreting lake isotope records of Holocene environmental change in the Eastern Mediterranean. *Quaternary International*. 181, 32-38.
- Jones, P.D. and Mann, M.E. (2004) Climate over past millennia. *Reviews of Geophysics*. 42, RG2002/2004.

- Jongman, R.H.G., Ter Braak, C.J.F. and van Tongeren, O.F.R. (Eds) (1995) *Data Analysis in Community and Landscape Ecology*. Cambridge University Press: UK.
- Juggins S. (2003). *C2 version 1.3: software for ecological and palaeoecological data analysis and visualisation*. (Computer Software) Department of Geography, University of Newcastle, Newcastle upon Tyne: UK.
- Juggins, S. (2008) *European Diatom Database*. [Online: [http:// craticula.ncl.ac.uk/Eddi/jsp/index.jsp](http://craticula.ncl.ac.uk/Eddi/jsp/index.jsp)]. Accessed: 24/10/05-29/01/09.
- Juggins, S., Battarbee, R.W., Fritz, S.C. and Gasse, F. (1994) The CASPIA project: diatoms, salt lakes and environmental change. *Journal of Palaeolimnology*. 12, 191-196.
- Kahya, E. and Karabörk, Ç. (2001) The analysis of El Niño and La Niña signals in streamflows of Turkey. *International Journal of Climatology*. 21, 1231-1250.
- Karabıyıkoglu, M., Kuzucuoglu, C., Fontugne, M., Kaiser, B., Mouralis, D. and Babayigit, S. (1999) Facies and depositional sequences of the Late Pleistocene Göçü shoreline system, Konya Basin, central Anatolia: lake level changes and climate implications. *Quaternary Science Reviews*, 18, 593-610.
- Karabörk, M.Ç. (2007) Trends in drought patterns of Turkey. *Journal of Environmental Engineering and Science*. 6, 45-52.

Karabörk, M.Ç. and Kahya, E. (2003) The teleconnections between the extreme phases of the Southern Oscillation and precipitation patterns over Turkey. *International Journal of Climatology*. 23, 1607-1625.

Karabörk, M.Ç., Kahya, E. and Karaca, M. (2005) The influence of Southern and North Atlantic oscillations on climate surface variables in Turkey. *Hydrological Processes*. 19, 1185-1211.

Karageorgis, A.P., Kaberi, H., Price, N.B., Muir, G.K.P., Pates, J.M. and Lykousis, V. (2005) Chemical composition of short sediment cores from Thermaikos Gulf (East Mediterranean): sediment accumulation rates, trawling and winnowing effects. *Continental Shelf Research*. 25, 2456-2475.

Kashima, K. (1996) Sedimentary diatom assemblages in freshwater and saline lakes of the Anatolian Plateau, central part of Turkey: an application for reconstruction of palaeosalinity change during Late Quaternary. In: Marino, D. and Montresor, M. (Eds) *Proceedings of the 13th International Diatom Symposium*. Biopress: Bristol. 93-100.

Kashima, K. (2003) The quantitative reconstruction of salinity changes using diatom assemblages in inland lakes in the central part of Turkey during the Late Quaternary. *Quaternary International*. 105, 13-19.

Kazancı, N. (2005) The Holocene climate of Anatolia deduced from lake level records and sediment compositions, Turkey. *Atlas Conferences*. [Online: <http://atlas-conferences.com/c/a/o/d/71.htm>]. Accessed: 02/09/08.

- Keatley, B.E., Douglas, M.S.V. and Smol, J.P. (2006) Early-20th century environmental changes inferred using subfossil diatoms from a small pond on Melville Island, N.W.T., Canadian High Arctic. *Hydrobiologia*. 553, 15-26.
- Kelly, M.G., Bennion, H., Cox, E.J., Goldsmith, B., Jamieson, J., Juggins, S., Mann, D.G. and Telford, R.J. (2005) *Common Freshwater Diatoms of Britain and Ireland: An Interactive Key*. Environment Agency: Bristol.
- Kent, M. and Coker, P. (1992) *Vegetation Description and Analysis: A Practical Approach*. Belhaven Press: UK.
- Ketterer, M.E., Hafer, K.M., Jones, V.J. and Appleby, P.G. (2004) Rapid dating of recent sediments in Loch Ness: inductively coupled plasma mass spectrometric measurements of global fallout plutonium. *Science of the Total Environment*. 322, 221-229.
- Keyantash, J. and Dracup, J.A. (2002) The Quantification of drought: an evaluation of drought indices. *American Meteorological Society*. 83, 1167–1180.
- Kilham, P., Kilham, S.S. and Hecky, R.E. (1986) Hypothesized resource relationships among African planktonic diatoms. *Limnology and Oceanography*. 31, 1169-1181.
- Kilham, P. and Kilham, S.S. (1990) Endless summer: internal loading processes dominate nutrient cycling in tropical lakes. *Freshwater Biology*. 23, 379-389.

- Kilham, S.S., Theriot, E.C. and Fritz, S.C. (1996) Linking planktonic diatoms and climate change in the large lakes of the Yellowstone ecosystem using resource theory. *Limnology and Oceanography*. 41, 1052-1062.
- Kirschtel, D. (1996) *Biovol. version 2.1*. (Computer Software). Illinois Institute of Technology: USA.
- Klein, B. (2003) Mediterranean climate variability and its connection to the eastern transient. *Geophysical Research Abstracts: European Geophysical Society*. 5, 10200.
- Klein, A.M.G., Wijngaard, J.B., Können, G.P., Böhm, R., Demarée, G., Gocheva, A., Mileta, M., Pashiardis, S., Hejkrlik, L., Kern-Hansen, C., Heino, R., Bessemoulin, P., Müller-Westermeier, G., Tzanakou, M., Szalai, S., Pálsdóttir, T., Fitzgerald, D., Rubin, S., Capaldo, M., Maugeri, M., Leitass, A., Bukantis, A., Aberfeld, R., van Engelen, A.F.V., Forland, E., Miletus, M., Coelho, F., Mares, C., Razuvaev, V., Nieplova, E., Cegnar, T., Antonio López, A., Dahlström, B., Moberg, A., Kirchhofer, W., Ceylan, A., Pachaliuk, O., Alexander, L.V. and Petrovic, P. (2002) Daily dataset of 20th-century surface air temperature and precipitation series for the European Climate Assessment. *International Journal of Climatology*. 22, 1441-1453.
- Koçak, M., Kubilay, N., Herut, B. and Nimmo, M. (2005) Dry atmospheric fluxes of trace metals (Al, Fe, Mn, Pb, Cd, Zn, Cu) over the Levantine Basin: A refined assessment. *Atmospheric Environment*. 39, 7330-7341.

- Kolbe, R.W. (1927) Cited in: Fritz, S.C., Cumming, B.F., Gasse, F. and Laird, K.R. (1999) Cht. 3: Diatoms as indicators of hydrologic and climate change in saline lakes. In: Stoermer, E.F. and Smol, J.P. (Eds) *The Diatoms: Applications for the Environmental and Earth Sciences*. Cambridge University Press: UK.
- Komuscu, A.Ü. (2001) An analysis of recent drought conditions in Turkey in relation to circulation patterns. *Drought Network News*. 13, 5-6.
- Kostopoulou, E. and Jones, P.D. (2007) Comprehensive analysis of the climate variability in the eastern Mediterranean. Part I: map-pattern classification. *International Journal of Climatology*. 27, 1189-1214.
- Kovach, W.L. (1995) Cht. 1: Multivariate data analysis. In: Maddy, D. and Brew, J.S. (Eds) *Statistical Modelling of Quaternary Science Data: Technical guide no. 5*. Quaternary Research Association: Cambridge. 1-38.
- Krammer, K. and Lange-Bertalot, H. (1991) Ettl, H., Gärtner, G., Gerloff, J., Heynig, H. and Mollenhauer, D. (Eds) *Vol. 3: Bacillariophyceae 3. Teil Centrales, Fragilariaceae, Eunotiaceae*. Gustav Fischer Verlag: Germany.
- Krammer, K. and Lange-Bertalot, H. (1991) Ettl, H., Gärtner, G., Gerloff, J., Heynig, H. and Mollenhauer, D. (Eds) *Vol. 4: Bacillariophyceae 4. Teil Achnantheaceae Kritische Ergänzungen zu Navicula (Lineolatae) und Gomphonema*. Gustav Fischer Verlag: Germany.

- Krammer, K. and Lange-Bertalot, H. (1997) Ettl, H., Gärtner, G., Gerloff, J., Heynig, H. and Mollenhauer, D. (Eds) *Vol. 1: Bacillariophyceae 1. Teil Naviculaceae*. Gustav Fischer Verlag: Germany.
- Krammer, K. and Lange-Bertalot, H. (1997) Ettl, H., Gärtner, G., Gerloff, J., Heynig, H. and Mollenhauer, D. (Eds) *Vol. 2: Bacillariophyceae 2. Teil Bacillariaceae, Epithemiaceae, Surirellaceae*. Gustav Fischer Verlag: Germany.
- Krammer, K. and Lange-Bertalot, H. (2000) Büdel, B., Gärtner, G., Krienitz, L. and Lokhorst, G.M. (Eds) *Vol. 5: Bacillariophyceae Part 5. English and French Translation of the Keys*. Gustav Fischer Verlag: Germany.
- Kuniholm, P.I. (1990) Archaeological evidence and non-evidence for climate change. *Philosophical Transactions of the Royal Society of London*. 330, 645-655.
- Kumke, T., Kienel, U., Weckstrom, J., Korhola, A. and Hubberten, H.W. (2004) Inferred Holocene palaeo-temperatures from diatoms at Lake Lama, central Siberia, Arctic. *Antarctic and Alpine Research*. 36, 624-634.
- Kutiel, H. and Benaroch, Y. (2002) North Sea-Caspian Pattern (NCP) – an upper level atmospheric teleconnection affecting the eastern Mediterranean: identification and definition. *Theoretical Applied Climatology*. 71, 17-28.
- Kutiel, H. and Türkeş, M. (2005) New evidence for the roles of the North Sea – Caspian pattern on the temperature and precipitation regimes in continental central Turkey. *Geografiska Annaler*. 87 A, 501-513.

- Kuzucuoglu, C., Pastre, J.F., Black, S., Ercan, T., Fontunge, M., Guillou, H., Hatté, C., Karabiyikoglu, M., Orth, P. and Türkecan, A. (1998) Identification and dating of tephra layers from Quaternary sedimentary sequences of inner Anatolia, Turkey. *Journal of Volcanology and Geothermal Research*. 85, 153-172.
- Laird, K.R., Fritz, S.C., Maasch, K.A. and Cumming, B.F. (2008) North American drought: a paleo perspective - the last 2,000 years. *NAOO Satellite and Information Service, National Climate Data Centre US Dept. of Commerce*. [Online: http://www.ncdc.noaa.gov/paleo/drought/drght_laird96.html]. Accessed: 10/08/2008.
- Laird, K.R., Fritz, S.C., Grimm, E.C. and Mueller, P.G. (1996) Century-scale palaeoclimatic reconstruction from Moon Lake, a closed-basin lake in the northern Great Plains. *American Society of Limnology and Oceanography*. 41, 890-902.
- Laird, K.R., Fritz, S.C. and Cummings, B.F. (1998) A diatom based reconstruction of drought intensity, duration and frequency from Moon Lake, North Dakota: a sub-decadal record of the last 2300 years. *Journal of Palaeolimnology*. 19, 161-179.
- Lamb, H.F. and van der Kaars, S. (1995) Vegetational response to Holocene climatic change: pollen and palaeolimnological data from the middle Atlas, Morocco. *The Holocene*. 5, 400-408.

- Lamb, A.L., Leng, M.J., Barker, P.B. and Morley, D.W. (2004) The potential of oxygen isotopes in diatoms as a palaeoclimate indicator in lake sediments. *PAGES News*. 12, 6-8.
- Lamoureux, S. (2001) Cht. 11: Varve chronological techniques. In: Last, M. and Smol, J.P. (Eds) *Tracking Environmental Change Using Lake Sediments. Vol 1: Basin Analysis, Coring and Chronological Techniques*. Kluwer Academic Publishers: Netherlands. 247-260.
- Landmann, G., Reimer, A., Lemcke, G. and Kempe, S. (1996) Dating Late Glacial abrupt climate changes in the 14,570 yr long continuous varve record of Lake Van, Turkey. *Palaeogeography, Palaeoclimatology, Palaeoecology*. 122, 107-118.
- Leng, M.J., Roberts, N., Reed, J.M. and Sloane, H.J. (1999) Late Quaternary palaeohydrology of the Konya Basin, Turkey, based on isotope studies of modern hydrology and Lacustrine carbonates. *Journal of Palaeolimnology*. 22, 187-204.
- Leng, M.J., Barker, P., Greenwood, P., Roberts, C.N. and Reed, J. (2001) Oxygen isotope analysis of diatom silica and authigenic calcite from Lake Pinarbasi, Turkey. *Journal of Palaeolimnology*. 25, 343-349.
- Leng, M.J. and Barker, P.A. (2006) A review of the oxygen isotope composition of lacustrine diatom silica for palaeoclimate reconstruction. *Earth-Science Reviews*. 75, 5-27.

- Leroy, S., Kazancı, N., İleri, Ö., Kibar, M., Emre, O., McGee, E. and Griffiths, H.I. (2002) Abrupt environmental changes within a late Holocene lacustrine sequence south of the Marmara Sea (Lake Manyas, N-W Turkey): possible links with seismic events. *Marine Geology*. 190, 531-552.
- Luterbacher, J., Dietrich, D., Xoplaki, E., Grosjean, M. and Wanner, H. (2004) European seasonal and annual temperature variability, trends and extremes since 1500. *Science*. 303, 1499-1503.
- Luterbacher, J., Xoplaki, E., Casty, C., Wanner, H., Pauling, A., Küttel, M., Rutishauser, T., Brönnimann, S., Fischer, E., Fleitmann, D. González-Rouco, F.J., García-Herrera, R., Barriendos, M., Rodrigo, F., Gonzalez-Hidalgo, J.C., Saz, M.A., Gimeno, L., Ribera, P., Brunet, M., Paeth, H., Rimbu, N., Felis, T., Jacobeit, J., Dünkeloh, A., Zorita, E., Guiot, J., Türkeş, M., Alcoforado, M.J., Trigo, R., Wheeler, D., Tett, S., Mann, M.E., Touchan, R., Shindell, D.T., Silenzi, S., Montagna, P., Camuffo, D., Mariotti, A., Nanni, T., Brunetti, M., Maugeri, M., Zerefos, C., De Zolt, S. and Lionello, P. (2006) Cht. 1 Mediterranean climate variability over the last centuries: a review. In: Lionello, P., Malanotte-Rizzoli, P. and Boscolo, R. (Eds) *The Mediterranean Climate: an overview of the main characteristics and issues*. Elsevier: Netherlands. 27-148.
- Lionello, P., Malanotte-Rizzoli, P.M. and Boscolo, R. (Eds) (2006 a) *Developments in Earth and Environmental Science 4; Mediterranean Climate Variability*. Elsevier: Netherlands.

- Lionello, P., Malanotte-Rizzoli, P.M., Boscolo, R., Alpert, P., Artale, V., Li, L., Luterbacher, J., May, W., Trigo, R., Tsimplis, M., Ulbrich, U. and Xoplaki, E. (2006 b) Cht. 1: The Mediterranean climate: an overview of the main characteristics and issues. In: Lionello, P., Malanotte-Rizzoli, P.M. and Boscolo, R. (Eds) *Developments in Earth and Environmental Science 4; Mediterranean Climate Variability*. Elsevier: Netherlands. 1-18.
- Little, J.L., Hall, R.I., Quinlan, R. and Smol, J.P. (2000) Past trophic status and hypolimnetic anoxia during eutrophication and remediation of Gravenhurst Bay, Ontario: comparison of diatoms, chironomids and historical records. *Canadian Journal of Fisheries and Aquatic Sciences*. 57, 333-341.
- Liu, X. and Yanai, M. (2001) Relationship between the Indian monsoon rainfall and the tropospheric temperature over the Eurasian continent. *Q. J. Royal Meteorological Society*. 127, 909-937.
- Livingstone, D.A. (1955) A lightweight piston sampler for lake deposits. *Ecology*. 36, 137-139.
- Lloyd-Hughes, B. and Saunders, M.A. (2002) A drought climatology for Europe. *International Journal of Climatology*. 22, 1571-1592.
- Luterbacher, J., Dietrich, D., Xoplaki, E., Grosjean, M. and Wanner, H. (2004) European seasonal and annual temperature variability, trends and extremes since 1500. *Science*. 303, 1499-1503.

- Mackay, A.W., Ryves, D.B., Battarbee, R.W., Flower, R.J., Jewson, D., Rioual, P. and Sturm, M. (2005) 1000 years of climate variability in central Asia: assessing the evidence using Lake Baikal (Russia) diatom assemblages and the application of a diatom-inferred model of snow cover on the lake. *Global and Planetary Change*. 46, 281.
- Mackereth, F.J.H. (1969) A short core sampler for subaqueous deposits. *Limnology and Oceanography*. 15, 145-151.
- Maddy, D. and Brew, J.S. (1995) *Statistical Modelling of Quaternary Science Data: Technical Guide no. 5*. Quaternary Research Association: Cambridge.
- Mann, M.E. (2002) Large-scale climate variability and connections with the Middle East in past centuries. *Climate Change*. 55, 287-314.
- Mann, M.E. (2007) Climate over the last two millennia. *Annual Review of Earth and Planetary Sciences*. 35, 111-136.
- Mann, M.E., Bradley, R.S. and Hughes, M.K. (1999) Northern Hemisphere temperatures during the past millennium: inferences, uncertainties and limitations. *Geophysics Research Letters*. 26, 759-762.
- Mann, M.E. and Jones, P.D. (2003) 2,000 year hemispheric multi-proxy temperature reconstructions, IGBP PAGES/World Data Centre for Paleoclimatology. *NOAA/NGDC Paleoclimatology Program*. [Online:

- ftp://ftp.ncdc.noaa.gov/pub/data/paleo/contributions_by_author/mann2003b/mann2003b.txt]. Accessed: 10/08/2008.
- Marcarelli, A.M., Wurtsbaugh, W.A. and Griset, O. (2006) Salinity controls phytoplankton response to nutrient enrichment in the Great Salt Lake, Utah, USA. *Canadian Journal of Fisheries and Aquatic Sciences*. 63, 2236-2248.
- Marchetto, A. and Musazzi, S. (2001) Comparison between sedimentary and living diatoms in Lago Maggiore (N. Italy): implications of using transfer functions. *Journal of Limnology*. 60, 19-26.
- Martin-Del Pozzo, A.L., Aceves, F., Espinasa, R., Aguayo, A., Inguaggiato, S., Morales, P. and Cienfuegos, E. (2002) Influence of volcanic activity on spring water chemistry at Popocatepetl Volcano, Mexico. *Chemical Geology*. 190, 207-229.
- Mayewski, P.A., Rohling, E.E., Stager, J.C., Karlen, W., Maasch, K.A., Meeker, L.D., Meyerson, E.A., Gasse, F., van Kreveld, S., Holmgren, K., Lee-Thorp, J., Rosqvist, G., Rack, F., Staubwasser, M., Schneider, R.R. and Steig, E.J. (2004) Holocene climate variability. *Quaternary Research*. 62, 243-255.
- McCune, B. and Mefford, M.J. (1999). *PC-ORD. Multivariate Analysis of Ecological Data. version 5.0* (Computer Software). MjM Software: U.S.A.
- Microsoft Corporation (2007) *MS Excel. version 2007*. (Computer software).

- Migowski, C., Stein, M., Prasad, S., Negendank, J.F.W. and Agnon, A. (2006) Holocene climate variability and cultural evolution in the Near East from the Dead Sea sedimentary record. *Quaternary Research*. 66, 421-431.
- Mitchell, T.D. and Jones, P.D. (2005) TS 2.1 0.5 degree global time-series high-resolution gridded meteorological data (1901-2002). *Climate Research Unit, University of East Anglia*. [Online: <http://www.cru.uea.ac.uk/cru/data/hrg.htm>]. Accessed: 06/05/08.
- Mizuno, M. (1991) Influence of cell volume on the growth and size reduction of marine and estuarine diatoms. *Journal of Phycology*. 27, 473-478.
- National Research Council (2006) *Surface Temperature Reconstructions for the Last 2,000 Years*. The National Academics Press: USA.
- Oksanen, J., Läärä, E., Huttunen, P. and Meriläinen, J. (2004) Estimation of pH optima and tolerances of diatoms in lake sediments by the methods of weighted averaging, least squares and maximum likelihood and their use for the prediction of lake acidity. *Journal of Palaeolimnology*. 1, 39-49.
- Oldfield, F. and Thompson, R. (2004) Cht. 2: Archives and proxies along the PEP III transect. In: Battarbee, R.W., Gasse, F. and Stickley, C.E. (Eds) *Past Climate Variability through Europe and Africa*. Springer: Netherlands. 7-29.

- Osborn, T. (2008) North Atlantic Oscillation index data. *Climate Research Unit, University of East Anglia*. [Online: http://www.cru.uea.ac.uk/~timo/projpages/nao_update.htm]. Accessed: 06/05/08.
- O'Sullivan, P.E. (1983) Annually-laminated lake sediments and the study of Quaternary environmental changes: a review. *Quaternary Science Reviews*. 1, 245-313.
- O'Sullivan, P.E., Moyeed, R., Cooper, M.C. and Nicholson, M.J. (2001) Comparison between instrumental, observational and high-resolution proxy sedimentary records of Late-Holocene climate change – a discussion of possibilities. *Quaternary International*. 88, 27-44.
- O'Sullivan, P.E. and Reynolds, C.S. (2003 a) *The Lakes Handbook. Vol. 2: Lake Restoration and Rehabilitation*. Blackwell Science: UK.
- O'Sullivan, P.E. and Reynolds, C.S. (2003 b) *The Lakes Handbook. Vol. 1: Limnology and Limnetic Ecology*. Blackwell Science: UK.
- Papineau, D., Walker, J.J., Mojzsis, S.J. and Pace, N.R. (2005) Composition and structure of microbial communities from stromatolites of Hamelin Pool in Shark Bay, Western Australia, *Applied and Environmental Microbiology*, 71, 4822-4832.
- Putyrskaya, V. and Klemm, E. (2007) Modelling ^{137}Cs migration processes in lake sediments. *Journal of Environmental Radioactivity*. 96, 54-62.

- Raev, I. (2003) Investigations on global climate change in Bulgaria. In: Bolle, H.J. (Ed.) *Mediterranean Climate: Variability and Trends*. Springer-Verlag: Germany. 241-243.
- Raichich, F., Pinardi, N. and Navarra, A. (2003) Teleconnections between Indian monsoon and Sahel rainfall and the Mediterranean. *International Journal of Climatology*. 23, 173-186.
- Raup, D.M. (1975) Taxonomic diversity estimation using rarefaction. *Paleobiology*. 1, 333-342.
- Reed, J.M. (1998) A diatom-conductivity transfer function for Spanish salt lakes. *Journal of Paleolimnology*. 19, 399-416.
- Reed, J.M., Roberts, N. and Leng, M.J. (1999) An evaluation of the diatom response to Late Quaternary environmental change in two lakes in the Konya Basin, Turkey, by comparison with stable isotope data. *Quaternary Science Reviews*. 18, 631-646.
- Reed, J.M., Stevenson, A.C. and Juggins, S. (2001) A multi-proxy record of Holocene climatic change in southwestern Spain: the Laguna de Medina, Cádiz. *The Holocene*. 11, 707-719.
- Renberg, I., Bindler, R. and Brännvall, M.L. (2001) Using the historical atmospheric lead-deposition record as a chronological marker in sediment deposits in Europe. *The Holocene*. 11, 511-516.

- Renberg, I., Brännvall, M.L., Bindler, R. and Emteryd, O. (2002) Stable lead isotopes and lake sediments- a useful combination for the study of atmospheric lead pollution history. *The Science of the Total Environment*. 292, 45–54.
- Reynolds, C.S. (1993) *Cambridge Studies in Ecology: The Ecology of Freshwater Phytoplankton*. Cambridge University Press: UK.
- Reynolds, C.S. (2006) *Ecology, Biodiversity and Conservation: Ecology of Phytoplankton*. Cambridge University Press: UK.
- Roberts, N. (1982) Lake levels as an indicator of Near Eastern palaeo-climates: a preliminary appraisal. In: Bintliff, J.L. and van Zeist, W. (Eds), *Palaeoclimates, Palaeoenvironments and Human Communities in the Eastern Mediterranean Region in Later Prehistory*. B.A.R. International: Oxford. 235–267.
- Roberts, N. (1990) Cht 5: Human-induced landscape change in south and southwest Turkey during the later Holocene. In: Bottema, S., Entjes-Nieborg, G. and van Zeist., W. (Eds) (1990) *Man's Role in the Shaping of the Eastern Mediterranean Landscape*. Balkema: Rotterdam. 53-68.
- Roberts, N. (2000) *The Holocene: An Environmental History. Second Edn*. Blackwell Publishers Ltd: UK.
- Roberts, N. and Wright, H.E. (1993) Vegetational, lake level and climatic history of the Near East and Southwest Asia. In: Wright, H.E., Kutzbach, J.E., Webb, T.,

- Kuddino, W.F., Street-Perrott, F.A. and Bartlein, P.J. (Eds) *Global Climates Since the Last Glacial Maximum*. University of Minnesota Press: Minneapolis. 194-220.
- Roberts, N., Eastwood, W.J., Lamb, H.F. and Tibby, J.C. (1997) The age and causes of mid-late Holocene environmental change in southwest Turkey. In: Nüzhet, D., Kukla, G. and Weiss, H. (Eds) *NATO ASI Series: Third Millennium BC Climate Change and Old World Collapse*. Springer-Verlag: Berlin Heidelberg. 149, 409-429.
- Roberts, N., Black, S., Boyer, P., Eastwood, W.J., Griffiths, H.I., Lamb, H.F., Leng, M.J., Parish, R., Reed, J.M., Twigg, D. and Yigitbasioglu, H. (1999) Chronology and stratigraphy of Late Quaternary sediments in the Konya Basin Turkey: results from the KOPAL project. *Quaternary Science Reviews*. 18, 611-630.
- Roberts, N., Reed, J.M., Leng, M.J., Kuzucuoglu, C., Fontugne, M., Bertaux, J., Woldring, H., Bottema, S., Black, S., Hunt, E. and Karabiyikoglu, M. (2001) The tempo of Holocene climate change in the eastern Mediterranean region: new high-resolution crater-lake sediment data from central Turkey. *The Holocene*. 11, 721-736.
- Roberts, N. and Karabiyikoğlu, M. (2004) Western-central Anatolian lake basins: climate and tectonics. *Final report to MTA General Directorate, Ankara, Turkey on co-project (2000-2002)*. 17.
- Roberts, N., Stevenson, T., Davis, B., Cheddadi, R., Brewster, S. and Rosen, A. (2004) Holocene climate, environment and cultural change in the circum-Mediterranean

- region. In: Battarbee, R.W., Gasse, F. and Stickley, C. (Eds) *Past Climate Variability through Europe and Africa: PAGES PEPIII conference volume*. Kluwer Academic Publishers: Netherlands. 343-362.
- Rohling, E.J., Sprovieri, M., Cane, T., Casford, J.S.L., Cooke, S., Bouloubassi, I., Emeis, K.C., Schiebel, R., Rogerson, M., Hayes, A., Jorissen, F.J. and Kroon, D. (2004) Reconstructing past planktonic foraminiferal habitats using stable isotope data: a case history for Mediterranean sapropel S5. *Marine Micropaleontology*. 50, 89-123.
- Romero-Viana, L., Julia, R., Camacho, A., Vicente, E. and Miracle, M.R. (2008) Climate signal in varve thickness: Lake La Cruz (Spain), a case study. *Journal of Paleolimnology*. 40, 703-714.
- Rosen, A.M. and Rosen, S.A. (2001) Determinist or not determinist?: climate, environment and archaeological explanation in the Levant. Cited in: Wolff, F. (Ed.) (2004) Studies in the archaeology of Israel and neighbouring lands in memory of Douglas L. Esse. In: Battarbee, R.W., Gasse, F. and Stickley, C. (Eds) *Past Climate Variability through Europe and Africa: PAGES PEP III conference volume*. Kluwer Academic Publishers: Netherlands. 343-362.
- Rossignol-Strick, M. (1993) Late Quaternary climate in the Eastern Mediterranean region. *Paléorient*. 19/1, 135-151.
- Round, F.E. (1984). (Ed.) *The Ecology of Algae*. Cambridge University Press: UK.

- Round, F.E., Crawford, R.M. and Mann, D.G. (1992). *The Diatoms: Biology and Morphology of the Genera*. Cambridge University Press: UK.
- Russell, J.M. and Johnson, T.C. (2003) Lake Edward, East Africa: carbonates, the silica cycle and late Holocene century-scale drought. *Geological Society of America conference abstracts*. 1, 62.
- Russell, J.M., Verschuren, D. and Eggermont, H. (2007) Spatial complexity of 'Little Ice Age' climate in East Africa: sedimentary records from two crater lake basins in western Uganda. *The Holocene*. 17, 183-193.
- Saarnisto, M. (1986) Annually laminated lake sediments. In: Berglund, B.E. (Ed.) *Handbook of Holocene Palaeoecology and Palaeohydrology*. Wiley: Chichester. 343-370.
- Sansal, B. (2005) Turkey's physical geography. *All About Turkey*. [Online: <http://www.allaboutturkey.com/cografya.htm>] Accessed: 10/12/05.
- Saros, J.E. and Fritz, S.C. (2000) Changes in the growth rates of saline-lake diatoms in response to variation in salinity, brine type and nitrogen form. *Journal of Plankton Research*. 22, 1071-1083.
- Sarris, D., Christodoulakis, D. and Körner, K. (2007) Recent decline in precipitation and tree growth in the eastern Mediterranean. *Global Change Biology*. 13, 1187-1200.

Schilman, B., Bar-Matthews, M., Almogi-Labin, A. and Luz, B. (2001) Global climate instability reflected by eastern Mediterranean marine records during the late Holocene. *Palaeogeography, Palaeoclimatology, Palaeoecology*. 176, 157-176.

Serieyssol, K.K. and Johansen, J.R. (1985-2008) *Diatom Research: The Journal of the International Society for Diatom Research*. Biopress Ltd: UK.

Shaw, G. and Wheeler, D. (2000) *Statistical Techniques in Geographical Analysis*. The Cromwell Press: UK.

Sinha, R. and Raymahashay, B.C. (2004) Evaporite mineralogy and geochemical evolution of the Sambhar Salt Lake, Rajasthan, India. *Sedimentary Geology*. 166, 59-71.

Smol, J. (2002) *Key Issues in Environmental Change: Pollution of Lakes and Rivers*. Hodder Headline Group: London.

Smol, J.P. and Cumming, B.F. (2000) Tracking long-term changes in climate using algal indicators in lake sediments. *Journal of Phycology*. 36, 986-1011.

Smol, J.P., Birks, H.J.B. and Last, W.M. (Eds) (2001) *Tracking Environmental Change Using Lake Sediments. Vol. 3: Terrestrial, Algal and Siliceous Indicators*. Kluwer Academic Publishers: Netherlands.

Snoeijs, P., Busse, S. and Potapova, M. (2002) The importance of diatom cell size in community analysis. *Journal of Phycology*. 38, 265-281.

- Sontakke, N.A., Pant, G.B. and Singh, N. (1993) Construction of all-India summer monsoon rainfall series for the period 1844-1991. *Journal of Climatology*. 6, 1807-1811.
- Ssemmanda, I., Ryves, D.B., Bennick, O. and Appleby, P.G. (2005) Vegetation history in western Uganda during the last 1200 years: a sediment-based reconstruction from two crater lakes. *The Holocene*. 15, 119-132.
- Stager, J.C., Cummings, B.F. and Meeker, L.D. (2003) A 10,000-year high-resolution diatom record from Pilkington Bay, Lake Victoria, East Africa. *Quaternary Research*. 59, 172-181.
- Staubwasser, M. and Weiss, H. (2006) Holocene climate and cultural evolution in late prehistoric–early historic West Asia. *Quaternary Research*. 66, 372-387.
- Stebich, M., Bruchmann, C., Kulbe, T. and Negendank, J.F.W. (2005) Vegetation history, human impact and climate change during the last 700 years recorded in annually laminated sediments of Lac Pavin, France. *Review of Palaeobotany and Palynology*. 133, 115-133.
- Stoermer, E.F. and Smol, J.P. (1999 a) Cht 1: Applications and uses of diatoms: prologue. In: Stoermer, E.F. and Smol, J.P. (Eds) *The Diatoms: Applications for the Environmental and Earth Sciences*. Cambridge University Press: UK. 3-8.

- Stoermer, E.F. and Smol, J.P. (Eds) (1999 b) *The Diatoms: Applications for the Environmental and Earth Sciences*. Cambridge University Press: UK.
- Street-Perrott, F.A. and Barker, P.A. (2008) Biogenic silica: a neglected component of the coupled global continental biogeochemical cycles of carbon and silicon. *Earth Surface Processes and Landforms*. 33, 1436-1457.
- Sweets, P.R. (1995-2008) *Diatom-L (list serve) Indiana University*. [Online: [http:// www.google.co.uk/search?hl=en&q=diatom+list+server&meta=](http://www.google.co.uk/search?hl=en&q=diatom+list+server&meta=)]. Accessed: 10/05-12/08.
- Telford, R.J. and Birks, H.J.B. (2005) The secret assumption of transfer functions: problems with spatial autocorrelation in evaluating model performance. *Quaternary Science Reviews*. 24, 2173-2179.
- The International Research Institute for Climate and Society. (2006) Indices India rainfall: summer monsoon rainfall data. *IRI*. [Online: <http://iridl.ldeo.columbia.edu/SOURCES/.Indices/.india/.rainfall/>]. Accessed: 10/08/2008.
- Toprak, V. (1998) Vent distribution and its relation to regional tectonics, Cappadocian Volcanics, Turkey. *Journal of Volcanology and Geothermal Research*. 85, 55–67.
- Touchan, R., Garfin, G.M., Meko, D.M., Funkhouser, G., Erkan, N., Hughes, M.K. and Wallin, B.S. (2003) Preliminary reconstructions of spring precipitation in

- southwestern Turkey from tree-ring width. *International Journal of Climatology*. 23, 157-171.
- Touchan, R., Akkemik, Ü., Hughes, M.K. and Erkan, N. (2007) May-June precipitation reconstruction of south-western Anatolia, Turkey during the last 900 years from tree rings. *Quaternary Research*. 68, 196-202.
- Tsukada, H., Tsujimura, S. and Nakahara, H. (2006) Seasonal succession of phytoplankton in Lake Yogo over 2 years: effect of artificial manipulation. *Limnology*. 7, 3-14.
- Türkeş, M. (1996) Spatial and temporal analysis of annual rainfall variations in Turkey. *International Journal of Climatology*. 16, 1057-1076.
- Türkeş, M. (1998) Influence of geopotential heights, cyclone frequency and Southern Oscillation on rainfall variations in Turkey. *International Journal of Climatology*. 18, 649-680.
- Türkeş, M. (2003) Cht. 5: Spatial and temporal variations in precipitation and aridity index series of Turkey. In: Bolle, H.J. (Ed.) *Mediterranean Climate – Variability and Trends. Regional Climate Studies*. Springer Verlag: Heidelberg. 181-213.
- Türkeş, M., Sümer, U.M. and Kilic, G. (1995) Variations and trends in annual mean air temperatures in Turkey with respect to climate variability. *International Journal of Climatology*. 15, 557-569.

- Türkeş, M., Sümer, U.M. and Demr, S. (2002) Re-evaluation of trends and changes in mean, maximum and minimum temperatures of Turkey for the period 1929-1999. *International Journal of Climatology*. 22, 947-977.
- Türkeş, M. and Erlat, E. (2003) Precipitation changes and variability in Turkey linked to the North Atlantic Oscillation during the period 1930-2000. *International Journal of Climatology*. 23, 1771-1796.
- Türkeş, M. and Erlat, E. (2005) Climatological responses of winter precipitation in Turkey to variability of the North Atlantic Oscillation during the period 1930-2001. *Theoretical Applied Climatology*. 81, 45-69.
- Türkeş, M. and Erlat, E. (2008) Influence of the Arctic Oscillation on the variability of winter mean temperatures in Turkey. *Theoretical and Applied Climatology*. 92, 75-85.
- Turner, R. (2007) *Late Quaternary Fire Histories in the Eastern Mediterranean Region from Lake Sedimentary Micro-Charcoals*. Ph.D. thesis: University of Plymouth.
- United Nations Environment Programme (UNEP) (1991) *High and Dry: Mediterranean Climate in the Twenty-first Century*. United Nations Environment Programme: Greece.
- US Dept. of Commerce: Climate prediction centre internet team. (2008) *NOAA National Weather Service*. Changes to the Oceanic Niño Index (ONI). [Online:

http://www.cpc.noaa.gov/products/analysis_monitoring/ensostuff/ensoyears.shtml
]. Accessed: 01/06/08.

Verschuren, D., Laird, K.R. and Cumming, B.F. (2000) Rainfall and droughts in equatorial east Africa during the past 1,100 years. *Nature*. 403, 410-414. [Online: <http://www.ncdc.noaa.gov/paleo/africa-drought.html>]. Accessed: 01/07/2008.

Wasylikowa, K. (2005) Palaeoecology of Lake Zeribar, Iran, in the Pleniglacial, Late-glacial and Holocene, reconstructed from plant macrofossils. *The Holocene*. 15, 720-735.

Wetzel, R.G. (2001) *Limnology: Lake and River Ecosystems. Third Edn.* Academic Press: USA.

Wick, L., Lemcke, G. and Sturm, M. (2003) Evidence of Late-glacial and Holocene climate change and human impact in eastern Anatolia: high-resolution pollen, charcoal, isotopic and geochemical records from the laminated sediments of Lake Van, Turkey. *The Holocene*. 13, 665-675.

Wilhite, D.A. (2000) *Drought: Vol. I.* Routledge: London.

Wolfe, A.P. (2003) Diatom community responses to late-Holocene climatic variability, Baffin Island, Canada: a comparison of numerical approaches. *The Holocene*. 13, 29-37.

- Wolin, J.A. and Duthie, H.C. (1999) Cht. 8: Diatoms as indicators of water level change in freshwater lakes. In: Stoermer, E.F. and Smol, J.P. (Eds) *The Diatoms: Applications for the Environmental and Earth Sciences*. Cambridge University Press: UK. 183-202.
- Xoplaki, E., Luterbacher, J., Burkard, R., Patrikas, I. and Maheras, P. (2000) Connection between the large-scale 500 hPa geopotential height fields and precipitation over Greece during winter-time. *Climate Research*. 14, 129-146.
- Xoplaki, E., Luterbacher, J. and González-Rouco, J.F. (2006) Mediterranean summer temperature and winter precipitation, large-scale dynamics, trends. *Il Nuovo Cimento*. 29, 45-54.
- Yang, X.D., Wang, S.M., Kamenik, C., Schmidt, R., Shen, J., Zhu, L.P. and Li, S.F. (2004) Diatom assemblages and quantitative reconstruction for palaeosalinity from a sediment core of Chencuo Lake, southern Tibet. *Science in China Series D-Earth Sciences*. 47, 522-528.
- Yano, T., Aydin, M. and Haraguchi, T. (2007) Impact of climate change on irrigation demand and crop growth in a Mediterranean environment of Turkey. *Sensors*. 7, 2297-2315.
- Yıldız, O. (2007) Investigating frequency and spatial characteristics of droughts in the central Anatolian region, Turkey. *International Congress River Basin Management*. 2, 22-24.

Zaccone, C., Cocozza, C., Cheburkin, A.K., Shotyk, W. and Miano, T.M. (2007)

Enrichment and depletion of major and trace elements and radionuclides in ombrotrophic raw peat and corresponding humic acids. *Geoderma*. 141, 235-246.

Zalasiewicz, J., Williams, M., Smith, A., Barry, T.L. Coe, A.L. Bown, P.R., Brenchley,

P. Cantrill, D. Gale, A., Gibbard, P., Gregory, J., Hounslow, M.W. Kerr, A.C.

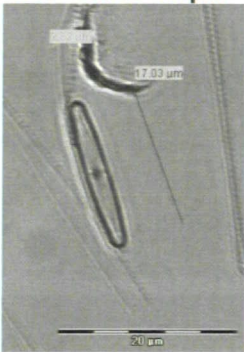
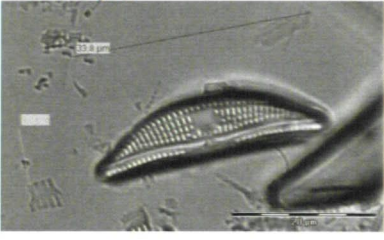
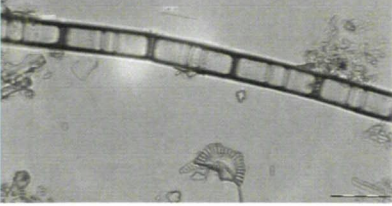
Pearson, P., Knox, R., Powell, J. Waters, C., Marshall, J., Oates, M., Rawson, P.

and Stone, P. (2008) Are we now living in the Anthropocene? *The Geological Society of America*. 18, 4-8.

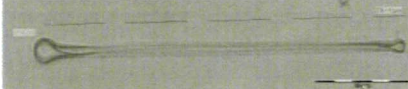
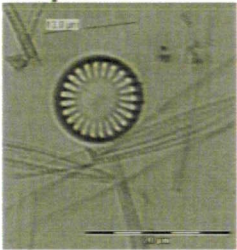
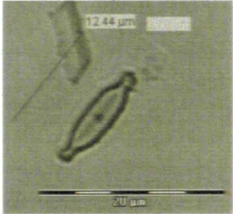
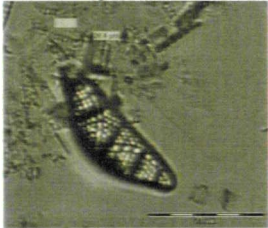
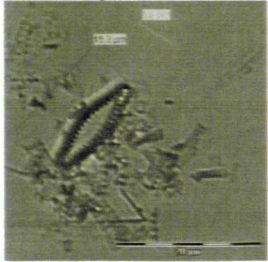
Appendix 1

Nar diatom species assemblage (>5% and important species according to biovolume)

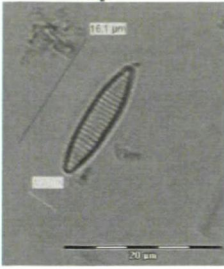
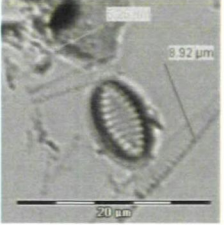
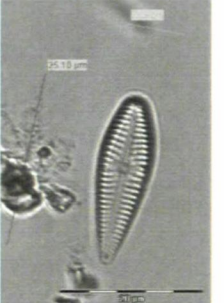
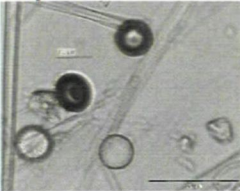
with illustrations (not to scale), synonyms, distinguishing features and taxonomic issues.

Species illustrations (LM) Typical size of Nar specimens	Distinguishing features (KLB)	Nar Gölü diatom assemblage taxonomic issues
<p><i>Achnantheidium minutissimum</i> (<i>Achnanthes minutissima</i> var. <i>minutissima</i>) Size: 17.03x2.83µm</p> 	<p>Pennate Size: 5-25x2-5µm Striae: 30 per 10µm</p> <p>Outline linear, linear-lanceolate to linear-elliptical. Striae not visible with LM.</p> <p>Habitat: planktonic and haptobenthic (attached).</p>	<p>The most common variety of this species was <i>A. minutissimum</i> var. <i>minutissimum</i>. However, the outline of many specimens was relatively variable; therefore it was not possible to split species varieties confidently. The key in KLB key does not split varieties, therefore specimens were grouped.</p>
<p><i>Amphora libyca</i> (<i>Amphora copulata</i>) (<i>Amphora ovalis</i> var. <i>affinis</i>) 33.8x9.0µm</p> 	<p>Pennate Size: 20-80x14-35µm Striae: 11-15 per 10µm</p> <p>Hyaline area in centre. Raphe branch strongly curved.</p> <p>Habitat: epiphytic, epilithic and epipelagic.</p>	<p>Taxonomy was straightforward for this species due to the distinguishing hyaline area.</p>
<p><i>Aulacoseira crenulata</i> (<i>Aulacoseira italica</i> f. <i>crenulata</i>) 12.48x8.37µm</p> 	<p>Centric Size: 5-32µm diameter Puncta: 9-13 per 10µm</p> <p>Striae appear slightly diagonal. Cells are joined by linking spines.</p> <p>Habitat: planktonic.</p>	<p>This species varied in terms of its length to width ratio. However, this is not a key taxonomic feature (Reed, per comm.); therefore species of different size ranges were grouped.</p>

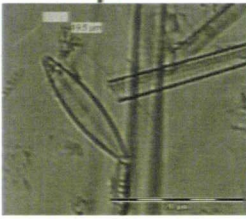
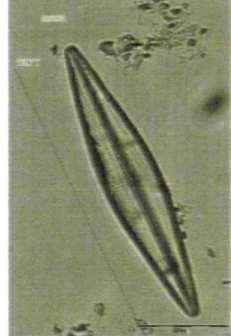
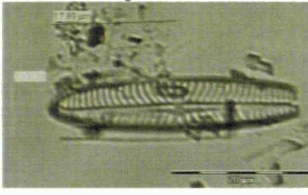
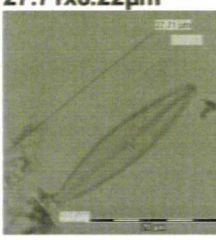
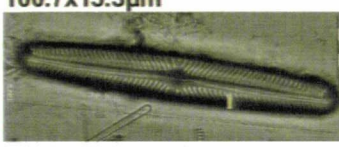
continued

<p><i>Asterionella formosa</i> 79.44x5.61µm</p> 	<p>Pennate Size: 30-160x1-6µm Striae: 24-28 per 10µm</p> <p>Cells heteropolar. Girdle view with triangular broadened ends.</p> <p>Habitat: forms stellate colonies, planktonic.</p>	<p>The taxonomy of this species was distinguished by its delicate appearance and bone-shape outline.</p>
<p><i>Cyclotella meneghiniana</i> (<i>Cyclotella kuetzingiana</i> var. <i>kuetzingiana</i>) (<i>Cyclotella stylorum</i>) 13.0µm</p> 	<p>Centric Size: 5-43µm diameter</p> <p>Coarse striae. Centre oval-shaped and undulating with numerous strutted processes.</p> <p>Habitat: free-living and forms filaments. Mainly planktonic.</p>	<p>Taxonomy was uncomplicated for this species due to the distinguishing coarse striae.</p>
<p><i>Cymbella microcephala</i> (<i>Navicula incompta</i>) 12.44x3.7µm</p> 	<p>Pennate Size: 10-30x2-4µm Striae: dorsal has 23-25 per 10µm and basal 30 per 10µm Puncta: 36-40 per 10µm</p> <p>Small with fine striae and capitate ends. Terminal raphe fissures bent towards ventral margin.</p> <p>Habitat: colonial, epiphytic, epilithic and epipellic.</p>	<p>Taxonomy was straightforward due to the distinguishing small size of this <i>Cymbella</i> species.</p>
<p><i>Epithemia argus</i> (<i>Eunotia argus</i>) 28.4x9.4µm</p> 	<p>Pennate Size: 20-130x4-18µm Striae: 10-14 per 10µm</p> <p>Central area of the raphe rises towards the dorsal and 4 rows of aerolae are present between ribs.</p> <p>Habitat: epiphytic and epipellic.</p>	<p>The characteristic raphe structure and number of aerolae rows between ribs allowed this species to be identified relatively easily.</p>
<p><i>Fragilaria brevistriata</i> (<i>Staurosira brevistriata</i>) (<i>Pseudostaurosira brevistriata</i>) 15.3x5.6µm</p> 	<p>Pennate Size: 11-30x3-5µm Striae: 12-17 per 10µm</p> <p>Rhomboid-shaped to broadly lanceolate. Striae are short around margin Ends are elongate and broadly rounded.</p> <p>Habitat: benthic and facultative planktonic.</p>	<p>This taxon was quite variable with regard to shape and size. Larger examples were straightforward to identify. However, smaller 'rugby ball-shaped' specimens were confused with similar species e.g. <i>F. pseudoconstruens</i> and <i>F. construens</i> var. <i>venter</i>.</p> <p>The short striae length was used as a distinguishing feature and smaller varieties were grouped with larger forms.</p>


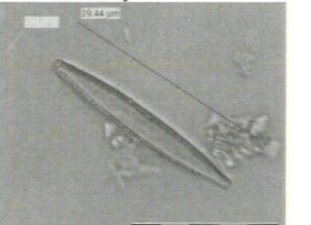
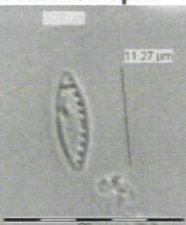
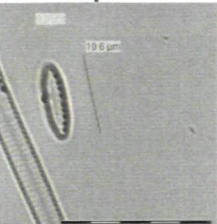
continued

<p><i>Fragilaria capucina</i> var. <i>rumpens</i> (<i>Synedra capucina</i> var. <i>rumpens</i>) 16.1x4.2µm</p> 	<p>Pennate Size: 10-100x2-6µm Striae: 18-20 per 10µm</p> <p>Outline is linear elliptical to lanceolate and narrowed towards the ends. Indistinctly or not punctate. Hyaline central area on one size of the raphe.</p> <p>Habitat: benthic and facultative planktonic.</p>	<p>This species was distinctive to identify. The KLB key does not split varieties of <i>Fragilaria capucina</i>. However, KLB illustrations reveal that this variety is very distinct due to the hyaline central area present on just one side of the raphe.</p>
<p><i>Fragilaria construens</i> var. <i>venter</i> (<i>Staurosira construens</i> var. <i>venter</i>) 8.92x5.25µm</p> 	<p>Pennate Size: 4-35x2-12µm Striae: 12-20 per 10µm</p> <p>Outline is variable with rounded ends. Puncta are difficult to distinguish.</p> <p>Habitat: benthic attached and facultative planktonic.</p>	<p>Initially this taxon was thought to be <i>F. elliptica</i>. However, specimens did not match all taxonomic features. Discussions with other diatomists (BDM, 2007) resulted in an attribution change to <i>F. construens</i> var. <i>venter</i>.</p> <p>Taxonomy remains problematic as the KLB key does not split <i>F. construens</i> varieties and examples were very small in relation to the size range of this species.</p>
<p><i>Gomphonema olivaceum</i> (<i>Gomphoneis olivacea</i>) 25.1x7.85µm</p> 	<p>Pennate Size: 8-45x3-13µm Striae: 9-16 per 10µm</p> <p>Central area is transversally widened and without stigmata.</p> <p>Habitat: colonial and haptobenthic.</p>	<p>This species was distinguished by the lack of stigmata in the central area. However, varieties were difficult to split and have therefore been grouped.</p>
<p><i>Clipeoparvus anatolicus</i> 8.0µm</p> 	<p>Centric 25-70µm diameter</p> <p>Habitat: <i>Melosira</i> is epibenthic.</p>	<p>This previously undescribed taxon identified at Nar had <i>Melosira</i>-type features. EM analysis suggested that it is a new genus.</p>

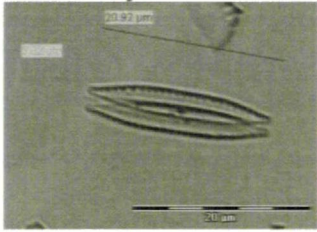
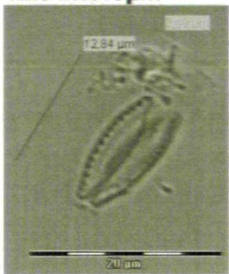
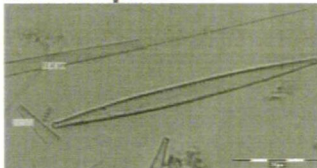
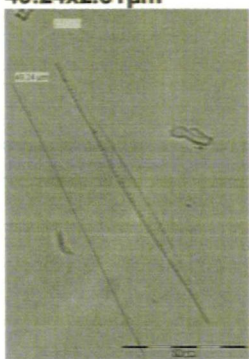
continued

<p><i>Navicula cryptotenella</i> (<i>Navicula radiosa</i> var. <i>tenella</i>) (<i>Navicula tenella</i>) 19.5x5.3µm</p> 	<p>Pennate Size: 14-40x5-7µm Striae: 14-16 per 10µm</p> <p>Striations are radial, particularly in centre and converge at the ends. A small central area is present.</p> <p>Habitat: epipelon.</p>	<p>The taxonomy of this species was quite straightforward; however, care was taken to avoid confusion with <i>N. cryptocephala</i>. Distinguishing features being the central area and striae arrangement.</p>
<p><i>Navicula halophila</i> (<i>Craticula halophila</i>) (<i>Navicula cuspidata</i> var. <i>halophila</i>) 67.74x12.97µm</p> 	<p>Pennate Size: 7-140x4.5-18µm Striae: 15-24 per 10µm</p> <p>No longitudinal ribs present. Striae are parallel in the centre and converge at the ends. Varies in shape and size.</p> <p>Habitat: epipelon and epipellic.</p>	<p>This species was confused with <i>N. cuspidata</i>. The distinguishing features between the two were <i>N. halophila</i>'s absence of longitudinal ribs.</p>
<p><i>Navicula digitoradiata</i> (<i>Pinnularia digitoradiata</i>) 17.89x7.49µm</p> 	<p>Pennate Size: 25-80x7-28µm Striae: 7-14 per 10µm</p> <p>Ends are blunt or rounded. Striae alternate in length at centre and converge at the ends.</p> <p>Habitat: epipelon.</p>	<p>Taxonomy was straightforward due to the distinctive striae arrangement.</p>
<p><i>Navicula elkab</i> (<i>Craticula elkab</i>) 27.71x8.22µm</p> 	<p>Pennate Size: 13-27x3.5-5.7µm Striae: 25-28 per 10µm</p> <p>Description according to European Diatom Database (Juggins, 2008): Small with fine striae. Lanceolate to elliptic-lanceolate-shaped with protracted or rostrate apices.</p> <p>Habitat: epipelon.</p>	<p>Species was confused with <i>N. accomoda</i>. <i>N. elkab</i> was distinguished by the shape and consistently small size.</p>
<p><i>Navicula oblonga</i> 100.7x15.3µm</p> 	<p>Pennate Size: 70-220x12-24µm Striae: 6-9 per 10µm</p> <p>Large with coarse striae. Striae are radiate in the centre and converge and kink at the ends.</p> <p>Habitat: epipelon.</p>	<p>This very distinctive taxon was identified without difficulty due to the large size and characteristic striae.</p>

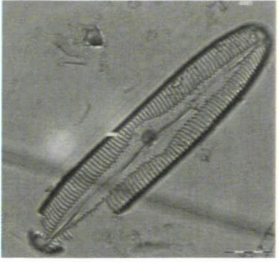

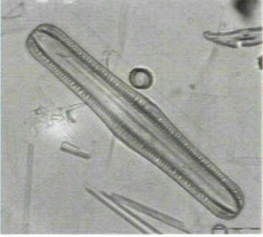
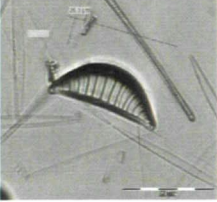
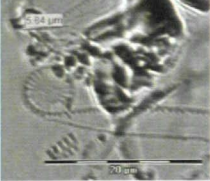
continued

<p><i>Nitzschia amphibia</i> 27.8x5.3µm</p> 	<p>Pennate Size: 6-50x4-6µm Striae: 13-18 per 10µm Fibulae: 7-9 per 10µm</p> <p>A pore is present in the centre of the fibulae. Striae are quite widely spaced and appear punctate.</p> <p>Habitat: epipellic and planktonic.</p>	<p>This distinctive taxon was characterised by coarse, punctate striae and a central pore in the fibulae.</p>
<p><i>Nitzschia capitellata</i> <i>(Nitzschia virgata var. capitellata)</i> 29.44x3.75µm</p> 	<p>Pennate Size: 20-70x3.5-6.5µm Striae: 23-40 per 10µm Fibulae: 10-18 per 10µm</p> <p>A pore is present in the centre of the fibulae. The largest forms are lanceolate or linear lanceolate. The ends are pointed and slightly capitate.</p> <p>Habitat: epipellic and planktonic.</p>	<p>This species was confused with a number of closely related <i>Nitzschias</i> and was distinguished by the characteristic shape.</p>
<p><i>Nitzschia af. fonticola</i> 11.27x3.28µm</p> 	<p>Pennate Size: 10-65x2-5µm Striae: 23-33µm Fibulae: 9-16 per 10µm</p> <p>More than one result in the KLB key: Lanceolate-linear lanceolate or distinctly lanceolate Poles sharply rounded or pointed to slightly capitate. Fibulae are point-like with a pore in the centre. Striae density is variable.</p> <p>Habitat: epipellic and planktonic.</p>	<p>This was a problematic taxon. Many specimens were too small to fit the KLB size range (<10µm) and occasionally there was no clear central pore on the fibulae. Discussions with different diatomists resulted in conflicting opinions. One suggestion was that this species could be <i>N. lacuum</i>, however, this species size is above 10µm and it does not have a central pore.</p> <p>Gasse (1986) described 3 types of <i>N. fonticola</i> on the basis of fibulae spacing. However, EM analysis is required to split these accurately and Gasse recognised transitional types between <i>N. sp. af. fonticola</i> and <i>N. af. frustulum</i>.</p>
<p><i>Nitzschia inconspicua</i> 10.6x3.0µm</p> 	<p>Pennate Size: 3-22x2-5µm Striae: 23-32 per 10µm Fibulae: 8-13 per 10µm</p> <p>Short with bluntly rounded ends. A pore is present in the centre of the fibulae.</p> <p>Habitat: epipellic and planktonic.</p>	<p>This species was confused with <i>N. af. fonticola</i> and was differentiated on the basis of shape, particularly the valve ends.</p>

continued

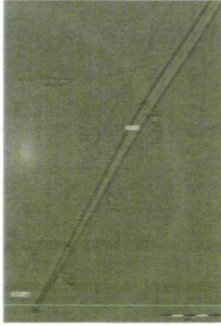
<p><i>Nitzschia palea</i> 20.92x3.02µm</p> 	<p>Pennate Size: 15-70x2-5µm Striae: 28-40 per 10µm Fibulae: 9-17 per 10µm</p> <p>Broadly lanceolate with fine, weakly visible striae. Usually large and elongated. No central pore in the fibulae.</p> <p>Habitat: epipellic and planktonic.</p>	<p>Typical specimens were very distinct. However, many examples varied with regard to their characteristics. This species was distinguished by the striae density and the absence of a pore in the fibulae.</p>
<p><i>Nitzschia cf. palea1 (small)</i> 12.84x3.49µm</p> 	<p>Pennate Size: 15-70x2-5µm Striae: 28-40 per 10µm Fibulae: 9-17 per 10µm</p> <p>Same characteristics as <i>N. palea</i>. There is a species listed on the European Diatom Database (Juggins, 2008) as <i>Nitzschia cf. palea (small)</i>.</p> <p>Habitat: epipellic and planktonic.</p>	<p>Specimens, at less than 15µm in length, were consistently too short to fit the KLB size range and striations were often distinctly visible. Transitional types were also recognised.</p> <p>Gasse (1986) described a small <i>N. frustulum type 1</i>, and <i>N. cf. fonticola type 1</i>, which lacks a fibulae pore and is slightly depressed in the centre.</p>
<p><i>Nitzschia palea var. major</i> 61.4x3.96µm</p> 	<p>Pennate Size: 15-70x2-µm Striae: 28-40 per 10µm Fibulae: 9-17 per 10µm</p> <p>Large form with the same characteristics as <i>N. palea</i>.</p> <p>Habitat: epipellic and planktonic.</p>	<p>Specimens were confused with <i>N. capitellata</i>. Distinctions were made based on the characteristic <i>N. capitellata</i> shape.</p>
<p><i>Nitzschia paleacea</i> (<i>Nitzschia subtilis</i> var. <i>paleacea</i>) 49.24x2.51µm</p> 	<p>Pennate Size: 8-55x1.5-4µm Striae: 44-55 per 10µm Fibulae: 14-18 per 10µm</p> <p>Outline is variable and can appear narrowly lanceolate to narrowly linear lanceolate. Valve width is typically narrow. Central pore present in fibulae. Striae are difficult to resolve with LM. Ends are elongate-rostate to capitate.</p> <p>Habitat: epipellic and planktonic.</p>	<p>Typical examples of this species were easily identified. However, valve ends were often variable. It was not possible to consistently place specimens in categories for end-shape due to the many transitional types. Therefore varieties were grouped.</p>

continued

<p><i>Pinnularia viridis</i> (<i>Navicula viridis</i>) 130x28 μm</p> 	<p>Pennate Size: 50-170x10-30μm Striae: 6-12 per 10μm</p> <p>Valve with longitudinal bands. Ends bluntly rounded to broadly capitate. Raphe strongly lateral. Large size range.</p> <p>Habitat: benthic</p>	<p>Species straightforward to identify due to the characteristically large shape and ornamentation.</p>
<p><i>Rhoicosphenia abbreviata</i> (<i>Gomphonema curvatum</i>) 33.6x5.9μm</p> 	<p>Pennate Size: 10-75x3-8μm Striae: 15-20 per 10μm</p> <p>Valve shape appears bent in girdle view. The outline of two frustules is visible in valve view.</p> <p>Habitat: epiphytic and epilithic.</p>	<p>This very distinctive taxon was easily identified by its 'bent' appearance.</p>
<p><i>Rhopalodia gibba</i> (<i>Cystopleura gibba</i>) (<i>Epithemia gibba</i>) 115x20 μm</p> 	<p>Pennate Size: 22-300x18-30μm Striae: 30 per 10μm</p> <p>Valves bracket-shaped, bent ventrally at the ends and sharply rounded. Large size range. Parallel striations.</p> <p>Habitat: epipelagic and epiphytic.</p>	<p>Distinctive taxon identified by large size and shape.</p>
<p><i>Rhopalodia operculata</i> (<i>Rhopalodia operculata</i> var. <i>constricta</i>) 25.3x10.2μm</p> 	<p>Pennate Size: 18-52x13-26μm Striae: 16-18 per 10μm Puncta: <45 per 10μm</p> <p>Puncta difficult to resolve with LM. The length to breadth ratio is less than five.</p> <p>Habitat: epipelagic and epiphytic.</p>	<p>This distinctive taxon was identified by the valve shape and ornamentation.</p>
<p><i>Stephanodiscus parvus</i> 5.84μm</p> 	<p>Centric Size: 5-11μm diameter</p> <p>Valves are small and flat with a regular margin. Strutted processes are present on the valve face.</p> <p>Habitat: planktonic.</p>	<p>This species was straightforward to identify due to its characteristic small size.</p>

continued

Synedra acus
(*Fragilaria acus*)
220x5.22µm



Pennate
Size: 27-600x2-9µm
Striae: 7-15 per 10µm

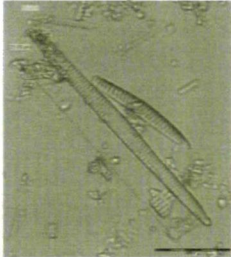
Very long and thin.
Usually larger than 100µm.

Habitat: planktonic and epiphytic.

KLB does not split *S. ulna* and *S. acus*, therefore identifications were based on EDDI illustrations.

S. acus is thinner, appears more delicate and has capitate valve ends in comparison with *S. ulna*.

Synedra ulna
(*Fragilaria ulna*)
71.55x4.78µm



Pennate
Size: 27-600x2-9µm
Striae: 7-15 per 10µm

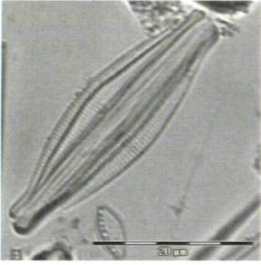
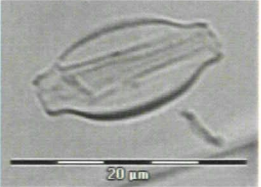
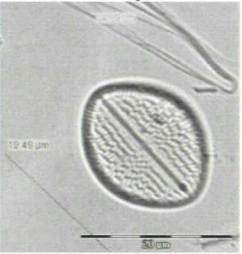

Variable characteristics.
Long and thin.
Usually greater than 100µm long.

Habitat: planktonic and epiphytic.

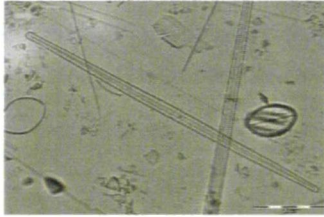
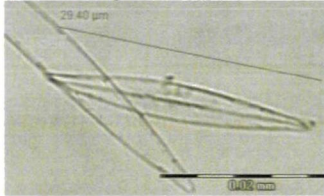
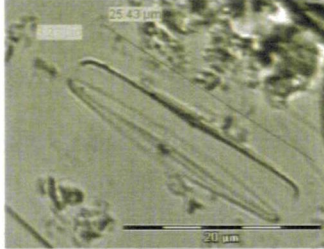
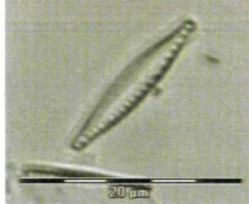
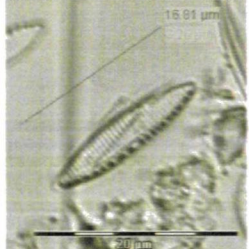
This taxon was distinguished from *S. acus* on the basis on its less delicate structure and the 'ladder' appearance of the striations.

Appendix 2

Kratergöl diatom species assemblage (>3%) with illustrations (not to scale), synonyms, distinguishing features and taxonomic issues.

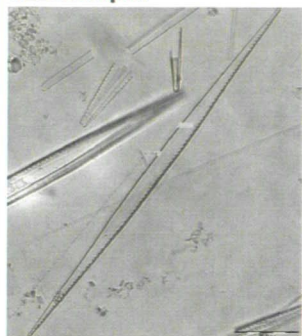
Species illustrations (LM) Typical size of Kratergöl specimens	Distinguishing features (KLB)	Taxonomic issues
<p><i>Amphora coffeaeformis</i> (<i>Frustulia coffeaeformis</i>) 36x4.71µm</p> 	<p>Pennate</p> <p>Size: 13-60x10-19µm Striae: 16-24 per 10µm</p> <p>Striae very finely punctate. Cells with intercalary bands.</p> <p>Habitat: epiphytic, epilithic and epipellic.</p>	<p>This species was initially confused with <i>A. acutisculata</i>. <i>A. coffeaeformis</i> was distinguished by its non-punctate striae appearance.</p>
<p><i>Amphora veneta</i> 15x5.5µm</p> 	<p>Pennate</p> <p>Size: 5-60x7-18µm Striae: 26-32 per 10µm</p> <p>Dorsal striae wider spaced at centre. Striae punctate. Valves have intercalary bands.</p> <p>Habitat: epiphytic, epilithic and epipellic.</p>	<p>This taxon was occasionally confused with <i>A. coffeaeformis</i>. Transitional types between the two species were recognised. Distinctions were based on the smaller size of <i>A. veneta</i>.</p>
<p><i>Cocconeis placentula</i> 19.49x14.99µm</p> 	<p>Pennate</p> <p>Size: 10-80x8-40µm Striae: 18-23 per 10µm</p> <p>Flat appearance with lanceolate central area. Raphe-less valve has >16s with transapically lengthened fine aerolae.</p> <p>Habitat: epiphytic and epilithic.</p>	<p>A few specimens of this species were thought to be <i>C. pediculus</i> (which has an arched appearance). However, it was not possible to consistently distinguish differences, therefore all were grouped as <i>C. placentula</i>.</p>
<p><i>Entomoneis paludosa</i> var. <i>Subsalina</i> (<i>Amphiprora paludosa</i>) 51.56x9.09µm</p> 	<p>Pennate</p> <p>Size: 40-130x20-50µm Striae: 18-23 per 10µm</p> <p>Delicately silicified. Keel not punctate. Striae very delicate in appearance.</p> <p>Habitat: epipellic.</p>	<p>This species was straightforward to identify due to its characteristic shape and ornamentation.</p>

continued

<p><i>Fragilaria fasciculata</i> (<i>Tabularia fasciculata</i>) 93.28x2.98µm</p> 	<p>Pennate Size: 20-400x2-8µm Striae: 7-26 per 10µm</p> <p>Striae short and not punctate. Large axial area.</p> <p>Habitat: epiphytic and planktonic.</p>	<p>This species was distinguished by the characteristic striae length and large size.</p>
<p><i>Navicula complanata</i> 29.4x4.04µm</p> 	<p>Pennate Size: 25-75x4-7.5µm Striae: 20 per 10µm</p> <p>Valve narrow lanceolate with pointed ends.</p> <p>Habitat: epilithic and epipellic.</p>	<p>This species was identified by its characteristic weakly silicified appearance and valve shape.</p>
<p><i>Navicula salinicola</i> 25.43x3.23µm</p> 	<p>Pennate Size: 7-17x2-3µm Striae: 17-20 per 10µm</p> <p>Striae parallel to weakly radial and converge at ends. Small central area.</p> <p>Habitat: epipellic.</p>	<p>The taxonomy of this species was complicated as specimens were often larger than the KLB size range. Therefore valve shape and striae appearance were used as distinguishing features.</p>
<p><i>Nitzschia fonticola</i> 15.81x3.09µm</p> 	<p>Pennate Size: 10-65x2-5µm Striae: 23-33µm Fibulae: 9-16 per 10µm</p> <p>See Appendix 1 for description.</p> <p>Habitat: epipellic and planktonic.</p>	<p>This species was identified as <i>N. fonticola</i> due to the characteristic capitate ends.</p>
<p><i>Nitzschia frustulum</i> 16.81x3.26µm</p> 	<p>Pennate Size: 5-60x2-5µm Striae: 19-30 per 10µm Fibulae: 10-16 per 10µm</p> <p>Lanceolate to linear lanceolate shaped. Ends blunt. Fibulae point-like and broader than the striae.</p> <p>Habitat: epipellic and planktonic.</p>	<p>The taxonomy of this species was complicated by its large size range and the fact that a central pore was not always visible. Smaller specimens without a central pore were split and identified as <i>N. liebethuthii</i>. Larger varieties were grouped as <i>N. frustulum</i>. Gasse (1986) split four morphological types of <i>N. frustulum</i>:</p> <ol style="list-style-type: none">1 – large with equidistant fibulae.2 – small and elliptical with fibulae irregularly spaced and no central pore.3 – small to medium sized, elliptical, and fibulae sometimes equidistant.4 – larger, typical of KLB type.

continued

Nitzschia wuellerstorffii
122x5.57µm



Pennate
Size: 140-250x8-8.5µm
Striae: 30-31.5 per 10µm
Fibulae: 4-7 per 10µm

Valves long and narrow.
Fibulae broad.

Habitat: epipellic and planktonic.

This species was confused with *N. sigma* and was distinguished by the characteristic valve shape.

Rhopalodia constricta
68.93x17.4µm



Pennate
Size: 24-75x15-48µm
Striae: 15-20 per 10µm

Large forms with straight ventral edge
and puncta irregularly arranged on
striae.

Valve outline semi-circular or
lanceolate.

Habitat: epipellic and epiphytic.

This species was straightforward to identify due to the characteristic size, shape and appearance.

Appendix 3

Nar Gölü and Kratergöl diatom species list with cell dimensions and biovolume.

Species without biovolume calculations were too rare in the datasets to derive reliable measurements of cell dimensions. Where different size ranges of the same species were encountered at Nar and Kratergöl both calculations are given.

Species	Biovolume (μm^3)	Surface area (SA) (μm^2)	S.A to vol. ratio (μm)	Height (μm)	Width (μm)	Length (μm)	Radius/centre to bottom
<i>Achnanthes exigua</i> var <i>elliptica</i>	91.925	151.787	1.651	1.83	2.835	5.64	
<i>Achnanthes exigua</i> var <i>exigua</i>	91.925	151.787	1.651	1.83	2.835	5.64	
<i>Achnanthes lanceolata</i> var <i>dubia</i> f <i>minuta</i>	35.951	91.861	2.555	1.07	2.3	4.65	
<i>Achnanthes lanceolata</i> forma <i>frequentissima</i>	134.437	226.899	1.688	1.83	2.455	9.525	
<i>Achnanthes lanceolata</i> var <i>lanceolata</i>	169.088	258.294	1.528	1.83	3.535	8.32	
<i>Achnanthidium minutissimum</i>	37.817	107.046	2.831	1.07	1.5	7.5	
<i>Achnanthes</i> sp				n.a			
<i>Actinocyclus normanii</i>				n.a			
<i>Amphora coffeaeformis</i>	209.08	952.536	4.556	5	2.355	18	
<i>Amphora commutata</i>	1174.853	1541.353	1.312	7	5.15	21.15	
<i>Amphora libyca</i>	716.754	1016.534	1.418	6	4.5	16.9	
<i>Amphora pediculus</i>	82.839	135.704	1.638	3	2.8	5.045	
(Nar) <i>Amphora veneta</i>	202.895	736.989	3.632	4.2	2.5	15.5	
(Kratergöl) <i>Amphora veneta</i>	150.796	265.808	1.763	3.2	3	8	
<i>Anomoeneis sphaerophora</i>	4061.75	2114.993	0.521	6	7.85	27.45	
<i>Asterionella formosa</i>	223.617	530.487	2.372	1.4	1.5	33.895	
<i>Aulacoseira crenulata</i>	402.124	301.593	0.75			8	4
<i>Caloneis bacillum</i>	528.182	538.421	1.019	3.4	3.365	14.695	
<i>Caloneis silicula</i>	720.275	682.536	0.948	3.4	4.05	16.65	
<i>Caloneis</i> sp				n.a			
<i>Campylodiscus clypeus</i>	57019.91	21080.09	0.37			6	55
<i>Cocconeis placentula</i> var <i>euglypta</i>	1100.151	950.843	0.864	3	8.32	14.03	

continued

<i>Cyclotella meneghiniana</i>	904.779	628.319	0.694			4.5	8
<i>Cyclotella ocellata</i>				rare			
<i>Cymbella cystula</i>	597.102	907.266	1.519	4	7.385	30.32	
<i>Cymbella microcephala</i>	12.814	57.562	4.492	1.5	1.89	6.78	
<i>Cymbella pusilla</i>	18.975	109.041	5.746	1	2.405	11.835	
<i>Denticula subtilis</i>	29.713	84.723	2.851	1	1.745	5.42	
<i>Diatoma moniliformis</i>	29.354	84.98	2.895	1	1.645	5.68	
<i>Diatoma tenue</i>	153.431	354.747	2.312	1.4	1.605	21.735	
<i>Entomoneis paludosa v subsalina</i>	1882.206	1406.786	0.747	5.5	7.1	30.685	
<i>Epithemia argus</i>	1550.779	1217.405	0.785	6	6.025	27.31	
<i>Fragilaria brevistriata</i>	168.232	225.069	1.338	2.5	2.8	7.65	
<i>Fragilaria capucina var capitellata</i>	42.849	122.453	2.858	1.145	1.285	9.27	
<i>Fragilaria capucina var gracilis</i>	81.273	250.527	3.083	1.145	1.06	21.315	
<i>Fragilaria capucina var rumpens</i>	100.906	176.445	1.749	1.9	2.1	8.05	
<i>Fragilaria capucina var vaucherie</i>	260.592	388.302	1.49	1.98	3.015	13.895	
<i>Fragilaria construens var exigua</i>	153.371	212.487	1.385	2.05	4.88	4.88	
<i>Fragilaria construens var venter</i>	51.459	94.415	1.835	1.75	2.4	3.9	
<i>Fragilaria elliptica</i>	34.672	66.626	1.922	1.805	2.29	2.67	
(Nar) <i>Fragilaria fasciculata</i>	597.282	1110.844	1.86	1.98	1.665	57.67	
(Kratergöl) <i>Fragilaria fasciculata</i>	481.595	895.778	1.86	1.98	1.665	46.5	
<i>Fragilaria montana</i>	175.504	410.212	2.337	1.3	1.775	24.21	
<i>Fragilaria pulchella</i>	1595.545	1627.723	1.02	3.3	3.425	44.935	
<i>Fragilaria sp</i>				n.a			
<i>Gomphonema gracile</i>	490.098	729.455	1.488	3.7	3.62	25.05	22
<i>Gomphonema olivaceum</i>	194.689	329.524	1.693	3.5	2.49	12	15.86
<i>Gomphonema parvulum</i>	299.743	480.539	1.603	3.2	3.79	13	17.75
<i>Gomphonema sp</i>				n.a			
<i>Gomphonema truncatum</i>	262.701	445.489	1.696	3.19	3.115	15	18.18
<i>Hantzschia amphioxys</i>	567.616	570.304	1.005	3.435	3.43	15.335	
<i>Mastogloia smithii</i>	1342.701	923.691	0.688	4.7	5.73	15.87	
<i>Mastogloia smithii var lacustris</i>	1246.982	928.527	0.745	4.7	4.565	18.5	
<i>Mastogloia sp</i>				n.a			
<i>Clipeoparvus anaticus</i>	113.103	113.13	1				3
<i>Navicula capitata</i>	457.19	482.721	1.056	3.2	3.385	13.435	

continued

<i>Navicula capitata</i> <i>var hungarica</i>	194.06	234.854	1.21	3.2	2.55	7.57	
<i>Navicula cari</i>	535.47	624.376	1.166	2.5	3.965	17.195	
(Nar) <i>Navicula</i> <i>cincta</i>	179.288	274.253	1.53	2.05	2.63	10.585	
(Kratergöl) <i>Navicula cincta</i>	302.145	383.186	1.268	2.5	3.115	12.35	
<i>Navicula</i> <i>clementoides</i>	180.294	262.473	1.456	2	3.325	8.63	
<i>Navicula</i> <i>complanata</i>	282.743	397.77	1.407	2.4	2.5	15	
(Nar) <i>Navicula</i> <i>cryptocephala</i>	139.817	284.886	2.038	1.29	3	11.5	
(Kratergöl) <i>Navicula</i> <i>cryptocephala</i>	391.324	499.63	1.277	2.4	3.255	15.945	
(Nar) <i>Navicula</i> <i>cryptotenella</i>	139.817	284.886	2.038	1.29	3	11.5	
(Kratergöl) <i>Navicula</i> <i>cryptotenella</i>	391.324	499.63	1.277	2.4	3.255	15.945	
<i>Navicula</i> <i>digitoradiata</i>	210.481	296.649	1.409	2	3.745	8.945	
<i>Navicula elkab</i>	215.036	369.338	1.718	1.6	3.1	13.8	
<i>Navicula</i> <i>elginensis</i>	973.126	929.633	0.955	2.8	6.215	17.8	
<i>Navicula halophila</i>	2070.124	1839.724	0.889	3	6.485	33.87	
<i>Navicula</i> <i>laevissima</i>	753.128	786.891	1.045	2.8	4.385	19.525	
<i>Navicula minima</i>	25.34	71.607	2.826	1	1.865	4.325	
<i>Navicula mutica</i>	179.583	251.375	1.4	2.1	3.45	7.89	
<i>Navicula nivalis</i>	198.126	279.365	1.41	2	3.79	8.32	
<i>Navicula oblonga</i>	14520.85	5135.339	0.354	12	7.65	50.35	
<i>Navicula pupula</i>	367.642	503.125	1.369	2	3.975	14.72	
<i>Navicula pupula</i> <i>var nyassensis</i>	239.377	345.798	1.445	2	3.31	11.51	
<i>Navicula</i> <i>pygmaea</i>	250.614	348.249	1.39	2	3.88	10.28	
<i>Navicula radiosa</i>	1584.244	1419.871	0.896	3.3	4.935	30.965	
<i>Navicula</i> <i>salinicola</i>	90.478	201.317	2.225	1.5	1.6	12	
<i>Navicula sp</i>				n.a			
(Kratergöl) <i>Navicula sp24</i>	218.716	275.954	1.262	2.625	2.985	8.885	
<i>Navicula</i> <i>vitabunda</i>	80.919	176.38	2.18	1.3	2.28	8.69	
<i>Nitzschia</i> <i>acidoclinata</i>	43.3	111.547	2.576	1.3	1.385	7.655	
<i>Nitzschia</i> <i>amphibia</i>	300.874	394.899	1.313	2.6	2.65	13.9	
<i>Nitzschia</i> <i>archibaldii</i>	50.967	146.865	2.882	1.2	1.17	11.555	
<i>Nitzschia bacillum</i>				rare			
<i>Nitzschia</i> <i>capitellata</i>	127.235	242.368	1.905	1.8	1.8	12.5	
<i>Nitzschia</i> <i>dissipata var</i> <i>dissipata</i>	43.832	106.751	2.435	1.33	1.855	6.165	
<i>Nitzschia</i> <i>dissipata var</i> <i>media</i>	504.439	850.463	1.686	1.77	2.55	35.575	
<i>Nitzschia</i> <i>elegantula</i>	64.298	127.464	1.982	1.7	1.82	6.615	

continued

<i>Nitzschia etoshensis</i>	143.381	269.74	1.881	1.7	2.03	13.225	
<i>Nitzschia filiformis</i>	2896.265	3180.369	1.098	3	3.28	93.69	
<i>Nitzschia filiformis</i> <i>var conferta</i>	86.688	175.034	2.019	1.7	1.705	9.52	
(Nar) <i>Nitzschia fonticola</i>	47.311	102.277	2.162	1.501	1.79	5.605	
(Kratergöl) <i>Nitzschia fonticola</i>	56.341	138.063	2.45	1.4	1.4	9.15	
<i>Nitzschia fonticola</i> 1	47.311	102.277	2.162	1.501	1.79	5.605	
(Nar) <i>Nitzschia frustulum</i>	76.936	158.585	2.061	1.7	1.625	8.865	
(Kratergöl) <i>Nitzschia frustulum</i>	102.805	196.273	1.909	1.8	1.8	10.1	
<i>Nitzschia frustulum</i> <i>var bulnheimiana</i>	117.822	240.068	2.038	1.7	1.655	13.33	
<i>Nitzschia heufleriana</i>	1203.602	1302.169	1.082	3.305	2.975	38.965	
<i>Nitzschia hungarica</i>	1594.743	1483.694	0.93	3.3	4.395	35	
<i>Nitzschia inconspicua</i>	37.463	86.66	2.313	1.5	1.5	5.3	
<i>Nitzschia inconspicua</i> 1	37.156	85.173	2.292	1.5	1.54	5.12	
<i>Nitzschia incognita</i>	91.439	227.797	2.491	1.5	1.225	15.84	
<i>Nitzschia laevis</i>	48.078	101.683	2.115	1.5	1.925	5.3	
<i>Nitzschia liebruthii</i>	41.469	93.465	2.254	1.5	1.6	5.5	
<i>Nitzschia linearis</i>				rare			
<i>Nitzschia microcephala</i>	52.432	122.851	2.343	1.4	1.58	7.545	
<i>Nitzschia palea</i>	111.024	251.824	2.268	1.5	1.52	15.5	
<i>Nitzschia palea</i> 1	68.094	138.194	2.029	1.7	1.7	7.5	
<i>Nitzschia palea</i> 4	72.612	152.908	2.106	1.7	1.545	8.8	
<i>Nitzschia palea</i> <i>var debilis</i>				rare			
<i>Nitzschia palea</i> <i>var major</i>	305.544	600.618	1.966	1.6	1.98	30.7	
<i>Nitzschia paleacea</i>	59.376	198.86	3.349	1	1.05	18	
<i>Nitzschia peisonis</i>	1731.332	1784.002	1.03	3.3	3.34	50	
<i>Nitzschia pusilla</i>	54.884	123.132	2.243	1.5	1.59	7.325	
<i>Nitzschia scalpelliformis</i>	6359.527	5483.147	0.862	3.1	6.53	100	
<i>Nitzschia sigma</i>	1407.434	1450.508	1.031	3.2	3.5	40	
<i>Nitzschia sigmoidea</i>	1203.602	1302.169	1.082	3.305	2.975	38.965	
<i>Nitzschia sp</i>				n.a			
<i>Nitzschia subinvicta</i>	98.96	199.521	2.016	1.6	1.875	10.5	
<i>Nitzschia thermaloides</i>	145.39	283.636	1.951	1.5	2.325	13.27	
<i>Nitzschia trybionella</i>	5022.54	3970.973	0.791	3	11.79	45.2	
<i>Nitzschia umbonata</i>	1559.368	1630.55	1.046	3	44.18	3.745	
<i>Nitzschia valdecostata</i>	64.782	145.418	2.245	1.6	1.44	8.95	
<i>Nitzschia wuellerstorffii</i>	5163.622	4878.569	0.945	3.805	3.375	127.99	

continued

<i>Pinnularia borealis</i> var <i>rectangularis</i>	601.467	573.597	0.954	3.7	3.52	14.7	
<i>Pinnularia ignobilis</i>	297.827	420.896	1.413	2.315	2.61	15.69	
<i>Pinnularia microstauron</i>	1822.617	1265.465	0.694	4.45	5.99	21.765	
<i>Pinnularia</i> sp				n.a			
<i>Pinnularia viridis</i>	44628.69	10338.85	0.232	15.5	14.1	65	
<i>Rhoicosphenia abbreviata</i>	357.459	485.487	1.358	4.6	2.95	17	16.6
<i>Rhopalodia constricta</i>	4243.271	2275.3	0.536	9	8.7	34.5	
<i>Rhopalodia gibba</i>	7761.359	4055.11	0.522	8.7	4.85	58.55	
<i>Rhopalodia operculata</i>	664.447	592.419	0.892	4.7	6	15	
<i>Rhopalodia</i> sp				n.a			
<i>Stauroneis anceps</i>				rare			
<i>Stephanodiscus alpinus</i>	970.929	1028.736	1.06			2.5	11.72
<i>Stephanodiscus minutulus</i>	75.398	138.23	1.833			1.5	4
<i>Stephanodiscus parvus</i>	26.786	71.92	2.685			1	2.92
<i>Stephanodiscus</i> sp				n.a			
<i>Synedra acus</i>	775.094	1891.525	2.44	1.285	1.6	120	
<i>Synedra ulna</i>	1717.924	2338.386	1.361	2.6	2.39	88	
<i>Synedra af ulna</i>	1717.924	2338.386	1.361	2.6	2.39	88	
<i>(Kratergöf) sp31</i>	753.982	774.507	1.027	3	4	20	

Appendix 4.1

NAR06 DCA ordination plots with sample symbol size weighted to the percentage of different diatom species.

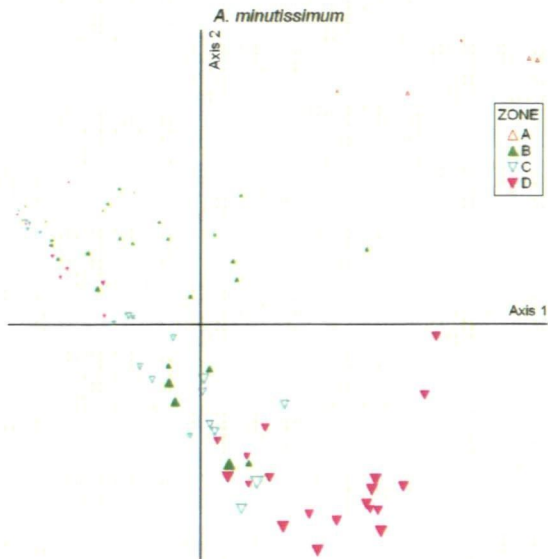


Figure a

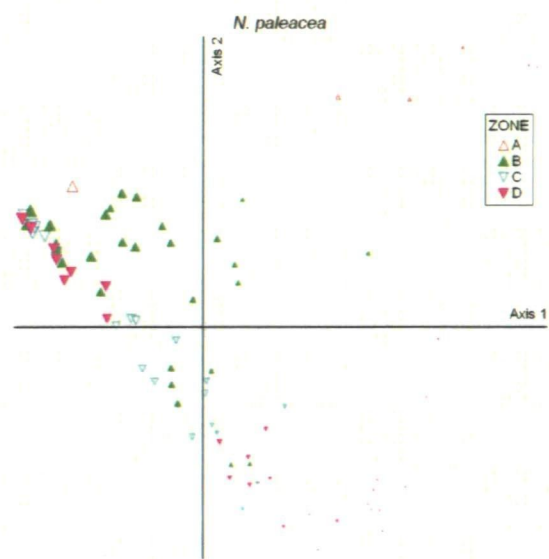


Figure b

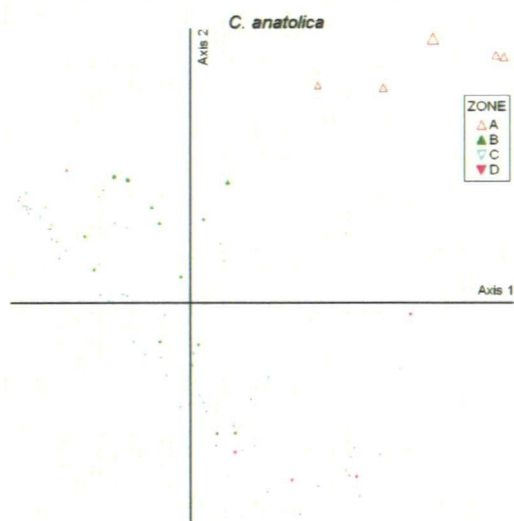


Figure c

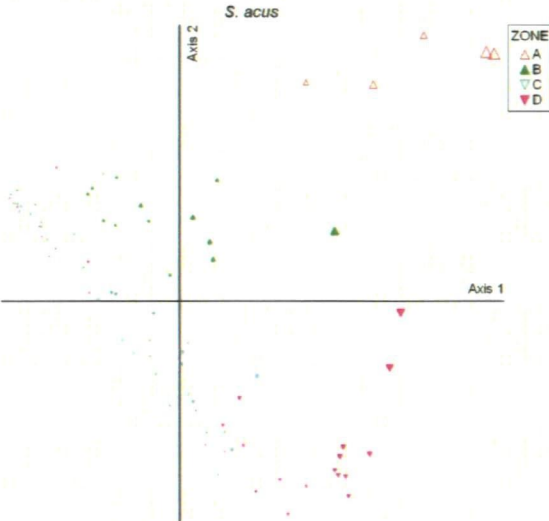
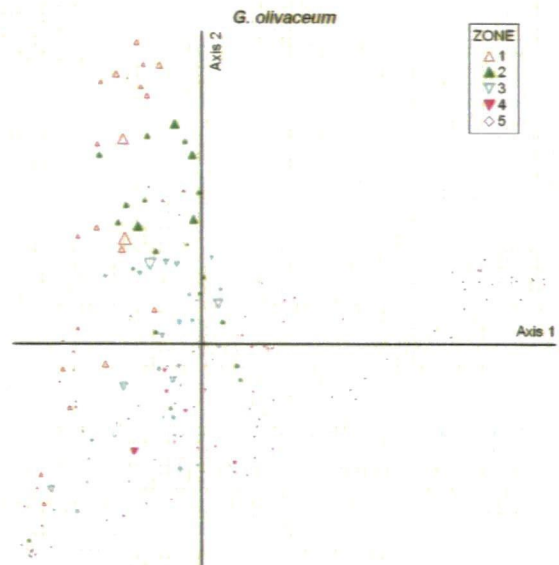
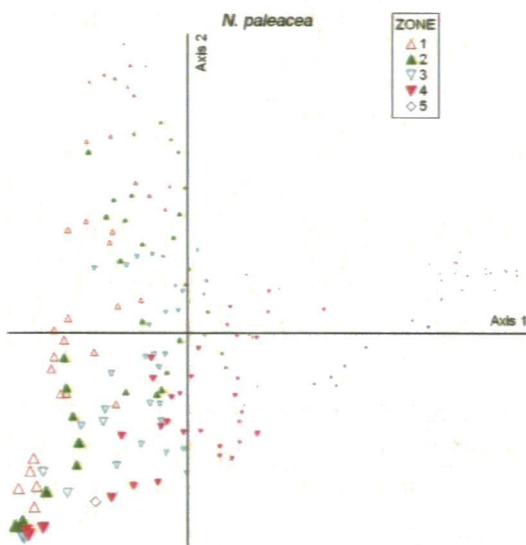
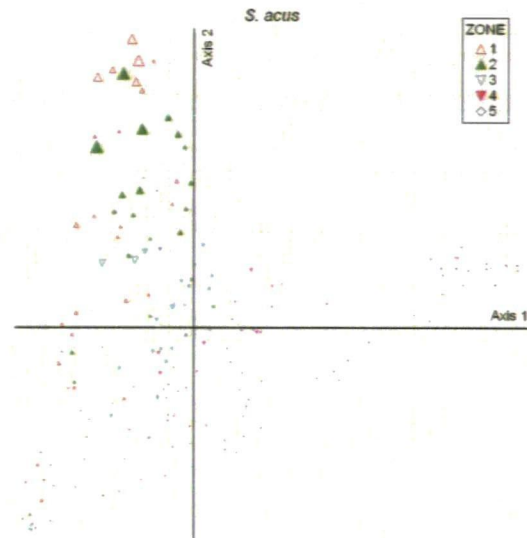
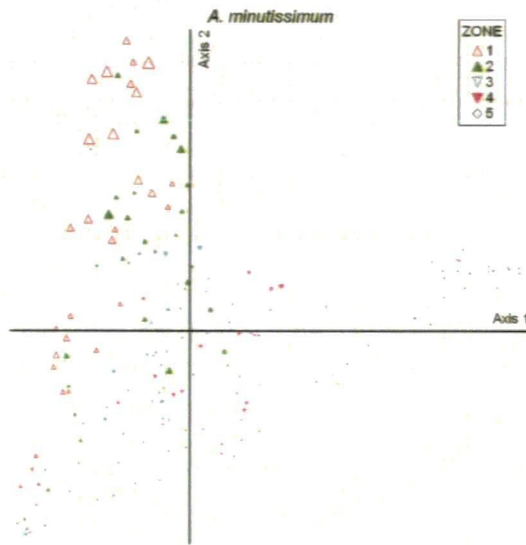


Figure d

Appendix 4.2

NAR01/02 DCA ordination plots with sample symbol size weighted to the percentage of different diatom species.



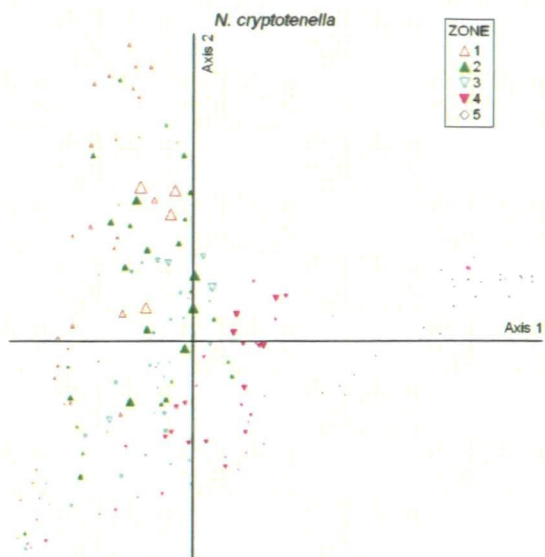


Figure e

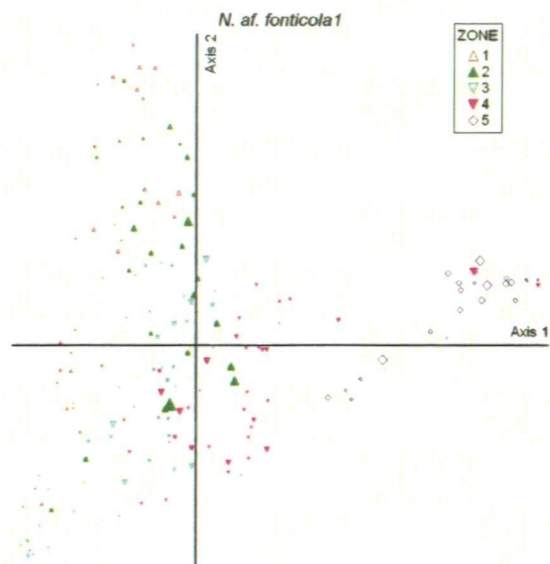


Figure f

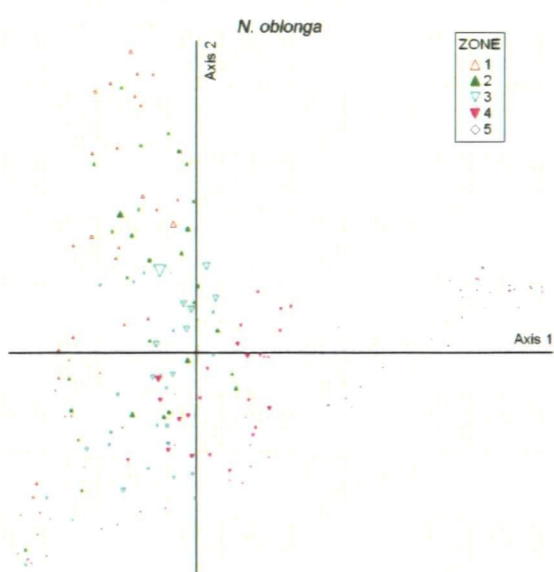


Figure g

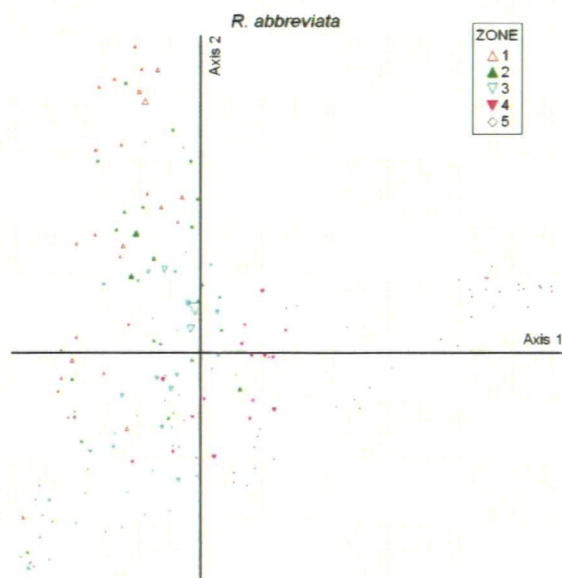


Figure h

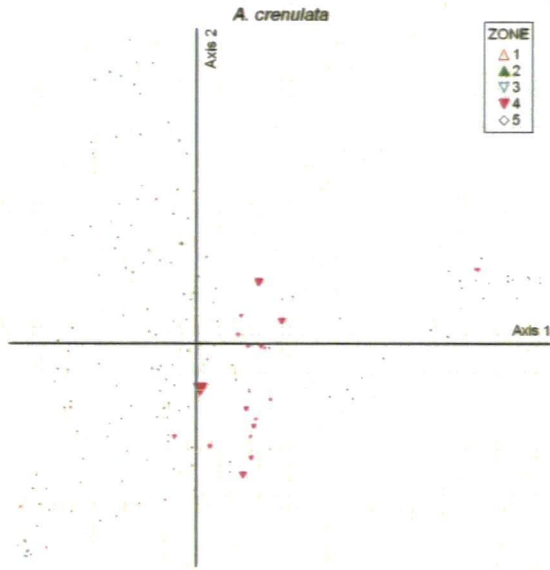


Figure i

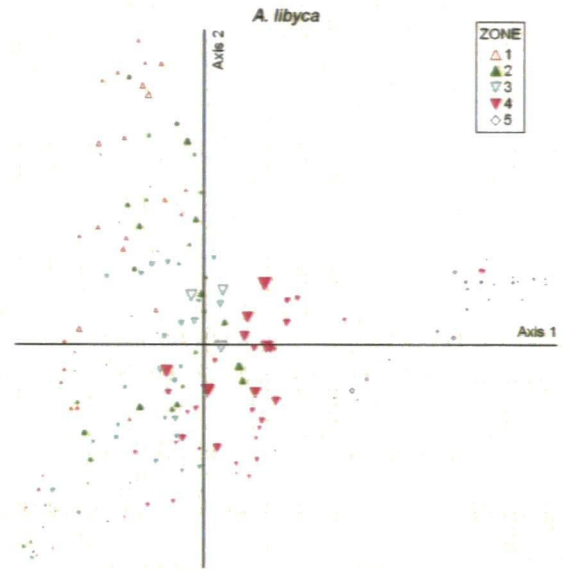


Figure j

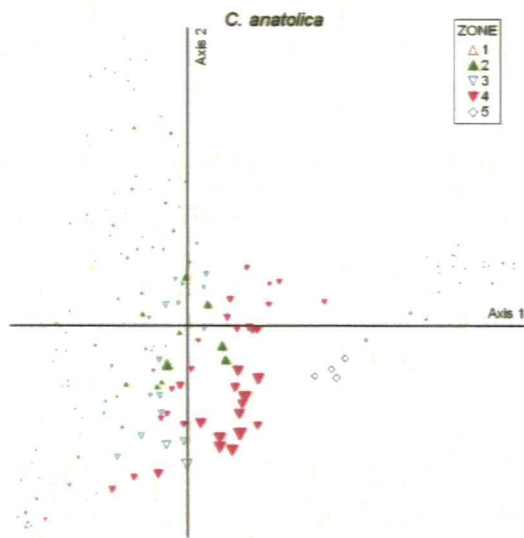


Figure k

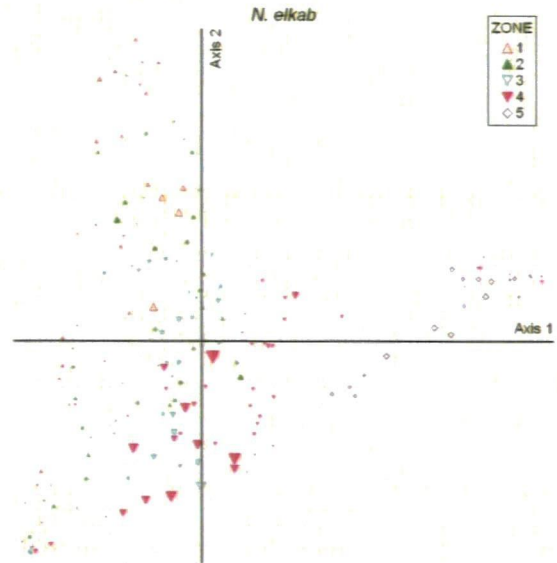


Figure l

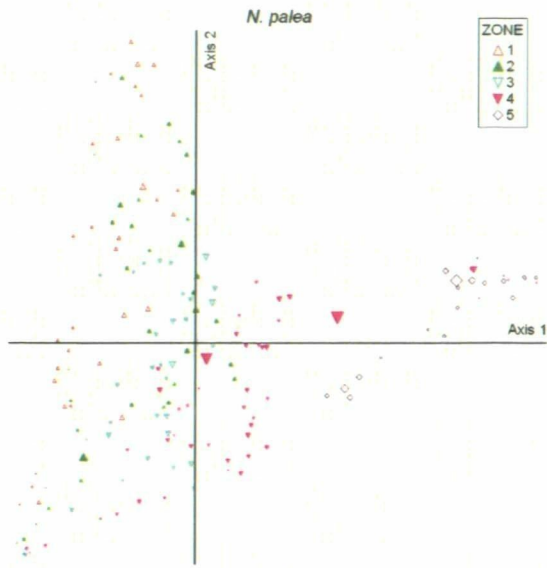


Figure m

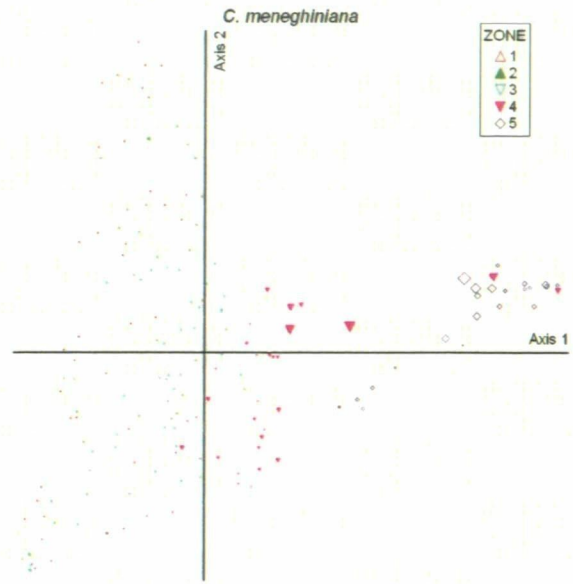


Figure n

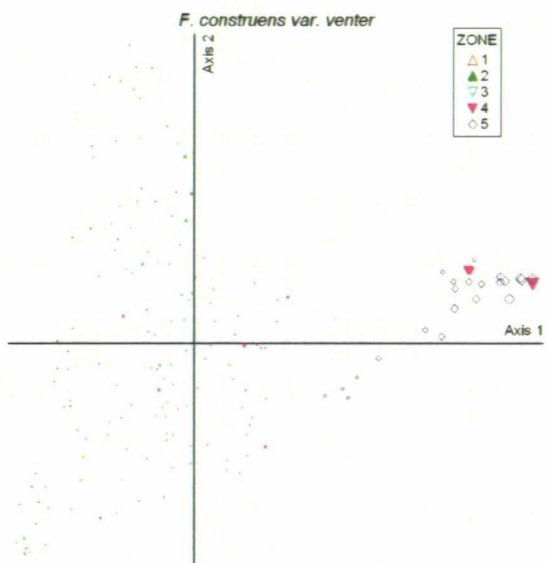


Figure o

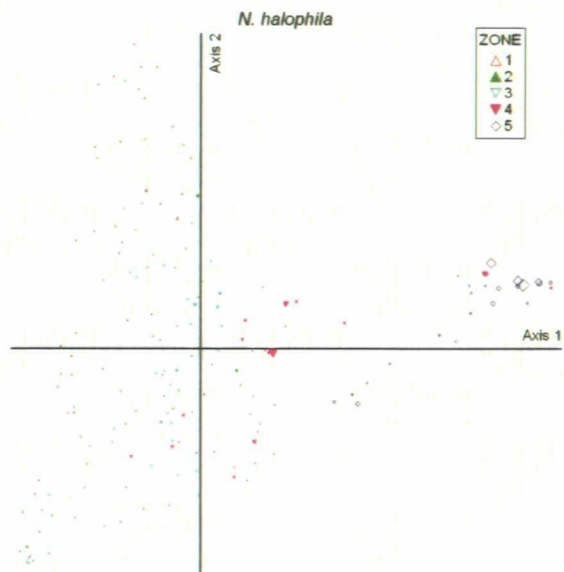


Figure p

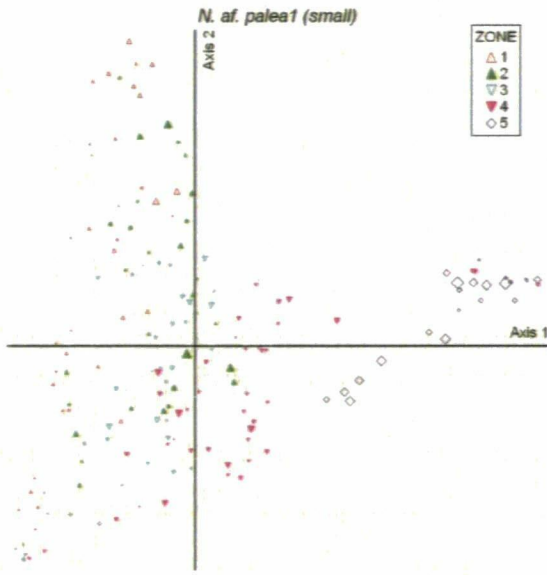


Figure q

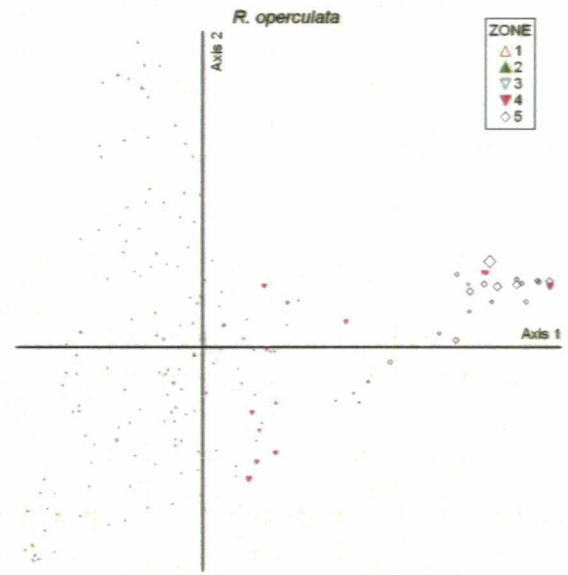


Figure r

Appendix 4.3

Kratergöl ACM99 DCA ordination plots with sample symbol size weighted to the percentage of different taxa.

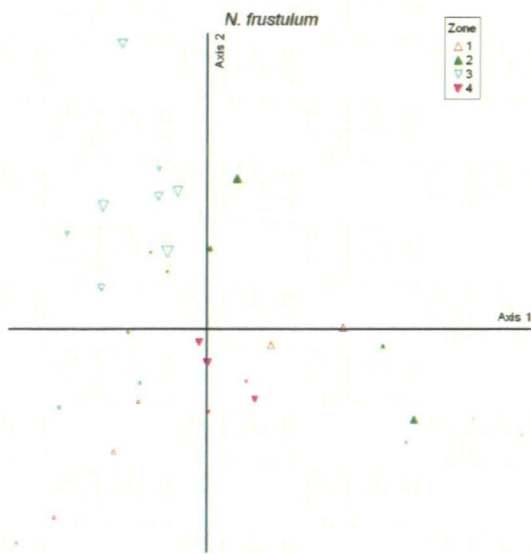


Figure a

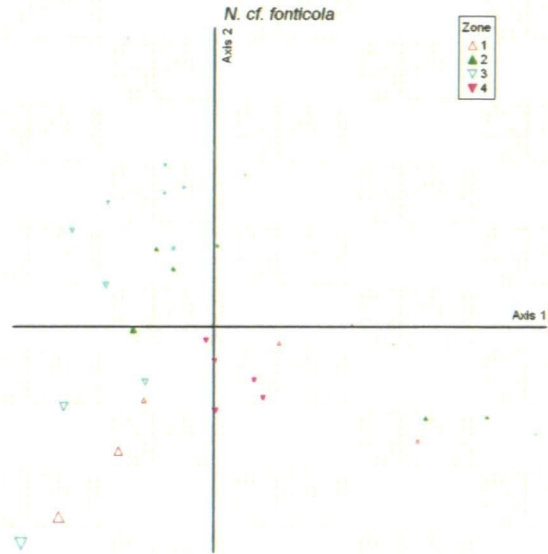


Figure b

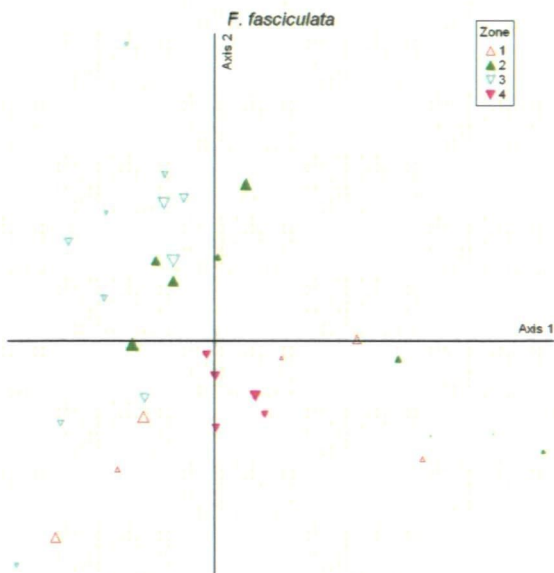


Figure c

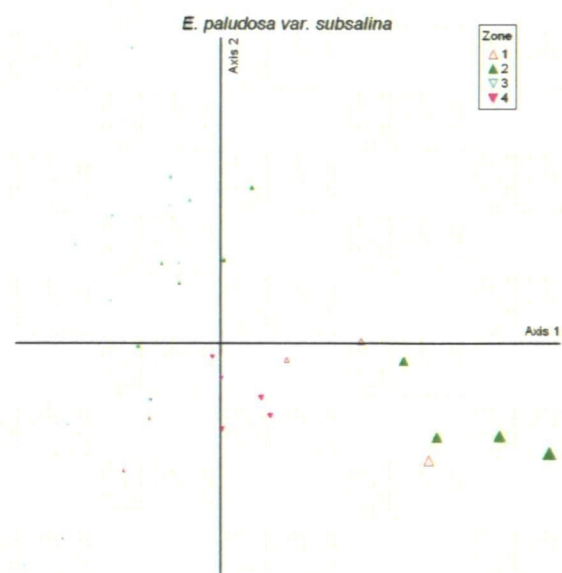


Figure d

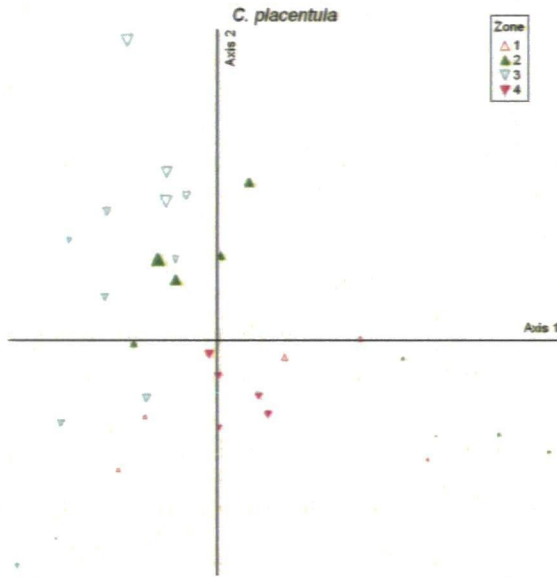


Figure e

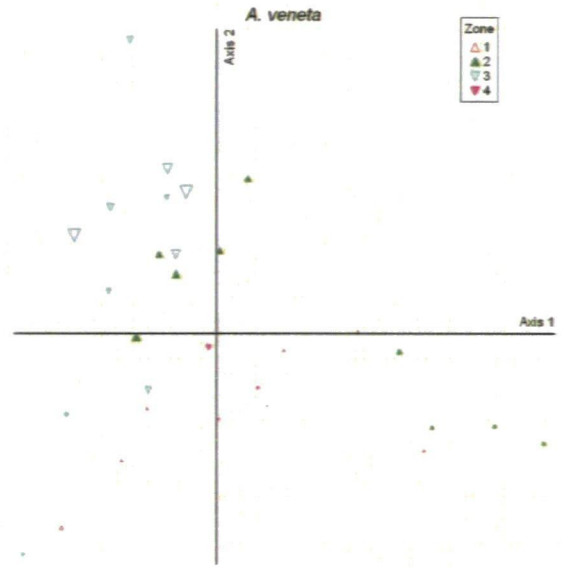


Figure f

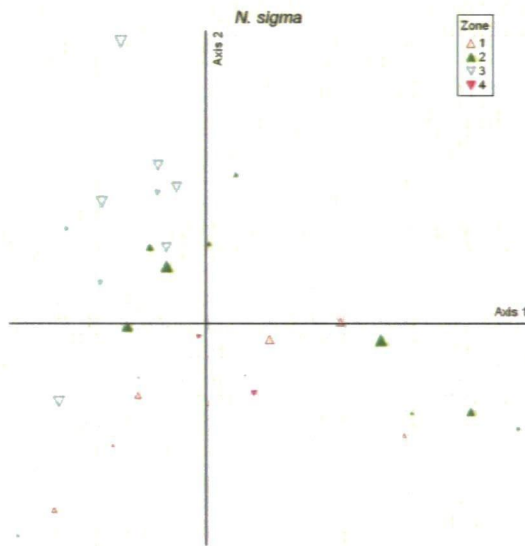


Figure g

Appendix 5.1

NAR01/02 minimum dissimilarity coefficient (min. DC) values for the combined salinity and TP reconstructions based on datasets from EDDI with number of matching analogues.

Depth VY	Combined salinity		Combined TP	
	Min. DC	Matching analogues	Min. DC	Matching analogues
1	111.035	No good	117.481	No close
10	111.845	No good	113.547	No close
20	112.382	No good	115.171	No close
30	109.179	No good	109.606	No close
40	95.6255	Good	110.253	No close
50	104.756	Good	114.261	No close
60	101.627	Good	114.974	No close
70	91.4585	Good	108.115	No close
80	78.6024	Good	103.357	No close
90	89.2522	Good	108.867	No close
100	70.7577	Good	111.768	No close
120	78.0368	Good	100.176	No close
130	108.677	Good	107.211	No close
140	106.474	Good	108.52	No close
150	110.34	No good	112.251	No close
160	105.673	No good	113.182	No close
170	97.8772	Good	105.511	No close
180	117.115	No good	107.213	No close
190	115.96	No good	106.249	No close
200	111.482	No good	99.9591	No close
210	79.0358	Good	106.202	No close
220	92.0156	Good	111.052	No close
230	98.0967	Good	108.769	No close
240	71.2192	Good	105.069	No close
250	114.058	No good	101.848	No close
260	66.2433	Good	109.036	No close
270	107.34	Good	113.706	No close
280	106.169	Good	120.702	No close
290	96.9587	Good	116.787	No close
300	114.986	No good	126.911	No close
310	123.182	No close	99.5048	No close
320	120.237	No good	109.162	No close
330	106.898	Good	116.742	No close
340	110.067	No good	106.205	No close
350	124.12	No close	108.765	No close
360	87.9487	Good	127.133	No close
370	107.958	Good	122.967	No close
380	102.632	Good	128.526	No close
390	108.049	Good	111.979	No close
400	105.617	Good	115.432	No close
410	110.028	No good	117.238	No close
420	110.84	No good	118.677	No close
430	101.248	Good	110.399	No close
440	71.4496	Good	114.758	No close
450	102.069	Good	106.181	No close
460	122.172	No close	118.745	No close
470	115.617	No good	106.904	No close
480	113.834	No good	110.765	No close
490	94.669	Good	111.136	No close

continued

500	92.0337	Good	122.825	No close
510	123.907	No close	107.099	No close
520	107.58	Good	114.998	No close
530	113.288	No good	106.012	No close
540	119.201	No good	115.777	No close
550	109.712	No good	116.984	No close
560	121.096	No close	117.9	No close
570	113.824	No good	129.197	No close
580	127.852	No close	129.256	No close
590	134.97	No close	122.747	No close
600	132.282	No close	125.361	No close
610	129.498	No close	133.618	No close
620	125.446	No close	112.207	No close
630	109.585	No good	122.241	No close
640	97.1499	Good	122.71	No close
650	132.778	No close	118.487	No close
660	126.985	No close	118.505	No close
670	126.435	No close	109.626	No close
680	114.962	No good	114.541	No close
690	94.3334	Good	118.342	No close
700	107.013	Good	116.932	No close
710	117.127	No good	105.957	No close
720	119.294	No good	111.479	No close
730	66.9612	Good	86.3855	No close
740	86.2842	Good	95.4753	No close
750	96.9299	Good	106.518	No close
760	172.191	No close	23.6167	Good
770	176.912	No close	17.0937	Good
780	124.547	No close	106.76	No close
790	109.005	No close	123.452	No close
800	123.234	No close	113.739	No close
810	110.136	No good	106.949	No close
820	127.437	No close	122.624	No close
830	127.52	No close	118.753	No close
840	122.75	No close	111.248	No close
850	143.017	No close	139.779	No close
860	124.215	No close	117.96	No close
870	120.869	No good	113.33	No close
880	125.878	No close	121.945	No close
890	127.839	No close	121.64	No close
900	126.787	No close	123.389	No close
910	123.366	No close	120.884	No close
920	118.211	No good	120.671	No close
930	128.017	No close	114.056	No close
940	130.481	No close	119.516	No close
950	119.93	No good	106.518	No close
960	114.973	No good	110.253	No close
970	123.975	No close	132.106	No close
980	135.717	No close	123.78	No close
990	124.933	No close	130.132	No close
1000	119.801	No good	128.691	No close
1010	107.047	Good	118.573	No close
1020	128.56	No close	119.387	No close
1030	115.509	No good	124.551	No close
1040	126.901	No close	132.889	No close
1050	130.155	No close	125.414	No close
1060	108.486	Good	121.883	No close
1070	105.357	Good	114.057	No close
1080	120.334	No good	127.642	No close
1090	126.355	No close	119.915	No close
1100	108.665	Good	117.282	No close
1110	111.929	No good	100.679	No close

1120	128.648	No close	120.694	No close
1130	129.13	No close	133.407	No close
1140	141.554	No close	144.286	No close
1150	121.559	No close	121.877	No close
1160	131.001	No close	123.735	No close
1170	132.52	No close	128.038	No close
1180	119.68	No good	127.708	No close
1190	108.194	Good	115.241	No close
1200	121.033	No close	133.196	No close
1210	118.842	No good	133.532	No close
1220	111.248	No good	122.686	No close
1230	127.725	No close	130.187	No close
1240	123.764	No close	114.771	No close
1250	115.661	No good	134.752	No close
1260	131.853	No close	128.229	No close
1270	145.616	No close	139.583	No close
1280	135.684	No close	141.638	No close
1290	128.614	No close	144.014	No close
1300	135.288	No close	131.14	No close
1310	114.37	No good	131.035	No close
1320	141.163	No close	133.13	No close
1340	131.929	No close	132.789	No close
1350	135.893	No close	134.117	No close
1360	128.558	No close	120.597	No close
1370	117.658	No good	132.012	No close
1380	133.154	No close	127.339	No close
1390	118.396	No good	139.776	No close
1400	130.402	No close	143.755	No close
1410	144.717	No close	144.641	No close
1420	146.471	No close	138.053	No close
1430	148.034	No close	139.481	No close
1440	139.466	No close	132.982	No close
1450	109.484	No good	139.08	No close
1460	128.318	No close	118.845	No close
1470	117.362	No good	102.849	No close
1480	141.234	No close	103.515	No close
1490	134.672	No close	85.6772	No close
1500	137.861	No close	93.2209	No close
1510	141.011	No close	92.9062	No close
1520	138.797	No close	128.669	No close
1530	125.027	No close	94.752	No close
1540	134.555	No close	104.784	No close
1550	140.112	No close	105.278	No close
1560	133.084	No close	104.302	No close
1570	133.24	No close	107.393	No close
1580	131.547	No close	103.511	No close
1590	133.096	No close	91.8214	No close
1600	147.979	No close	124.683	No close
1610	138.698	No close	129.065	No close
1620	144.208	No close	132.101	No close
1630	135.817	No close	127.242	No close
1640	134.518	No close	128.716	No close
1650	139.82	No close	116.367	No close
1660	121.441	No close	113.297	No close
1670	107.654	No good	110.589	No close
1680	121.81	No close	102.016	No close
1690	111.489	No good	105.679	No close
1700	123.26	No close	109.147	No close
1710	93.3248	Good	115.919	No close
1720	97.0393	Good	115.014	No close

Appendix 5.2

NAR06 min. DC values for the combined salinity and TP reconstructions based on datasets from EDDI with number of matching analogues.

Depth VY	Combined salinity		Combined TP	
	Min. DC	Matching analogues	Min. DC	Matching analogues
1	78.5902	Good	127.916	No close
2	62.1851	Good	127.645	No close
3	59.4266	Good	123.803	No close
4	87.9002	Good	135.554	No close
5	106.664	Good	126.456	No close
6	110.758	No good	122.759	No close
7	116.397	No good	115.226	No close
8	115.426	No good	103.666	No close
9	117.089	No good	115.918	No close
10	107.542	No good	115.716	No close
11	111.684	No good	109.109	No close
12	111.675	No good	106.23	No close
13	77.1584	Good	119.718	No close
14	104.784	Good	118.521	No close
15	110.848	No good	119.721	No close
16	109.267	No good	111.467	No close
17	111.995	No good	112.012	No close
18	107.764	Good	118.463	No close
19	121.196	No close	120.96	No close
20	118.319	No good	115.099	No close
21	101.323	Good	114.881	No close
22	102.835	Good	110.503	No close
23	101.932	Good	116.388	No close
24	104.717	Good	106.406	No close
25	115.509	No good	118.824	No close
26	108.541	Good	109.722	No close
27	103.975	Good	105.574	No close
28	114.39	No good	109.729	No close
29	93.4223	Good	106.373	No close
30	99.3179	Good	106.629	No close
31	102.312	Good	116.098	No close
32	106.559	Good	120.585	No close
33	102.882	Good	113.691	No close
34	98.9895	Good	107.062	No close
35	109.163	No good	110.93	No close
36	109.488	No good	105.286	No close
37	90.9485	Good	111.57	No close
38	101.9	Good	116.269	No close
39	111.878	No good	98.5196	No close
40	107.197	Good	107.217	No close
41	80.1221	Good	105.153	No close
42	95.2939	Good	109.052	No close
43	93.2009	Good	99.4843	No close
44	110.22	No good	101.287	No close
45	103.077	Good	112.51	No close
46	105.075	Good	113.407	No close
47	103.66	Good	117.648	No close
48	102.78	Good	116.603	No close
49	122.979	No close	119.831	No close
50	113.868	No good	112.708	No close
51	107.355	Good	118.827	No close
52	95.4359	Good	104.355	No close
53	105.279	Good	106.852	No close
54	89.2999	Good	107.417	No close
55	109.016	No good	108.667	No close
56	88.9445	Good	108.884	No close
57	64.0403	Good	106.075	No close
58	83.3108	Good	103.65	No close

continued

59	76.2765	Good	101.064	No close
60	76.2108	Good	99.9549	No close
61	110.877	No good	120.345	No close
62	107.723	Good	115.014	No close
63	107.084	Good	119.867	No close
64	106.235	Good	114.873	No close
65	106.547	Good	111.403	No close
66	108.999	Good	117.5	No close
67	112.489	No good	121.36	No close
68	113.287	No good	122.46	No close
69	104.216	Good	114.076	No close
70	111.317	No good	110.304	No close
71	106.419	Good	117.472	No close
72	88.1242	Good	107.948	No close
73	105.193	Good	110.934	No close
74	102.46	Good	108.831	No close
75	92.7832	Good	117.717	No close
76	94.8761	Good	114.474	No close
77	73.7423	Good	109.296	No close
78	88.0998	Good	108.106	No close
79	57.8272	Good	103.755	No close
80	89.9635	Good	111.81	No close

Appendix 5.3

Kratergöl ACM99 min. DC and number of matching analogues based on the EDDI combined salinity and TP training sets.

Depth cm	Combined salinity		Combined TP	
	Min. DC	Matching analogues	Min. DC	Matching analogues
0	111.246	No good	136.846	No close
1	121.73	No close	153.193	No close
2	108.552	Good	142.037	No close
4	109.81	No good	137.532	No close
6	119.422	No good	141.61	No close
8	127.226	No close	150.119	No close
10	135.625	No close	155.826	No close
12	132.431	No close	152.459	No close
14	126.133	No close	149.298	No close
16	135.543	No close	156.451	No close
18	99.1462	Good	125.069	No close
20	94.6843	Good	124.745	No close
22	86.8778	Good	121.805	No close
24	105.234	Good	134.053	No close
26	100.601	Good	130.28	No close
28	105.181	Good	131.776	No close
30	106.805	Good	131.464	No close
32	92.4229	Good	125.927	No close
34	80.6843	Good	120.841	No close
36	100.948	Good	132.741	No close
38	102.912	Good	135.732	No close
40	102.303	Good	141.695	No close
42	92.3914	Good	124.309	No close
44	105.307	Good	145.917	No close
46	100.108	Good	134.644	No close
48	99.9972	Good	133.524	No close
50	109.16	No good	135.119	No close
52	107.717	Good	137.427	No close
54	108.988	Good	138.942	No close
56	107.982	Good	137.843	No close
58	105.368	Good	134.946	No close

Appendix 6.1

Nar Gölü diatom species (>5%) habitat, salinity and ecological preferences.

Species	Habitat	Conductivity optimum (EDDI) (μS^{-1})	Ecological preferences
Nar Gölü			
<i>Achnanthydium minutissimum</i>	Attached benthic Epiphytic on algae or macrophytes Common in plankton and periphyton Widespread and abundant	Fresh/brackish Low to moderate salinity Optimum conductivity 1,044	Circumneutral/alkaline/ weakly acidic Eutrophic-dystrophic, moderate nutrient levels Well-oxygenated water
<i>Amphora libyca</i>	Attached or non-attached periphyton Colonises mud at the edges of ponds Widely distributed	Brackish/fresh Medium/low conductivity Optimum conductivity 3,541	Alkaliphilous and calciphilous Tolerant of mild pollution Favours dilute waters
<i>Aulacoseira crenulata</i>	Cells linked, non-attached Planktonic Entangled among macrophytes	Freshwater Optimum conductivity 139	Common in spring plankton when silica levels are high
<i>Asterionella formosa</i>	Solitary or forms colonies Freely motile Planktonic	Freshwater Optimum conductivity 800	Mesotrophic and eutrophic water Alkaliphilous Typical in plankton spring bloom
<i>Craticula halophila</i>	Motile in periphyton Thermal springs	Brackish Oligohalobous-indifferent Tolerates high salinity Optimum conductivity 5,639	Tolerant of moderate pollution Alkaliphilous Various mineral content, high sodium carbonate content Temperatures up to 50°C
<i>Cyclotella meneghiniana</i>	Solitary cells, non-attached Floating or freely motile Plankton or littoral Fairly widespread	Brackish Halophilous, oligohaline to mesohaline Wide salinity range Optimum conductivity 6,599	Wide range of alkalinity and pH Medium to high mineral content Nitrogen rich waters Eurythermal, tolerates hot springs Also in freshwater, pollution indicator (Reed, <i>per. comm.</i>)
<i>Cymbella microcephala</i>	Epilithon, epiphytic or benthic	Fresh/brackish Oligohalobous-indifferent Optimum conductivity 1,607	Low nutrient concentrations Aerophilous Alkaliphilous Tolerant of chloride and mild pollution
<i>Epithemia argus</i>	Solitary or short chains Attached to macrophytes, epiphyton, epilithon, periphyton	Varied, fresh/brackish Optimum conductivity 1,590	Various chemical conditions Neutral to high pH
<i>Fragilaria brevistriata</i>	Facultative plankton or periphyton in shallow lakes	Sometimes tolerates high salinity Optimum conductivity 1,193	Varied ecological conditions Dilute, circumneutral to slightly alkaline waters of different chemical types Associated with disturbance

continued			
<i>Fragilaria construens</i> var. <i>venter</i>	Wide distribution Pioneering species in shallow lakes and freshwater springs	Freshwater Optimum conductivity 633	Favours freshwaters of medium pH and alkalinity Tolerates wide range of chemical conditions Associated with disturbance
<i>Gomphonema olivaceum</i>	Solitary cells Epiphytic	Fresh Optimum conductivity 131	Tolerant of pollution Circumneutral pH
<i>Clipeoparvus anatolicus</i>	Non-chain forming and non-planktonic	Modern Nar Gölü conductivity ~3,300	Typical of modern conditions at Nar Gölü: Circumneutral pH and brackish
<i>Navicula cryptotenella</i>	Solitary, non-attached Motile Epiphytic, often colonises biofilms on rocks	Fresh/brackish Optimum conductivity 5,136	Eutrophic and alkaliphilous
<i>Navicula digitoradiata</i>	Solitary, non-attached Motile Thermal springs	Brackish, mesohalobous or euryhalobous Optimum conductivity 2,418	Tolerant of pollution Alkaliphilous Temperatures up to 33.5°C
<i>Navicula elkab</i>	Periphyton or plankton Thermal springs	Saline water Optimum conductivity 14,844	Indicates strongly saline/alkaline waters
<i>Navicula oblonga</i>	Solitary, non-attached Epipelagic/plankton	Oligohalobous, fresh/slightly brackish Optimum conductivity 2,671	Alkaliphilous High mineral content Sensitive to pollution
<i>Nitzschia amphibia</i>	Solitary or colonies Non-attached Widespread, epipelagic or planktonic, found in literal mud of freshwater lakes and hot springs	Fresh/brackish Oligohalobous, can tolerate high salt content and fluctuating osmotic pressure Optimum conductivity 633	Leptomeshalobous, in water of various chemical types Euryhalobous-indifferent to ionic ratios Alkaliphilous or alkalibiontic, Favours high nutrient levels and tolerates pollution
<i>Nitzschia capitellata</i>	Solitary, motile, non-attached Benthic	Brackish Optimum conductivity 3,079	High acidity Alkaliphilous Tolerant of heavy metal and organic pollution
<i>Nitzschia fonticola</i>	Solitary, motile, non-attached Benthic, plankton, and periphyton	Fresh/brackish Optimum conductivity 7,436	Variety of habitats, water chemistry and temperatures Alkaline and meso/eutrophic waters Tolerates pollution
<i>Nitzschia inconspicua</i>	Solitary, non-attached Motile Benthic	Brackish/fresh Optimum conductivity 4,439	Pollution tolerant and alkaliphilous

continued

<i>Nitzschia palea</i>	Solitary, non-attached Motile Benthic, common epipelagic, epilithic or epiphytic species	Tolerates wide range of conductivity Fresh/brackish Optimum conductivity 1,093	Tolerates wide range of pH, alkalinities, and temperatures Favours circumneutral to slightly alkaline water Found in water of various chemical types Indicator of eutrophic conditions Favours very high nutrient levels and tolerant of heavy pollution
<i>Nitzschia paleacea</i>	Solitary or linked cells Motile Periphyton, bottom mud, epiphytic, epipelagic or planktonic	Oligohalobous Fresh/brackish Optimum conductivity 240	Cosmopolitan Alkaliphilous Low to medium pH Pollution tolerant Eutrophic
<i>Pinnularia viridis</i>	Solitary cells, non-attached Floating or freely motile	Oligohalobous-indifferent Optimum conductivity 242	pH indifferent - circumneutral High mineral content
<i>Rhoicosphenia abbreviata</i>	Filamentous or stalked Epiphytic, epilithic or epipelagic In bottom mud of shallow lakes	Freshwater or brackish Oligohalobous or halophilous Optimum conductivity 1,828	Alkaliphilous Eutrophic
<i>Rhopalodia gibba</i>	Cells solitary, attached or free-living. Epipelagic and epiphytic.	Moderate to high conductivity Optimum conductivity: 916	Favours oligotrophic, alkaline water of carbonate-bicarbonate type
<i>Rhopalodia operculata</i>	Solitary, attached or periphytic forms Free-living in epilimon	Brackish and saline Optimum conductivity - only 2 occurrences at 6.3 and 40	Freshwater specimens are found in high pH water
<i>Stephanodiscus parvus</i>	Cells form chains Common planktonic species	Freshwater Optimum conductivity 1,170	Typical in spring plankton Common in nutrient-rich water
<i>Synedra acus</i>	Non-attached Typically epiphytic Also in plankton and bottom mud	Fresh/brackish Dilute conditions Oligohalobous-indifferent Optimum conductivity 272	Tolerant of mild pollution Alkaliphilous
<i>Synedra capucina var. rumpens</i>	Linked cell to cell, non attached, non-motile Floating or freely-motile	Fresh Optimum conductivity 1,617	Circumneutral water Low to moderate nutrient levels Twisted varieties tolerant to heavy metals
<i>Synedra ulna</i>	Non-attached Widespread Free-living or epiphytic Also in periphyton and plankton	Fresh/brackish Oligohalobous indifferent, Low conductivity Optimum conductivity 272	Tolerant of moderate pollution Alkaliphilous Eutrophic, eurythermal, mesohaline and euryonic Water of carbonate-bicarbonate type

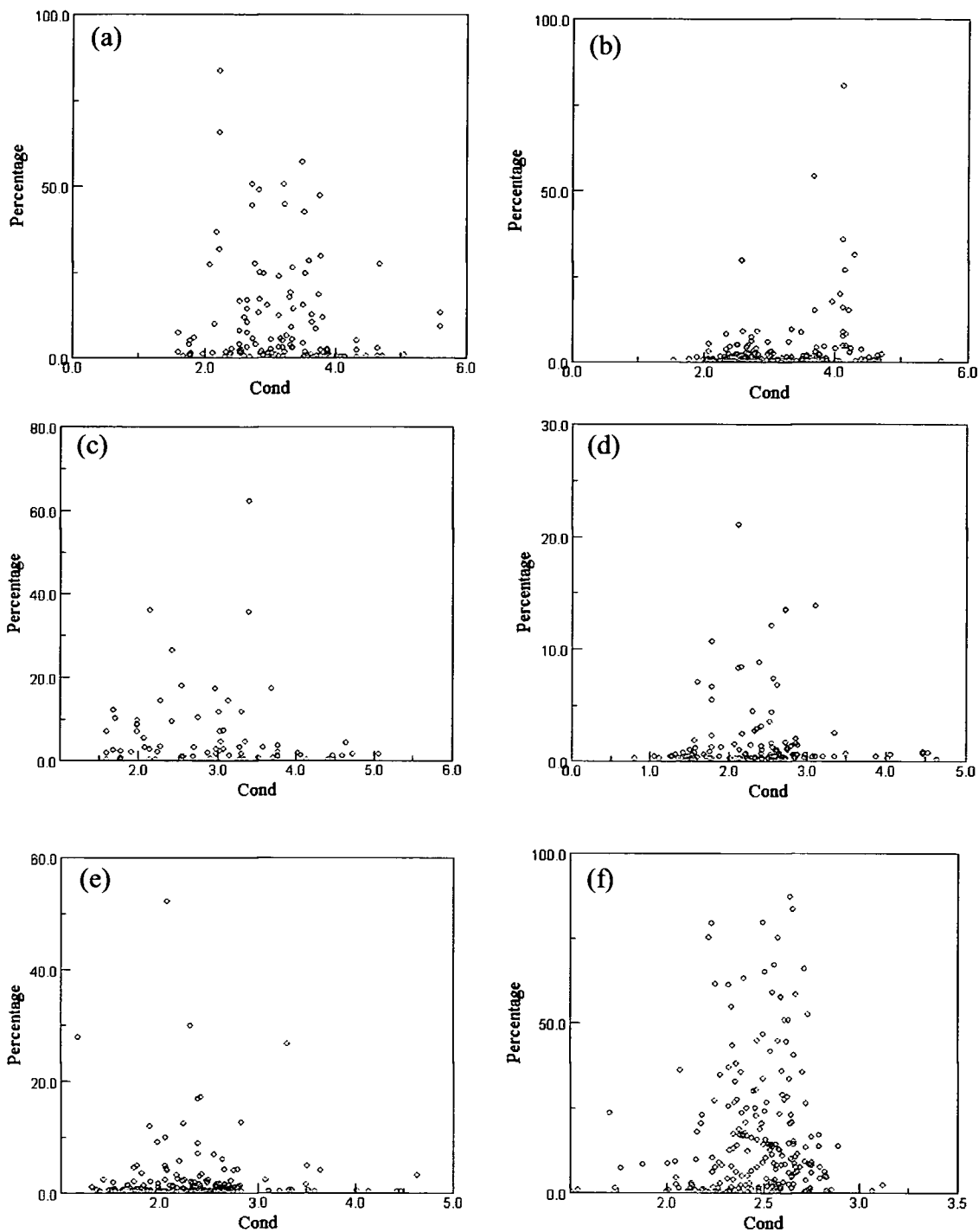
Appendix 6.2

Kratergöl diatom species (>3%) habitat, salinity and ecological preferences.

Species	Habitat	Conductivity optimum (EDDI) (μS^{-1})	Ecological preferences
Kratergöl			
<i>Amphora coffeaeformis</i>	Epiphytic, epilithic or epipelagic Found in hot springs	Medium to high conductivity Optimum conductivity 10,753	High mineral content, in sodium chloride and carbonate water Circumneutral pH Eurythermal - temperature up to 44°C
<i>Amphora veneta</i>	Non-attached Widely distributed in lake periphyton Epipelagic, epiphytic or epilithic in springs	Brackish/saline Optimum conductivity 2,773	Tolerant of organic pollution Alkalibiontic
<i>Cocconeis placentula</i>	Solitary cells, attached to plants and rocks Motile Widely-distributed Fast-growing, pioneer species Benthic - periphyton, epiphytic and epilithic	Freshwater, brackish and saline Oligohalobous-indifferent Mesohaline waters Optimum conductivity 2,964	Circumneutral or alkaline Alkaliphilous and calciphilous Tolerant of moderate organic pollution
<i>Entomoneis paludosa var. subsalina</i>	Solitary cells Epipelagic	Brackish, marine, occasionally freshwater Optimum conductivity 45,910	Typically a marine species Low nutrients
<i>Fragilaria fasciculata</i>	Forms colonies in freshwater plankton Also epiphytic	Recognised in salt lakes Optimum conductivity 15,942	An indicator of high salinity
<i>Navicula complanata</i>	Solitary cells, motile Epilithic and epipelagic	Recognised in salt lakes Not listed on EDDI	An indicator of high salinity
<i>Navicula salinicola</i>	Epipelagic, benthic and motile	Marine Optimum conductivity 125,762	Associated with marine bio-fouling.
<i>Nitzschia frustulum</i>	Solitary and non-attached Motile Benthic, epipelagic and planktonic	Fresh and brackish Sometimes very high conductivity Optimum conductivity 4,881	Alkaline Sodium carbonate or saline sodium chloride waters Hot springs
<i>Nitzschia wuellerstorffii</i>	Epipelagic and planktonic	No information on EDDI	
<i>Rhopalodia constricta</i>	Solitary, attached epiphytic or periphytic forms Free-living in epipelagic	No information on EDDI	Typically a coastal/marine species

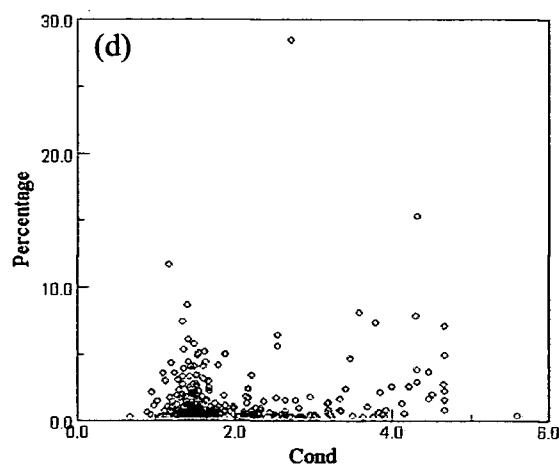
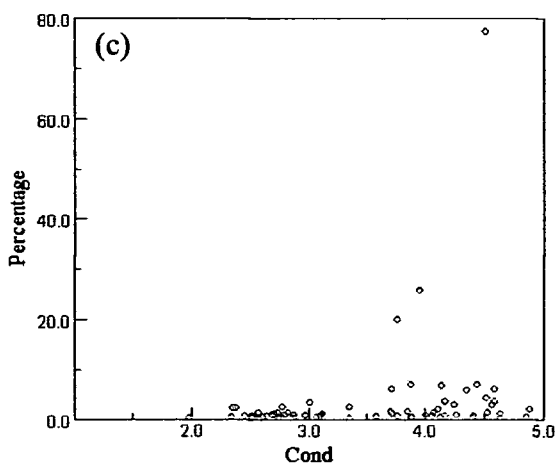
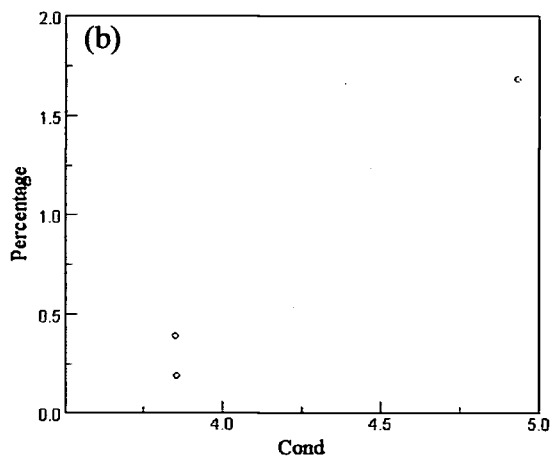
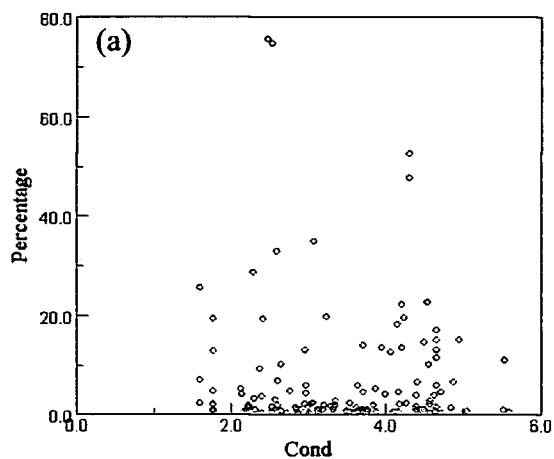
Appendix 7.1

Dominant Nar species conductivity (\log_{10}) optima based on % abundance at lakes sites in the EDDI combined salinity training set. (a) *A. minutissimum*, (b) *C. meneghiniana*, (c) *F. construens*, (d) *N. paleacea*, (e) *S. acus*, (f) *S. parvus*.



Appendix 7.2

Dominant Kratergöl species conductivity (\log_{10}) optima based on % abundance at lakes sites in the EDDI combined salinity training set. (a) *C. placentula*, (b) *E. paludosa* var. *subsalina*, (c) *F. fasciculata*, (d) *N. fonticola*.



Appendix 8

Significant relationships between the Nar diatom record and gridded meteorological data.

	Annual average			Total precip.
	Min. temp.	Ave. temp.	Max. temp.	
N. paleacea bloom	<u>0.267</u>	<u>0.300</u>	<u>0.311</u>	-0.037
	<u>0.020</u>	<u>0.008</u>	<u>0.006</u>	0.754
S. acus bloom	-0.017	-0.148	<u>-0.253</u>	0.181
	0.886	0.203	<u>0.028</u>	0.117
Grey layer	-0.151	-0.113	-0.075	<u>-0.253</u>
	0.194	0.331	0.521	<u>0.027</u>

Table 1 Relationships between annual average gridded climate data for central Anatolia and the NAR01/02 diatom thin section record (Pearson's coefficient, r and p values) (significant relationships highlighted $p < 0.05$). (Only diatom numerical analyses that showed a significant relationship are included).

	Annual average			Total precipitation
	Min. temp.	Ave. temp.	Max. temp.	
N. paleacea bloom	<u>0.244</u>	<u>0.274</u>	<u>0.278</u>	-0.058
	<u>0.034</u>	<u>0.017</u>	<u>0.015</u>	0.620
S. acus bloom	-0.010	-0.160	<u>-0.275</u>	0.198
	0.932	0.168	<u>0.016</u>	0.086

Table 2 Relationships between annual average climate data for the grid containing Nar Gölü and the NAR01/02 diatom thin section record (Pearson's coefficient, r and p values) (significant relationships highlighted $p < 0.05$). (Only diatom numerical analyses that showed a significant relationship are included).

	Spring (MAM)				Summer (JJA)			
	Min. temp.	Ave. temp.	Max. temp.	Total precip.	Min. temp.	Ave. temp.	Max. temp.	Total precip.
N. paleacea bloom	0.226	<u>0.231</u>	0.219	-0.043	<u>0.425</u>	<u>0.446</u>	<u>0.431</u>	-0.132
	0.050	<u>0.045</u>	0.057	0.714	<u>0.000</u>	<u>0.000</u>	<u>0.000</u>	0.256
Varve thickness	0.171	0.140	0.105	-0.069	<u>0.348</u>	<u>0.296</u>	<u>0.233</u>	-0.064
	0.139	0.228	0.368	0.554	<u>0.002</u>	<u>0.009</u>	<u>0.043</u>	0.580
Carbonate	0.095	0.075	0.054	-0.029	<u>0.335</u>	<u>0.284</u>	0.226	0.048
	0.415	0.520	0.644	0.803	<u>0.003</u>	<u>0.013</u>	0.050	0.679

Table 3 Relationships between spring and summer gridded climate data from central Anatolia and the NAR01/02 thin section diatom record (Pearson's coefficient, r and p values) (significant relationships highlighted $p < 0.05$). (Only diatom numerical analyses that showed a significant relationship are included).

	Autumn (SON)				Winter (DJF)			
	Min. temp.	Ave. temp.	Max. temp.	Total precip.	Min. temp.	Ave. temp.	Max. temp.	Total precip.
S. acus bloom	-0.042	-0.203	<u>-0.324</u>	<u>0.231</u>	-0.155	-0.216	<u>-0.273</u>	-0.125
	0.720	0.078	<u>0.004</u>	<u>0.044</u>	0.183	0.061	<u>0.017</u>	0.283

Table 4 Relationships between autumn and winter gridded climate data for central Anatolia and the NAR01/02 thin section diatom record (Pearson's coefficient, r and p values) (significant relationships highlighted $p < 0.05$). (Only diatom numerical analyses that showed a significant relationship are included).

	Spring (MAM)				Summer (JJA)			
	Min. temp.	Ave. temp.	Max. temp.	Total precip.	Min. temp.	Ave. temp.	Max. temp.	Total precip.
N. paleacea bloom	<u>0.236</u>	<u>0.230</u>	0.208	-0.019	<u>0.412</u>	<u>0.448</u>	<u>0.428</u>	-0.121
	<u>0.040</u>	<u>0.046</u>	0.071	0.873	<u>0.000</u>	<u>0.000</u>	<u>0.000</u>	0.300
S. acus bloom	<u>0.232</u>	0.167	0.099	0.134	0.117	-0.019	-0.122	0.086
	<u>0.043</u>	0.149	0.393	0.250	0.316	0.871	0.294	0.462
Varve thickness	0.186	0.143	0.097	-0.096	<u>0.372</u>	<u>0.316</u>	<u>0.239</u>	-0.075
	0.107	0.218	0.406	0.410	<u>0.001</u>	<u>0.005</u>	<u>0.038</u>	0.518
Carbonate	0.098	0.061	0.027	-0.071	<u>0.356</u>	<u>0.303</u>	<u>0.231</u>	0.031
	0.401	0.598	0.815	0.542	<u>0.002</u>	<u>0.008</u>	<u>0.045</u>	0.794

Table 5 Relationships between spring and summer climate data for the grid containing Nar Gölü and the NAR01/02 thin section diatom record (Pearson's coefficient, r and p values) (significant relationships highlighted $p < 0.05$). (Only diatom numerical analyses that showed a significant relationship are included).

	Autumn (SON)				Winter (DJF)			
	Min. temp.	Ave. temp.	Max. temp.	Total precip.	Min. temp.	Ave. temp.	Max. temp.	Total precip.
S. acus bloom	-0.004	-0.188	<u>-0.327</u>	<u>0.242</u>	-0.174	<u>-0.237</u>	<u>-0.295</u>	-0.098
	0.974	0.104	<u>0.004</u>	<u>0.035</u>	0.132	<u>0.039</u>	<u>0.010</u>	0.399
Organic	0.113	0.154	0.177	0.017	0.069	0.067	0.063	<u>0.269</u>
	0.330	0.183	0.125	0.882	0.554	0.567	0.587	<u>0.019</u>

Table 6 Relationships between autumn and winter climate data for the grid containing Nar Gölü and the NAR01/02 thin section diatom record (Pearson's coefficient, r and p values) (significant relationships highlighted $p < 0.05$). (Only diatom numerical analyses that showed a significant relationship are included).

	Spring (MAM)				Summer (JJA)			
	Min. temp.	Ave. temp.	Max. temp.	Total precip.	Min. temp.	Ave. temp.	Max. temp.	Total precip.
DCA axis								
2	0.139	0.098	0.059	0.095	<u>0.352</u>	<u>0.319</u>	<u>0.273</u>	-0.035
	0.229	0.397	0.611	0.413	<u>0.002</u>	<u>0.005</u>	<u>0.017</u>	0.762
C.								
anatolicus	0.096	0.096	0.090	0.028	<u>0.396</u>	<u>0.302</u>	0.211	<u>0.229</u>
%	0.409	0.408	0.440	0.808	<u>0.000</u>	<u>0.008</u>	0.068	<u>0.047</u>
S. acus %	0.208	<u>0.231</u>	<u>0.234</u>	-0.124	0.198	0.158	0.116	-0.143
	0.071	<u>0.044</u>	<u>0.042</u>	0.285	0.087	0.172	0.317	0.217
	Autumn (SON)				Winter (DJF)			
Total biovolume	0.109	0.203	<u>0.266</u>	<u>-0.315</u>	-0.071	-0.037	-0.001	0.035
	0.350	0.078	<u>0.020</u>	<u>0.006</u>	0.544	0.750	0.994	0.767
S. acus %	<u>0.240</u>	0.167	0.092	0.097	-0.175	-0.175	-0.169	-0.158
	<u>0.037</u>	0.149	0.431	0.406	0.129	0.130	0.145	0.173

Table 7 Seasonal relationship between gridded climate data for central Anatolia and the NAR06 diatom record (Pearson's correlation, r and p values) (significant relationships highlighted $p < 0.05$). (Only diatom numerical analyses that showed a significant relationship are included).

	Spring (MAM)				Summer (JJA)			
	Min. temp.	Ave. temp.	Max. temp.	Total precip.	Min. temp.	Ave. temp.	Max. temp.	Total precip.
D-I salinity	-0.022	0.024	0.060	-0.038	-0.150	-0.155	-0.142	<u>0.226</u>
	0.852	0.835	0.605	0.741	0.196	0.182	0.219	<u>0.049</u>
DCA axis 2	0.102	0.053	0.007	0.037	<u>0.332</u>	<u>0.305</u>	<u>0.252</u>	-0.092
	0.381	0.652	0.955	0.751	<u>0.003</u>	<u>0.007</u>	<u>0.028</u>	0.429
Rarefaction	-0.078	-0.014	0.040	-0.045	-0.077	-0.096	-0.100	<u>0.242</u>
	0.502	0.902	0.733	0.697	0.508	0.407	0.390	<u>0.035</u>
<i>C. anaticus</i> %	0.097	0.085	0.066	-0.004	<u>0.373</u>	<u>0.287</u>	0.190	0.201
	0.405	0.466	0.568	0.974	<u>0.001</u>	<u>0.012</u>	0.100	0.082
<i>S. acus</i> %	0.187	0.220	<u>0.230</u>	-0.033	0.206	0.159	0.110	-0.113
	0.106	0.056	<u>0.045</u>	0.780	0.075	0.170	0.344	0.330
	Autumn (SON)				Winter (DJF)			
Total biovolume	0.079	0.195	<u>0.272</u>	<u>-0.372</u>	-0.059	-0.019	0.019	0.003
	0.498	0.092	<u>0.017</u>	<u>0.001</u>	0.615	0.868	0.870	0.980

Table 8 Seasonal relationship between climate data for the grid containing Nar Gölü and the NAR06 diatom record (Pearson's correlation, r and p values) (significant relationships highlighted $p < 0.05$). (Only diatom numerical analyses that showed a significant relationship are included).

Appendix 9

Paper submitted to *Diatom Research*

MORPHOLOGY AND ECOLOGY OF A NEW CENTRIC DIATOM FROM CAPPADOCIA (CENTRAL TURKEY)

Jessie Woodbridge¹

Neil Roberts¹

Eileen J. Cox²

School of Geography, University of Plymouth, Drake Circus, Plymouth PL4 8AA UK¹

Department of Botany, The Natural History Museum, Cromwell Road, London

SW7 5BD UK²

ABSTRACT

A previously unidentified, small, centric diatom from Cappadocia, Central Turkey is described as a new species and genus (*Clipeoparvus anatolicus*). Cells of this diatom are sub-spherical, often linked in pairs and covered with irregular spines. Striae radiate around a hyaline area on the valve face. Neither rimoportulae nor fultoportulae were found. Specimens have been placed in the Natural History Museum (London) diatom collection.

Clipeoparvus anatolicus is highly abundant within a modern brackish crater-lake (Nar Gölü), where it appears to grow benthically or epiphytically in the silica-rich, eutrophic, circumneutral waters. It is also common in late Holocene sediment cores, reaching over 40% of the total assemblage in samples of medieval age. This taxon also increased in abundance in the lake between 2001 and 2008.

INTRODUCTION

Knowledge of modern diatom species assemblages within lacustrine ecosystems is paramount for palaeoenvironmental proxy-reconstructions from lake sediment material. Spaulding et al. (2003) discussed a number of studies on the diatom flora of central Turkey and highlighted that few have concentrated on detailed taxonomy, and that the diatom species diversity of the region is probably underestimated. Many studies have concentrated on describing the diatom community of Turkish lakes (e.g. Çetin & Şen 1998; Şahin 2000; Kiliç & Sivaci 2001; Akbulut & Yildiz 2002; Çelekli et al. 2007; and Çevik et al. 2007), however, less attention has been given to species ecology. Diatoms have also been utilised in various palaeoecological studies based in Turkey (e.g. Kashima 1995; 2003; Kashima et al. 1999; Reed et al. 1999; and Roberts et al. 1999; 2001). Such research has strengthened our knowledge of palaeoclimatic variability in the Eastern Mediterranean region and highlighted the effectiveness of diatoms as proxy indicators of environmental change. The description of this new diatom contributes to our

knowledge of diatom diversity, while the physico-chemical data on its locality will allow future work to utilise this taxon as an indicator of environmental change.

STUDY AREA AND METHODS

Site description

The inland area of Cappadocia, located in Anatolia (Central Turkey), experiences a semi-arid and sub-humid dry climate (Kutiel & Türkeş 2005). The modern climate of Cappadocia (recorded at Nevşehir meteorological station) is strongly seasonal, with average summer (JJA) and winter (DJF) temperatures of +20.3°C and +0.4°C (data from Turkish State Meteorological Service). Average precipitation, for the period AD 1960-2006, was 409 mm per year, the majority of which accumulates between October and May. The Cappadocia region is volcanic and includes several crater lakes, which provide extensive archives of Holocene environmental change.

Nar Gölü (Fig. 1, Table 1) is a small, extant, volcanic crater-lake situated 25 km west of the town of Derinkuyu (38°22'30"N; 34°27'30"E). The lake is thermally and chemically stratified with hypolimnetic, anoxic bottom water. Seasonal varves comprising authigenic carbonate, organic matter and diatoms are deposited annually. The lake lacks any surface outlets and its modern catchment experiences relatively minor human impact. Lake diatoms were studied from collections of living material and specimens preserved in sediments spanning the late Holocene. Annual fieldwork at the lake has revealed that the water level of Nar Gölü decreased by 3.4 m between 2001 and 2008. Water chemistry analyses carried out between 1999 and 2008 demonstrate that the lake is weakly alkaline to circumneutral and slightly saline with sodium, chloride and bicarbonate as the major ions (Tables 1, 2).

Sample collection, preparation, and analysis

Living diatoms were collected from various habitats at Nar Gölü during summer 2006-2008. Surface sediments from the centre and edge of the lake, aquatic macrophytes, marginal surface gravel, rock scrapings and water samples containing plankton were collected and stored in plastic bottles and polythene bags. Algae growing on an aquatic macrophyte were grown in the laboratory. The sample was cultured in a Petri dish with adequate exposure to light and warmth, adding 5 ml of ultrapure water weekly. Algal growth was visible to the naked eye as a brown/yellow colouring. Seston sediment traps, installed in the lake annually, were used to collect detritus and organic matter falling through the water column. Traps comprise plastic tubing with a funnel inserted and are attached to ropes and floats at different points in the lake.

Palaeoecological analysis of Nar Gölü sediments was carried out using a number of lake cores collected between 1999 and 2002 (NAR01/02) and an additional short core collected in September 2006 (NAR06). ²¹⁰Pb and ¹³⁷Cs radioisotopic dating of the NAR01/02 sequence confirmed that varves are formed annually (Jones et al. 2005). The NAR06 core was analysed at annual resolution for the most recent 80 varve years (VY) (AD 1926-2006) for diatom analysis by taking subsamples of successive laminations from half-sections. Samples comprising three adjoining VYs were taken from the NAR01/02 sequence at decadal intervals over the last 1720 VY (AD 280-2001).

For light microscopy (LM) of live material, a small sample of the cultured algae was suspended in water on a microscope slide under a coverslip. Specimens were examined with a Zeiss Universal microscope and photographed using a Kodak DCS Pro SLR/c (NHM). For permanent preparations of fossil, modern, cultured and sediment trap material, samples were prepared for diatom analysis by heating in 30% H₂O₂ to dissolve organic material, and 10% HCl to remove carbonates and oxides. The material was washed repeatedly with distilled water (method adapted from Battarbee 1986; Battarbee et al. 2001). A 500 µl (diluted appropriately) sample of the processed material was allowed to dry on a coverslip. Samples were then inverted

and mounted in NAPHRAX on microscope slides for LM analysis. An Olympus BX50 LM was used to analyse diatoms at 1000x magnification (oil immersion). LM analysis was supported with the use of an eyepiece reticule for measuring diatoms, a Leica DFC280 microcam and analySIS computer software (1986-2002) for digital photography.

For scanning electron microscopy (SEM) a small drop of processed sample in suspension was evaporated directly onto an aluminium stub. Samples were then coated with gold ready for inspection (Battarbee et al. 2001). Photomicrographs were taken at 7000-25000x magnification using a JEOL 5600 low vacuum SEM at the University of Plymouth Electron Microscopy Centre and a Philips XL30 field emission SEM at the Natural History Museum (London).

RESULTS

Morphology

When viewed under LM, live cells often occur in pairs or short chains and are sometimes clumped together in mucilage masses (Figs 2-6). Cells are circular in valve view, domed and strongly biconvex in girdle view, without a distinct girdle region (Figs 7-12). Each cell has two yellow-brown chloroplasts that lie closely associated with the inner surface of the valves. After cleaning, valve surfaces are found to be covered with short spines and are porous apart from a small central zone (Figs 13-18 and 25-28). The valves are robust and thick-walled for their size, 6-10 μm diameter (e.g. Fig. 15), with radiate striae that extend from the edge of the central zone to the valve margin.

When observed in girdle view with SEM, the two valves form a sub-hemispherical shape with a size range of 4-6 x 6-10 μm (Figs 19-24 and 29-34). Heterovalvy is evident as the degree of doming can differ between the two valves (e.g. Fig. 29). SEM confirms the presence of short irregular spines over the external valve surface. The spines are numerous, robust and are irregularly distributed around the outer part of the valve face, they may or may not be present over the central zone. The valves are perforated by radiating rows of rounded pores, although these may be externally obscured by the spines and by external granules.

Internally the valve surface is smooth with radiating rows of rounded pores containing 10-12 pores (approx. 5 in 1 μm), except in the central zone (e.g. Fig 15). Pores may be internally occluded (Fig. 16), but no processes are visible. The edge of the valves is thick and smooth. There are numerous (1-20) relatively narrow, split, ligulate, non-porous girdle bands (e.g. Fig. 22), the number varying according to whether or not they span two sibling cells. The valvocopula seems to lap over the edge of the valve.

Morphological variability

Cultured modern examples and fossil specimens of the genus differ slightly in the size ranges of their features. However, the overall cell structure is very similar, which implies that the same species spans the palaeo and the modern lake environment. The main difference between cells from the modern and palaeo-environment is the length of the spines and the dissimilar structure of the silica granules that attach to the valve surface (e.g. Figs 14 and 26). Fossil specimens appear to have longer spines and granules attached to cultured cells are globule-shaped whereas on fossil examples granules are almost star-shaped. These differences cannot be detected using LM and they may be associated with temporal changes in environmental conditions or resource availability. Variability in valve shape and copulae number is evident when comparing specimens from the same environment (e.g. Figs 19 and 21). Additionally, variation in the extent of granule covering is apparent, e.g. when comparing Fig. 25 with Fig. 27.

Comparisons with existing genera

Features of *Clipeoparvus* have been compared with various published genera from the class Coscinodiscophyceae (Table 4) (Round 1992). The main characteristics of *Clipeoparvus* that

distinguish it from others are the lack of portulae, the small size, the non-chain forming life-form and the absence of pores on the copulae.

Similarities were recognised with the genus *Melosira*. Comparing Krammer & Lange-Bertalot (1991; 2000) and Round et al.'s (1992) descriptions of *Melosira* there appear to be several features which comply with *Clipeoparvus*. For example, similarities exist in the valve shape and the presence of spines or granules. However, the internal pore structures and girdle bands differ. *Clipeoparvus* copulae are split and ligulate, but no pores are present. Additionally, *Clipeoparvus* does not possess rimoportulae, spines are always present and cells do not form filaments.

The paired or solitary life-form of *Clipeoparvus* cells appears more closely related to the genera *Hyalodiscus* and *Podosira*. However, these genera differ from *Clipeoparvus* due to the absence of spines and granules on the valve face and differences in the copulae structure.

According to Crawford (1988) the underlying feature of *Melosira* is the linking of cells in chains. Additionally, *Melosira* often possess a ring of rimoportulae and a milled edge. Crawford (1988) split *Ellerbeckia* from the *Melosira* genus based on the absence of these features and the presence of heterovalvy. Similarly, *Clipeoparvus* does not have a milled edge and heterovalvy is frequently evident. However, *Ellerbeckia* is large, cylindrical and forms chains and therefore does not correspond with the features of *Clipeoparvus*. Another centric taxon that does not possess rimoportulae is *Chrysanthemodiscus*. However, the cell shape and ornamentation of this diatom differ considerably from *Clipeoparvus*.

Servant-Vildary et al. (1986) reported encountering a very small (10-11 x 4-5 μm) diatom closely related to *Melosira jouseana*, within Miocene lake deposits from central Turkey. The description of this species matches *C. anatolicus* well with spines observed and a similar size range. However, this species did not have a hyaline area on the valve surface. Akbulut & Yildiz (2002) and Çetin & Şen (1998) recorded *Melosira sp.* in their research on Turkish diatoms and mentioned that unidentified *Melosira* species have been recorded in other studies in Turkey. Therefore it appears that *C. anatolicus*, although not previously described, may have been encountered by other researchers.

ECOLOGY

Modern environment

Clipeoparvus anatolicus is very abundant in the modern environment of Nar Gölü. This diatom was also previously noted at the lake by Jane Reed (pers. comm.). According to Reed, this species was not present at any other lake sites that she analysed in Anatolia. Therefore, within this region, *C. anatolicus* appears to be limited to Nar Gölü. However, further analysis of other lakes is required in order to confirm this.

The relative percentage abundance of *C. anatolicus* in modern samples (collected during summer 2006-2008) representing benthos from surface sediment samples (epipelon), gravel and a rock scraping from the lake edge (epilithon), plankton from the water column and aquatic macrophytes (epiphyton) is presented in Fig. 35. Highest percentages were identified in the epiphyton, epipelon and gravel and lowest values were observed in the plankton and rock scraping samples. This suggests that *C. anatolicus* is typically non-planktonic and prolific in multiple habitats. Table 3 illustrates the percentage of *C. anatolicus* observed in Nar Gölü sediment traps between 2003 and 2007 and highlights that this taxon has been an important member of the diatom community throughout the last 5 years.

The high abundance of *C. anatolicus* in the current lake environment, comprising >40% of the integrated surface sediment diatom assemblage, implies that its ecological preferences are characteristic of modern conditions at Nar Gölü (Tables 1 and 2). This includes average conductivity of 3.3 μS^{-1} , weakly alkaline to circum-neutral pH and a silica-rich environment.

Palaeoecology

Clupeoparvus anatolicus is well preserved within lake sediment cores from Nar Gölü. Within the NAR06 annual record, *C. anatolicus* was most abundant during the most recent five years (5-1 VY, AD 2001-2006) and throughout the NAR01/02 decadal record, highest values were identified between 1660-1600 VY (AD 340-400) and 1460-550 VY (AD 540-1450) (Fig. 36). Elevated abundance of *C. anatolicus*, contributing above 40% of the population, throughout the last 1720 years was generally associated with low numbers of most other species. The increase in *C. anatolicus* during the most recent five years coincides with a rise in *Synedra acus*. Throughout the NAR01/02 record *C. anatolicus* increased concordant with higher abundance of *Amphora libyca*, *Aulacoseira crenulata*, and *Nitzschia paleacea* (1470 VY, AD 530). *C. anatolicus* then decreased with the appearance of *Achnantheidium minutissimum* and *S. acus* at 550 VY (AD 1450).

The ecological preferences of the species with which *C. anatolicus* peaks may reveal the conditions that this diatom favours. *A. libyca* is a widespread alkaliphilous taxon that favours low to moderate conductivity. *A. crenulata* favours fresher water and *N. paleacea* also favours alkaliphilous conditions, moderate conductivity and is a eutrophic species. Additionally, *S. acus* is alkaliphilous and favours dilute conditions. Therefore it appears that *C. anatolicus* may favour weakly alkaline, brackish, eutrophic waters. Analysis of NAR01/02 core thin section slides, which allow the diatom assemblage to be microscopically observed *in situ* without disturbance to the sediment, revealed that *C. anatolicus* does not form filaments and is common in the lake during the period when a mixed diatom community is present and abundant organic material, such as plant remains, are deposited. Therefore it appears that *C. anatolicus* could be most prolific during spring and summer.

FORMAL DESCRIPTION

Clupeoparvus Woodbridge, E.J. Cox and Roberts

Cellulae saepe pares vel series breve formantes, aspectu valvari circulares, aspectu cingulari plus minusque biconvexae. Cellula unaquaeque duobus chloroplastibus rotundatis instructa. Valvae circulares, valde tholiformes, parietibus comparate crassis, zona centrali parvula hyaline et poris rotundatis probabiliter interne oclusis seriatim radiantibus ornatis. Valvae pagina externa spinis brevibus irregularibus plerumque obtectis, saepe super paginam spinasque granulis instructis. Copulae angustae fissae ligulatae, sine poris.

Cells often in pairs or forming short chains, circular in valve view and more or less biconvex in girdle view. Each cell with two rounded chloroplasts. Valves circular, strongly domed and relatively thick-walled with a small hyaline central zone and radiating rows of round pores that are probably occluded internally. External valve surface usually covered with short irregular spines, with granules often present over the surface and the spines. Girdle bands narrow, split and ligulate, lacking pores.

Clupeoparvus anatolicus Woodbridge, E.J. Cox and Roberts

Cellulae characteres generi parabentes, aspectu valvari 6-10 μm in diametro, aspectu cingulari 4-6 μm latae, circa 40 striis radiantibus per 10 μm ornatis, poris secus strias leviter artiore circa 5 per 1 μm dispositis.

Cells showing the generic characters, 6-10 μm diameter, 4-6 μm deep in girdle view. Approximately 40 radiating striae in 10 μm , pores slightly more closely spaced along the striae, about 5 in 1 μm .

HOLOTYPE: BM 101379; Nar Gölü, Turkey, on surface of gravel at margin of lake, summer 2008, Neil Roberts.

Also present on BM 101380-BM 101383. Modern and core samples from Nar Gölü, Turkey.

Etymology and systematics

The genus (*Clipeoparvus*) and species (*anatolicus*) have been named according to frustule characteristics and in relation to the region in which the diatom was identified. 'Clipeo' relates to the round/shield-like shape of the frustule and 'parvus' refers to the small size of the diatom. The species name relates to the Anatolia region of Turkey. Systematically, *Clipeoparvus* belongs to the Bacillariophyta and due to its typical centric features is placed in the class Coscinodiscophyceae. It cannot be placed more precisely at order or family level based on current definitions of these taxa.

CONCLUSION

The morphology of *Clipeoparvus* does not correspond with any previously described genus. Distinguishing features of *Clipeoparvus* include its small size, the lack of portulae and the absence of pores in the copulae. Based on analysis of the modern environment, core thin sections and comparisons with other species, it appears that *Clipeoparvus* is largely encountered in benthic habitats, favours brackish water, circumneutral to weakly alkaline pH and could be most abundant during spring and summer. *Clipeoparvus anatolicus* is an important component of the diatom flora at Nar Gölü and has fluctuated significantly in abundance throughout the last 1720 years. This diatom may therefore be an important indicator of environmental change. Further research is required to strengthen our understanding of its modern ecology and thereby our studies of environmental fluctuations.

ACKNOWLEDGEMENTS

This research was funded by a University of Plymouth Ph.D. studentship and fieldwork was supported financially by the British Institute at Ankara. The authors would like thank the University of Plymouth technical and Cartographic staff, Quaternary Environments Research Group, Electron Microscopy Centre and various individuals who have contributed towards this research including Adam Fisher, Matt Jones, Francoise Gasse, Jane Reed, Ann England, Warren Eastwood and Martin Kent. Additionally, the Natural History Museum (London) provided access to microscopical facilities, and we thank Elliot Shubert for his help with the light microscopy, and Norman Robson for checking and correcting the Latin diagnoses. We would also like to thank those diatomists who commented on the identity of this taxon by responding to posted images on Diatom-L, and for discussions at the annual British Diatomists' Meeting.

REFERENCES

- AKBULUT, A. & YILDIZ, K. (2002). The planktonic diatoms of Lake Çıldır (Ardahan-Turkey). *Turkish Journal of Botany*, **26**, 55-75.
- BARBER, H.G. & HAWORTH, E.Y. (1981). *A Guide to the Morphology of the Diatom Frustule*, Freshwater Biological Association, UK.
- BATTARBEE, R.W. (1986). Diatom Analysis. In: *Handbook of Holocene Palaeoecology and Palaeohydrology*, (B.E. Berglund, ed.), 527-570. Wiley, Chichester.
- BATTARBEE, R.W., JONES, V.J., FLOWER, R.J., CAMERON, N.G. & BENNION, H. (2001). Diatoms. In: *Tracking Environmental Change Using Lake Sediments, Vol 3: Terrestrial, Algal and Siliceous Indicators*. (J. Smol, ed.), 155-202. Kluwer Academic Publishers, Netherlands.
- ÇELEKLİ, A., OBALI, O. & KÜLKÖYLÜOĞLU, O. (2007). The phytoplankton community (except Bacillariophyceae) of lake Abant (Bolu, Turkey). *Turkish Journal of Botany*, **31**, 109-124.

- ÇETIN, A. K. & ŞEN, B. (1998). Diatoms (Bacillariophyta) in the phytoplankton of Keban Reservoir and their seasonal variations. *Turkish Journal of Botany*, **22**, 25-33.
- ÇEVİK, F., WHITTON, B.A. & ÖZTÜRK, O. (2007). A new genus record for the freshwater algal flora of Turkey. *Turkish Journal of Botany*, **31**, 149-152.
- COX, E.J. (1996). *Identification of Freshwater Diatoms from Live Material*, Chapman and Hall, UK.
- CRAWFORD, R. M. (1988). Reconsideration of *Melosira arenaria* and *M. teres*; resulting in a proposed new genus *Ellerbeckia*. In: *Algae and the Aquatic Environment*, (F.E. Round, ed.), 413-433. Biopress Ltd., Bristol.
- ENGLAND, A. (2006). Ph.D. thesis: *Late Holocene palaeoecology of Cappadocia (Central Turkey): an investigation of annually laminated sediments from Nar Gölü crater lake*, University of Birmingham.
- ENGLAND, A. EASTWOOD, W.J., ROBERTS, C.N., TURNER, R. & HALDON, J.F. (2008). Historical landscape change in Cappadocia (central Turkey): a palaeoecological investigation of annually-laminated sediments from Nar Lake. *The Holocene*, **18**, 1229-1245.
- GASSE, F. (1986). *Bibliotheca Diatomologica: East African Diatoms*, Gebrüder Borntraeger, Berlin.
- GERMAIN, H. (1981). *Flore Des Diatomées, eaux douces et saumâtres*, Société Nouvelle Des éditions Boubée, Paris.
- HARTLEY, B. (1996). *An Atlas of British Diatoms*, Henry Ling Ltd., UK.
- HAWORTH, E.Y. (1981). *A Guide to the Morphology of the Diatom Frustule*, Freshwater Biological Association Scientific Publications, UK.
- JONES (2004). Ph.D. thesis: *High-resolution records of climate change from lacustrine stable isotopes through the last two millennia in western Turkey*, University of Plymouth.
- JONES, M.D., LENG, M.J., ROBERTS, C.N., and TÜRKEŞ, M. (2005) A coupled calibration and modelling approach to the understanding of dry-land lake oxygen isotope records. *Journal of Palaeolimnology*, **34**, 391-411.
- JONES, M.D., ROBERTS, C.N., LENG, M.J. & TÜRKEŞ, M. (2006). A high-resolution late Holocene lake isotope record from Turkey and links to North Atlantic and monsoon climate. *Geology*, **34**, 361-364.
- KASHIMA, K. (1995). Sedimentary diatom assemblages in freshwater and saline lakes of the Anatolia plateau, central part of Turkey: an application for reconstruction of palaeosalinity change during Late Quaternary. In: *Proceedings of the 13th International Diatom Symposium*, (D. Marino & M. Montresor, eds.) 93-106, Biopress Ltd., Bristol.
- KASHIMA, K., KUZUCUOĞLU, C. & KARABIYIKOĞLU, M. (1999). Diatom assemblages from lake and marsh sediments at the central part of Turkey: and their sedimentary environments. In: *Proceedings of the 14th International Diatom Symposium*, (S. Mayama, M. Idei & I. Koizumi, eds.) 457-466, Koeltz Scientific Books, Koenigstein.
- KASHIMA, K. (2003). The quantitative reconstruction of salinity changes using diatom assemblages in inland saline lakes in the central part of Turkey during the Late Quaternary. *Quaternary International*, **105**, 13-19.

- KILINÇ, S. & SIVACI, E.R. (2001). A study on the past and present diatom flora of two alkaline lakes. *Turkish Journal of Botany*, **25**, 373-378.
- KOLAYLI, S., BAYSAL, A. & ŞAHİN, B. (1998). A study on the epipelagic and epilithic algae of Şana River (Trabzon, Turkey). *Turkish Journal of Botany*, **22**, 163-170.
- KUTIEL, H. & TÜRKEŞ, M. (2005). New evidence for the role of the North Sea Caspian Pattern on the temperature and precipitation regimes in continental central Turkey. *Geografiska Annaler*, **87** A, 501-513.
- KRAMMER, K. & LANGE-BERTALOT, H. (1991). *Bacillariophyceae, 3. Teil: Centrales, Fragilariaceae, Eunotiaceae*, Gustav Fischer, Germany.
- KRAMMER, K. & LANGE-BERTALOT, H. (2000). *Bacillariophyceae, Part 5: English and French Translation of the Keys*, Gustav Fischer, Germany.
- REED, J.M., ROBERTS, C.N. & LENG, M. (1999). An evaluation of the diatom response to Late Quaternary environmental change in two lakes in the Konya Basin, Turkey, by comparison with stable isotope data. *Quaternary Science Reviews*, **18**, 631-646.
- ROBERTS, N., BLACK, S., BOYER, P., EASTWOOD, W.E., GRIFFITHS, H.I., LAMB, H.F., LENG, M.J., PARISH, R., REED, J.M., TWIGG, D. & YİĞİTBAŞIOĞLU, H. (1999). Chronology and stratigraphy of Late Quaternary sediments in the Konya Basin, Turkey: results from the KOPAL project. *Quaternary Science Reviews*, **18**, 611-630.
- ROBERTS, N., REED, J.M., LENG, M.J., KUZUCUOĞLU, C., FONTUGNW, M., BERTAUX, J., WOLDRING, H., BOTTEMA, S., BLACK, S., HUNT, E. & KARABIYIKOĞLU, M. (2001). The tempo of Holocene climate change in the Eastern Mediterranean region: new high-resolution crater-lake sediment data from central Turkey. *The Holocene*, **11**, 721-736.
- ROUND, F.E. (1984). (ed.) *The Ecology of Algae*, Cambridge University Press, Cambridge.
- ROUND, F.E., CRAWFORD, R.M. & MANN, D.G. (1992). *The Diatoms: Biology and Morphology of the Genera*, Cambridge University Press, Cambridge.
- ŞAHİN, B. (2000). Algal flora of lakes Aygır and Balıklı (Trabzon, Turkey). *Turkish Journal of Botany*, **24**, 35-45.
- ŞAHİN, B. (2007). Two new records for the freshwater algae of Turkey. *Turkish Journal of Botany*, **31**, 153-156.
- SERVANT-VILDARY, S., PAICHELER, J.C. & SEMELIN, B. (1986). Miocene lacustrine diatoms from Turkey. In: *Proceedings of the 9th International Diatom Symposium*. (F.E. Round, ed.) Biopress, Bristol.
- SPAULDING, S.A., KOCIOLEK, J.P. & DAVIS, D.R. (2002). A new diatom (Bacillariophyceae) genus with two new species from New Mexico, USA. *European Journal of Phycology*, **37**, 135-143.
- SPAULDING, S.A., AKBULUT, A. & KOCIOLEK, J.P. (2003). A new diatom species of *Aneumastus* D.G. Mann & Stickle from central Turkey. *Diatom Research*, **18**, 149-160.
- VAN DER WERFF, A. & HULS, H. (1976). *Diatomeeënflora van Nederland*, Otto Koeltz Science Publishers, Germany.
- WERNER, D. (1977). *The Biology of Diatoms*, Blackwell Scientific Publications, UK.

WETZEL, R.G. (2001). *Limnology: Lake and River Ecosystems, Third Edn.*, Academic Press, USA.

WITKOWSKI, A., LANGE-BERTALOT, H. & METZELTIN, D. (2000). *Diatom Flora of Marine Coasts I*, A.R.G. Gantner Verlag K.G., Germany.

FIGURE CAPTIONS

Fig. 1. Map of Turkey highlighting location of Nar (Gölü) crater lake.

Figs 2-6. Living specimens of *Clipeoparvus anatolicus* within marginal lake surface gravel in valve and girdle view (LM). **Fig 2.** Cells in mucilage forming loose colony. **Figs 3-6.** Solitary and paired cells in valve and girdle view.

Figs 7-12. Modern lake and sediment core fossil specimens of *Clipeoparvus anatolicus* in valve and girdle view (LM). **Figs 7-10.** Cultured specimens. **Figs 11-12.** Fossil specimens.

Fig 13-18. Cultured modern lake specimens of *Clipeoparvus anatolicus*. External and internal valve views (SEM). Arrow highlights occluded internal pore opening.

Figs 19-24. Cultured modern lake specimens of *Clipeoparvus anatolicus* presented in girdle view (SEM). Arrow highlights ligulate girdle band.

Figs 25-28. Lake sediment fossil specimens of *Clipeoparvus anatolicus*. External and internal valve views (SEM).

Figs 29-34. Lake sediment fossil specimens of *Clipeoparvus anatolicus* in girdle view (SEM).

Fig. 35. *Clipeoparvus anatolicus* relative % abundance recorded in different lake habitats at Nar Gölü during summer 2006-2008.

Fig. 36 Relative % abundance of *C. anatolicus* throughout the NAR01/02 decadal 1720 varve year (AD 280-2001) and NAR06 annual 80 varve year (AD 1926-2006) lake sediment sequences.



Fig 1 (13.3x6.1cm)

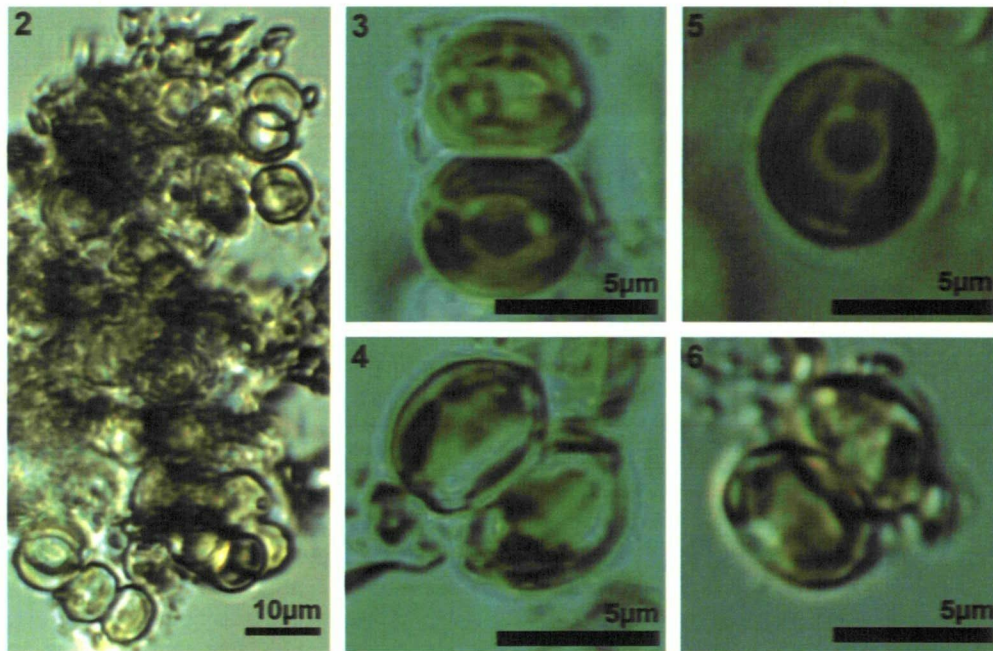


Fig 2-6 (13x8.6cm)

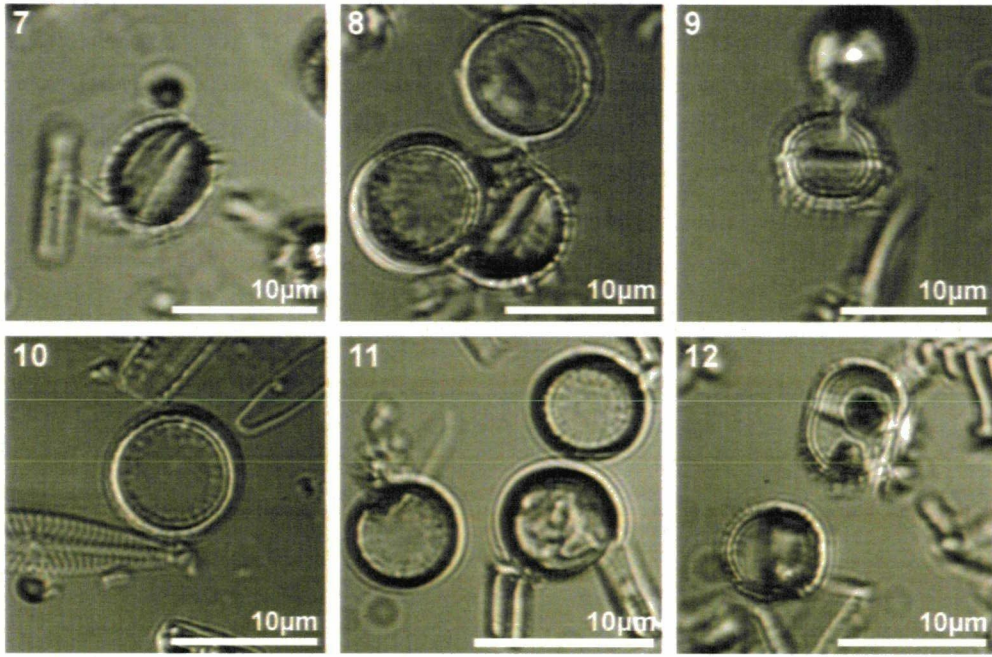


Fig 7-12 (13x8.6cm)

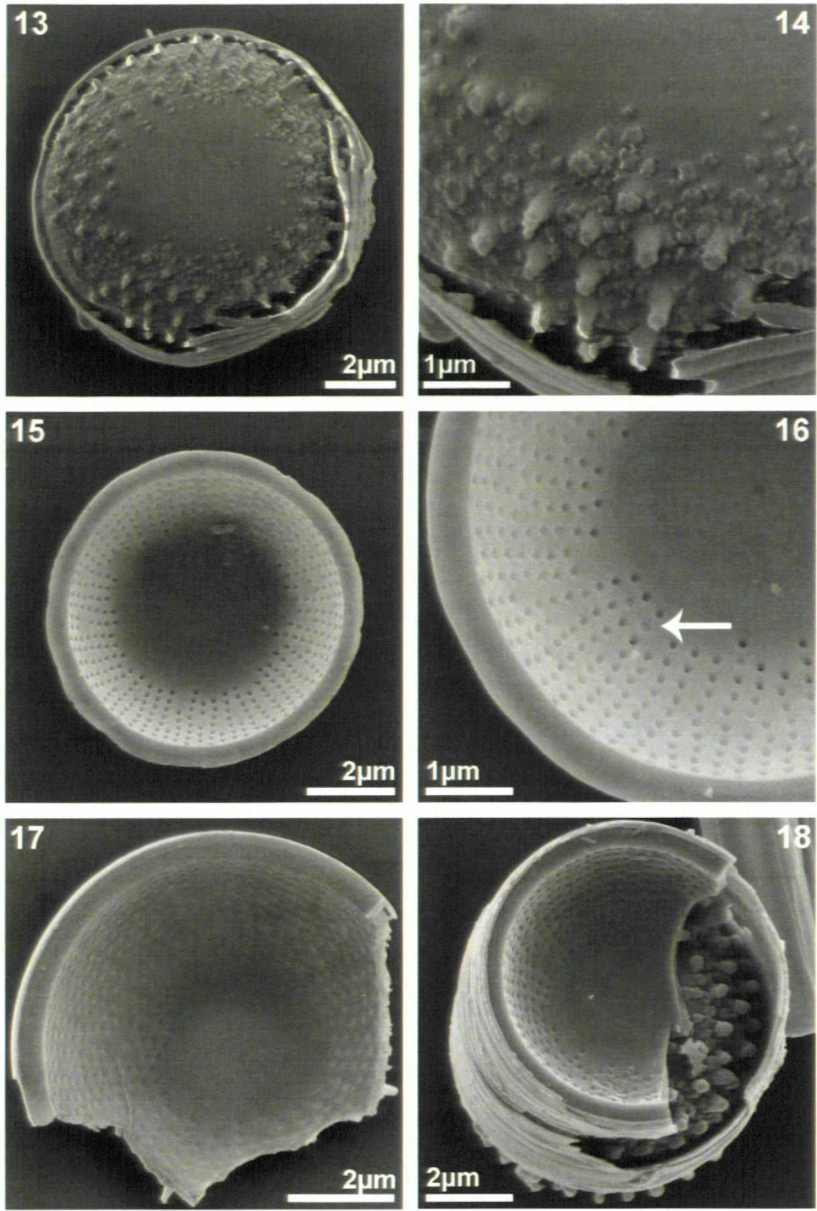


Fig 13-18 (10.6x16cm)

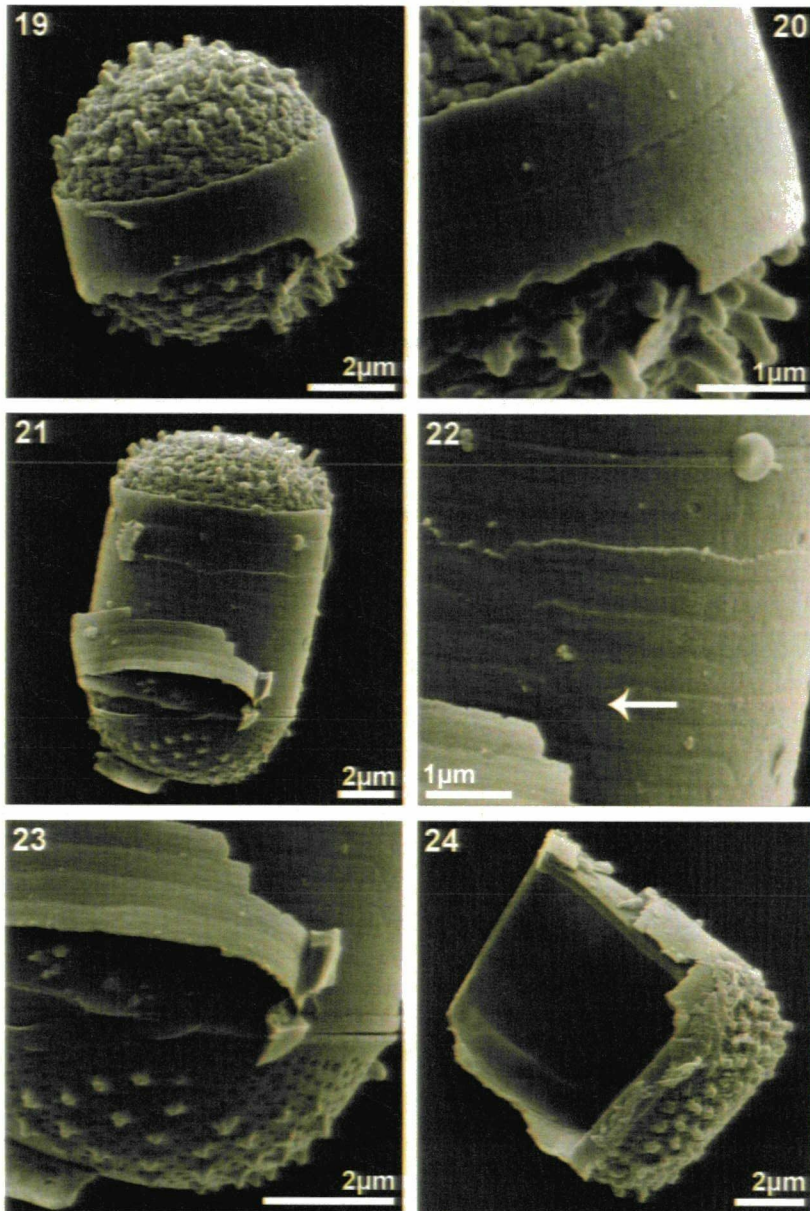


Fig 19-24 (10.6x16cm)

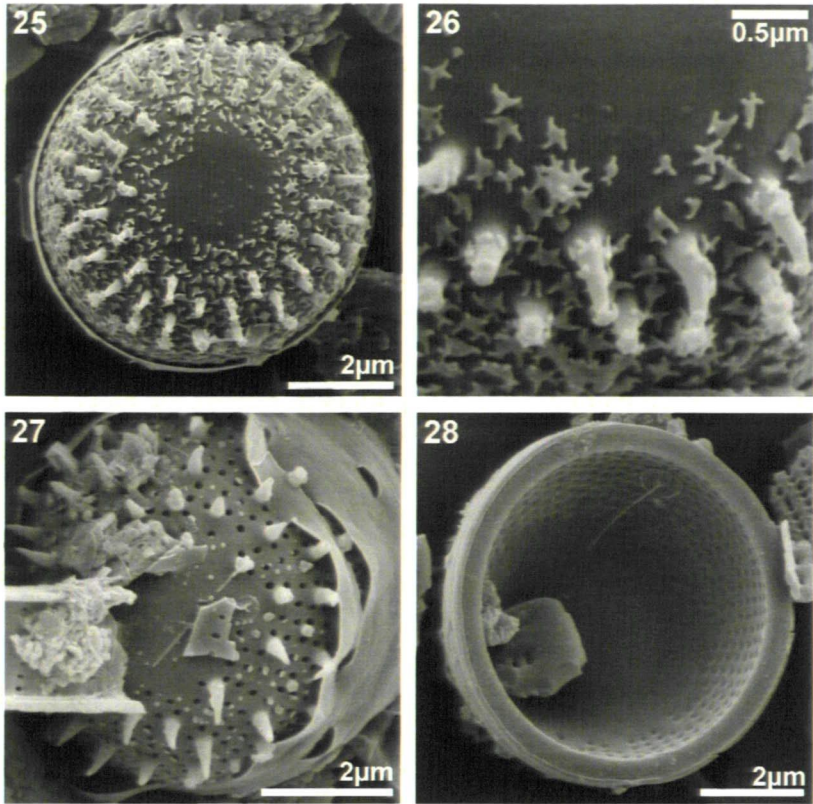


Fig 25-28 (10.6x10.6cm)

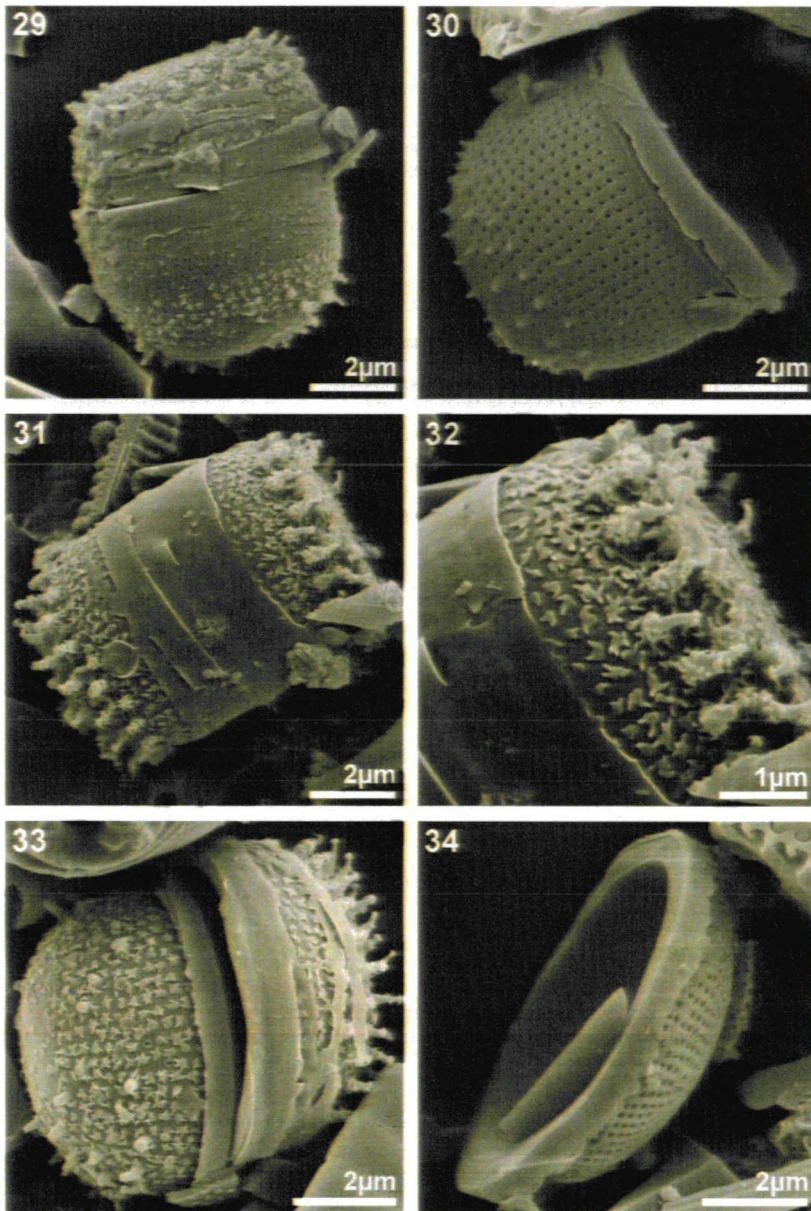


Fig 29-34 (10.6x16cm)

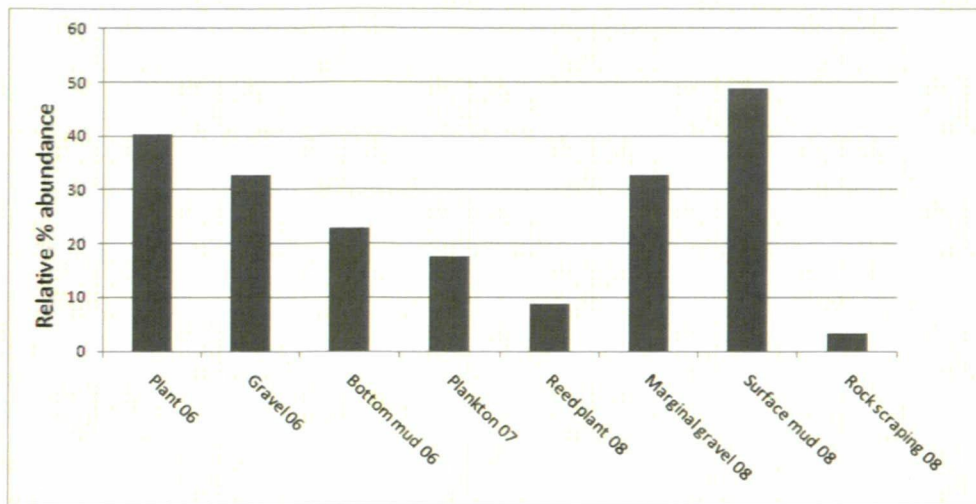


Fig 35 (6.02x3.12cm)

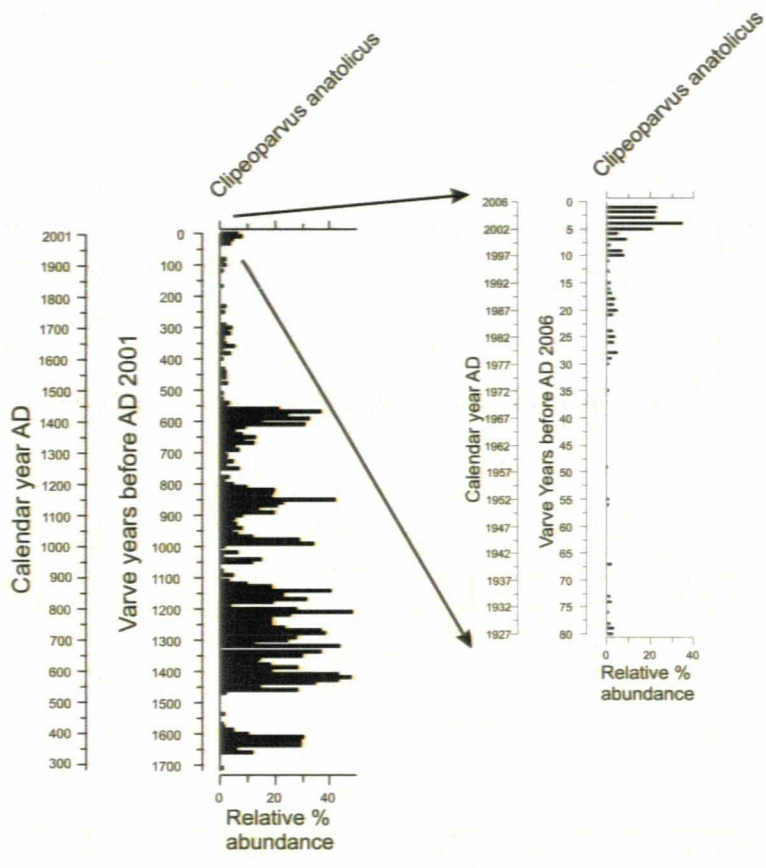


Fig 36 (9.83x11.08cm)

Table 1. Lake characteristics of Nar Gölü, including data from Jones (2004) and England (2006).

<i>Lake area (m²)</i>	<i>Lake volume (m³)</i>	<i>Catchment area (m²)</i>	<i>Residence time (yrs)</i>	<i>Elevation (m above sea level)</i>	<i>Max. water depth (m)</i>
5.6x10 ⁵	7.7x10 ⁵	2.4x10 ⁶	8-11	1,363	26 (2001) 22.6 (2008)

<i>Water sample location</i>	<i>Water depth (m)</i>	<i>Temperature (°C)</i>	<i>Conductivity (mS)</i>	<i>pH</i>
Lake centre (mean summer values, 2001-2008)	0	23.3	3.3	7.9
	10	18.2	3.6	7.3
	20	12.4	3.4	6.8

Table 2. Nar Gölü major ion water chemistry (mg/l⁻¹) summer 1999 (analysis by Jane Reed) and summer 2008 (analyses conducted at the University of Plymouth).

<i>Lake water sample location</i>	<i>0.5 m 1999</i>	<i>0.5 m depth 2008</i>	<i>20 m depth 2008</i>
<i>mg/l⁻¹</i>			
Cl ⁻	970.0		
Na ⁺	380.0		
SO ₄ ²⁻	154.0	160.7	163.4
K ⁺	144.4		
Mg ²⁺	103.4		
Ca ²⁺	59.8		
SiO ₂	58.14	79.2	72.9
Sr ²⁺	31.3		
Phosphate		0.000	0.000
Nitrate		0.046	0.023
Phenolphthalein alkalinity	83.84	54.3	4.2
Total alkalinity	455.90	591.5	645.8

Table 3. Average percentage *C. anaticus* in diatom population identified in Nar Gölü sediment traps between 2003 and 2007.

<i>Sediment trap summer installation and collection date</i>	<i>Percentage C. anaticus</i>
2006-2007	37.6
2005-2006	34.0
2004-2005	31.2
2002-2003	36.4

Table 4. Comparison of *C. anaticus* and a number of centric genera in the class Coscinodiscophyceae as described by Round et al. (1992).

Genus	<i>Clupeoparvus</i>	<i>Melosira</i>	<i>Hyalodiscus</i>	<i>Podosira</i>	<i>Chrysanthemodiscus</i>
Shape	Sub-spherical to cylindrical	Cylindrical to sub-spherical	Lens-shaped	Spherical to sub-spherical	Cylindrical, convex
Heterovalvy	Occasionally	No	No	No	Occasionally
Milled edge	No	Yes	No	No	No
Valve face	Domed, convex	Flat or domed	Deep, hemi-spherical	Hemispherical	Domed, undulating
Central area	Non-porous, flat	Porous	Non-porous, flat	Sometimes flat	Porous
Corona	Absent	Sometimes	Absent	Absent	Absent
Spines	Present, irregular	Present, irregular	Absent	Absent	Absent
Granules	Present	Present	Absent	Absent	Absent
External pores	Present in rows	Present	Present	Present in radial sectors	Present, radiating rows
Loculate (chambered)	No	Yes	Yes	Yes	Unknown
Internal pores	Sometimes covered	Larger pores than outside	Round pores with rotae	Pores open via rotae	Little detail evident
Portulae	Absent	Present	Present	Present	Absent
Copulae	Numerous		Very thin	Numerous	Numerous
Ligulate	Yes	Yes	Unknown	Yes	No
Porous	No	Yes	Yes	Yes	Yes
Split	Yes	Yes	Unknown	Yes	No
Colony					
Filamentous	No	Yes	Yes		Yes
Solitary	Yes		Yes	Yes	
Pairs/short chains	Yes		Yes	Yes	
Mucilage mass	Yes				
Ecology					
FW	Yes	Yes			
M		Yes	Yes	Yes	Yes
Epiphytic	Yes		Yes		Yes
Benthic	Yes	Yes	Yes	Yes	
Planktonic					

continued

Genus	<i>Coscinodiscus</i>	<i>Stellarima</i>	<i>Ellerbeckia</i>	<i>Pleurosira</i>	<i>Minidiscus</i>
Shape	Discoid, thin, barrel-shaped	Discoid	Large, short, cylindrical	Cylindrical	Barrel-shaped
Heterovalvy	No	No	Occasionally	No	No
Milled edge	No	No	No	No	No
Valve face	Flat, sometimes depressed	Convex face, radial striae	Flat with radial markings, grooves	Flat, deep mantle, radial striae	Slightly convex
Central area	Porous	Porous	Different from margin, no pores	Porous, two ocelli present	Raised pores
Corona	Absent	Absent	Absent	Absent	Absent
Spines	Absent	Absent	Absent	Absent	Absent
Granules	Absent	Absent	Absent	Sometimes	Absent
External pores	Present	Present, with cribra	Absent	Present	Present, raised
Loculate (chambered)	Yes	Yes	Yes	No	Yes
Internal pores	Foramina	Sometimes covered	Dome-like projections	Simple	Fine pores
Portulae	Present	Present	Absent	Present	Present
Copulae		Not studied			Not studied
Ligulate	Yes		No	Yes	
Porous	Yes		Yes	Yes	Yes
Split	Yes		Yes	Yes	
Colony					
Filamentous			Yes	Yes	Yes
Solitary	Yes	Yes			
Pairs/short chains					Yes
Mucilage mass					
Ecology					
FW			Mainly	Brackish	Yes
M	Yes	Yes			
Epiphytic					
Benthic					Yes
Planktonic	Yes	Yes			

continued

Genus	<i>Minidiscus</i>	<i>Thalassiosira</i>	<i>Porosira</i>	<i>Cyclotella</i>	<i>Cyclostephanos</i>	<i>Stephanodiscus</i>
Shape	Barrel-shaped	Discoid, cylindrical	Short, cylindrical	Short, drum-shaped	Short, disc-shaped	Discoid, shallow, barrel-shaped
Heterovalvy	No	No	No	No	No	No
Milled edge	No	No	No	No	No	No
Valve face	Slightly convex	Flat, ribbed	No real mantle	Undulating	Undulating	Undulate and almost flat, edge vertically grooved
Central area	Raised pores	Porous	Porous	Often non-porous	Porous	Porous or non-porous
Corona	Absent	Absent	Absent	Absent	Absent	Absent
Spines	Absent	Sometimes	Absent	Often present	Present	Present
Granules	Absent	Absent	Absent	Often present	Absent	Absent
External pores	Present, raised	Present with foramina	Present with foramina	Present	Raised pores	Present
Loculate (chambered)	Yes	Yes	Yes	No	No	No
Internal pores	Fine pores	Open	Closed	Closed	Domed cribra	Domed cribra
Portulae	Present	Present	Present	Present	Present	Present
Copulae	Not studied	Numerous	Numerous	Numerous		
Ligulate		Yes	No	No	Yes	Yes
Porous	Yes	Sometimes	Yes	No	Yes	Yes
Split		Yes	Yes	Yes	Yes	Yes
Colony						
Filamentous		Yes	Yes	Yes	Yes	Yes
Solitary	Yes	Yes		Yes	Yes	
Pairs/short chains					Yes	
Mucilage mass	Yes	Yes				
Ecology						
FW		Yes		Yes	Yes	Yes
M	Yes	Yes	Yes			
Epiphytic						
Benthic						
Planktonic	Yes	Yes	Yes	Yes	Yes	Yes